United States
Environmental Protection
Agency

Air Pollution Training Institute (APTI)
MD 17
Environmental Research Center
Research Triangle Park, NC 27711

January 2000

Air

Control of Particulate Matter Emissions

Student Manual

APTI Course 413
Third Edition

Author
John R. Richards, Ph.D., P.E.
Air Control Techniques, P.C.

Developed by

ICES Ltd.
EPA Contract No. 68D99022

ICES Ltd.
The Multimedia Group
Customized Multimedia Information and Training Solutions

Control of Particulate Matter Emissions

Student Manual

APTI Course 413

Third Edition

Author
John R. Richards, Ph.D., P.E.
Air Control Techniques, P.C.

Developed by
ICES Ltd.
EPA Contract No. 68D99022

Acknowledgments

The author acknowledges the contributions of Dr. James A. Jahnke and Dave Beachler, who authored the first edition of *Control of Particulate Emissions* in 1981 under contract to Northrop Services Inc. (EPA 450/2-80-068). In 1995, the second edition of this text was published, authored by Dr. John R. Richards, P.E., under contract to North Carolina State University (funded by EPA grant).

TABLE OF CONTENTS

	Section	Sub-Section	Contents	Page
			List of Tables	vi
			List of Figures	vii
			List of Acronyms	viii
Chapter 1			**Introduction**	
	1.1		Particulate Matter Control Regulations	1-1
	1.2		General Types of Particulate Matter Sources	1-8
	1.3		Particle Size	1-10
	1.4		Particle Size Distributions	1-14
	1.5		Particle Formation	1-17
			Review Exercises	1-22
			Review Answers	1-24
Chapter 2			**Particle Collection Mechanisms**	
	2.1		Steps in Particulate Matter Control	2-1
	2.2		Gravity Settling	2-4
	2.3		Centrifical Inertial Force	2-14
	2.4		Inertial Impaction	2-16
	2.5		Particle Brownian Motion	2-17
	2.6		Electrostatic Attraction	2-18
	2.7		Thermophoresis and Diffusiophoresis	2-20
	2.8		Particle Size-collection Efficiency Relationships	2-21
			Review Exercises	1-22
			Review Answers	1-24
Chapter 3			**Air Pollution Control Systems**	
	3.1		Flowcharts	3-1
		3.1.1	Flowchart Symbols	3-2
		3.1.2	Diagrams	3-6
	3.2		Gas Pressure, Gas Temperature, and Gas Flow Rate	3-15
	3.3		Hoods	3-20
		3.3.1	Hood Operating Principles	3-22
		3.3.2	Monitoring Hood Capture Effectiveness	3-26
	3.4		Fans	3-33
		3.4.1	Types of Fans and Fan Components	3-33
		3.4.2	Centrifugal Fan Operating Principles	3-37
		3.4.3	Effect of Gas Temperature and Density on Centrifugal Fans	3-47
Chapter 4			**Fabric Filters**	
	4.1		Types and Components	4-1
		4.1.1	Pulse Jet Fabric Filters	4-1
		4.1.2	Cartridge Filters	4-8
		4.1.3	Reverse Air Fabric Filters	4-10
		4.1.4	Fabric Types	4-13
	4.2		Operating Principles	4-18
		4.2.1	Particle Collection	4-18
		4.2.2	Emissions through Holes, Tears and Gaps	4-20
		4.2.3	Filter Media Blinding and Bag Blockage	4-24
		4.2.4	Fabric Filter Applicability Limitations	4-25

	Section	Sub-Section	Contents	Page
	4.3		Capability and Sizing	4-25
		4.3.1	Air-to-Cloth Ratio	4-25
		4.3.2	Gas Approach Velocity	4-29
		4.3.3	Bag Spacing and Length	4-32
		4.3.4	Bag "Reach" and Accessibility	4-34
		4.3.5	Cleaning System Design	4-34
		4.3.6	Reverse Air Fabric Filters Cleaning System Design	4-40
		4.3.7	Air Filtration	4-42
		4.3.8	Hopper Design	4-44
		4.3.9	Instrumentation	4-45
		4.3.10	Baghouse Bypass Dampers	4-47
			Review Exercises	4-48
			Review Answers	4-51
			Bibliography	4-55
Chapter 5			**Electrostatic Precipitators**	
	5.1		Types and Components	5-1
		5.1.1	Dry, Negative Corona Precipitators	5-1
		5.1.2	Wet, Negative Corona Precipitators	5-9
		5.1.3	Wet, Positive Corona Precipitators	5-14
	5.2		Operating Principles	5-15
		5.2.1	Precipitator Energization	5-15
		5.2.2	Particle Charging and Migration	5-17
		5.2.3	Dust Layer Resistivity	5-20
		5.2.4	Electrostatic Precipitator Applicability Limitations	5-25
	5.3		Electrostatic Precipitator Capability and Sizing	5-26
		5.3.1	Specific Collection Area	5-26
		5.3.2	Sectionalization	5-31
		5.3.3	Aspect Ratio	5-35
		5.3.4	Gas Superficial Velocity	5-36
		5.3.5	Collection Plate Spacing	5-36
		5.3.6	Flue Gas Conditioning Systems	5-37
		5.3.7	Evaporative Coolers	5-40
		5.3.8	Rapping Systems	5-40
		5.3.9	High Voltage Frame Support Insulators	5-41
		5.3.10	Discharge Electrodes	5-42
		5.3.11	Hoppers	5-43
		5.3.12	Instrumentation	5-43
			Review Exercises	5-45
			Review Answers	5-50
			Bibliography	5-54
Chapter 6			**Particulate Wet Scrubbers**	
	6.1		Types and Components of Wet Scrubber Systems	6-1
		6.1.1	Characteristics of Wet Scrubber Systems	6-1
		6.1.2	Types of Scrubbers Vessels	6-5
		6.1.3	Mist Eliminators	6-22
		6.1.4	Liquid Recirculation Systems, Alkali Addition Systems, and Wastewater Treatment Systems	6-25
		6.1.5	Fans, Ductwork and Stacks	6-28
		6.1.6	Instrumentation	6-29

	Section	Sub-Section	Contents	Page
	6.2		Particulate Matter Wet Scrubber Operating Principles	6-31
		6.2.1	Particle Collection Mechanisms	6-31
		6.2.2	Liquid-to-Gas Ratio	6-32
		6.2.3	Static Pressure Drop	6-32
		6.2.4	Particulate Matter Wet Scrubber Capabilities and Limitations	6-37
	6.3		Particulate Matter Wet Scrubber Sizing and Design	6-38
		6.3.1	Particulate Matter Removal Capability	6-38
		6.3.3	Liquid Purge Rates	6-45
		6.3.4	Mist Eliminator Velocities	6-46
		6.3.5	Alkali Requirements	6-47
		6.3.6	Instrumentation	6-48
			Review Exercises	6-51
			Review Answers	6-54
			Bibliography	6-57
Chapter 7			**Mechanical Collectors**	
	7.1		Types and Components of Mechanical Collectors	7-1
		7.1.1	Large Diameter Cyclones	7-1
		7.1.2	Small Diameter Multi-Cyclone Collectors	7-5
	7.2		Operating Principles	7-8
		7.2.1	Particle Collection	7-8
		7.2.2	Static Pressure Drop	7-11
		7.2.3	Capabilities and Limitations of Cyclonic Collectors	7-12
	7.3		Capability and Sizing of Mechanical Collectors	7-13
		7.3.1	Collection Efficiency	7-13
		7.3.2	Instrumentation	7-20
			Review Exercises	7-24
			Review Answers	7-28
			Bibliography	7-34
Chapter 8			**Particulate Matter Emission Testing and Monitoring**	
	8.1		Particle Size Distribution Measurement	8-1
		8.1.1	Cascade Impactors	8-1
		8.1.2	Microscopy	8-3
		8.1.3	Optical Counters	8-5
		8.1.4	Electrical Aerosol Analyzer	8-5
	8.2		Emission Testing Procedures	8-6
		8.2.1	General Testing Requirements	8-7
		8.2.2	Total Particulate Matter Emissions	8-14
		8.2.3	PM_{10} Particulate Matter Emissions	8-15
		8.2.4	$PM_{2.5}$ Particulate Matter	8-17
	8.3		Emission Monitoring	8-18
		8.3.1	Opacity	8-18
		8.3.2	Particulate Matter Continuous Emission Monitors	8-21
			Review Exercises	8-25
			Review Answers	8-27
			Bibliography	8-29
			References	8-29

LIST OF TABLES

			Page
Chapter 1	Table 1-1	Spherical Particle Diameter, Volume, and Surface Area	1-12
	Table 1-2	Aerodynamic Diameters of Differently Shaped Particles	1-13
	Table 1-3	Aerodynamic Diameters of Particles with Different Densities	1-13
	Table 1-4	Example Particle Size Data	1-15
Chapter 2	Table 2-1	Terminal Settling Velocities at 25°C	2-14
Chapter 3	Table 3-1	Codes for Utility Streams	3-2
	Table 3-2	Minor Components	3-4
	Table 3-3	Instrument Codes	3-5
	Table 3-4	Codes for Construction Materials	3-6
	Table 3-5	Baseline Data for the Hazardous Waste Incinerator	3-9
	Table 3-6	Gas Temperature Profile for the Hazardous Waste Incinerator (ºC)	3-9
	Table 3-7	Gas Static Pressure Profile for the Hazardous Waste Incinerator (in. W.C.)	3-9
	Table 3-8	Static Pressures and Static Pressure Drops (in. W.C.)	3-13
	Table 3-9	Gas Temperatures (ºF)	3-14
	Table 3-10	Units of Pressure	3-16
	Table 3-11	Commonly Recommended Transport Velocity	3-32
	Table 3-12	Relationship Between Fan Speed and Air Flow Rate	3-37
	Table 3-13	Relationship Between Fan Speed and Fan Static Pressure Rise	3-38
	Table 3-14	Gas Densities at Different Gas Temperatures	3-47
Chapter 4	Table 4-1	Temperature and Acid Resistance Characteristics	4-16
	Table 4-2	Fabric Resistance to Abrasion and Flex	4-17
	Table 4-3	General Summary of Air-to-Cloth Ratios in Various Industrial Categories	4-29
	Table 4-4	Common Sites of Air Infiltration	4-43
Chapter 5	Table 5-1	Effective Migration Velocities for Various Industries	5-28
	Table 5-2	Data Used in EPA/RTI Computerized Performance Model for Electrostatic Precipitators	5-29
	Table 5-3	Calculation Results for Problem 5-2	5-30
	Table 5-4	Typical Sizing Parameters Dry Negative Corona ESPs	5-37
Chapter 6	Table 6-1	Gas Velocities Through Mist Eliminators	6-46
Chapter 7	Table 7-1	Efficiency Estimates, Problem 7-1	7-18
	Table 7-2	Efficiency Estimates, Problem 7-2	7-19

LIST OF FIGURES

Chapter 1 **Page**

Figure 1-1. Community near a steel mill in the northeast U.S., 1967 1-1
Figure 1-2. Particulate matter emissions from a stationary source, 1970 1-2
Figure 1-3. Typical fuel burning curve particulate matter regulation 1-3
Figure 1-4. Opacity of a plume emitted from a stationary source 1-4
Figure 1-5. Fugitive particulate matter escaping a hood 1-4
Figure 1-6. Fugitive particulate matter from an unpaved road 1-5
Figure 1-7. Typical ambient air particulate matter size distributions 1-7
Figure 1-8. Comparison of ambient particulate matter size range definitions 1-7
Figure 1-9. Traditionally inventoried PM_{10} emissions in the U.S. 1-9
Figure 1-10. Complete inventory of PM_{10} sources 1-9
Figure 1-11. Very large particle and rain drop 1-10
Figure 1-12. 1 and 10 μm particles compared to a 100 μm particle 1-11
Figure 1-13. Scanning electron microscopy photomicrograph of coal fly ash 1-12
Figure 1-14. Different shapes of particles 1-14
Figure 1-15. Particle size distribution 1-14
Figure 1-16. Histogram of a lognormal size distribution 1-15
Figure 1-17. Cumulative lognormal size distribution 1-16
Figure 1-18. Multi-normal particle size distribution 1-17
Figure 1-19. Grinding wheel 1-17
Figure 1-20. Tertiary crusher 1-18
Figure 1-21. Combustion process 1-19
Figure 1-22. Chemical composition resulting form heterogeneous nucleation 1-20
Figure 1-23. Approximate particle size distributions resulting from various formation mechanisms ... 1-21

Chapter 2

Figure 2-1. Steps in particulate matter collection in a pulse jet fabric filter 2-2
Figure 2-2a. Side elevation view of an electrostatic precipitator 2-3
Figure 2-2b. Precipitator plate dust layer 2-3
Figure 2-3. Drag force on particle 2-5
Figure 2-4. Relationship between C_D and N_{Rep} for spheres 2-8
Figure 2-5. Relationship between particle size, temperature, and the Cunningham Correction Factor, C_c 2-10
Figure 2-6. Balance of gravitational and drag forces 2-12
Figure 2-7. View of spinning gas in a cyclone 2-15
Figure 2-8. Inertial impaction and interception 2-16
Figure 2-9. General characteristics of the impaction efficiency curve 2-17
Figure 2-10. Brownian motion 2-17
Figure 2-11. General relationship between collection efficiency and particle size 2-21

Chapter 3

Figure 3-1. Material stream symbols 3-2
Figure 3-2. Major equipment symbols 3-3
Figure 3-3. Identification of emission points 3-3
Figure 3-4. Minor component symbols 3-4
Figure 3-5. Gauge symbols. 3-5
Figure 3-6. Example flowchart of a waste solvent system 3-7
Figure 3-7. Example flowchart of an asphalt plant 3-7
Figure 3-8. Example flowchart of a hazardous waste incinerator and pulse jet baghouse system 3-8
Figure 3-9. Static pressure and temperature profile for present data 3-10
Figure 3-10. Example flowchart of a hazardous waste incinerator and venturi scrubber system 3-13

Figure 3-11. Static pressure profiles 3-14
Figure 3-12. Definition of positive and negative pressure 3-16
Figure 3-13. Example gas velocity calculation using ACFM 3-19
Figure 3-14. Stationary hood in an industrial process 3-20
Figure 3-15. Role of hoods in an industrial process 3-21
Figure 3-16. Hood capture velocities 3-23
Figure 3-17. Beneficial effect of side baffles on hood captive velocities 3-25
Figure 3-18. Push-pull hood 3-26
Figure 3-19. Plain duct end with a hood entry loss coefficient of 0.93 3-27
Figure 3-20. Flanged opening with a hood entry loss coefficient of 0.49 3-28
Figure 3-21. Bell-mouth inlet with a hood entry loss coefficient of 0.04 3-28
Figure 3-22. Relationship between hood static pressure and flow rate 3-29
Figure 3-23. Axial fans 3-34
Figure 3-24. Centrifugal fan components 3-34
Figure 3-25. Centrifugal fan and motor sheaves 3-35
Figure 3-26. Types of fan wheels 3-36
Figure 3-27. Centrifugal fan with radial blade 3-37
Figure 3-28. Fan static pressure rise 3-38
Figure 3-29. Total system static pressure drop 3-39
Figure 3-30. System characteristic curve 3-40
Figure 3-31. Fan static pressure rise profile 3-40
Figure 3-32. Portion of a typical multi-rating table 3-41
Figure 3-33. Operating point 3-41
Figure 3-34. Fan characteristic curve 3-42
Figure 3-35. Changes in the system resistance curve 3-43
Figure 3-36. Changes in the fan speed 3-43
Figure 3-37. Changes in the inlet damper position 3-44
Figure 3-38. Portion of a ventilation system 3-45
Figure 3-39. Example of a brake horsepower curve 3-46
Figure 3-40. Example flowchart 3-51

Chapter 4

Figure 4-1. Typical pulse jet fabric filter 4-2
Figure 4-2. View of the bottoms of pulse jet bags 4-3
Figure 4-3a. Worm drive clamp type attachment 4-4
Figure 4-3b. Snap ring type attachment 4-4
Figure 4-4. Damage to the compressed air delivery tube position relative to the bag inlet 4-5
Figure 4-5. Gravity settling during cleaning of pulse jet bags 4-6
Figure 4-6. Compartmentalized pulse jet baghouse 4-7
Figure 4-7. Magnehelic® static pressure drop gauge 4-8
Figure 4-8. Pleated cartridge filter element 4-9
Figure 4-9. Flat cartridge filter element 4-9
Figure 4-10. Reverse air fabric filter 4-10
Figure 4-11. Reverse air bag 4-10
Figure 4-12a. Clamp-and-thimble-type bag attachment 4-11
Figure 4-12b. Snap-ring type bag attachment 4-11
Figure 4-13. Pyramidal type hopper 4-12
Figure 4-14a. Rotary discharge valve 4-12
Figure 4-14b. Double flapper valve 4-13
Figure 4-15. Woven fabric 4-14
Figure 4-16. Felted fabric 4-15
Figure 4-17. Membrane fabric at 500x magnification 4-15
Figure 4-18. Particle size to efficiency relationship 4-18

Figure 4-19. Emissions as a function of air-to-cloth ratio 4-19
Figure 4-20. Gas flow through holes, tears, and gaps....4-20
Figure 4-21. Flange-to-flange and filter media static pressure drops 4-22
Figure 4-22. Static pressure drop profile 4-24
Figure 4-23. Gas approach velocity for pulse jet baghouse 4-30
Figure 4-24. Gas approach velocity in reverse air baghouse 4-31
Figure 4-25. Possible problems with tall pulse jet bags....4-33
Figure 4-26. Pulse jet bag-to-bag contact 4-34
Figure 4-27. Layout of reverse air bags 4-35
Figure 4-28. Process fugitive emissions caused by increased gas flow resistance through a baghouse....4-35
Figure 4-29. Major components of a pulse jet baghouse cleaning system....4-36
Figure 4-30. Vulnerable position of diaphragm valve relative to compressed air manifold in certain designs. 4-38
Figure 4-31. Damper in a reverse air baghouse 4-40
Figure 4-32. A standard poppet valve in open and closed positions....4-41
Figure 4-33. Top access hatches on a top-load pulse jet baghouse....4-43
Figure 4-34. Corroded area on the sidewall of a baghouse....4-44
Figure 4-35. Hopper design features....4-45
Figure 4-36. Triboflow® type bag break detector 4-46

Chapter 5

Figure 5-1. Gas passage composed of discharge electrode and collection plates....5-2
Figure 5-2. Typical dry, negative corona type electrostatic precipitator 5-2
Figure 5-3. Gas distribution screens at the precipitator inlet 5-3
Figure 5-4. Arrangement of fields and chambers in a dry, negative corona precipitator....5-4
Figure 5-5. Transformer-rectifier set, support insulator discharge electrode frames, and discharge electrodes 5-4
Figure 5-6. Types of gauges present on the control cabinet for each precipitator field....5-5
Figure 5-7. Measurement of an alignment position 5-6
Figure 5-8. Sketch of high voltage frame support insulators....5-6
Figure 5-9. Anti-sway insulator suffering electrical short-circuiting across the surface 5-7
Figure 5-10. Components of a precipitator hopper....5-8
Figure 5-11. Roof-mounted rapper 5-8
Figure 5-12. Side-mounted collection plate rappers 5-9
Figure 5-13. General flowchart of a wet, negative corona precipitator 5-10
Figure 5-14. Vertical, wet negative corona precipitator 5-11
Figure 5-15. Side view of a horizontal gas flow wet, negative corona precipitator 5-12
Figure 5-16. View of the traversing header sprays on a wet, negative corona precipitator....5-13
Figure 5-17. Wet, positive corona precipitator 5-14
Figure 5-18. Precipitator field energization....5-15
Figure 5-19. Voltage-current curve....5-16
Figure 5-20. Corona discharges 5-18
Figure 5-21. Typical particle size efficiency relationship for electrostatic precipitators 5-19
Figure 5-22. Trajectories of particles redispersed from upper portions of inlet field collection plates....5-21
Figure 5-23. Terminal settling velocities of particles 5-21
Figure 5-24. Effect of dust layer resistivity on migration velocity....5-22
Figure 5-25. Paths of current flow through the dust layers....5-23
Figure 5-26. Example resistivity-temperature relationship....5-24
Figure 5-27. Collection plate area calculation 5-31
Figure 5-28. Applied secondary voltage before and after an electrical spark 5-32
Figure 5-29. Precipitator with poor aspect ratio 5-36

Figure 5-30. Sulfur trioxide conditioning system 5-38
Figure 5-31. Pellitized sulfur type sulfur trioxide conditioning system 5-39
Figure 5-32. High voltage support insulator 5-41
Figure 5-33. Electrical resistance heater for a high voltage support insulator 5-42
Figure 5-34. Protective shroud on a wire-type discharge electrode 5-42

Chapter 6

Figure 6-1. Example particulate matter wet scrubber system 6-2
Figure 6-2. Venturi scrubber and mist eliminator vessel 6-4
Figure 6-3. Spray tower scrubber 6-7
Figure 6-4. Mechanically aided scrubber 6-8
Figure 6-5. Common types of packing material 6-8
Figure 6-6. Vertical packed bed scrubber system 6-9
Figure 6-7. Crossflow packed bed scrubber 6-10
Figure 6-8. Composite fiber pad 6-10
Figure 6-9. Four stage fiber bed scrubber 6-11
Figure 6-10. Wet-ionizing scrubber 6-12
Figure 6-11. Impingement tray scrubber 6-13
Figure 6-12. Catenary grid scurbber 6-14
Figure 6-13. Fixed throat venturi scrubber 6-16
Figure 6-14. Adjustable throat venturi scrubber 6-16
Figure 6-15. Flow restrictor-type adjustable throat venturi scrubber 6-17
Figure 6-16. Rod deck scrubber 6-18
Figure 6-17. Collision scrubber 6-19
Figure 6-18. Orifice scrubber vessel 6-19
Figure 6-19. Nozzle in a high energy liquid atomization scrubber 6-20
Figure 6-20. Example of a condensation growth scrubber system 6-21
Figure 6-21. Cyclonic mist eliminator 6-23
Figure 6-22. Radial vane mist eliminator with heavy solids accumulation 6-23
Figure 6-23. Chevron mist eliminator 6-24
Figure 6-24. Mesh pad mist eliminator 6-25
Figure 6-25. Centrifugal pump 6-26
Figure 6-26. Spray pattern of full cone nozzle 6-27
Figure 6-27. Relationship between contact power and number of transfer units, cyclonic and venturi scrubbers serving ferrosilicon furnaces. 6-34
Figure 6-28. Relationship between pressure drop and particulate emissions for flooded disc scrubbers serving lime kilns 6-34
Figure 6-29 Particulate emissions versus pressure drop, venturi scrubber serving coal driers 6-35
Figure 6-30. Emissions versus pressure drop for three venturi scrubbers serving Q-BOF processes 6-36
Figure 6-31. Particle size-collection efficiency relationships 6-37
Figure 6-32. Penetration versus particle size for an example venturi scrubber 6-41
Figure 6-33 Definition of the liquid-to-gas ratio 6-44
Figure 6-34 Psychrometric chart method of estimating adiabatic saturation temperature 6-49

Chapter 7

Figure 7-1. Large diameter cyclones 7-1
Figure 7-2. Types of cyclone inlets 7-2
Figure 7-3. Four types of solids discharge valves 7-3
Figure 7-4. Special outlet configurations for large diameter cyclones 7-4
Figure 7-5. Series and parallel arrangements of cyclones 7-4
Figure 7-6. Multi-cyclone collector 7-5
Figure 7-7. Small diameter cyclone tube for a multi-cyclone collector 7-6
Figure 7-8. Gasket between a multi-cyclone tube and a dirty side tube sheet 7-7

Figure 7-9. Outlet tube: clean side tube sheet seals for multi-cyclone collectors 7-8
Figure 7-10. View of spinning gas in a cyclone 7-9
Figure 7-11. Particle size-collection efficiency relationship for cyclonic collectors 7-10
Figure 7-12. Cyclone efficiency versus particle size, experimental results, and theoretical predictions 7-13
Figure 7-13. Cyclone efficiency versus particle size ratio 7-17
Figure 7-14. Problems 7-1 and 7-2 efficiency curves 7-19
Figure 7-15. Cross-hopper gas flow 7-22
Figure 7-16. Hopper baffles to prevent cross-hopper flow 7-23
Figure 7-17. Side stream baghouses 7-23

Chapter 8

Figure 8-1. Schematic diagram, operation of a cascade impactor 8-2
Figure 8-2. Sketches of two commercial types of cascade impactors 8-2
Figure 8-3. Optical microscope used for PLM analyses 8-4
Figure 8-4. SEM photomicrograph fly ash 8-4
Figure 8-5. Operating principle for an optical particle counter 8-5
Figure 8-6. Coaxial cylinder mobility analyzer 8-6
Figure 8-7. Minimum number of traverse points for particulate traverse 8-8
Figure 8-8. Example calculation of the number of sampling points 8-8
Figure 8-9. Location of traverse points in a circular stack 8-9
Figure 8-10a. Parallel flow 8-10
Figure 8-10b. Cyclonic flow 8-10
Figure 8-11. Type S pitot tube 8-10
Figure 8-12. Velocity traverse form 8-12
Figure 8-13. Complete sampling train for particulate emission testing 8-13
Figure 8-14. Isokinetic sampling bias 8-14
Figure 8-15. Method 5 particulate sampling train 8-14
Figure 8-16. Method 17 particulate sampling train 8-15
Figure 8-17. Method 201A particulate sampling train 8-16
Figure 8-18. Dual cyclone sampling head for PM_{10} and PM_{25} 8-17
Figure 8-19. Double-pass opacity monitor 8-19
Figure 8-20. Siting for opacity monitor 8-20
Figure 8-21. Light scattering type particulate CEM 8-21
Figure 8-22. Scintillation monitor 8-22
Figure 8-23. Beta gauge instrument 8-23
Figure 8-24. Oscillating microbalance particulate CEMS 8-23

LIST OF ACRONYMS

ACRONYM		DEFINITION
ACFM	-	actual cubic feet per minute
BACT	-	best available control technology
CAAA	-	Clean Air Act Amendments
cgsu	-	centimeter gram second units
DSCFM	-	dry standard cubic feet per minute
EAA	-	electric aerosol analyzer
EDS	-	energy dispersive X-ray spectroscopy
ESP	-	electrostatic precipitator
FGC	-	flue gas conditioning
FRP	-	fiberglass reinforced plastics
LEL	-	lower explosive limit
MACT	-	maximum achievable control technology
MMD	-	mass median diameter
MND	-	median number diameter
MVD	-	median volume diameter
NAAQS	-	National Ambient Air Quality Standards
NASHAP	-	National Emissions Standards for Hazardous Air Pollutants
NSPS	-	New Source Performance Standards
PLM	-	plarizing light microscopy
psi	-	pounds per square inch
PTFE	-	polytetrafluoroethylene
SCFM	-	standard cubic feet per minute
SCA	-	specific collection area
SCR	-	silicon controlled rectifier
SEM	-	scanning electron microscopy
SIP	-	state implementation plan
SMD	-	Sauter mean diameter
SNCR	-	selective non-catalytic reduction
STP	-	standard temperature and pressure

T-R	-	transformer rectifier
TSP	-	total suspended particle
W.C.	-	water column

Chapter 1
Introduction

The regulation of particulate matter matter emissions dates back to the early stages of the industrial revolution. Even in the 1600s, people could see the relationship between particulate matter emissions and problems such as solids deposition, fabric soiling, material corrosion, and building discoloration. As technology and public awareness expanded, it became apparent that particulate matter emissions also contributed to certain types of lung disease and related illnesses. Particulate matter emissions were an important factor in the air pollution-related fatalities that occurred during a multi-day atmospheric inversion in Donora, Pennsylvania in 1947. Since that time, particulate matter emissions have been identified as causal factors in many toxicological and epidemiological studies, and there continues to be a strong public demand for particulate matter control.

In the late 1940s, many types of particulate matter control systems advanced from relatively rudimentary designs to forms that resemble modern-day, high efficiency systems. For example, electrostatic precipitators advanced from one-field, tubular units for acid mist control to one- and two-field, plate-type precipitators. Venturi scrubbers also began to be used for particulate matter control. These control systems were installed primarily to satisfy local health department requirements and to minimize nuisance dust problems.

1.1 PARTICULATE MATTER CONTROL REGULATIONS

Conditions such as those shown in Figures 1-1 and 1-2 were common in the United States until particulate matter control devices began to be installed. The environmental awareness that began to increase during the 1950s and 1960s culminated in the enactment of the Clean Air Act Amendments of 1970, which substantially increased the pace of particulate matter control. Since 1970, there have been substantial advancements in the capability and reliability of particulate matter control devices. Many new types of systems have been commercialized. Increasingly efficient control systems are being developed and installed in response to the stringent requirements that will be imposed by regulations adopted in accordance with the Clean Air Act Amendments of 1990.

Figure 1-1. Community near a steel mill in the northeast U.S., 1967

Figure 1-2. Particulate matter emissions from a stationary source, 1970

The emissions of particulate matter from sources similar to the one shown in Figure 1-2 combined with other particulate matter emissions have created high ambient levels of total suspended particulate matter (TSP) in many communities. Due to increasing concerns about the possible health and welfare effects of ambient particulate matter, regulatory agencies in the late 1960s began to measure the ambient concentrations of TSP using High-Volume (Hi-Vol) ambient samplers that provided a single concentration value for a 24-hour sampling period. Particulate matter that was sufficiently small to remain suspended in the atmosphere and captured in the sampling systems of the Hi-Vol samplers was defined as TSP. Particles smaller than approximately 45 micrometers (45µm)—approximately the diameter of a human hair—are considered to be TSP.

On November 25, 1971, the newly formed U.S. Environmental Protection Agency (EPA) promulgated primary and secondary National Ambient Air Quality Standards (NAAQS) for TSP. Both types of standards were designed to set upper limits to the permissible ambient concentrations of TSP. The primary standards were more restrictive and were designed to protect health. The secondary standards were intended to reduce adverse material effects (crop damage, building soiling, dustfall) of particulate matter. These standards were based on the available ambient monitoring and health/welfare effects research data. Based on the available information, all areas of the country were divided into Air Quality Control Regions. Areas having measured ambient concentrations of TSP above the primary or secondary standards were labeled as nonattainment areas. Nonattainment areas were required to devise a set of emission regulations and other procedures that would reduce ambient levels of particulate matter below the NAAQS specified limits.

Control strategies for the achievement of the NAAQS were developed and adopted as part of the State Implementation Plans (SIPs) required by the Clean Air Act Amendments of 1970. These control strategies were designed by each state and local regulatory agency having areas above the NAAQS limits. Particulate matter emission regulations were adopted by the states and local agencies to implement the SIP control strategies.

These particulate matter emission limitations took many regulatory forms, many of which are still in effect today. For stationary combustion sources, conventional "fuel burning curve" regulations were made more stringent. This type of regulation limits the total particulate matter emissions based on a fuel heat input basis. Moderate emissions are allowed for small sources where air pollution control is especially expensive. Lower emissions are required for larger sources where particulate matter control

equipment is more applicable and economical. Typical fuel burning emission regulatory limits are shown in Figure 1-3.

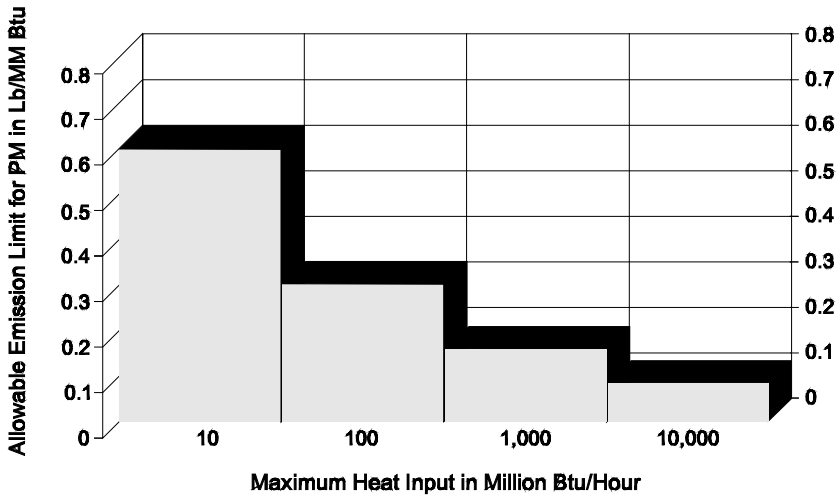

Figure 1-3. Typical fuel burning curve particulate matter regulation

It is apparent that the allowable emission rate (in terms of pounds per million BTU of heat input) is much lower for large sources than for small sources. However, the total quantity of emissions in terms of pounds per hour is proportional to the combustion source operating rate. Higher mass emissions are allowed at higher boiler or furnace loads. Compliance is determined by means of a stack-type emission test.

A process weight-based particulate matter emission regulation is used for industrial process sources. It is conceptually similar to the fuel burning regulation because the allowable emissions are a function of the process operating rate. The emission rates are also larger for small sources. Process weight emission limitations are expressed mathematically using equations similar to Equation 1-1 and Equation 1-2.

$$E_1 = 4.9445\ (P)^{0.4376} \tag{1-1}$$

Where:

E_1 = allowable emissions for asphalt plants (lb_m/hr)
P = process operating rate (ton/hr)

$$E_2 = 9.377\ (P)^{0.3067} \tag{1-2}$$

Where:

E_2 = allowable emissions for chemical fertilizer plants (ton/hr)
P = process operating rate (ton/hr)

Opacity regulations were adopted along with fuel burning, process weight, and other emission rate type regulations. Opacity is a measure of the extent to which the particulate matter emissions reduce the ambient light passing through the plume as indicated in Figure 1-4.

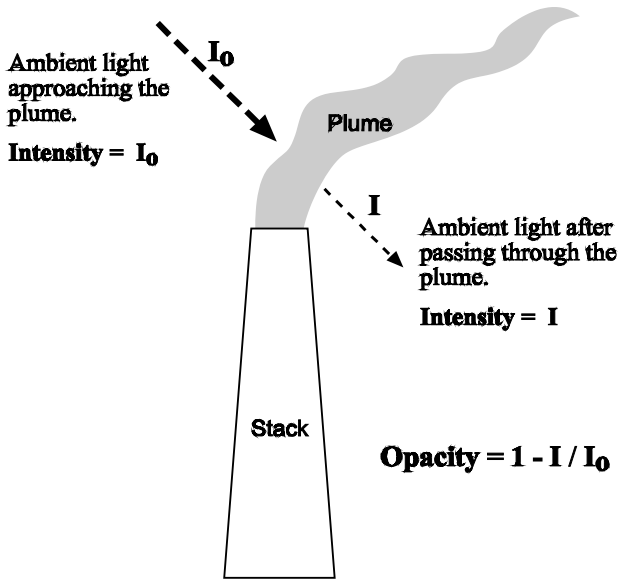

Figure 1-4. Opacity of a plume emitted from a stationary source

Opacity is a convenient indirect indicator of particulate matter emissions and can be determined by a trained visible emissions observer without the need for special instruments. Initially, opacity regulations were used primarily as general indicators of particulate matter problems. As the regulations evolved, however, opacity has become a separately enforceable emission characteristic.

In addition to regulations applying to particulate matter emitted from stacks and vents, the regulations included in the SIPs applied to fugitive particulate matter emissions. As illustrated in Figures 1-5 and 1-6, fugitive emission sources include (1) sources where a portion of the particulate matter generated escapes collection hoods and is emitted directly to the atmosphere and (2) unpaved roads and similar dust sources that cannot be captured by hoods and controlled by air pollution control systems.

Figure 1-5. Fugitive particulate matter escaping a hood

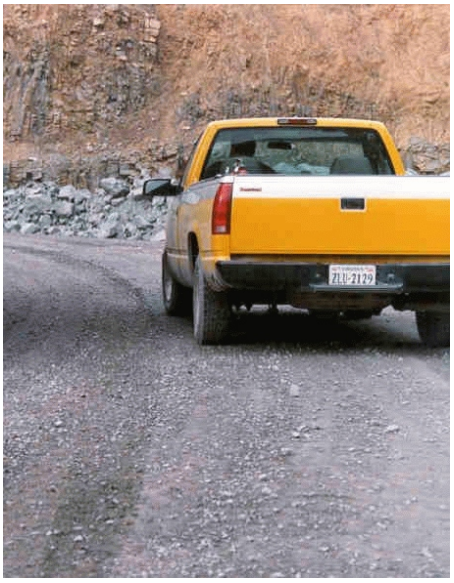

Figure 1-6. Fugitive particulate matter from an unpaved road

Fugitive emission regulations were adopted to control process related fugitive emissions. Due to the diversity of these sources and the difficulty in measuring fugitive emissions, regulations have taken many forms. Regulations include but are not limited to (1) required work practices, (2) visible emission (opacity) limits at plant boundary lines, and (3) visible emission limits at the process source.

All of the regulation types discussed above apply to existing sources included within the scope of the SIPs. Substantial differences in the stringency of regulations existed from jurisdiction to jurisdiction, depending on the particulate matter control strategy believed necessary and advantageous to achieve the NAAQS. The Clean Air Act Amendments of 1970 also stipulated emission limitations that would apply to new (and substantially modified) sources on a nationwide basis. The purpose of these regulations was to ensure continued reductions in the total particulate matter emissions as new sources replaced existing sources. These new source-oriented standards were titled "New Source Performance Standards" (NSPS). These stringent standards were adopted by the U.S. EPA on a source category-by-category basis. Sources subject to these regulations are required to install air pollution control systems that represent the “best demonstrated technology” for that particular type of industrial source category. In addition to particulate matter mass emission standards, the U.S. EPA also included opacity limits and continuous opacity monitoring requirements in many of the NSPS standards.

The Clean Air Act of 1970 authorized the promulgation of especially stringent regulations for pollutants that are considered highly toxic or "hazardous." The U.S. EPA was charged with the responsibility of identifying these pollutants and developing appropriate regulations to protect human health. This set of regulations is titled “National Emission Standards for Hazardous Air Pollutants” (NESHAPS). Due to regulatory complexities occurring from 1971 to 1990, only a few of these regulations were promulgated. The Clean Air Act Amendments of 1990 (CAAA of 1990) required a major revision and expansion of these regulations. The CAAA of 1990 specified 189 specific pollutants and categories of pollutants. In June of 1996 the chemical caprolactam was removed from the list. Title III provisions of the CAAA of 1990 require that regulations be developed for the present 188 specific pollutants and categories of pollutants. This list includes many compounds and elements that are generally in particulate matter form. These regulations were adopted on a source category-by-category basis starting in 1991. Sources subject to the regulation are required to install “Maximum Achievable Control Technology” (MACT) as defined

by the U.S. EPA for that source category. These regulations are a major driving force for particulate matter control in the future. While the MACT regulations are not directed at the control of particulate matter per se, they will require the high efficiency control of the toxic compounds (listed in Title III) that are included in the particulate matter.

The U.S. EPA defines PM_{10} as particulate matter with a diameter of 10 micrometers collected with 50% efficiency by a sampling collection device. However, for convenience purposes, the remainder of this course will consider PM_{10} to include particles having an aeordynamic diameter of less than equal to 10 micrometers. $PM_{2.5}$ will include particles having an aeordynamic diameter of 2.5 micrometers or less.

In 1987, the U.S. EPA revised the NAAQS for particulate matter to include only particles equal to or smaller than 10 micrometers (m). This change was made to focus regulatory attention on those particles that are sufficiently small to penetrate into the respiratory system and, therefore, contribute to adverse health effects. Particles larger than 10 m are effectively filtered out by the nose and upper respiratory tract. Therefore, only particles equal to or smaller than 10 m were measured in evaluating ambient air quality levels with respect to the NAAQS. These particulate matters are collectively designated as PM_{10} to differentiate them from TSP. A few of the source-oriented particulate matter emission regulations, such as fuel burning curves and process weight curves, have also been revised to address only PM_{10}.

In 1997, the U.S. EPA added a new NAAQS applicable to particulate matter equal to or less than 2.5 m and termed $PM_{2.5}$. The U.S. EPA concluded that the $PM_{2.5}$ NAAQS were needed in response to health effects research indicating that particulate matter in this size category was most closely associated with adverse health effects.

Health effects attributed to $PM_{2.5}$ are believed to result from both their small size and their composition. Small size increases the probability that the particles will penetrate deeply into the respiratory tract and be retained. There are also data indicating that materials present in $PM_{2.5}$ particles are considerably more toxic than those present in the larger particles.

The difference in particle composition is due to quite different particle formation mechanisms. This is indicated by the distinct tri-modal ambient particle size distributions that are generally observed in research studies. As indicated in Figure 1-7, there are ultrafine particles smaller than 0.1 micrometer (nuclei mode), fine particles approximately 0.1 to 2.5 micrometers (accumulated and nuclei modes), and coarse particles larger than 2.5 micrometers.

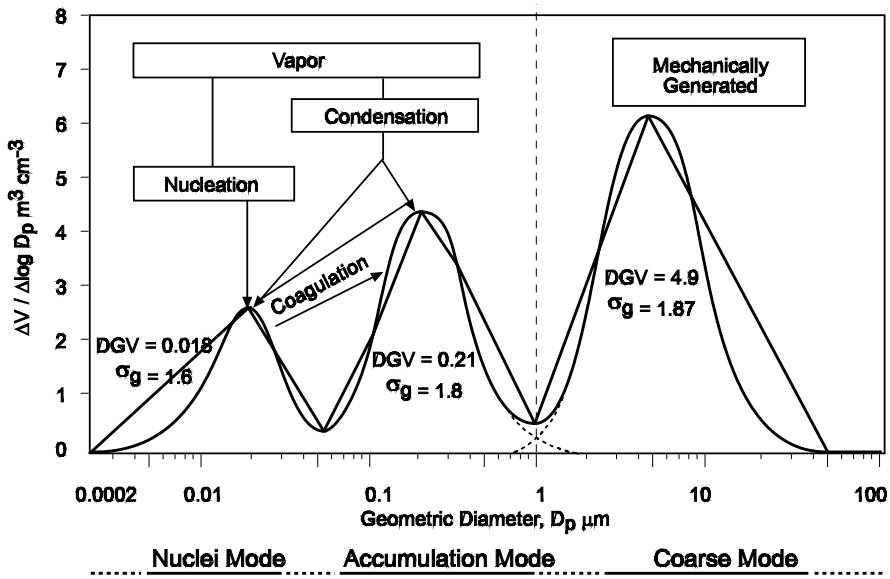

Figure 1-7. Typical ambient air particulate matter size distributions
(Source: U.S. EPA, Criteria Document, 1997)

The particles in the ultrafine and fine distributions are formed mainly by chemical reactions between gases in the atmosphere. The particles in the coarse distribution are formed primarily by physical grinding (attrition) and by combustion burnout of ash particles.

State and local agencies are now deploying ambient air monitors to measure the 24-hour average $PM_{2.5}$ concentrations. These data will be used in the future to determine areas that are not in attainment with the NAAQS. State and local agencies will formulate control strategies and adopt control regulations to control $PM_{2.5}$. This regulatory process is quite similar to the process used in the development of TSP and PM_{10} controls in the past. However, due to the differences in the sources of $PM_{2.5}$, these new regulations might concern a quite different set of sources.

A summary of the ambient particulate matter size ranges that have been subject to NAAQS are provided in Figure 1-8. The TSP NAAQS were retired in 1987 when the PM_{10} standard was first adopted. The NAAQS apply to PM_{10} and $PM_{2.5}$.

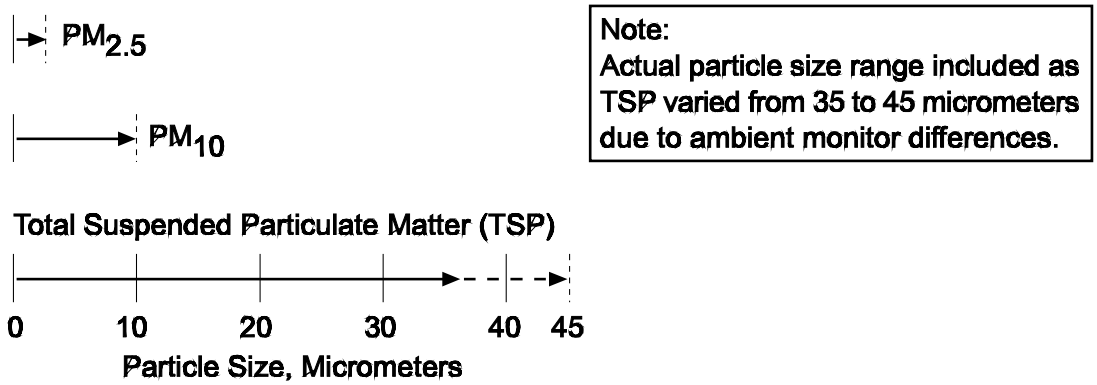

Figure 1-8. Comparison of ambient particulate matter size range definitions

1.2 GENERAL TYPES OF PARTICULATE MATTER SOURCES

Particulate matter can be divided into the following two categories:

1. Primary particulate matter
2. Secondary particulate matter

Primary particulate matter is material emitted directly in to the atmosphere. These emissions have been the focus of all particulate matter control programs prior to 1997. Primary particulate matter can consist of particles less than 0.1 micrometer to more than 100 micrometers; however, most of the primary particulate matter is in the coarse mode shown in Figure 1-7.
With the promulgation of the $PM_{2.5}$ standard aimed at fine and ultrafine particles, there is increasing attention concerning "secondary" particulate matter. This is particulate matter that forms in the atmosphere due to reactions of gaseous precursors. Secondary formation processes can result in the formation of new particles or the addition of particulate material to pre-existing particles. The gases most commonly associated with secondary particulate matter formation include sulfur dioxide, nitrogen oxides, ammonia, and volatile organic compounds. Most of these gaseous precursors are emitted from anthropogenic sources; however, biogenic sources also contribute some nitrogen oxides, ammonia, and volatile organic compounds.

Secondary particulate matter can be further subdivided into two categories.

1. Secondary particulate matter formed from condensed vapors emitted from anthropogenic and biogenic sources
2. Secondary particulate matter formed due to atmospheric reactions of gaseous precursors

Volatile organic compounds and sulfuric acid are two common examples of emissions that can condense to form secondary particulate matter. These materials pass through particulate matter control systems, including high efficiency devices, due to their vapor form in the stationary source gas stream. However, the vapor phase material can, under some conditons, potentially condense in the ambient air to form particles measured by ambient sampling systems. The relative importance of condensable particulate matter is just beginning to be evaluated.

Sulfates, nitrates, and ammonium compounds are three of the main types of material present in secondary particles formed by atmospheric reactions. These materials appear to form over periods of hours to days as gaseous precursors in plumes and in large air masses move across the country. Particulate matter formed in atmospheric reactions is important with respect to the ambient $PM_{2.5}$ concentrations. However, the relative importance of stationary and mobile sources in emitting the precursors for this type of secondary particulate matter has not been fully evaluated.

More data are available for the main sources of particulate matter in the coarse and supercoarse mode. This material is inventoried by the U.S. EPA as PM_{10}. In the most recent edition of the emission trends report (U.S. EPA, 1997c), the U.S. EPA has divided these sources into the following two categories:

1. Traditionally Inventoried
2. Other

The traditionally inventoried sources of PM_{10} include stationary source fuel combustion (e.g., utility and industrial boilers), stationary industrial processes (e.g., steel mills, foundries), and transportation sources (e.g., cars, trucks, airplanes). As indicated in Figure 1-9, stationary source fuel combustion accounts for approximately 35%, industrial processes 42%, and transportation sources 23% of the total U.S. emissions

of PM_{10}. There are substantial area-to-area differences in the relative emissions due to the distribution of industrial sources in various geographical areas and the concentration of transportation sources in urban regions.

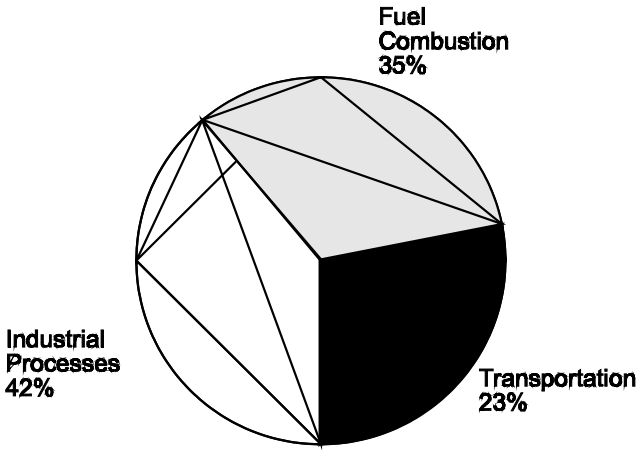

Figure 1-9. Traditionally inventoried PM_{10} emissions in the U.S. (Source: U.S. EPA, 1997c)

As indicated by the U.S. EPA's estimates shown in Figure 1-10, fugitive PM_{10} emissions account for approximately 58%, wind erosion (natural emission) approximately 16%, and agricultural operations for 14% of the total U.S. emissions. The traditionally inventoried stationary sources (Figure 1-9) account for only 9% of this total. Other combustion sources, such as wood burning stoves, account for an additional 3% of this total.

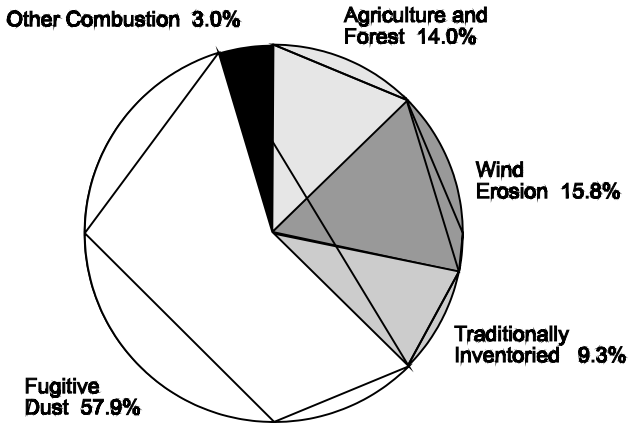

Figure 1-10. Complete inventory of PM_{10} sources (Source: U.S. EPA, 1997c)

The general inventory of PM_{10} sources indicated in Figure 1-10 represents only a snapshot of the emissions. Since emissions from these major sources are extremely difficult to measure accurately. Furthermore, this inventory does not take into account the possible long range transport of particulate matter in air masses. Accordingly, these data provide only a general indication of the relative importance of different categories of PM_{10}.

1.3 PARTICLE SIZE

Particulate matter regulations adopted over the last thirty years have gradually shifted from regulating the coarse mode particles that comprised TSP to regulating the very small particles in the PM_{10} and $PM_{2.5}$ size ranges. This shift has occured primarily because health effects research data indicated that small particles are most closely related to adverse health effects.

The range of particle sizes of concern in air pollution control is extremely broad. Some of the droplets collected in the mist eliminators of wet scrubbers and the solid particles collected in large diameter cyclones are as large as raindrops. Some of the small particles created in high temperature incinerators and metallurgical processes are so small that more than 500 particles could be lined up across the diameter of a human hair.

To appreciate the difference in sizes, it is helpful to compare the diameters, areas, and volumes of a variety of particles. Assume that all of the particles are simple spheres. The "typical" raindrop shown in Figure 1-11 is 500 mm in diameter. The term "micrometer" (mm) simply means one millionth of a meter. One thousand micrometers are equivalent to 0.1 cm or 1.0 mm. In some texts, the term "micron" is often used as an abbreviation for "micrometer."

A 100 mm particle shown next to the raindrop in Figure 1-11 looks like a small speck compared to the pushpin in the background. However, both the raindrop and the 100 mm particle are on the large end of the particle size range of interest in air pollution control.

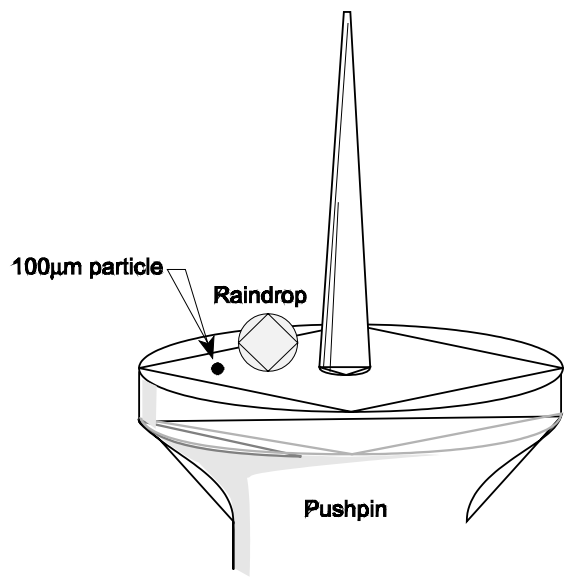

Figure 1-11. Very large particle and raindrop

Particles in the range of 10-100 mm are also on the large end of the particle size scale of interest in this course. The particle size range between 1 and 10 mm is especially important in air pollution control. A major fraction of the particulate matter generated in some industrial sources is in this size range. Furthermore, all particles less than or equal to 10 mm are considered respirable and are regulated as PM_{10}.

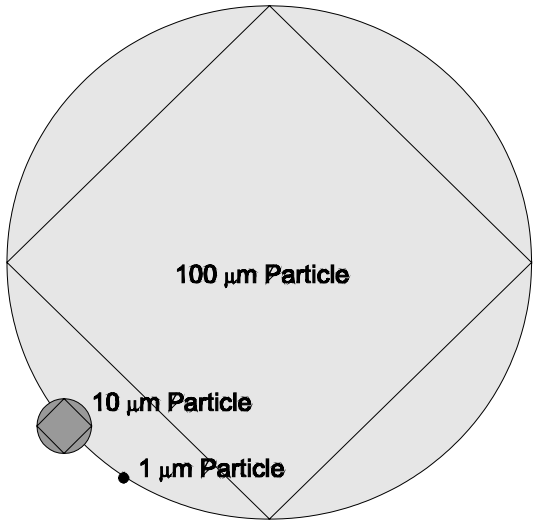

Figure 1-12. 1 and 10 m particles compared to a 100 m particle

Figure 1-12 shows a comparison of 1, 10, and 100 m particles. It is apparent that there is a substantial difference in size between these particles.

Particles in the range of 0.1 to 1.0 m are important in air pollution control because they can represent a significant fraction of the particulate matter emissions from some types of industrial sources and because they are relatively hard to collect.

Particles can be much smaller than 0.1 m, as indicated by the ultrafine mode in Figure 1-7. Some industrial processes, such as combustion and metallurgical sources, generate particles in the range of 0.01 to 0.1 m. These sizes are approaching the size of individual gas molecules, which are in the range of 0.0002 to 0.001 m. However, particles in the size range of 0.01 to 0.1 m tend to agglomerate rapidly to yield particles in the greater than 0.1 m range. Accordingly, very little of the particulate matter entering an air pollution control device remains in the ultrafine small size range of 0.01 to 0.1 m.

Throughout this manual, small particles are defined as less than 1 m, moderately-sized particles are classified as 1 to 10 m, and large particles are classified as 10 to 1000 m. The volumes and surface areas of particles over this size range are shown in Table 1-1.

The data in Table 1-1 indicate that particles of 1000 m are more than 1,000,000,000,000 times (one trillion) larger in volume than 0.1 m particles. As an analogy, assume that a 1000 m particle was a large domed sports stadium. A basketball in this "stadium" would be equivalent to a 5 m particle. Approximately 100,000 spherical particles of 0.1 m diameter would fit into this 5 m "basketball." The entire 1000 m "stadium" is the size of a small raindrop. Particles over this extremely large size range of 0.1 to 1000 m are of interest in air pollution control.

Table 1-1. Spherical Particle Diameter, Volume, and Surface Area		
Particle Diameter, µm	**Particle Volume, cm^3**	**Particle Area, cm^2**
0.1	5.23×10^{-16}	3.14×10^{-10}
1.0	5.23×10^{-13}	3.14×10^{-8}
10.0	5.23×10^{-10}	3.14×10^{-6}
100.0	5.23×10^{-7}	3.14×10^{-4}
1000.0	5.23×10^{-4}	3.14×10^{-2}

Particle size itself is difficult to define in terms that accurately represent the types of particles. This difficulty stems from the fact that particles exist in a wide variety of shapes, not just as spheres as shown earlier. The photomicrograph shown in Figure 1-13 has a variety of spherical particles and irregularly shaped particles. For spherical particles, the definition of particle size is easy: it is simply the diameter. For the irregularly shaped particles, size can be defined in a variety of ways. For example, when measuring the size of particles on a microscope slide, size can be based on the particle width that divides the particle into equal areas (Martin's diameter) or the maximum edge-to-edge distance of the particle (Feret's diameter).

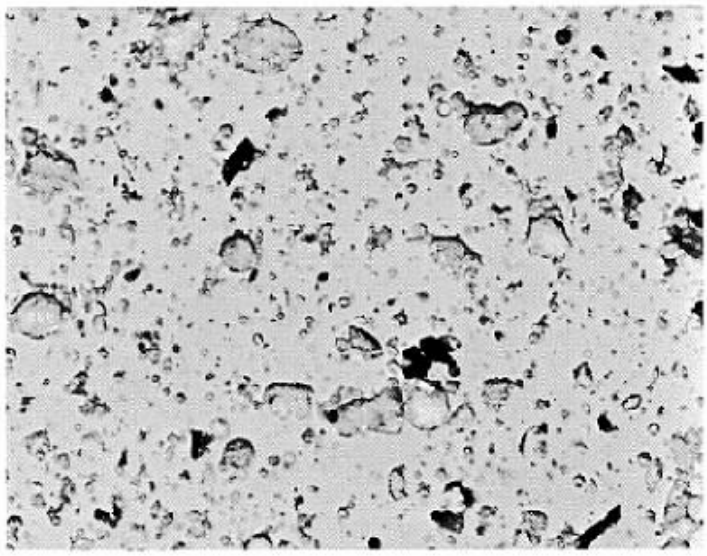

Figure 1-13. Scanning electron microscopy photomicrograph of coal fly ash (Reprinted courtesy of Research Triangle Institute)

Neither of these microscopically based size definitions, however, is directly related to how particles behave in a fluid such as air. The particle size definition that is most useful for evaluating particle motion in a fluid is termed the *aerodynamic diameter*. For all particles greater than 0.5 µm, the aerodynamic diameter can be approximated by Equation 1-3.

$$d_p = d\sqrt{\rho_p C_c} \tag{1-3}$$

Where:

d_p = aerodynamic particle diameter (m)

d = Stokes (physical) diameter (m)

$_p$ = particle density (gm/cm^3)

Particle density affects the motion of a particle through a fluid and is taken into account in Equation 1-3. The Stokes diameter is based on the aerodynamic drag force caused by the difference in velocity of the particle and the surrounding fluid. For smooth spherical particles the Stokes diameter is identical to the physical diameter. As is the case for most textbooks, the remainder of this course will use the term *physical diameter* or *actual diameter* to describe a smooth spherical particle.

The aerodynamic diameter is determined by inertial sampling devices such as the cascade impactor, which is discussed in Chapter 8 of this manual. Particles that appear to be different in physical size and shape can have the same aerodynamic diameter (as illustrated in Table 1-2).

Table 1-2. Aerodynamic Diameters of Differently Shaped Particles

	Solid sphere	$_p$ = 2.0 gm/cm^3 d = 1.4 µm	d_p = 2.0 µm
	Hollow sphere	$_p$ = 0.50 gm/cm^3 d = 2.80 µm	
	Irregular shape	$_p$ = 2.3 gm/cm^3 d = 1.3 µm	

Conversely, some particles that appear to be visually similar can have somewhat different aerodynamic diameters (as illustrated in Table 1-3).

Table 1-3. Aerodynamic Diameters of Particles with Different Densities

	= 1.0 gm/cm^3 d = 2.0 µm	d_p = 2.0 µm
	= 2.0 gm/cm^3 d = 2.0 µm	d_p = 2.8 µm
	= 3.0 gm/cm^3 d = 2.0 µm	d_p = 3.5 µm

The term *aerodynamic diameter* is useful for all particles including the fibers and particle clusters shown in Figure 1-14. The aerodynamic diameter provides a simple means of categorizing the sizes of particles with a single dimension and in a way that relates to how particles move in a fluid. Unless otherwise noted, particle size is expresed in terms of aerodynamic diameter throughout the remainder of this manual.

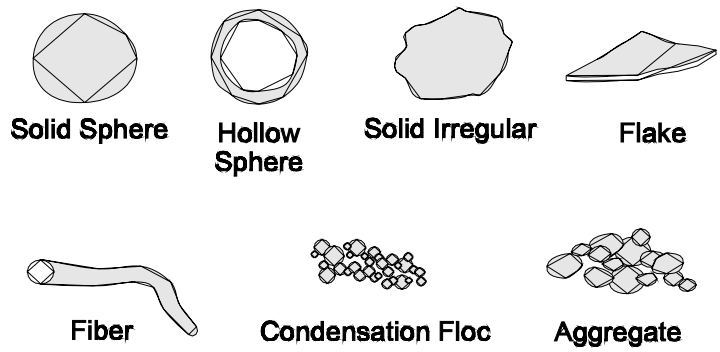

Figure 1-14. Different shapes of particles

1.4 PARTICLE SIZE DISTRIBUTIONS

Particulate matter emissions from both anthropogenic and biogenic sources do not consist of particles of any one size. Instead, they are composed of particles over a relatively wide size range. It is often necessary to describe this size range.

One of the simplest means of describing a particle size distribution is a histogram as shown in Figure 1-15. This simply shows the number of particles in a set of arbitrary size ranges specified on the horizontal axis. The terms used to characterize the particle size distribution are also shown in Figure 1-15.

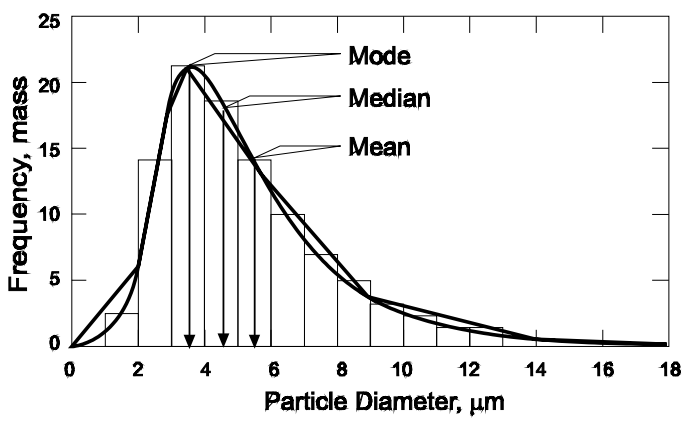

Figure 1-15. Particle size distribution
(Reprinted by permission from Silverman L., C.E. Billings, and M.W. First, Particle Size Analysis in Industrial Hygiene, Academic Press, 1971, p. 237)

The median particle size divides the frequency distribution in half: 50% of the aerosol mass has particles with a larger diameter, and 50% of the aerosol mass has particles with a smaller diameter. The **mean** is the mathematical average of the distribution. The value of the mean is sensitive to the quantities of particulate matter at the extreme lower and upper ends of the distribution.

For many stationary and mobile sources, the observed particulate matter distribution in the effluent gas stream approximates a lognormal distribution. When the log of the particle diameter is plotted against the frequency of occurrence, a normal bell-shaped curve is generated. The histogram for a lognormal curve is shown in Figure 1-16. This type of distribution can be described in terms of the geometric mean diameter, which is calculated simply by summing the logs of frequency observations and dividing by the number of size categories.

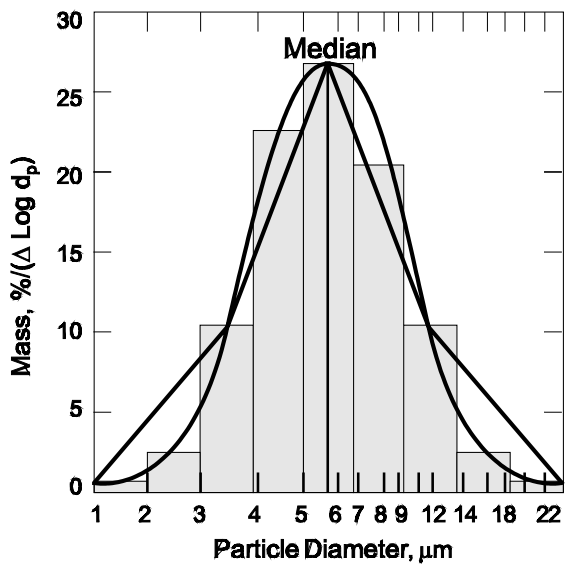

Figure 1-16. Histogram of a lognormal size distribution

Both the geometric mean and the standard deviation of a lognormal distribution can be determined by plotting the distribution data on log-probability paper. (Standard deviation is introduced in the U.S. EPA, APTI course SI:100 *Mathematics Review for Air Pollution Control*.) The data plotted in Figure 1-17 are based on the particle size data listed in Table 1-4.

Table 1-4. Example Particle Size Data

Size Range, mm	Concentration, (µgm/m^3)	Percent Weight in Size Range	Cumulative Percent Weight Larger than $d_p$max
0 to 2	1.0	0.5	99.5
>2 to 4	14.5	7.25	92.25
>4 to 6	24.7	12.35	79.9
>6 to 10	59.8	29.90	50
>10 to 20	68.3	34.15	15.85
>20 to 40	28.9	14.45	1.4
>40	2.8	1.4	--
TOTAL	200 µgm/m^3	100.0	

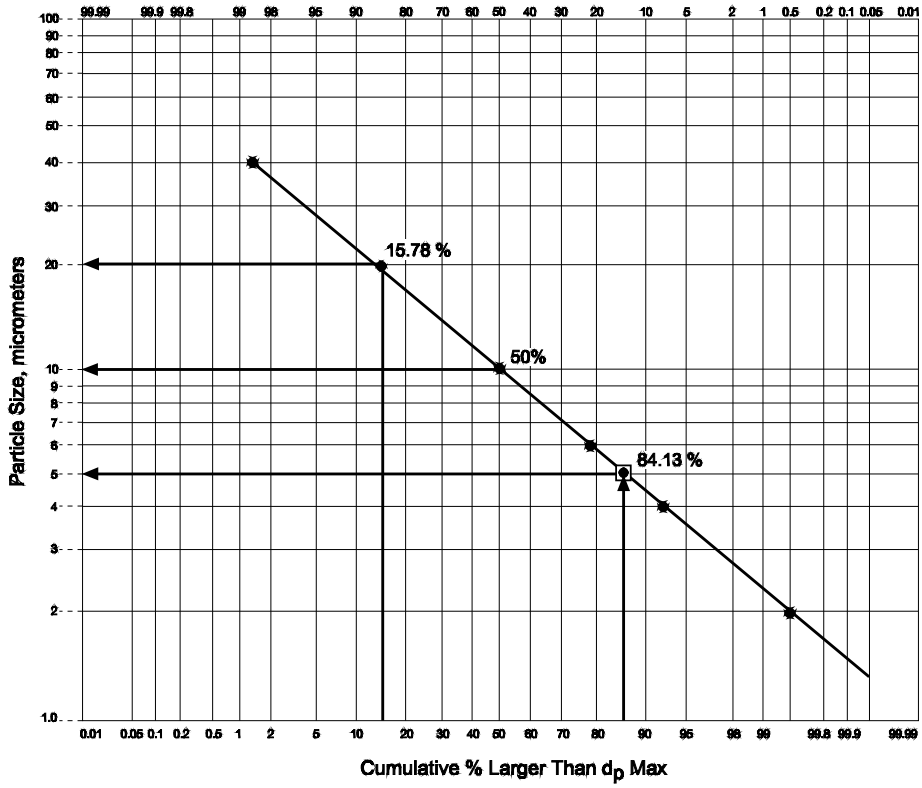

Figure 1-17. Cumulative lognormal size distribution

The geometric mean is the particle diameter that is equivalent to the 50 % probability point. This indicates that half of the particulate matter mass is composed of particles larger than this value, and half of the mass is composed of particles with smaller diameters. The diversity of the particle sizes is described by the standard deviation. A distribution with a broad range of sizes has a larger standard deviation ($_g$) than one in which the particles are relatively similar in size. The standard deviation is determined by dividing the geometric mean by the particle size at the 15.78 percent probability or by dividing the particle size at the 84.13 percent probability by the geometric mean size.

$$\sigma_g = d_{50} / d_{15.78} \quad (1\text{-}4)$$

$$\sigma_g = d_{84.13} / d_{50} \quad (1\text{-}5)$$

Where:

σ_g = standard deviation of particle mass distribution
d_{50} = median sized particle
$d_{15.78}$ = diameter of particle is equal to or greater than 15.78% of the mass of particles present
$d_{84.13}$ = diameter of particle is equal to or greater than 84.13% of the mass of particles present

Particle size distributions resulting from complex particle formation mechanisms or several simultaneous formation mechanisms may not be lognormal. As shown in Figure 1-18, these distributions may exhibit more than one peak. In these cases, plots of the data on log-probability paper will not yield a straight line.

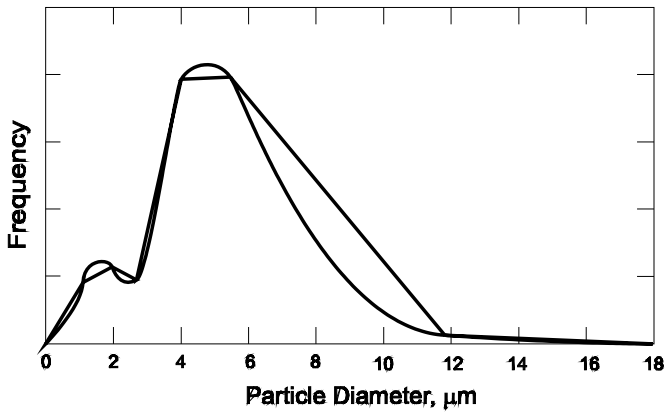

Figure 1-18. Multi-modal particle size distribution

1.5 PARTICLE FORMATION

The range of particle sizes formed in a process is largely dependent on the types of particle formation mechanisms present. It is possible to estimate the general size range simply by recognizing which of these is important in the process being evaluated. The most important particle formation mechanisms in air pollution sources include the following:

- Physical attrition/mechanical dispersion
- Combustion particle burnout
- Homogeneous condensation
- Heterogeneous nucleation
- Droplet evaporation

Physical attrition occurs when two surfaces rub together. For example, the grinding of a rod on a grinding wheel (as shown in Figure 1-19) yields small particles that break off from both surfaces. The compositions and densities of these particles are identical to the parent materials.

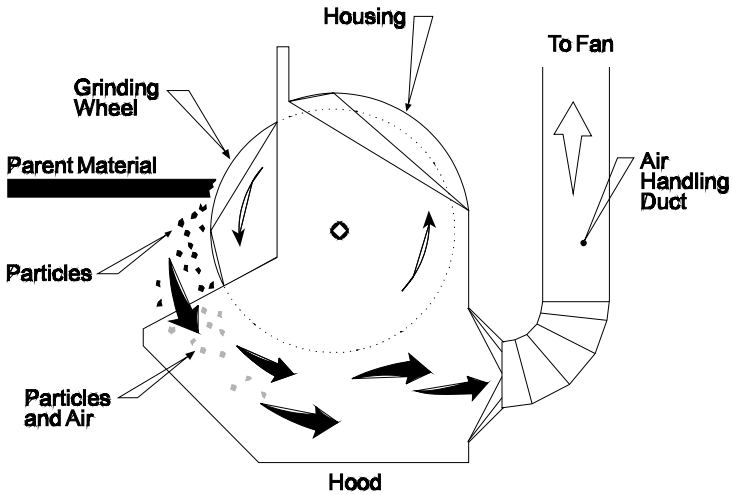

Figure 1-19. Grinding wheel

The tertiary stone crusher shown in Figure 1-20 is an example of an industrial source of particles that involves only physical attrition. The particles formed range from approximately 1 m to almost 1,000 m. However, the limited energy used in the crushing operation, very little of the particulate matter is less than 10 m. Physical attrition generates primarily large particles.

Figure 1-20. Tertiary crusher

In order for fuel to burn, it must be pulverized (solid fuel) or atomized (liquid fuel) so that sufficient surface area is exposed to oxygen and high temperature. As indicated in Table 1-1, the surface area of particles increases substantially as more and more of the material is reduced in size. Accordingly, most industrial-scale combustion processes use one or more types of physical attrition in order to prepare or introduce their fuel into the furnace. For example, coal-fired boilers use pulverizers to reduce the chunks of coal to sizes that can be burned quickly. Oil-fired boilers use atomizers to disperse the oil as fine droplets. In both cases, the fuel particle size range is reduced primarily to the 100-1,000 m range. Coal pulverizers and oil burner atomizers are examples of physical attrition and mechanical dispersion.

When the fuel particles are injected into the hot furnace area of the combustion process (Figure 1-21), most of the organic compounds are vaporized and oxidized in the gas stream. The fuel particles get smaller as the volatile matter leaves. The fuel particles are quickly reduced to only the incombustible matter (ash) and slow burning char composed of organic compounds. Eventually, most of the char will also burn, leaving primarily the incombustible material. As oxidation progresses, the fuel particles, which started as 100-1,000 m particles, are reduced to ash and char particles that are primarily in the 1 to 10 m range. This mechanism for particle formation can be termed combustion fuel burnout.

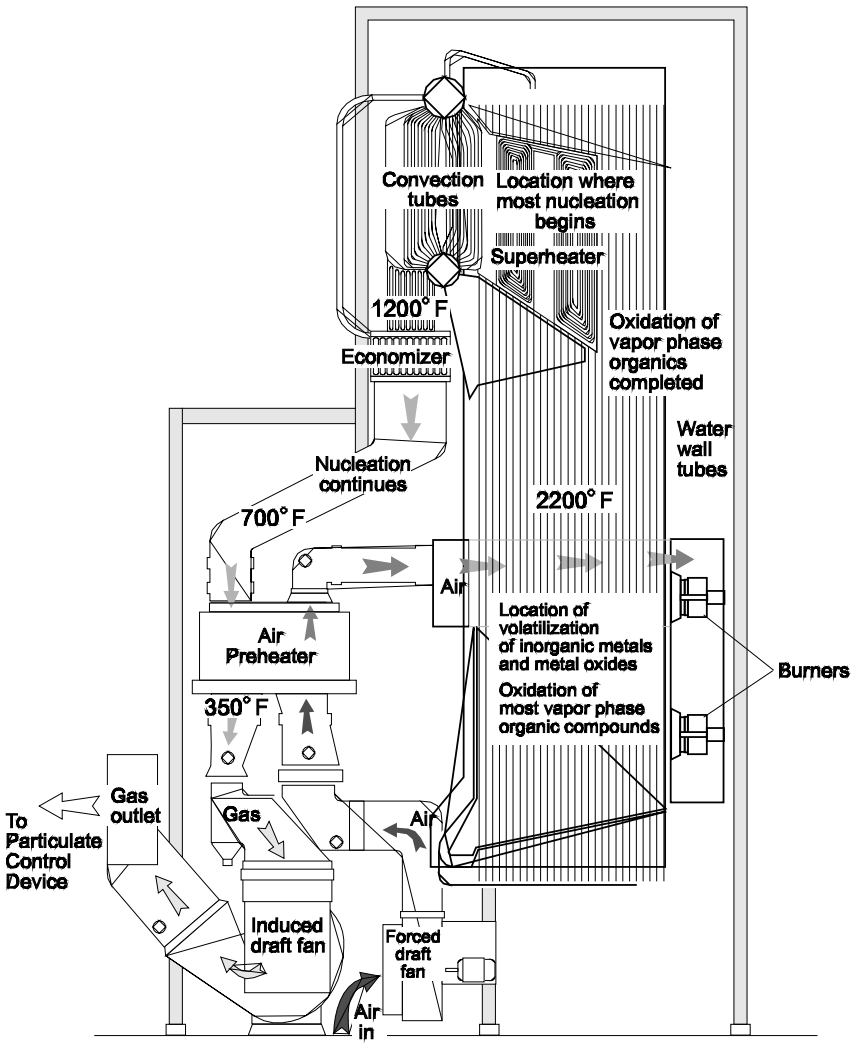

Figure 1-21. Combustion process

Homogeneous nucleation and heterogeneous nucleation involve the conversion of vapor phase materials to a particulate matter form. Homogeneous nucleation is the formation of new particles composed almost entirely of the vapor phase material. Heterogeneous nucleation is the accumulation of material on the surfaces of particles that have formed due to other mechanisms. In both cases, the vapor-containing gas streams must cool to the temperature at which nucleation can occur. The temperature at which vapors begin to condense is called the dew point, and it depends on the concentration of the vapors. The dew point increases with increases in the vapor concentration. Some compounds condense in relatively hot gas zones (>1000°F), while others do not reach their dew point temperature until the gas stream cools below 300°F.

There are three main categories of vapor phase material that can nucleate in air pollution source gas streams: (1) organic compounds, (2) inorganic metals and metal compounds, and (3) chloride compounds. For example, in a waste incinerator organic vapor that has volatilized from the waste due to the high temperature is generally oxidized completely to carbon dioxide and water. However, if there is

a combustion upset, a portion of the organic compounds or their partial oxidation products remain in the gas stream as they leave the incinerator. These organic vapors can condense in downstream equipment. Volatile metals and metal compounds such as mercury, lead, lead oxide, cadmium, cadmium oxide, cadmium chloride, and arsenic trioxide can also volatilize in the hot incinerator. Once the gas stream passes through the heat exchange equipment used to produce steam, the organic vapors and metal vapors can homogeneously or heterogeneously condense. Generally, the metals and metal compounds reach their dew point first and begin to nucleate in relatively hot zones of the unit. The organic vapors and/or chloride compounds begin to condense in downstream areas of the process where the gas temperatures are cooler. These particles must then be collected in the downstream air pollution control systems. Homogeneous and heterogeneous nucleation generally creates particles that are very small, often between 0.05 and 1.0 m.

Heterogeneous nucleation facilitates a phenomenon called "enrichment" in particles in the submicrometer size range. The elemental metals and metal compounds volatilized during high temperature operations (e.g., fossil fuel combustion, incinerator, and metallurgical processes) nucleate preferentially on these very small particles. This means that these particles have more of these materials than the very large particles leaving the processes. These small particles are described as enriched with respect to their concentration of metals and metal compounds. Heterogeneous nucleation contributes to the formation of particle distributions that have quite different chemical compositions in different size ranges.

Another consequence of heterogeneous nucleation is that the metals are deposited in small quantities on the surfaces of a large number of small particles (Figure 1-22). In this form, the metals are available to participate in catalytic reactions with gases or other vapor phase materials that are continuing to nucleate. Accordingly, heterogeneous nucleation also increases the types of chemical reactions that can occur as the particles travel in the gas stream from the process source and through the air pollution control device.

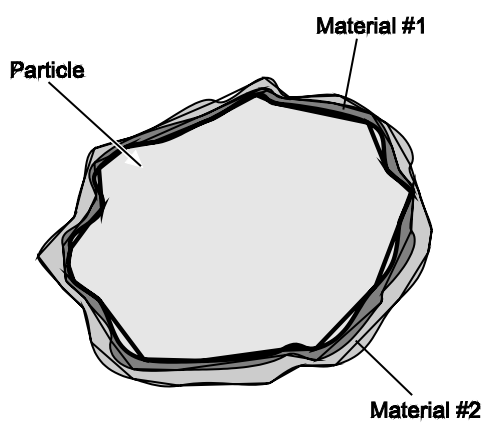

Figure 1-22. Chemical composition resulting from heterogeneous nucleation

Some air pollution control systems use solids-containing water recycled from wet scrubbers to cool the gas streams. This practice inadvertently creates another particle formation mechanism that is very similar to fuel burnout. The water streams are atomized during injection into the hot gas streams. As these small droplets evaporate to dryness, the suspended and dissolved solids are released as small particles. The particle size range created by this mechanism has not been extensively studied; however, it probably creates particles that range in size from 0.1-2.0 m. All of these particles must then be collected in the downstream air pollution control systems.

A summary of the particle size ranges generated by the different formation mechanisms is provided in Figure 1-23. Several particle formation mechanisms can be present in many air pollution sources. As a result, the particles created can have a wide range of sizes and chemical compositions.

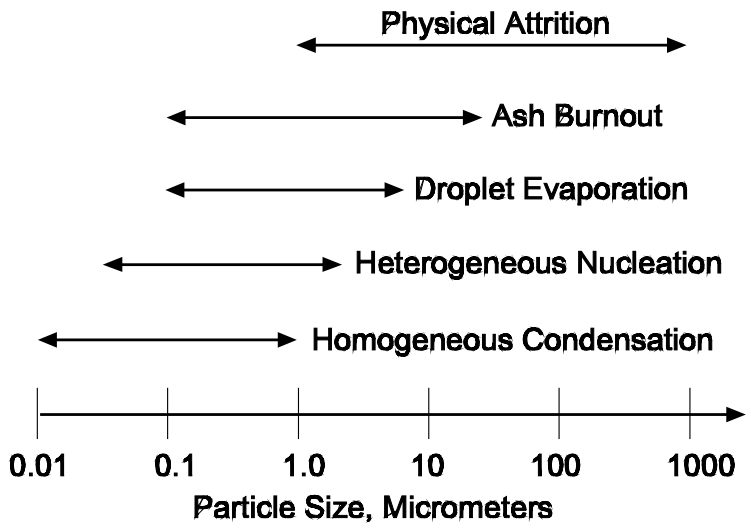

Figure 1-23. Approximate particle size distributions resulting from various formation mechanisms

Review Exercises

1. How many 1 m particles can fit across a 1-inch space?
2. Calculate the total volume of a 1 m spherical particle and a 10 m spherical particle.
3. Calculate the surface area of a 1 m spherical particle and a 10 m spherical particle.
4. Calculate the aerodynamic diameter of a spherical particle having a true diameter of 2 m and a density of 2.7 gm/cm^3.
5. What is total suspended particulate matter?
   a. Particulate matter measured in the ambient air having a size less than approximately 1,000 micrometers
   b. Particulate matter measured in the ambient air having a size less than approximately 100 micrometers
   c. Particulate matter measured in the ambient air having a size less than approximately 45 micrometers
   d. Particulate matter measured in the ambient air having a size less than approximately 10 micrometers
   e. None of the above
6. What are ultrafine particles?
   a. Particulate matter measured in the ambient air having a size less than approximately 10 micrometers
   b. Particulate matter measured in the ambient air having a size less than approximately 0.1 micrometers
   c. Particulate matter measured in the ambient air having a size less than approximately 0.01 micrometers
   d. Particulate matter measured in the ambient air having a size less than approximately 0.001 micrometers
   e. None of the above
7. Particles that form by homogeneous condensation and/or heterogeneous nucleation are mainly in which size range?
   a. Greater than 10 micrometers
   b. Between 1 and 10 micrometers
   c. Between 0.1 and 10 micrometers
   d. Betweeen 0.01 and 0.1 micrometers
   e. None of the above

8. What types of mechanisms are responsible for the formation of condensable particulate matter? Select all that apply.
   a. Condensation of vapor phase material emitted from stationary sources
   b. Condensation of organic vapors emitted from stationary sources
   c. Atmospheric reactions involving sulfur dioxide and ammonia
   d. Grinding of one material against another (attrition)
   e. All of the above

9. The accurately measured ambient concentration of PM_{10} is 78 micrograms per cubic meter. Which of the following could be true?
   a. The ambient concentration of $PM_{2.5}$ is 125 micrograms per cubic meter.
   b. The ambient concentration of $PM_{2.5}$ is 26 micrograms per cubic meter.
   c. The ambient concentration of $PM_{2.5}$ is 158 micrograms per cubic meter.
   d. The ambient concentration of total suspended particulate matter is 65 micrograms per cubic meter.

10. Which compounds are known to participate in atmospheric reactions that result in the formation of secondary particulate matter? Select all that apply.
   a. Sulfur dioxide
   b. Nitrogen oxides
   c. Ammonia
   d. All of the above

Review Answers

1. How many 1 m particles can fit across a 1-inch space?

   2.54×10^4 particles

   Solution:

$$\frac{1\,\text{inch}}{} \left| \frac{2.54\,\text{cm}}{\text{inch}} \right| \frac{10^4\,\mu\text{m}}{\text{cm}} \left| \frac{\text{particle}}{1\,\mu\text{m}} \right. = 2.54 \times 10^4 \text{ particles}$$

2. Calculate the total volume of a 1 m spherical particle and a 10 μm spherical particle.

   5.23 10^{-13} cm^3 and 5.23×10^{-10} cm^3

   Solution:

   Volume of a sphere = $\frac{\pi}{6} d^3$

   Where:

   π = 3.14

   1 cm = 10,000 μm

   For a 1 m particle,

$$\text{Volume} = \frac{3.14}{6}\left[(1\mu\text{m})\left(\frac{\text{cm}}{10{,}000\mu\text{m}}\right)\right]^3 = 5.23 \times 10^{-13}\,\text{cm}^3$$

   For a 10 m particle,

$$\text{Volume} = \frac{3.14}{6}\left[(10\mu\text{m})\left(\frac{\text{cm}}{10{,}000\,\mu\text{m}}\right)\right]^3 = 5.23 \times 10^{-10}\,\text{cm}^3$$

3. Calculate the surface area of a 1 m spherical particle and a 10 m spherical particle.

   3.14×10^{-8} cm^2 and 3.14×10^{-6} cm^2

   Solution:

   Surface area = d^2

   For a 1 m particle,

$$\text{Surface area} = 3.14\left[(1\mu\text{m})\left(\frac{\text{cm}}{10{,}000\mu\text{m}}\right)\right]^2 = 3.14 \times 10^{-8}\,\text{cm}^2$$

For a 10 m particle,

$$\text{Surface area} = 3.14\left[(10\,\mu\text{m})\left(\frac{\text{cm}}{10{,}000\,\mu\text{m}}\right)\right]^2 = 3.14\times10^{-6}\ \text{cm}^2$$

4. Calculate the aerodynamic diameter of a spherical particle having a physical diameter of 2 m and a density of 2.7 gm/cm^3.

   3.29 m

   Solution:

   Aerodynamic diameter $= d(\rho_p)^{0.5}$

   Aerodynamic diameter $= 2\ \mu\text{m}\ (2.7)^{0.5} = 3.29$ m

5. What is total suspended particulate matter?
   c. Particulate matter measured in the ambient air having a size less than approximately 45 micrometers

6. What are ultrafine particles?
   b. Particulate matter measured in the ambient air having a size less than approximately 0.1 micrometers

7. Particles that form by homogeneous condensation and/or heterogeneous nucleation are mainly in which size range?
   c. Between 0.1 and 10 micrometers

8. What types of mechanisms are responsible for the formation of condensable particulate matter? Select all that apply.
   a. Condensation of vapor phase material emitted from stationary sources
   b. Condensation of organic vapors emitted from stationary sources
   c. Atmospheric reactions involving sulfur dioxide and ammonia

9. The accurately measured ambient concentration of PM_{10} is 78 micrograms per cubic meter. Which of the following could be true?
   b. The ambient concentration of $PM_{2.5}$ is 26 micrograms per cubic meter.

10. What compounds are known to participate in atmospheric reactions that result in the formation of secondary particulate matter? Select all that apply.
   d. All of the above

Chapter 2

Particle Collection Mechanisms

Air pollution control systems apply forces to particles in order to remove them from the gas stream. The forces listed below are basically the "tools" that can be used for particulate collection. All of these collection mechanism forces are strongly dependent on particle size.

- Gravity settling
- Inertial impaction and interception
- Particle Brownian motion
- Electrostatic attraction
- Thermophoresis
- Diffusiophoresis

Applying one or more of these forces, such as electrostatic force or inertial force, accelerates the particle in a direction where it can be collected. The extent to which the particle is accelerated is indicated by the Equation 2-1. The more the particle (or agglomerated mass of particles) is accelerated, the more effective and economical the air pollution control device can be.

$$F = m_p \, a_p \tag{2-1}$$

Where:

F = force on the particle (gm•cm/sec^2)

m_p = mass of the particle (gm)

a_p = acceleration of the particle (cm/sec^2)

Air pollution control devices are designed to apply the maximum possible force on the particles in the gas stream.

2.1 STEPS IN PARTICULATE MATTER CONTROL

Three fundamental steps are involved in the collection of particulate matter in high efficiency particulate control systems such as fabric filters and electrostatic precipitators.

1. Initial capture of particles on vertical surfaces
2. Gravity settling of solids into the hopper
3. Removal of solids from the hopper

The particle collection mechanisms described in this section control the effectiveness of the first two steps; initial capture of incoming particles and gravity settling of collected solids. Particle size distribution is important in each of these steps. As indicated in the following examples, there are significant differences in the particle size ranges involved.

A typical pulse jet fabric filter is illustrated in Figure 2-1. Using inertia, electrostatic attraction, and Brownian diffusion particles in the entire size range of 100 m to less than 0.01 m are captured onto the vertical dust layers present on the exterior surfaces of the bags.

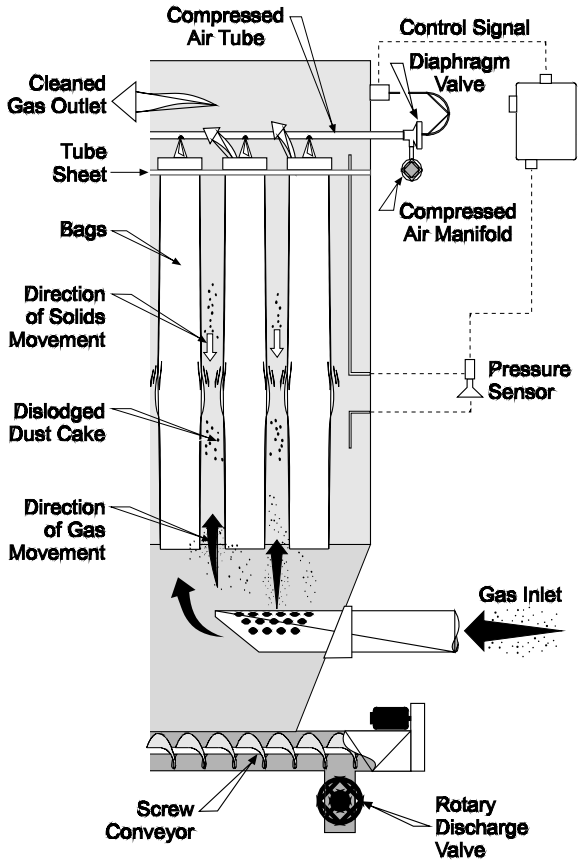

Figure 2-1. Steps in particulate matter collection in a pulse jet fabric filter

At regular intervals, the bag cleaning cycle is activated. Large chunks of dust cake are dislodged from the bag surface and fall into the hopper. These agglomerated chunks of solids are usually in the range of 10,000 to 50,000 micrometers (1.0 cm to 5.0 cm). Due to their relatively large size, they fall rapidly into the hopper. However, if the bag compartment is cleaned improperly, the solids can be dislodged in very small agglomerates that might settle too slowly. Proper gravity settling of the solids, step 2 of particle collection, is crucial to the proper operation of the fabric filter.

In electrostatic precipitators, the dust is collected as a layer on vertical collection plates (Figures 2-2a and 2-2b) by electrostatic attraction forces. The initial capture of particles is efficient over the entire size range of 0.1 to 100 micrometers. The particulate matter that accumulates on these vertical collection plates must be discharged to the hoppers below during routine intervals. The cleaning systems in precipitators create disturbances that break off layers or clumps of accumulated solids that fall by gravity into the hopper. As the solids fall downward, they are swept toward the outlet of the precipitator by the horizontally moving gas stream. If the solids clumps are too small, gravity settling is too slow to allow the solids to reach the hopper before the gas stream carries them out of the collector. For this reason, gravity settling is an important second step in particulate matter control in electrostatic precipitators.

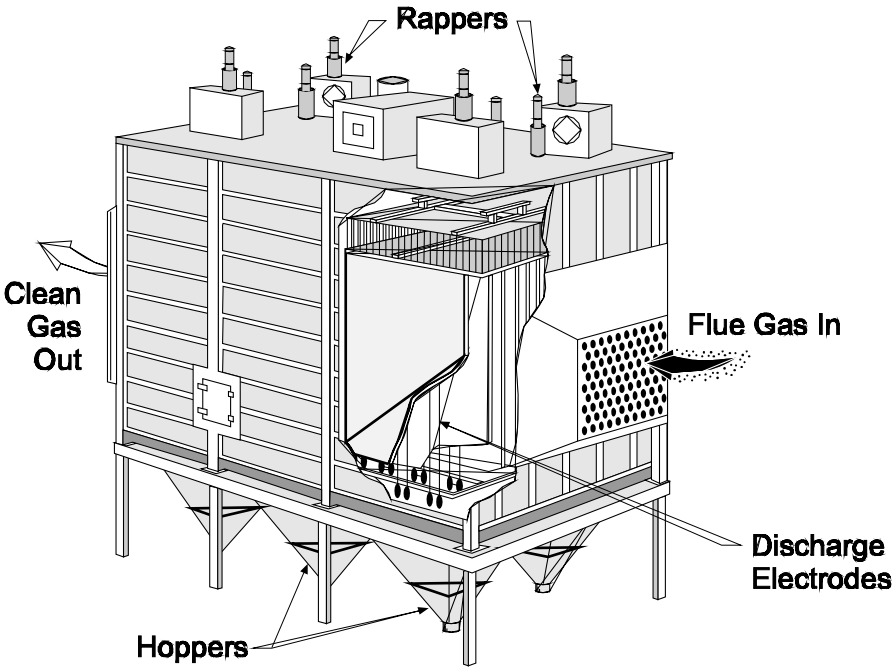

Figure 2-2a. Side elevation view of an electrostatic precipitator

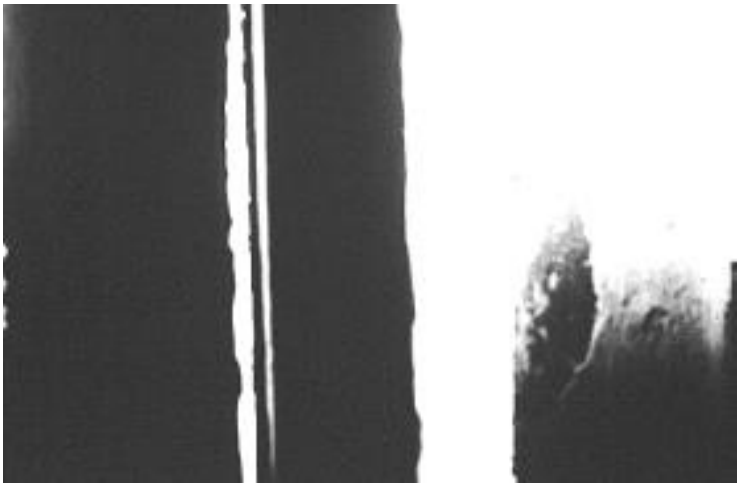

Figure 2-2b. Precipitator plate dust layer

The performance of air pollution control equipment is dependent on all three of these steps. Inertial impaction, electrostatic attraction, and Brownian motion primarily control the effectiveness of initial capture. Gravity settling is responsible for settling of large clunks of solids during step 2.

2.2 GRAVITY SETTLING

To determine the extent to which a particle or agglomerated solid clumps can be collected in an air pollution control device, it is necessary to calculate the force exerted on the material. The gravitational force F_G, which causes particles and masses to fall, can be expressed in the form of Equation 2-2.

$$F_G = m_p\, g \tag{2-2}$$

Where:
F_G = force of gravity (gm•cm/sec^2)
m_p = mass of the particle (gm)
g = acceleration of particle due to gravity, 980 cm/sec^2

The mass of the particle is equal to the particle density (ρ_p) multiplied by the particle volume (V_p).

$$m_p = \rho_p\, V_p \tag{2-3}$$

To simplify aerosol calculations, particles are assumed to be spheres. The volume of a spherical particle is equal to:

$$V_p = \frac{4}{3}\pi r_p^{\,3} = \frac{\pi d^3}{6} \tag{2-4}$$

Where:
d = physical diameter

Equation 2-2, which is the equation for gravitational force, can then be written as:

$$F_G = \frac{\pi \rho_p d^3 g}{6} \tag{2-5}$$

Where:
ρ_p = density of the particle (gm/cm^3)
d = physical particle diameter (cm)
g = acceleration of particle due to gravity, 980 cm/sec^2

This ignores the bouyancy of the particle, which is appropriate because the density of air and other gas streams of interest in air pollution control is well below the density of the particles. Accordingly, ignoring bouyancy causes an error considerably less than 1%.

Problem 2-1

Calculate the gravitational force on a unit density sphere with a diameter of 2 m.

Solution:

$$\begin{aligned} F_G &= [1\ \text{gm/cm}^3 \times 3.14 \times (2\ \text{m})^3 \times 980\ \text{cm/sec}^2]\ 1/6 \\ &= [1\ \text{gm/cm}^3 \times 3.14 \times (2 \times 10^{-4}\ \text{cm})^3 \times 980\ \text{cm/sec}^2]\ 1/6 \\ &= 4.1 \times 10^{-9}\ \text{gm•cm/sec}^2 \end{aligned}$$

Drag Force, F_D - Whenever there is particle motion in a gas stream due to gravitational force or any other force, there will be a force caused by the fluid (gas) molecules resisting the motion of the particle (Figure 2-3). Note that the sizes of the gas molecules in Figure 2-3 are exaggerated for illustrative purposes. Actual gas molecules have relative sizes well below that indicated by this figure.

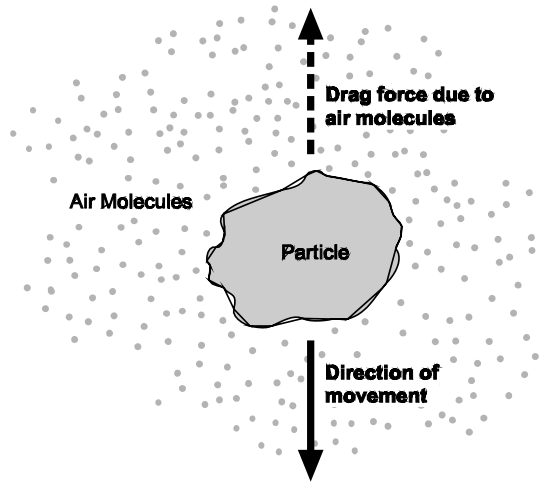

Figure 2-3. Drag force on particle

The resistive force caused by the fluid on the particle is called the drag force, or F_D. The drag force is given by the following expression:

$$F_D = \frac{\pi d_p^2 \rho_g v_p^2 C_D}{8} \tag{2-6}$$

Where:

d_p = particle diameter (cm)
ρ_g = density of the fluid (gm/cm^3)
v_p = particle velocity (cm/sec)
C_D = drag coefficient (dimensionless)
F_D = drag force (gm•cm/sec^2)

As Equation 2-6 illustrates, the drag force is greatly influenced by particle size and velocity. The fluid density and drag coefficient have a less pronounced effect, but these will vary with temperature and pressure changes.

Drag coefficient, (C_D) and particle Reynolds number (N_{REP}) - The value of C_D is related to the velocity of the particle and the flow pattern of the fluid around the particle. The Reynolds number of the particle, N_{REP} , is used as an indicator of this flow pattern and, like the fluid Reynolds number, is dimensionless. The Reynolds number of the particle is a function of the fluid density, fluid viscosity and particle diameter, particle velocity relative to the gas stream it is suspended in. The particle Reynolds number is given as:

$$N_{REP} = \frac{\rho_g \, v_p \, d_p}{\mu} \tag{2-7}$$

Where:

ρ_g = density of the fluid (gm/cm^3)
v_p = particle velocity relative to the gas stream (cm/sec)
d_p = particle diameter (cm)
= fluid viscosity (gm/(cm•sec))

The density of air at 20°C is 0.001205 gm/cm^3. Values for fluid density at other temperatures can be determined using the Ideal Gas Law.

Viscosity is a measure of the resistance provided by a fluid to shear. The viscosity of air at 20°C is 1.8 × 10^{-4} gm/cm•sec. The viscosity of air and other gases important in air pollution control application can be calculated using Equation 2-8 over the range of 0°F to 500°F.

$$\mu = 51.05 + 0.207T_S + 3.24x10^{-5}(T_S)^2 - 74.14x + 53.417y \qquad (2\text{-}8)$$

Where:

= fluid viscosity (micropoise)

T_S = stack temperature (°R)

x = water vapor content of gas stream (fraction) (i.e., 10% H_20 = 0.10 fraction)

y = oxygen content of gas stream (fraction)

Note: 1 micropoise = 1.0 x 10^{-6} gm/(cm•sec)

Problem 2-2

Calculate the particle Reynolds number for a unit density particle moving through air at 10°C. The physical particle diameter is 2 m, and its velocity is 6 m/sec.

Solution:

$$N_{REP} = \frac{\rho_g \, v_p \, d_p}{\mu}$$

First, calculate the air density at 10°C (283°K). If the density at 20°C (293°K) is 0.001205 gm/cm^3, the density at 10°C (assuming no change in pressure) is as follows:

(293°K/283°K) × 0.001205 gm/cm^3 = 0.001248 gm/cm^3 = density at 10°C

A value of 1.77 × 10^{-4} gm/cm·sec is estimated based on viscosity data from Equation 2-8. Substituting into Equation 2-7 gives:

$$N_{REP} = \frac{\left(\frac{0.001248 \text{ gm}}{\text{cm}^3}\right)\left(\frac{600 \text{ cm}}{\text{sec}}\right)(0.0002 \text{ cm})}{(1.77 \text{ x } 10^{-4} \text{ gm/cm} \bullet \text{sec})}$$

$$N_{REP} = 0.85$$

Problem 2-3

Calculate the particle Reynolds number for a particle moving through air at 240°C. Use the same particle diameter and particle velocity as Problem 2-2. Assume that the water vapor content is 4% (0.04 fraction) and the oxygen content is 20.9% (0.209 fraction).

Solution:

First, calculate the air density at 240°C (513°K). If the density at 20°C (293°K) is 0.001205 gm/cm^3, the density at 240°C (assuming no change in pressure) is as follows:

$(293°K/513°K) \times 0.001205\ gm/cm^3 = 0.00069\ gm/cm^3$ = density at 240°C

Calculate the viscosity at 240°C using Equation 2-8.

$$= 51.05 + 0.207\ (923.4) + 324 \times 10^{-5}\ (923.4)^2 - 74.14\ (0.04) + 53.417\ (0.209)$$

$$\mu = 278 \text{ micropoise } = 2.78 \times 10^{-4} \frac{gm}{(cm \bullet sec)}$$

A value of 2.78×10^{-4} gm/cm·sec is estimated based on gas temperature and composition data stated in the problem. Substituting into Equation 2-7 gives:

$$N_{RE_p} = \frac{\left(\frac{0.00069\ gm}{cm^3}\right)\left(\frac{600\ cm}{sec}\right)(0.0002\ cm)}{\frac{2.78 \times 10^{-4}\ gm}{cm \bullet sec}} = 0.3$$

The particle Reynolds number in Problem 2-3 is lower than in Problem 2-2 due to the decreased gas density and the increased gas viscosity present at the higher gas temperature.

The particle Reynolds numbers calculated using Equation 2-7 are quite different from the fluid Reynolds numbers used in fluid mechanics. The particle Reynolds numbers describe the characteristics of fluid flow in the vicinity of the particle surface. The fluid Reynolds number describes the relationship between the inertial and viscous forces in the entire fluid stream. The fluid Reynolds numbers are calculated using Equation 2-9.

$$N_{RE_f} = \frac{\rho_g V d_d}{\mu} \tag{2-9}$$

Where:

= fluid viscosity (gm/(cm•sec))
ρ = fluid density (gm/cm^3)
V = fluid velocity in duct or pipe (cm/sec)
d_d = characteristic dimension of pipe or duct (cm)
N_{REP} = Reynolds number of fluid (dimensionless)

The calculation of fluid Reynolds numbers and the relationship between fluid and particle Reynolds number is illustrated in Problem 2-4.

Problem 2-4

Calculate the particle and fluid Reynolds numbers for a gas stream moving through a 200-cm diameter duct at a velocity of 1500 cm/sec. Assume that the particles are moving at the same velocity as the gas stream and are not settling due to gravity. Use a gas temperature of 20°C and standard pressure.

Solution:

The particle Reynolds number = 0. There is no difference in velocity between the gas stream and the particle.

The fluid Reynolds number is calculated using Equation 2-9.

$$N_{RE} = \frac{\rho V d_d}{\mu}$$

Where:

Density = 0.001205 gm/cm^3 from Problem 2-2

Viscosity = 1.77 x 10^{-4} gm/(cm•sec) from Problem 2-2

$$N_{RE} = \frac{\left(\frac{0.001205\,gm}{cm^3}\right)\left(\frac{1500\,cm}{sec}\right)(200\,cm)}{\frac{1.77x10^{-4}\,gm}{(cm\bullet sec)}} = 2.04\,x10^4$$

The fluid Reynolds number calculated in Problem 2-4 is well into the turbulent range. The particle Reynolds number is negligible because the particle is "at rest," moving along with the gas stream.

It is important not to confuse particle and fluid Reynolds numbers. Each has an important but different purpose in analyzing movement of fluids.

The particle Reynolds number calculated using the procedures illustrated in Problems 2-2 and 2-3 is used to estimate the value of the drag coefficient. Values of C_D can be estimated by using plots of C_D versus Reynolds numbers constructed from experimental data. It is essential to determine C_D so that one can solve for F_D, the drag force, as in Equation 2-6.

From experimentation, it has been observed that three particle flow ranges exist: laminar (sometimes termed *Stokes*), transition, and turbulent. These ranges are related to the Reynolds number of the particle N_{REP}. The relationship of C_D versus N_{REP} is shown in Figure 2-4.

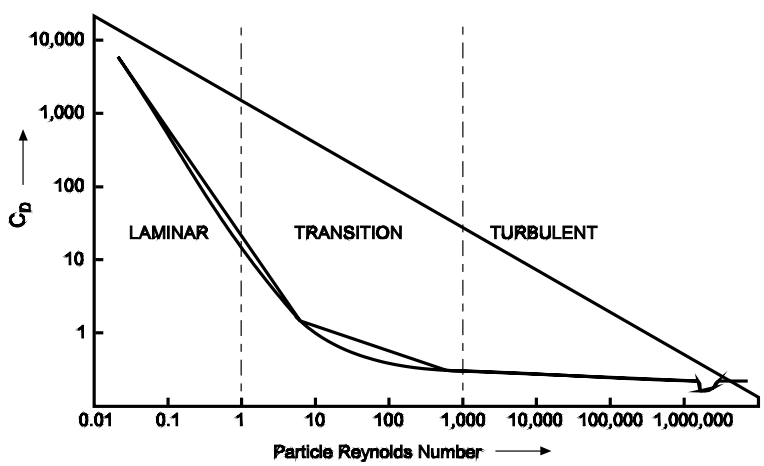

Figure 2-4. Relationship between C_D and N_{REP} for spheres

For low values of the particle Reynolds number $(N_{REP} \leq 1.0)$, the flow is considered laminar. Laminar flow is defined as flow in which the fluid moves in layers smoothly over an adjacent particle surface. For much higher values of the particle Reynolds number $(N_{REP} > 1000)$, the flow is turbulent. Turbulent flow is

characterized by erratic motion of fluid with a violent interchange of momentum throughout the fluid near the particle surface. For particle Reynolds numbers between 1 and 1000, the flow pattern is said to be in the transition range.

In most air pollution control applications, particles less than 100 m are in the laminar flow range. Intermediate and turbulent flow conditions are relevant primarily to the gravity settling of large agglomerates in fabric filters and electrostatic precipitators.

Mathematical expressions relating the values of C_D and N_{REP} can be derived from the data illustrated in Figure 2-4. Equations for determining C_D in each flow range are as follows:

$$C_D = \frac{24}{N_{REP}} \quad \text{Laminar } (N_{REP} < 1.0) \tag{2-10}$$

$$C_D = \frac{24}{N_{REP}} + \frac{4}{(N_{REP})^{1/3}} \quad \text{Transition} \quad (1.0 < N_{REP} < 1000) \tag{2-11}$$

$$C_D = 0.44 \quad \text{Turbulent } (N_{REP} > 1000) \tag{2-12}$$

Cunningham slip correction factor, C_c - If the size of the particle is greater than approximately 3 m in diameter, the fluid appears *continuous* around the particle. This means that the particle is not affected by collisions with individual air molecules that occur frequently on all sides of the particle.

If the particles are smaller than 3 m in diameter, the fluid appears *discontinuous*. This often occurs for particles in the laminar flow range. In this case, the particles are affected by collisions with air molecules. These collisions cause the particle to move in a direction related to the combined forces acting on the particle. The particle is said to be "slipping" between the fluid molecules. To correct for this, Cunningham deduced that the drag coefficient should be reduced. Thus the drag coefficient equation includes a term called the *Cunningham slip correction factor,* C_c. In the laminar flow range, Equation 2-10 is corrected to include C_c. The drag coefficient for the laminar range then becomes:

$$C_D = \frac{24}{N_{REP}\ C_c} \tag{2-13}$$

The Cunningham slip correction factor can be estimated by:

$$C_c = 1 + \frac{(6.21 \times 10^{-4})(T)}{d_p} \tag{2-14}$$

Where:

T = absolute temperature (°K)

d_p = particle diameter m)

Calculation of F_D - The drag force can be calculated by substituting the proper C_D expression into Equation 2-6. The equations for calculating F_D in all three flow ranges are shown in Equations 2-15, 2-16, and 2-17.

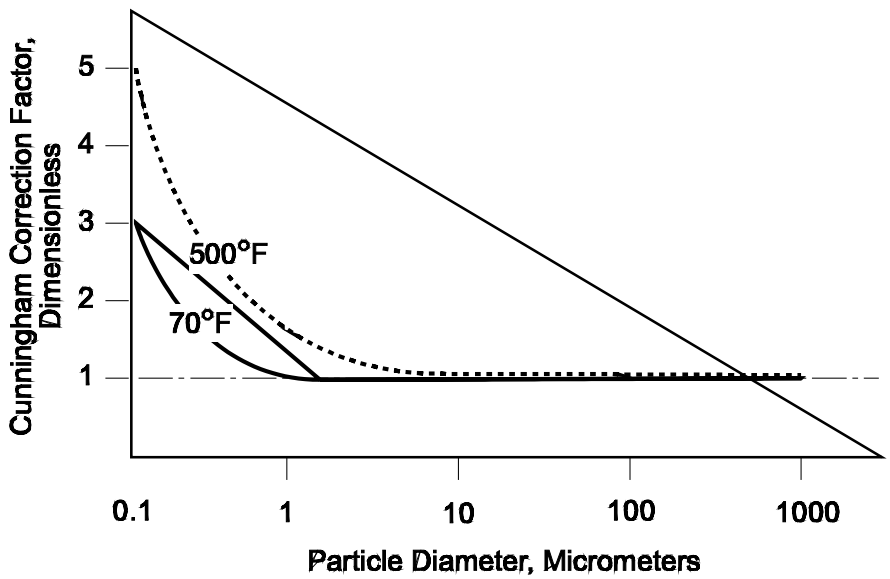

Figure 2-5. Relationship between particle size, temperature, and the Cunningham Correction Factor, C_c

$$F_D = \frac{3\,\pi\,\mu\,v_p\,d}{C_c} \qquad \text{Laminar} \tag{2-15}$$

$$F_D = 2.31\,\pi\,(d\,v_p)^{1.4}\,\mu^{0.6}\,\rho_a^{0.4} \qquad \text{Transition} \tag{2-16}$$

$$F_D = 0.055\,\pi\,(d\,v_p)^2\,\rho_a \qquad \text{Turbulent} \tag{2-17}$$

Where:

g = gravitational acceleration, 980 cm/sec^2
= fluid viscosity (gm/(cm-sec))
d = physical particle diameter (cm)
$_p$ = particle density (gm/cm^3)
$_g$ = gas density (gm/cm^3)
v_p = velocity of particle relative to gas stream (cm/sec)

The streamline (laminar) flow of a fluid around a sphere (particle) was investigated by G. Stokes in 1845 for small values of the Reynolds number. Stokes found that the drag force of the fluid around a particle is a function of the gas viscosity, particle velocity, and particle diameter. Equation 2-15 expresses this finding known as Stokes' Law, which is valid for particle Reynolds numbers equal to or less than 1.0. Particles less than approximately 100 m in air pollution control devices generally have particle Reynolds numbers less than 1.0. Therefore, Stokes' Law generally applies only for the initial collection of particles. The agglomerated masses of particles that are dislodged during cleaning are larger than 100 m, and these "particles" have Reynolds numbers greater than 1.0. Therefore, the drag force on these agglomerated materials must usually be calculated using either Equation 2-16 or 2-17, depending on the size of the particles or agglomerated particles.

Problem 2-5

Calculate the drag force experienced by a 2 m unit density particle moving through 100°C air at 10 m/sec.

Solution:

Air at 100°C has a viscosity of 2.2×10^{-4}gm/cm·sec. The C_c for a 2 m particle moving in 100°C air is:

$$C_c = 1 + \frac{6.21x10^{-4}(373°K)}{2\mu m} = 1.12$$

Substituting these values into the drag equation for laminar flow gives:

$$F_D = \frac{3\ \pi\ (2.2x10^{-4} gm/cm \cdot sec)(1x10^{3} cm/sec)(2x10^{-4} cm)}{1.12}$$

$$= 3.70\ \ x\ 10^{-4} g \cdot cm / sec^2$$

Verify that the laminar flow assumption is valid.

Air density at 100°C = (293°K/373°K) × 0.001205 gm/cm^3 = 9.47×10^{-4}gm/cm^3.

$$Re_p = \frac{(9.47x10^{-4} gm/cm^3)1x10^{3} \frac{cm}{sec}(2x10^{-4} cm)}{2.2x10^{-4} gm/cm \cdot sec}$$

$$= 0.86$$

Since N_{REP} is less than 1.0, the assumption is valid.

Balance of Forces on a Particle. Newton's second law of motion states that the acceleration produced in a given mass by the action of a given force is proportional to the force and in the direction of that force. The second law is simply a statement of the equation *F = ma.* The sum of the forces can be written as follows:

$$\sum F = ma = m\frac{dv}{dt} \qquad (2\text{-}18)$$

Where:

dv/dt = acceleration or change in velocity with respect to time

A particle in motion in a fluid will be affected by a number of forces such as gravitational, drag, and electrostatic forces. The simplest example involves a particle falling through still air (Figure 2-6).

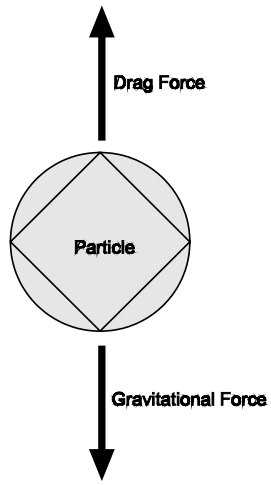

Figure 2-6. Balance of gravitational and drag forces

The vector sum of the forces is equal to a resultant force, F_R. Note that the effect of bouyancy has been ignored because the density of particles is substantially greater than the density of air or other gases.

$$F_R = F_G - F_D = m\frac{dv}{dt} \tag{2-19}$$

As the particle accelerates, the velocity will increase. The drag force on the particle also increases with increasing velocity. At some point, a velocity value will be reached where the drag force will be as large as the gravitational force. At this point, the resultant force will be zero, and the particle will no longer accelerate. If the particle is not accelerating, it is at a constant velocity. This constant velocity, where all the forces balance out, is called the terminal settling velocity.

$F_R = F_G - F_D = 0$ at terminal settling velocity

Then: $F_G = F_D$

A parachutist relies on the phenomenon of terminal settling velocity. After jumping from the plane, there is a short period of acceleration. Then the gravitational force pulling the parachutist down is balanced by the drag force of the air resisting his or her fall. In the absence of additional forces, free fall at a constant velocity results. Eventually, the person opens the parachute to increase the drag force and establish a lower terminal velocity. With particles much smaller than human bodies, the settling velocity is much slower. This can be seen with smoke plumes that remain aloft for long periods. Without the resisting drag force, these plumes would fall to the ground immediately.

The particle settling velocity equation is derived by setting F_G equal to F_D. Substitute the values for F_G from Equation 2-5 and F_D (for laminar conditions) from Equation 2-15.

$$F_G = \frac{\rho_p \pi d^3 g}{6}$$

$$F_D = \frac{3\pi\mu v_p d}{C_c}$$

$$\frac{\rho_p \pi d^3 g}{6} = \frac{3\pi\mu v_p d}{C_c}$$

Solving for v_p (which is now v_t):

$$v_t = \frac{g \rho_p d^2}{18 \mu} C_c \qquad (2\text{-}20)$$

Where:

g = gravitational acceleration, 980 cm/sec^2
= fluid viscosity (gm/(cm•sec))
d = physical particle diameter (cm)
$_p$ = particle density (gm/cm^3)
C_c = Cunningham slip correction factor (dimensionless)
v_t = terminal settling velocity (cm/sec)

Problem 2-6

Calculate the terminal settling velocity of a 2 m unit density particle in air at 20°C.

Solution:

The Cunningham slip correction factor is:

$$C_c = 1 + \frac{6.21 \times 10^{-4} (293°K)}{2\mu m} = 1.09$$

The viscosity of air at 20°C is 1.8×10^{-4}gm/cm•sec. The terminal settling velocity then equals:

$$v_t = \frac{(980 cm/sec^2)1(gm/cm^3)(2 \times 10^{-4} cm)^2 (1.09)}{18(1.8 \times 10^{-4} gm/cm \bullet sec)} = 0.013 \text{ cm/sec}$$

Although less commonly used, similar derivations for the settling velocity for the other ranges result in:

$$v_t = \frac{0.153\ g^{0.71}\ d^{1.14}\ \rho_p^{0.71}}{\mu^{0.43}\ \rho_g^{0.29}} \quad \text{Transition} \qquad (2\text{-}21)$$

$$v_t = 1.74\left(\frac{g\ d\ \rho_p}{\rho_g}\right)^{0.5} \quad \text{Turbulent} \qquad (2\text{-}22)$$

Where:

g = gravitational acceleration, 980 cm/sec^2
= fluid viscosity (gm/(cm•sec))
d = physical particle diameter (cm)
$_p$ = particle density (gm/cm^3)
$_g$ = gas density (gm/cm^3)
v_t = terminal settling velocity (cm/sec)

The gravity settling equations have been used to calculate the terminal settling velocities of particles from 0.1 to 100,000 m. The data in Table 2-1 clearly indicates that the terminal settling velocities are virtually negligible for particles less than 10 m, moderate for particles in the size range of 10 - 80 m, and relatively fast only for particles larger than 80 m.

Table 2-1. Terminal Settling Velocities at 25˚C

Particle Size, mm	Terminal Settling Velocity at 25˚C, cm/sec	Flow Condition
0.1	0.000087	Laminar
1.0	0.0035	Laminar
10.0	0.304	Laminar
50.0	7.5	Laminar
80.0	19.3	Laminar
100	31.2	Transitional
200	68.8	Transitional
1000	430.7	Transitional
10000	1583	Turbulent
100000	5004	Turbulent

It is for this reason that air pollution control devices are not designed to use gravity settling to accomplish initial separation. Instead, gravity settling is employed only for the second step in particulate control, which is the removal of large agglomerated masses or clumps of dust (1,000 to 100,000 micrometers) that have been collected on bags, precipitator plates, or other collection surfaces. These large clumps of material have high terminal settling velocities.

2.3 CENTRIFUGAL INERTIAL FORCE

Inertial force can be an effective collection mechanism when a particulate-laden gas stream is made to flow in a circular manner within a cylinder, as shown in Figure 2-7. Inertial force that is applied in a spinning gas stream is often termed *centrifugal force*.

The movement of particles due to inertial force in a spinning gas stream is estimated using the same procedure described for terminal settling velocity due to gravitational force. The equation for centrifugal force is:

$$F_c = \frac{m_p u_T^2}{R} \qquad (2\text{-}23)$$

Where:

F_c = centrifugal force (gm•cm/sec^2)
m_p = mass of the particle (gm)
u_T = tangential velocity of the gas (cm/sec)
R = cylinder radius (cm)

Note that for centrifugal force, the term "u_t^2/R" is similar to the gravitation force term "g" used in the discussion of gravity settling.

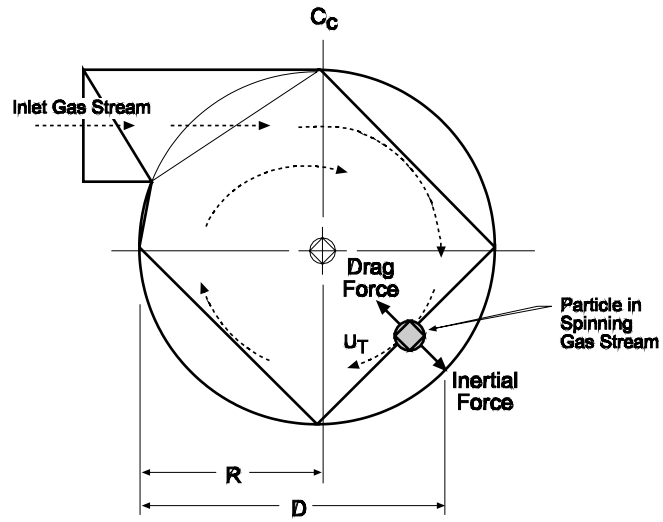

Figure 2-7. View of spinning gas in a cyclone
(top view)

Expressing the mass of the particle (m_p) in Equation 2-23 in terms of the particle density and the particle volume (see Equations 2-3 and 2-4) yields the following equation:

$$F_C = \frac{\frac{\pi}{6} d^3 \rho_p u_T^2}{R} \tag{2-24}$$

Where:

d = physical particle diameter (cm)

ρ_p = particle density (gm/cm^3)

For small particles that have particle Reynolds numbers in the laminar range, the drag force opposing motion introduced in Equation 2-15 and is as follows:

$$F_D = \frac{3\pi\mu\ v_p\ d}{C_c}$$

The velocity of the particle radially across the gas streamlines and toward the wall of the cyclonic chamber is then given by Equation 2-25.

$$v_c = \frac{d^2\ \rho_p\ u_T^2\ C_c}{18\mu R} \tag{2-25}$$

This equation illustrates that the velocity of the particle moving across the gas stream lines in the cyclone and toward the cyclone wall is proportional to the square of the particle size. This means that cyclones will be substantially more effective for large particles than for small particles. At any given particle size, the particle radial velocity will be proportional to the square of the gas stream tangential velocity and inversely proprotional to the cyclone radius. These two parameters determine the extent to which the gas

stream is spinning within the cyclone. High velocities increase the spinning action and therefore increase particle radial velocity and particle collection. A small cyclone radius makes the gas stream turn more sharply and therefore also increases cyclone efficiency.

2.4 INERTIAL IMPACTION

The inertia of a particle in motion in a gas stream can cause it to strike slow-moving or stationary obstacles in the path of the gas stream. As the gas stream deflects around the obstacle, the particle is displaced across the gas streamlines toward the direction of the target. If it has sufficient inertia, the particle contacts the obstacle and is captured. The general movement of the particles is illustrated in Figure 2-8.

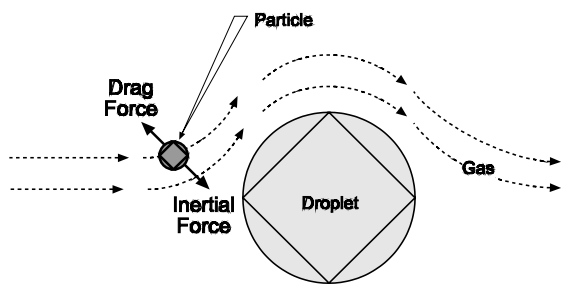

Figure 2-8. Inertial impaction and interception

The motion of the particle across the gas streamlines is similar to that in a cyclone. The particles are displaced in a radial direction. The extent of displacement is related directly to the efficiency of capture in the target. Large particles are captured more easily than small particles due to their greater inertia.

The efficiency of impaction can be evaluated using the same general procedures used to evaluate gravity settling and centrifugal force. For particles having a Reynolds number less than 1 (drag force Equation 2-8), the effectiveness of impaction can be related to the impaction parameter shown in Equation 2-26. As the value of this parameter increases, particles have a greater tendency to move radially toward the target. As the value of the parameter approaches zero, the particles have a tendency to remain on the gas streamlines and pass around the target.

$$K_I = \frac{C_c\, d^2\, v\rho_p}{18\,\mu\, D_c} \qquad (2\text{-}26)$$

Where:

K_I = impaction parameter (dimensionless)
C_c = Cunningham slip correction factor (dimensionless)
d = physicalparticle diameter (cm)
v = difference in velocity between the particle and the target (cm/sec)
D_c = diameter of target (cm)
= gas viscosity (gm/(cm•sec))
$_p$ = particle density (gm/cm^3)

Note that, in some texts, the impaction parameter is termed the “Stokes number” and has a value that is one-half the value shown in Equation 2-26.

This equation basically indicates that the extent of movement of the particle across gas streamlines is related to the square of the particle diameter for particles that have Reynolds numbers equal to less than 1. Evaluating the efficiency of impaction based on the impaction parameter yields a curve similar to that shown in Figure 2-9.

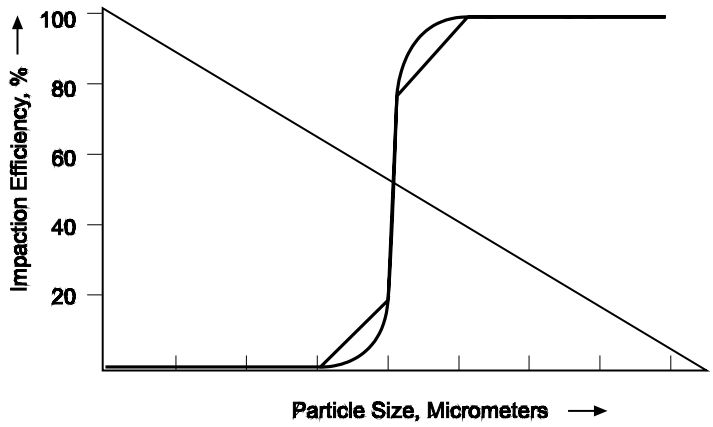

Figure 2-9. General characteristics of the impaction efficiency curve

2.5 PARTICLE BROWNIAN MOTION

Very small particles (0.2 to 0.002 micrometers) deflect slightly when they are struck by gas molecules. The deflection is caused by the transfer of kinetic energy from the rapidly moving gas molecule to the small particle. An exaggerated illustration of this motion is shown in Figure 2-10.

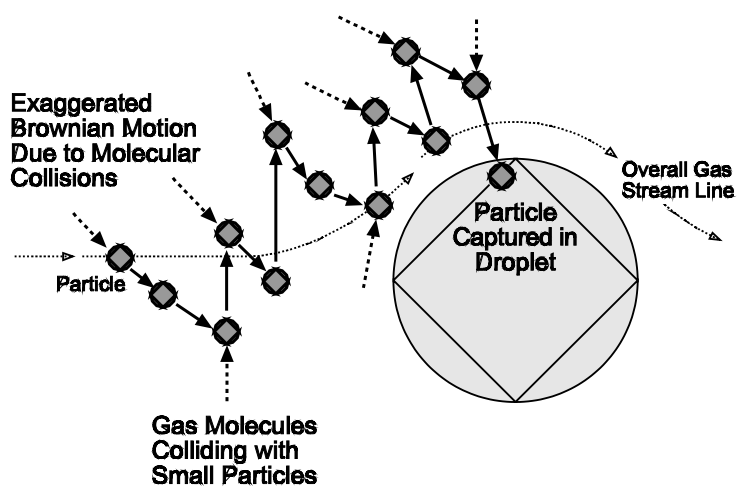

Figure 2-10. Brownian motion

Brownian motion and diffusion are important only for particles less than 0.3 micrometers. The rate of diffusion is related to the diffusivity parameter shown in Equation 2-27. This indicates that the rate of particle diffusion is inversely proportional to the particle diameter and directly proportional to the absolute gas temperature.

$$D_p = \frac{C_c\ K\ T}{3\ \pi\ \mu\ d} \tag{2-27}$$

Where:

D_p = diffusivity of particles (cm^2/sec)
K = Boltzmann constant ($gm \cdot cm^2/sec^2 \cdot °K$)
T = absolute temperature (°K)
C_c = Cunningham slip correction factor (dimensionless)
= gas viscosity (kg/m•sec)
d = physical particle diameter (μm)

Brownian motion and particle diffusion are responsible for a slight increase in the observed collection efficiencies of air pollution control devices in the size range less than 0.3 micrometers. However, diffusion rates are low even for particles in the 0.3 to 0.01 size range. Accordingly, particle Brownian motion and diffusion are not significant influences in the majority of air pollution control systems.

2.6 ELECTROSTATIC ATTRACTION

The following two particle charging mechanisms are active in air pollution control devices used to collect particulate matter.

- Diffusion charging
- Field dependent charging

Diffusion charge is the result of the collisions of unipolar ions with particles in a gas stream. The collisions are caused by the random Brownian motion of both the ions and the particles. Diffusional charging continues until electrical charges on the surface of the particle are sufficiently strong to repel most approaching ions. The number of electrical charges that accumulate on the surface of the particle due to these charging mechanisms is indicated by the relationship shown in Equation 2-28.

$$n = \frac{d_p kT}{2e^2} \log_{10}\left(1 + \frac{\pi d_p c_i e^2 N_i t}{2kT}\right) \tag{2-28}$$

Where:

d_p = diameter of particles (cm)
k = Boltzmann constant ($gm \cdot cm^2/sec^2 \cdot °K$)
T = absolute temperature (°K)
c_i = ion velocity (rms value)
e = charge of an electron (stC)
t = time (sec)
N_i = ion concentration

The extent of diffusional charging is related to the particle diameter. This is the most important charging mechanism for particles less than approximately 0.4 micrometers.

Diffusional charging does not require an electrical field. However, the particles that acquire an electrical charge will be influenced by a field that exists in the area of diffusional charging. These particles will move along the electrical field lines to an area of lower field strength (e.g., collection surface).

Field dependent charging occurs when particles are placed in a strong electrical field with a high concentration of unipolar ions. The ions are move along electric field lines that intersect the particle in the field. The transfer of electrical charge continues until the electrical field on the particle is sufficient to repel the field. This point is termed the *saturation charge* and is calculated using Equation 2-29.

$$n_s = \left(\frac{3\varepsilon}{\varepsilon + 2}\right)\left(\frac{E d_p^{\,2}}{4\varepsilon}\right) \tag{2-29}$$

Where:

d_p = diameter of particles (cm)
= dielectric constant of the particle (dimensionless)
E = electrical field strength (kv/cm)
n_s = saturation charge (number)

Equation 2-29 indicates that the number of electrical charges placed on a particle due to field dependent charging is related to the square of the particle diameter. This level of charging is achieved extremely quickly. Once charged, the particles will be influenced by the electrical field and will move along the electrical field lines toward the area of reduced electrical field strength.

Field dependent charging is the dominant charging mechanism for particles larger than 2 micrometers. It becomes progressively less important as the particle size decreases. Conversely, diffusional charge is more effective on particles smaller than 0.4 micrometers, and it becomes progressively more important as particle size decreases.

The charge on a particle is usually expressed as *n* times the smallest unit of charge, the charge on an electron, *e* (4.8×10^{-10} statcoulombs). The force on a particle with *n* units of charge in an electrical field, *E*, is given by:

$$F_E = n\,e\,E \tag{2-30}$$

Where:

F_E = electrostatic force (statcoulomb^2/cm^2)
n = number of charges
e = 4.8×10^{-10} stC
E = electric field strength (kv/cm)

The forces created in an electric field can be thousands of times greater than gravity. The velocity with which particles in the electric field migrate can be determined in a manner similar to that shown for gravity settling and centrifugal force. Setting the electrostatic force (F_E) equal to the drag force (F_D) and solving for terminal electrostatic velocity provides:

$$F_E = F_D \tag{2-31}$$

$$n\,e\,E = \frac{3\pi\mu d\, v_p}{C_c} \tag{2-32}$$

$$v = \frac{n\,e\,E\,C_c}{3\,\pi\,\mu\,d} \tag{2-33}$$

This equation applies to particles in the laminar region. When $N_{REP} > 1.0$, a more complicated procedure is required.

Problem 2-7

Determine the terminal electrostatic velocity of a 2 m unit density particle carrying 800 units of charge in an electric field of 2 kV/cm. Assume that the gas temperature is 20°C. To solve this problem, the following relationships are used:

300 V = 1 statvolt
statvolt = statcoulomb/cm
dyne = statcoulomb^2/cm^2 = gm·cm / sec^2
C_c = 1.09 (as calculated in Problem 2-4)

The electric field in centimeter-gram-second units (cgsu) is:

$$E = 2\,\frac{kV}{cm}\left(\frac{1\ stV}{.3\ kV}\right) = 6.7\ \frac{stV}{cm} = 6.7\ \frac{stC}{cm^2}$$

Using Equation 2-33,

$$V_p = \frac{800\left(4.8\times10^{-10}\,stC\right)\left(6.7\,stC/cm^2\right)\left(1.09\right)}{3\pi\left(1.8\times10^{-4}\,gm/cm\times sec\right)\left(2\times10^{-4}\,cm\right)} = 8.3\ \ cm/sec$$

It is apparent that the velocity for the 2 m particle discussed in Problem 2-7 is substantially greater than the gravity settling velocity for the same size particle. This is due to the much greater force imposed by the electrostatic field. Electrostatic force can be used for the initial separation of particles due to the magnitudes of the forces that can be imposed on small particles.

2.7 THERMOPHORESIS AND DIFFUSIOPHORESIS

Thermophoresis and diffusiophoresis are two relatively weak forces that can affect particle collection. Thermophoresis is particle movement caused by thermal differences on two sides of the particle. The gas molecule kinetic energies on the hot side of the particle are higher than they are on the cold side. Therefore, collisions with the particle on the hot side transfer more energy than molecular collisions on the cold side. Accordingly, the particle is deflected toward the cold area.

Diffusiophoresis is caused by an imbalance in the kinetic energies being transmitted to the particles by the surrounding molecules. When there is a strong difference in the concentration of molecules between two sides of the particle, there is a difference in the number of molecular collisions. The particle moves toward the area of lower concentration. Diffusiophoresis can be important when the evaporation or condensation of water is involved since these conditions create substantial concentration gradients. The normal differences in pollutant concentration are not sufficient to cause significant particle movement.

2.8 PARTICLE SIZE-COLLECTION EFFICIENCY RELATIONSHIPS

Due to the combined action of the various collection mechanisms described in the previous section, the performance of particulate control devices often has the particle size-efficiency relationship shown in Figure 2-11. Above 100 m, particles are collected with very high efficiency by inertial impaction, electrostatic attraction, and even gravity settling. Efficiency remains high throughout the range of 10 - 100 m due to the inertial and/or electrostatic forces (depending on the type of collector), both of which are approximately proportional to the square of the particle diameter. For particles less than 10 m, the limits of inertial forces and electrostatic forces begin to become apparent, and the efficiency drops. Efficiency of these collection mechanisms reaches low levels between 1 and 0.1 m, depending on such factors as gas velocities (inertial forces) and electrical field strengths (electrostatic attraction). Below 0.3 m, Brownian displacement begins to become effective. Accordingly, the overall efficiency curve begins to rise in the very small size range.

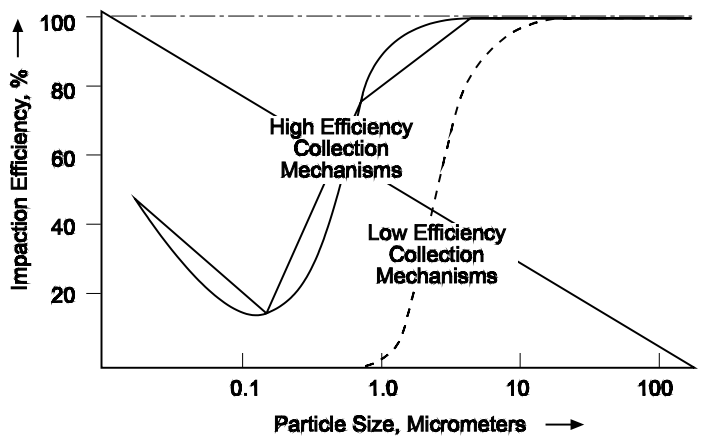

Figure 2-11. General relationship between collection efficiency and particle size

The combined result of these various collection mechanisms is a minimum collection efficiency in the particle size range of 0.1 to 0.5 m. Collection mechanisms in many devices are not highly efficient for particles in this range. These particles can be classified as "difficult-to-control" due to the inherent limitations of the collection mechanisms. This relationship, which can be seen in a number of studies of actual sources, indicates that stationary sources generating high concentrations of particles in the 0.1 to 0.3 m range may be an especially challenging control problem.

The actual extent of this gap in particulate control capability varies substantially among the types of particulate control systems. The gap is most noticeable in wet scrubbers and electrostatic precipitators. Fabric filters generally have a minimal decrease in overall efficiency in this range due to the multiple-collection mechanisms inherently present. Cyclonic collectors generally are inefficient for particles less than 1 to 3 m (low efficiency mechanism curve).

Operators of stationary sources that generate large fractions of the total particulate matter in the 0.1 to 0.3 m range may need to modify the process to alter the particle size distribution or use a pretreatment system to "grow" the particles to a more easily collected size range. These options are discussed in Chapter 6.

Review Exercises

1. What is the main role of gravity settling in high efficiency particulate control systems?
   a. Initial capture of particles in the gas stream being treated
   b. Collection of solids dislodged from the components (e.g., bags, collection plates) during the cleaning cycle
   c. Minimization of the particulate matter in the gas stream prior to the inlet to the particulate matter control device.
   d. None of the above.

2. How does the particle Reynolds number change when the gas temperature is increased?
   a. Increases
   b. Decreases
   c. Remains unchanged

3. A particle is being transported in a gas stream moving horizontally at 50 feet per second. Calculate the particle Reynolds number for a gas temperature of 115°C, a water vapor content of 10%, and an oxygen content of 7%. Ignore particle gravitational settling in the gas stream.

4. How does the gas viscosity change as the temperature is increased?
   a. Increases
   b. Decreases
   c. Remains unchanged

5. How is the collection efficiency of a cyclonic collector related to the particle size?
   a. It increases proportional to the cube of the particle diameter.
   b. It increases proportional to the square of the particle diameter.
   c. It increases proportional to the particle diameter.
   d. It is independent of the particle diameter.

6. How is the collection efficiency of an air pollution control device using inertial impaction (e.g., particulate wet scrubber) related to the particle size?
   a. It increases proportional to the cube of the particle diameter.
   b. It increases proportional to the square of the particle diameter.
   c. It increases proportional to the particle diameter.
   d. It is independent of the particle diameter.

7. How does the effectiveness of Brownian motion and diffusion relate to the particle size?
   a. It increases proportional to the cube of the particle diameter.
   b. It increases proportional to the square of the particle diameter.
   c. It increases proportional to the inverse of the particle diameter.
   d. It increases proportional to the inverse of the square of the particle diameter.

8. Calculate the particle Reynolds numbers for the following unit density particles. Assume a gas density of 0.001205 gm/cm^3 at 20°C.
   a. 10 µm particle moving at 1 ft/sec
   b. 10 µm particle moving at 10 ft/sec
   c. 100 µm particle moving at 1 ft/sec
   d. 100 µm particle moving at 10 ft/sec

9. Calculate the coefficient of drag at a particle Reynolds number of 0.5.

10. Calculate the terminal settling velocities of spherical particles having the following physical diameters. Assume a gas density of 0.001205 gm/cm^3 at 20°C. Also assume that the particle Reynolds number is < 1 and that the particle density = 1 gm/cm^3.
    a. 1 µm
    b. 10 µm
    c. 100 µm

Review Answers

1. What is the main role of gravity settling in high efficiency particulate control systems?
   b. Collection of solids dislodged from the components (e.g. bags, collection plates) during the cleaning cycle

2. How does the particle Reynolds number change when the gas temperature is increased?
   b. Decreases

3. A particle is being transported in a gas stream moving horizontally at 50 feet per second. Calculate the particle Reynolds number for a gas temperature of 115°C, a water vapor content of 10%, and an oxygen content of 7%. Ignore particle gravitational settling in the gas stream.

   Solution:

   The particle Reynolds number is zero because the particle is moving at the same speed as the gas stream.

4. How does the gas viscosity change as the temperature is increased?
   a. Increases

5. How is the collection efficiency of a cyclonic collector related to the particle size?
   b. It increases proportional to the square of the particle diameter

6. How is the collection efficiency of an air pollution control device using inertial impaction (e.g. particulate wet scrubber) related to the particle size?
   b. It increases proportional to the square of the particle diameter

7. How does the effectiveness of Brownian motion and diffusion related to the particle size?
   c. It increases proportional to the inverse of the particle diameter

8. Calculate the particle Reynolds numbers for the following unit density particles. Assume a gas density of 0.001205 gm/cm^3 at 20°C.
   a. 10 µm particle moving at 1 ft/sec = N_{REP} = 0.203
   b. 10 µm particle moving at 10 ft/sec = N_{REP} = 2.03
   c. 100 µm particle moving at 1 ft/sec = N_{REP} = 2.03
   d. 100 µm particle moving at 10 ft/sec = N_{REP} = 20.3

   Solution (general):

   All four parts of this problem use the following equation to calculate the particle Reynolds number:

$$\text{particle Reynolds number} = \frac{\rho_g v_p d_p}{\mu}$$

From Equation 2-8, the gas viscosity at 20°C is 1.81×10^{-4} gm/(cm•sec).

Solution for part a:

$$N_{REP} = \frac{0.001205\ gm/cm^3 \times [1\ ft/sec \times 12\ in./ft \times 2.54\ cm/in.] \times 0.001\ cm}{1.81 \times 10^{-4}\ gm/(cm \bullet sec)}$$

$$= 0.203$$

Solution for part b:

$$N_{REP} = \frac{0.001205\ gm/cm^3 \times [10\ ft/sec \times 12\ in./ft \times 2.54\ cm/in.] \times 0.001\ cm}{1.81 \times 10^{-4}\ gm/(cm \bullet sec)}$$

$$= 2.03$$

Solution for part c:

$$N_{REP} = \frac{0.001205\ gm/cm^3 \times [1\ ft/sec \times 12\ in./ft \times 2.54\ cm/in.] \times 0.01\ cm}{1.81 \times 10^{-4}\ gm/(cm \bullet sec)}$$

$$= 2.03$$

Solution for part d:

$$N_{REP} = \frac{0.001205\ gm/cm^3 \times [10\ ft/sec \times 12\ in./ft \times 2.54\ cm/in.] \times 0.01\ cm}{1.81 \times 10^{-4}\ gm/(cm \bullet sec)}$$

$$= 20.3$$

9. Calculate the coefficient of drag at a particle Reynolds number of 0.5.

   $C_D = 48$

   Solution:

   $C_D = 24/N_{REP}$ if $N_{REP} < 1.0$

   $C_D = 24/0.5 = 48$

10. Calculate the terminal settling velocities of spherical particles having the following physical diameters. Assume a gas density of 0.001205 gm/cm^3 at 20°C. Also, assume that the particle Reynolds number is < 1 and that the particle density = 1 gm/cm^3

    a. 1 µm = The terminal settling velocity (v_t) = 0.0035 cm/sec.
    b. 10 µm = The terminal settling velocity (v_t) = 0.307 cm/sec.
    c. 100 µm = The terminal settling velocity (v_t) = 30.5 cm/sec.

Solution for part a:

For a 1 m particle,

$$C_c = 1 + (6.21 \times 10^{-4}\ T)/d_p = 1 + (6.21 \times 10^{-4})\ (293^{\circ}K)/1\mu m = 1.18$$

$$v_t = \frac{g \rho_p d^2\ C_c}{18\mu}$$

$$v_t = \frac{(980\ \text{cm/sec}^2)\,(1\ \text{gm/cm}^3)\,(1\times10^{-4}\ \text{cm})^2(1.18)}{18\ \ (1.81\times10^{-4}\ \text{gm/cm}\bullet\text{sec})} = 0.0035\ \text{cm/sec}$$

particle Reynolds number = $\dfrac{\rho_g v_p d_p}{\mu}$

$$N_{REP} = \frac{(0.001205\ \text{gm/cm}^3)\,(0.0035\ \text{cm/sec})\,(0.0001\ \text{cm})}{1.81\times10^{-4}\ \text{gm/cm}\bullet\text{sec}}$$

$$N_{REP} = 2.3\times10^{-6}$$

Therefore, use of the laminar form of the gravity settling equation is correct, and 0.0035 cm/sec is the correct terminal settling velocity of this particle.

Solution for part b:

For a 10 m particle,

$C_c = 1 + (6.21 \times 10^{-4}\ T)/d_p = 1 + (6.21 \times 10^{-4})\ (293^{\circ}K)/10 = 1.02$

$$v_t = \frac{g\,\rho_p\,d^2\,C_c}{18\,\mu}$$

$$v_t = \frac{(980\ \text{cm/sec}^2)(1\ \text{gm/cm}^3)\,(1\times10^{-3}\,\text{cm})^2\ (1.02)}{18\,(1.81\times10^{-4}\ \text{gm/cm}\bullet\text{sec})} = 0.307\ \text{cm/sec}$$

particle Reynolds number = $\dfrac{\rho_g v_p d_p}{\mu}$

$$N_{REP} = \frac{(0.001205\ \ \text{g/cm}^3)(0.307\ \ \text{cm/sec})(0.001\ \ \text{cm})}{1.81\times10^{-4}\ \text{gm/cm}\bullet\text{sec}}$$

$$N_{REP} = 2.0\times10^{-3}$$

Therefore, use of the laminar form of the gravity settling is correct, and 0.307 cm/sec is the correct terminal settling velocity of this particle.

Solution for part c:

For a 100 m particle,

$C_c = 1 + (6.21 \times 10^{-4}\ T)/d_p = 1 + (6.21 \times 10^{-4})\ (293°K)/100 = 1.00$

$$v_t = \frac{g\,\rho_p\,d^2\,C_c}{18\,\mu}$$

$$v_t = \frac{(980\ \text{cm/sec}^2)\ (1\,\text{gm/cm}^3)\,(1\times10^{-2}\ \text{cm})^2\ (1.0)}{18\,(1.81\times10^{-4}\ \text{gm/cm}\ \bullet\text{sec})} = 30.1\ \ \text{cm / sec}$$

particle Reynolds number = $\frac{\rho_g \; v_p \; d_p}{\mu}$

$$N_{REP} = \frac{(0.001205 \;\; gm/cm^3)\,(30.1 \; cm/sec)\,(0.01 \;\; cm)}{1.81 \times 10^{-4} \; gm/cm \bullet sec}$$

$$N_{REP} = 2.00$$

Therefore, use of the laminar form of the gravity settling equation is not correct.

Assume that the flow near the particle is in the transitional range.

$$v_t = \frac{0.153 \; g^{0.71} \, d^{1.14} \, \rho_p^{0.71}}{\mu^{0.43} \, \rho_g^{0.29}}$$

$$v_t = \frac{0.153 (980 \; cm/sec^2)^{0.71} \;\; (0.01 cm)^{1.14} \;\; (1 \, gm/cm^3)^{0.71}}{(1.81 \times 10^{-4} \; gm/cm \bullet sec)^{0.43} \;\; (0.001205 \, gm/cm^3)^{0.29}}$$

$$v_t = 30.5 \;\; cm/sec$$

particle Reynolds number = $\frac{\rho_g \; v_p \; d_p}{\mu}$

$$N_{REP} = \frac{(0.001205 \;\; gm/cm^3)\,(30.3 \; cm/sec)\,(0.01 \;\; cm)}{1.81 \times 10^{-4} \; gm/cm \bullet sec}$$

$$N_{REP} = 2.03$$

Therefore, use of the transitional form of the gravity settling equation is correct, and 30.5 cm/sec is the correct terminal settling velocity for this particle.

Chapter 3

Air Pollution Control Systems

Industrial process systems consist of the process equipment, which generates the pollutants, the air pollution control equipment that removes them, and the fan that moves the gas stream.

The process equipment and the air pollutant control devices do not work independently. The operating conditions of all the system components are closely linked together by the fans, hoods, and ductwork.

In addition to discussing how hoods and fans operate in an industrial system, this chapter introduces you to the preparation and use of industrial source system flowcharts. Flowcharts provide an important tool for evaluating the overall system.

Some reasons for understanding and evaluating the entire industrial process as a whole are given below.

- Changes in the process equipment can have a major impact on the efficiency of the control device.
- Changes in the air pollution control device can affect the ability of the process hoods to capture the pollutants at the point of generation.
- The operating data from one unit in the system can be valuable in evaluating the operating conditions in another unit in the system.
- Hoods and fans can influence the efficiency of the air pollution control equipment and the release of fugitive emissions from the process equipment.

3.1 FLOWCHARTS

Flowcharts are a useful tool when you want to evaluate the performance of an entire system because they provide a means for organizing and presenting operating data. More specifically, flowcharts can be used for the following purposes:

- Evaluating process operating changes that are affecting control device performance
- Identifying instruments that are not working properly
- Identifying health and safety problems
- Communicating effectively

As discussed later (see lesson on Flowchart Diagrams) an expanded block diagram flowchart has been adopted for use in this Course. Major components such as baghouses are shown as a simple block rather than a complex sketch resembling the actual baghouse. A set of conventional instrument symbols and major equipment symbols have been adopted primarily from conventional chemical engineering practice.

Most of the standard symbols are reproduced on the back of the flowchart sheet so that you do not need to remember any of the specific information included within this course. The form is basically "self contained."

3.1.1 Flowchart Symbols

A complete flowchart consists of several symbols representing major and minor pieces of equipment and numerous material flow streams. It is important to be able to differentiate between the various types of material flow streams without sacrificing simplicity and clarity.

Material Streams

The recommended symbols selected for the material streams are presented in Figure 3-1.

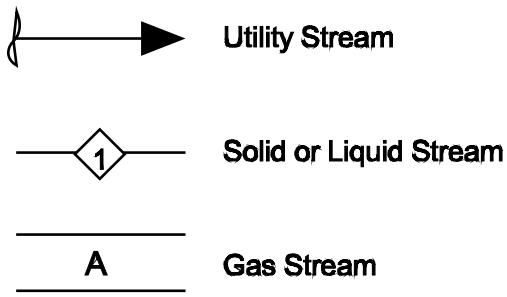

Figure 3-1. Material stream symbols

Gas flow streams are shown as two parallel lines spaced slightly apart and therefore appear larger than other streams. This size difference is important so that the inspector can quickly scan the flowchart and differentiate between gas and liquid material flow streams. Segments of ductwork connecting one major piece of equipment to another are labeled with an alphabetic character.

Important liquid and solid material flow streams are shown as solid, single lines. Diamonds with enclosed numbers are used to identify each of the streams.

To avoid cluttering the drawing, some of the liquid and solid material streams for which operating data will not be necessary are unnumbered. These types of streams are often called *utility streams* for a couple of reasons. They provide necessary materials to the system being shown and the characteristics of these streams are relatively constant. Typical utility streams for air pollution control equipment systems include make-up water, cooling water, and low-pressure steam. Natural gas, oil, and other fossil fuels can also be treated as utility streams to simplify the drawings. Instead of the numbered diamonds, these utility streams are identified either by using one of the codes listed in Table 3-1 or by a one- or two-word title. The codes or work titles are placed next to a "stretched S" symbol, which is used to indicate that the source of the utility stream is outside the scope of the drawing.

Table 3-1. Codes for Utility Streams

Cal	- Compressed calibration gas	HS	- High pressure steam
CA	- Compressed air	IA	- Instrument air
CD	- Condensate	LS	- Low pressure steam
CW	- City (or plant) fresh water	Oil	- No. 2 or No. 6 oil
Gas	- Natural Gas		

Major Components of Systems

A square or rectangle is used to denote major equipment such as the air pollution control devices, tanks and vessels, or process equipment. Fans are denoted using a relatively large circle with a set of tangential lines to indicate the discharge point. A stack is shown as a slightly tapered rectangle. All of these symbols are shaded or filled with crosshatched diagonal lines so that it is easy to pick out the major equipment items from the gas handling ductwork and other streams leaving these units as shown in Figure 3-2.

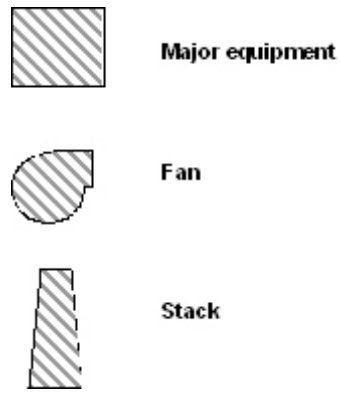

Figure 3-2. Major equipment symbols

The items treated as major equipment depend on the overall complexity of the system being drawn and on individual preferences. These decisions are determined based primarily on the types of data and observations that are possible and the level of detail that is necessary to evaluate the performance of the overall system.

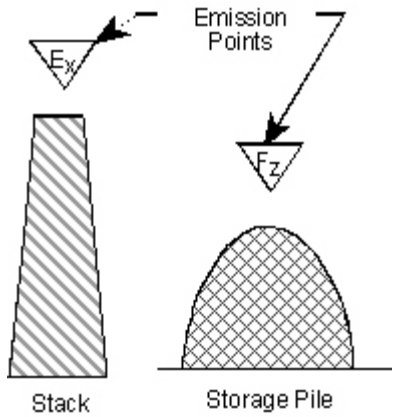

Figure 3-3. Identification of emission points

The stack (or emission discharge point) is obviously important due to the visible emission observations and the presence of continuous emission monitors and stack sampling ports in some systems. The emission points, which should be subject to Method 9 or Method 22 visible emission observations, are identified by a set of inverted triangles immediately above the source as shown in Figure 3-3. These are numbered whenever there is any possibility of confusing different sources within a single industrial complex. The numbers used in the triangles should correspond with the emission point identification

numbers used in the inspector's working files. Typical identification numbers E_1, E_2, ... E_n are used for enclosed emission points such as stacks and F_1, F_2... F_n are used for fugitive emission points such as storage piles and material handling operations.

Minor Components of Systems

A number of relatively small components in air pollution control systems should be shown on the block-diagram-type flowcharts in order to clarify how the system operates. A partial list of these minor equipment components is provided in Table 3-2.

Table 3-2. Minor Components

Fabric Filters	Wet Scrubbers
• Bypass dampers	• Pumps
• Relief dampers	• Nozzles
• Outlet dampers	• Manual valves
• Reverse air fans	• Automatic valves
Carbon adsorbers and Oxidizers	
• Indirect heat exchangers	
• Fans	

Symbols for the minor components listed in Table 3- 2 are shown in Figure 3-4. Note that all of these symbols are relatively simple and quick to draw.

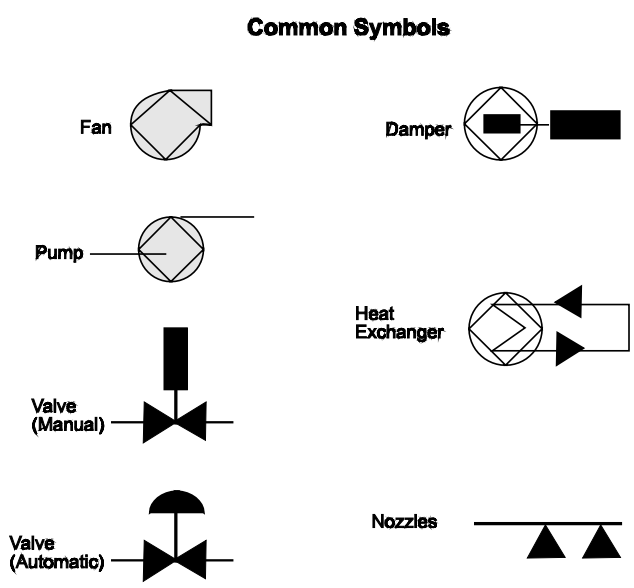

Figure 3-4. Minor component symbols

Instruments

The presence of an instrument or a sampling port is indicated by a small circle connected to a stream line by a short dashed line as shown in Figure 3-5.

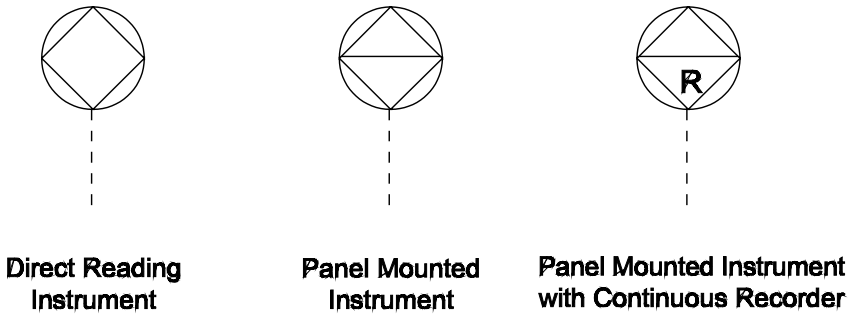

Figure 3-5. Gauge symbols

The type of instrument is indicated using the symbols listed in Table 3-3.

Table 3-3. Instrument Codes

A	- Motor current	pH	- Liquid or slurry pH
CEM	- Continuous emission monitor	Δp	- Static pressure drop
Den	- Density	SP	- Gas static pressure
F	- Flow	SSP	- Stack sampling port
L	- Liquid level	T	- Temperature
LEL	- Lower explosive limit	V	- Vacuum gauge
MP	- Measurement port	VOC	- Low concentration VOC monitor
Op	- Opacity	W	- Weight
P	Gas or liquid pressure		

Instruments such as manometers and dial-type thermometers can only be read at the gauge itself. These indicating gauges, shown in Figure 3-5, are simply denoted by the instrument circle and the instrument code. More sophisticated instruments with panel-mounted readout gauges (normally in the control room) are indicated using a line horizontally bisecting the instrument circle. In this case, the instrument code is placed directly above the line. When the instrument readout is a continuous strip chart recorder or data acquisition system, the letter "R" for "Recording" is placed below the line.

Materials of Construction

The materials of construction are relevant whenever there has been or may be a serious corrosion problem that could affect either system performance or safety. On a single-page-format-type of flowchart, it is impractical to specify the exact types of material and protective coatings on each vulnerable component because there are several hundred combinations of materials and coatings in common use. However, the general type of material in certain selected portions of the system may be important. For example, it would be helpful to know that a stack discharging high concentrations of sulfuric acid vapor is composed of carbon steel because this material is easily attacked by sulfuric acid. The stack platform and access

ladders could be vulnerable to failure as the corrosion problem gets progressively worse. A small set of symbols is presented in Table 3-4 for identifying materials of construction.

Table 3-4. Codes for Construction Materials

CS - Carbon steel	RL - Rubber lined
FRP- Fiberglass reinforced plastic	SS - - Stainless steel
N - Nickel alloy	WD - Wood

These symbols should be placed next to the major equipment item (e.g., stack, fan, air pollution control device) or the gas handling ductwork segment.

3.1.2 Diagrams

Basic Flowcharting Techniques

Flowcharts can serve many purposes and therefore many levels of sophistication in flowchart preparation exist. Some of the most complex are design-oriented piping and instrumentation drawings (termed *P & I drawings*), which show every major component, valve, and pipe within the system. Even a drawing for a relatively simple system (or part of a system) can have more than 500 separate items shown on it. Conversely, a simple block diagram used as a field sketch may have only 3 to 5 symbols on the drawing.

Flowcharts for air pollution control studies should be relatively simple. Generally, you need more equipment detail than shown on a simple block diagram, but far less information than provided by the standard P & I drawing. The flowcharts should not be so cluttered with system design details that it is difficult to include present system operating conditions to help identify health and safety risks and performance problems. Since these are primarily "working" drawings, they must be small enough to be carried easily while walking around the facility. The flowcharts should not also require a lot of time to prepare or to revise.

For these reasons, an expanded block diagram flowchart has been adopted for use in this course. In this type of flowchart, only the system components directly relevant to the study are included. Major components such as baghouses are shown as a simple block rather than a complex sketch resembling the actual baghouse. Most minor components and material flow streams are omitted to avoid cluttering the drawing.

The size of the flowchart is designed so that it fits entirely on a single 8½ by 11 inch page and can be carried on a standard clipboard or in a notebook. Furthermore, most of the standard symbols are reproduced on the back of the flowchart sheet.

Flowchart Diagrams

An example flowchart for a relatively complicated air pollution source, a waste solvent incinerator, is shown in Figure 3-6. The process equipment in this example consists of a starved air modular incinerator with primary and secondary chambers. The air pollution control system consists of a venturi scrubber followed by a mist eliminator.

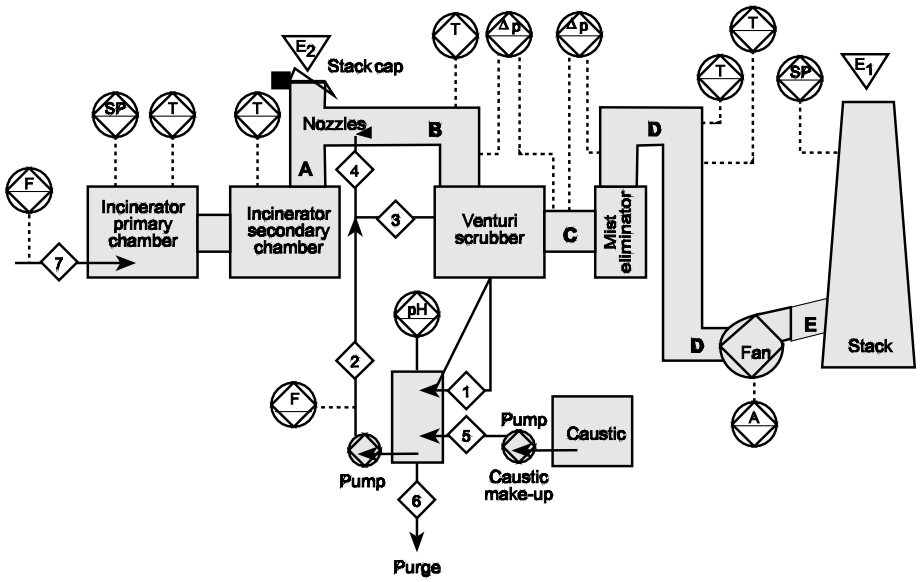

Figure 3-6. Example flowchart of a waste solvent system

The primary and secondary chambers of the waste solvent incinerator have been shown separately because data from each chamber is important to the inspection. However, many components of the incinerator and wet scrubber systems have not been shown because their operating conditions are not central to the potential air pollution emission problems or health and safety problems.

Another flowchart example is shown in Figure 3-7. This is a simple wet scrubber system serving a recycle operation in a hot mix asphalt plant. Most of the plant is not shown since the scrubber only controls the particulate emissions from the mixing of hot, new aggregate with cold, aged recycled asphaltic concrete.

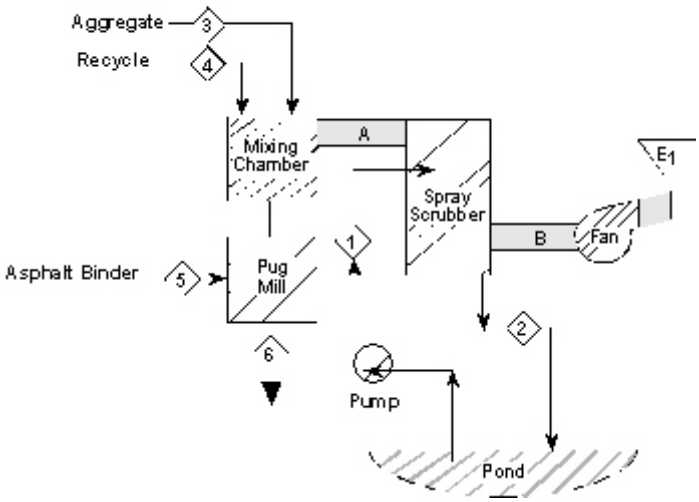

Figure 3-7. Example flowchart of an asphalt plant

It is apparent in Figure 3-7 that the duct labeled as section C serves as the discharge point. The liquid recycle pond is shown using an irregular shape and with a slightly different form of cross hatching so that it is easy to differentiate between the pond and the major equipment items.

It should be noted that the symbols for the major pieces of equipment and the symbols for other parts of the system should be located in logical positions. For example, the pond in Figure 3-7 is placed near the bottom of the sketch, and the stack is in a relatively high location.

The following problems illustrate how flowcharts can be helpful during the inspection of air pollution control systems. They serve as a tool for organizing relevant data and determining what needs further investigation.

Follow these steps when evaluating the overall system:

1. Determine whether or not the operating data is consistent and logical.
2. Compare current data against site-specific baseline data.
3. Determine specific areas that may need emphasis during the inspection.
4. Determine potential health and safety problems that may be encountered during the inspection.

Problem 3-1

A regulatory agency is conducting an inspection of a soil remediation unit at a hazardous waste site. This site is an abandoned chemical plant where several nonvolatile carcinogens (chlorinated organic compounds) are present in old lagoons. The plant uses a rotary kiln for destruction of the carcinogens and two side-by-side pulse jet fabric filters for control of particulate matter generated in the kiln. Based on the data shown in Figure 3-8 (Present Situation) and Table 3-5 (Baseline Data), determine the following:

A. Is the operating data for the system consistent and logical?

B. Do any important discrepancies exist between the current and baseline data?

C. What areas of the facility should be emphasized during the inspection?

D. What health and safety issues should be considered during the inspection?

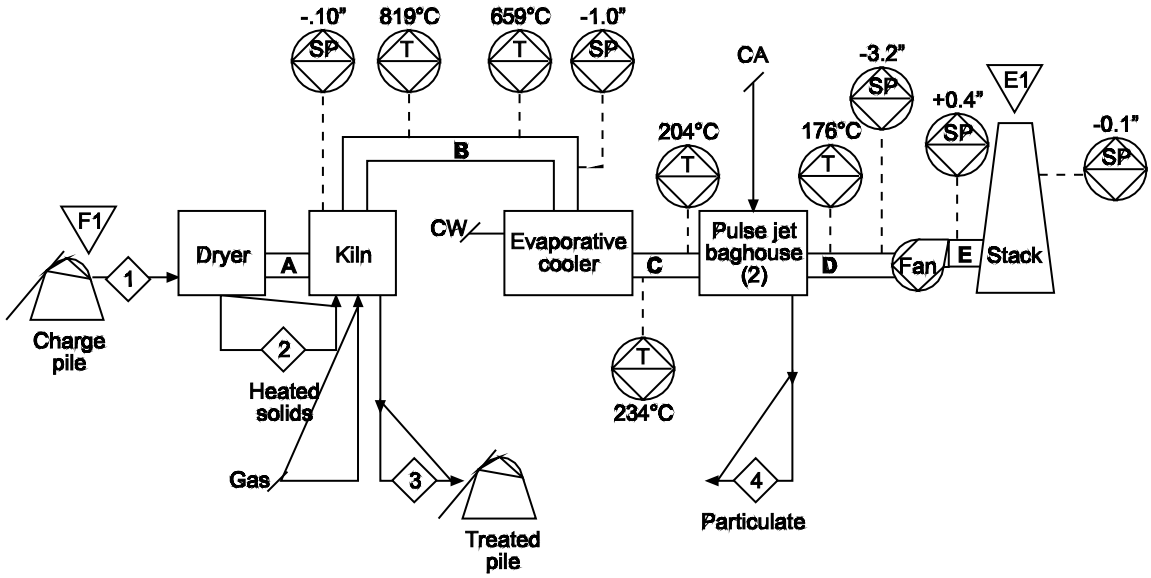

Figure 3-8. Example flowchart of a hazardous waste incinerator and pulse jet baghouse system

Table 3-5. Baseline Data for the Hazardous Waste Incinerator		
Location	**Temperature (°C)**	**Static Pressure (in. W.C.)**
Kiln hood	810	-0.1
Evaporative cooler inlet	785	-1.0
Evaporative cooler outlet	240	No Data
Baghouse inlet	195	No Data
Baghouse outlet	190	-5.1
Duct E	No Data	-1.5
Stack	No Data	-1.0

Solution:

Part A

Determine if the operating data for the system is consistent and logical. There should be logical trends in the gas temperatures, gas static pressures, gas oxygen concentrations (combustion sources) and other parameters along the direction of gas flow.

For this example, the gas temperature and static pressure data are listed in Tables 3-6 and 3-7 in the direction of gas flow.

Table 3-6. Gas Temperature Profile for the Hazardous Waste Incinerator (°C)		
	Present	**Baseline**
Kiln hood	819	810
Evaporative cooler inlet	659	785
Evaporative cooler outlet	234	240
Baghouse inlet	204	195
Baghouse outlet	176	190

Table 3-7. Gas Static Pressure Profit for the Hazardous Waste Incinerator (in. W.C.)		
	Present	**Baseline**
Kiln hood	-0.10	-0.10
Evaporative cooler inlet	-1.0	-1.0
Evaporative cooler outlet	No Data	No Data
Baghouse inlet	No Data	No Data
Baghouse outlet	-3.2	-5.1
Duct E	+0.4	-1.5
Stack	-0.1	-1.0

The gas temperature and static pressure trends through the system are both logical. The gas temperatures are at a maximum at the discharge of the combustion source, and they decrease throughout the system. The gas temperature at the fan outlet is not provided for this example. Note that sometimes gas temperature at the fan outlet is *higher* than that at the fan inlet due to compression that occurs as the gas moves through the fan (the Joule-Thompson effect)[2]. The static pressures become progressively more negative as the gas approaches the fan. After the fan, the static pressure of the system significantly increases, as expected. Since the set of plant instruments provides consistent and logical profiles through the system, they are probably relatively accurate.

Solution:

Part B

Compare the current data against the site-specific baseline data to the extent that it is available.

Step 1. Compare the current temperature data against the site-specific baseline data.

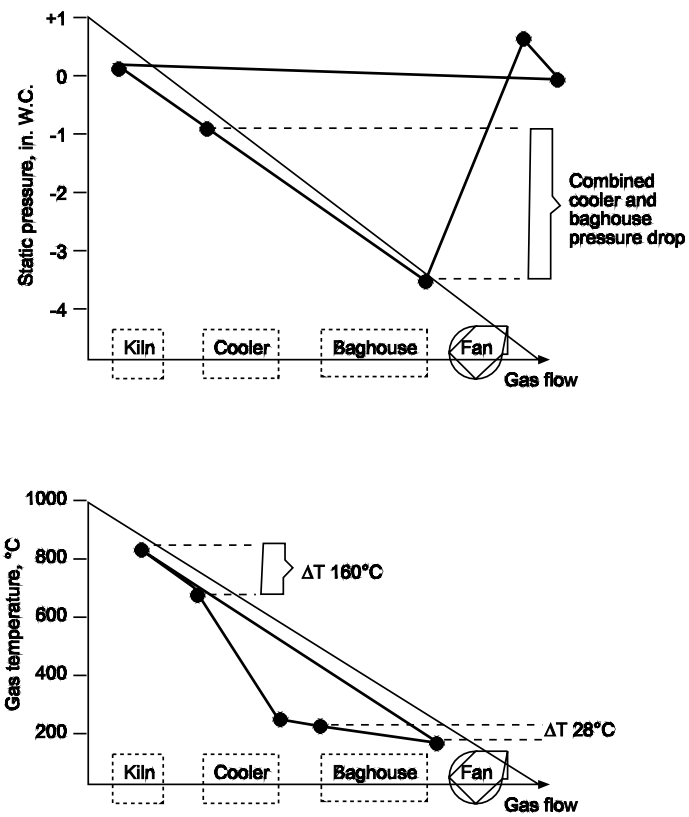

Figure 3-9. Static pressure and temperature profile for present data

a. Evaluate the temperature data for Duct B using Figure 3-9 and Table 3-6

The 160˚C temperature drop (from 819°C to 659°C) in the short duct (B) between the kiln and the evaporative cooler is relatively new. The baseline data indicates that the previous temperature drop was 25°C due to radiative and convective heat losses from the refractory-lined duct. The significantly higher temperature drop presently occurring across this short section of ductwork indicates that air

infiltration is probably happening. This air infiltration could reduce the amount of combustion being pulled from the kiln and thereby cause fugitive emissions from the kiln. A check for fugitive emissions should be included in the scope of the inspection.

b. Evaluate the destruction efficiency of the rotary kiln using the kiln outlet temperature data using Figure 3-9 and Table 3-6.

The primary function of this portable plant is to incinerate the contaminated soil. It is apparent from the flowchart that the most useful single parameter for evaluating the destruction efficiency of the rotary kiln system is the kiln outlet temperature monitored by the temperature gauge on the left side of duct B. The present value of 819°C compares well with the baseline data obtained during the trial burn tests in which the unit demonstrated good performance. Accordingly, it appears that the unit is presently in compliance.

c. Evaluate the temperature data for the evaporative cooler. See Figure 3-9 and Table 3-6.

The evaporative cooler is important primarily because it protects the temperature-sensitive Nomex® bags used in the downstream pulse jet baghouses. It is clear from the flowchart that presently there is a gas temperature drop of 425°C across the evaporative cooler. This fact combined with an observed outlet gas temperature of 234°C demonstrates that this unit is operating as intended. It is not necessary to climb to the top of the unit to check the spray nozzles.

d. Evaluate the temperature data for the baghouse. See Figure 3-9 and Table 3-6

The flowchart data indicates there is a severe temperature drop across the baghouse (28°C). This should be included in the field evaluation.

Step 2. Compare the current pressure drop data against the site-specific baseline data.

a . Evaluate the static pressure data across the kiln using Figure 3-9 and Table 3-7.

The pressure readings are in agreement for the baseline data and the present data.

b. Evaluate the static pressure data from the evaporative cooler inlet to the baghouse outlet. See Figure 3-9 and Table 3-7.

The baseline static pressure drop is 4.1 in. W.C. compared with a present pressure drop reading of 2.2 in. W.C. Pressure drops across evaporative coolers tend to remain constant. However, the pressure drop across baghouses can vary due to changes in emission loading or a malfunction. Emission loading is directly related to a pressure drop increase. A decrease in pressure drop may result from air inleakage at the bag connention points. Air inleakage can also occur due to worn or torn bags.

c. Evaluate the static pressure data from the baghouse exit to the stack. See Figure 3-9 and Table 3-7.

The static pressure increase created by the fan (3.6 in. W.C.) is similar for the baseline and present conditions. The static pressure drop from the fan exit to the stack is also in agreement.

Solution:

Part C

Determine the areas that should be emphasized during inspection. They are as follows:

1. Check for air infiltration in Duct B.

2. Check for fugitive emissions from rotary kiln.

3. Investigate reasons for temperature drop of the pulse jet baghouses.

4. Check for air inleakage across the pulse jet baghouse

Solution:

Part D

Determine what health and safety issues should be considered during the inspection.

The pulse jet baghouse should be one of the main areas evaluated during the field portion of the inspection. However, this work must be conducted carefully in order to minimize safety hazards. The roof of the unit should be avoided because it is an uninsulated metal surface at 176°C (349°F). The soles of safety shoes could begin to melt and thereby cause a fall. Furthermore, there is a slight possibility of falling through the roof of the baghouse. The gas temperature drop of 28°C across the baghouse indicates severe air infiltration that may be caused by corrosion. If so, the roof may have been weakened. Corrosion is very likely in this process due to the formation of hydrochloric acid and water vapor in the kiln.

The waste being burned in this portable plant includes several suspected carcinogens. This should be noted on the flowchart to serve as a reminder to stay out of areas where inhalation problems or skin absorption hazards could exist.

Summary of Health and Safety Issues

1. Avoid roof of pulse jet baghouse.

2. Remain aware that chemicals in process are possible carcinogens. Avoid areas where inhalation or absorption may become dangerous.

Problem 3-2

A company is routinely evaluating the performance of a venturi scrubber serving a hazardous waste incinerator. They are using an Enhanced Monitoring Protocol that is based on the static pressure drop gauge across the venturi. Answer the following questions based on the data shown in Figure 3-10.

A. Is there any reason to believe that the venturi scrubber pressure drop gauge is malfunctioning?

B. Is there any reason to be concerned about fugitive emissions from the emergency bypass stack? (The emergency bypass stack has the stack cap covering the outlet.)

The present data and the corresponding baseline data are provided in Tables 3-8 and 3-9.

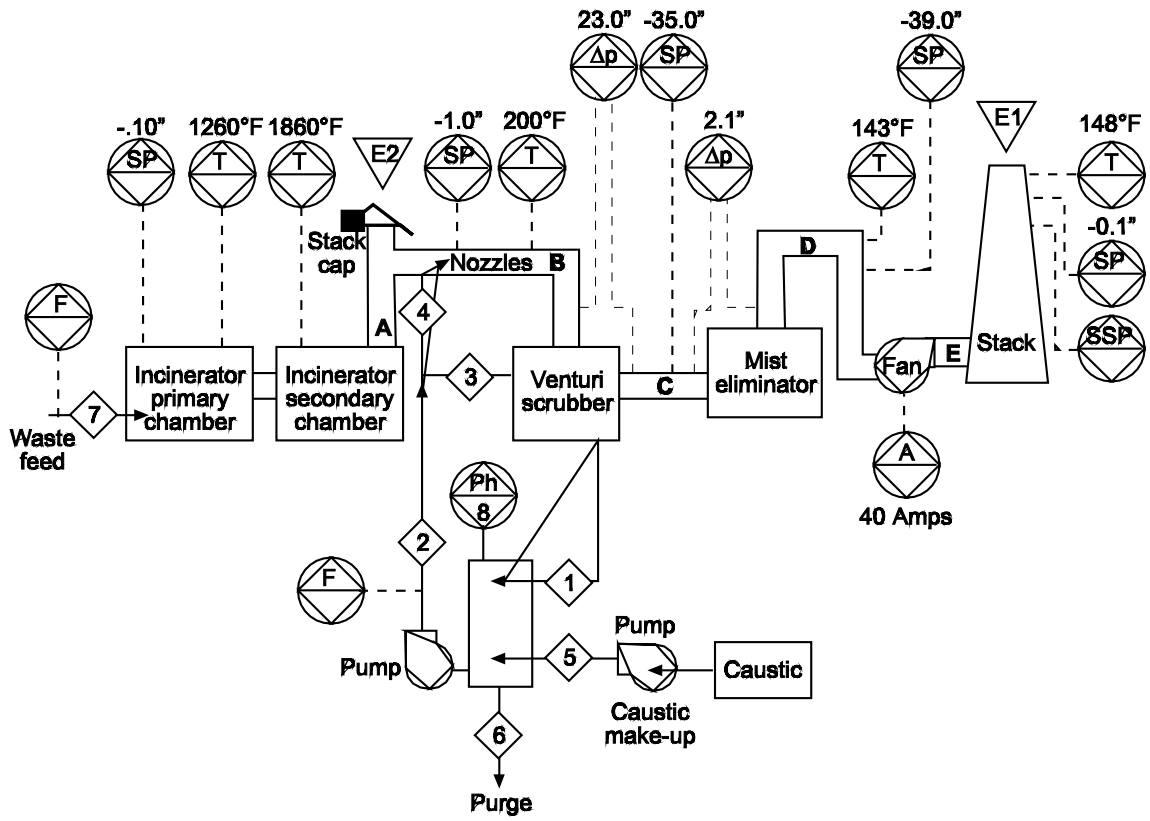

Figure 3-10. Example flowchart of a hazardous waste incinerator and venturi scrubber system

Table 3-8. Static Pressures and Static Pressure Drops (in. W.C.)		
	Present	**Baseline**
Static Pressures		
Incinerator primary chamber	-0.10	-0.12
Duct B	-1.0	-1.10
Mist eliminator inlet	-35.0	-38.0
Fan Inlet (Duct D)	-39.0	-40.0
Stack	-0.1	-0.1
Static Pressure Drop		
Venturi scrubber	23.0	36.0
Mist eliminator	2.1	1.6

Table 3-9. Gas Temperatures (°F)		
	Present	**Baseline**
Incinerator secondary chamber	1860	1835
Duct B	200	197
Fan Inlet	143	142
Stack	148	147

Solution:

Part A

First, evaluate the quality of data before attempting to evaluate the system. There should be logical trends for the static pressures, gas temperatures, and other relevant parameters.

The static pressure and pressure drop data have been combined into a single graph (Figure 3-11), which can be used to evaluate the static pressures along the entire gas flow path. It is apparent that present static pressure drop data for the venturi scrubber does not make sense. The present mist eliminator inlet static pressure and fan inlet static pressure data suggest that the static pressure drop across the venturi scrubber should be higher than indicated by the gauge. It is quite possible that the venturi scrubber pressure drop gauge is malfunctioning and that the actual static pressure drop is relatively similar to the baseline value of 36 in. W.C.

Solution:

Part B

There is no reason to suspect fugitive emissions from the emergency bypass stack. The static pressures upstream and downstream of the bypass stack are negative. Accordingly, ambient air could leak into a poorly sealed stack. Untreated combustion gas could not escape through gaps in the stack seal.

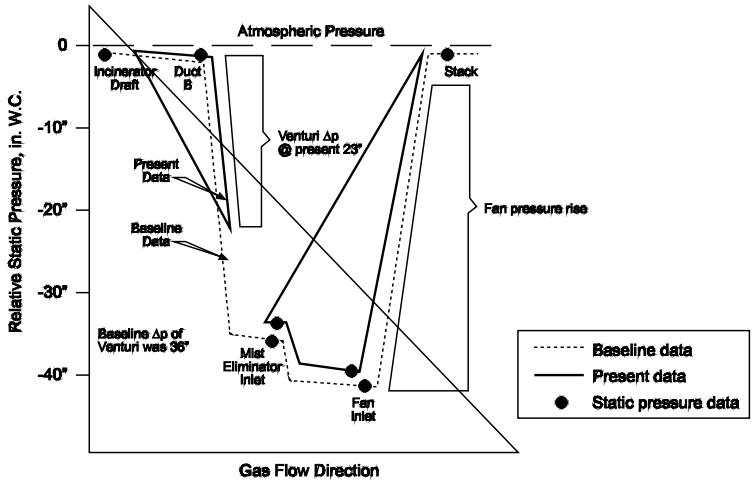

Figure 3-11. Static pressure profiles

Flowcharts Summary

A flowchart of the process system can be used to:

- Identify changes in control device performance due to process changes
- Identify instruments that are not consistent with other similar instruments in the system
- Communicate effectively with other personnel
- Avoid potential health and safety hazards

Flowcharts used for agency inspections should be prepared prior to or in the early stages of the inspection. If flowcharts for the system being inspected have been prepared previously, they should be reviewed prior to the on-site work and updated as necessary.

3.2 GAS PRESSURE, GAS TEMPERATURE, AND GAS FLOW RATE

Gas pressure, gas temperature, and gas flow rate data are used in essentially all projects concerning the performance of a particulate control device.

Gas Pressure

The pressures of the gas streams throughout the particulate control system are very important. Throughout this course, gas pressure data will be used to evaluate operating conditions.

The total pressure of a gas stream is the sum of the static pressure and velocity pressure of the gas stream as indicated in Equation 3-1. Velocity pressure is exerted only in gas streams that are in motion. This part of the total pressure is of concern only during emission tests and gas flow rate measurements and is not routinely monitored by plant personnel.

$$\text{Total Pressure} = \text{Static Pressure} + \text{Velocity Pressure} \tag{3-1}$$

The term *static pressure* is used to describe the pressure exerted by gases in all directions. This pressure is related to the number of gas molecules in a given volume and at a given temperature. If the number of molecules in the space increases, the pressure increases. An increase in the gas temperature increases the kinetic energy of the molecules, and the static pressure increases. All gas streams exert a static pressure. The static pressure exerted by ambient air is termed either *atmospheric* or *barometric pressure*. The latter term is often used since atmospheric pressure is measured by a barometer.

When fans used in industrial systems create gas static pressures above the prevailing atmospheric pressure, the condition is termed *positive pressure*. When the fans create a gas static pressure below the prevailing atmospheric pressure, *negative pressure* exists. Both positive and negative pressures are considered relative terms since the static pressure is being described in a form that is compared to the atmospheric pressure. The atmospheric pressure is an absolute term since it is directly related to the number of molecules and their kinetic energy.

$$\text{SP(absolute)} = \text{SP (barometric)} + \text{SP(relative)} \tag{3-2}$$

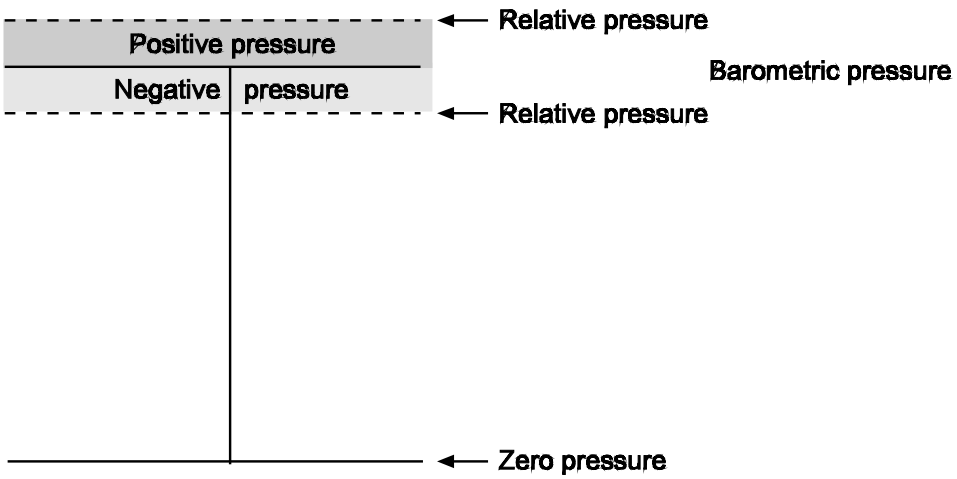

Figure 3-12. Definition of positive and negative pressure

Standard atmospheric pressure is defined as 14.7 pounds per square inch (psi). This is the average pressure that exists at sea level at 45° latitude. On a mountain, the atmospheric pressure is lower than 14.7 psi since the column of air above the measuring point is smaller. When weather systems pass over, there are slight variations in the atmospheric pressure that are slightly above or slightly below 14.7 psi. Nevertheless, the value of 14.7 psi will be used as a "standard."

The absolute and relative air pressures can be expressed in a number of units which are listed in Table 3-10. The values of the atmospheric pressure under standard conditions are listed in the second column.

Table 3-10. Units of Pressure

Units	Value at Standard Conditions
Psi	14.70
in. Hg	29.92
mm Hg	760.00
ft W.C.	33.92
in. W.C.	407.00

The most useful of these units is 407 inches of water (in. W.C.). This format is most convenient due to the magnitudes of the positive and negative relative pressures commonly found in industrial source systems. For example, the normal positive pressure gas streams are generally from +1 to +20 in. W.C., which is equivalent to the awkward values of +0.036 to +0.722 psi or +0.0735 to +1.47 inches of mercury (in. Hg). The normal negative pressures range from -0.20 to -60 in. W.C. which are equivalent to -0.0072 to -2.17 psi. Generally, the inches of water units for pressure are most convenient. Furthermore, gauges often used in air pollution control, and industrial ventilation systems indicate relative pressure directly in inches of water.

Problem 3-3

An air pollution control device has an inlet static pressure (relative) of –25 in. W.C. What is the absolute static pressure at the inlet of the air pollution control device if the barometric pressure at the time is 29.85 in. Hg?

Solution:

Convert the barometric pressure to in. W.C.

$$SP(\text{barometric}) = \left(\frac{407 \text{ in.W.C.}}{29.92 \text{ in Hg.}}\right) 29.85 \text{ in. Hg.} = 406 \text{ in.W.C.}$$

$$SP\ (\text{absolute}) = SP\ (\text{barometric}) + SP\ (\text{relative})$$

$$SP(\text{absolute}) = SP(406 \text{ in. W.C.}) + SP(-25 \text{ in. W.C.}) = 381 \text{ in. W.C.}$$

Generally, the inches of water units for pressure are most convenient. Furthermore, gauges often used in air pollution control, and industrial ventilation systems indicate relative pressure directly in inches of water.

Gas Temperature

Gas temperature can be expressed using both absolute and relative scales. The absolute scales start at absolute zero. These include the Kelvin scale for the centimeter-gram-second system (cgs) of measurements and the Rankine scale for the American engineering system of measurements.

The commonly used Celsius and Fahrenheit temperature units are relative scales. Both of these have arbitrary values that apply to the freezing and boiling points of water at standard conditions. When recording temperature values, it is important to note the units as well as the values. Many of the calculations performed in this course and in later APTI courses will require the conversion of the relative temperatures to absolute temperatures. The relationships between these various temperature scales are indicated by Equation 3-3 through Equation 3-9.

$$\Delta°F = \Delta°R \tag{3-3}$$

$$\Delta°C = \Delta°K \tag{3-4}$$

$$°R = 460 + °F \tag{3-5}$$

$$°K = 273 + °C \tag{3-6}$$

$$°F = 32 + 1.8\ (°C) \tag{3-7}$$

$$°C = (°F-32)/1.8 \tag{3-8}$$

$$\Delta°R = 1.8(\Delta°K) \tag{3-9}$$

Problem 3-4

The gas temperature in the stack of a wet scrubber system is 130°F. What is the absolute temperature in degrees Rankine and degrees Kelvin?

Solution:

Absolute Temperature, °R = 460°R + 130°F=590°R

Absolute Temperature, °K = 590°R/1.8 = 327.8°K

Gas Flow Rate

The gas flow rate can be expressed either in terms of standard cubic feet per minute (SCFM) or actual standard cubic feet per minute (ACFM).

The SCFM value is directly related to the number of gas molecules being handled per minute. It is the measure of the total quantity of gas being handled. It is also the volume that this amount of gas occupies at standard temperature (20°C or 68°F) and pressure (14.7 psi or 407 in. W.C.). Quantities in standard cubic feet per minute can be handled, added, and subtracted as necessary to describe the industrial source system. For example, if 1000 SCFM enter an air pollution control device, and none is reacted or lost, then 1000 SCFM exit the control device. If there is a negative pressure control device which is suffering air inleakage of 125 SCFM, and the inlet gas flow rate is 2000 SCFM, then the outlet gas flow rate is 2125 SCFM. The SCFM quantity can be calculated directly from the ideal gas law as indicated in Equation 3-10 and 3-11.

$$n = x / MW_{Avg.} \tag{3-10}$$

$$V = (n)(R)(T)/P \tag{3-11}$$

Where:

n = number of pound moles

x = pounds of gas per minute

MW_{Avg} = average molecular weight (usually between 28 and 30 for air and combuston gases)

V = gas volume in SCFM

R = universal gas constant (10.73 (psi)(cf)/(lb×moles)(°R))

T = absolute temperature (°R)

P = absolute pressure (psi)

It is possible to convert between SCFM and ACFM values using the ideal gas law relationship. This has been expressed in the form of simple ratios shown in Equations 3-12 and 3-13.

$$ACFM = SCFM\left(\frac{T_{Actual}}{T_{STP}}\right)\left(\frac{P_{STP}}{P_{Actual}}\right) \tag{3-12}$$

$$SCFM = ACFM\left(\frac{T_{STP}}{T_{Actual}}\right)\left(\frac{P_{Actual}}{P_{STP}}\right) \tag{3-13}$$

Where:

T_{Actual} = gas temperature at actual conditions (°R)

T_{STP} = gas temperature at standard conditions (°R)

P_{Actual} = gas pressure at actual conditions (in. W.C.)

P_{STP} = gas pressure at standard conditions (in. W.C.)

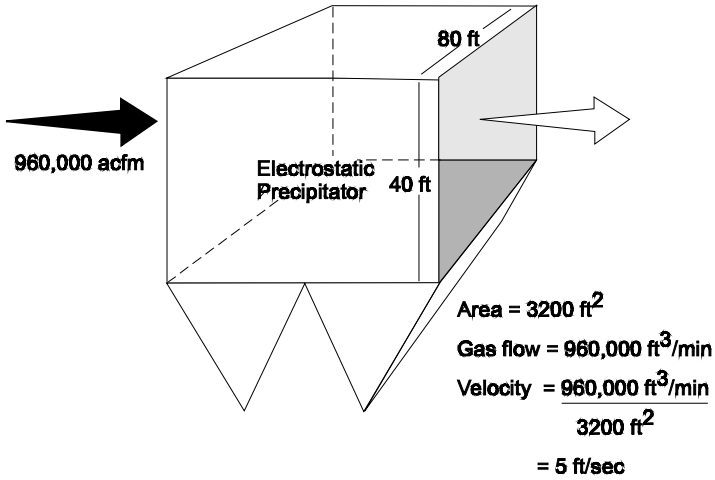

Figure 3-13. Example gas velocity calculation using ACFM

The SCFM form for gas flow rate is used whenever it is necessary to describe the *quantity* of gas. However, this form is not very useful when evaluating the gas flow characteristics inside the ductwork, air pollution control devices, and process equipment. When it is necessary to evaluate gas velocities and other flow conditions, the gas flow rate is expressed in terms of ACFM. This is the total *volume* of gas passing through the area of concern in one minute. The usefulness of the ACFM form is illustrated by the example shown in Figure 3-18. In this case, the velocity of 5 ft/sec through the electrostatic precipitator is calculated simply by dividing the gas flow rate in ACFM by the cross sectional area of the precipitator. The gas flow rates must be expressed in ACFM whenever *velocity* is calculated.

Problem 3-5

A particulate control system consists of a hood, ductwork, fabric filter, fan, and stack. The total gas flow entering the fabric filter is 8,640 SCFM and the total gas flow rate entering the fan downstream of the fabric filter is 11,340 SCFM. What is the rate of air infiltration into the fabric filter and the ductwork between the fabric filter and the fan?

Solution:

Prepare a material balance around the fabric filter and its outlet ductwork using SCFM.

Gas flow into the fabric filter and outlet ductwork= 8,640 SCFM + air infiltration

Gas flow out of the fabric filter and outlet ductwork = 11,340 SCFM

Gas flow in = Gas flow out

8,640 SCFM + air infiltration = 11, 340 SCFM

Air infiltration = 2,700 SCFM

Problem 3-6

The same system described in Problem 3-5 has a rectangular fabric filter inlet duct with inside dimensions of 3 feet by 4 feet. What is the velocity into the fabric filter? The gas temperature in the inlet duct is 320°F, the relative static pressure is –10 in. W.C. and the barometric pressure is 28.3 in. Hg.

Solution:

Convert the relative pressure to absolute pressure

$$SP(\text{absolute}) = \left(\frac{407 \text{ in. W.C.}}{29.92 \text{ in. Hg.}}\right) 28.3 \text{ in. Hg} + (-10 \text{ in. W.C.}) = 375 \text{ in. W.C.}$$

Convert the relative gas temperature to absolute temperature

$$T_{actual} = 460\,°R + 320\,°F = 780\,°R$$

Convert the fabric filter inlet flow rate to ACFM

$$ACFM = SCFM(T_{Actual}/T_{STP})(P_{STP}/P_{Actual})$$

$$ACFM = 8{,}640 \text{ SCFM}\left(\frac{780\,°R}{528\,°R}\right)\left(\frac{407 \text{ in. W.C.}}{375 \text{ in. W.C.}}\right) = 13{,}853 \text{ ACFM}$$

Calculate the velocity

$$\text{Velocity} = \frac{\text{Gas flow rate (ACFM)}}{\text{Area (ft}^2)} = \frac{13{,}853 \text{ ft}^3/\text{min}}{12 \text{ ft}^2} = 1{,}154 \text{ ft/min}$$

3.3 HOODS

The pollutants generated or released in process equipment must be captured so that they can be transported to the air pollution control device. Pollutant capture occurs in hoods.

Hoods are normally an integral part of the process equipment. The hood can consist of a simple, stationary plenum mounted above or to the side of the source, a large moveable plenum, or the process equipment itself.

Figure 3-14. Stationary hood in an industrial process

If hoods do not capture pollutants generated by process equipment, the pollutants disperse directly into the plant air and eventually pass through roof vents and doors into the atmosphere. Evaluation of the ability of the hoods to capture pollutants at the point of generation is important in many inspections and engineering studies. The EPA defines fugitive emissions as "emissions that (1) escape capture by process equipment exhaust hoods; (2) are emitted during material transfer; (3) are emitted to the atmosphere from the source area; and (4) are emitted directly from process equipment."[3]

$$\text{Fugitive emissions} = \text{Total emissions} - \text{Emissions captured by hood} \tag{3-14}$$

$$\text{Stack emissions} = \text{Emissions captured by hood} \times \left(\frac{100\% - \eta}{100\%}\right) \tag{3-15}$$

Where:

η = Collection efficiency (%)

The importance of hood performance is illustrated by Problems 3-7 and 3-8, which are based on the simplified industrial process shown in Figure 3-15. This system consists of a process unit that generates pollutants, several hoods surrounding the process equipment, the ductwork, an air pollution control device, a fan, and a stack.

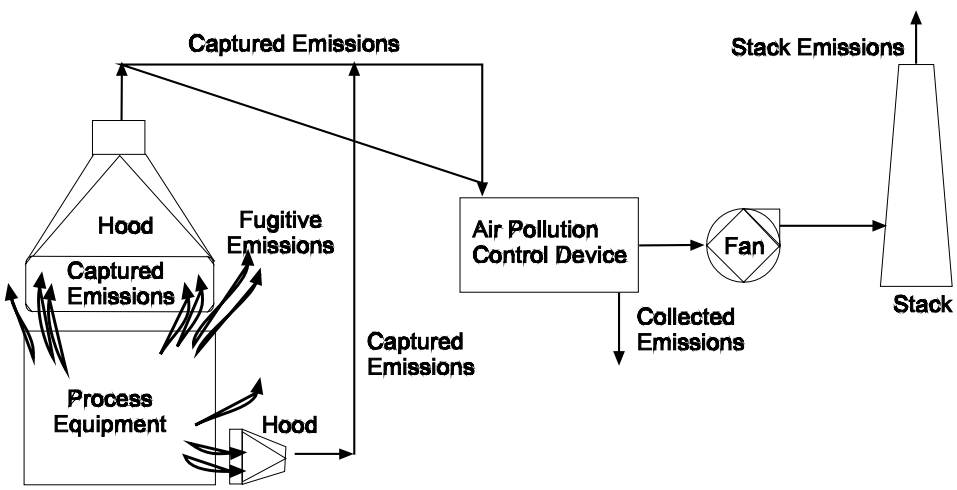

Figure 3-15. Role of hoods in an industrial process

Problem 3-7

Calculate the fugitive emissions and the stack emissions if the process equipment generates 100 lb_m/hr of volatile organic compounds (VOCs), the hood capture efficiency is 95%, and the collection efficiency of the air pollution control device is 95%.

Solution:

1. Calculate fugitive emissions.

Fugitive emissions = Total emissions - Emissions captured by hood

= 100 lb_m/hr-95 lb_m/hr = 5 lb_m/hr

2. Calculate stack emissions.

$$\text{Stack emissions} = \text{Emissions captured by hood} \times \left(\frac{100\% - \eta}{100\%}\right)$$

Where:

η = Collection efficiency

$$\text{Stack emissions} = (95\ \text{lb}_m/\text{hr})\frac{(100\% - 95\%)}{100\%}$$
$$= 4.75\ \text{lb}_m/\text{hr}$$

The capture of fugitive emissions is the key step in an air pollution control system. It is crucial that all the fugitive emissions are captured and transported to the air pollution control device. Problem 3 shows that even with hood capture efficiencies approaching 100%, fugitive emissions can be higher than emissions leaving the stack.

Problem 3-8

Calculate the stack emissions and fugitive emissions if the process equipment generates 100 lb_m/hr of VOCs, the hood capture efficiency is 90%, and the collection efficiency of the air pollution control device is 95%.

Solution:

Fugitive emissions = 100 lb_m/hr-90 lb_m/hr = 10 lb_m/hr

$$\text{Stack emissions} = \frac{(100\% - 95\%)}{100\%}(90\ \text{lb}_m/\text{hr}) = 4.5\ \text{lb}_m/\text{hr}$$

These two problems illustrate the importance of hoods. Slight changes in the ability of the hood to capture the pollutants can have a large impact on the total fugitive and stack emissions released into the atmosphere.

Unfortunately, it is not always possible to see the fugitive emissions. Gaseous and vapor emissions such as carbon monoxide, sulfur dioxide, hydrogen chloride, and nitric oxide are not visible. Even particulate emissions may be hard to see under the following circumstances:

- If there are numerous small fugitive sites
- If there is one major site that cannot be seen from normal areas accessible to personnel
- If the particulate matter is not in the size range that causes light scattering

Techniques for monitoring hood capture effectiveness are important because the quantities of fugitive emissions can be high, and these emissions are often hard to see.

3.3.1 Hood Operating Principles

Hoods are generally designed to operate under negative pressure. The air is drawn into the hood due to static pressures that are lower inside the hood than those in the process equipment and the surrounding air. Since air from all directions moves toward the low-pressure hood, the hood must be as close as possible to the process equipment in order to capture the pollutant-laden air and not just the surrounding air. At approximately one-hood-diameter away from the hood entrance, the gas velocities are often less than 10% of the velocity at the hood entrance. Figure 3-16 illustrates how quickly the gas velocity decreases as distance from the hood increases.

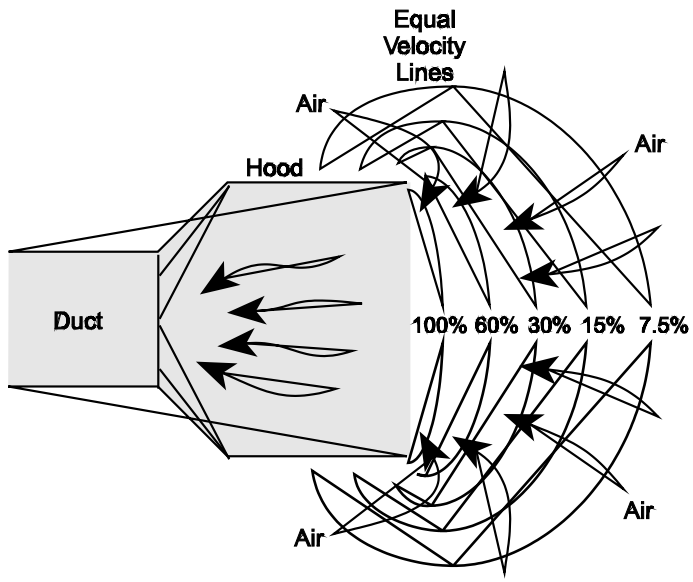

Figure 3-16. Hood capture velocities

Figure 3-16 indicates that the hood has very little influence on gas flow except in the area very close to the hood entrance. In order to ensure good capture of the pollutant-laden gas streams, the hood must be close to the emission source. The capture velocity of a hood is defined as *the air velocity at any point in front of the hood or at the hood opening necessary to overcome opposing air currents and to capture the contaminated air at that point by pulling it into the hood.*[1]

The following examples show conditions that would help determine what part of the capture velocity range for a particular operation should be used, low end of the capture velocity range vs. upper end of the capture velocity range.[1]

- The surrounding air currents
  - Minimal room air currents vs. disturbing room air currents
- The level of toxicity of the pollutant to be captured
  - Nuisance value only vs. high toxicity
- The amount of pollutant
  - Intermittent (low production) vs. high production (heavy use)
- Area of the hood opening
  - Large hood (large air mass in motion) vs. small hood (local control only)

The following flow/capture velocity equation for a freely suspended hood without a flange demonstrates the importance of the proximity of the hood to the source.

$$Q = v_h(10X^2+A_h) \qquad (3\text{-}16)$$

Where:

Q = volumetric flow rate (ACFM)

X = distance from hood face to farthest point of contaminant release (ft)

v_h = hood capture velocity at distance X (ft/min)

A_h = area of hood opening (ft^2)

It should be noted that the correlation between distance, gas flow rate, and capture velocity should be used for *estimation purposes only* because the vacuum from a hood does not create equal velocity lines or points. Equation 3-16 is also limited to the distance (X) being less than or equal to 1.5 hood diameters.[1]

Problem 3-9

The recommended capture velocity for a certain pollutant is 300 fpm entering a 16-inch diameter hood. What is the required volumetric flow rate and capture velocity for the following distances from the hood face (X)? Assume X is the farthest distance from the hood face to the emission source.

A. X = 12 in. (75% of hood diameter)

B. X = 24 in. (150% of hood diameter)

Solution:

Part A.

$$Q = v_h(10X^2+A_h)$$

1. Calculate the area of the hood opening.

$$\text{Area} = \frac{\pi D^2}{4}$$
$$= \frac{3.14(16\text{ in.})^2}{4} = 201\text{ in.}^2$$

2. Calculate the volumetric flow rate, Q, required to obtain the recommended capture velocity of 300 fpm at a distance of 12 inches from the hood.

$$Q = \frac{300\text{ ft}}{\text{min}}\left[10(1\text{ ft})^2 + (201\text{ in.}^2)\left(\frac{1\text{ ft}^2}{144\text{ in.}^2}\right)\right]$$
$$= 3{,}419\text{ ACFM}$$

Solution:

Part B.

$$Q = v_h(10X^2 + A_h)$$

1. Calculate the volumetric flow rate, Q, required to obtain the recommended capture velocity of 300 fpm at a distance of 24 inches from the hood.

$$Q = \frac{300\text{ ft}}{\text{min}}\left[10(2\text{ ft})^2 + (201\text{ in.}^2)\left(\frac{1\text{ ft}^2}{144\text{ in.}^2}\right)\right]$$
$$= 12{,}419\text{ ACFM}$$

The volumetric flow rate requirements increased approximately <u>four times</u> when the distance between the hood and the contaminant source <u>doubled</u>.

The capture velocity equations for a variety of hoods with different locations and arrangements can be obtained from the ACGIH, *Industrial Ventilation Manual*, 23rd edition.

Hood Designs for Improved Performance

There are many ways to design hoods to improve capture effectiveness. When the pollutant-laden gas stream is hot, the hood is often positioned above the point of pollutant release to take advantage of the buoyancy of the low-density hot gas stream.

Side baffles or **flanges** can be used to block the movement of clean air into the hood. The possible beneficial effect of side baffles on the gas velocities near the hood entrance is shown in Figure 3-17.

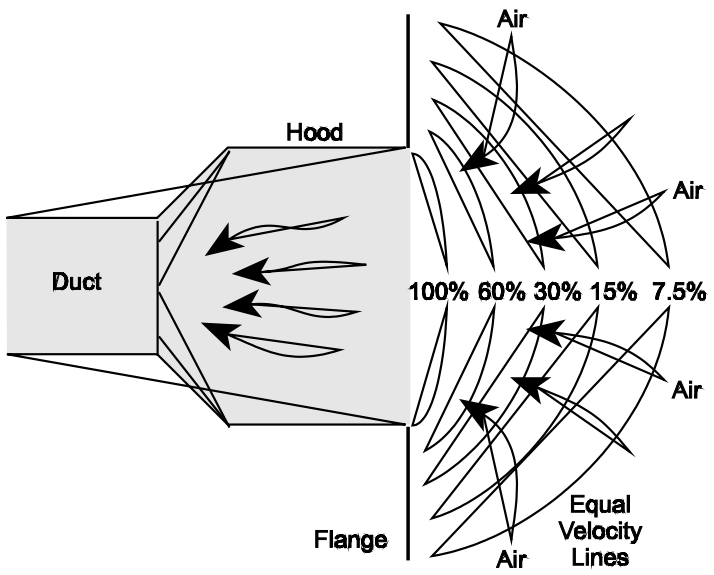

Figure 3-17. Beneficial effect of side baffles on hood capture velocities

Hood capture is greatly improved when the enclosure comprised of the hood and the side baffles can encompass the point of pollutant generation. These side baffles can be in the form of metal sheets, strips of fabric or plastic, or any other materials that block the movement of clean air into the low-pressure area of the hood. In addition to reducing the unintentional capture of clean air, these side baffles prevent cross drafts, which can prevent the intended movement of the pollutant-laden gas into the hood. The recommended width of a flange for most situations should be equal to the square root of the hood area.

Some process equipment inherently creates an entirely enclosed area for pollutant-laden gas capture. For example, coal-fired boilers generate pollutants in an enclosed furnace area that is maintained at a slightly negative static pressure of -0.05 to -0.25 in. W.C. In this case, the boiler walls serve as the hood.

Another hood design that is used to improve capture effectiveness is called the **push-pull hood**. As shown in Figure 3-18, a high-velocity clean air stream is blown across the area of pollutant generation into the hood on the opposite side.

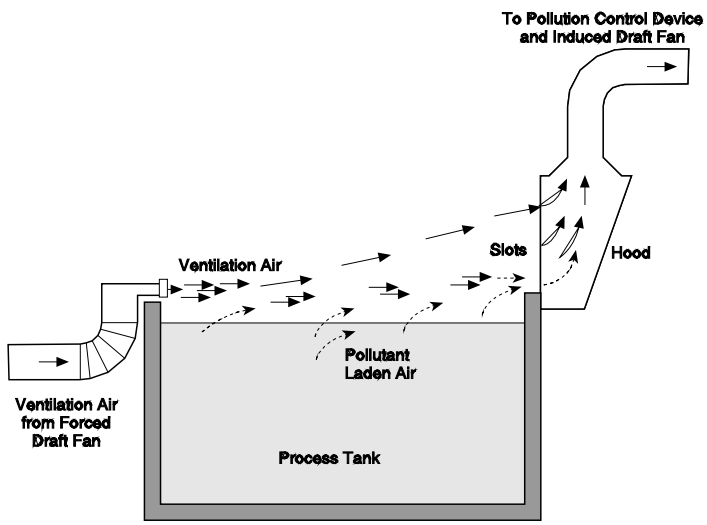

Figure 3-18. Push-pull hood

The high-velocity gas stream does not inherently disperse rapidly. Therefore, it flows toward the hood and is captured. The hood also effectively captures the pollutant-laden gas that is trapped in this strong cross draft. These types of hoods are sometimes used on open tanks and other sources where access from the top is necessary in order to operate the equipment. However, they may not be appropriate for tanks and other processes handling materials where the cross draft could significantly increase the quantities vaporized. Push-pull hoods can provide very high capture efficiencies where they are applicable.

3.3.2 Monitoring Hood Capture Effectiveness

There are several effective ways to confirm that the hood capture effectiveness has not decreased since it was installed or tested. Visible emission observations for fugitive emissions should be conducted in the case of particulate sources. In general, you should confirm that the hood has not been moved away from the point of pollutant generation and that side baffles and other equipment necessary to maintain good operation have not be damaged or removed.

The hood static pressure should be monitored to ensure that the appropriate gas flow rate is being maintained. The *hood static pressure* is simply the static pressure in the duct immediately downstream from the hood. This static pressure is entirely dependent on the hood geometry and the gas flow rate. As long as the hood has not been damaged or altered, the hood static pressure provides an indirect, but relatively accurate measurement of the gas flow rate. As indicated in Equation 3-17, the hood static pressure is determined by (1) the velocity pressure in the duct from the hood and (2) the hood entry loss. The loss of pressure caused by airflow moving into a system is referred to as entry loss.

$$SP_h = -(VP_d) - h_e \tag{3-17}$$

Where:

SP_h = hood static pressure (in. W.C.)

VP_d = duct velocity pressure (in. W.C.)

h_e = overall hood entry loss (in. W.C.)

$$h_e = (F_h)(VP_d) \tag{3-18}$$

Where:

F_h = hood entry loss coefficient (dimensionless)
VP_d = duct velocity pressure (in. W.C.)

The hood entry loss term is calculated using the coefficient of entry, F_h, which is tabulated in standard texts concerning hoods and ventilation systems.

$$SP_h = -(VP_d) - (F_h)(VP_d) \tag{3-19}$$

Where:

SP_h = hood static pressure (in. W.C.)
VP_d = duct velocity pressure (in. W.C.)
F_h = hood entry loss coefficient (dimensionless)

The velocity pressure term in Equation 3-18 is due to the energy necessary to accelerate the air from zero velocity to the velocity in the duct.

When air enters a negative pressure duct, the airflow converges as shown in Figures 3-19 through 3-21. The area where air converges upon entering a duct is referred to as *vena contracta*. After the vena contracta, the airflow expands to fill the duct and some of the velocity pressure converts to static pressure. The vena contracta is dependent on the hood geometry, which determines the resistance to airflow entering the hood.

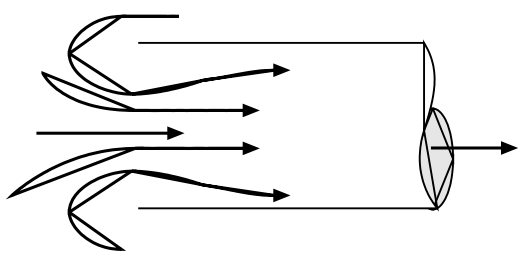

Figure 3-19. Plain duct end with a hood entry loss coefficient of 0.93

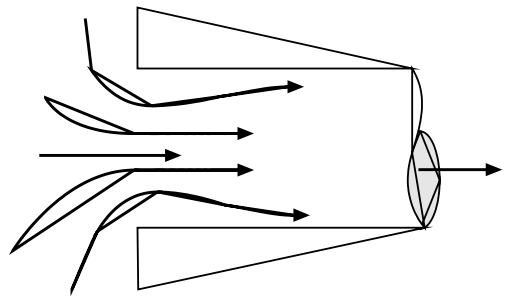

Figure 3-20. Flanged opening with a hood entry loss coefficient of 0.49

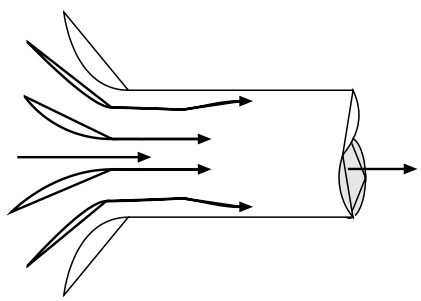

Figure 3-21. Bell-mouth inlet with a hood entry loss coefficient of 0.04

The velocity pressure is related to (1) the square of the velocity of the gas stream in the duct and (2) the gas density. The velocity pressure is calculated using Equation 3-20.

$$VP_d = \left(\frac{v}{4005}\right)^2 \frac{\rho_{Actual}}{\rho_{Standard}} \tag{3-20}$$

Where:

VP_d = velocity pressure of duct (in. W.C.)

v = gas velocity (ft/min)

$_{Actual}$ = density at actual conditions (lb_m/ft^3)

$_{Standard}$ = density at standard conditions (lb_m/ft^3)

$$VP_d = \left(\frac{v}{4005}\right)^2 \frac{\rho_{Actual}}{0.075\,lb_m}/ft^3$$

As the gas flow rate into the hood increases, the hood static pressure increases (see Figure 3-22). In this figure, a hood with an entry loss coefficient (F_h) of 0.49 has been assumed in evaluating the gas flow rate versus hood static pressure curve.

The hood static pressure can be measured by relatively simple gauges such as water-filled manometers and Magnehelic® gauges. The normal range of hood static pressures is -0.2 to -2.0 in. W.C.

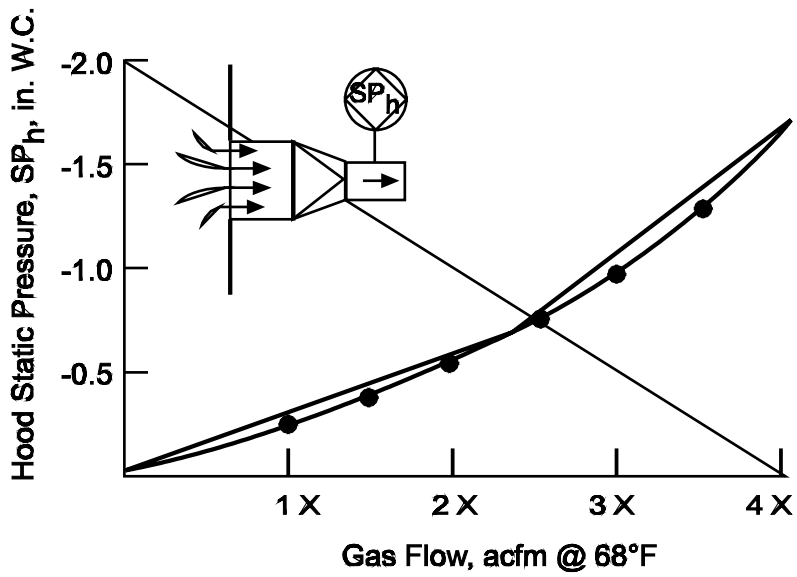

Figure 3- 22. Relationship between hood static pressure and flow rate

A decrease in hood static pressure (i.e., a less negative value), corrected for gas density changes, usually indicates that the gas flow rate entering the hood has decreased from previous levels. This may reduce the effectiveness of the hood by reducing the capture velocities at the hood entrance.

Problem 3-10

A hood serving a paint dipping operation has a hood static pressure of -1.10 in. W.C. The baseline hood static pressure was -1.70 in. W.C. Estimate the gas flow rate under the following two conditions:

A. At present operating conditions

B. At baseline levels

Use the data provided below:

Hood F_h = 0.93

Baseline air temperature = 68°F

Duct diameter = 2 ft (inside diameter)

Solution:

Part A.

Step 1. Calculate the gas velocity and flow rate at present conditions.

1. Calculate the velocity pressure (VP) using the following equation.

$$SP_h = -(VP_d) - h_e$$

Calculate the value for the hood entry loss, h_e, as follows.

$$h_e = (F_h)(VP_d)$$
$$= (0.93)(VP_d)$$

$$SP_h = -VP_d - 0.93(VP_d) = -1.93(VP_d)$$

Given: SP_h = -1.10 in. W.C.

$$-1.1 \text{ in. W.C.} = -1.93(VP_d)$$

$$VP_d = \frac{-1.1 \text{ in. W.C.}}{-1.93} = 0.57 \text{ in. W.C.}$$

2. Calculate the gas velocity using a variation of Equation 3-19 at standard conditions $_{Actual}$ = 0.075 lb_m/ft^3.)

$$v = 4005\sqrt{VP}$$

$$v = 4005\sqrt{0.57}$$
$$v = 3{,}024 \text{ ft/min}$$

3. Calculate the gas flow rate as follows:

Flow rate = Velocity × Area of duct

$$\text{Area of duct} = \frac{\pi D^2}{4}$$
$$= \frac{3.14(2\text{ft})^2}{4}$$
$$= 3.14 \text{ ft}^2$$

$$\text{Flow rate} = 3{,}024 \text{ ft/min } (3.14 \text{ ft}^2) = 9{,}495 \text{ ACFM}$$

Solution:

Part B.

Step 1. Calculate the gas flow rate at baseline conditions.

1. Calculate the velocity pressure using the following.

$$SP_h = -(VP_d) - h_e$$

$$SP_h = -(VP_d) - (0.93)(VP_d)$$
$$= -(VP_d) - 0.93\,VP_d = -1.93(VP_d)$$

Given: $SP_h = -1.7$ in. W.C.

$$-1.7 \text{ in. W.C.} = -1.93(VP_d)$$

$$VP_d = 0.88 \text{ in. W.C.}$$

2. Calculate the gas velocity using a variation of Equation 3-19 at standard conditions

$\rho_{Actual} = 0.075 \quad lb_m/ft^3$

$$v = 4005\sqrt{VP}$$

$$v = 4005\sqrt{0.88}$$

$$v = 3{,}757 \text{ ft/min}$$

3. Calculate the gas flow rate. The duct area was calculated in Part A.

$$\begin{aligned}\text{Flow rate} &= \text{Velocity} \times \text{Area}\\ &= 3{,}757 \text{ ft/min} \times (3.14 \text{ ft}^2)\\ &= 11{,}797 \text{ ACFM}\end{aligned}$$

The change in hood static pressure from -1.7 in. W.C. to -1.1 in. W.C. indicates a drop in the gas flow rate from 11,797 ACFM to 9,495 ACFM. This is a 20% decrease in the gas flow rate.

Flow / Capture Velocity Equation

The flow / capture velocity equation that was used in Problem 3-9 can be modified to determine the gas flow rate with different hood designs. A hood with a wide flange would use the following equation:

$$Q = v_h(0.75)(10X^2 + A_h) \tag{3-21}$$

Using the information given in Problem 3-9 (Part A)

Calculate the volumetric flow rate, Q, required to obtain the recommended capture velocity of 300 fpm at a distance of 12 inches from the hood.

$$\begin{aligned}Q &= \frac{300 \text{ ft}}{\text{min}}(0.75)\left[10(1 \text{ ft})^2 + (201 \text{ in.}^2)\left(\frac{1 \text{ ft}^2}{144 \text{ in.}^2}\right)\right]\\ &= 2{,}564 \text{ ACFM}\end{aligned}$$

The volumetric flow requirements decreased by approximately 25% when a flanged hood was used.

Transport Velocity

When the contaminant is captured by the hood system and enters the ductwork, a minimum transport velocity must be maintained to keep the contaminant from settling out of the gas flow stream and building up deposits in the ductwork. The minimum transport velocity is particularly important when handling particulate-laden gas streams. If the minimum transport velocity is not maintained in the ductwork, then the particulate matter will settle out in the ductwork due to decreased flow rate. This will lead to

decreased hood capture efficiencies and increased fugitive emissions. Systems with heavy particulate-laden gas streams should have clean-out ports installed to remove particulate that has settled out.

$$v = \frac{Q}{A} \tag{3-22}$$

Where:

v = gas velocity (ft/min)

Q = volumetric gas flow rate (ACFM)

A = cross-sectional area of duct or equipment (ft^2)

The proper duct diameter is a key element when addressing minimum transport velocity. If a section of ductwork has a larger than necessary diameter, then settling out will most likely occur. If a section of ductwork is too small, the pressure drop will increase across this section, thus requiring the fan to handle more static pressure. Another concern when dealing with transport velocities is the abrasion of the ductwork, especially of the bends or elbows. The amount of abrasion that occurs is dependent upon several factors: the duct velocity, the amount and type of particulate in the gas stream, and the construction of the ductwork.

Minimum transport velocities for different types of particulate matter can be obtained from standard texts concerning hoods and ventilation systems. Examples of transport velocities are listed below.

Table 3-11. Commonly Recommended Transport Velocity

Type of Pollutant	Transport Velocity
Gaseous Gases	~1000 – 2000ft/min
Light Particulate Loading	~3000 – 3500ft/min
Normal Particulate Loading	~3500 – 4500ft/min

Problem 3-11

Transport Velocity

A duct system transporting a very light dust requires a minimum transport velocity of 2,800 ft/min. The volumetric flow rate for the system is 978 ACFM. What is the necessary duct diameter in inches for this section of ductwork to maintain the minimum transport velocity?

Given: Minimum transport velocity = 2,800 ft/min
Volumetric flow rate = 978 ACFM

Solution:

Step 1. Calculate the duct area.

1. Calculate the duct area.

$$\text{Duct area} = \frac{\text{Gas flow rate, actual}}{\text{Gas velocity}}$$
$$= \frac{978\ \text{ft}^3/\text{min}}{2800\ \text{ft/min}}$$
$$= 0.349\ \text{ft}^2$$

2. Calculate the duct diameter.

$$\text{Duct area} = \frac{\pi D^2}{4}$$
$$D^2 = \frac{4\left(0.349\ \text{ft}^2\right)}{3.14}$$
$$D = 8\ \text{in.}$$

Summary

Hoods are the first component of the air pollution control system and are of critical importance. If they fail to capture the pollutant, the overall collection efficiency of the system is reduced. Pollutants not captured by hoods become fugitive emissions. Many factors affect a hood's capture efficiency; however, one of the key factors is the distance between the pollutant source and the hood.

The geometry of a hood opening influences the hood entry loss coefficient and the hood static pressure due to the formation of the vena contracta. Comparing the hood static pressure against baseline condition provides a good indicator if the system has developed any problems.

Maintaining a system's minimum transport velocity is necessary to ensure that all of the captured pollutant reaches the air pollution control device and to prevent build-up of the pollutants in the ductwork.

3.4 FANS

Fans are the heart of the system. They control the gas flow rate at the point of pollutant generation in the process equipment and through the air pollution control devices. Fans provide the necessary energy for the gas stream to overcome the resistance to gas flow caused by the ductwork and air pollution control devices. Data concerning fan performance is important during inspections and all other technical evaluations of system performance.

3.4.1 Types of Fans and Fan Components

There are two main types of fans: axial and centrifugal. Most fans used in air pollution control systems are centrifugal fans.

An axial fan is shown in Figure 3-23. The term, axial, refers to the use of a set of fan blades mounted on a rotating shaft. A standard house ventilation fan is an axial fan.

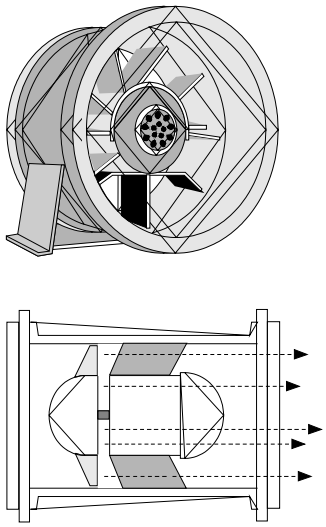

A. Axial Fan

Figure 3-23. Axial fans

A centrifugal fan has a fan wheel composed of a number of fan blades mounted around a hub. As shown in Figure 3-24, the hub turns on a shaft that passes through the fan housing. The gas enters from the side of the fan wheel, turns 90° and is accelerated as it passes over the fan blades. The term, centrifugal, refers to the trajectory of the gas stream as it passes out of the fan housing.

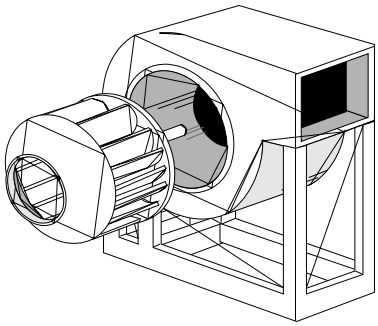

B. Centrifugal Fan

Figure 3-24. Centrifugal fan components

Centrifugal fans can generate high-pressure rises in the gas stream. Accordingly, they are well-suited for industrial processes and air pollution control systems. The remainder of this section concerns centrifugal fans.

The major components of a typical centrifugal fan include the fan wheel, fan housing, drive mechanism, and inlet dampers and/or outlet dampers. A wide variety of fan designs serve different applications.

The fan drive determines the speed of the fan wheel and the extent to which this speed can be varied. The types of fan drives can be grouped into three basic categories:

1. Direct drive
2. Belt drive
3. Variable drive

In a **direct drive** arrangement, the fan wheel is linked directly to the shaft of the motor. This means that the fan wheel speed is identical to the motor rotational speed. With this type of fan drive, the fan speed cannot be varied.

Belt driven fans use multiple belts which rotate in a set of sheaves mounted on the motor shaft and the fan wheel shaft. This type of drive mechanism is illustrated in Figure 3-25.

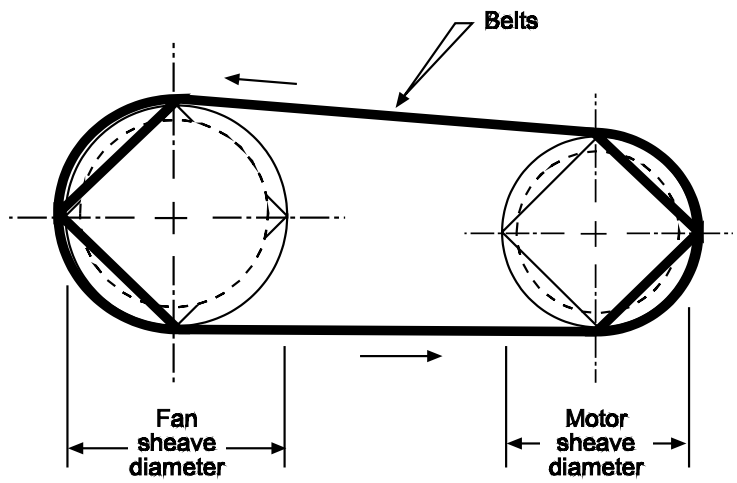

Figure 3-25. Centrifugal fan and motor sheaves

The belts transmit the mechanical energy from the motor to the fan. The fan wheel speed is simply the ratio of the fan wheel sheave diameter to the motor sheave diameter as indicated in Equation 3-23.

$$RPM_{(Fan)} = RPM_{(Motor)} \frac{D_{(Motor)}}{D_{(Fan)}} \tag{3-23}$$

Where:

$RPM_{(Fan)}$ = Fan speed (revolutions per minute)

$RPM_{(Motor)}$ = Motor speed (revolutions per minute)

$D_{(Fan)}$ = Diameter of fan sheave (inches)

$D_{(Motor)}$ = Diameter of motor sheave (inches)

Fan wheel speeds in belt-driven arrangements are fixed unless the belts slip. Belt slippage normally reduces fan wheel speed several hundred rpm and creates a noticeable squeal. If it is necessary to change the fan wheel speed in a belt-driven arrangement, the motor and/or fan wheel sheaves must be replaced with units having different diameters. However, there are very definite safety limits to the extent to which the fan speed can be increased. If the fan rotational speed is excessive, the fan can disintegrate.

Variable speed fans use hydraulic or magnetic couplings that allow operator control of the fan wheel speed independent of the motor speed. The fan speed controls are often integrated into automated systems to maintain the desired fan performance over a variety of process operating conditions.

Fan dampers are used to control gas flow into and out of the centrifugal fan. These dampers can be on the inlet side and/or on the outlet side of the fan. Dampers on the outlet side simply impose a flow resistance that is used to control gas flow. Dampers on the inlet side are designed to control gas flow and to change how the gas enters the fan wheel at different operating conditions. Inlet dampers conserve fan energy due to their ability to affect the airflow pattern into the fan.

The fan wheel consists of a hub and a number of fan blades. The fan blades on the hub can be arranged in three different ways:

- Forward
- Backward
- Radial

Forward-curved fans (Figure 3-26a) use blades that curve toward the direction of rotation of the fan wheel. These are especially sensitive to particulate and are not used extensively in air pollution control systems.

Backward-curved fan blades (Figure 3-26b) use a straight plate, a curved plate, or a curved airfoil. These types of fan wheels are used in fans designed to handle gas streams with relatively low particulate loadings because they are prone to solids build-up. Backward-curved fans are more energy efficient than radial blade fans.

Radial blades are fan wheel blades that extend straight out from the hub. A radial blade fan wheel, as shown in (Figure 3-26c), is often used on particulate-laden gas streams because it is the least sensitive to solids build-up on the blades.

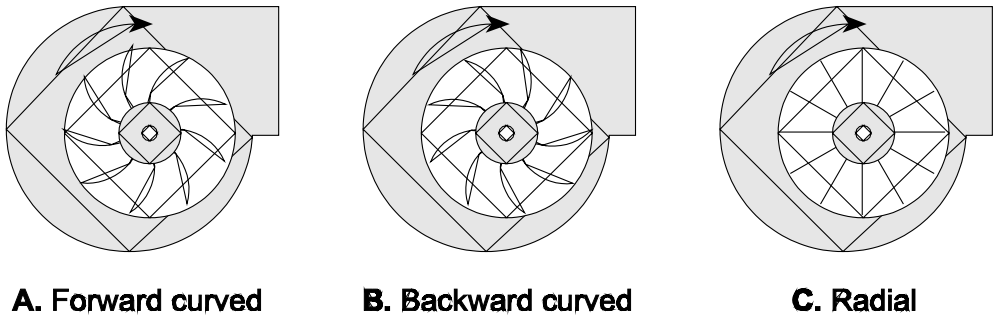

Figure 3-26. Types of fan wheels

3.4.2 Centrifugal Fan Operating Principles

A basic understanding of fan operating principles is necessary to evaluate the performance of an industrial ventilation system. The fan operating speed is one of the most important operating variables. Most fans, such as the example radial blade centrifugal fan shown in Figure 3- 27, can operate over a modest range of speeds.

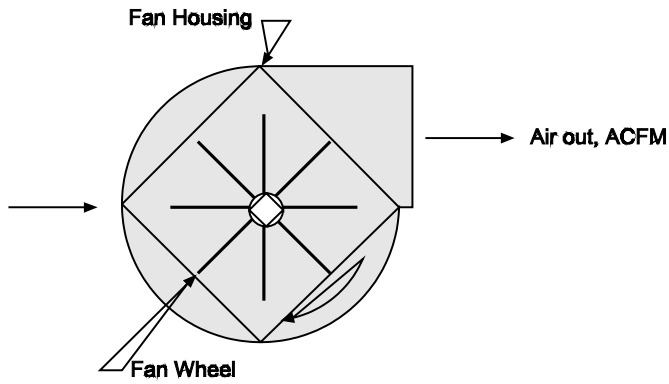

Figure 3-27. Centrifugal fan with radial blade

The flow rate of air moving through the fan depends on the fan wheel rotational speed. As the speed increases, the air flow rate increases as indicated in the example data in Table 3-12.

Table 3-12. Relationship Between Fan Speed and Air Flow Rate

Fan Wheel Speed	Air Flow Rate, ACFM
800	16,000
900	18,000
1000	20,000
1100	22,000
1200	24,000

It is important to recognize that a 10% decrease in fan speed results in a 10% decrease in the air flow rate through the ventilation system. This relationship is expressed as one of the major fan laws shown below as Equation 3-24.

$$Q_2 = Q_1(RPM_2/RPM_1) \quad (3\text{-}24)$$

Where:

Q_1 = Baseline air flow rate (ACFM)

Q_2 = Present air flow rate (ACFM)

RPM_1 = Baseline fan wheel rotational speed (revolutions per minute)

RPM_2 = Present fan wheel rotational speed (revolutions per minute)

The rate of air flow through a fan is always expressed in terms of ACFM. This is helpful because this value does not change regardless of the air density. In this respect, a fan is much like a shovel. It moves a specific amount of air per minute regardless of whether the air is dense cold air or light hot air.

The air stream moving through the fan has a static pressure rise due to the mechanical energy expended by the rotating fan wheel. As indicated in Figure 3-28, the static pressure at the outlet is always higher than the static pressure at the inlet. For the purposes of this course, the static pressure rise across the fan is denoted Fan ΔSP.

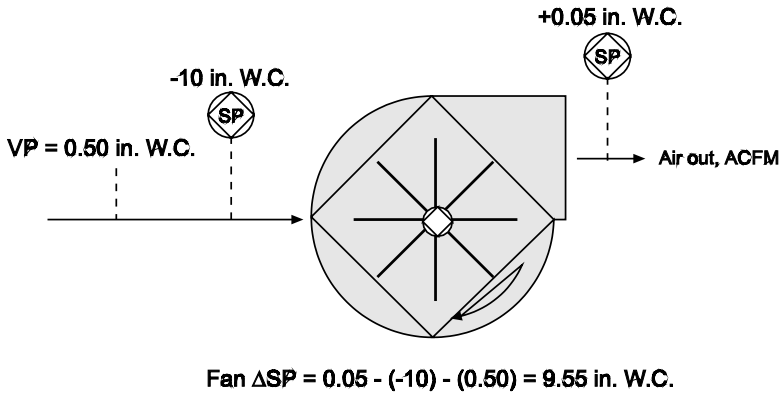

Figure 3-28. Fan static pressure rise

The Fan ΔSP is related to the square of the fan speed as indicated in the second fan law shown below as Equation 3-25. The fan static pressure rise is usually expressed in units of inches of water column (in. W.C.).

$$\text{Fan } \Delta SP_2 = \text{Fan } \Delta SP_1 (RPM_2/RPM_1)^2 \qquad (3\text{-}25)$$

Where:

ΔSP_1 = baseline fan static pressure rise (in. W.C.)

ΔSP_2 = present fan static pressure rise (in. W.C.)

RPM_1 = baseline fan wheel rotational speed (revolutions per minute)

RPM_2 = present fan wheel rotational speed (revolutions per minute)

The static pressure rise across the fan increase rapidly as the fan speed is increased. This is illustrated using example data shown in Table 3-13.

Table 3-13. Relationship Between Fan Speed and Fan Static Pressure Rise

Fan Wheel Speed	Fan ΔSP In. W.C.
800	5
900	5.6
1000	6.3
1100	6.9
1200	7.5

The specific fan for an industrial ventilation system must be selected based on the specific air flow rate and fan static pressure rise needed to properly capture, transport, and control the emissions. As indicated in the block type flowcharts introduced earlier in this chapter, each industrial ventilation system includes one or more capture hoods, ductwork, air pollution control systems, the fan, and a stack. The gas flow rate through the ventilation system must be sufficient to provide adequate pollutant capture at the hoods and to ensure proper transport of the pollutant-laden air to the air pollution control systems.

The fan static pressure rise must be sufficient to accelerate the air entering the hoods and to overcome the flow resistances of the hoods, ductwork, air pollution control systems, and stack at the prescribed hood, ductwork, and air pollution control system air flow velocities.

The changes in the air stream static pressure from the point of entry into the hood to the point of discharge from the stack are illustrated in Figure 3-29. This static pressure profile of the system is useful in illustrating the necessary fan static pressure rise.

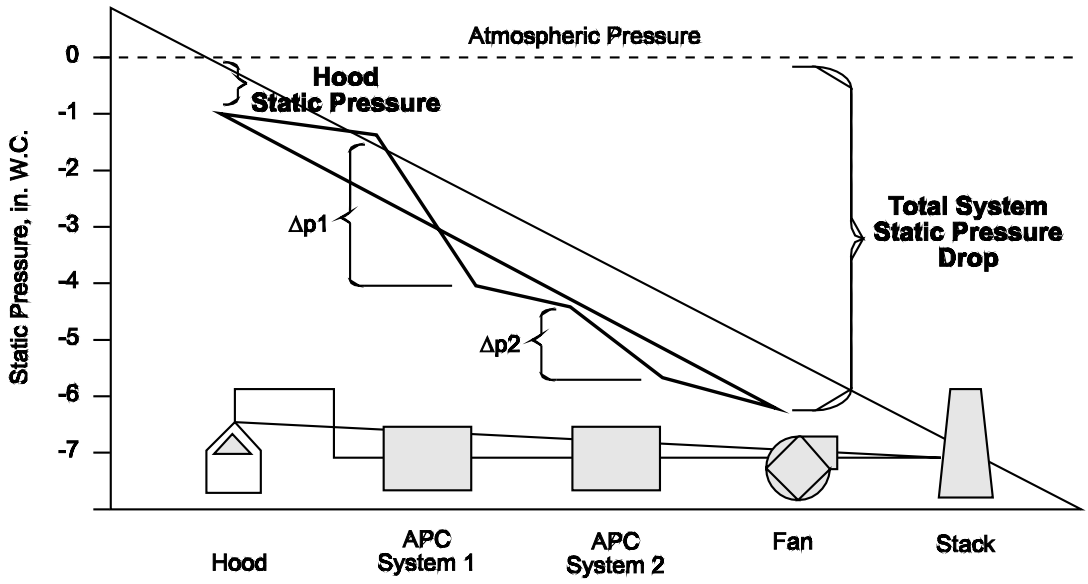

Figure 3-29. Total system static pressure drop

The designer of a system, such as the one shown at the bottom of Figure 3-29, starts by specifying the air velocities in the hoods, ductwork, air pollution control system, and stack. These velocities are selected based on established engineering design principles to ensure high efficiency hood capture, proper operation of the air pollution control systems, and proper dispersion of the effluent gas stream from the stack. The overall static pressure drop across each component of the overall system is related to the square of the air flow rate. This is illustrated in Figure 3-30.

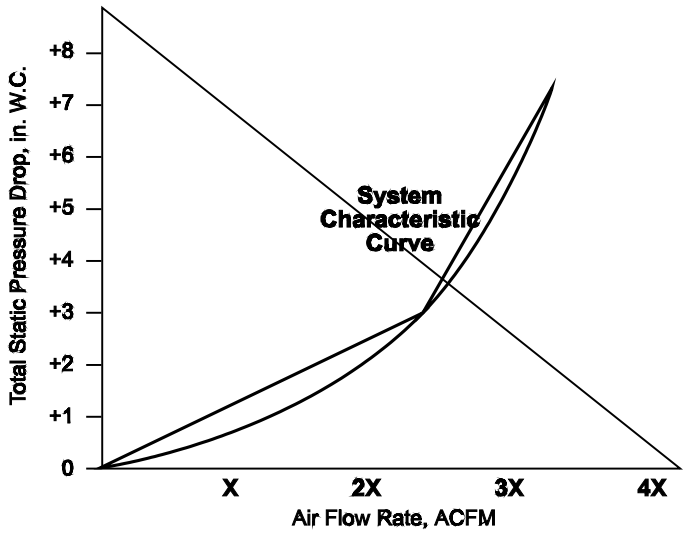

Figure 3-30. System characteristic curve

This general relationship between total system static pressure drop and air flow rate is term the system characteristic curve. For example, if the designer of the system needed 12,000 ACFM to achieve the necessary velocities in the system, he or she would know that the total static pressure drop across the system would be 10 in. W.C. Therefore, a fan would have to be found to generate an air flow of 12,000 ACFM at a fan static pressure rise of at least 10 in. W.C.

The use of the fan allows the air static pressure to be increased from the low level exiting the last air pollution control system, to a static pressure close to, or even slightly above ambient absolute pressure levels. This is illustrated in Figure 3-31 which is simply the completed version of the static pressure profile chart shown in Figure 3-29.

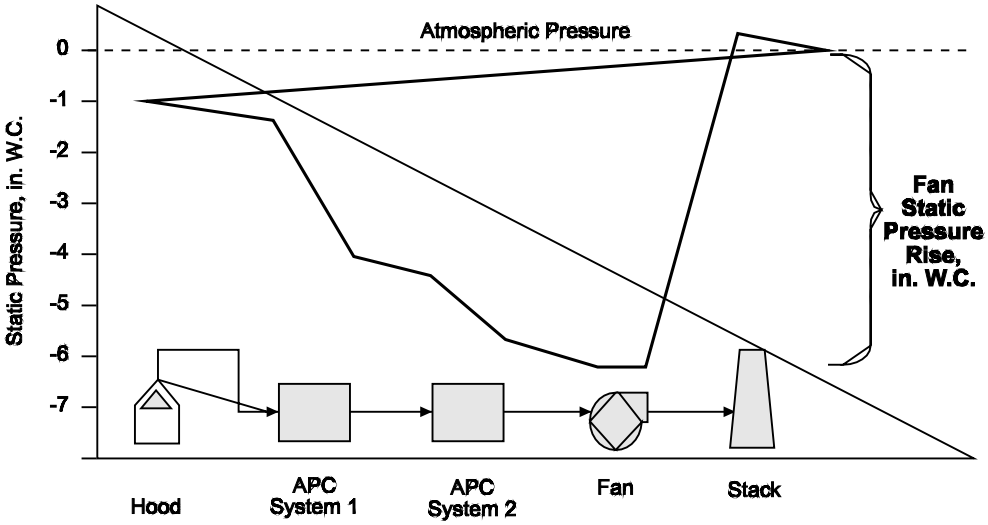

Figure 3-31. Fan static pressure rise profile

An appropriate fan is selected based on fan manufacturer's performance data. Usually, these data are provided in terms of multi-ratings tables published for each specific fan model and size. Based on these data it is possible to select a fan model, the specific model size, and the fan speed necessary to achieve the air flow rates and static pressure rise conditions necessary for the overall air pollution control system. An excerpt from a multi-rating table for a centrifugal fan is shown below in Figure 3-32.

194 LS

Inlet diameter: 11" O.D. | Wheel diameter: 19⅛"
Outlet area: .660 sq. ft. inside | Wheel circumference: 5.01 ft

CFM	OV	2"SP		4"SP		6"SP		8"SP		10"SP		12"SP		14"SP		16"SP		18"SP	
		RPM	BHP	RPM	BHP	RPM	BHP	RPM	BHP	RPM	BHP	RPM	BHP	RPM	BHP	RPM	BHP	RPM	BHP
660	1000	995	0.48	1392	1.01	1698	1.60	1960	2.27	2191	2.98	2399	3.74	2592	4.55	2769	5.38	2938	6.27
792	1200	1008	0.55	1398	1.11	1703	1.75	1962	2.45	2192	3.20	2398	3.99	2588	4.83	2767	5.71	2936	6.65
924	1400	1023	0.62	1405	1.23	1708	1.90	1965	2.64	2194	3.43	2401	4.27	2589	5.14	2766	6.05	2932	7.01
1056	1600	1042	0.71	1418	1.35	1716	2.07	1971	2.84	2197	3.67	2401	4.53	2593	5.46	2769	6.42	2935	7.41
1188	1800	1061	0.80	1431	1.49	1726	2.24	1980	3.06	2203	3.92	2407	4.83	2593	5.78	2771	6.79	2936	[illegible]
1320	2000	1084	0.90	1447	1.64	1739	2.44	1987	3.29	2209	4.19	2414	5.15	2600	6.13	2773	7.16	2940	[illegible]
1452	2200	1109	1.01	1465	1.80	1753	2.65	1999	3.54	2221	4.49	2422	5.47	2607	6.50	2778	7.55	2943	
1584	2400	1136	1.13	1485	1.98	1769	2.87	2012	3.80	2229	4.78	2431	5.82	2612	6.87	2786	7.98	2949	
1716	2600	1162	1.26	1505	2.16	1784	3.10	2025	4.08	2242	5.11	2441	6.18	2623	7.28	2791	8.40	2956	
1980	3000	1223	1.56	1554	2.58	1824	3.62	2059	4.70	2272	5.82	2464	6.95	2644	8.14	2815	9.38	2973	
2244	3400	1290	1.91	1606	3.04	1867	4.19	2098	5.38	2305	6.59	2495	7.83	2671	9.09	2838	10.4	299[illegible]	
2508	3800	1361	2.33	1661	3.56	1917	4.84	2141	6.12	2345	7.44	2531	8.78	2703	10.1	2866	11.5	3[illegible]	
2772	4200	1439	2.83	1723	4.16	1968	5.54	2189	6.95	2387	8.37	2569	9.80	2740	11.3	2900	12.8	[illegible]	
3036	4600	1519	3.40	1788	4.84	2025	6.32	2239	7.85	2432	9.36	2611	10.9	2780	12.5	2937	14.1		
3300	5000	1603	4.07	1855	5.58	2086	7.20	2294	8.83	2483	10.5	2660	12.1	2825	13.8	2978	15.5		
3564	5400	1691	4.84	1929	6.45	2148	8.14	2350	9.88	2536	11.6	2708	13.4	2869	15.2	3024	17.0		
3828	5800	1781	5.73	2005	7.41	2214	9.18	2409	11.0	2591	12.9	2759	14.8	2917	16.7	3069	18[illegible]		

Figure 3-32. Portion of a typical multi-rating table.
(Reprinted courtesy of The New York Blower Company)

The match between the fan performance data and the system characteristic curve is illustrated in Figure 3-33 for the specific fan rotational speed chosen. As long as the overall system remains in good condition and the fan remains in good condition, the system will operate at the point shown in Figure 3-33. This is termed the *operating point*.

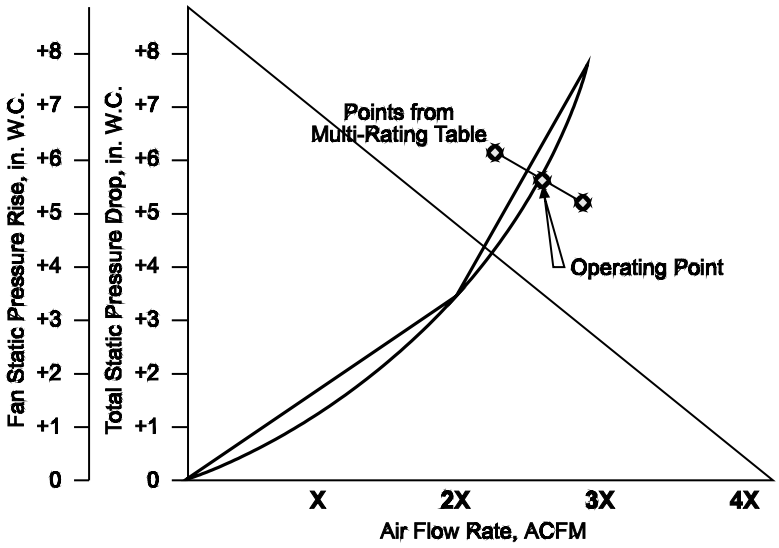

Figure 3-33. Operating point

When the total system static pressure drop and the fan static pressure rise are shown on the same graph, as in the case with Figure 3-33, it is convenient to simply delete the total system static pressure drop axis.

Figure 3-34 illustrates an example fan curve for a given fan speed. The multi-rating data used to select the fan represented a subset of the total data set that defines this fan curve. There is a specific fan curve for each fan model, model size, and speed. The intersection of the fan curve and the system characteristic curve is illustrated as Point A. This is the point that was determined previously by the system designer selecting the fan.

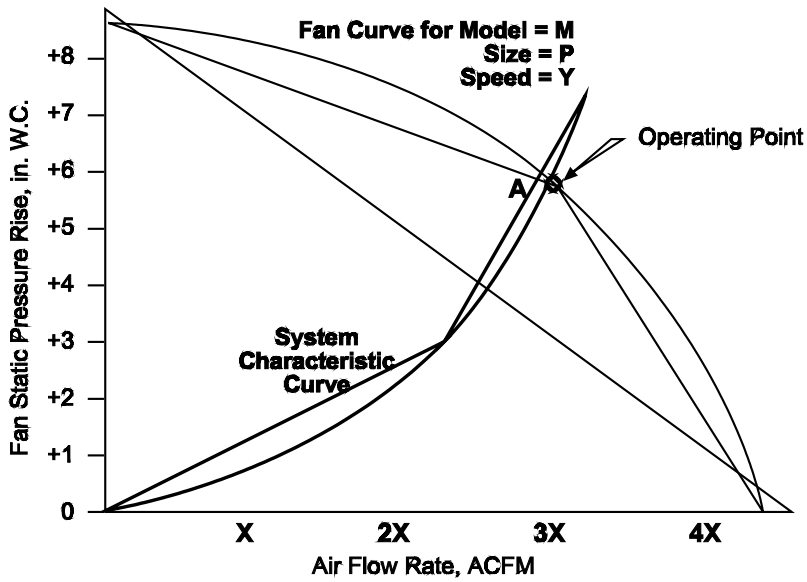

Figure 3-34. Fan characteristic curve

Air pollution control systems and other types of industrial ventilation systems, however, do not necessarily remain exactly at the conditions anticipated by the system designer and the fan manufacturer. A number of normal operating changes and operating problems can cause changes in the overall system air flow rates and the static pressure rises across the fan. The extent of the air flow and static pressure rise changes depend on the fan's performance conditions and the system characteristic curve. Some of these changes are illustrated in Figures 3-35 through 3-37.

If the gas flow resistance increases due to the build-up of dust in an air pollution control device or because a damper is closed, the system characteristic curve will shift upwards as indicated in Figure 3-35. With this increased gas flow resistance there will be a new operating point, labeled "B" in Figure 3-35. At this new operating point, the fan static pressure rise will be slightly higher while the air flow rate will be slightly lower.

If the air flow resistance decreases due to changes in an air pollution control device or opening of a damper, the system characteristic curve will shift downwards. This results in a new operating point (labeled "C") that has a slightly reduced fan static pressure and increased air flow rate.

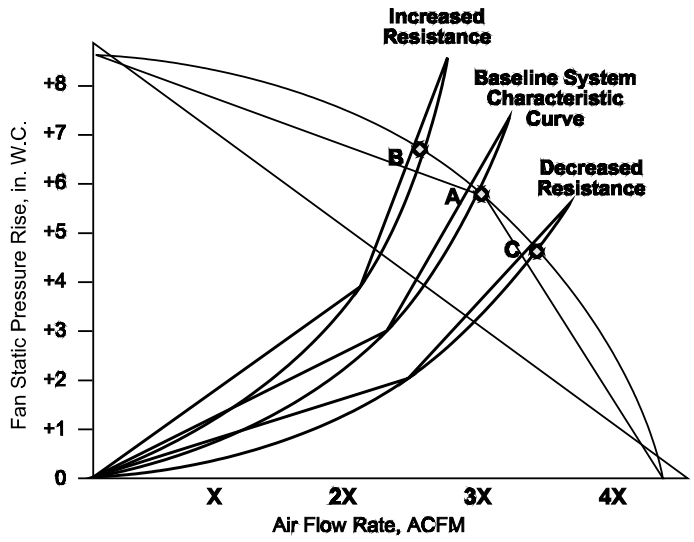

Figure 3-35. Changes in the system resistance curve

Some changes in the system characteristic curve are normal due to factor such as (1) air pollution control system cleaning cycles, (2) gradually increasing air infiltration between maintenance cycles, and (3) the opening and closing of individual dampers on individual process sources ducted into the overall ventilation system. The system must be designed to provide adequate pollutant capture even at the lowest normally occurring air flow rates.

When changes in the system characteristic curve are outside of the anticipated range, operators often have the option of modifying the fan to increase its capability. Most fans on industrial systems are selected to operate at a speed near the middle of its safe operating range. Slight increases in the fan speed can improve air flow rates and static pressure rises without exceeding the safe operating speed limits. The impact of a slight increase in the fan speed is illustrated in Figure 3-36.

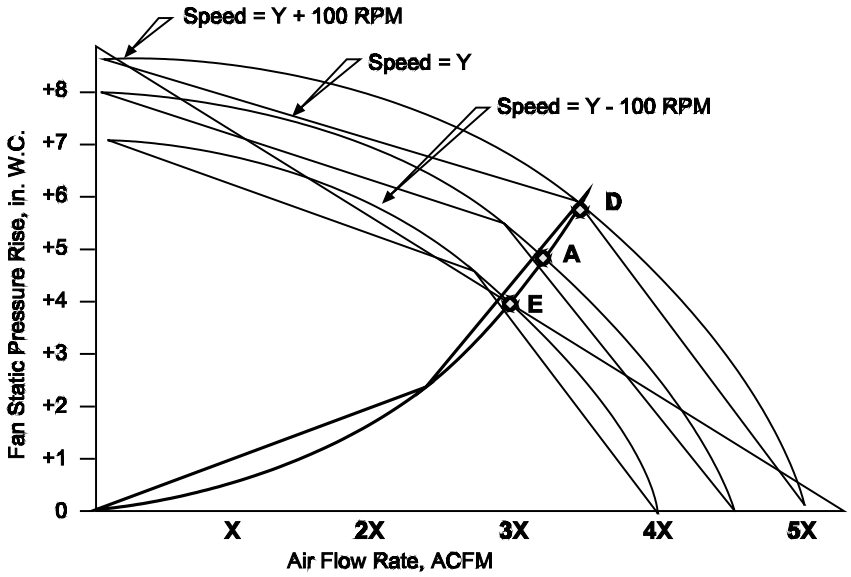

Figure 3-36. Changes in the fan speed

It is apparent that the increased fan speed results in a new operating point (labeled "D") having an air flow rate and fan static pressure rise that are both larger than the conditions represented by operating point "A." Not all fans can be easily adjusted to change the fan speed. For example, direct drive fans where the fan wheel shaft is directly driven by the fan motor operate only at the motor rotation speed and can not be adjusted. Belt driven fans can be adjusted but only by changing one or both of the sheaves on the fan and motor. Some large fans with hydraulic or magnetic drives have easily adjusted fan speeds.

Some inadvertent reductions in fan speed are possible for belt driven fans. If the drive belts become slightly loose, they can slip as they move across the sheaves. This often results in a decreased air flow rate of 100 to 200 rpm. The decrease in the air flow rate is directly proportional to the decrease in the fan speed.

The operating point of a system can also be changed due to the opening and closing of a fan inlet damper. This is a special damper mounted immediately ahead of the fan and this damper changes how air enters fan wheel. Changes caused by the opening and closing of a fan inlet damper are illustrated in Figure 3-37. It is apparent that the operating point changes to lower air flow rates and fan static pressure rises as the inlet damper is closed.

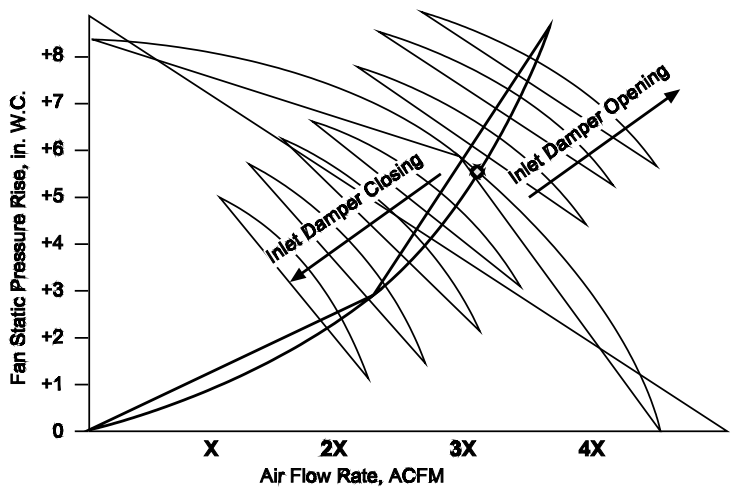

Figure 3-37. Changes in the inlet damper position

The fan inlet damper is often used to ensure safe opening of a fan that operates with air streams at elevated gas temperatures. During start-up when the air is cold, the fan inlet damper is kept partially closed to minimize the quantity of heavy cold air moved through the system. As the air heats and becomes less dense, the fan inlet damper opens to increase the air flow rate and fan static pressure rise. This approach minimizes the electrical power demand on the fan motor. Starting with the fan inlet dampers wide open would often exceed the safe current levels for the motor and thereby result in burnout of the motor windings. It is very important to avoid overloading fan motor currents.

Problem 3-12

A portion of a ventilation system is shown in Figure 38. The static pressure drop across the system measured at the fan inlet is -16.5 in. W.C. at a gas flow rate of 8,000 ACFM. Estimate the static pressure drop if the flow rate increased to 12,000 ACFM.

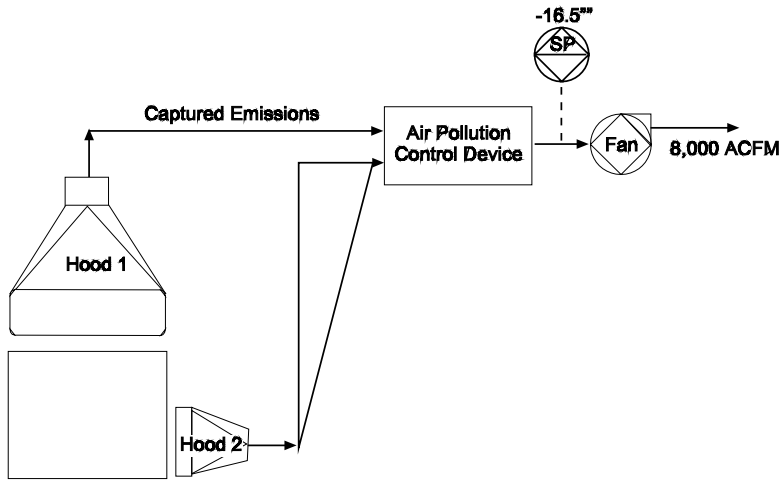

Figure 3-38. Portion of a ventilation system

Solution:

$$\frac{SP_{@\,High\ flow}}{SP_{@\,Low\ flow}} = \frac{(12{,}000\ ACFM)^2}{(8{,}000\ ACFM)^2} = 2.25$$

$$SP_{@\,High\ flow} = SP_{@\,Low\ flow}(2.25)$$

$$= -16.5\,in.\ W.C.\,(2.25)$$

$$= -37.13\,in.\ W.C.$$

Note: This solution is based on the assumption that there are no significant changes in gas density due to the increase in gas flow rate.

Problem 3-12 illustrates that an increase in the gas flow rate of 50% more than doubled the static pressure drop across the system.

The static pressure drop for a set of hoods, ductwork, and air pollution control devices can be calculated using the "velocity pressure" methods described in the (ACGIH Industrial Ventilation Manual, 23rd edition). This calculation method takes into account the energy losses throughout the ventilation system. A partial list of these energy losses include the following:

- Turbulence at the hood inlet
- Acceleration of the gas from zero velocity to the velocity of the duct
- Frictional losses on the surfaces of the duct
- Turbulence losses at duct expansions and contractions
- Static pressure drop across the air pollution control device

Decreased system resistance can also be a problem. In this situation, the system operating point shifts to the right to a position of higher gas flow rate and lower static pressure rise. While this change would favor improved hood capture, it could reduce the collection efficiency of the air pollution control device.

High gas velocities through certain types of air pollution control systems such as fabric filters, electrostatic precipitators, carbon bed adsorber, and catalytic oxidizers can reduce efficiency slightly.

It is helpful to be able to determine when the system characteristic curve has shifted. The most direct way to check the fan performance is to measure the gas flow rate. However, this is time consuming. The fan motor current data provides an indirect, but nevertheless very useful, indication of gas flow changes from the baseline conditions. An increase in fan motor current is generally associated with an increase in the gas flow rate. Decreases in fan current occur when the gas flow rate drops. Unfortunately, the relationship between gas flow rate and motor current is not linear. The nonlinear characteristic of the relationship is indicated by the **brake horsepower curve** shown in Figure 3-39. The fan motor current is directly proportional to the brake horsepower as indicated by Equation 3-26, which applies to three-phase motor[5].

$$BHP = \frac{I \times E \times 1.73 \times Eff \times P.F.}{745} \tag{3-26}$$

Where:

BHP = brake horsepower (total power consumed by the fan)

I = fan motor current (amperes)

E = voltage (volts)

Eff = efficiency expressed as decimal

P.F. = power Factor

While the shape of the horsepower curve varies for different types of fan wheels, the general relationship applies to all centrifugal fans in their normal operating range. As the horsepower increases, the gas flow rate increases.

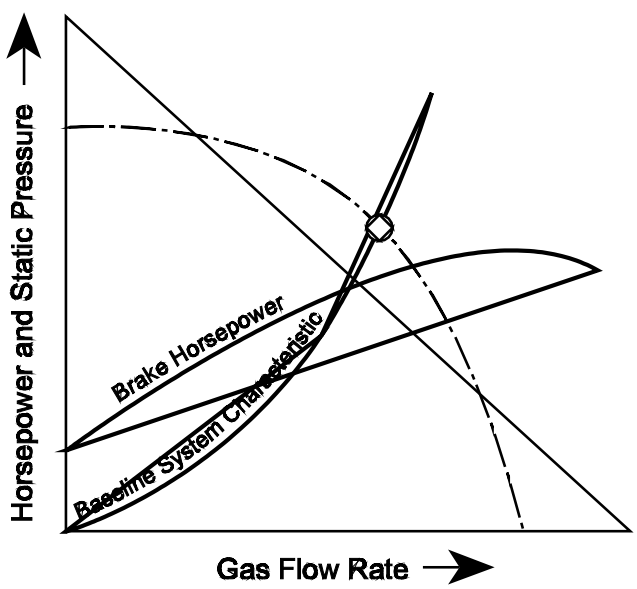

Figure 3-39. Example of a brake horsepower curve

The fan motor current is related directly to brake horsepower as indicated by Equation 3-26. Therefore, it provides a good indicator of changes in the gas flow rate. When the fan motor current has increased, the brake horsepower has probably increased, and, therefore, the gas flow rate has probably increased. However, the extent of the change cannot be determined from the simple relationship due to the nonlinearity of the brake horsepower curve and the variations in the power factor.

The brake horsepower is related to the cube of the fan speed as indicated in the third fan law shown below as Equation 3-27.

$$BHP_2 = BHP_1(RPM_2/RPM_1)^3 \quad (3\text{-}27)$$

Where:

BHP_1 = baseline brake horsepower (bhp)

BHP_2 = present brake horsepower (bhp)

RPM_1 = baseline fan wheel rotational speed (revolutions per minute)

RPM_2 = present fan wheel rotational speed (revolutions per minute)

The fan motor current is measured by the fan ammeter, which is monitored either in the main control room or in a remote fan control room.

3.4.3 Effect of Gas Temperature and Density on Centrifugal Fans

A fan operates like a high-speed shovel. Every rotation of the fan wheel at a given operating point moves a constant volume of air. While the volume is constant, the weight of the air being moved may not be constant. The density of the gas being handled by the fan is a strong function of the gas temperature. At high gas temperatures, the gas has a low density, and the gas is relatively light. When the gas temperature is cold, for example at ambient temperature, the gas is dense, and its weight is substantial.

Table 3-14. Gas Densities at Different Gas Temperatures

Gas Temperature °F	Gas Density[1] lb_m/ft^3	Gas Temperature °F	Gas Density[1] lb_m/ft^3
32	0.081	600	0.037
60	0.076	700	0.034
68	0.075	800	0.032
70	0.075	900	0.029
100	0.071	1000	0.027
150	0.065	1200	0.024
200	0.060	1400	0.021
250	0.056	1600	0.019
300	0.052	1800	0.018
400	0.046	2000	0.016
500	0.041	2500	0.013

1. Gas density at standard pressure of 407 in. W.C. and zero moisture level

In addition to gas temperature, gas density is also a function of the absolute gas pressure. The absolute pressure can be taken into account using Equation 3-28.

$$\rho_{Actual} = \rho_{STP}\left(P_{Actual} / P_{STP}\right) \tag{3-28}$$

Where:

ρ_{Actual} = gas density at actual conditions (lb_m/ft^3)
ρ_{STP} = gas density at standard conditions (lb_m/ft^3)
P_{STP} = gas pressure at standard conditions (in. W.C.)
P_{Actual} = gas pressure at actual conditions (in. W.C.)

The gas density has a direct effect on the fan motor current. The current will be high when the gas stream is cold such as the times when the process is starting up. If steps are not taken to minimize gas flow during cold operating periods, the fan motor could burn out due to excessive current flow. To prevent this, the fan inlet or outlet dampers are usually partially closed during start-up to restrict the amount of "dense" air being handled. As the process heats up and the gas stream becomes less dense, the dampers can be opened to permit normal gas flow rates.

When using the fan motor current as an indicator of gas flow rate, it is important to correct the motor currents at the actual conditions back to standard conditions. This correction can be performed using Equation 3-9.

$$I_{STP} = I_{Actual}\left(\rho_{STP} / \rho_{Actual}\right) \tag{3-29}$$

Where:

I_{STP} = fan motor current at standard conditions (amperes)
I_{Actual} = fan motor current at actual conditions (amperes)
ρ_{STP} = gas density at standard conditions (lb_m/ft^3)
ρ_{Actual} = gas density at actual conditions (lb_m/ft^3)

Problem 3-13

A fan motor is operating at 80 amps and the gas flow rate through the system is 10,000 ACFM at 300°F and -10 in. W.C. (fan inlet). What is the motor current at standard conditions?

Solution:

Step 1. Calculate the gas density at actual conditions. As a basis, use 1 lb mole of gas. Assume 1 lb mole of gas has a mass of 29 pounds.

1. Convert pressure from inches of water to psia.

$$\text{psia} = \frac{(407\text{ in. W.C.} - 10\text{ in. W.C.})}{407\text{ in. W.C.}} \times (14.7\text{ psia})$$
$$= 14.34\text{ psia}$$

2. Calculate the gas volume at actual conditions using the ideal gas law equation.

$V = nRT/P$

$$V = \left(\frac{10.73\ \text{psia} \cdot \text{ft}^3}{°\text{R} \bullet \text{lb mole}}\right)\frac{(460°\text{F} + 300°\text{F})}{14.34\ \text{psia}}$$
$$= 568.7\ \text{ft}^3/\text{lb mole}$$

3. Calculate the gas density, ρ.

$$\rho = \frac{\text{Mass}}{\text{Volume}}$$

$$\text{Mass} = 29\ \text{lb}_m/\text{lb mole}$$

$$\text{Volume} = 568.7\ \text{ft}^3/\text{lb mole}\ (\text{at actual conditions})$$

$$\rho = \frac{29\ \text{lb}_m}{568.7\ \text{ft}^3}$$
$$= 0.051\ \text{lb}_m/\text{ft}^3$$

Step 2. Calculate the gas density at standard conditions.

1. Calculate the gas volume at standard conditions using the ideal gas law.

$$V = \left(\frac{10.73\ \text{psia} \bullet \text{ft}^3}{°\text{R} \bullet \text{lb mole}}\right)\frac{(460°\text{F} + 68°\text{F})}{14.7\ \text{psia}}$$
$$= 385.4\ \text{ft}^3/\text{lb mole}$$

2. Calculate the gas density,ρ.

$$\rho = 29\ \text{lb}_m / 385.4\ \text{ft}^3 = 0.075\ \text{lb}_m/\text{ft}^3$$

Step 3. Correct the motor current for the change in gas density.

$$I_{STP} = I_{Actual}(\rho_{STP} / \rho_{Actual})$$

$$I_{STP} = 80\ \text{amps}\ \frac{0.075\ \text{lb}_m/\text{ft}^3}{0.051\ \text{lb}_m/\text{ft}^3}$$
$$= 80\ \text{amps}\ (1.47)$$
$$= 118\ \text{amps}$$

Note 1: The problem could have been solved quickly by using tabulated values of the gas density. However, this approach also reduces the risk of a gas density error caused by not taking into account the effect of pressure changes.

Note 2: The gas composition in Problem 3-13 could be taken into account by calculating the weighted average molecular weights of the constituents rather than assuming 29 pounds per pound mole, which is close to the value for air. This correction is important when the gas stream has a high concentration of compounds such as carbon dioxide or water, which have molecular weights that are much different than air.

The gas temperature and gas pressure corrections for gas density must also be used when selecting a fan. The fan multi-ratings tables are expressed in standard temperatures and pressures. These corrections are needed to ensure that the fan will deliver the necessary gas flow rates and absolute pressure increases under the actual operating conditions anticipated in the process.

The temperature of a gas may increase, decrease, or remain constant when a pressure change occurs. When the gas flow reaches the fan, the gas flow changes from negative to positive pressure. This increase in pressure can cause the temperature to increase slightly.

Summary

Centrifugal fans are the most commonly used type of fan in industrial processes due to their ability to generate high-pressure rises in the gas stream. The major components of a typical centrifugal fan include the fan wheel, fan housing, drive mechanism, and inlet dampers and/or outlet dampers.

The intersection of the fan characteristic curve and the system characteristic curve is called the operating point for the fan. The factors that affect the fan characteristic curve are the type of fan wheel and blade, the fan wheel rotational speed, and the shape of the fan housing. The system characteristic curve takes into account the energy losses throughout the ventilation system. These curves are helpful indicators in determining if a change in the system has occurred. A change in the system can also be detected through the fan motor current data that corresponds with the gas flow rate, however not linearly.

The fan laws can predict how a fan will be affected by a change in an operating condition. The fan laws apply to fans having the same geometric shape and operating at the same point on the fan characteristic curve.

A fan will move a constant volume of air; however the amount of work required to move the gas flow is dependent on the density of the gas. Two factors that affect density are temperature and pressure. The gas flow density has a direct effect on the fan motor current.

Review Exercises

Use the drawing shown below to answer questions 1-3.

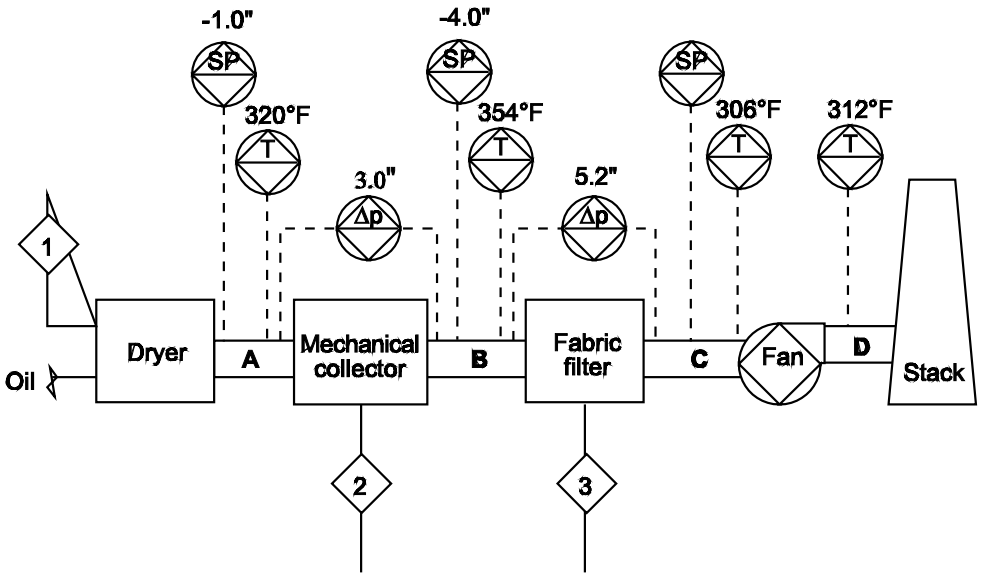

Figure 3-40. Example flowchart

1. Which static pressure reading appears to be illogical according to the flowchart?
   a. Duct A
   b. Duct B
   c. Duct D
   d. They all appear logical.

2. Calculate the static pressure at the inlet to the centrifugal fan. (Exclude frictional losses of ducts and entry losses.)
   a. 0.7 in. W.C.
   b. -1.7 in. W.C.
   c. -9.2 in. W.C.
   d. none of the above

3. The temperature in Duct A was checked by plant personnel and determined to be correct. Which of the other temperature readings appears to be illogical according to the flowchart?
   a. Duct B
   b. Duct C
   c. Duct D
   d. They all appear logical.

4. The gas flow rate is duct A is 5,000 SCFM, the gas temperature is 350°F and the gas pressure is –32 in.W.C.. The gas flow rate in duct B is 4,000 ACFM, the gas temperature is 400°F, and the gas pressure is –35 in. W.C. Calculate the total gas flow rate in a combined duct C handling the flows from ducts A and B. Use a barometric pressure of 29.15 in Hg..

5. Calculate the hood static pressure if the hood coefficient of entry is 0.49, and the gas flow rate through a 1.5-foot diameter duct from the hood is 6,200 ft^3/min. Use standard temperatures and pressures.

   a. -2.1 in W.C.
   b. -1.15 in. W.C.
   c. -0.38 in W.C.
   d. 0.85 in W.C.

6. Find the farthest distance away that a flanged hood, 6 in. by 12 in., can be placed away from the contaminant source and maintain the capture velocity of 300 fpm and a volumetric flow rate of 2000 ACFM. The equation for a flanged hood is

$$Q = (0.75)v_h\left[10(X)^2 + A_h\right]$$

   a. 15 inches
   b. 24 inches
   c. 3 inches
   d. 11 inches

7. Estimate the rotational speed of a belt-driven centrifugal fan based on the following data:

   Motor rotational speed, RPM_{Motor} = 1778 rpm

   Motor sheave diameter, D_{Motor} = 8 in.

   Fan sheave diameter, D_{Fan} = 14 in.

   a. 1239 rpm_{fan}
   b. 2000 rpm_{fan}
   c. 400 rpm_{fan}
   d. 1016 rpm_{fan}

8. A system consists of the following components (in order): hood, fabric filter, centrifugal fan, and stack. The fabric filter static pressure drop has increased from 4.5 inches of water to 6.5 inches of water. If the fan dampers do not move to compensate for this change, what will happen to the hood static pressure?

   a. It will be less negative (closer to zero).
   b. It will be more negative.
   c. It will become positive.
   d. It will remain unchanged.

9. A centrifugal fan is moving 1,000 cubic feet of air per minute at a temperature of 450°F and a fan inlet pressure of -15 inches of water. What will the actual air flow rate be if the gas temperature decreases to 68°F, the inlet pressure remains unchanged, and the fan rotational speed remains the same?
   a. The air flow rate will increase to 1,5800 ACFM.
   b. The air flow rate will decrease to 580 ACFM.
   c. The air flow rate will remain at 1000 ACFM.

10. A centrifugal fan is operating with a motor current of 120 amps. The gas density entering the fan during normal operation is 0.045 pounds per cubic foot. Estimate the motor current at standard conditions when the gas density is approximately 0.075 pounds per cubic foot.
   a. 500 amps
   b. 200 amps
   c. 159 amps
   d. 90 amps

11. The static pressure drop through a section of ductwork is -1.2 inches of water when the gas flow rate is 5,000 ACFM. Estimate the static pressure drop across this section of ductwork if the gas flow rate increases to 8,000 ACFM. Assume that there are no gas density changes associated with the increased gas flow rate.
   a. 3.07 in W.C.
   b. 1.1 in W.C.
   c. 2 in W.C.
   d. 4 in W.C.

12. The hood capture efficiency is 92% and the wet scrubber control system has collection efficiency of 95%. If the process served by this system is generating 140 pounds of pollutant per hour, calculate the fugitive emissions and the stack emissions.
   a. 20.50 lb_m/hr Fugitive emissions and 9.80 lb_m/hr Stack emissions
   b. 1.50 lb_m/hr Fugitive emissions and 0.80 lb_m/hr Stack emissions
   c. 11.2 lb_m/hr Fugitive emissions and 6.4 lb_m/hr Stack emissions
   d. 14.0 lb_m/hr Fugitive emissions and 3.54 lb_m/hr Stack emissions

13. Assume a fan is presently operating with the following conditions, 20,000 ACFM, -2.5 in. W.C. static pressure, 400 RPM, and 12 brake horsepower. Using the fan laws determine the new RPM, brake horsepower, and static pressure when the volumetric increases to 22,500 ACFM.
   a. 490 rpm, 19.1 hp, -5.7 in. W.C.
   b. 350 rpm, 9.5 hp, -3.9 in. W.C.
   c. 400 rpm, 10.2 hp, -2.8 in. W.C.
   d. 450 rpm, 17.1 hp, -3.2 in. W.C.

14. What would happen to the desired operating point of a fan if a hole developed in the ductwork. Which characteristic curve will shift, what will happen to the "operating point", volumetric flow rate, and hood static pressure.

    a. The system characteristic curve will shift down, the volumetric flow rate will increase, and the hood static pressure will increase.

    b. The system characteristic curve will shift down, the volumetric flow rate will decrease, and the hood static pressure will decrease.

    c. The system characteristic curve will shift down, the volumetric flow rate will increase, and the hood static pressure will decrease.

    d. The system characteristic curve will shift up, the volumetric flow rate will increase, and the hood static pressure will decrease.

Review Answers

1. Which static pressure reading appears to be illogical according to the flowchart?

   d. They all appear logical.

   The gas stream decreases in pressure as it approaches the fan inlet.

2. Calculate the static pressure at the inlet to the centrifugal fan. (Exclude frictional losses of ducts and entry losses.)

   c. -9.2 in. W.C.

   Solution:

$$SP_{DuctC} = SP_{DuctB} - \Delta p_{Fabricfilter}$$

$$= -4.0 \text{ in. W.C.} - 5.2 \text{ in. W.C.}$$

$$= -9.2 \text{ in. W.C.}$$

3. The temperature in Duct A was checked by plant personnel and determined to be correct. Which of the other temperature readings appears to be illogical according to the flowchart?

   a. Duct B

   The temperatures should decrease as the gas moves through the system since no significant source of heat is added to the gas. There is no reason for the gas stream in Duct B to be hotter than the gas stream in Duct A. Other wise the temperature trend appears logical.

4. The gas flow rate is duct A is 5,000 SCFM, the gas temperature is 350°F and the gas pressure is –32 in.W.C.. The gas flow rate in duct B is 4,000 ACFM, the gas temperature is 400°F, and the gas pressure is –35 in. W.C. Calculate the total gas flow rate in a combined duct C handling the flows from ducts A and B. Use a barometric pressure of 29.15 in Hg..

   Solution:

   Calculate the absolute pressure in Duct B

$$SP = \left(\frac{407 \text{ in.W.C.}}{29.92 \text{ in.Hg.}}\right) 29.15 \text{ in. H.G.} + (-32 \text{in.W.C.}) = 364.5 \text{ in. W.C.}$$

   Convert the flow in duct B to SCFM

$$SCFM = ACFM\left(\frac{528°R}{460°R + 400°F}\right)\left(\frac{407 \text{ in. W.C.}}{364.5 \text{ in.W.C.}}\right) = 2{,}742 \text{ SCFM}$$

   Flow in Duct C = Flow in Duct A + Flow in Duct B =5,000 SCFM + 2,740 SCFM = 7,740 SCFM

5. Calculate the hood static pressure if the hood coefficient of entry is 0.49, and the gas flow rate through a 1.5-foot diameter duct from the hood is 6,200 ft^3/min. Use standard temperatures and pressures.

   b. -1.15 in. W.C.

   Solution:

   To calculate the hood static pressure (SP_h), use the following equation:

$$SP_h = -VP_d - h_e$$

1. Calculate the velocity pressure (VP) using the following equation. At standard conditions, $_{Actual}$ = 0.075 lb_m/ft^3.

$$VP_d = \left[\frac{v}{4005}\right]^2 \times \frac{\rho_{Actual}}{0.075}$$

$$\text{Velocity} = \frac{6{,}200\ ft^3/min}{\pi D^2/4}$$

$$= \frac{6{,}200\ ft^3/min}{(3.14)(1.5\ ft)^2/4}$$

$$= 3{,}510\ ft/min$$

$$VP_d = \left[\frac{3{,}510}{4{,}005}\right]^2 = 0.77 in.\ W.C.$$

2. Calculate the hood entry loss (h_e) as follows:

$$h_e = F_h(VP)$$

Given: F_h = 0.49

$$h_e = 0.49(0.77\ in.\ W.C.)$$

$$= 0.38\ in.\ W.C.$$

3. Calculate the hood static pressure (SP_h).

$$SP_h = -0.77\ in.\ W.C. - 0.38\ in.W.C.$$

$$= -1.15\ in.\ W.C.$$

6. Find the farthest distance away that a flanged hood, 6 in. x 12 in., can be placed away from the contaminant source and maintain the capture velocity of 300 fpm and a volumetric flow rate of 2000 ACFM. The equation for a flanged hood is

$$Q = (0.75)v_h\left[10(X)^2 + A_h\right]$$

d. 11 inches

Solution:

1. Solve for X using the following equation.

$$Q = (0.75)v_h\left[10(X)^2 + A_h\right]$$

$$\frac{2000\ \text{ACF}}{\text{min}} = \left(\frac{0.75}{1}\right)\left(\frac{300\ \text{ft}}{\text{min}}\right)\left[10(X\ \text{ft})^2 + \left(\frac{72\ \text{in}^2}{1} \times \frac{1}{144\ \text{in}^2}\right)\right]$$

$$2000\ \text{ACFM} = \left(\frac{225\ \text{ft}}{\text{min}}\right)\left[10(X\ \text{ft})^2 + 0.5\ \text{ft}^2\right]$$

$$8.89\ \text{ft}^2 = 10(X\ \text{ft})^2 + 0.5\ \text{ft}^2$$

$$8.39\ \text{ft}^2 = 10(X\ \text{ft})^2$$

$$0.839\ \text{ft}^2 = (X\ \text{ft})^2$$

$$X = 0.916\ \text{ft} \times \frac{12\ \text{in.}}{1\ \text{ft}} = 11\ \text{in.}$$

7. Estimate the rotational speed of a belt-driven centrifugal fan based on the following data:
Motor rotational speed, RPM_{Motor} = 1778 rpm
Motor sheave diameter, D_{Motor} = 8 in.
Fan sheave diameter, D_{Fan} = 14 in.

d. 1016 rpm_{fan}

Solution:

Calculate the fan speed (RPM_{fan}) using the following equation.

$$RPM_{Fan} = RPM_{Motor} \times \frac{D_{Motor}}{D_{Fan}}$$

$$= \frac{1778}{1}\left|\frac{8\ \text{in.}}{14\ \text{in.}}\right. = 1016\ \text{rpm}$$

8. A system consists of the following components (in order): hood, fabric filter, centrifugal fan, and stack. The fabric filter static pressure drop has increased from 4.5 inches of water to 6.5 inches of water. If the fan dampers do not move to compensate for this change, what will happen to the hood static pressure?

   a. It will be less negative (closer to zero).

   The hood static pressure will decrease due to reduced gas flow rate caused by the increased blockage of airflow from the fabric filters.

9. A centrifugal fan is moving 1,000 cubic feet of air per minute at a temperature of 450°F and a fan inlet pressure of -15 inches of water. What will the actual air flow rate be if the gas temperature decreases to 68°F, the inlet pressure remains unchanged, and the fan rotational speed remains the same?

   c. The air flow rate will remain at 1000 ACFM

   Fans move a constant volume of air.

10. A centrifugal fan is operating with a motor current of 120 amps. The gas density entering the fan during normal operation is 0.045 pounds per cubic foot. Estimate the motor current at standard conditions when the gas density is approximately 0.075 pounds per cubic foot.

    b. 200 amps

    Solution:

$$I_{STP} = I_{Actual}\left(\rho_{STP} / \rho_{Actual}\right)$$

$$= 120 \text{ amps} \frac{\left(0.075\ lb_m / ft^3\right)}{\left(0.045\ lb_m / ft^3\right)} = 200 \text{ amps}$$

11. The static pressure drop through a section of ductwork is -1.2 inches of water when the gas flow rate is 5,000 ACFM. Estimate the static pressure drop across this section of ductwork if the gas flow rate increases to 8,000 ACFM. Assume that there are no gas density changes associated with the increased gas flow rate.

    a. 3.07 in W.C.

    Solution:

$$\frac{SP_{@\,High\ flow}}{SP_{@\,Low\ flow}} = \frac{(8{,}000\ ACFM)^2}{(5{,}000\ ACFM)^2} = 2.56$$

Given: $SP_{@\,Low\ flow}$ = -1.2 in. W.C.

$$SP_{@\,High\ flow} = -1.2 \text{ in. W.C.}(2.56) = -3.07 \text{ in. W.C.}$$

12. The hood capture efficiency is 92% and the wet scrubber control system has collection efficiency of 95%. If the process served by this system is generating 140 pounds of pollutant per hour, calculate the fugitive emissions and the stack emissions.

c. 11.20 lb_m/hr Fugitive emissions and 6.44 lb_m/hr Stack emissions

Solution:

Fugitive emissions = 0.08 (140 lb_m/hr) = 11.2 lb_m/hr

Capture emissions = 140 lb_m/hr - 11.20 lb_m/hr = 128.8 lb_m/hr

Stack emissions = 0.05 (128.80 lb_m/hr) = 6.4 lb_m/hr

13. Assume a fan is presently operating with the following conditions, 20,000 ACFM, -2.5 in. W.C. static pressure, 400 rpm, and 12 brake horsepower. Using the fan laws determine the new RPM, brake horsepower, and static pressure when the volumetric increases to 22,500.

d. 450 rpm, 17.1hp, -3.2 in. W.C.

Solution:

New fan speed:

$$\frac{Q_1}{Q_2} = \frac{RPM_1}{RPM_2}$$

$$\frac{20{,}000\ ACFM}{22{,}500\ ACFM} = \frac{400\ rpm}{RPM_2}$$

$$RPM_2 = 450\ rpm$$

Brake horsepower:

$$\frac{BHP_1}{BHP_2} = \left(\frac{RPM_1}{RPM_2}\right)^3$$

$$\frac{12\ hp}{BHP_2} = \frac{64{,}000{,}000}{91{,}125{,}000}$$

$$BHP_2 = 17.1\ bhp$$

Static pressure:

$$\frac{SP_1}{SP_2} = \left(\frac{RPM_1}{RPM_2}\right)^2$$

$$\frac{-2.5\text{ in. W.C.}}{SP_2} = \left(\frac{400}{450}\right)^2 = \frac{160{,}000}{202{,}500}$$

$$SP_2 = -3.2\text{ in. W.C.}$$

14. What would happen to a fan's desired operating point if a hole developed in the ductwork? Which characteristic curve will shift, what will happen to the "operating point", volumetric flow rate, and hood static pressure.

    c. The system characteristic curve will shift down, the volumetric flow rate will increase, and the hood static pressure will decrease.

    The system characteristic curve will shift down due to a decrease in the system resistance, causing the static pressure to decrease and the gas flow rate to increase. The hood static pressure will decrease because the hole in the ductwork will allow air to enter the system prior to the hood. The gas flow rate will increase due to the air inleakage

References

1. American Conference of Governmental Industrial Hygienists, *Industrial Ventilation - A Manual of Recommended Practice*, 23rd Edition, 1998.

2. Cengel, Yunus A., Boles, Michael A., *Thermodynamics An Engineering Approach*. McGraw-Hill Publishing. 1989

3. Code of Federal Regulations, 40 Part 60, Method 22, July 1, 1997.

Chapter 4
Fabric Filters

Fabric filters are capable of high-efficiency particulate matter removal in a wide variety of industrial applications. Uses for fabric filters have steadily expanded since the 1960s, because of the development of new, highly effective fabrics capable of efficiently collecting particles over the size range of 0.1 – 1,000 m. This particle collection efficiency, even in the difficult-to-control range of 0.2 to 0.5 m, is due to (1) the multiple opportunities for a particle to be captured as it attempts to pass through a dust cake and fabric and (2) the multiple modes of particle capture that occur within the dust cake and fabric. These modes of capture include impaction, Brownian diffusion, and electrostatic attraction.

The conceptual simplicity of fabric filters belies the complexity of the equipment design and the operating procedures necessary to achieve and maintain high particulate removal efficiencies. Serious performance problems can develop relatively rapidly. Holes and tears in the bags can develop due to chemical attack, high temperature excursions, or abrasion/flex damage. Cleaning system problems can result in excessive static pressure drops. Particles can also "bleed" through the dust cake and fabric due to improper design or cleaning.

This section emphasizes three of the major types of fabric filters: pulse jet, cartridge, and reverse air units. There are many other types that are not explicitly discussed in this manual. However, the operating principles, sizing practices, and performance evaluation procedures discussed with respect to pulse jet, cartridge, and reverse air units are generally applicable to all types of fabric filters.

4.1 TYPES AND COMPONENTS

4.1.1 Pulse Jet Fabric Filters

Pulse jet fabric filters, invented during the early 1960s, are used for a wide variety of small-to-medium size industrial applications. These include asphalt plants, cement plant clinker coolers, and industrial boilers. The baghouses are termed *pulse jet* since a pulse of compressed air is used for cleaning each of the bags.

There are two major design types: top access and side access. The top access design includes a number of large hatches across the top of the baghouse for bag replacement and maintenance. The side access design has one large hatch on the side for access to the bags. The side access units often have a single small hatch on the top of the baghouse shell for routine inspection.

A cutaway drawing of a typical top access type pulse jet fabric filter is shown in Figure 4-1. The inlet gas stream enters in the upper portion of the hopper and passes vertically up between the bags during filtering. Dust accumulates on the outside surfaces of the bags shown in Figure 4-2.

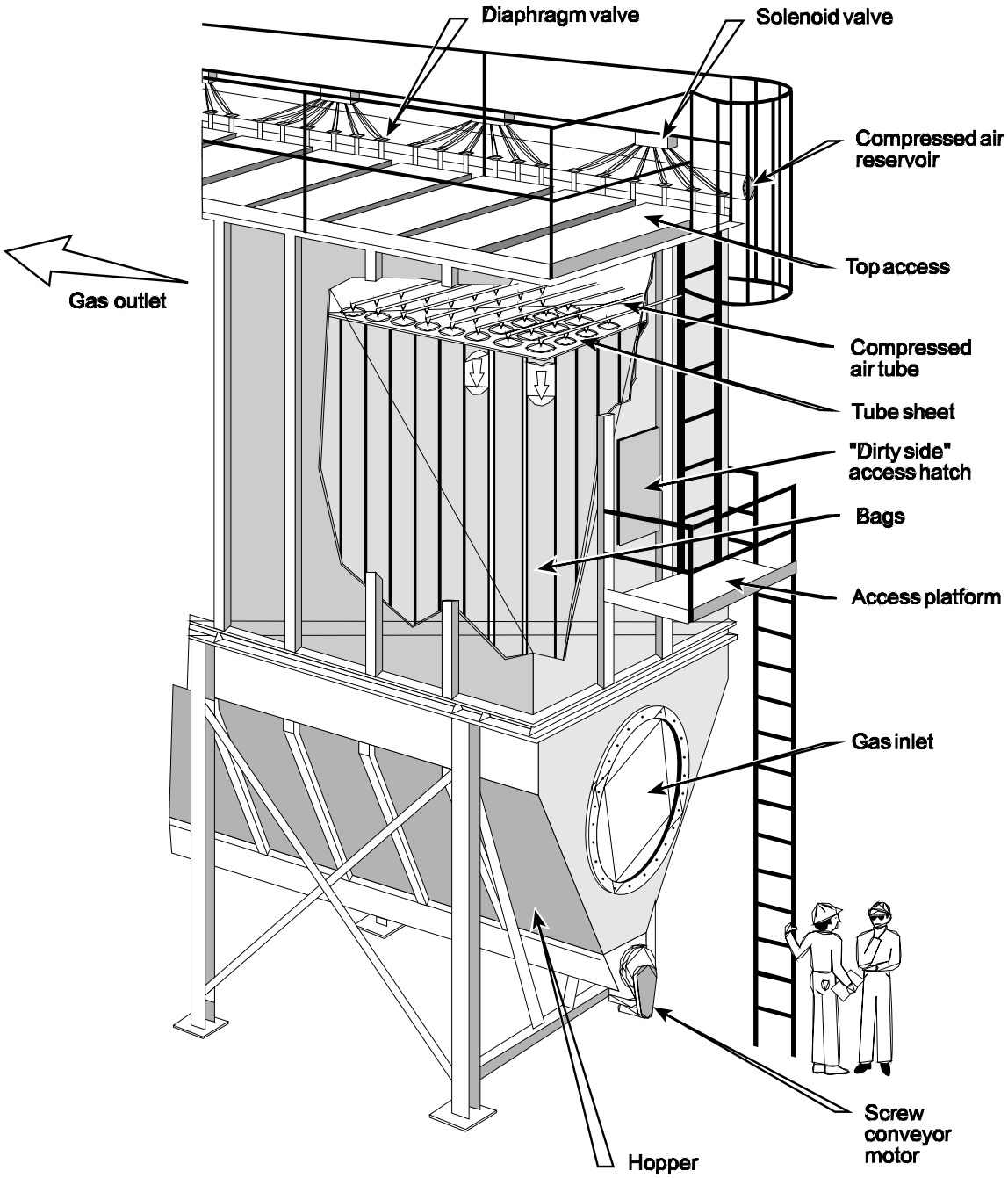

Figure 4-1. Typical pulse jet fabric filter

Figure 4-2. View of the bottoms of pulse jet bags
(note flex around inner cages)

The cleaned gas enters the cylindrical bags and moves upward into the clean gas plenum at the top of the baghouse. The outlet duct from this plenum takes the cleaned gas to the fan and stack.

A portion of the dust must occasionally be removed from the bags in order to avoid excessively high gas flow resistances. The bags are cleaned by introducing a high-pressure pulse of compressed air at the top of each bag. The sudden pulse of air generates a pressure wave that travels down inside the bag. The pressure wave also induces some filtered gas to flow downward into the bag. Due to the combined action of the pressure wave and the induced gas flow, the bags are briefly deflected outward. This cracks the dust cake on the outside of the bags and causes some of the dust to fall into the hopper. Cleaning is normally performed on a row-by-row basis while the baghouse is operating.

The compressed air at pressures from 60 to 90 pounds per square inch gauge (20 to 40 psig compressed air is used in low pressure-high volume designs) is generated by an air compressor and stored temporarily in the compressed air manifold. When the pilot valve (a standard solenoid valve) is opened by the controller, the diaphragm valve connected to the pilot valve opens suddenly. This lets compressed air into the delivery tube that services a row of bags. There are holes in the delivery tube above each bag. The cleaning system controller can operate on the basis of a differential pressure sensor (static pressure drop), or it can simply be operated on a timer. In either case, bags are cleaned on a relatively frequent basis with each row being cleaned from once every five minutes to once every several hours. Cleaning usually starts with the first row of bags and continues through the remaining rows in the order the bags are mounted.

The bags are supported on metal cages as shown in Figure 4-2. These cages prevent the bags from collapsing due to the movement of the gas stream through the bags. Because the fabric flexes around the cage wires during filtering, some fabric wear is possible. To minimize this potential problem, cages with closely-spaced wires are used for fabrics that are especially vulnerable to flex-type wear. More economical cages are used for fabrics that are very tolerant of flex.

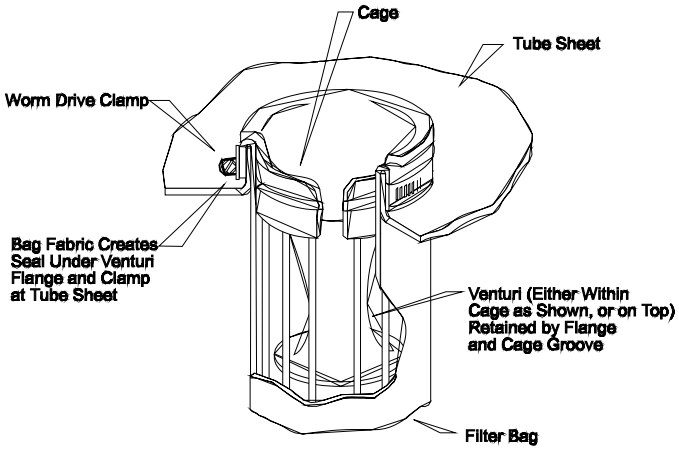

Figure 4-3a. Worm drive clamp type attachment

There are no frames or attachments at the bottom of the pulse jet bags. This free-hanging design is necessary in order to facilitate bag replacement, to allow gas stream movement upward, and to eliminate any abrasive surfaces near the bottom of the bags.

The pulse jet bags are suspended from a metallic plate called the *tube sheet*. In top access designs, the bags are clamped and sealed to the top of the tube sheet. This allows for bag removal and replacement from the top of the unit. Two of the many techniques for bag attachment at the top are shown in Figures 4-3a and 4-3b.

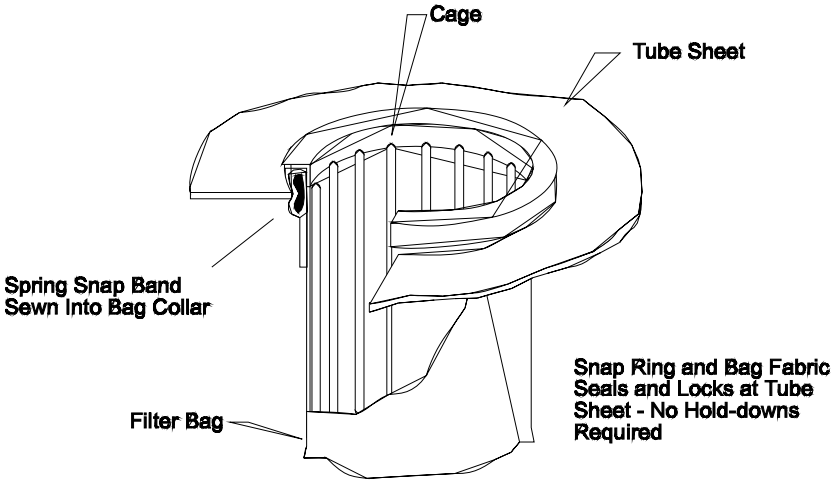

Figure 4-3b. Snap ring type attachment

Figure 4-4. Damage to the compressed air delivery tube position relative to the bag inlet

A proper bag seal is very important, for preventing dust-laden inlet gas from short-circuiting from the "dirty" side to the "clean" side of the baghouse without passing through the dust cake and bag. Even small leak sites can cause significant particulate emissions due to the two- to six-inch static pressure drop across pulse jet baghouses.

Proper cleaning of pulse jet bags is very important to achieve maximum particulate removal efficiency and to extend bag service life. Excessive cleaning intensity or very frequent pulsing can physically damage the pulse jet bags, especially near the top where the pulse enters. As shown in Figure 4-4, the compressed air delivery tube is generally mounted close to the bag opening. Damage due to excessive compressed air pressure or a misdirected (non-plumb) pulse can cause damage in the top several feet of the bag.

Compressed air used for bag cleaning can be contaminated by compressor lubricating oil or by condensed water. The water comes from the ambient air that was compressed and heated in the compressor. As the compressed air and water vapor stream passes through the aftercooler (if present) or the cold piping leading to the baghouse, some of the moisture condenses. It often accumulates in the compressed air manifolds and can be entrained in the compressed air stream passing through the manifold. After entering the bags, the water can create muddy areas near the top of the bag. These areas allow little or no gas flow. The lubricating oil creates sticky deposits near the top of the bags, which also prevent normal gas flow through the affected area. In order to minimize both compressed air quality problems, it is common for pulse jet collectors to have air dryers on the compressed air supply, coalescing filters for oil removal, and water drains on the compressed air manifolds.

Excessive cleaning intensities and frequencies can cause removal efficiency problems even before bag holes and tears develop. Severe cleaning practices result in the dispersion of small particles or agglomerates of particles from the dust cake. Due to the physical arrangement of the pulse jet bags, it is very difficult for these small particles or agglomerates to settle by gravity into the hopper. Only the large clumps will fall through the gas stream, which is rising upward and opposing gravity settling. The settling problem becomes increasingly difficult near the bottom of the bag, because this is the point of

maximum gas velocity as shown in Figure 4-5. Due to the opposed gravity settling, some very small particles or agglomerates with low terminal settling velocities (see Chapter 2) can turn around and return to the remaining dust cake, where they will remain until they bleed through the dust cake and the fabric to the clean side of the baghouse.

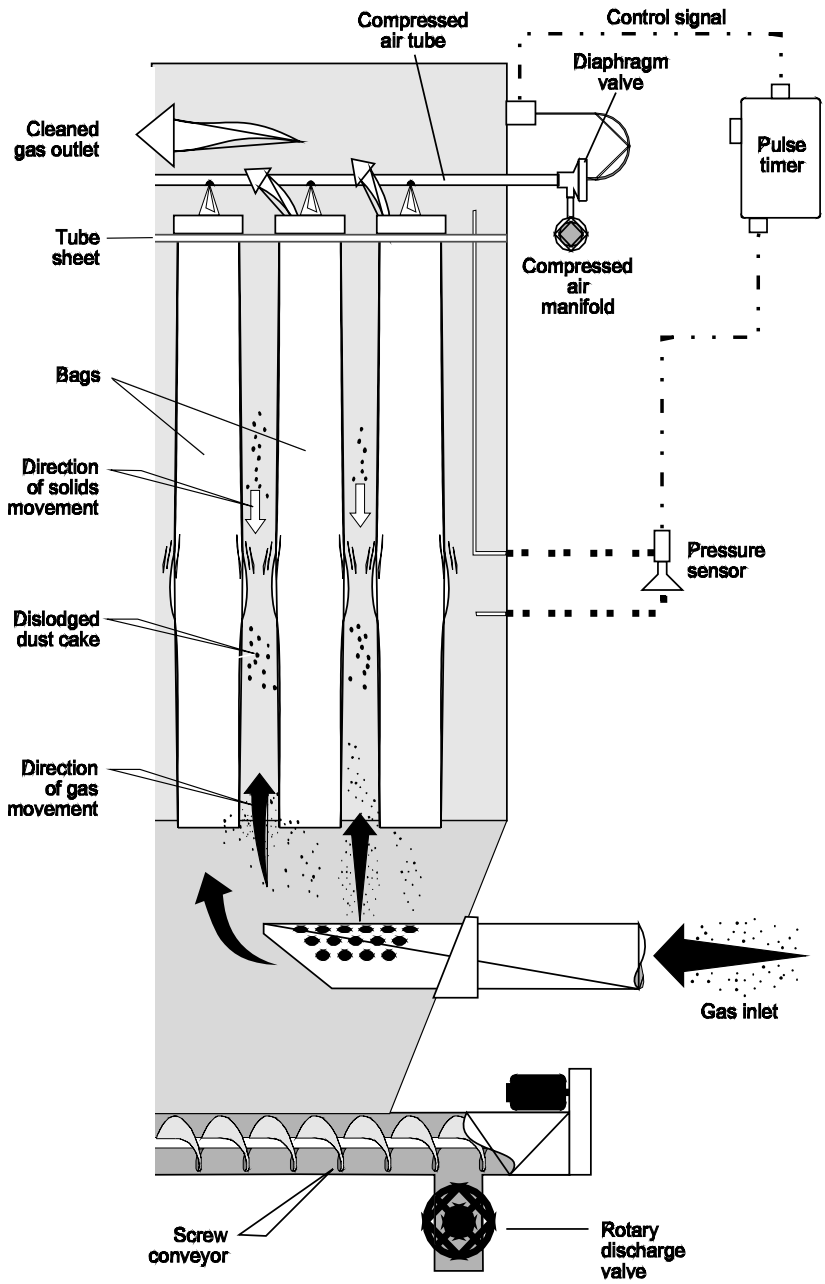

Figure 4-5. Gravity settling during cleaning of pulse jet bags

Actually, baghouse operation can be described as three separate sequential steps: (1) filtration of particles from the gas stream, (2) gravity settling of the dust cake, and (3) removal from the hopper. Each of these steps must be performed properly to ensure high efficiency particulate collection.

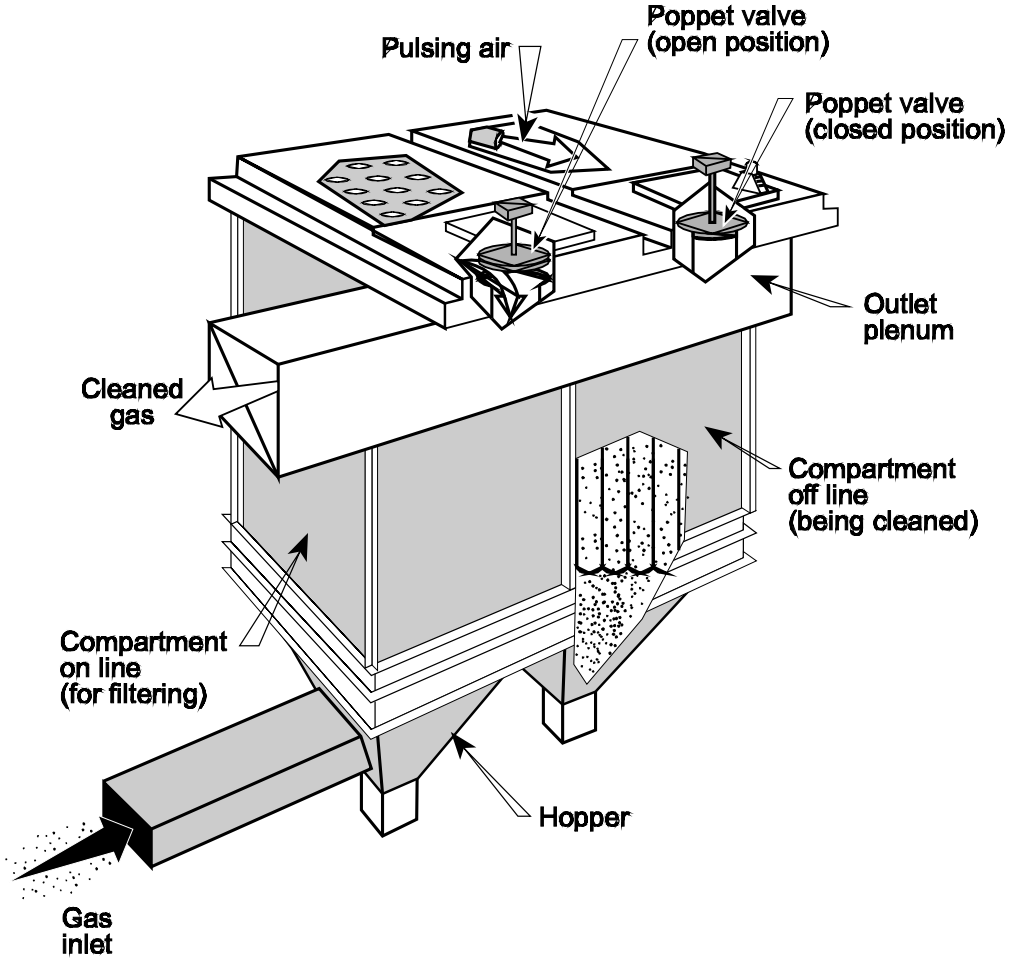

Figure 4-6. Compartmentalized pulse jet baghouse

In most small pulse units, the rows are cleaned one-by-one while the adjacent rows continue to filter the gas stream. However, with this operating practice, dust released from one row of bags can either return to the bag (because of gravity settling problems) or be recollected on a bag in an adjacent row that remains in filtering service. Both problems can be avoided by using off-line cleaning. This is accomplished by dividing the pulse jet baghouse into compartments and isolating the compartment being cleaned to prevent gas flow through it. A two-compartment pulse jet baghouse is shown in Figure 4-6. Most units have between four and 10 compartments. As shown in Figure 4-6, poppet dampers are usually used at the outlet of each compartment to shut off gas flow during cleaning.

The instruments used on pulse jet fabric filters are relatively simple. A static pressure gauge, such as that shown in Figure 4-7, is used to measure the overall static pressure drop across the entire baghouse. Other types of instruments that are often used include the following.

- Inlet gas stream temperature monitor
- Outlet gas stream (or fan inlet) temperature monitor)
- Compressed air pressure gauge

Figure 4-7. Magnehelic® static pressure drop gauge

Pyramidal or trough-type hoppers are often used on pulse jet baghouses. Units serving hot gas streams need thermal insulation and weatherproof lagging in order to keep the collected dust warm and free-flowing. Essentially all pulse jet baghouses need a solids discharge valve that prevents air movement up through the hopper and into the bag area.

Overall, pulse jet fabric filters are relatively small units for a given gas flow rate. This is due to the use of felted type fabrics that can be used at relatively high gas flow rates per unit of cloth. Sizing of pulse jet fabric filters is discussed later in this chapter.

4.1.2 Cartridge Filters

Cartridge filter systems are similar to pulse jet fabric filter systems. The filter elements are supported on a tube sheet that is usually mounted near the top of the filter housing. The gas stream to be filtered passes from the outside of the filter element to the inside. Filtering is performed by the filter media and the dust cake supported on the exterior of the filter media. The filter media is usually a felted material composed of cellulose, polypropylene, or other flex-resistant material.

The unique feature of a cartridge filter is the design of the filter element. Essentially all cartridges are shorter than pulse jet bags. Some cartridges have simple cylindrical designs. Others can have a large number of pleats as shown in Figure 4-8 or other complex shapes as shown in Figure 4-9 in order to increase the filtering surface area. Due to the shortness of the cartridge filter elements, they are usually less vulnerable to abrasion caused by the inlet gas stream. The shorter length also facilitates cleaning by a conventional compressed air pulsing system identical to those used on pulse jet collectors.

Cartridge filter elements are used in a wide variety of industrial applications. Due to their inherently compact design, they can be used in small collectors located close to the point of particulate matter generation. They are generally used on gas streams less than approximately 400°F. This temperature limit is due to the capabilities of the flex resistant, high temperature fabrics and by the limitation of the gasketing material used to seal the cartridge filter element to the tube sheet.

Figure 4-8. Pleated cartridge filter element
(Reprinted courtesy of Pneumafil, Inc.)

Figure 4-9. Flat cartridge filter element
(Reprinted courtesy of Airguard Industries, Inc.)

4.1.3 Reverse Air Fabric Filters

Reverse air fabric filters must be compartmentalized. During cleaning, the gas flow through a compartment is stopped, and filtered gas is passed in a reverse direction through the bags in the compartment. This cleaning procedure is the basis for the name "reverse air." A cutaway sketch of a typical reverse air fabric filter is shown in Figure 4-10.

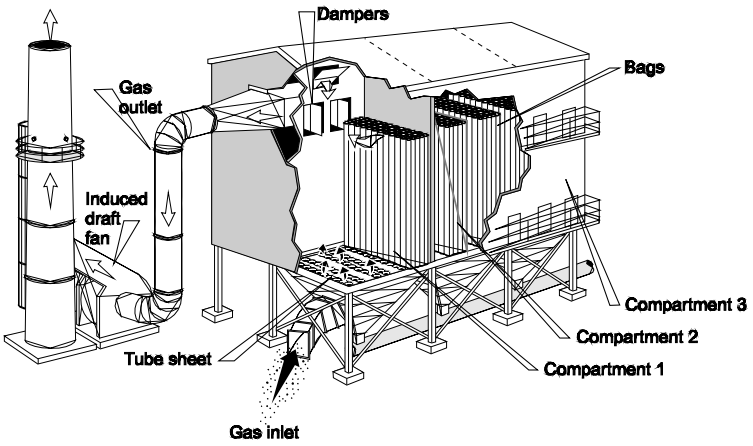

Figure 4-10. Reverse air fabric filter

Reverse air bags are hung from support frames near the tops of the compartments. The bags are tensioned to 60 to 120 pounds force by spring assemblies on the top frame as shown in Figure 4-11. Tension minimizes mechanical flexing and abrasion of the vulnerable fabrics.

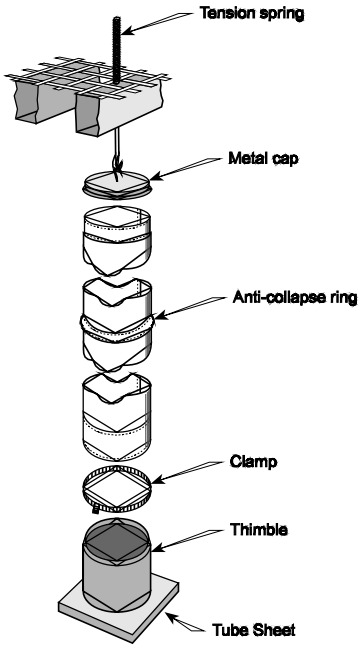

Figure 4-11. Reverse air bag

Reverse air bags do not have support cages. Instead, they have a set of anti-collapse rings sewn into the bags to prevent them from flattening during cleaning. There are usually between five and eight anti-collapse rings in a bag, depending on bag height and design. Most reverse air bags have heights ranging from 20 to 35 ft.

The bottoms of the bags are attached to a metallic plate called a *tube sheet*, which is mounted directly above the hopper. A clamp-and-thimble arrangement (shown in Figure 4-12a) or a snap ring arrangement (Figure 4-12b) secures each bag bottom to the tube sheet. As in the case with pulse jet bags, the seal provided by these attachments is important in preventing the movement of unfiltered gas to the clean side.

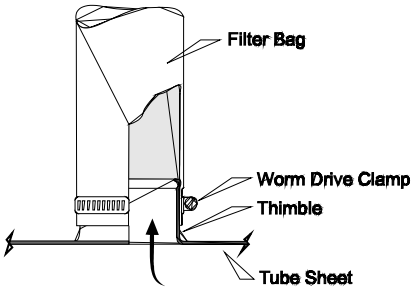

Figure 4-12a. Clamp-and-thimble-type bag attachment

The inlet unfiltered gas stream enters the baghouse near the top of the hopper and then enters the inside of each of the reverse air bags. A dust cake accumulates on the interior surfaces of the bags. The dust cake causes most of the filtration.

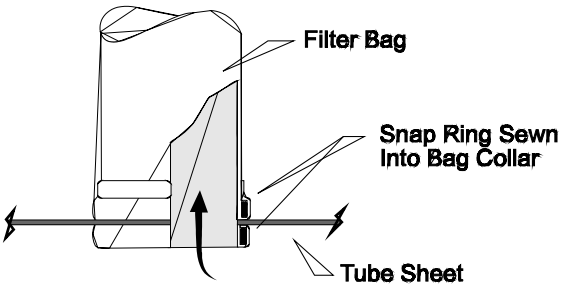

Figure 4-12b. Snap-ring-type bag attachment

During the filtering mode, the compartment's outlet and inlet gas dampers are open. When it is time to clean the compartment, the outlet damper is closed to block gas flow. After a short time to allow the bags to relax, the reverse air damper located near the top of the compartment is opened to permit filtered gas from the baghouse outlet to be recycled through the compartment. This reverse flow is sustained for as little as 30 seconds or as long as several minutes. During this time, large clumps of dust cake from the interior of the bags are dislodged and fall by gravity into the hopper. Gravity settling is obviously important during the cleaning operation. However, reverse air baghouses are less vulnerable than pulse jet baghouses to small particle gravity settling problems because particle movement is aided by the reverse gas movement downward in the bag. As long as the reverse air flow rate is adequate, the particles are carried out of the bag by this gas stream.

The reverse air passes through the compartment's inlet damper (which remains open during cleaning) and reenters the duct leading to the inlet side of other compartments, which continue on-line in the filtering mode. Large clumps and sheets of dust cake dislodged during cleaning are collected in the hopper underneath the compartment. Usually, pyramidal-type hoppers such as the one shown in Figure 4-13 are used for dust collection. Thermal insulation and hopper heaters are used to keep the solids warm until they can be dislodged. Solids discharge valves below the hoppers are needed to prevent ambient air from rushing upward into the baghouse.

Figure 4-13. Pyramidal type hopper

A variety of solids-handling systems are used to empty hoppers and transport the solids. Large reverse air baghouses usually have either pneumatic or pressurized solids-handling systems, both of which empty one hopper at a time. The solids-handling system often cycles continuously between the hoppers in order to minimize solids build-up problems.

Small reverse air units often have screw conveyors with either rotary discharge valves or double flapper valves to prevent air infiltration. Rotary valves use either metal blades or flexible wipers on metal blades to maintain an air seal (Figure 4-14a). The sections of the double flapper valve

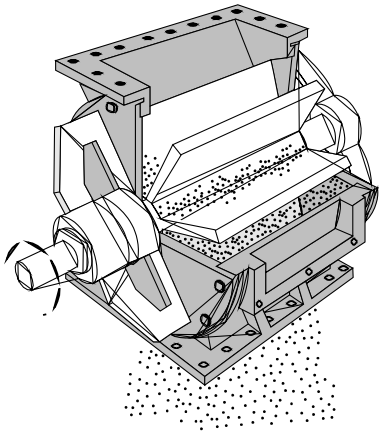

Figure 4-14a. Rotary discharge valve

move in an alternating fashion so that one is always in place to provide an air seal (Figure 4-14b).

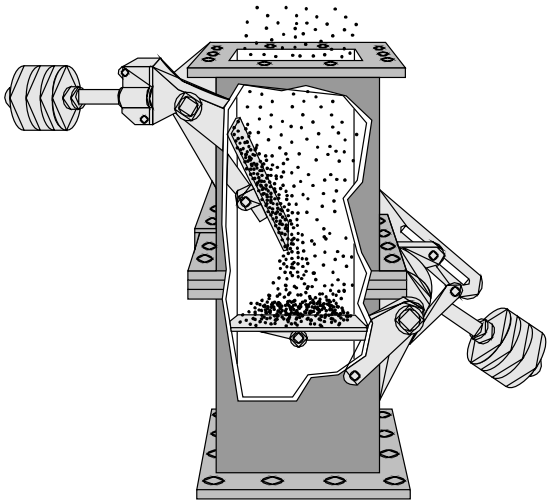

Figure 4-14b. Double flapper valve

Reverse air fabric filters contain gas stream bypass dampers that seal the connecting passageway from the inlet and outlet ducts of the unit. Typically, large poppet dampers are used; however, some units have a double set of louvered dampers. These dampers are especially important because they are subjected to the maximum static pressure drop across the entire baghouse. Slight leaks through poorly sealing bypass dampers can result in relatively low overall particulate removal efficiency. The bypass dampers are needed to protect the baghouse during malfunction and start-up periods when the bags could be damaged.

The instruments used on large reverse air fabric filters are often more sophisticated than the instruments on small-to-moderately sized pulse jet baghouses. In some cases, double-pass transmissometers are used to monitor opacity in the breachings and/or stack downstream from the baghouse. Bag-break monitors are often used when double-pass type opacity monitors are not required. Static pressure gauges are used to monitor the overall static pressure drop and the compartment-by-compartment static pressure drops during both filtering and cleaning. Static pressure gauges are also used to monitor the pressure of the reverse air stream being supplied to the compartments during cleaning. Inlet and outlet gas temperature monitors are used to ensure that the temperature remains within the acceptable range for the fabric being used.

4.1.4 Fabric Types

A wide variety of fabrics is commercially available. These can be categorized into five different groups based on the general type of “fabric” (media) construction.

1. Woven
2. Felted
3. Membrane
4. Sintered metal fiber
5. Ceramic cartridge

A **woven fabric** is composed of interlaced yarns as shown in Figure 4-15. The yarns in the “warp” direction provide strength to the fabric, and the yarns in the "fill" direction determine the characteristics of the fabric.

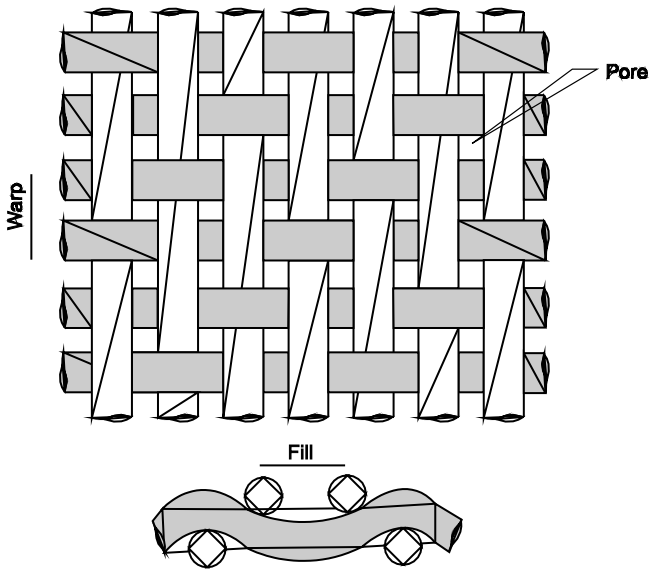

Figure 4-15. Woven fabric

The pores, which are the gaps between the yarns, can be more than 50 m in size. Small particles can easily pass through these pores until particles are captured on the sides of the yarns and bridge over the openings. The dust cake is critical for proper filtration by woven cloths.

There are a variety of weave types used to modify the characteristics of the fabric. For example, the twill weave shown in Figure 4-15 is less vulnerable than other weaves to fabric blinding due to the penetration of fine particles into the fabric. Overall, the weave characteristics influence the strength of the cloth, the difficulty of dust cake release during cleaning, and the resistance to gas flow.

Felted fabrics are composed of randomly oriented fibers attached to a very open weave termed the **scrim**. The felted fabrics are usually much thicker than woven cloths due to the layer of fibers on both sides of the scrim. With this type of fabric construction, there are no pores as indicated in Figure 4-16. The fibers on the filtering ("dirty") side provide a large number of targets for particle impaction, Brownian diffusion, and electrostatic attraction. However, even with felted fabrics, the dust cake that accumulates on the surface is primarily responsible for particle capture.

Membranes are another major category of fabrics used in air pollution control. These are composed of a polytetrafluoroethylene (PTFE) membrane that is laminated to either a woven or felted support fabric (Figure 4-17). The membrane is placed on the filtering side of the fabric. Particle collection occurs primarily due to the sieving action of the membrane's very small pores (less than 5 mm). In membrane fabrics, the dust layer is not especially important in particulate removal. Furthermore, static pressure drop is relatively low due to the good dust cake release properties.

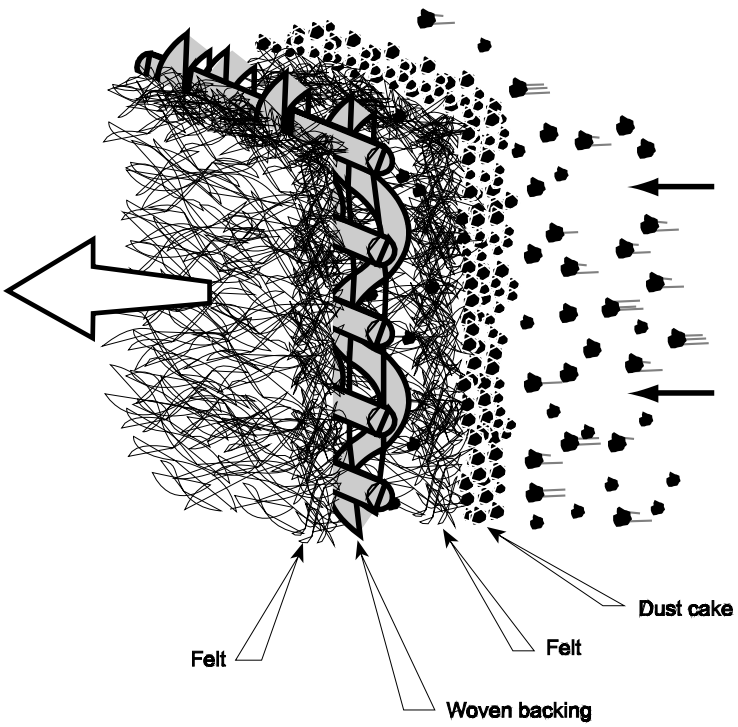

Figure 4-16. Felted fabric

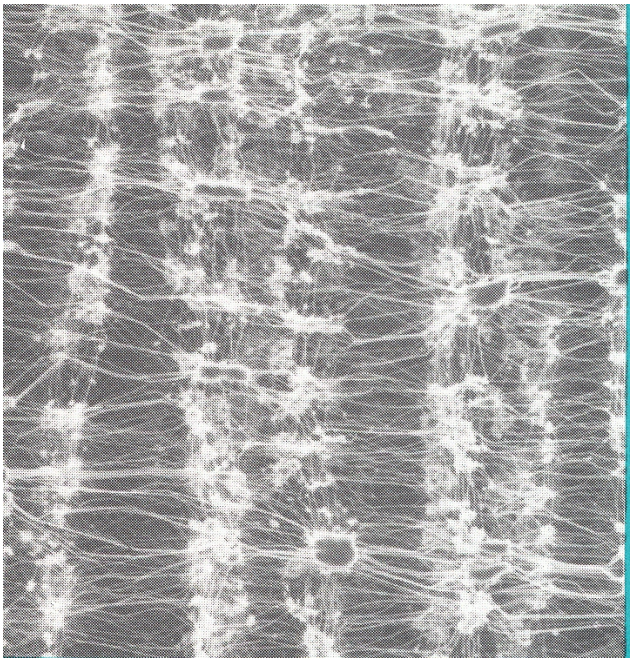

Figure 4-17. Membrane fabric at 500x magnification
(Reprinted courtesy of W.L. Gore & Associates, Inc.)

Sintered metal fiber bags are composed of small metal fibers randomly oriented on a cylindrical surface. The bags are heated to high temperatures to bond the fibers together. The bags are rigid and require specially designed pulse jet type cleaning systems. Sintered metal fiber bags can be used for hot gas streams. They can also be aggressively cleaned if they become blinded by sticky or moist dust.

Ceramic cartridge filters are fabricated in cylindrical candle or honeycomb forms. Particle capture occurs as the dust passes through the dust cake on the exterior surface and through the pores through the ceramic media. These filters are designed for applications where the gas temperatures are extremely hot.

The fabrics used for baghouses can be composed of a variety of synthetic and natural materials. Selection of the fabric material is based primarily on three criteria.

- Maximum gas temperatures of the gas stream
- Corrosive chemical concentrations in the gas stream
- Physical abrasion and fabric flex conditions

The various fabrics differ substantially with respect to their ability to tolerate temperature, chemical attack, and physical abrasion/flex. The temperature and acid-resistant capabilities of some of the commercially available types of fabrics are summarized in Table 4-1.

Table 4-1. Temperature and Acid Resistance Characteristics

Generic Name	Common or Trade Name	Maximum Temperature, °F		Acid Resistance
		Continuous	Surges	
Natural Fiber, Cellulose	Cotton	180	225	Poor
Polyolefin	Polyolefin	190	200	Good to Excellent
Polypropylene	Polypropylene	200	225	Excellent
Polyamide	Nylon®	200	225	Excellent
Acrylic	Orlon®	240	260	Good
Polyester	Dacron®	275	325	Good
Aromatic Polyamide	Nomex®	400	425	Fair
Polyphenylene Sulfide	Ryton®	400	425	Good
Polyimide	P-84®	400	425	Good
Fiberglass	Fiberglass	500	550	Fair
Fluorocarbon	Teflon®	400	500	Excellent
Stainless Steel	Stainless Steel	750	900	Good
Ceramic	Nextel®	1300	1400	Good

The continuous temperature rating shown in Table 4-1 is intended only as a general indicator of the fabric's capability. To optimize bag life, the normal operating temperatures should be slightly below this limit.

The capability with respect to temperature surges is a function mainly of the fabric's dimensional stability and protective coatings. For example, the limiting maximum surge (or short-term) temperatures for fiberglass fabrics is due, in part, to the need to avoid volatilization of lubricants on the fiber surfaces (lubricants are necessary to prevent fiber-fiber abrasion during cleaning). Also, the ability of the fabric to withstand short-term temperature spikes depends on the quantity of dust cake present. The dust can absorb some of the heat and thereby moderate the maximum temperature while slightly extending the time period that the fabric is exposed to elevated temperature.

The resistance to acids is oriented primarily toward inorganic acids such as sulfuric acid and hydrochloric acid. Most of the fabrics listed in Table 4-1 have a low resistance to hydrofluoric acid.

The ability of fabrics to withstand physical abrasion and flex is summarized in Table 4-2. Fabrics listed as fair must be cleaned gently, and the bags must be handled carefully during installation.

Table 4-2. Fabric Resistance to Abrasion and Flex

Generic Name	Common or Trade Name	Resistance to Abrasion and Flex
Natural Fiber, Cellulose	Cotton	Good
Polyolefin	Polyolefin	Excellent
Polypropylene	Polypropylene	Excellent
Polyamide	Nylon®	Excellent
Acrylic	Orlon®	Good
Polyester	Dacron®	Excellent
Aromatic Polyamide	Nomex®	Excellent
Polyphenylene Sulfide	Ryton®	Excellent
Polyimide	P-84®	Excellent
Fiberglass	Fiberglass	Fair
Fluorocarbon	Teflon®	Fair
Stainless Steel	Stainless Steel	Excellent
Ceramic	Nextel®	Fair

Most of the fabrics have good to excellent capability with respect to abrasion and flex. The two main exceptions are fiberglass, Teflon® fabrics, and ceramic which are often used for moderate-to-high gas temperature applications.

Some of the fabrics are coated to improve their ability to withstand acid attack and abrasion/flex type physical damage. All fiberglass fabrics must have coatings to protect the relatively brittle fibers that can easily be broken by fiber-to-fiber abrasion. Silicone-graphite finishes for fiberglass fabrics have been used for more than 40 years. Other coatings that have been developed and used successfully over the last 20 years include Teflon-B® coating, I-625®, Blue Max®, and Chemflex®. Some of these newer coatings also protect the fabric from acid attack.

4.2 OPERATING PRINCIPLES

4.2.1 Particle Collection

Multiple-capture mechanisms are responsible for particle capture within dust layers and fabrics. Impaction is effective because there are many sharp changes in flow direction as the gas stream moves around the various particles and fibers. Unlike some types of particulate collection devices, there are multiple opportunities for particle impaction due to the numbers of individual dust cake particles and fabric fibers in the gas stream path.

Brownian diffusion is moderately effective for collecting submicrometer particles because of the close contact of the gas stream and the dust cake. The particle does not have to be displaced a long distance in order to come into contact with a dust cake particle or fiber. Furthermore, the displacement of submicrometer particles can occur over a relatively long time as the gas stream moves through the dust cake and fabric.

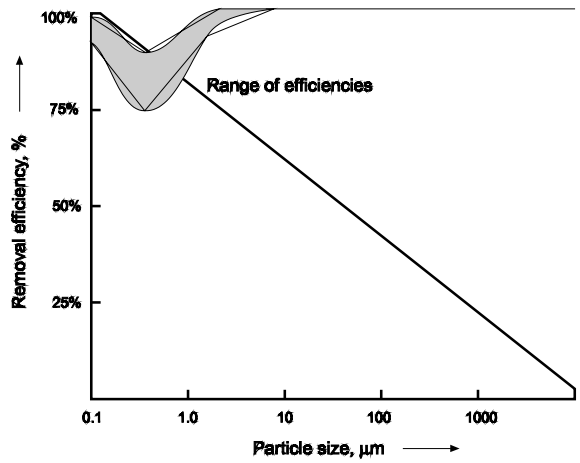

Figure 4-18. Particle size to efficiency relationship

Electrostatic attraction is another particle collection mechanism. Particles can be attracted to the dust layer and fabric due to the moderate electrical charges that accumulate on the fabrics, the dust layers, and the particles. Both positive and negative charges can be generated, depending on the chemical make-up of the materials. Particles are attracted to the dust layer particles or fabric fibers when there is a difference in charge polarity or when the particle has no electrical charge.

Sieving of particulate matter can occur after the dust cake is fully established. The net result of the various types of collection mechanisms is a particle size-efficiency curve, which has relatively high removal efficiency levels even in the difficult-to-control particle size range of 0.2 to 0.5 m as shown in Figure 4-18.

For new bags, the initial particle removal efficiency is not nearly as high as suggested in Figure 4-18. Time is needed to establish residual dust cakes on the surfaces of the fabric. These particles provide the foundation for the accumulation of the operating mode dust cake, which is ultimately responsible for the high efficiency particulate matter removal. The particles on the fabric surface are termed the “residual dust cake” because they remain after normal cleaning of the bag.

The particle size-efficiency curve shown in Figure 4-18 applies only when an adequate dust cake has been established. Immediately after cleaning, patchy areas of the fabric surface may be exposed. Only the residual dust cake remains in these patchy areas. Depending on the particulate matter concentration, it may take several seconds to a minute for the dust cake to "heal" or "repair" over these patchy areas and thereby reduce emissions. During the time that the dust cake is being reestablished, particle removal efficiency can be low, especially for small particles. For this reason, excessive cleaning intensity, frequency, and/or duration can increase particulate emissions.

Particulate matter emissions can be increased dramatically by related phenomena such as particle bleed-through (bleeding) and pore collapse. Both phenomena are related to the quantity of gas passing through a given area of the cloth. This gas flow rate is normally expressed as the air-to-cloth ratio, as defined in Equation 4-1.

$$A/C = \frac{\text{Gas Flow Rate, } ft^3/min \text{ (Actual)}}{\text{Fabric Area, } ft^2} \tag{4-1}$$

As the air-to-cloth ratio increases, the localized gas velocities through the dust cake and fabric increase. At high air-to-cloth values, some particles, especially small particles, can gradually migrate through the dust layer and fabric. This is possible because dust particles within the cake are retained relatively weakly. After passing through the dust cake and fabric, these particles are re-entrained in the clean gas stream leaving the bag. Some of the factors that increase the tendencies for particle bleed-through include the following.

- Small particle size distribution
- Fabric flexing and movement
- Small dust cake quantities

Pore collapse in woven fabrics is also caused by high air-to-cloth ratios. At high air-to-cloth levels, the forces on the particle bridges that span the pores can be too large. Once a bridge is shattered and pushed through the fabric, a pinhole is created in the fabric. The gas stream channels through this low resistance path through the bag.

The net result of bleed-through and pore collapse is increased particulate matter emissions at high air-to-cloth ratios. The general nature of the relationship is shown in Figure 4-19.

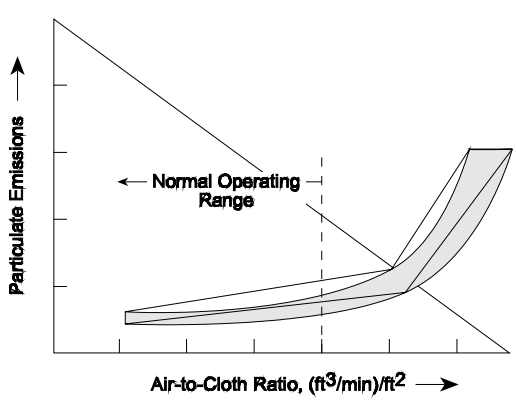

Figure 4-19. Emissions as a function of air-to-cloth ratio

The effect of bleed-through and pore collapse is relatively minor until a threshold air-to-cloth ratio is reached. Above this value, these emissions can increase rapidly.

The curve shown in Figure 4-19 indicates that there is a limit to the air-to-cloth ratio. A baghouse that is severely undersized for the gas flow being treated (high air-to-cloth ratio) can have abnormally low removal efficiency.

4.2.2 Emissions Through Holes, Tears, and Gaps

Low resistance paths for gas flow are created when holes or tears develop in the bags. Gaps in bag seals or in the welds around the tube sheet also create paths for unfiltered gas to pass through the baghouse. As shown in Figure 4-20, the fraction of the total gas stream passing through these openings will increase until the pressure drop across the opening is equivalent to the average pressure drop across the undamaged bags in the compartment.

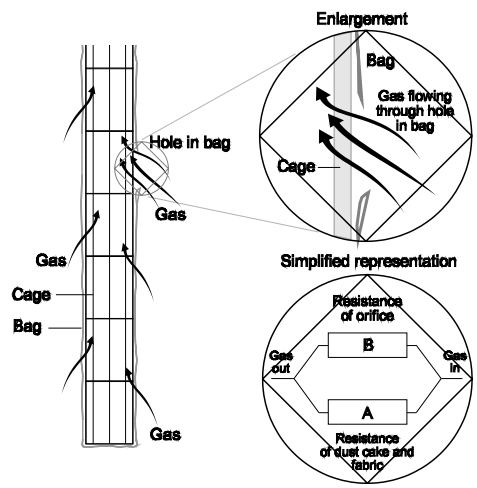

Figure 4-20. Gas flow through holes, tears, and gaps

The quantity of the gas passing through openings can be approximated using the standard orifice equation shown in Equation 4-2.

$$V_o = C\sqrt{\frac{2g_c \Delta p}{\rho_g}} \tag{4-2}$$

Where:

V_o = velocity through the orifice, ft/sec
C = orifice coefficient, dimensionless (usually 0.61)
g_c = gravitation constant, 32.2 ft-lb_m/lb_f-sec^2
p = static pressure drop, lb_f/ ft^2
$_g$ = gas density, lb_m/ft^3

The pressure drop value used in Equation 4-2 is the reduced pressure drop after the hole has developed. However, this is very close to the pre-tear pressure drop except in cases where the area of the hole (or holes) is very large. The velocities and gas flow rates through these holes, tears, and gaps can be quite high, as illustrated in Problem 4-1.

Problem 4-1

Calculate the gas flow rate and gas velocity though a one-inch hole in a bag operating at a pressure drop of 5 in. W.C. Assume that the gas density is 0.05 lb_m/ft^3. Use 0.61 as the orifice coefficient.

Solution:

$$\Delta p = \frac{5\,\text{in. W.C.}}{} \left| \frac{\text{Atm.}}{407\,\text{in. W.C.}} \right| \frac{14.7\,\text{lb}_f/\text{in.}^2}{\text{Atm.}} \left| \frac{(144\,\text{in.}^2)}{\text{ft}^2} \right.$$

$$= 26.0\ \text{lb}_f/\text{ft}^2$$

$$V_O = 0.61\sqrt{\frac{2\left(\frac{32.2\,\text{ft}\cdot\text{lb}_m}{\text{lb}_f \bullet \text{sec}^2}\right)26.0\,\frac{\text{lb}_f}{\text{ft}^2}}{\frac{0.05\,\text{lb}_m}{\text{ft}^3}}}$$

$$= 112\ \text{ft/sec}$$

The area of a one-inch hole is simply $D^2/4$

$$\text{Area} = 3.14\ \frac{[(1\,\text{in.})(\text{ft}/12\,\text{in.})]^2}{4}$$

$$= 0.00545\ \text{ft}^2$$

Solving for the flow rate:

Flow Rate = Velocity Area

= (112 ft/sec) (0.00545 ft^2) (60 sec/min)

= 36.6 ft^3/min

The gas velocity calculated in Problem 4-1 is sufficient to cause fabric abrasion as the particle-laden gas stream passes through the hole. Over time the hole or tear can increase in size because of the abrasion.

The gas flow rate calculated in Problem 4-1 is a significant fraction of the total gas flow rate handled by a normally sized bag operating at an air-to-cloth ratio of approximately 2 ft/min. If there are many of these holes in the bags, particulate emissions can be substantial.

It is important to note that holes, tears, and gaps can allow significant particulate emissions without major changes in the observed static pressure drop across the fabric filter. Because of the balancing of the gas flows between the opening and the undamaged cloth, the overall static pressure drop does not decrease dramatically. It is often difficult to identify these slight drops since the static pressure drop across a baghouse is not usually a constant value.

There are two alternative monitoring locations for both the overall system static pressure drop gauge and the compartment specific static pressure drop gauges. As indicated in Figure 4-21, the gauge can be mounted across the tube sheet that supports the bag and separates the clean side from the unfiltered side of the unit. An instrument in this location is termed the *media static pressure drop gauge* because it indicates the resistance to gas flow caused only by the filter media and the dust cake on the filter media. A gauge that monitors the static pressure drop from the inlet duct to the outlet duct, also shown in Figure 4-21, is termed the *overall static pressure drop gauge*. In this location, the static pressure drop gauge monitors the following flow resistances:

- Frictional losses at the inlet of the fabric filter
- Pressure drop across the media and the dust cake on the media
- Frictional losses at the entrance of the outlet duct
- Acceleration losses at the entrance of the outlet duct

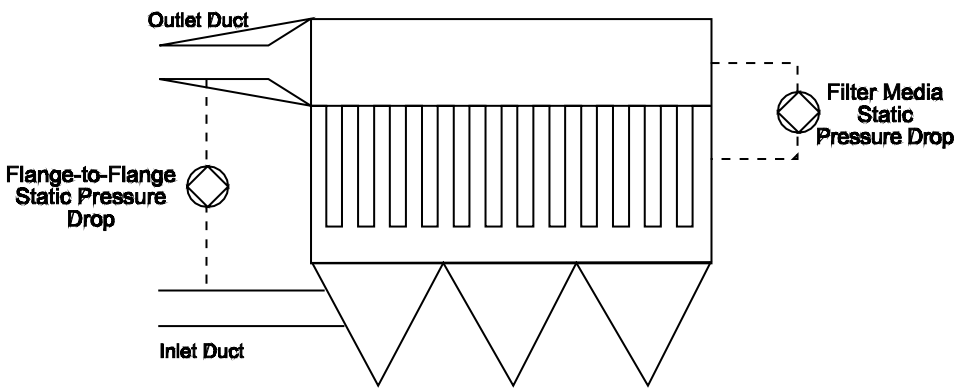

Figure 4-21. Flange-to-flange and filter media static pressure drops

The overall static pressure drop value is usually 1 to 3 in. W.C. higher than the media static pressure drop value. This difference is due primarily to the acceleration losses and frictional losses at the entrance of the outlet duct.

The static pressure drop across the fabric filter system is important for several reasons. Higher-than-expected static pressure drop increases the overall system resistance to gas flow. Decreased gas flow from the process area will result if the centrifugal fan and damper system cannot compensate for this increased resistance. Fugitive emissions can occur when the capture velocities at the hood are too low.

High static pressure drop is also important because electrical energy is needed for the centrifugal fan. This can represent a significant operating cost for the system.

The total static pressure drop across the fabric filter system is the sum of the inlet and outlet ductwork static pressure losses and the static pressure drop across the bags. This is summarized in Equation 4-3.

$$p_{total} = p_{inlet} + p_{outlet} + p_{media\ and\ dust\ cake} \quad (4\text{-}3)$$

The static pressure drop across the bag is the sum of the pressure drops across the fabric and the dust cake. The basic formula for the pressure drop across the clean fabric and dust cake is based on Darcy's law as shown in Equation 4-4.

$$p_f \quad S_E \, v_f$$

Where:

p_f = pressure drop across fabric and residual dust layer (in. W.C.)
S_E = filter drag (in. W.C.•min/ft)
v_f = velocity through filter (ft/min)

Equation 4-4 indicates that the pressure drop across the residual dust layer should be directly proportional to the gas velocity through the fabric. The S_E factor is dependent on the fabric characteristics such as thickness and porosity, which can vary from 0.2 to 2.0 in. W.C.

The static pressure drop across the dust cake is approximated by Equation 4-5.

$$p_c = k_2 \, c_i \, v_f^2 \, t \qquad (4\text{-}5)$$

Where:

p_c = pressure drop across dust cake (in. W.C.)
k_2 = dust cake resistance (in. W.C./(ft/min) lb_m/ft)
v_f = velocity through filter (ft/min)
c_i = particulate concentration (lb_m/ft^3)
t = filtration time (min)

The dust cake resistance parameter is dependent on a variety of factors such as the particle size distribution and the gas velocity. The k_2 factor increases when the dust cake is tightly packed together due to large quantities of small particles or high gas velocities through the dust cake. Gas stream characteristics can also influence the k_2 factor. The k_2 parameters can vary from values as low as 1 to 40 (Turner et al., 1987).

The pressure drop across the dust cake will increase steadily over time as indicated by Equation 4-5. It is necessary to clean the bags when the static pressure drop reaches the design maximum value, which is generally in the range of 5 to 6 in. W.C.

During cleaning, a portion of the dust cake is removed, and the overall pressure drop due to the dust cake is reduced. If the gas flow rate remains constant throughout this filtration-cleaning cycle, a sawtooth-type pressure drop relationship is generated over time. This is illustrated in Figure 4-22.

The variability of the static pressure variations depends on the frequency of cleaning, the intensity of cleaning, and the fraction of bags cleaned at any given time. It should be noted that the particulate removal efficiency does not vary significantly despite these static pressure drop fluctuations. The high efficiency performance characteristics of fabrics are reestablished very soon after dust cake “repair.”

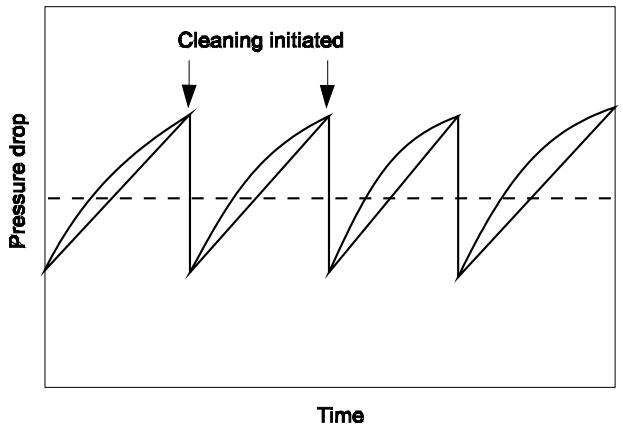

Figure 4-22. Static pressure drop profile

Particulate matter removal efficiency does not increase as the static pressure drop across the baghouse increases. For example, a fabric filter operating at 9 in. W.C. pressure drop does not necessarily have a higher particulate matter removal efficiency than a unit operating at 4 in. W.C. pressure drop. In fact, quite the opposite can be true. Because of the bleed-through and pore collapse modes of emission, particulate matter removal efficiency is often lower when the pressure drop is in the high range. Fabric filters are usually designed for maximum filter media static pressure drops below 6 in. Higher values may indicate cleaning system malfunctions or higher air-to-cloth ratio conditions.

4.2.3 Filter Media Blinding and Bag Blockage

Water droplets in the dust cake can severely increase the resistance to gas flow. At the very least, the water can fill the voids in the dust cake where the gas would normally flow. If the quantity of water is high, the dust cake can be packed tightly together or even form a muddy layer. At this point, the affected portion of the bag is essentially impervious to gas flow. This is termed *fabric blinding*.

Water is not the only substance that can cause blinding, but it is one of the most common. Condensed water droplets can be entrained from the process being treated, or they can be carried in with the compressed air in pulse jet fabric filters. Excessive gas cooling in baghouses serving combustion sources and other sources generating high vapor concentrations can cause water condensation in the dust cakes.

Another common blinding agent is the lubricating oil often present in pulse jet fabric filter compressed air supplies. The oil droplets can deposit in the upper, clean side surfaces of the bags and prevent gas flow. The entire inlet gas stream must, therefore, be filtered in the unaffected lower portions of the pulse jet bag.

“Wet” materials are not the only blinding agents. Submicrometer particles can be driven deep into the fabric if the bag is exposed to a high velocity particulate-laden gas stream before a protective residual dust layer is present. This type of blinding often occurs when a new bag is installed in a compartment with a large number of seasoned bags. Due to the resistance caused by the seasoned bags’ residual dust cakes, the gas velocities through the new bag are excessively high. Submicrometer particle blinding can occur following the installation of new bags at sources that generate high concentrations of submicrometer particulate matter. In these cases, the new bags can be conditioned prior to service by exposing them to resuspended large diameter particulate.

Hopper overflow or solids bridging in hoppers can cause high dust levels. A portion of the filtering area will be inadvertently isolated if these solids block some of the bag inlets in reverse air baghouses. This occurs most often around the exterior walls of the hoppers where cooling of the solids is most severe. If moisture is present, these deposits can become crusty and remain even after the solids in the hopper have been removed. Proper hopper design and frequent emptying are important in minimizing the occurrence of this condition.

4.2.4 Fabric Filter Applicability Limitations

There are several limitations that should be considered when working with fabric filters. Clogging or blinding of the fabric can occur when the particulate is sticky or if moisture is present. Blinding can also occur when large quantities of small particles (0.1 to approximately 2 m) pass through new bags that are not protected by a dust cake. Fabric filters can be designed to operate with moderate blinding conditions. However, they may not be appropriate for very sticky conditions.

Excessive quantities of large particles moving at high velocities can be abrasive and cause erosion of the fabric, especially near the bottoms of the bags. In reverse air units and most pulse jet units, the gas velocities are usually highest near the bottom because of the way the particulate-laden gas stream enters the baghouse. Large particles are the most abrasive and can strike exposed fabric yarns and fibers with considerable force.

Fires and explosions can occur in fabric filters due to the high concentration of dust on the bags and in the upper elevations of the hoppers. These fires and explosions can be ignited by embers from process equipment and even by static electricity generated inside the baghouse. Baghouses can be designed to minimize the risks of fires and explosions. However, when the risk is very high, alternative particulate control systems or combinations of control systems may be necessary.

There are gas temperature limits to the application of fabric filters because of the limits of the fabric itself. At high temperatures, the fabric can thermally degrade, or the protective finishes can volatilize. Accordingly, fabric filters have usually been limited to gas temperatures below approximately 500˚F, which is the maximum long-term temperature of the most temperature-tolerant fabric. Recently commercialized fabrics should tolerate much higher temperatures.

4.3 CAPABILITY AND SIZING

4.3.1 Air-to-Cloth Ratio

The air-to-cloth ratio is the main sizing parameter used for fabric filters. Low values of the air-to-cloth ratio indicate that the velocity of gas passing through a given area of the fabric is relatively low. This favors proper particulate matter capture and moderate static pressure drops.

The gross air-to-cloth ratio is defined as the total fabric area in the baghouse divided by the actual gas flow rate at maximum operating conditions. This is summarized in Equation 4-6.

$$(A/C)_{gross} = \frac{G_{maximum}}{A_{total}} \tag{4-6}$$

Where:

$(A/C)_{gross}$ = gross air-to-cloth ratio ($(ft^3/min)/ft^2$)
$G_{maximum}$ = maximum gas flow rate (ft^3/min (actual temperature and pressure))
A_{total} = total fabric area (ft^2)

The net air-to-cloth ratio is often used for multi-compartment fabric filters where one or more of the compartments is isolated from the gas flow due to cleaning or maintenance. This sizing parameter is defined in Equation 4-7.

$$(A/C)_{net} = \frac{G_{maximum}}{A_{net}} \tag{4-7}$$

Where:

$(A/C)_{net}$ = net air-to-cloth ratio ($(ft^3/min)/ft^2$)
$G_{maximum}$ = maximum gas flow rate (ft^3/min (actual temperature and pressure))
A_{net} = fabric area in filtering service (ft^2)

The gross and net air-to-cloth ratios can be calculated using basic information concerning the number of bags, the dimensions of the bags, and the actual gas flow rate at maximum process operating conditions. The bag areas for cylindrical pulse jet bags and reverse air bags are calculated based on the formula shown in Equation 4-8.

$$A = Dh \tag{4-8}$$

Where:

A = bag area (ft^2)
D = bag diameter (ft)
h = bag height (ft)

Equation 4-8 is the formula for the area of the side of a cylinder. In using this equation, it is assumed that filtration occurs only on the side of the bag, not on the circular top (reverse air) or bottom (pulse jet). This is a reasonable approach because both types of bags usually have a solid cup across the circular area.

The formula for calculating the fabric area of a pleated cylindrical cartridge filter (Figure 4-8) is provided in Equation 4-9. This takes into account the area of the pleats in the filter.

$$A=2nhd \tag{4-9}$$

Where:

A = cartridge area (ft^2)
n = number of pleats
d = depth of pleat (ft)
h = pleat height (ft)

For other types of cartridges, the filter area should be calculated by applying standard geometrical relationships to the shape of the filter surfaces.

Problem 4-2 illustrates the calculation of the gross and net air-to-cloth ratios for a reverse air baghouse. Problem 4-3 illustrates procedures for calculating the gross and net air-to-cloth ratios for a cartridge baghouse.

Problem 4-2

Calculate the gross and net air-to-cloth ratios for a reverse air baghouse with 20 compartments, 360 bags per compartment, a bag length of 30 ft, and a bag diameter of 11 inches. Use an actual gas flow rate of 1.2×10^6 ft^3/min. Assume that two compartments are out of service when calculating the net air-to-cloth ratio.

Solution:

Bag area Dh
Area/bag = 3.14 (11 inches)(ft/12 in.) 30 ft
Area/bag = 86.35 ft^2/bag

The gross air-to-cloth ratio is calculated assuming that all the bags are in service.

$$\text{Total number of bags} = \frac{360\,\text{bags}}{\text{compartment}} \Bigg| \frac{20\ \text{compartments}}{}$$

Total number of bags = 7,200 bags

$$\text{Total fabric area} = \frac{7{,}200\ \text{bags}}{} \Bigg| \frac{86.35\ \text{ft}^2}{\text{bag}}$$

$$= 621{,}720\ \text{ft}^2$$

$$(A/C)_{gross} = \frac{1.2\times10^6\ \text{ft}^3/\text{min}}{621{,}720\ \text{ft}^2} = 1.93(\text{ft}^3/\text{min})/\text{ft}^2$$

The net air-to-cloth ratio is calculated by subtracting the compartments that are not in filtering service.

$$\text{Total number of bags} = \frac{360\ \text{bags}}{\text{compartment}} \Bigg| \frac{18\ \text{compartments}}{}$$

Total number of bags = 6,480 bags

$$\text{Total fabric area} = \frac{6{,}480\ \text{bags}}{} \Bigg| \frac{86.35\ \text{ft}^2}{\text{bag}}$$

$$= 559{,}548\ \text{ft}^2$$

$$(A/C)_{net} = \frac{1.2\times10^6\ \text{ft}^3/\text{min}}{559{,}548\ \text{ft}^2} = 2.14(\text{ft}^3/\text{min})/\text{ft}^2$$

Problem 4-3

Calculate the gross and net air-to-cloth ratios for a cartridge baghouse with 4 compartments, 16 cartridges per compartment, a cartridge length of 2 ft, and a cartridge diameter of 8 inches. Use a pleat depth of 1.25 inches and a total of 36 pleats in the cartridge. Use an actual gas flow rate of 4,000 ft/min. Assume one compartment is out of service when calculating the net air-to-cloth ratio.

Solution:

Bag area = 2nhd
Area/bag = 2 (36 pleats)(2 ft)(1.5 in./(12 in. per ft)
Area/bag = 18 ft^2

The gross air-to-cloth ratio is calculated assuming that all the bags are in service.

$$\text{Total number of bags} = \frac{16 \text{ cartridges}}{\text{compartment}} \left| \frac{4 \text{ compartments}}{} \right.$$

$$\text{Total number of bags} = 64 \text{ cartridges}$$

$$\text{Total fabric area} = \frac{64 \text{ cartridges}}{} \left| \frac{18 \text{ ft}^2}{\text{cartridge}} \right.$$

$$= 1{,}152 \text{ ft}^2$$

$$(A/C)_{gross} = \frac{4{,}000 \text{ ft}^3/\text{min}}{1{,}152 \text{ ft}^2} = 3.47 \text{ (ft}^3/\text{min)/ft}^2$$

The net air-to-cloth ratio is calculated by subtracting the compartments that are not in filtering service.

$$\text{Total number of bags} = \frac{16 \text{ cartridges}}{\text{compartment}} \left| \frac{3 \text{ compartments}}{} \right.$$

$$\text{Total number of bags} = 48 \text{ cartridges}$$

$$\text{Total fabric area} = \frac{48 \text{ cartridges}}{} \left| \frac{18 \text{ ft}^2}{\text{cartridge}} \right.$$

$$= 864 \text{ ft}^2$$

$$(A/C)_{net} = \frac{4{,}000 \text{ ft}^3/\text{min}}{864 \text{ ft}^2} = 4.62 \text{ (ft}^3/\text{min)/ft}^2$$

The appropriate air-to-cloth ratio for a given application depends on the particle size distribution, fabric characteristics, particulate matter loadings, and gas stream conditions. Low values for a design air-to-cloth ratio are generally used when the particle size distribution includes a significant fraction of submicrometer particulate matter or when the particulate loading is high. The air-to-cloth ratios for cartridge filters are usually maintained at values less than approximately 4 $(ft^3/min)/ft^2$. A summary of air-to-cloth ratio values for pulse jet and reverse air fabric filters in a variety of industries is provided in Table 4-3. Some caution is warranted in reviewing any table of this type, because the design air-to-cloth ratios were gradually decreased over the past 20 years, and there can be significant site-to-site differences in the particle size distributions, particulate loadings, and fabric characteristics. Furthermore, the regulations based on the Clean Air Act Amendments of 1990 place even greater demands on fabric filter performance. Accordingly, historical design data may not be strictly applicable to a specific application.

Table 4-3. General Summary of Air-to-Cloth Ratios in Various Industrial Categories

Industry	Reverse Air[1]	Pulse Jet[2]
Basic Oxygen Furnaces	1.5 – 2.0	6 – 8
Brick Manufacturers	1.5 – 2.0	9 – 10
Coal-Fired Boilers	1.0 – 1.5	3 – 5
Electric Arcs	1.5 – 2.0	6 – 8
Feed Mills	–	10 – 15
Grey Iron Foundries	1.5 – 2.0	7 – 8
Lime Kilns	1.5 – 2.0	8 – 9
Municipal Incinerators	1.0 – 2.0	2.5 – 4.0
Phosphate Fertilizer	1.8 – 2.0	8 – 9
Portland Cement	1.2 – 1.5	7 – 10

Source: EPA 450/3-76-014.
Notes:
1. Usually woven fabrics
2. Usually felted fabrics

In sizing a fabric filter system, the “quality” of fabric utilization can be as important as the "quantity" of fabric (indicated by the air-to-cloth ratios). A variety of other design factors should be considered, such as:

- Gas approach velocity
- Bag spacing and length
- Bag "reach" and accessibility

4.3.2 Gas Approach Velocity

Gravity settling of dust cake agglomerates, sheets, and particles released during bag cleaning is a critical step in the fabric filtration process. If fine particles with inherently poor terminal settling velocities (Chapter 2) return to the bag-dust cake surface, there can be adverse effects on both collection efficiency and static pressure drop.

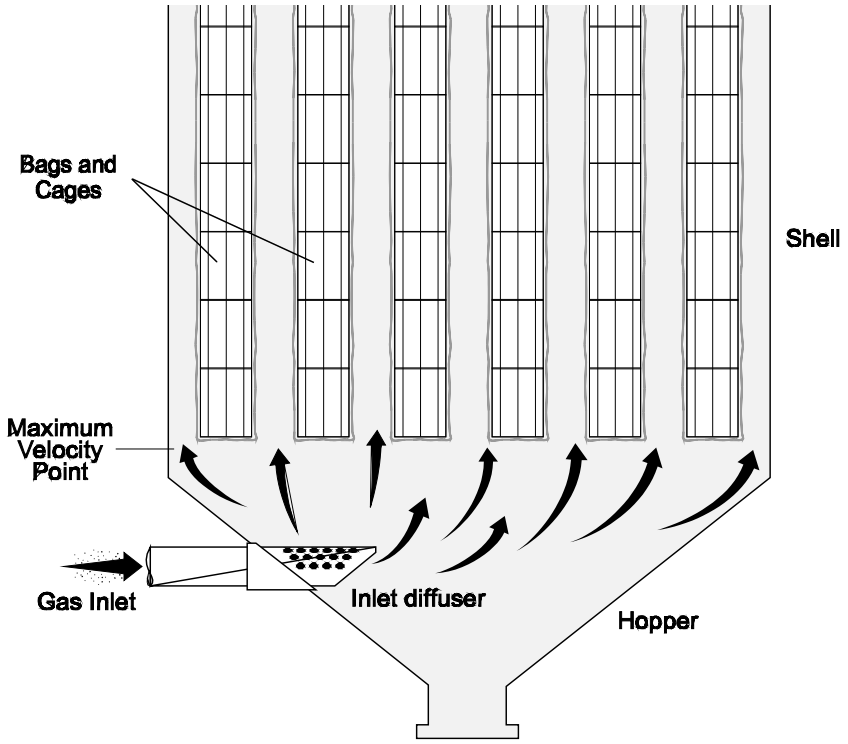

Figure 4-23. Gas approach velocity for pulse jet baghouse (on-line cleaning)

In both pulse jet and reverse air fabric filters, there is a point of maximum inlet gas velocity. In pulse jet units, the point of maximum velocity is the area around the bottoms of the bags. As shown in Figure 4-23, all the particulate-laden gas to be filtered by the bags must pass through this area in order to reach the bag surfaces. For units that use on-line cleaning (compartment remains in filtering mode while row-by-row cleaning is in progress), the dust released during cleaning must fall through this area as it settles by gravity. If the upward velocity of the inlet gas stream exceeds the downward terminal settling velocity, the particles will be caught and return to the bag-dust cake surface.

A similar, although less severe, problem can exist in reverse air fabric filters. In this case, the maximum velocity area is the bag inlet at the tube sheet. All the gas filtered by the bag must enter through this area as shown in Figure 4-24. During cleaning, all the dust released must settle through the inside of the bag, pass through the tube sheet opening, and enter the hopper.

The following design features are just two of the many factors that minimize gravity settling problems in reverse air units.

- The compartment is isolated from inlet gas flow during cleaning.
- The downward movement of the reverse air carries small particles at velocities greater than their terminal settling velocities.

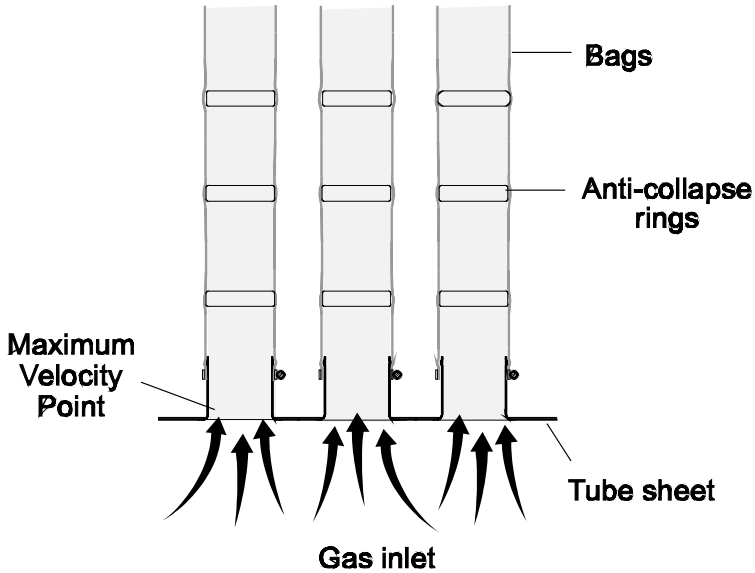

Figure 4-24. Gas approach velocity in reverse air baghouse

Gravity settling problems can also occur in reverse air fabric filters when there are inadequate reverse air flow rates and when the dampers do not seal properly. In these cases, small particles are not aided by the downward movement of the reverse air, and their settling may even be opposed by modest inlet gas flow into the bags during the cleaning cycle.

The air-to-cloth ratio is one factor that affects the severity of gravity settling problems, especially in pulse jet fabric filters. The gas approach velocity is directly proportional to the air-to-cloth ratio, as illustrated in Problem 4-4. A comparison of the calculated approach velocity indicates that even 100 m particles released from the dust cake will not settle by gravity (Chapter 2). It is important that the large dust agglomerates or sheets be released, not just small agglomerates or individual particles.

Problem 4-4

What is the difference in gas approach velocities for two identical pulse jet fabric filters with the following design characteristics?

Characteristic	Unit A	Unit B
Compartment area, ft^2	130	130
Number of bags	300	300
Bag diameter, in.	6	6
Bag height, ft	10	10
Air-to-cloth ratio, $(ft^3/min)/ft^2$	5	8

***Solution**:*

The bag area for both units is identical. It is calculated using the circumference of the bag times the height.

$$\text{Bag area} = Dh = \frac{3.14}{}\left|\frac{6\text{inches}}{}\right|\frac{1\text{ foot}}{12\text{inches}}\left|\frac{10\text{ feet}}{}\right.$$

$$= 15.7\ \text{ft}^2/\text{bag}$$

$$\text{Total bag area} = \frac{300\text{ bags}}{}\left|\frac{15.7\ \text{ft}^2}{\text{bag}}\right. = 4{,}710\ \text{ft}^2$$

$$\text{Total gas flow rate, Unit A} = \frac{5\left(\text{ft}^3/\text{min}\right)}{\text{ft}^2}\left(4{,}710\ \text{ft}^2\right)$$

$$= 23{,}550\ \text{ft}^3/\text{min}$$

$$\text{Total gas flow rate, Unit B} = \frac{8\left(\text{ft}^3/\text{min}\right)}{\text{ft}^2}\left(4{,}710\ \text{ft}^2\right)$$

$$= 37{,}680\ \text{ft}^3/\text{min}$$

The area for gas flow at the bottom of the pulse jet bags is identical in both units.

Area for flow = total area – bag projected area
= total area – no. of bags circular area of bag at bottom
= 130 ft^2 – 300 ($D^2/4$)
= 130 ft^2 – 58.9 ft^2
= 71.1 ft^2

$$\text{Gas approach velocity for Unit A} = \frac{23{,}550\ \text{ft}^3/\text{min}}{71.1\ \text{ft}^2} = 331\ \text{ft/min}$$

$$\text{Gas approach velocity for Unit B} = \frac{37{,}680\ \text{ft}^3/\text{min}}{71.1\ \text{ft}^2} = 530\ \text{ft/min}$$

4.3.3 Bag Spacing and Length

In pulse jet baghouses, the bag arrangement in the baghouse and the length of the bag affects gravity settling problems and causes bag abrasion.

The approach velocity is directly proportional to the height of the bag. For example, an increase in the bag height to 16 ft from 10 ft in Unit B (Problem 4-4) would increase the approach velocity 60% to approximately 850 ft/min as long as the air-to-cloth ratio remained constant. Furthermore, particles and small dust cake agglomerates would have a longer distance to travel with the taller bag. Both factors increase the susceptibility to gravity settling-related emission and pressure drop problems.

Approach velocities are also a function of bag spacing. Units that crowd the bags close together have high approach velocities because there is very little area between the bags for the inlet gas stream to pass through. For example, the velocities calculated in Problem 4-4 were based on a unit having bags on 8-inch centers (8 in. from center of bag to center of adjacent bag). If the bags in Problem 4-4 were spaced on 7-inch centers, the approach velocities for Units A and B would be 571 and 913 ft/min, respectively.

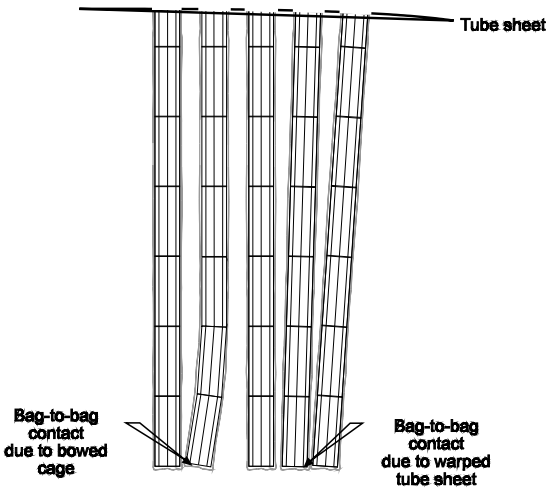

Figure 4-25. Possible problems with tall pulse jet bags

Gravity settling and bag cleaning in general would be significantly more difficult at these high velocities. It is usually preferable to space the bags far apart to minimize this potential problem. However, there are practical limits to the bag spacing because wide spacings increase the size of the baghouse shell and the area needed for the baghouse.

Pulse jet bag height and spacing are important for reasons that are entirely separate from the gas approach velocity. Bag-to-bag abrasion can occur at the bottoms of the bags because they hang freely from the tube sheet. Slight bows in the pulse jet bag support cages or slight warpage of the supporting tube sheet can cause bag-to-bag contact at the bottom, as illustrated in Figures 4-25 and 4-26. Abrasion damage can occur due to the slight movement of the fabric and cage during each pulse cycle. Holes can develop within several weeks to several months of routine operation, depending on the abrasion sensitivity of the fabric being used. Pulse jet units with relatively short bags are less vulnerable to this mode of bag failure.

A variety of other practical problems limit bag height. Very tall bags are often difficult to install in a pulse jet baghouse when there is limited overhead clearance to remove the failed bag mounted on the rigid cage. In some cases, failed bags partially fill with solids and, in the case of tall bags, the weight can be substantial. For all these reasons, relatively short bags of 8 to14 ft are preferable to tall bags, which can be as high as 20 ft.

Bag height and spacing are also important for reverse air fabric filters. However, the problems with height are less severe because reverse air bags are fixed at both the top and the bottom. Tall reverse air bags are vulnerable to bag tension problems caused by the weight of dust on the bag. This can lead to bag sagging if the support springs become overloaded. Once this happens, bag abrasion can be rapid because the folds of sagging fabric are usually in the direct path of the bag inlet gas stream. Reverse air bags are usually less than 32 ft. in height.

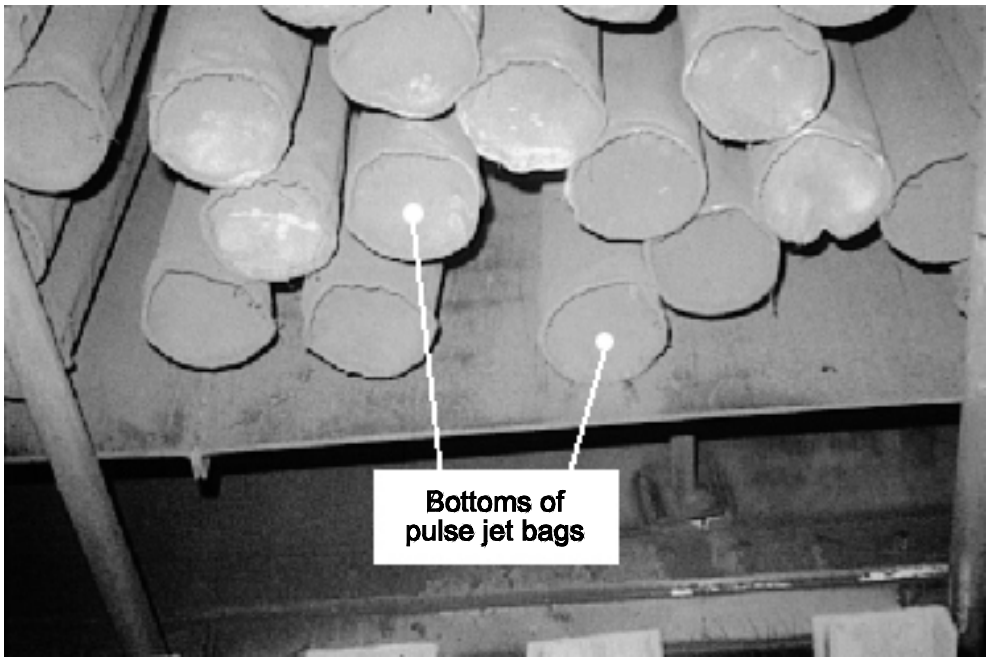

Figure 4-26. Pulse jet bag-to-bag contact

4.3.4 Bag "Reach" and Accessibility

Access for bag inspection and replacement is important. In the case of reverse air baghouses, sufficient space should be allowed so that each bag can be checked visually and either capped off (bag opening sealed) or replaced if necessary. One measure of the accessibility provided for the maintenance staff is termed the *bag reach*. This is simply the maximum number of rows of bags from the nearest access walkway. For example, the plan view (top view) drawing of a single baghouse compartment shown in Figure 4-27 has a reach of three. Each row of bags in the center of the compartment is no more than three rows deep from the nearest walkway. Accordingly, it is possible for plant maintenance staff to find and correct bag problems. Units with less accessible bags are difficult to service. Furthermore, it is possible to damage bags in the outer rows while attempting to work on bags in rows far from the access walkways. There is no single value for bag reach that is considered appropriate for reverse air baghouses. However, units with a minimum reach are easier to maintain.

4.3.5 Cleaning System Design

Proper bag cleaning is critical to ensuring minimum stack emissions, minimum process fugitive emissions, and minimum bag damage. Over-cleaning removes too much of the dust cake and permits short-term emissions during dust cake repair. If over-cleaning has been chronic, bag holes and tears can be caused by cleaning-related abrasion and flex. If the cleaning system fails to operate or if cleaning is too gentle, high static pressure drops will result from the heavy dust layers. If the system fan dampers cannot compensate for this change in gas flow resistance, the gas flow will drop as shown in Figure 4-28. This can reduce pollutant capture at the process hood.

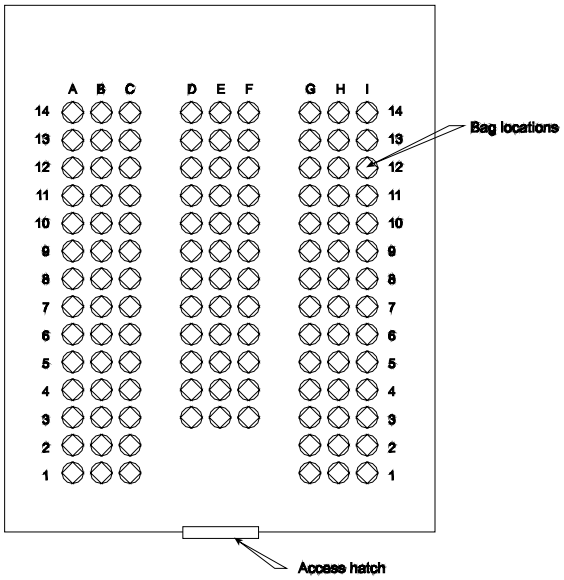

Figure 4-27. Layout of reverse air bags

As discussed in Chapter 3, a small increase in the fugitive emissions can significantly affect total emissions to the atmosphere from the process equipment being controlled.

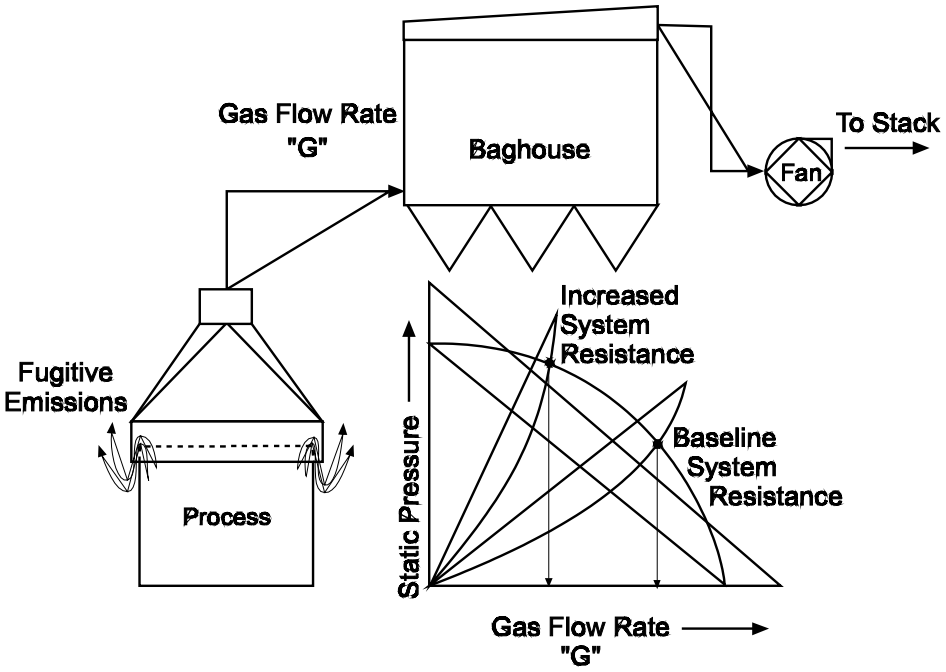

Figure 4-28. Process fugitive emissions caused by increased gas flow resistance through a baghouse

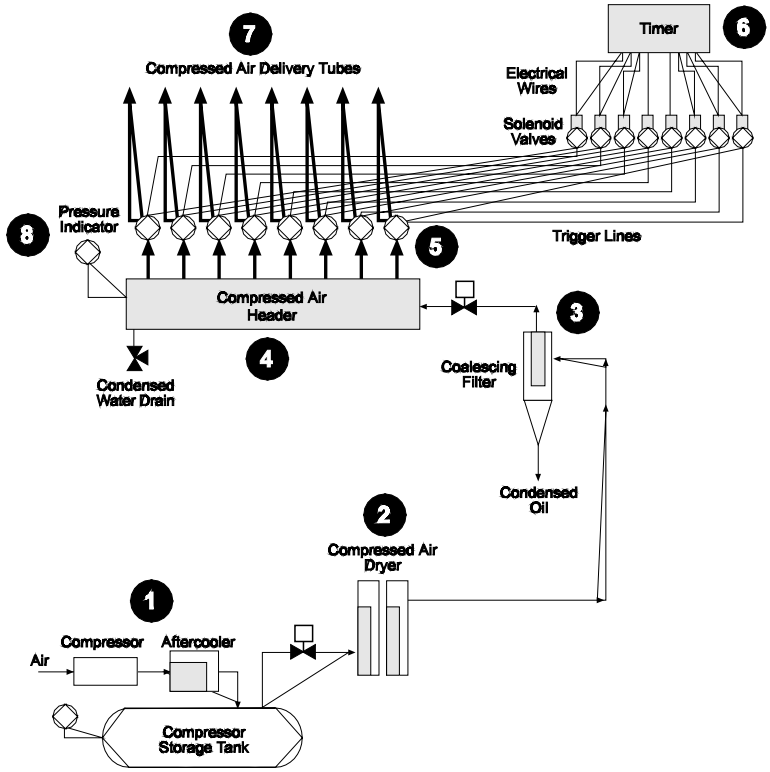

Figure 4-29. Major components of a pulse jet baghouse cleaning system

The main components of the pulse jet and cartridge cleaning system are illustrated in Figure 4-29. The major components include (1) a source of compressed air, (2) a drier, (3) a coalescing filter, (4) a compressed air header, (5) diaphraghms and solenoid valves, (6) a solenoid valve controller, (7) compressed air delivery tubes, and (8) instrumentation.

The source of compressed air for bag cleaning can be an air compressor dedicated to the specific baghouse or the plant air system. Dedicated compressors are often used for very large systems, but they are rarely economically practical for systems handling less than approximately 100,000 ACFM.

Dedicated compressors usually include an aftercooler to reduce the high temperature caused by compression, a pressure regulator to control the compressor, and a compressed air storage tank. The compressed air is usually located within a plant building that may be far removed from the location of the baghouse itself. The compressed air is piped from the storage tank to the compressed air headers mounted on the side walls of the pulse jet or cartridge filter units.

A drier is sometimes used on a compressed air supply (plant air or dedicated compressor) to reduce the water content. Ambient moisture compressed along with the air can condense once the compressed air stream begins to cool. This moisture can accumulate in the compressed air header and be entrained in the cleaning air injected into the bags or cartridges. Water entering the bags can cause blockage of the filter due to the formation of muddy deposits. The types of driers used on compressed air supplies include refrigerant and dessicant driers. These driers usually reduce the water vapor dewpoint of the gas stream to levels 20°F to 30°F below the lowest ambient wintertime temperature at the location of the baghouse. These low water vapor dewpoints mean that the water vapor levels are less than 5% of the levels of

untreated compressed air.

A coalescing filter is often used after the compressor to remove entrained oil droplets. The oil is introduced into the compressed air stream by the vaporization of lubricating oil used in certain types of compressors. After the compressed air cools, the oil vapor can condense to form oil droplets. If they are not removed, the oil droplets can accmulate on the bag surface and eventually cause blockage of gas flow.

A typical compressed air header is shown in Figure 4-30. These provide a reservior of compressed air to support the operation of the diaphragm valves during a cleaning cycle. There is a connection to each diaphragm valve serving each row of the baghouse. It is important that these connections and the header itself be leak free to ensure that the header remains at the necessary air pressure. In most systems, the compressed air pressure is in the range of 60 to 120 psig.

For baghouses that do not have driers on the compressed air supply, the compressed air header is usually mounted below the elevation of the diapragm valves to prevent condensed water carryover into the bags. The quantity of condensed water in these headers can be quite large as illustrated in Problem 4-5.

Problem 4-5

What is the total quantity of water that accumulates in a compressed air header over a one-week operating period for a header serving a pulse jet baghouse with 10 rows of bags and 10 bags per row? Assume that the compressed air usage during each pulse is approximately 1 SCFM per bag and that the ambient moisture level is 3% by volume. Assume that the cleaning frequency is one complete pulsing cycle (10 rows cleaned) every 15 minutes.

Solution:

The quantity of air used per hour is:

10 SCFM/row (10 row/15 min)(60 min/hr) = 400 SCF/hr

The quantity of air used in a week is:

400 SCF/hr (168 hr/week)=67,200 SCF/week

The moisture content is: (0.03) 67,200=2016 SCF water/week

If 100% of the water vapor is condensed in the header, the total quantity of water accumulating in a one-week period would be:

(2016 SCF water/week)(lb mole/385.4 SCF)(18 lb mole water/lb mole)
= 94.2 lb water/week

(94.2 lb water/week)(gal/8.76 lb) = 10.7 gallons per week

It is apparent that a large quantity of water can accumulate in this area. Therefore, it is important to minimize the vulnerability of the cleaning system to carryover of the condensed water to the bags or cartridges in the baghouse. A drain with a valve is often mounted on a low spot of the compressed air manifold to facilitate routine draining of this condensed moisture.

The opening and closing of the diaphragm valve serving each row of bags or cartridges is controlled by a solenoid valve. As indicated in Figure 4-30, there is one solenoid valve for each diaphragm valve. The solenoid is a "normally closed" design. The cleaning cycle controller sends an electrical signal to the solenoid (often termed the "pilot" valve) to open this valve. This allows compressed air to flow from the trigger line that connects the diaphragm valve to the solenoid valve. The release of compressed air from the back of the diaphragm valve causes an imbalance of forces on the diaphragm plate which causes it to snap backwards. This allows compressed air from the compressed air header to move through the open diaphragm valve and enter the delivery tube passing above the row of bags.

There are a number of different designs for the diaphragm and solenoid valves. They can be separate as indicated in Figure 4-30, or they can be mounted together in a "double acting" valve. In the double acting units, the trigger line is a short connecting piece located within the body of the valve assembly. The size (compressed air capacity) of the valve depends on the number of bags in the row to be cleaned, the compressed air quantity for each bag being cleaned, and the design characteristics of the delivery tubes.

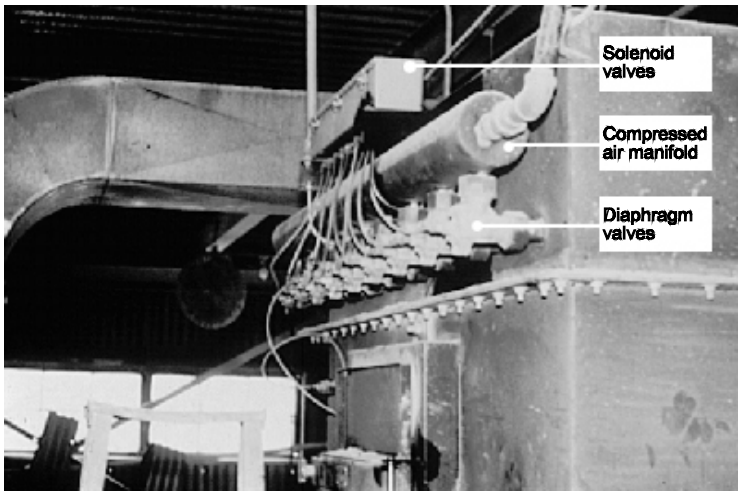

Figure 4-30. Vulnerable position of diaphragm valve relative to compressed air manifold in certain designs

The cleaning cycle for pulse jet and cartridge type baghouses can be either a standard timing board or a differential pressure transmitter and controller. The timing board simply activates the cleaning cycle on a frequency set by the operator. The differential pressure transmitter and controller monitors the media static pressure drop and activates the cleaning cycle whenever the static pressure drop exceeds the maximum level set by the operator.

The compressed air delivery tube transports the compressed air from the discharge side of the diaphragm valve to the inlet of each bag or cartridge in the row. These tubes have either a small orifice or an extension tube on the lower side. This hole or extension tube directs the compressed air to the center of the bag or cartridge. The actual pressure generated at the bag or cartridge inlet depends on the quantity of compressed air in the pulse, the size of the hole or extension tube, and the distance between the hole or extension tube attaches to the inlet of the bag or cartridge.

It is important to orient the delivery tube so that the orifice or extension tube points straight into the bag

or cartridge. Rotation of the delivery tube could cause abrasion of the filter media due to the force of the incoming compressed air pulse. For this reason, many types of pulse jet and cartridge fabric filters have a mounting on the delivery tube to ensure that it can only be placed in the proper orientation.

It is also important to securely fasten the compressed air delivery tube in the baghouse. This tube experiences a pressure rise from ambient pressure (approximately 14.7 psia at standard conditions) to more than 60 psig in a time period of 10 to 50 milliseconds. If this tube is not firmly secured, it can break free. Most baghouses have a fastener on the end of the delivery tube to ensure that it does not move. This same fastener is often used to ensure that the delivery tube is properly rotated. The use of the clamps and other fasterers is important because baghouse operators must remove and reinstall the delivery tubes each time it is necessary to change one or more bags (or cartridges) in the row served by the delivery tube.

The instrumentation for the compressed air pulsing system is usually quite limited. There is usually a compressed air pressure gauge on the storage tank of the compressor and on each compressed air header serving the baghouse. The compressed air pressure data can be used in conjuction with the overall static pressure drop data for the baghouse to confirm that the baghouse cleaning system is performing properly.

Diaphragm valve freezing is a problem that can significantly increase static pressure drop. Diaphragm valve freezing can be minimized by one or more of the following actions:

- Using a compressed air drier
- Relocating the compressed air manifold below the elevation of the diaphragm valves
- Enclosing the diaphragm valves, manifold, and solenoid valves in a weatherproof enclosure and, if necessary, providing heat
- Using drains on manifolds to remove accumulated water on a routine basis

Misrotation of the compressed air tubes contributes to high pulse jet baghouse static pressure drop, regardless of the compressed air pressure or the operability of the diaphragm valves. If the tubes are not installed properly, the orifice or nozzle above the bags can be rotated out of the necessary plumb position. This causes the compressed air pulse to strike the side of the bag near the top, and bag holes are created. This problem is minimized by proper design of the tube and its mounts so that maintenance staff can determine the proper orientation of the tube during reinstallation.

Breakage of the small diameter tubes (also called “trigger lines”) between the diaphragm valve and solenoid valve can adversely affect cleaning by leaking compressed air needed for cleaning other bag rows. When the solenoid valve is closed, compressed air fills these trigger lines and a small portion of the diaphragm valve. This pressure keeps the diaphragm valve closed. When it is necessary to activate the diaphragm valve, the solenoid valve is opened, and the compressed air in the trigger line is exhausted to the atmosphere. The diaphragm valve snaps open at this time and allows compressed air to flow into the delivery tube above the row of bags. A fraction of a second later, the solenoid valve is closed, the trigger line again fills with compressed air, and the diaphragm valve closes. If the trigger line is broken, the diaphragm valve cannot be closed, and compressed air continues to flow through the affected valve.

Excessive cleaning of pulse jet bags can simultaneously cause higher-than-normal emissions, higher-than-normal static pressure drop, and accelerated bag wear. If there is insufficient dust cake on the bag when it is cleaned, particles or small agglomerates of particles can be dispersed. These particles do not settle by gravity and simply return to the bag at an area where the dust cake is thin; they can accumulate

as a low porosity cake, thereby increasing pressure drop. Over time, these fine particles can bleed through the bag and cause opacity spiking after the cleaning pulse. The bleeding mode of emissions is caused, in part, by the deceleration shock occurring when the just-pulsed bag crashes back against the cage as the bag returns to filtering service (on-line cleaning units only).

The frequency of cleaning should be set by balancing the limits on high static pressure drop with the need to allow a moderate dust cake to accumulate on the bags between each cleaning cycle.

4.3.6 Reverse Air Fabric Filters Cleaning System Design

The main components of the cleaning system for a reverse air fabric filter are shown in Figure 4-31. This system consists of one or more reverse air fans, a set of dampers to control gas flow to each compartment, and instrumentation to monitor compartment conditions before and after cleaning.

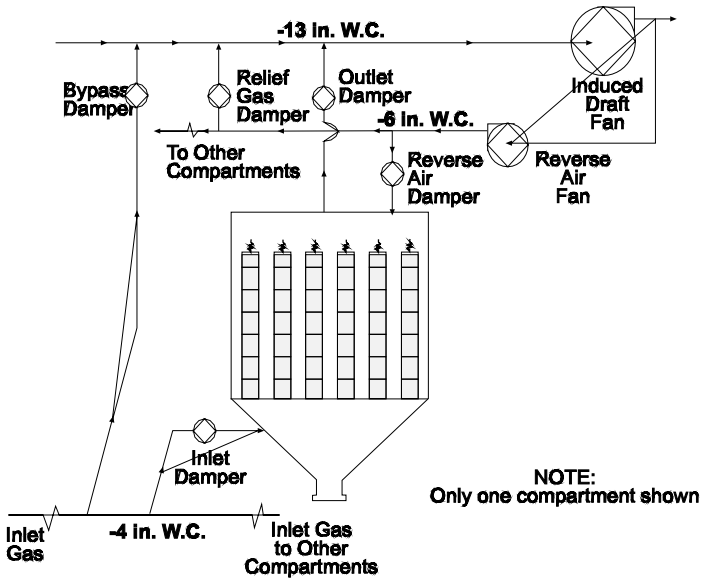

Figure 4-31. Damper in a reverse air baghouse
(typical static pressures shown)

The cleaning cycle is initiated by closing the outlet damper(s) on the compartment to be cleaned. During normal operating conditions, the static pressure drop should drop to zero because no gas is flowing through the compartment. There is usually a short null period to allow the fabric to "relax." Then the reverse air damper is opened, and filtered gas is passed from the outside of the bags to the inside in order to remove some of the dust and drive the dust into the hopper. The reverse gas then passes through the open inlet damper and reenters the gas stream inlet duct leading to other compartments that are in the filtering mode.

During the reverse gas flow period, the normal static pressure drop should be 0.25 to 3 in. W.C. in the reverse direction (negative direction in Figure 4-32). After reverse gas cleaning, there is a second null period to allow time for particles to settle by gravity out of the bags. The outlet damper(s) for the compartment is then reopened, and it returns to filtering service.

The reverse air fans are sized considerably smaller than the main system fan (usually induced draft). The reverse air fan needs only to supply sufficient gas flow to clean a single compartment at a time. The gas flow needed to dislodge the dust cake from the interior of the bags and to carry the particulate matter into the hopper is usually less than 1/3 to1/2 the gas flow rate that passes through the compartment during on-line filtration. Specific sizing criteria for a given system are site specific because they depend on factors such as (1) the difficulty in dislodging dust from the bags, (2) the bag dust cake retention characteristics, (3) the residual dust cake characteristics in the bag, (4) the particulate mass loading at the inlet of the fabric filter, and (5) the anticipated frequency of cleaning needed.

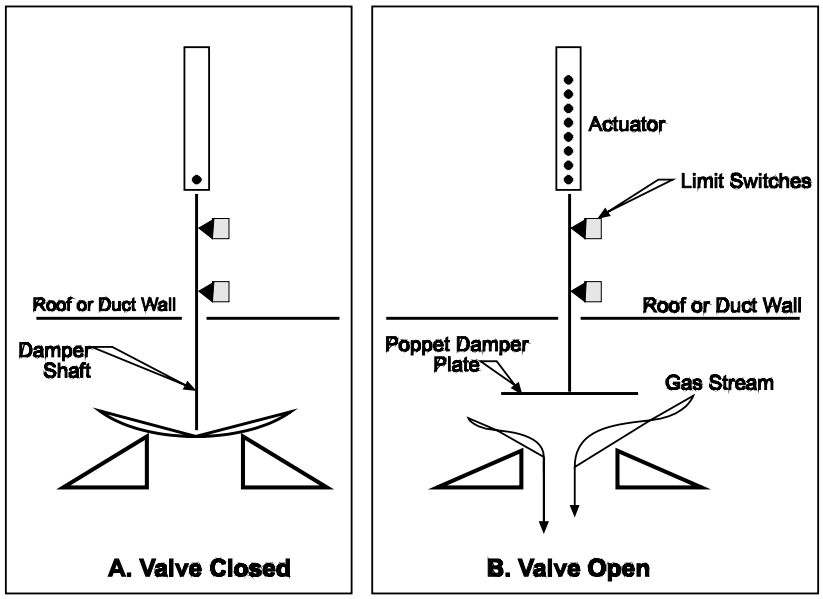

Figure 4-32. A standard poppet valve in open and closed positions

The design of the dampers used to control gas flow in and out of the compartment is very important in ensuring that the reverse air fabric filter will perform properly. A typical poppet damper is illustrated in Figure 4-32. This consists of a damper seat, a damper plate, the support rod, an actuator, and limit switches. The poppet damper can be oriented to use either the upper or lower surface of the damper plate for sealing against the damper seat. The damper shown in part A of Figure 4-32 uses the lower surface for sealing. When the damper is closed (part B), the damper sealing plate often deflects slightly. The maximum gap around the circumference of the sealing surface is minimized to prevent improper gas movement through the closed damper. When it is necessary to open the damper, the actuator lifts the support rod until the limit switch indicates that the damper plate is fully lifted. A second limit switch is used during closing of the damper to shut off the actuator when the damper has returned to the closed (sealed) position.

Proper sealing of the compartment dampers is critical to ensuring proper operation of the cleaning cycle. For example, Problem 4-6 illustrates the static pressures that exist in a typical system during a cleaning cycle.

Problem 4-6

Based on the static pressure data shown in Figure 4-31, calculate the static pressure for the cleaning air passing through the bags. Calculate the static pressure drop for the cleaning air stream leaking through a partially open outlet damper (shown with an arrow) at the top of the compartment.

Solution:

Static pressure drop for normal cleaning direction

$$= |-6 \text{ in. W.C.} - (-4 \text{ in. W.C.})|$$

$$= 2 \text{ in. W.C.}$$

Static pressure drop for leakage flow through outlet damper

$$= |-4 \text{ in. W.C.} - (-13 \text{ in. W.C.})|$$

$$= 9 \text{ in. W.C.}$$

Poorly sealing outlet dampers can cause especially serious cleaning system problems. If they leak significantly, the compartment is not fully isolated from the inlet gas stream. Particulate-laden air can continue to flow into the bags. This movement opposes any gravity settling of particulate. Furthermore, the cleaning effectiveness is almost entirely compromised since the reverse gas flow is simply exhausted through these partially open dampers. Due to the prevailing static pressures, the reverse gas stream is pulled strongly toward the outlet dampers rather than through the bags and toward the inlet duct.

Whenever reverse gas cleaning is impaired, high dust cake quantities can accumulate in the bags. This can overload the support springs and cause the bags to sag. This causes premature bag failure due to flexing at the fabric creases, and abrasion of particulate in the inlet gas stream that is blasting the slack portions of the bag.

4.3.7 Air Infiltration

Fabric filters that operate under negative static pressure (lower than atmospheric pressure) are vulnerable to air infiltration-related bag damage. In severe cases, air infiltration can also cause significant process fugitive emissions. Baghouses must be designed properly to minimize their vulnerability to these problems.

Bag damage is caused by localized areas within the baghouse that are at or below the sulfuric acid dew point for a significant portion of the operating time because of air infiltration. When sulfuric acid condenses on the surfaces of the bags, it can chemically attack the fabric. For most coal-fired boilers, the acid dew point is in the range of 200°F to 300°F. The dew point is generally related to the coal sulfur content, with high dew points associated with high sulfur levels. However, there are large differences between units in the concentration of sulfuric acid generated. It is usually necessary to maintain baghouse temperatures 20°F to 50°F above the estimated dew point to account for spatial gas temperature differences. Common sites for air infiltration in pulse jet and reverse air fabric filters are listed in Table 4-4.

Table 4-4. Common Sites of Air Infiltration
Pulse Jet Fabric Filters
• Hopper solids discharge valves and poke holes
• Top access hatches
• Inlet duct and outlet duct expansion joints
• Improperly welded shell
• Improperly sealed electrical conduits
Reverse Air Fabric Filters
• Hopper solid discharge valves and poke holes
• Side access hatches
• Compartment ventilation air ducts
• Improperly welded or gasketed shell
• Corroded shell

The access hatches for a top-load pulse jet baghouse are shown in Figure 4-33. These hatches are especially prone to leakage because they are directly above the clean gas plenum, which handles the filtered gas going to the fan (negative pressure units only). At this position, the gas stream is at the lowest static pressure of the entire system. Accordingly, there is a large pressure difference between the ambient air above the hatch and the filtered gas below the hatch. To minimize air infiltration, the hatches should be designed with a number of latches or clamps to ensure that they can be firmly secured in position. Many commerical units use stiffeners in the hatches to minimize warpage. Gaskets around the periphery of the hatch can also help minimize air infiltration.

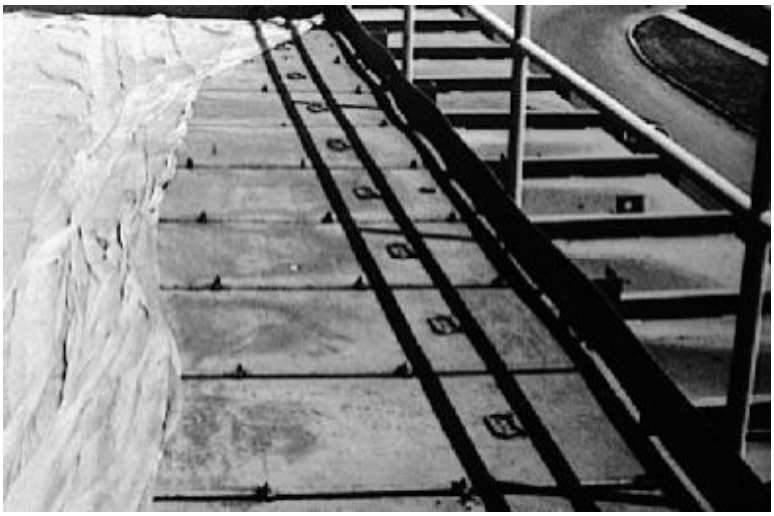

Figure 4-33. Top access hatches on a top-load pulse jet baghouse

Other common sites of air infiltration are the corroded holes on the side walls of fabric filters, as shown in Figure 4-34. These holes initially form due to the condensation and absorption of sulfuric acid or other acid gases into the moisture that accumulates on the interior of poorly insulated surfaces. As cold ambient air rushes through the hole, additional cooling and acid vapor condensation occurs. Accordingly, the hole can grow rapidly.

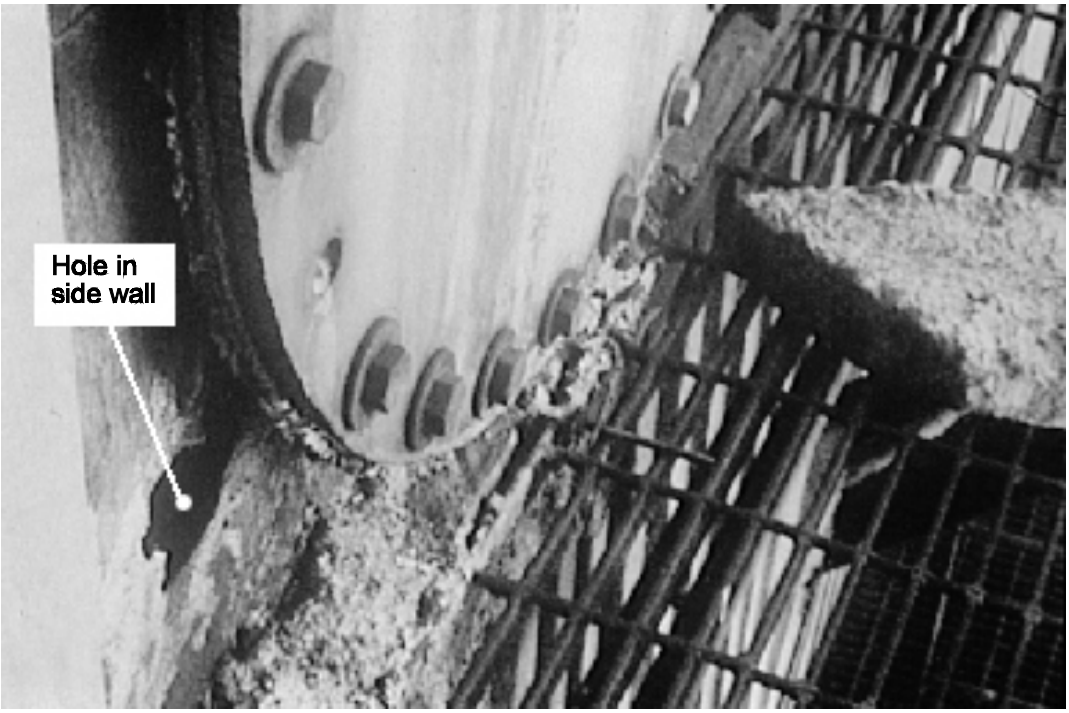

Figure 4-34. Corroded area on the side wall of a baghouse

These air infiltration sites can be minimized by proper thermal insulation of the shell and access hatches. It is important to prevent moisture accumulation on cold spots on the interior surfaces of the shell. Acid gases can absorb into condensed moisture and can cause corrosion of the metal.

4.3.8 Hopper Design

Hoppers must be designed to facilitate proper solids discharge. High solids levels due to blockage in the baghouse hoppers are very undesirable. The solids can be reentrained by the inlet gas stream and contribute to abrasion damage at the lower portions of both pulse jet and reverse air bags. The bag inlets of reverse air bags can be blocked as the solids levels increase. Some useful hopper design features are shown in Figure 4-35.

Thermal insulation and hopper heaters keep solids hot prior to discharge. Hot air keeps the solids in a free-flowing condition. It moves the material through the constricted area of the hopper and the hopper throat. Outer lagging over the insulation keeps the insulation dry and prevents air from passing upward along the outside wall due to a chimney effect (warm air rises; cold air replaces it).

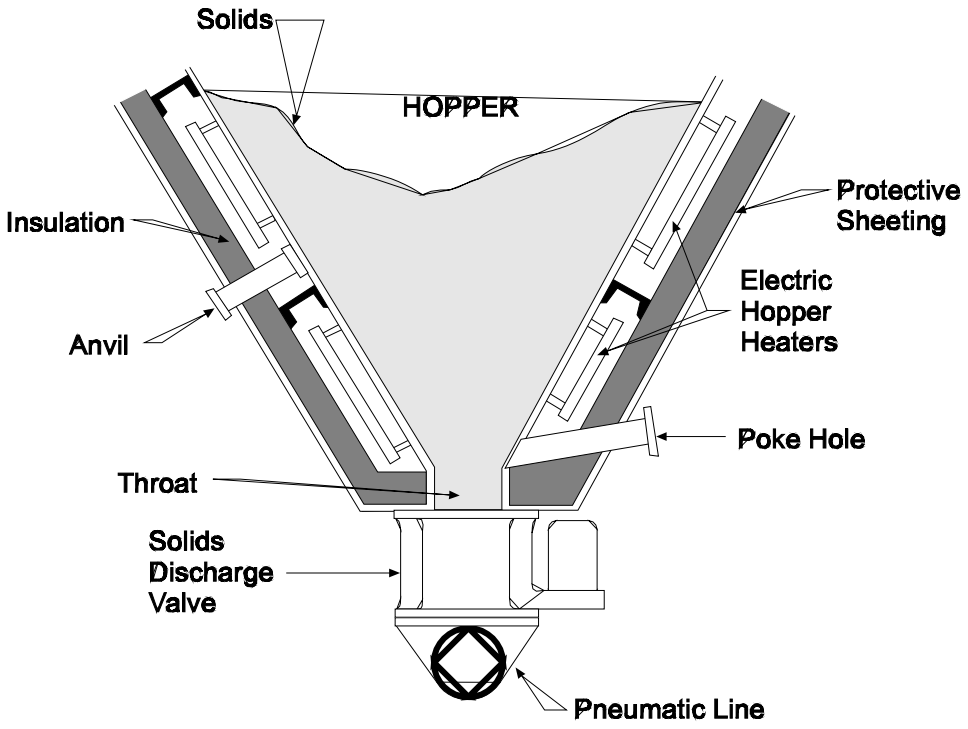

Figure 4-35. Hopper design features

Vibrators are often mounted on the side walls of hoppers in order to facilitate solids movement while the hopper is being discharged. However, these should not be operated when the discharge valve is closed because the solids may be compacted into a dense, non-moving mass.

Air infiltration problems can be especially severe in the hopper area and in the solids discharge valves. This is partially due to the relatively cold temperatures that can be present and due to the physical wear caused by the material being handled. Once air infiltration starts, hopper discharge problems can quickly become more severe due to the cooling influence of the ambient air.

One of the main sources of air infiltration is the solids discharge valve at the bottom of the hopper. The primary purpose of this valve is to provide an air seal when solids are not being discharged.

4.3.9 Instrumentation

Static pressure drop gauges are used to monitor the overall air resistance through the entire fabric filter and the through separate compartments. As indicated in Figure 4-31, a multi-compartment reverse air or pulse jet fabric filter can have numerous static pressure gauges.

Some fabric filter systems have bag break indicator systems to provide an early warning of increased particulate emissions. The types of instruments used for bag break monitoring include Triboflow®, single pass light scattering, and scintillation instruments. The Triboflow® instrument (Figure 4-36) uses a probe inserted in the outlet duct of a compartment or of the overall fabric filter.

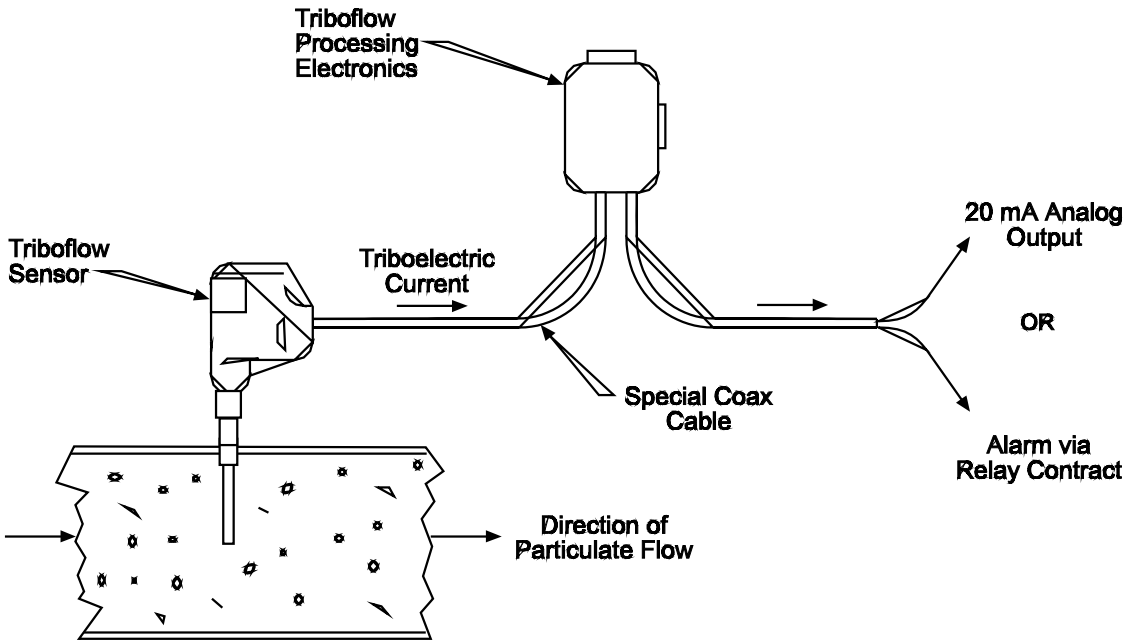

Figure 4-36. Triboflow® type bag break detector
(Reprinted courtesy of Auburn Systems, LLC)

In a Triboflow® unit, the transfer of electrical charge from the particulate emitted from the fabric filter to the probe provides an indication of the particulate matter concentration in the outlet gas stream. An increase in the instrument signal provides a qualitative indication of increased emissions.

In the single pass light scattering detectors, a visible light source is mounted on one side of the outlet duct, and a light detector is mounted on the oppositte side. A decrease in light intensity due to the presence of particulate matter in the gas stream provides an indication of a failed bag. These instruments often have an output scale expressed in terms of opacity. However, these instruments do not satisfy a number of the Performance Specifications applying to opacity monitors, and the output value is intended to be qualitative.

A scintillation type bag break indicator is also a light scattering, cross-stack monitor. The frequency of the light is varied to provide a means to evaluate the particulate mass concentration. This instrument provides data in the form of mass concentration values rather than opacity. However, these data are considered qualitative.

On large fabric filter systems, a double-pass transmissometer is often used to continuously monitor the effluent gas stream opacity. These systems use visible light that is projected across the stack, reflected off the surface of a mirror, and returned to a detector. The loss in light due to absorption and scattering during this double pass across the stack is measured as percent transmittance and is mathematically converted to opacity. These instruments are designed and installed in accordance with U.S. EPA Performance Specification 1 (40 CFR Part 60, Appendix A). They are usually located in either an outlet duct or the stack serving the fabric filter system.

4.3.10 Baghouse Bypass Dampers

The bypass dampers are mounted in short connecting ductwork that leads from the baghouse inlet duct to the outlet duct. These dampers provide important protection for the baghouse during periods of adverse gas temperatures or other conditions that could severely damage the bags. For example, the dampers are usually open during start-up and shut down when the gas stream is below the acid dew point, and the particulate matter can be sticky (prompting bag blinding).

During routine operation, it is important that these dampers seal tightly. They are subjected to a static pressure differential that is equivalent to the overall static pressure drop across the entire baghouse. Slight gaps in the poppet or louvered dampers can allow relatively large quantities of unfiltered air to "short circuit" around the baghouse. This problem is often indicated by a constant opacity of several percent.

Review Exercises

Types and Components of Fabric Filters

1. What types of fabric filter systems collect the dust cake on the exterior surface of the filter media? Select all that apply.
   a. Pulse jet
   b. Cartridge
   c. Reverse air

2. What is the purpose of using offline cleaning in a multicompartment pulse jet collector? Select all that apply.
   a. Minimize solids build-up problems in hoppers.
   b. Minimize gravity settling problems during cleaning of the bags.
   c. Minimize high static pressure drop problems.
   d. Minimize variability of the overall static pressure drop across the baghouse during the cleaning cycle.

3. What fabrics have a long term temperature limitation above 400 F? Select all that apply.
   a. Fiberglass
   b. Cellulose
   c. Nomex
   d. P84
   e. Stainless steel
   f. Ceramic
   g. Teflon

4. A static pressure drop gauge is mounted on the side wall of a pulse jet baghouse. One side of the gauge is connected to the side wall of the baghouse at a location just below the tube sheet. The other side of the gauge is located just above the tube sheet. The data provided by this intrument is termed the _____.
   a. Overall baghouse static pressure drop
   b. Filter media static pressure drop
   c. Compressor discharge static pressure
   d. Compressor header static pressure

5. What types of contaminants can be present in untreated compressed air used to clean pulse jet fabric filters and cartridge fabric filters? Select all that apply.
   a. Condensed water droplets
   b. Sulfur dioxide
   c. Carbon monoxide
   d. Condensed oil droplets

6. What problem or problems are created if a pulse jet bag does not seal properly to the tube sheet? Select all that apply.
   a. Unfiltered gas could leak around the bag into the clean gas plenum.
   b. The bags could fall into the hoppers due to inadequate support.
   c. The filter media static pressure drop would decrease.

7. A reverse bag constructed of fiberglass has very low tension and is sagging severely at the connection to the tube sheet thimble. What problem or problems could be created by this condition? Select all that apply.
   a. The bag could develop holes due to its vulnerability to flex failure.
   b. The bag could be abraded by the high velocity inlet gas stream.
   c. The sagging bag could choke off flow of unfiltered air into the bag.
   d.. All of the above

Operating Principles of Fabric Filters

8. How much gas will flow through a 4-inch diameter hole in the side of a baghouse if the internal static pressure is -12 in. W.C., and the gas density is 0.052 lb_m/ft^3?

9. What forces are used to remove particles in woven and felted bags? Select all that apply.
   a. Inertial impaction
   b. Brownian diffusion
   c. Electrostatic attraction
   d. Sieving

10. What forces are used to remove particles in a membrane bag? Select all that apply.
   a. inertial impaction
   b. Brownian diffusion
   c. Electrostatic attraction
   d. Sieving
   e. All of the above

11. What problem occurs at excessive air-to-cloth ratios?
   a. Accelerated bag failure
   b. Decreased static pressure drop
   c. Increased particulate emissions through the filter media
   d. All of the above

Design and Sizing of Fabric Filters

12. Calculate the net air-to-cloth ratio for a reverse air baghouse with 12 compartments containing 276 bags each. The diameter of each bag is 11 in., and the bag height is 28 ft. One of the compartments is always off-line for cleaning, and another is off-line for maintenance. Use a gas flow rate of 350,000 ACFM.

13. Calculate the gas approach velocity for a pulse jet baghouse having a single compartment, 60 rows of bags with 10 bags each, and a bag diameter of 6 in. Assume that the internal dimensions of the compartment are 6.5 ft times 40 ft. Use a gas flow rate of 66,000 ACFM.

14. Would a 150 m size particle or particle agglomerate successfully settle by gravity in the pulse jet baghouse described in Problem 13? Assume a gas density of 0.001205 gm/cm^3 at a temperature of 20°C. Also, assume that the particle density is 1.0 and that the transitional version of the terminal settling equation is appropriate for this particle size.

15. Calculate the static pressure difference between the clean gas plenum of a top access type pulse jet baghouse and the ambient air. Assume that the inlet static pressure to the baghouse is - 4 in. W.C. and the static pressure drop across the baghouse is 5 in. W.C.

Review Answers

1. What types of fabric filter systems collect the dust cake on the exterior surface of the filter media? Select all that apply.

   a. Pulse jet

   b. Cartridge

2. What is the purpose of using offline cleaning in a multicompartment pulse jet collector? Select all that apply.

   b. Minimize gravity settling problems during cleaning of the bags.

   c. Minimize high static pressure drop problems.

3. What fabrics have a long term temperature limitation above 400°F?

   a. Fiberglass

   e. Stainless steel

   f. Ceramic

4. A static pressure drop gauge is mounted on the side wall of a pulse jet baghouse. One side of the gauge is connected to the side wall of the baghouse at a location just below the tube sheet. The other side of the gauge is located just above the tube sheet. The data provided by this intrument is termed the _____.

   b. Filter media static pressure drop

5. What types of contaminants can be present in untreated compressed air used to clean pulse jet fabric filters and cartridge fabric filters? Select all that apply.

   a. Condensed water droplets

   d. Condensed oil droplets

6. What problem or problems are created if a pulse jet bag does not seal properly to the tube sheet? Select all that apply.

   a. Unfiltered gas could leak around the bag into the clean gas plenum.

7. A reverse bag constructed of fiberglass has very low tension and is sagging severely at the connection to the tube sheet thimble. What problem or problems could be created by this condition? Select all that apply.

   d. All of the above

Operating Principles of Fabric Filters

8. How much gas will flow through a 4-inch diameter hole in the side of a baghouse if the internal static pressure is -12 in. W.C., and the gas density is 0.052 lb_m/ft^3. Use 0.61 as the orifice coefficient.

   Answer: 887 ft^3/min

Solution:

$$V_o = C\sqrt{\frac{2g_c\Delta p}{\rho_g}}$$

$$\Delta p = 12\,\text{in. W.C.}\left|\frac{14.7\ \text{lb}_f/\text{in.}^2}{407\ \text{in.W.C.}}\right|\frac{144\ \text{in.}^2}{\text{ft}^2}$$

$$= 62.4\ \text{lb}_f/\text{ft}^2$$

$$V_o = 0.61\sqrt{\frac{(2)(32.2\ \text{ft}\bullet\text{lb}_m/\text{lb}_f\bullet\text{sec}^2)(62.4\ \text{lb}_f/\text{ft}^2)}{0.052\ \text{lb}_m/\text{ft}^3}}$$

$$= 170\ \text{ft/sec}$$

Gas flow rate = Area Velocity

$$\text{Area} = \pi D^2/4 = 3.14\ \frac{\left[(4\ \text{in.})\left(\frac{1\ \text{ft}}{12\ \text{in.}}\right)\right]^2}{4} = 0.087\ \text{ft}^2$$

$$\text{Gas flow rate} = 0.087\ \text{ft}^2 \times 170\ \text{ft/sec} \times 60\ \text{sec/min}$$

$$= 887\ \text{ft}^3/\text{min}$$

9. What forces are used to remove particles in woven and felted bags? Select all that apply.
   a. Inertial impaction
   b. Brownian diffusion
   c. Electrostatic attraction

10. What forces are used to remove particles in a membrane bag?
    e. All of the above

11. What occurs at excessive air-to-cloth ratios?
    c. Increased particulate emissions through the filter media

Design and Sizing of Fabric Filters

12. Calculate the net air-to-cloth ratio for a reverse air baghouse with 12 compartments containing 276 bags each. The diameter of each bag is 11 in., and the bag height is 28 ft. One of the compartments is always off-line for cleaning, and another is off-line for maintenance. Use a gas flow rate of 350,000 ACFM.

    Answer: 1.57

Solution:

$$\text{Bag area} = \pi Dh = 3.14\,(11\text{ in.})\left(\frac{1\text{ ft}}{12\text{ in.}}\right)(28\text{ ft})$$

$$= 80.6\ \text{ft}^2/\text{bag}$$

$$\text{Number of bags in service} = \frac{276\text{ bags}}{\text{compartment}} \times 10\text{ compartments}$$

$$= 2{,}760\ \text{bags}$$

$$\text{Net total bag area} = \frac{80.6\text{ ft}^2}{\text{bag}}\,(2{,}760\text{ bags})$$

$$= 222{,}500\ \text{ft}^2$$

$$\text{Net air-to-cloth ratio} = \frac{\text{Gas flow rate}}{\text{Net bag area}}$$

$$= \frac{350{,}000\ \text{ft}^3/\text{min}}{222{,}500\ \text{ft}^2}$$

$$= 1.57\ (\text{ft}^3/\text{min})/\text{ft}^2$$

13. Calculate the gas approach velocity for a pulse jet baghouse having a single compartment, 60 rows of bags with 10 bags each, and a bag diameter of 6 in. Assume that the internal dimensions of the compartment are 6.5 ft times 40 ft. Use a gas flow rate of 66,000 ACFM.

Answer: 464.2 ft/min or 7.73 ft/sec

Solution:

Total baghouse shell area = 6.5 ft (40 ft) = 260 ft^2

$$\text{Bottom areas of bag (circular cup)} = \frac{\pi D^2}{4}$$

$$= \frac{3.14\left[(6\text{ in.})\left(\frac{1\text{ ft}}{12\text{ in.}}\right)\right]^2}{4}$$

$$= 0.196\ \text{ft}^2/\text{bag}$$

Total bottom area of bags $= \frac{0.196\ ft^2}{bag}(600\ bags) = 118\ ft^2$

Area available for gas flow = total area – bag bottom cups

$= 260\ ft^2 - 118\ ft^2 = 142\ ft^2$

$$\text{Gas approach velocity} = \frac{\text{Gas flow rate}}{\text{Area}} = \frac{66{,}000\ ft^3/min}{142\ ft^2}$$

= 465 ft/min or 7.75 ft/sec

14. Would a 150 m size particle or particle agglomerate successfully settle by gravity in the pulse jet baghouse described in Problem 13? Assume a gas density of 0.001205 gm/cm^3 at a temperature of 20°C. Also, assume that the particle density is 1.0 and that the transitional version of the terminal settling equation is appropriate for this particle size.

Answer: No.

The 150 m particle will not settle. The upward velocity of the unfiltered gas stream is much higher than the terminal settling velocity.

$$v_t = \frac{0.153\ g^{0.71}\ d^{1.14}\ \rho_p^{0.71}}{\mu^{0.43}\ \rho_g^{0.29}}$$

$$v_t = \frac{0.153(980\ cm/sec^2)^{0.71}\ (0.0150\ cm)^{1.14}\ (1.0\ gm/cm^3)^{0.71}}{(1.81\times10^{-4}\ gm/cm\bullet sec)^{0.43}\ (0.001205\ gm/cm^3)^{0.29}} = 48.41$$

$$v_t = 48.41\ cm/sec \quad \frac{1\ in.}{2.54\ cm}\times\frac{1\ ft}{12\ in.}$$

= 1.588 ft/sec

15. Calculate the static pressure difference between the clean gas plenum of a top access type pulse jet baghouse and the ambient air. Assume that the inlet static pressure to the baghouse is –4 in. W.C. and the static pressure drop across the baghouse is 5 in. W.C.

Answer: Static pressure difference = 9 in. W.C.

Static pressure in the clean gas plenum

= -4 in. W.C. – 5 in. W.C.

Static pressure in the ambient air

= 0 in. W.C.

Difference = 9 in. W.C.

Bibliography

Bundy, R.P. *Operation and Maintenance of Fabric Filters, Proceedings, Operating and Maintenance Procedures for Gas Cleaning.* Air Pollution Control Association Specialty Conference (1980): 139-152.

Campbell, P.R. *Make Fiberglass Filter Bags Last Longer by Maintaining Proper Tension.* Power, (March, 1980): 92-93.

Carr, Robert C. Second Conference on Fabric Filter Technology for Coal-Fired Power Plants, Conference Summary. Journal of the Air Pollution Control Association. Volume 33, No. 10, (October 1983): 949-954.

Dennis, R., Cass, R.W., and Hall, R.R. *Dust Dislodgement from Woven Fabrics Versus Filter Performance.* Journal of the Air Pollution Control Association. Volume 28, No. 1, (January, 1978): 47-52.

Makansi, J. *Match Bag Material for Your Fabric Filter to Type of Service.* Power, (October, 1983): 115-118.

Perkins, R.P. *State-of-the-Art of Baghouses for Industrial Boilers.* Presented at the Industrial Fuel Conference. West Lafayette, Indiana. October 5-6, 1972.

Perkins, R.P. and Imbalzano, J.F. *Factors Affecting Bag Life Performance in Coal-Fired Boilers. Proceedings, the User and Fabric Filtration Equipment III.* Air Pollution Control Association Specialty Conference (1978): 120-144.

Turner, James H., Viner, Andrew S., McKenna J.D., Jenkins, R.E., and Vatavuk, W.M. *Sizing and Costing of Fabric Filters.* Journal of the Air Pollution Control Association, Volume 37, No. 6 (June, 1987): 749-759.

Viner, A.S., Donovan, R.P., Ensor, D.S. and Hovis, L.S. Comparison of Baghouse *Test Results with the GCA/EPA Design Model.* Journal of the Air Pollution Control Association Volume 34, No. 8 (August, 1984): 872-880.

Weber, G. F. and Schelkoph G. L. *Performance/Durability Evaluation of 3M Company's High-Temperature Nextel Filter Bags.* Presented at the Eighth Symposium on the Transfer and Utilization of Particulate Control Technology. San Diego, California. March 30-23, 1990.

Chapter 5
Electrostatic Precipitators

Electrostatic precipitators are used in many industries for the high efficiency collection of particulate matter. They were originally developed in the early 1900s for acid mist control. During the 1940s, precipitators began to be used for particulate matter control at coal-fired boilers, cement kilns, and kraft recovery boilers. The applications of precipitators has steadily increased since the 1940s due to their ability to impart large electrostatic forces for particle separation without imposing gas flow resistance. Electrostatic precipitator efficiency and reliability have improved steadily since the 1970s as a result of research and development programs sponsored by equipment manufacturers, trade associations, and the U.S. EPA.

5.1 TYPES AND COMPONENTS

There are three categories of electrostatic precipitators (ESPs). These units serve entirely different industrial applications.

- Dry, negative corona
- Wet, negative corona
- Wet, positive corona

General operating characteristics and components of these three ESPs as well as operating procedures and performance problems, are discussed in this chapter. The emphasis is on dry, negative corona units since this type is used on the largest systems and these are the most common type of units presently in service.

Dry, negative corona units are used in large industrial facilities such as cement kilns, kraft pulp mills, and coal-fired utility boilers. They are termed "dry" because the collected solids are removed from the collection plates as a dry material. The term "negative corona" means that the particles are collected by forcing them to move from a high negatively charged area to a electrically grounded collection plate.

Wet, negative corona units use water on the collection plates to remove the collected solids. This approach eliminates several of the major problems that can affect dry, negative corona units. However, it adds to the complexity involved with the use of water in close proximity to high voltage insulators, and it increases the potential problems associated with corrosion. Most wet, negative corona units are used for small-to-moderately-sized industrial sources.

Wet, positive corona units are sometimes termed two-stage precipitators. Particle charging occurs in a pre-ionizer section, and particle collection occurs in a downstream collection plate section. The pre-ionizer operates at a high positive voltage. The wet, positive corona units are used to remove organic compound mists. The collected material drains from the vertical collection plates. These precipitators are used on small sources.

5.1.1 Dry, Negative Corona Precipitators

A dry, negative corona electrostatic precipitator consists of a large number of parallel gas passages with discharge electrodes mounted in the center and grounded collection surfaces called plates on either side. The discharge electrodes are spaced 4.5 to 6 in. away from each of the collection plates as shown in Figure 5-1. A high negative voltage is applied to the discharge electrodes. The voltage difference between the discharge electrodes and plates creates continuous electrical discharges termed *coronas*.

Figure 5-1. Gas passage composed of discharge electrode and collection plates

Negatively charged gas ions formed in and near the corona discharge impart an electrical charge to the particles and cause them to move toward the electrically grounded collection plates. Mechanical hammers called *rappers* are used to remove a portion of the dust layer accumulating on these plates and the small quantities of dust that also collect on the discharge electrodes. Particle agglomerates and dust layer sheets fall by gravity into the hoppers during rapping.

The dry, negative corona electrostatic precipitator shown in Figure 5-2 is typical of units used on large-scale processes such as coal-fired utility boilers, coal-fired industrial boilers, kraft pulp mill recovery boilers, cement kilns, and municipal incinerators. They are generally quite large and are often designed for gas flow rates from 100,000 ACFM to more than 3,000,000 ACFM.

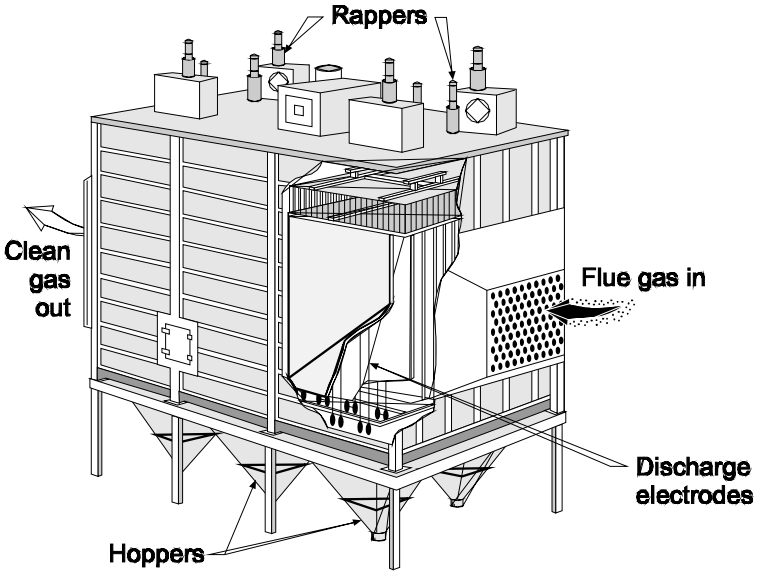

Figure 5-2. Typical dry, negative corona type electrostatic precipitator

The gas stream passing through the duct toward the precipitator is moving too fast for effective treatment. Deceleration occurs in the inlet nozzle section immediately upstream of the precipitator by expanding the gas flow area. The gas velocity decreases by a factor of approximately 10 so that the average velocity through the treatment zone is usually between 3 to 6 feet per second.

In addition to slowing down the gas stream, the inlet nozzle is used to distribute the gas flow as uniformly as possible so that there are no significant side-to-side or vertical variations in the gas velocities at the entrance of the precipitator.

Proper gas distribution is achieved by proper inlet nozzle design, by proper inlet ductwork design, by turning vanes in the inlet nozzle, and by a series of gas distribution screens mounted in the inlet nozzle. Perforated plate gas distribution screens are shown in Figure 5-3.

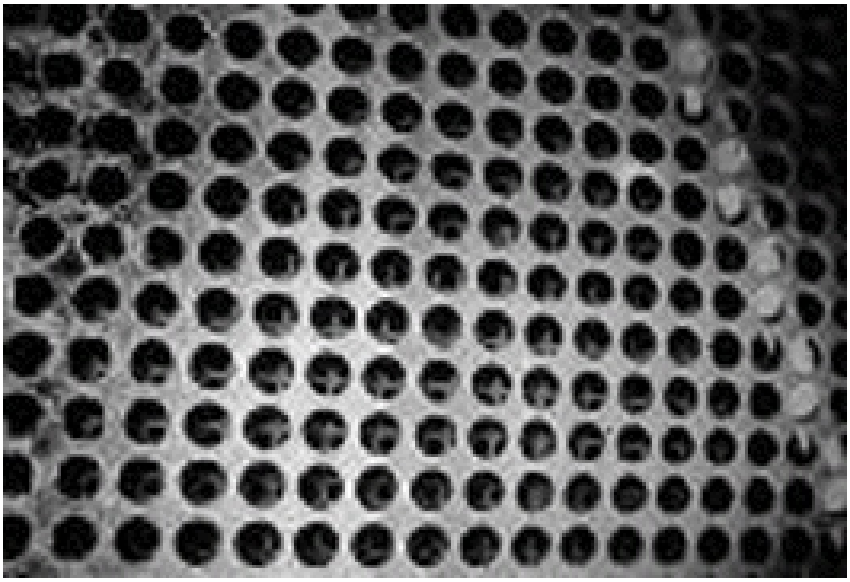

Figure 5-3. Gas distribution screens at the precipitator inlet

As the gas stream enters the precipitator, it goes through passages formed by the large, parallel collection plates. High voltage discharge electrodes are centered between each of the plates. In this type of precipitator, small diameter wires serve as the discharge electrodes. In other precipitator designs, rigid masts or wires in rigid frames are used. The high voltages applied to the discharge electrodes create localized electrical discharge points called **coronas**. Negative gas ions are formed in the coronas. These ions cluster around the particles attempting to move through the precipitator passages.

Once the ions are on the particle surfaces, the particles are held by the electrical field that exists between the high voltage discharge electrodes and the electrically grounded collection plates. Accordingly, the particles migrate over to the plates and build-up as dust layers on the plate surfaces. A small fraction of the particulate matter also accumulates on the discharge electrodes.

The discharge electrodes are divided into fields. These are portions of the precipitator energized by a single transformer-rectifier (T-R) set power supply. Most units have three to four fields in series as shown in Figure 5-4. However, some especially large units have as many as fourteen fields in series. The precipitator can also be divided into separate chambers that are separated by a solid wall. Chambers may also be designed as separate precipitator shells.

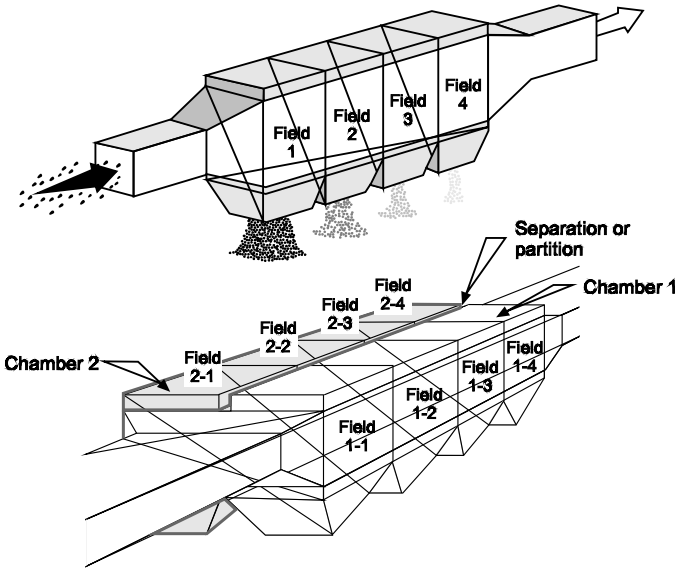

Figure 5-4. Arrangement of fields and chambers in a dry, negative corona precipitator

Each of the fields is energized by a T-R set (Figure 5-5). The primary control cabinet circuitry controls the voltage in the alternating current power line applied to one side of the transformer in the T-R set. The high voltage generated in the transformer is converted into direct current in the rectifier and is then sent to the precipitator field.

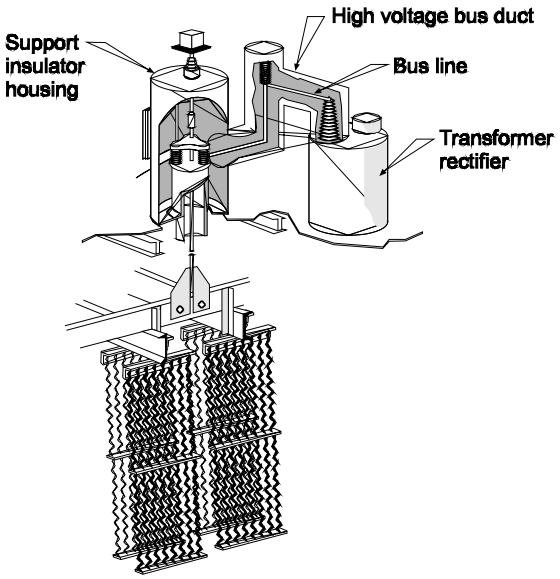

Figure 5-5. Transformer-rectifier set, support insulator discharge electrode frames, and discharge electrodes

The primary control cabinet includes silicon-controlled rectifiers (SCRs) to control the alternating current line to the T-R set. These SCRs are controlled by an automatic voltage controller that maintains the unit at the maximum voltage possible and by the SCR trigger and pulse controller that adjust the waveforms. The following list includes other major electrical components in the primary control cabinet.

- Linear reactor to control normal current surges
- Under-voltage protection to protect against short circuits
- Indicator gauges to provide data concerning the electrical operating conditions in the field

The gauges on the control cabinet for each T-R set provide much of the data necessary to evaluate performance. Figure 5-6 illustrates the analog gauges common in many older units. Some new precipitators have digital gauges used alone or in combination with the analog gauges.

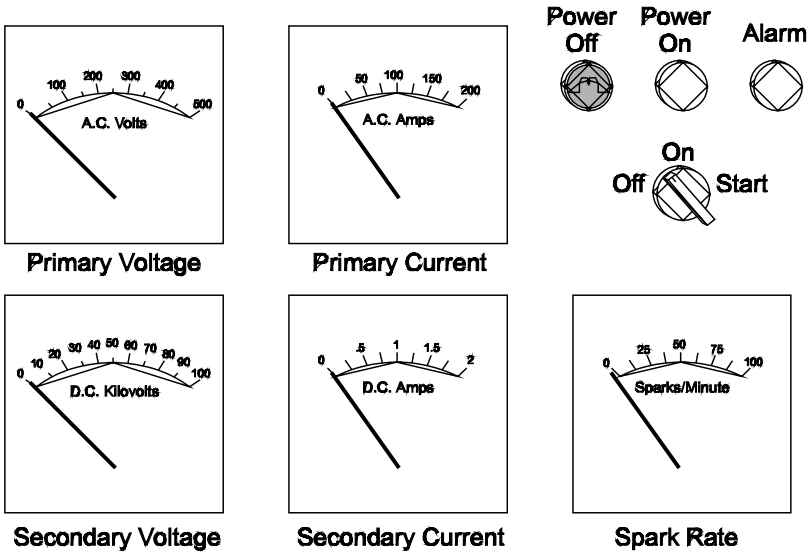

Figure 5-6. Types of gauges present on the control cabinet for each precipitator field

The distance between the high voltage discharge electrodes and the grounded collection plates affects the electrical charging and migration of the particles. If some portions of the discharge electrodes and collection plates are closer than others, a spark will occur frequently at the close approach point. The automatic voltage controller will respond to this condition by reducing the applied voltage. This reduces the affected field's ability to electrically charge and collect particles. For example, if the designers intended discharge electrode spacing to the collection plates is 4.5 in., it is usually necessary to maintain all the discharge electrodes at this point with an allowable spacing deviation of only ± 0.5 in. All discharge electrodes in this unit must be between 4 and 5 in. away from all portions of the adjacent collection plates. This is not easy to maintain.

The wire being measured in Figure 5-7 is approximately 2 in. from the collection plate rather than the intended 4.5 in. This can seriously impair the performance of the precipitator field.

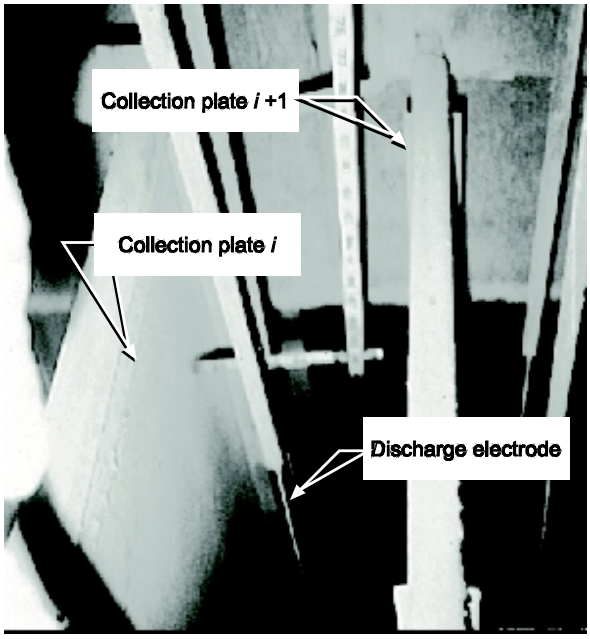

Figure 5-7. Measurement of an alignment position

The discharge wires are suspended between the grounded collection plates using insulators called high voltage frame support insulators. There are usually at least two high voltage frame support insulators for each bus section in a field. The location of these insulators is shown in Figure 5-8.

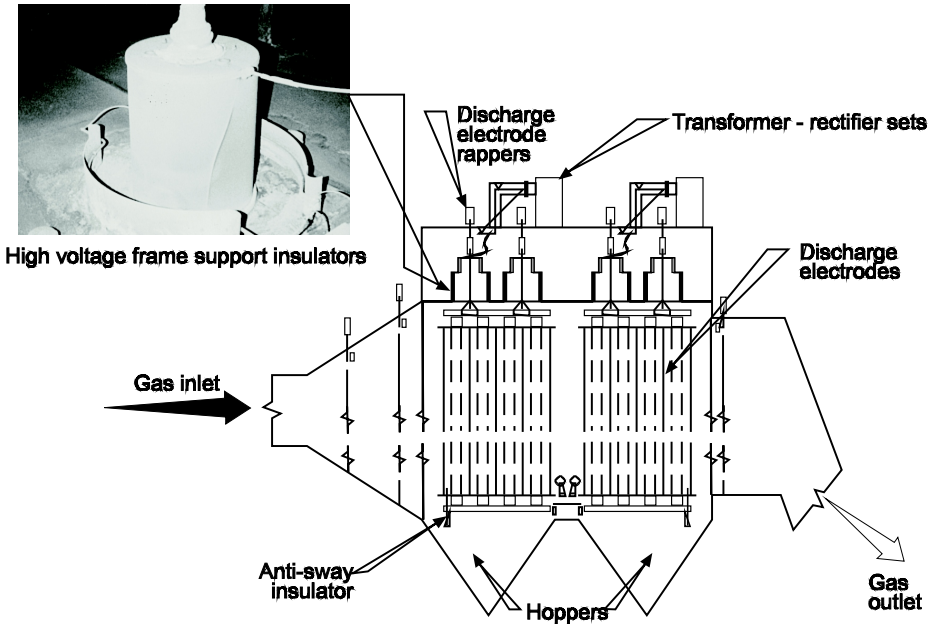

Figure 5-8. Sketch of high voltage frame support insulators

The accumulation of moisture or dust on the surfaces of support insulators can cause a short circuit. These shorts start as a small current and are identified by reduced voltage in the field and reduced spark rates. As the current flow increases, it heats the surface of the insulator. This heating can cause the insulator to shatter. The development of a short circuit across the insulator surface can also cause the field to automatically shut down. The high voltage frame support insulator must be kept clean at all times to prevent these problems.

Electrical heaters are often used around each insulator to reduce moisture accumulation. Purge air blowers are used to provide a constant flow of hot air into the insulator penthouse or compartment. This hot air flows through holes in the insulator top cover in order to purge out the interior area of the insulators.

There are usually several anti-sway insulators at the bottom of each high voltage frame to prevent a pendulum action that reduces clearances between the high voltage electrodes and the grounded plates. The anti-sway insulators must inherently be located in the hopper area where it is difficult to provide supplemental heat or hot purge air. Accordingly, these insulators are vulnerable to electrical leakage and failure. For example, the anti-sway insulator shown in Figure 5-9 have electrical short-circuiting lines (leakage current) across the surface, which disabled the precipitator field. Short-circuits are normally minimized by using relatively long anti-sway insulators.

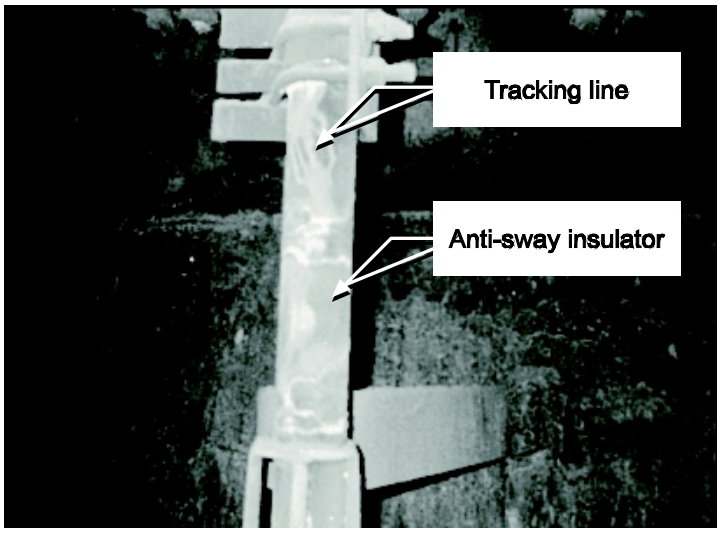

Figure 5-9. Anti-sway insulator suffering electrical short-circuiting across the surface

Movement of the wire-type discharge electrodes is minimized by hanging bottle weights on each wire. These provide 25 to 30 lb_f of tension on the wire so that it does not move excessively. In other precipitator designs, the discharge electrodes are mounted in rigid frames or are constructed as rigid masts.

The hoppers have very steep slopes to facilitate solids movement into the solids discharge valves leading out of the hoppers. A center division plate is used in each hopper to prevent untreated gas from evading the electrically energized zone by passing through the upper regions of the hopper. This is termed the anti-sneakage hopper baffle. There are also hopper heaters to keep solids hot to facilitate hopper discharge. The components of a typical hopper are illustrated in Figure 5-10.

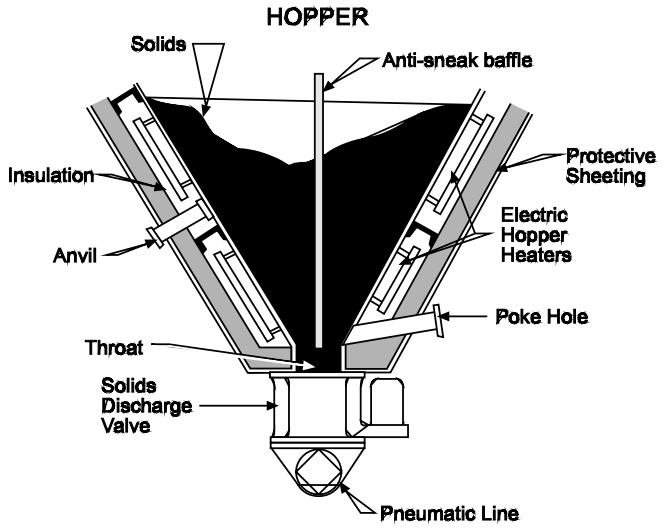

Figure 5-10. Components of a precipitator hopper

The side walls of the precipitator also have anti-sneakage baffles to prevent untreated gas from passing along the side walls of the precipitator, where it is impossible to mount discharge electrodes.

The rapping systems are especially important components of a precipitator. Separate groups of rappers are used to clean the collection plates, discharge electrode frames, and gas distribution plates. There are two basic categories of rappers: (1) roof-mounted rappers and (2) side-mounted rappers. Roof-mounted rapper designs incorporate a large number of individual rappers, each connected to a single high voltage discharge electrode frame or a section of collection plates. For collection plate rappers, the energy of roof-mounted rappers (Figure 5-11) is transmitted down a metallic rod. For discharge electrodes, the energy must be transmitted through an insulator rod to prevent carrying high voltage to the rapper and the accessible areas on the roof of the precipitator.

Figure 5-11. Roof-mounted rapper

A side-mounted rapper system is shown in Figure 5-12. Motors are mounted on the exterior of the precipitator. These motors turn shafts that run across the precipitator. A set of hammers is mounted to these rotating shafts in order to rap each individual collection plate and discharge electrode frame.

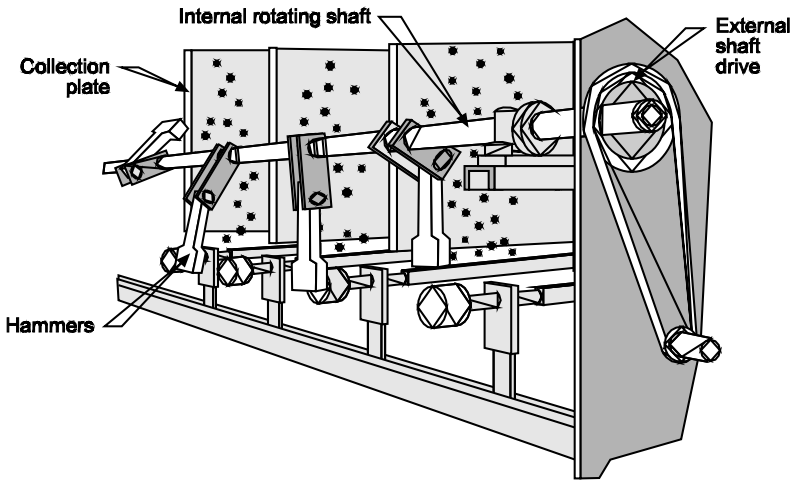

Figure 5-12. Side-mounted collection plate rappers

For both types of rapper designs, the frequency and intensity of rapping must be carefully controlled in order to achieve proper precipitator removal efficiency. The frequency of rapping must take into account that approximately 50-80% of the particulate is removed in each separate field. Accordingly, the inlet fields remove much greater quantities of dust than the outlet fields.

For example, assume that the field-by-field efficiencies in a four-field unit are 80%, 70%, 60%, and 50%, respectively, from inlet to outlet. If the inlet particulate loading is 10,000 lb/hr, the quantities of dust removed would be the following:

- Inlet - 8,000 lb/hr (80% of inlet quantity)
- Second - 1,400 lb/hr (70% of inlet field effluent)
- Third - 360 lb/hr (60% of second field effluent)
- Outlet - 120 lb/hr (50% of third field effluent)

This simplistic example illustrates the need to rap the inlet field collection plates and discharge electrodes much more frequently than the middle and outlet fields.

There is usually one or more opacity monitors at the outlet of the precipitator. These monitors are especially useful for evaluating performance of electrostatic precipitators. The opacity data are used in conjunction with the electrical data from each of the fields to diagnose problems.

5.1.2 Wet, Negative Corona Precipitators

A wet, negative corona precipitator is useful for industrial applications where (1) mists or fogs must be controlled or (2) solid particulate matter in the gas stream has undesirable electrical or physical properties. Undesirable physical properties include moderate stickiness or a high carbonaceous composition. A washing system, rather than rappers, is used for dust removal. These units, termed either *wet* or *wetted wall*, use power supplies that generate high negative voltages on the small discharge electrodes. The power supplies are essentially identical to those used on dry, negative corona precipitators.

Wet, negative corona ESPs are usually preceded by a quench chamber to ensure that the gas stream is saturated prior to entering the unit. This quench chamber can either be a separate stand-alone vessel as shown in Figure 5-13 or an initial compartment within the wet ESP itself. Due to the presaturation sprays, the operating gas temperatures are usually 130°F - 170°F. This substantially reduces the vulnerability of the system to drying of the collection surfaces. Some systems use a liquid recirculation system and liquid additives to maintain the proper pH in the collection plate sprays. Liquid additives can also help minimize the viscosity of the materials draining from the collection plates and can help minimize foaming in some industrial applications.

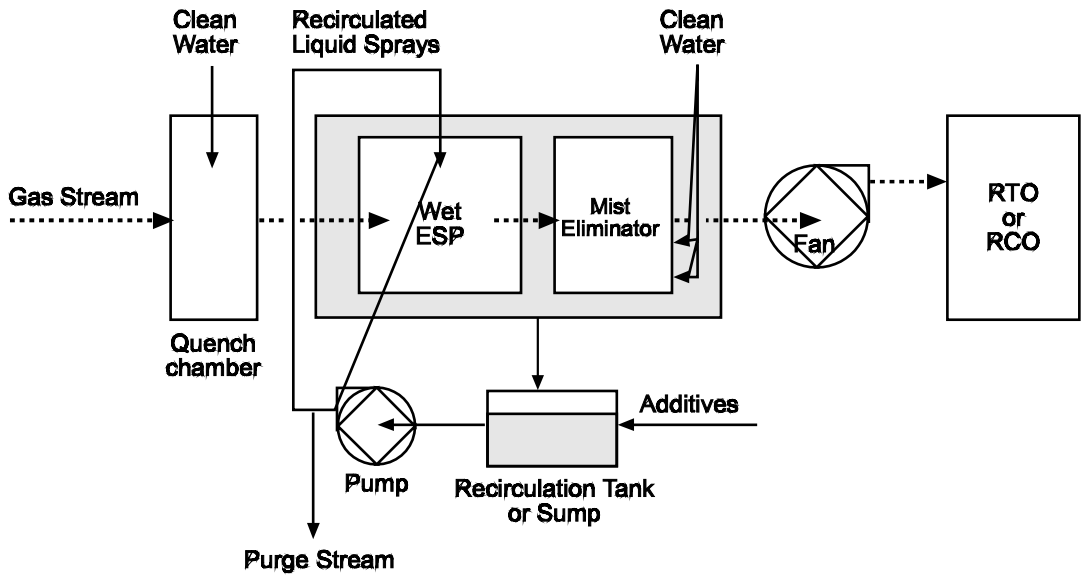

Figure 5-13. General flowchart of a wet, negative corona precipitator

Recirculation liquid must be purged to maintain the solids levels. The rate of liquid purge depends primarily on the rate of collection of solids. Usually, the rate of purge is quite small because the overall recirculation rate of liquid is quite small. A normal liquid-to-gas ratio for a wet, negative corona precipitator is less than 2 gallons per thousand ACFM.

The gas passages in wet precipitators can be concentric circles, tubes, or parallel rows. Alignment of the negatively charged discharge electrodes and the electrically grounded collection plates is very important to ensure that the field can operate at the necessary voltage. The alignment tolerances are similar to those for dry precipitators.

There are two main design styles for wet, negative corona electrostatic precipitators: (1) downflow and (2) horizontal flow. A conventional downflow design is illustrated in Figure 5-14. The gas stream enters the cyclonic presaturator chamber at the top of the unit. The saturated particulate-laden gas stream is distributed to a set of vertical tubes leading to the bottom of the unit. High voltage discharge electrodes are mounted in the center of each tube to generate the negative corona that electrically charges the particles moving down each tube. The charged particles migrate to the wet inner surface of the tube and are collected. Liquid moving down the tube surfaces carries the collected material to the wet ESP sump. Sprays above the tubes are activated on a routine frequency to further clean the tube surface and thereby maintain the required electrical clearances between the high voltage electrode and the electrically grounded tube surface.

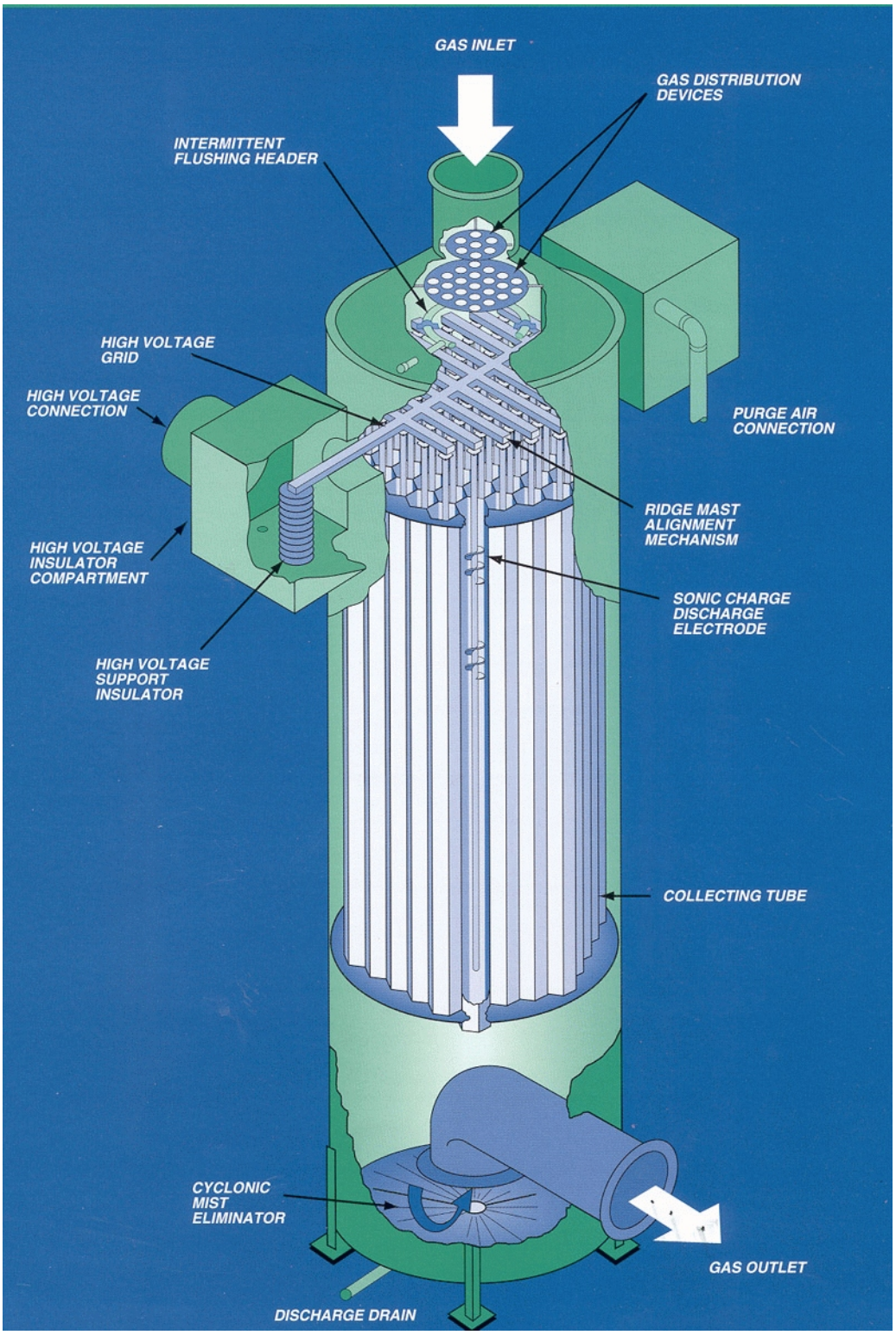

Figure 5-14. Vertical, wet negative corona precipitator
(Reprinted courtesy of TurboSonics)

Vertical flow wet ESPs have three or more support insulators to suspend the high voltage frame energizing each of the tube discharge wires. These insulators are similar to those used in dry, negative corona units. It is especially important to provide heat and purge air to these insulators due to the relatively cold gas temperatures and the presence of liquid sprays near the tops of the gas passage tubes.

Vertical flow wet, negative corona precipitators use electrical sectionalization differently than dry, negative corona systems. The wet ESPs often have two fields arranged in parallel and only one field in the direction of gas flow. This approach is due, in part, to the difficulty of protecting the high voltage frame support insulators in vertically stacked fields from descending liquid from an upper field.

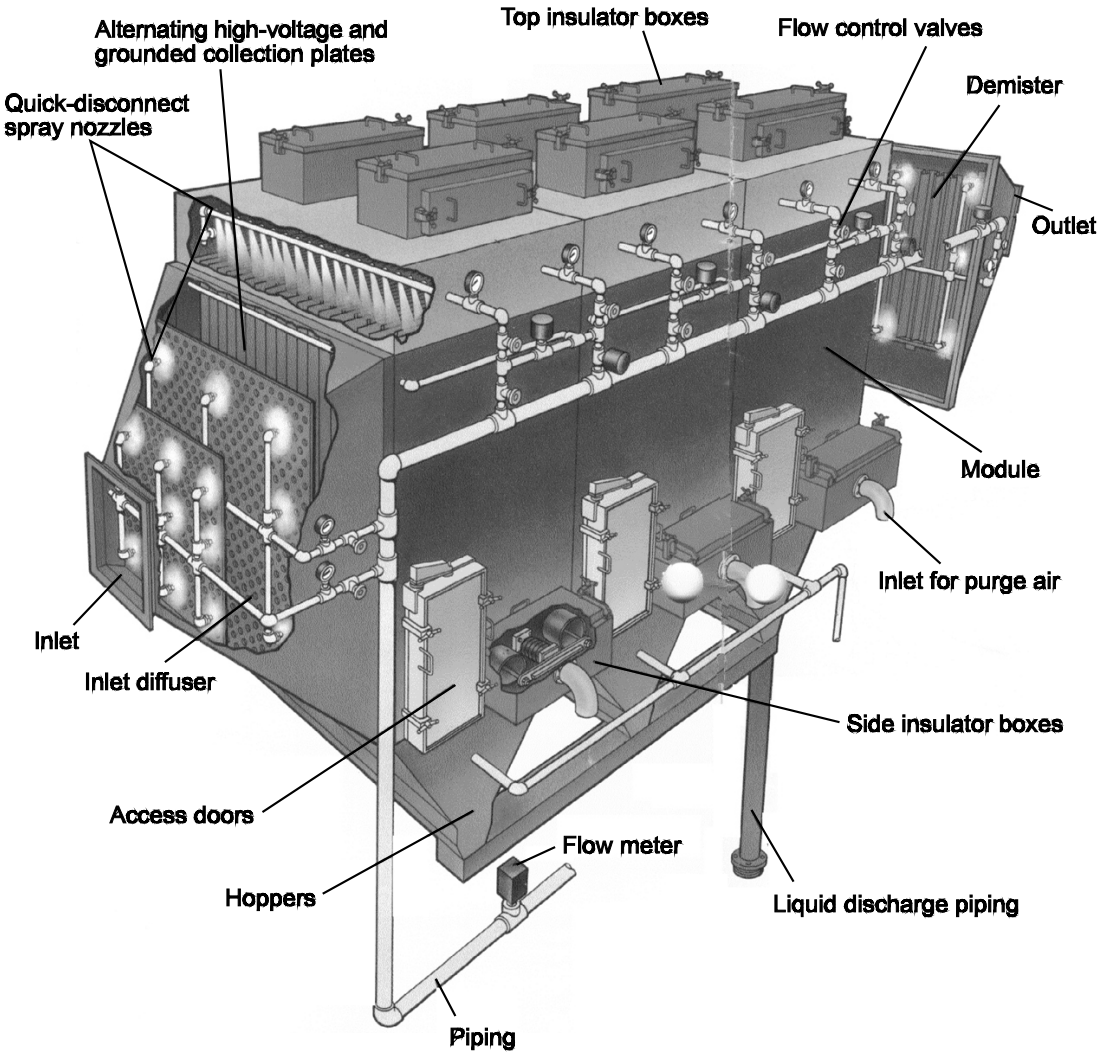

Figure 5-15. Side view of a horizontal gas flow wet, negative corona precipitator
(Reprinted courtesy of McGill AirClean Corporation)

A horizontal gas flow wet, negative corona precipitator is shown in Figure 5-15. This unit uses alternating high voltage plates and electrically grounded collection plates to form gas passages. The high voltage plates have discharge electrode points extending from the leading edge of each plate. These discharge points are energized by a conventional T-R set. The negative corona generated around these discharge points electrically charges particles passing through the unit. The particulate matter is collected

on electrically grounded collection plates and drains into the ESP sump. Cleaning of the collection plates is performed by a set of overhead sprays (Figure 5-16) and by a set of sprays on a traversing header (Figure 5-16) on the inlet side of each field.

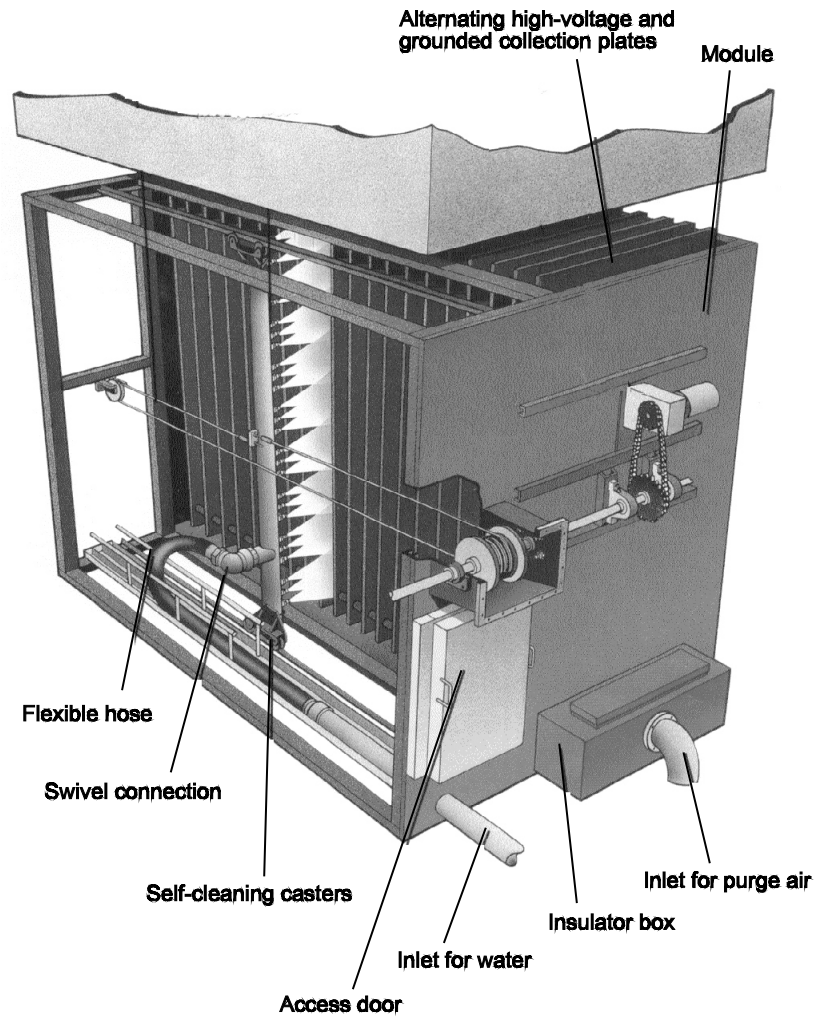

Figure 5-16. View of the traversing header sprays on a wet, negative corona precipitator
(Reprinted courtesy of McGill AirClean Corporation)

Horizontal wet ESPs usually have two or more fields in series. The sectionalization of the fields is similar to the design approach used in dry, negative corona units. The high voltage collection plate support insulators are mounted in insulator boxes on the roof of the unit. As with all wet ESPs, the insulators are heated to minimize the vulnerability to electrical tracking across wet insulator surfaces. Both vertical and horizontal gas flow wet ESPs often use perforated plates to distribute the gas flow entering the units. Sprays are used to occasionally clean these plates.

A set of mist eliminators is often used immediately after a wet, negative corona ESPs. The mist eliminators remove the entrained spray droplets and other solids-containing droplets that would otherwise be emitted to the atmosphere. Mist eliminators have clean water sprays to occasionally clean the droplet-contacting surfaces. Common types of mist eliminators used in wet ESPs include chevrons, tube banks, and baffle plates.

Wet, negative corona electrostatic precipitators are often used on industrial driers and boilers. They are used either as primary collectors or as particulate matter collectors ahead of regenerative thermal oxidizers and regenerative catalytic oxidizers. The regenerative systems are prone to solids accumulation at the bed inlet.

5.1.3 Wet, Positive Corona Precipitators

Wet, positive corona precipitators are used for the collection of organic mists from relatively small industrial applications such as textile mill tenter frames. As shown in Figure 5-17, the discharge electrodes are separated from the electrically grounded collection plates. Electrical charges are applied to particles as they pass through the preionizer discharge electrodes. These particles are then collected on the downstream collection plates. Since wet, positive corona precipitators only collect liquid particles that drain from the plates, they do not require rappers or liquid distributors.

Electrically, these units are quite different from the conventional negative corona. A positive electrical charge is applied to the discharge electrodes in order to charge the particles. Due to this charge, particles are attracted to the electrically grounded collection plates downstream from the preionizer section. The positive voltages applied to the discharge electrodes of the preionizer are in the range of 12 to 15 kilovolts, considerably lower than the negative voltages used in the dry, negative corona or wet, negative corona designs.

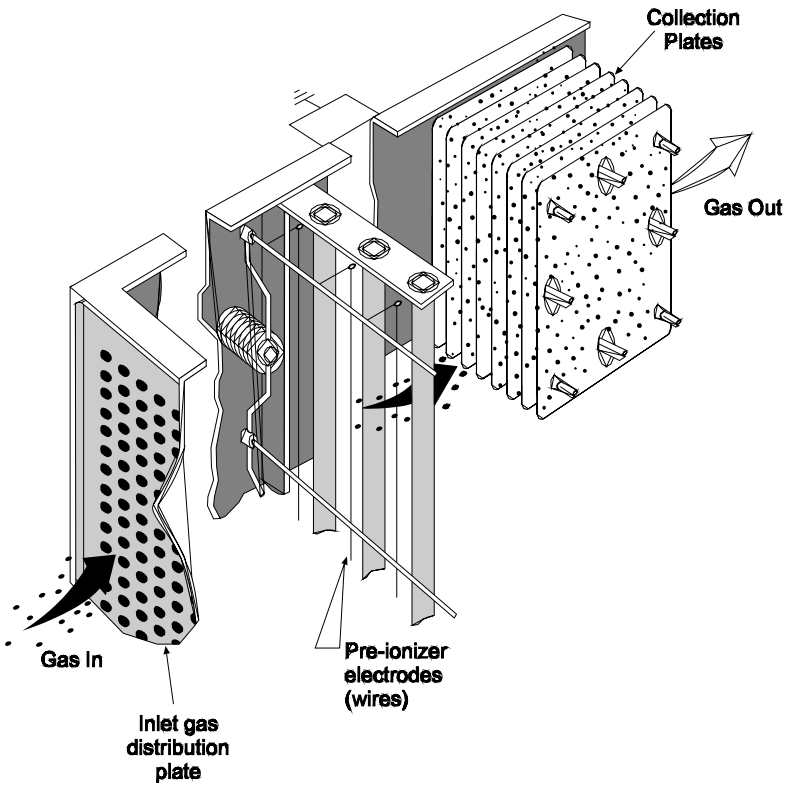

Figure 5-17. Wet, positive corona precipitator

The collection plates are designed to allow for easy removal and manual cleaning. The plates are often cleaned on a weekly or monthly basis, depending on the stickiness and viscosity of the collected material.

Wet, positive corona precipitators can have fire detection and suppression systems. The units are vulnerable to fires due to the collection or organic liquids.

5.2 OPERATING PRINCIPLES

In all three types of electrostatic precipitators, there are three basic steps to particulate matter collection.

- **Step 1** is the electrical charging and migration of particles toward a vertical collection surface.
- **Step 2** involves the gravity settling (or draining in the case of liquids) of the collected material from the vertical collection surfaces.
- **Step 3** is the removal of the accumulated solids or liquids from the hopper or sump below the electrically energized zone.

5.2.1 Precipitator Energization

The purpose of the high voltage equipment of an electrostatic precipitator is to cause particle-charging and migration (Step 1). A simplified drawing of the circuitry from the primary control cabinet to the precipitator field is shown in Figure 5-18.

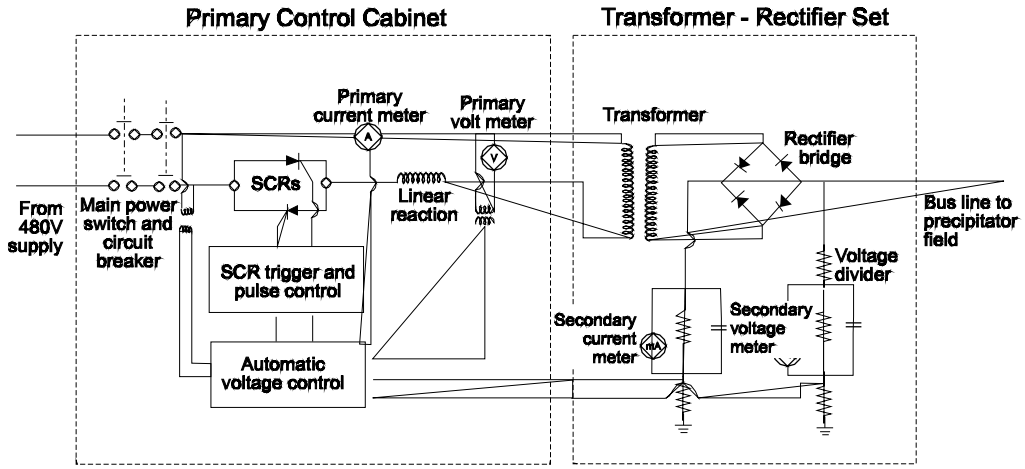

Basic Steps in Energizing a Precipitator Field

- Open/close 480 volt A.C. power supply to the primary control cabinet
- Control voltage and adjust voltage and current waveforms in primary line to the transformer
- Control current flow during sparking
- Increase voltage
- Convert electricity to direct current form

Components

- Main power switch and circuit breaker
- Automatic voltage controller, silicon controlled rectifiers (SCRs), trigger/pulse control for SCRs
- Linear reactor (located adjacent to primary control cabinet)
- Transformer
- Rectifier bridge

Figure 5-18. Precipitator field energization

The alternating current power line to the primary control cabinet is at a constant 480 volts and 60 cycles per second. This electrical power is supplied to the T-R set when the main switch and the circuit breaker in the primary control cabinet are both on. If an electrical problem is sensed in the power supply or the precipitator field, the circuit breaker automatically opens. This is called tripping the field.

In the primary control cabinet, the automatic voltage controller, the SCRs, and the SCR trigger/pulse controller alter the A.C. line voltage and adjust the waveform of the voltage to control electrical conditions on the primary side of the transformer in the T-R set. The result is a primary voltage that can range from zero to more than 400 volts. In the transformer, the relatively low primary voltage is stepped up to a secondary voltage of more than 50,000 volts.

The electricity on the secondary side of the transformer is converted from alternating current to direct current in a rectifier located in the T-R set. As a result of the T-R set, the electrical power going to the discharge electrodes is a pulse-type direct current.

The voltage applied to the discharge electrodes is called the secondary voltage because the electrical line is on the secondary side (high voltage generating side) of the transformer. This voltage is sensed using a voltage divider mounted inside the T-R set. For convenience, the secondary voltage gauge is located on the primary control cabinets.

As the primary voltage applied to the transformer increases, the secondary voltage applied to the discharge electrodes increases. Stable electrical discharges begin to occur when the secondary voltage exceeds the onset voltage, which can be between 15,000 and 25,000 volts depending partially on the "sharpness" or extent of curvature of the discharge electrode. The relationship between the secondary voltage and the secondary current is shown in Figure 5-19.

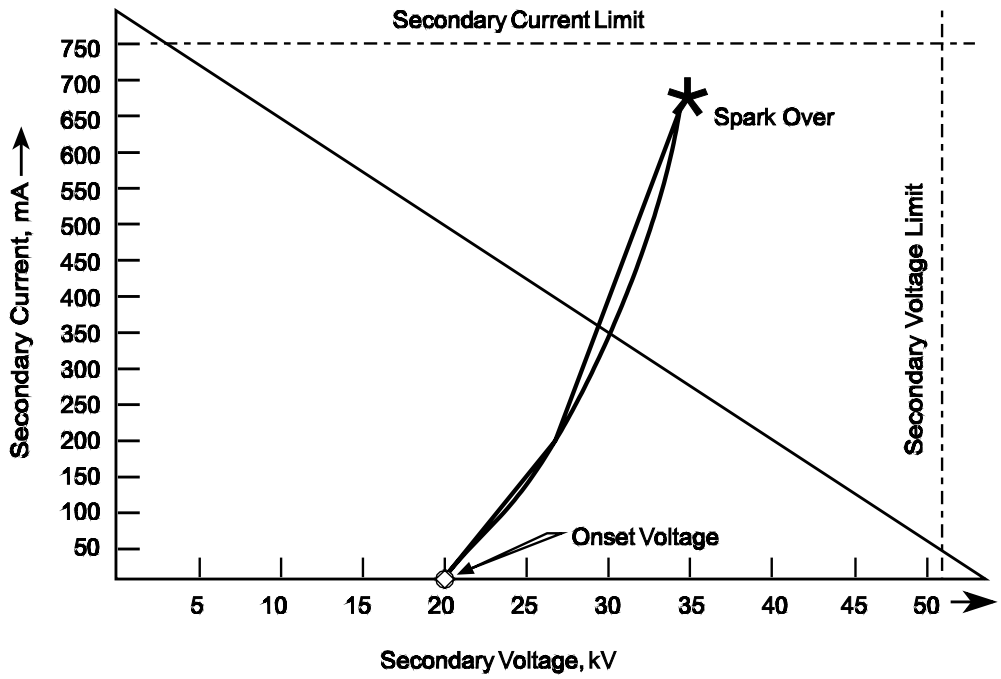

Figure 5-19. Voltage-current curve

The automatic voltage controller in the primary control cabinet is designed to increase the primary voltage applied to the T-R set to the maximum point possible at any given time. One of the following six factors will always limit the maximum secondary voltage.

- Primary voltage limit
- Primary current limit
- Secondary voltage limit
- Secondary current limit
- Spark rate limit
- SCR conduction angle

The upper limit of the primary voltage is set by the 480 volts of the power line leading to the primary control cabinet. The primary current limit is set by the operator at a level below the current value that could damage the primary control cabinet components. The secondary voltage and current limits are also set at levels necessary to protect the T-R set components.

The spark rate limit is an arbitrary limit selected by the operator to optimize performance. Some electrical sparking is generally indicative of good operation. Excessive sparking can cause premature component failure. Whenever any one of these limits is reached, the automatic voltage controller decreases the applied primary voltage to protect the electrical circuitry. The applied primary voltage moves up the voltage-current curve until one of the limits is reached.

Operating conditions at any given time are determined by one of the six operating limits. The primary voltage, primary current, secondary voltage, secondary current, and spark rate at this prevailing limit are indicated by gauges mounted on the front of the primary control cabinet. Most of the new installations also have indicator lights to show the operating limit that is presently limiting the secondary voltage. The electrical conditions and the limiting factor vary at any one field over time, and they vary substantially from field-to-field. This information is very useful for evaluating precipitator performance and is, therefore, discussed in more detail later in this chapter.

If there is no electrical sparking in a field, the electrical conditions in the field will remain very stable until dust loadings or other changes affect the electrical conditions. If electrical sparking occurs, there will be short-term variations in these indicated operating conditions. After each spark in a precipitator field, the automatic voltage controller shuts off the primary voltage for a short period of time (milliseconds) to prevent the short-term spark from becoming a sustained, damaging power arc. Once this quench period is over, the voltage is ramped up quickly to a voltage very close to the previous point at which the spark occurred. The voltage is then gradually increased to the point where another spark occurs. Generally, these variations appear as very brief fluctuations in the secondary voltage meter.

Protective equipment is included in the primary control cabinet. If a problem is sensed in the power supply of the precipitator field, this protective circuitry trips the power supply and the T-R set off-line. For example, a short circuit across the surface of a high voltage frame support insulator would create very low voltages and high currents. The under-voltage sensors would detect this condition and shut down the field to prevent damage to the insulator or to the power supply itself.

5.2.2 Particle Charging and Migration

The corona electrical discharges on the precipitator discharge electrodes are needed to electrostatically charge the particles. Within this corona discharge (see Figure 5-20), electrons accelerated by the very strong electrical field strike and ionize gas molecules. Each collision of a fast-moving electron and a gas molecule generates an additional electron and a positively charged gas ion. The corona discharges are often described as an electron "avalanche" since large numbers of electrons are generated during multiple electron-gas molecule collisions. The positive ions generated in the ionization process move back toward the discharge electrode and are neutralized.

Some of the electrons released in the corona discharges are later captured by gas molecules in areas slightly farther away from the discharge electrode where the electrical field strength is lower. These negatively-charged gas ions move rapidly toward the grounded collection plates.

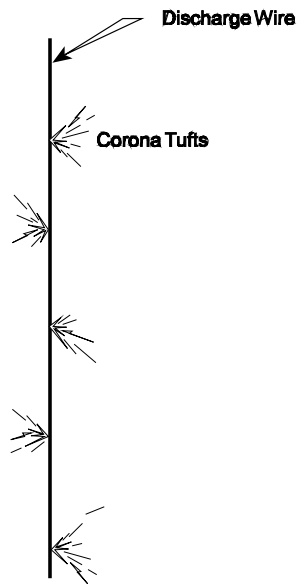

Figure 5-20. Corona discharges

Some of the negatively charged gas ions are captured by particles as the ions attempt to move toward the grounded collection plate. The particles quickly reach a maximum charge called the field dependent saturation charge. This is the charge at which the electrical field created by the captured ions is strong enough to deflect additional gas ions that are approaching the particle. The magnitude of the saturation charge is dependent on the particle size, as indicated by Equation 5-1.

$$q = (12\pi\varepsilon_0 E_0)\, d_p^2 \qquad (5\text{-}1)$$

Where:

q = charge on particle

$_0$ = permitivity of free space

E_0 = electric field strength

d_p = particle diameter

Small particles have a low saturation charge since the ions are bunched closely together on a small surface. As shown in Equation 5-1, the saturation charge increases with the square of the particle diameter. Large particles are easier to collect in electrostatic precipitators since they accumulate higher electrical charges on their surface and, therefore, are more strongly affected by the applied electrical field.

Diffusion of the negatively charged gas ions to the surface of the particles can increase the electrical charge above the level created by the field dependent charging. This charging mechanism, usually termed *diffusional charging*, is important primarily for particles of less than 2 m (MacDonald and Dean, 1980).

Once the particles have attached ions with a negative electrical charge, the particles are influenced by the strong, nonuniform electrical field between the discharge electrode and the grounded collection plate.

Accordingly, the charged particles begin to migrate toward the grounded plates. Large particles move faster than small particles due to the greater electrical charge on the large particles. The migration velocities of particles are indicated in Equation 5-2.

$$\omega = \frac{qE_pC_c}{6\pi d_p\mu} \tag{5-2}$$

Where:

= migration velocity

q = charge on particle

E_p = electric field near collection plate

C_c = Cunningham slip correction factor

= gas viscosity

d_p = particle diameter

The field strength at the discharge electrode is dependent primarily on the peak voltage applied to the discharge electrodes. The field strength at the collection surface depends on the applied peak voltage and on the electrical field created by the negatively charged ions streaming toward the collection plates along the electrical field lines. The electrical field created by the negative gas ions is termed the ionic space charge.

The combined effect of field dependent charging and diffusional charging creates a typical particle size-collection efficiency relationship similar to Figure 5-21. There are very high collection efficiencies above 0.5 micrometers due to the increasing effectiveness of field dependent charging for large particles. Diffusional charging is especially beneficial for particles less than 0.1 micrometers. There is a difficult-to-control range between 0.1 to 0.5 micrometers due to the size dependent limitations of both of these charging mechanisms. As indicated in Figure 5-21, the precipitator is least effective for the particles in this size range.

The extent of this efficiency limit in the difficult-to-control size range is related to the size of the precipitator, the extent of sectionalization, the operating conditions, and the physical conditions. Well designed and operated precipitators can have size-efficiency relationships with only a slight efficiency decrease in the difficult-to-control size range. Undersized precipitators or units in poor condition can have a more pronounced efficiency decrease in this size range.

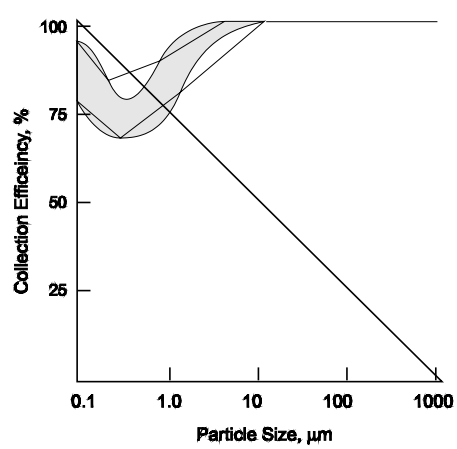

Figure 5-21. Typical particle size efficiency relationship for electrostatic precipitators

5.2.3 Dust Layer Resistivity

The gas ions arriving on the surfaces of particles and arriving as uncaptured ions must pass through the dust layers on the collection plates. As the electrical charges pass slowly through this dust layer, they create an electrostatic field.

At the metal surface of the collection plate, the voltage is zero since the plate is electrically grounded. At the outer surface of the dust layer where new particles and ions are arriving, the electrostatic voltage caused by the gas ions on the dust layer can be more than 10,000 volts.

It is this electrostatic voltage difference across the dust layer that holds the dust layer on the vertical surface of the collection plate. The same type of voltage difference is created when a child rubs a birthday balloon on his or her hair and then sticks the balloon on a wall. It does not fall because of the electrostatic field created by the very slight difference between the side of the balloon and the wall. Eventually, however, the balloon falls off the wall. The electrons that were initially trapped on one side of the balloon find a path for reaching the wall. As the electrons flow off the balloon, the electrostatic field holding it to the wall becomes weak.

Essentially the same phenomenon occurs in the dust layers on precipitator collection plates. When the electrical charges from the gas ions can readily move through the dust layer to the plate, the electrostatic field across the dust layer is relatively weak (i.e., several thousand volts). This means that the dust layer can be easily dislodged. When the electrical charges move very slowly through the dust layer, there are a large number of electrical charges on the outer surface, and the voltage difference can be very high (more than 10,000 volts). This means that the dust layer is held very tenaciously.

The ability of the electrical charges (electrons) to move through the dust layer is measured in terms of the dust layer resistivity. When the resistivity is very low, the electrons are conducted very readily, and only a slight electrostatic field is maintained across the dust layer. When the resistivity is very high, the electrons have difficulty moving through the dust layer and create a very high electrostatic field as they accumulate on the outer surface of the dust layer.

Very high and very low resistivity conditions are harmful to electrostatic precipitator performance. Electrostatic precipitators work best when the dust layer resistivity is in the moderate range: not too high and not too low. This is because of the various ways that the dust layer electrostatic field affects both dust layer rapping and particle charging migration.

During rapping of weakly held low resistivity dust layers, many of the particles are redispersed back into the gas stream as individual particles or small agglomerates that do not settle by gravity fast enough to reach one of the hoppers before the gas stream leaves the precipitator. The problem associated with gravity settling of the redispersed particles is illustrated in Figure 5-22, which shows the possible trajectories for 1, 10, and 100 m particles rapped from the top of the inlet field of a precipitator. The limited settling is due to the low terminal setting rates shown in Figure 5-23. It is apparent that even large particles of 100 m diameter do not fall sufficiently fast to reach the hoppers.

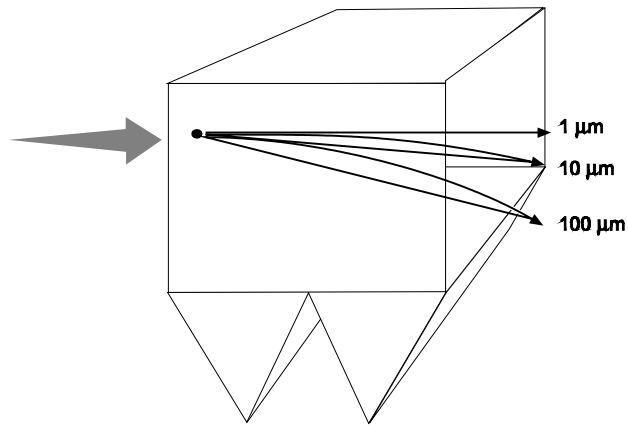

Figure 5-22. Trajectories of particles redispersed from the upper portions of the inlet field collection plates

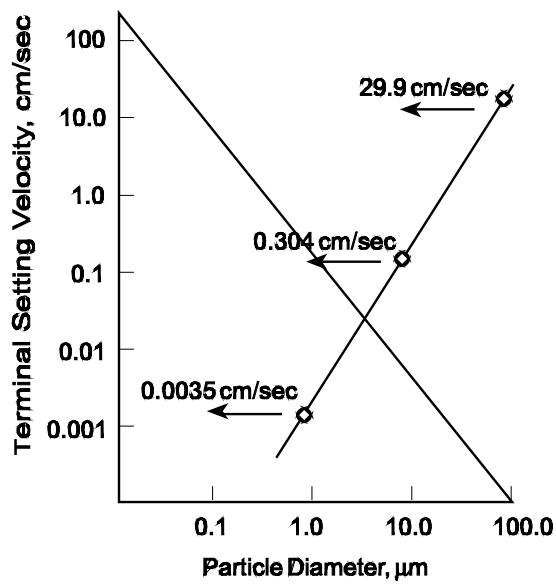

Figure 5-23. Terminal settling velocities of particles

It should be noted that most particles entering the precipitator are smaller than 100 µm. Accordingly, it is very important that the particles agglomerate in the dust layer and settle as large clumps or sheets rather than as discrete particles. If the resistivity is too low and particles (or even small agglomerates of particles) are redispersed, there can be a short term emission spike, called a puff, due to the emission of these particles immediately after rapping. As the resistivity increases into the moderate range, the voltage drop across the dust layer increases, and the dust cake is dislodged as cohesive sheets or clumps that are large enough to fall rapidly and be collected in the hoppers of the precipitator.

If the voltage drop across the dust layers becomes too high (high resistivity), there can be a number of adverse effects. First, it reduces the voltage difference between the discharge electrode and the dust layer and, thereby, reduces the electrostatic field strength used to drive the gas ion-carrying particles over to the

dust layer. As the dust layer builds up, and the electrical charges accumulate on the surface, the voltage difference decreases. The migration velocities of small particles is especially affected by the reduced field strength. The general impact of high resistivity on the migration velocity is illustrated in Figure 5-24.

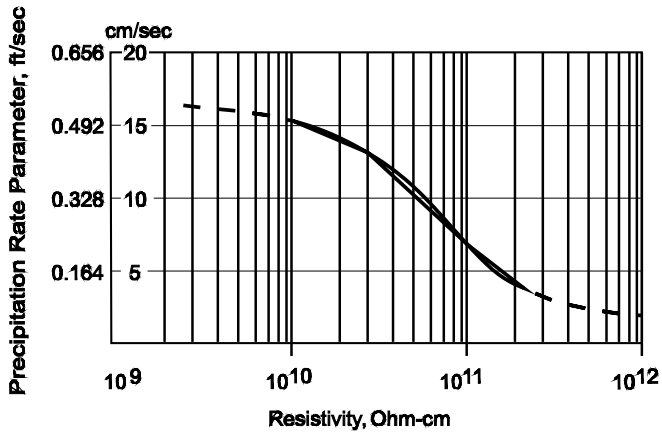

Figure 5-24. Effect of dust layer resistivity on migration velocity (White, 1977)

Another adverse impact of high resistivity dust layers is called back corona, which occurs when the electrostatic voltage across the dust layer is so great that corona discharges begin to appear in the gas trapped within the dust layer (MacDonald and Dean, 1980. White, 1977). When the voltage in the dust layer reaches sufficient levels, electrons are accelerated and ionization begins. However, when this happens in the dust layer, some of the positive ions formed by the electron collisions stream toward the negatively charged discharge electrode. Along the way, these positive ions neutralize some of the negative charges on the dust layer particles. They also neutralize some of the negative ions on the particles approaching the dust layer and reduce the ionic space charge near the dust layer surface (MacDonald and Dean, 1980; White, 1977). The net result of back corona is severely impaired particulate matter removal efficiency.

The third and generally most common adverse impact of high resistivity dust layers is increased electrical sparking. Once the sparking reaches the arbitrarily set spark rate limit, the automatic controllers limit the operating voltages of the field. This causes reduced particle charging effectiveness and reduced particle migration velocities toward the collection plates. High resistivity-related sparking is due primarily to the concentration of electrical field lines in localized portions of the dust layer on the collection plates (Hall, 1983. MacDonald and Dean, 1980. Katz, 1979). Any misalignment problems or protrusions of the collection plate surface make this localized area especially vulnerable to sparking. The location on the dust layer where the spark hits is not random, just as it is not random in nature. For example, lightning often strikes tall metal towers. Likewise, factors that cause the dust layer surfaces to be just a little closer to the discharge electrodes make these sites vulnerable to a spark under high resistivity conditions. These factors include bows or warps in the collection plate, misaligned discharge electrodes, and even small welding splashes on the surface of the collection plate. Anything that reduces the distance between the dust layer and the discharge electrodes makes the unit more susceptible to sparking. This is why proper alignment of precipitator collection plates and discharge electrodes is so important when the resistivity is high. The sparking created by these close approach points reduces the possible operating voltage of the unit and therefore severely limits the ability to charge and collect particles.

There is another adverse characteristic of high resistivity dust layers. Since the dust layers are so strongly held by the electrostatic fields, it is hard to dislodge the dust. As more negative ion-carrying dust

continues to arrive, the depth of the dust layer increases, and it becomes even harder for electrons to pass through to the collection plates. There can be some temptation to rap the collection plates frequently and severely to reduce the dust layer quantities. In severe cases, this practice can have very little beneficial impact on the dust layer depths, and it can lead to rapid mechanical failure of the rappers and/or misalignment of the collection plates. If in some cases this practice causes misalignment, the problems caused by high resistivity become even greater.

Electrostatic precipitators work best when the dust layer resistivity is in the moderate range. It should resist current flow a little but not too much. It is helpful to describe the dust layer resistivity based on units of ohm-centimeters (ohm-cm). This is simply the ohms of resistance created by each centimeter of dust in the dust layer. High resistivity is generally considered to be equal to or above 5×10^{10} ohm-cm (MacDonald and Dean, 1980. White, 1977). Low resistivity is generally considered to be equal to or below 5×10^{8} ohm-cm. The region between 5×10^{8} and 5×10^{10} ohm-cm is, therefore, the moderate or preferred range.

There are actually two basic paths that electrons can take in passing through the dust layer to the collection plate surface. They can pass directly through each particle until they reach the metal surface. This is called bulk conduction, which occurs only when there are one or more constituents in the particles that can conduct electricity. Conversely, the electrons can pass over the surfaces of various particles until they reach the metal surface. This is called surface conduction, which occurs when vapor phase compounds that can conduct electricity adsorb onto the surfaces of the particles. Both paths of current dissipation are illustrated in Figure 5-25.

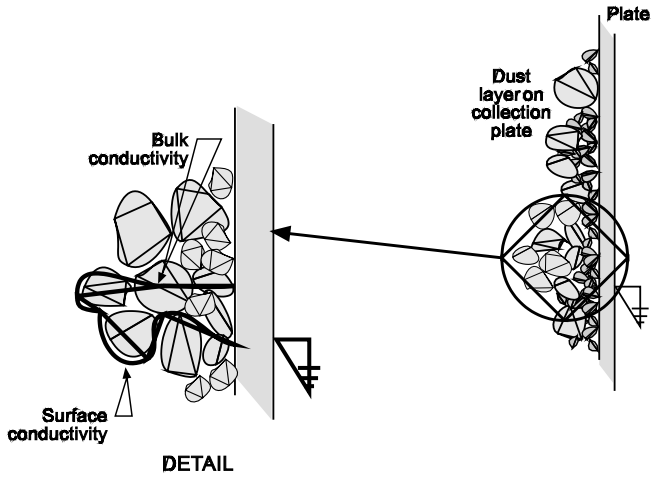

Figure 5-25. Paths of current flow through the dust layers

One of the most common electrical conductors responsible for bulk conduction in particles is carbonaceous material. If the concentration of this material is sufficiently high, the electrons can pass from particle to particle to reach the collection plate (White, 1977). Electrical conduction through the inorganic oxides and other compounds that comprise the majority of ash particles from combustion sources and other industrial sources is sufficiently rapid when the temperatures are above 400°F and preferably in the range of 500°F and 700°F. This resistivity-temperature relationship is indicated in Figure 5-26.

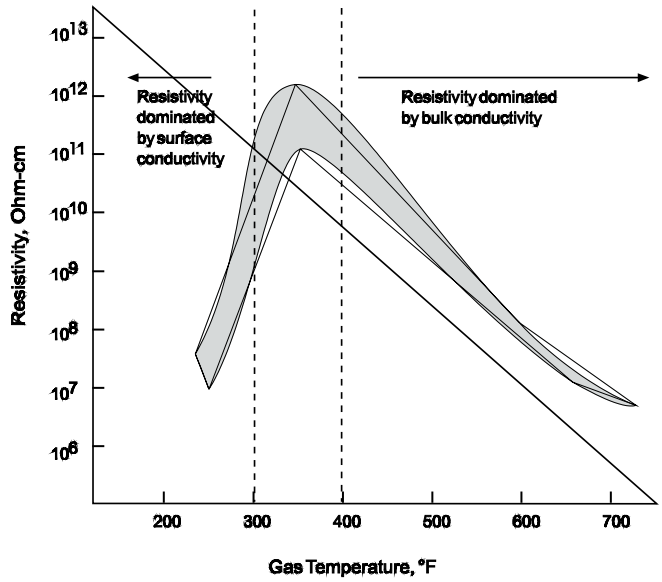

Figure 5-26. Example resistivity-temperature relationship

On the low temperature side of the typical resistivity curve, the resistivity can decrease dramatically as the gas temperature drops slightly (Katz, 1979). This is due to the increased adsorption of electrically conductive materials originally present as vapors in the gas stream. One of the most common vapor phase compounds responsible for surface conduction is sulfuric acid. It adsorbs to particle surfaces very readily, even at gas temperatures of 250°F to 350˚F. Even vapor phase concentrations of only 5 to 10 ppm are often sufficient to affect the dust layer resistivity. The ability of sulfuric acid to electrically condition the particle surfaces is due, in part, to its hygroscopic tendencies. Each sulfuric acid molecule can be attached to a cluster of water molecules, which can also be electrically conductive.

Many air pollution sources using electrostatic precipitators generate enough sulfuric acid or other particle surface conditioning agents to reduce the dust layer resistivities into the moderate range at operating temperatures of 250°F to 350˚F. However, if they generate too much sulfuric acid vapor, or if the gas temperature drops too much, the resistivity can be too low. If, for some reason, enough sulfuric acid is not generated, or the gas temperature is relatively high, the resistivity can be very high.

It is clear that dust layer resistivity can be very strongly influenced by gas temperature when surface conduction is the main path of electrical current movement through the dust layer. Also, resistivity is sensitive to the quantity of vapor phase compounds that can adsorb on the surface.

In sources that do not inherently generate enough vapor phase compounds for surface conditioning, it is necessary to inject the materials into the precipitator inlet. The most common material used to condition precipitators is sulfur trioxide, which quickly forms vapor phase sulfuric acid upon entering the inlet gas stream (Fletcher, 1982. Weyers and Cook, 1981. Eskra and McKinney, 1982). Ammonia is also used either alone or in combination with sulfur trioxide (Fletcher, 1982). These materials adsorb on the surfaces of the particles as they enter the precipitator and are being collected. Once the particle is in the dust layer, electrons pass through these adsorbed molecules.

The very strong temperature dependence of surface conditioning can create some very non-uniform dust layer resistivities in different portions of the unit. It is common for portions of the precipitator to be 30 to 50˚F different from the average temperature indicated by the plant instrumentation. In the hot areas, very little vapor phase material adsorbs, and the resistivity can be relatively high. In the cold areas, too much conductive material can be on the particle surfaces, and the resistivity can be relatively low. In one case,

spatial differences of more than three orders of magnitude in dust layer resistivity have been found (Beak, Krawcyzk, and Richards, 1988).

5.2.4 Electrostatic Precipitator Applicability Limitations

Electrostatic precipitators can provide high efficiency, reliable particulate matter control in a wide variety of industrial applications. However, there are a few conditions that limit their industrial applicability.

- Extremely low flyash resistivities
- Potential fire and explosion hazards
- Sticky particulate matter
- Ozone formation

In industrial sources that generate highly carbonaceous particulate matter, the flyash resistivities can be extremely low due to the high bulk conductivity of this material at all temperatures. These resistivities can be below the levels where good performance can be obtained by flue gas conditioning. Severe rapping reentrainment problems can persist during routine operation due to the weak electrical forces bonding the dust layer to the collection plate and the ease of particle dispersion during rapping. Electrostatic precipitators are not an ideal choice for particulate matter control in these applications due to the probable emission problems.

Applications involving the routine or intermittent presence of highly carbanaceous particulate matter or other easily combusted material should be approached with caution. Fires can occur in dust layers on the collection plates or in the accumulated solids in a hopper. These fires can create high temperature areas in the affected part of the unit, which can result in severe warpage and misalighnment of the collection plates. Electrostatic precipitators are not appropriate for sources that have potentially explosive concentrations of gases and/or vapors. The routine electrical sparking in the fields provides numerous opportunities to ignite the explosive materials. For these reasons, electrostatic precipitators are rarely used for sources generating highly combustible and/or potentially explosive contaminants in the gas streams.

The presence of highly sticky material such as some oils and compounds like ammonium bisulfate can present major operating problems in dry, negative corona precipitators. Rapping of the solids from the collection plates must be readily possible. The accumulation of sticky material on the collection plates and other components in the precipitator would soon cause collection plate-to-discharge electrode clearance problems that would adversely affect the electrical conditions in the affected field. For this reason, dry, negative corona precipitators are rarely used on sources that generate high concentrations of sticky particulate matter. Wet, negative corona precipitators and wet, positive corona precipitators can operate very well with moderately sticky material. However, it must be possible to remove the contaminants either by normal drainage or by occasional cleaning sprays.

Dry, negative corona and wet, negative corona precipitators generate very small quantities of ozone due to the characteristics of the corona discharge. Generally, the concentration of ozone is limited by the relatively low oxygen levels in the gas stream being treated. Due to the presence of ozone, these types of electrostatic precipitators are not used for standard air cleaning operations where the oxygen concentrations are at ambient levels, and it is necessary to recirculate the treated air stream to an occupied work area.

5.3 ELECTROSTATIC PRECIPITATOR CAPABILITY AND SIZING

The size of an electrostatic precipitator is important since there is a general relationship between the size of the unit and the attainable particulate matter removal efficiency. Particle charging and migration (Step 1 in electrostatic precipitation) is greater in large units since the migration velocities of particles less than 10 m are relatively low. Large electrostatic precipitators also provide longer gravity settling times for solids rapped from the collection plates and discharge wires (Step 2 in electrostatic precipitation). However, there are practical limits to precipitator size. Units that are too large are extremely expensive. Other problems associated with oversized units include-but are not limited to-corrosion caused by excessive convective and conductive gas cooling, corrosion caused by multiple air infiltration sites, and gas maldistribution caused by very low gas velocities at the precipitator inlet. Purchasers and designers of electrostatic precipitators must determine the optimum size that balances the requirements for high efficiency with the need for reasonable cost and reliability.

Several of the following precipitator sizing parameters are generally used to characterize the unit. It is not possible, however, to independently select specific values for all of these parameters due to their interrelationships.

- Specific collection area
- Sectionalization
- Aspect ratio
- Gas superficial velocity

The specific collection area is selected using experience-based empirical methods and/or computerized performance models. The other parameters are selected based primarily on empirical factors.

5.3.1 Specific Collection Area

The specific collection area (often termed the SCA) is defined as the ratio of the collection surface area to the gas flow rate passing through the unit. As shown in Equation 5-3, it is usually expressed in terms of square feet per 1000 ACFM of gas flow.

$$SCA = A/G \tag{5-3}$$

Where:

SCA = specific collection area (ft^2/1000 ACFM)

A = total collection plate area (ft^2)

G = total gas flow rate ((ft^3/min)×0.001)

There has been a substantial increase in the design of SCAs from levels of 100 to 200 ft^2 per 1000 ACFM in the 1960s to present-day levels of 300 to 1400 ft^2 per 1000 ACFM. There is no single value of SCA that guarantees adequate performance for all precipitators. Instead, the SCA must be based on unit-specific factors such as the dust layer resistivities and the particle size distribution.

Sources that generate particulate matter with high resistivities generally use a high SCA. The presence of large quantities of fine particulate also usually requires larger-than-average SCAs.

Empirical methods used to estimate the necessary SCA for a given application have been based on the Deutsch-Anderson equation. This equation is based on probability theory and generally applies to particles less than approximately 10 m in diameter (White, 1977). Particles less than this size have migration velocities of 0.3 to 0.8 ft/sec, which is well below the gas velocities through the passages of 3 to 6 ft/sec. Due to the turbulent nature of the gas flow through the passages, the motion of these particles is dependent primarily on the turbulent mixing of the eddy currents. However, particles close to the

collection plate may be captured due to electrostatic forces. The extent of particle capture is expressed by Equation 5-4.

$$\eta = 1 - e^{-\omega \frac{A}{G}} \tag{5-4}$$

Where:

= efficiency (decimal form)

= migration velocity (ft/sec)

A = total collection plate area (ft^2)

G = total gas flow rate (ft^3/sec)

e = base of natural logarithm = 2.718

The Matts-Ohnfield equation is another version of the Deutsch-Anderson equation. As shown in Equation 5-5, an additional exponent is used to provide a more conservative estimate of removal efficiency. Typical values of this "k" factor range from 0.4 to 0.6 (Szabo and Gerstle, 1977).

$$\eta = 1 - e^{-\left[\omega\left(\frac{A}{G}\right)\right]^k} \tag{5-5}$$

Where:

k = dimensionless constant

The migration velocity depends on the electrical field strength, the electrical charge on the particle, and other factors described earlier in Equation 5-2. Accordingly, Equation 5-4 and Equation 5-5 are applicable only for particles of a single size. The migration velocity calculated for a submicrometer particle is well below the migration velocity of larger particles due to the limited number of electrical charges on the small particles.

The migration velocities for particles that create low dust layer resistivities are high since these conditions increase the electrical field strength near the collection plate. As was shown in Figure 5-23, the migration velocities are in the 0.6 to 0.8 ft/sec range for low resistivity dusts and drop rapidly to the 0.2 to 0.3 ft/sec range for high resistivity dusts.

Due to variations in particle size distributions and in dust layer resistivities, it is difficult to use the Deutsch-Anderson type equations directly to determine the necessary precipitator size. Furthermore, this approach does not take into account particulate emissions due to rapping reentrainment, gas sneakage around the fields, and other non-ideal operating conditions.

To take these conditions into account, the migration velocity is often used as an empirical factor. Particulate removal data from a variety of similar units installed previously are reviewed to determine the effective migration velocity. This empirically derived migration velocity is then used to calculate the necessary collection plate area of a new installation. The variability of these values is illustrated in Table 5-1. The following exercise (Problem 5-1) illustrates the use of the effective migration velocity data.

Table 5-1. Effective Migration Velocities for Various Industries		
	Effective Migration Velocity	
Application	ft/sec	cm/sec
Utility Coal-Fired Boiler	0.13 - 0.67	4.0 - 20.4
Pulp and Paper Mill	0.21 - 0.31	6.4 - 9.5
Sulfuric Acid Mist	0.19 - 0.25	5.8 - 7.6
Cement (Wet Process)	0.33 - 0.37	10.1 - 11.3
Cement (Dry Process)	0.19 - 0.23	5.8 - 7.0
Gypsum	0.52 - 0.64	15.8 - 19.5
Open-Hearth Furnace	0.16 - 0.19	4.9 - 5.8
Blast Furnace	0.20 - 0.46	6.1 - 14.0

Source: Theodore and Buonicore, 1976

Problem 5-1

Calculate the expected particulate efficiency for an electrostatic precipitator serving a utility coal-fired boiler. The gas flow rate is 250,000 ACFM. The total collection plate area is 100,000 ft^2. Use an effective migration velocity of 0.20 ft/sec.

Substituting into the standard Deutsch-Anderson equation

$$\eta = 1 - e^{-\left[(0.20\,\text{ft/sec.})(100{,}000\,\text{ft}^2/250{,}000\,\text{ft}^3/\text{min.})\right]}$$

Converting ft^3/min to ft^3/sec)

$$\eta = 1 - e^{-\left[(0.20\,\text{ft/sec.})(100{,}000\,\text{ft}^2/4{,}167\,\text{ft}^3/\text{sec.})\right]}$$

$$= 1 - e^{-4.8}$$

$$= 1 - 0.00823$$

$$= 0.99177 = 99.177\%$$

This indicates that the overall efficiency of the precipitator would be 99.17% if the effective migration velocity were 0.20 feet per second. The estimated efficiencies for assumed effective migration velocities of 0.25 and 0.30 ft/sec would be 99.75% and 99.93% respectively. This illustrates the importance of the assumed effective migration velocity.

In the past, this precipitator sizing approach was sufficient to obtain an initial estimate of the required collection plate area as long as the equipment manufacturer had an extensive data base to select an appropriate effective migration velocity. These plate area data were then refined and adjusted in designing the unit. A variety of other design factors such as average gas flow rate, number of fields in

series, number of chambers, and aspect ratio were considered in determining the specifications of the precipitator.

Sizing calculations based only on Deutsch-Anderson type equations have significant limitations in present-day applications due primarily to the very stringent particulate control requirements. There can be substantial variations in all of the non-ideal modes of particulate emissions that are lumped together in the effective migration velocity term. Also, there can be significant differences in the energization of the precipitator fields. These site-specific energization and non-ideal emission mode variations can be large enough to cause a new unit to fail to meet the required performance specifications.

A computerized performance model, the EPA/RTI model (Lawless, 1992), has been developed. It provides a more fundamentally correct representation of the precipitation process than the Deutsch-Anderson type equations. The EPA/RTI model is based on the localized electrical field strengths and current densities prevailing throughout the precipitator (Lawless, 1992). These data can be input based on actual readings from operating units, or it can be calculated based on electrode spacing and resistivity. These data are used to estimate the combined electrical charging on each particle size range due to field dependent charging and diffusional charging. Particle size dependent migration velocities are then used in a Deutsch-Anderson type equation to estimate particle collection in each field of the precipitator. This model takes into account a number of the site-specific factors including gas flow maldistribution, particle size distribution, and rapping reentrainment.

The use of these performance models requires detailed information concerning the anticipated configuration of the precipitator and the characteristics of the gas stream. Information needed to operate the model is provided in Table 5-2. It is readily apparent that not all these parameters are needed in each case since some can be calculated from several of the others.

Table 5-2. Data Used in EPA/RTI Computerized Performance Model for Electrostatic Precipitators

ESP Design

- Specific collection area
- Collection plate area
- Collection height and length
- Gas velocity
- Number of fields in series
- Number of discharge electrodes
- Type of discharge electrodes
- Discharge electrode-to-collection plate spacing

Particulate Matter and Gas Stream Data

- Resistivity
- Particle size mass median diameter
- Particle size distribution standard deviation
- Gas flow rate distribution standard deviation
- Actual gas flow rate
- Gas stream temperature
- Gas stream pressure
- Gas stream composition

Problem 5-2

For comparison with Problem 5-1, the computerized model has been used to predict the precipitator removal efficiency for the gas flow rate and collection plate area used in Problem 5-1. The results are shown in Table 5-3.

Table 5-3. Calculation Results for Problem 5-2

Efficiency	99.60%
Total Particulate Matter Emissions	0.01124 gr/acf, or 0.0360 $lb_m/10^6$ Btu
PM_{10} Emissions	0.007 gr/acf
Rapping Contribution	16.7%

The efficiency shown in Table 5-3 is based on a moderate dust layer resistivity of 1.0×10^{10} ohm-cm and an average superficial velocity of 5 ft/sec. Both conditions are within the generally accepted range for proper precipitator performance. The other precipitator design and gas flow characteristics have been based on relatively typical values. Factors adversely affecting precipitator performance such as misalignment, severe gas maldistribution, and severe rapping reentrainment have not been included. Accordingly, the estimated efficiency in this specific calculation should be near the optimum level for the assumed case.

The EPA/RTI model is available through the U.S. EPA Technical Transfer Network (TTN) at http:www.epa.gov/ttn/. Copies of the instruction manual can be downloaded. This model should be useful for both permit review and precipitator problem evaluation.

The U.S. EPA has also published a computerized model for estimating fly ash resistivity based on ash composition data and on gas stream characteristics. This model is also available from EPA and from the National Technical Information Center.

In order to use any computerized model or the simple Deutsch-Anderson equation, the collection plate area and average gas velocities must be calculated from the precipitator specifications. The average gas velocity is simply the total gas flow rate in actual cubic feet per minute divided by the area of the precipitator inlet. This calculation is shown in Equation 5-6.

$$v = \frac{\text{actual gas flow}}{\text{area}} = \frac{(G\ ft^3/min)\left(\frac{min}{60\ sec}\right)}{HW} = \frac{(G\ ft^3/min)\left(\frac{min}{60\ sec}\right)}{(H)\left[\frac{S}{12}\times n\right]} \tag{5-6}$$

Where:

- v = gas velocity (ft/sec)
- G = gas flow rate (ft^3/min) (actual)
- H = collection plate height (ft)
- S = passage width, inches (normally 9, 10, 12 or 16 in.)
- n = number of passages
- W = precipitator width (ft)

In calculating the plate area, start by counting the number of gas passages in each field as shown in Figure 5-27. If there are "n" collection plates across the unit, there will be "n-1" passages since gas does not flow next to the exterior walls of the precipitator.

The collection plate area is calculated based on the dimensions of the plate. Since dust collects on both sides of the collection plates in the passages, the collection plate area is calculated using Equation 5-7.

$$A_p = 2\ (n-1)\ (H)\ (L) \qquad (5\text{-}7)$$

Where:

A_p = collection plate area in field i (ft^2)

n = number of collection plates across unit

H = height of collection plates (ft)

L = length of collection plate in direction of gas flow (ft)

The collection plate area for the unit chamber of the precipitator is calculated simply by summing the areas of each of the fields.

5.3.2 Sectionalization

The performance of an electrostatic precipitator is not solely a function of the quantity of collection plate surface areas. It is also dependent on how that surface area is used. There are a variety of design factors that must be taken into account to ensure proper particulate matter removal capability. Proper sectionalization is one of the most important of these design factors.

The electrostatic precipitator is divided into separately energized areas termed “fields.” The fields are arranged in series along the direction of gas flow as indicated in Figure 5-4. Almost all commercial precipitators have at least three fields in series. Some large units used for coal-fired boilers with high resistivity conditions can have has many as fourteen fields in series.

The inlet field removes 60% to 75% of the incoming particulate matter. This is due primarily to the collection of large diameter particles that acquire a high saturation charge and have high migration

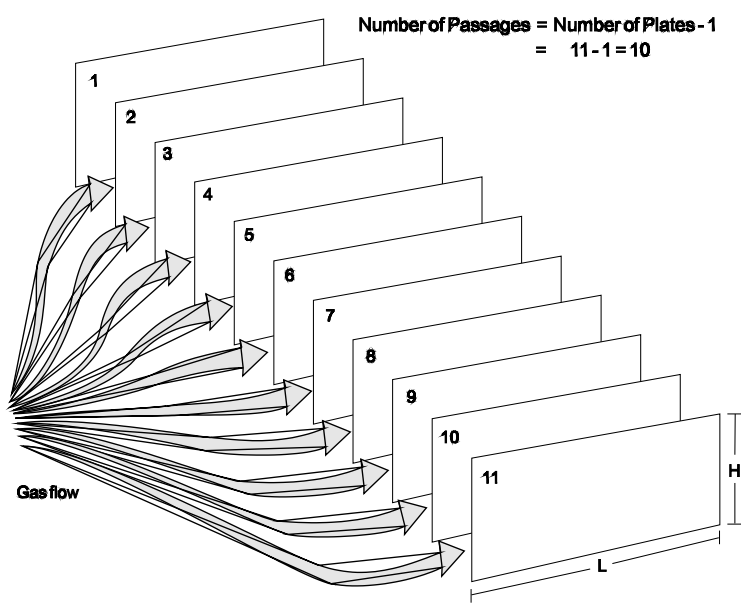

Figure 5-27. Collection plate area calculation

velocities toward the collection plates. The large particles are easily removed in the first field along with some small diameter particles. Each subsequent field in series removes 50% to 80% of the particulate matter penetrating through the preceding field. The outlet field has very low inlet mass concentrations; however, this material is comprised mainly of very small diameter particles that had low saturation charges and thereby were able to penetrate the upstream precipitator fields. A general representation of the removal of particulate matter from the fields of a precipitator is provided in Figure 5-4.

Due to these differences in mass collection rates, there can be significantly more dust on the collection plates in the fields on the inlet side of the precipitator than on the outlet side. The thick dust layers on the fields on the inlet side suppress current flow. The particles migrating toward the dust layers on the collection plates of the inlet fields can also suppress current flow. The presence of electrical charges on slow moving particles creates an electrical field that has the same polarity as the discharge electrode. The electrical charges residing on the particles moving through the space between the discharge electrode and the collection plate dust layer are termed the "space charge." This electrical phenomenon also suppresses current flow in the inlet fields. By dividing the precipitator into separate electrical fields in series, the effect of the heavy dust layers and the particle space charge can be minimized.

Electrical sparking occurs preferentially on the inlet side of the precipitator. This sparking is due primarily to the accumulation of electrical charge on the outer surface of the dust layer on the collection plate. Sparking near the inlet is also due to the disturbances caused when large quantities of dust are dislodged during each rapping cycle. Rapping in the inlet fields is more frequent than in the outlet fields. The automatic voltage controller detects the electrical spark as a current surge and shuts down the applied secondary voltage as shown in Figure 5-28.

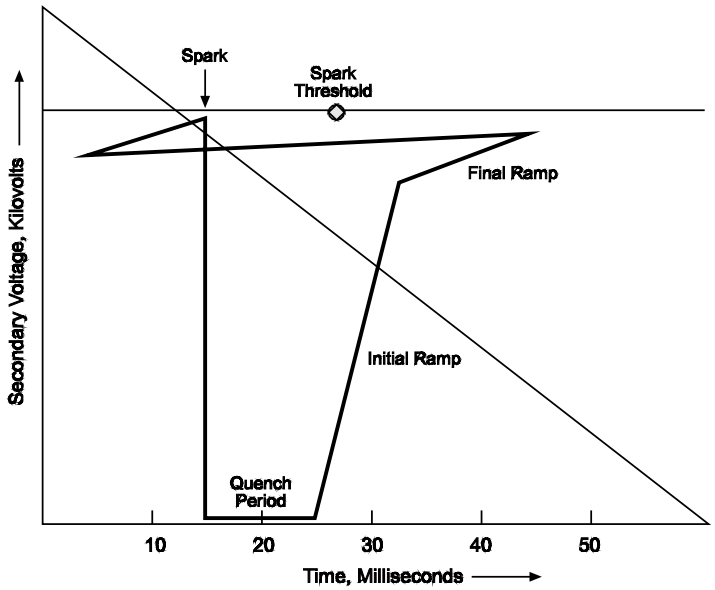

Figure 5-28. Applied secondary voltage before and after an electrical spark

There is a short period that lasts 10 to 20 milliseconds when the field is entirely shutdown. There is also a short period when the secondary voltage is ramping back to its maximum pre-spark levels. During these short time periods, the field strength is not at optimum levels for collection of particulate matter. By sectionalizing the precipitator into separate fields along the direction of gas flow, the field energization

problems associated with frequent sparking can be isolated to the first few fields with high spark rates while the outlet fields are relatively unaffected by their very low spark rates.

On an infrequent basis, an internal mechanical problem in a field can cause an electrical short circuit. Several conditions can cause "shorts."

- Mechanical flex failure of a discharge wire
- Chemical corrosion failure of a discharge wire
- Electrical sparking related erosion failure of a discharge wire
- Electrical tracking and failure across a support insulator surface or an anti-sway insulator surface
- Presence of solids bridging between the high voltage frame and the grounded collection plates due to hopper overflow

The field is automatically taken offline (sometimes termed "tripped") by the primary control cabinet to prevent component damage caused by the high current condition. The field can not be reenergized until maintenance personnel enter the unit to retrieve the failed wire, fix the insulators, or clear the hopper solids bridged material. Often the precipitator must operate for a long period of time before this maintenance work can be completed. If the precipitator has a high degree of sectionalization, the amount of the unit out-of-service is relatively small, and the emission rates do not increase substantially. If there are only a few fields in service, the impact of the loss of a field on performance can be quite high. This is illustrated in Problem 5-3.

Problem 5-3

One electrostatic precipitator serving a coal-fired boiler has a gas stream of 500,000 ACFM, an inlet particulate mass concentration of 2 grains per ACF, and an SCA of 300 ft^2/1000 ACFM. What is the increase in the emission rate if one of the four fields trips offline due to an internal mechanical-electrical problem?

A second electrostatic precipitator serving a similar coal-fired boiler also has a gas flow rate of 500,000 ACFM, an inlet particulate mass concentration of 2 grains per ACF, and an SCA of 300 ft^2/1000 ACFM. However, this unit only has three fields in series. What is the increase in the emission rate if the inlet field has an efficiency of 85%, the middle field has an efficiency of 81%, and the outlet field has an efficiency of 75%?

Solution:

For the first precipitator, the efficiency of four fields in series during routine operation can be estimated as follows.

$$\text{Emissions}_{\text{Routine}} = \frac{2\text{ grains}}{\text{ACF}}\left(1-\frac{\text{eff}_1}{100}\right)\left(1-\frac{\text{eff}_2}{100}\right)\left(1-\frac{\text{eff}_3}{100}\right)\left(1-\frac{\text{eff}_4}{100}\right)$$

$$\text{Emissions}_{\text{Routine}} = \frac{2\text{ grains}}{\text{ACF}}\left(1-\frac{80}{100}\right)\left(1-\frac{70}{100}\right)\left(1-\frac{70}{100}\right)\left(1-\frac{60}{100}\right)$$

$$\text{Emissions}_{\text{Routine}} = \frac{2\text{ grains}}{\text{ACF}}(0.20)(0.30)(0.30)(0.40) = 0.0072\left(\frac{2\text{ grains}}{\text{ACF}}\right) = 0.0144\text{ grains / ACF}$$

When one of the four fields is out of service, the performance of the precipitator can be calculated as follows:

$$\text{Emissions}_{\text{Upset}} = \frac{2\ \text{grains}}{\text{ACF}}\left(1-\frac{\text{eff}_1}{100}\right)\left(1-\frac{\text{eff}_2}{100}\right)\left(1-\frac{\text{eff}_3}{100}\right)\left(1-\frac{\text{eff}_4}{100}\right)$$

$$\text{Emissions}_{\text{Upset}} = \frac{2\ \text{grains}}{\text{ACF}}\left(1-\frac{80}{100}\right)\left(1-\frac{70}{100}\right)\left(1-\frac{70}{100}\right)\left(1-\frac{0}{100}\right)$$

$$\text{Emissions}_{\text{Upset}} = \frac{2\ \text{grains}}{\text{ACF}}(0.20)(0.30)(0.30)(1.0) = 0.0018\left(\frac{2\ \text{grains}}{\text{ACF}}\right) = 0.036\ \text{grains/ACF}$$

In this case, the emissions increased from 0.014 to 0.036 grains/ACF.

In this general calculation approach, it is assumed that the outlet field, the one with the lowest efficiency, is not available. This is an appropriate calculation approach regardless of which of the four is tripped offline. The roles of the four fields in series will shift as soon as one is lost. For example, the second field becomes the first field if the inlet field trips offline. If one of the middle fields in lost, the gas stream entering the outlet field has high mass loadings and larger sized particulate than during routine operation. Accordingly, the outlet field operates at the efficiency of a middle field.

For the second precipitator, the efficiency during routine operation and during upset conditions after the loss of one of the fields is estimated as follows:

$$\text{Emissions}_{\text{Routine}} = \frac{2\text{grains}}{\text{ACF}}(1-\frac{\text{eff}_1}{100})(1-\frac{\text{eff}_2}{100})(1-\frac{\text{eff}_3}{100})$$

$$\text{Emissions}_{\text{Routine}} = \frac{2\text{grains}}{\text{ACF}}(1-\frac{85}{100})(1-\frac{81}{100})(1-\frac{75}{100})$$

$$\text{Emissions}_{\text{Routine}} = \frac{2\text{grains}}{\text{ACF}}(0.15)(0.19)(0.25) = 0.014\,\text{grains/ACF}$$

$$\text{Emissions}_{\text{Upset}} = \frac{2\text{grains}}{\text{ACF}}(1-\frac{85}{100})(1-\frac{81}{100})$$

$$\text{Emissions}_{\text{Upset}} = \frac{2\text{grains}}{\text{ACF}}(0.15)(0.19) = 0.057\,\text{grains/ACF}$$

The second precipitator has an emission increase from 0.014 to 0.057 grains/ACF. This is a substantially higher increase than the first precipitator.

It is apparent from the relatively simple calculation that the emission increases resulting from the loss of a field are more severe for units with limited sectionalization, such as the second unit in Problem 5-3.

Sectionalization of precipitators is also necessary due to the practical limits to the size of the T-R set. Modern precipitators are quite large, and it would be difficult to build a T-R set that would be electrically stable and provide power to the entire precipitator. Sectionalization provides more stable electrical conditions and minimizes the vulnerability to operating problems.

In addition to standard sectionalization, most electrostatic precipitators also divide individual fields into bus sections. A precipitator field has either one or two bus sections. This is the smallest section of the field that can be energized by the T-R set serving the field. The term “bus section” is derived from the fact that each of these sections has a separate electrical bus (electrical conduit line) from the T-R set. Precipitators often have two bus sections per field so that these two different areas can be separately

energized using half-wave rectified power. The advantages and disadvantages of half wave versus full wave rectification are outside the scope of this course.

5.3.3 Aspect ratio

The aspect ratio is the relationship between the precipitator length and height. It is calculated in Equation 5-8. A typical problem involving the calculation of the precipitator aspect ratio is provided in Problem 5-4.

$$A.R. = \frac{\sum_{i=1}^{n} L_i}{H} \tag{5-8}$$

Where:

A.R. = aspect ratio (dimensionless)

L_i = length of plates in field i (ft)

H = collection plate height (ft)

n = number of fields in series

Problem 5-4

An electrostatic precipitator serving a cement kiln has four fields in series. All of the fields have collection plates that are 24 feet high. The first two fields have collection plate lengths of 9 feet each. The last two fields have collection plate lengths of 6 feet. What is the aspect ratio?

Solution:

$$A.R. = \frac{\sum_{i=1}^{n} L_i}{H} = \frac{(9+9+6+6)}{24} = 1.25$$

The aspect ratio is important because it directly affects the ability of the precipitator to capture solids rapped from the collection plates and falling toward the hoppers. If the aspect ratio is too low, the small particles or small agglomerates of particles are swept out of the precipitator before they can reach the hopper. This increases rapping reentrainment emissions.

The vulnerability of precipitators to these reentrainment emissions can be seen simply by looking at the side of the unit (Figure 5-29). Due to the height and short length, some of the solids rapped from the collection plates and discharge electrodes will invariably be redispersed into the outlet gas stream.

Figure 5-29. Precipitator with poor aspect ratio

Modern precipitators are being designed with aspect ratios of at least 1.0, and the normal range extends to more than 1.5 (Katz, 1979). This means that these precipitators are longer than they are high. This improves gravity settling, which is the important second step in the overall electrostatic precipitator process.

5.3.4 Gas Superficial Velocity

High gas velocities adversely affect the performance of precipitators. They reduce the time available for particle charging and migration. High velocities through the gas passages can scour particles from the outer surfaces of the dust layers and, thereby, add to reentrainment emissions. Furthermore, high gas velocities reduce the time available for rapped solids to settle by gravity into the hoppers. The average gas velocities in modern precipitators are generally between 3 and 6 ft/sec. (Katz, 1979; Szabo and Gerstle, 1977).

Variations in the gas velocity should be minimized. Localized high velocity zones in the precipitator could significantly increase particulate emissions. The variations should be limited to ± 20% of the average gas velocity.

In the past, equipment manufacturers have used 1/32 and 1/16 scale models in order to optimize gas flow rates. During the last 10 years, air flow computational fluid dynamic models (often termed CFD models) have also been successfully applied to correct gas flow maldistribution problems (Schwab and Johnson, 1994).

5.3.5 Collection Plate Spacing

A trend toward increased plate-to-plate spacings (increased gas passage width) started in the 1980s because of the interest in rigid frame type discharge electrode supports. Due to the width of the support tube, the plate spacings were increased from a typical value of 9 in. to the 11 to 12 in. range to allow space for these tubes. This practical consideration was not the only motivation for increased plate spacings. It has been recognized for more than 30 years that improved electrical field strengths could be obtained by increased discharge electrode-to-collection plate spacings (Feldman and Kumar, 1990; Makansi, 1986; Engelbrecht, 1983). Due, in part, to stringent particulate matter control requirements, many new units will have plate-to-plate spacings in the range of 10 to 20 in. (Makansi, 1986).

A summary of the typical sizing parameters for electrostatic precipitators is provided in Table 5-4. However, some caution is warranted in comparing an existing unit with the ranges shown in this table. The necessary precipitator size and design characteristics vary substantially from site-to-site due to factors such as differences in particulate resistivity distributions, particle size distributions, and process operating rate variations.

Table 5-4.Typical Sizing Parameters Dry Negative Corona ESPs

Sizing Parameter	Common Range
Specific Collection Area, (ft^2/1000 ACFM)	400 - 1000
Number of Fields in Series	3 - 14
Aspect Ratio	1 - 1.5
Gas Velocity, ft/sec	3 - 6
Plate-to-plate spacing, inches[1]	9 - 16

Note: 1. One manufacturer uses 6 in. spacing.

5.3.6 Flue Gas Conditioning Systems

These systems are used exclusively to adjust the resistivity conditions in cold side electrostatic precipitators serving coal-fired boilers. These units operate at gas temperatures between 200°F and 400°F and are vulnerable to both low and high resistivity conditions under some boiler operating conditions. These resistivities can be adjusted back into the moderate range where precipitators work well by injecting either sulfur trioxide and/or ammonia. Sulfur trioxide reacts to form sulfuric acid vapor and heterogeneously nucleates on the surfaces of particles to adjust the surface conductivity. Ammonia reacts with sulfur trioxide in the flue gas stream to form ammonium sulfate and ammonium bisulfate, which also nucleates on particle surfaces and adjusts the surface conductivity. Sulfur trioxide injection and ammonia injection have been used successfully since the 1970s (Fletcher, 1982; Weyers and Cook, 1981; Eskra and McKinney, 1982).

A conventional sulfur trioxide system is shown in Figure 5-30. Elemental sulfur is melted and pumped to the oxidation chamber where sulfur dioxide is formed. The gas stream then enters a vanadium pentoxide catalyst bed where the sulfur dioxide is oxidized further to yield sulfur trioxide. This is transported at a temperature range of 600°F to 700°F to a set of injection nozzles placed upstream of the precipitator inlet. As the sulfur trioxide disperses into the gas stream, it cools and forms vapor phase sulfuric acid as indicated by Reaction 5-1. The sulfuric acid molecules are highly hygroscopic and attract water molecules as indicated in Reaction 5-2.

$$SO_3 + H_2O \rightarrow (H_2SO_4)_{vapor}$$ Reaction 5-1

$$(H_2SO_4)_{vapor} + xH_2O \rightarrow (H_2SO_4 \bullet xH_2O)_{vapor}$$ Reaction 5-2

$$(H_2SO_4 \bullet xH_2O)_{vapor} \rightarrow (H_2SO_4 \bullet xH_2O)_{particle\,surface}$$ Reaction 5-3

The sulfuric acid then adsorbs on the surfaces of the particles. The sulfur trioxide injection rates provide concentrations of 5 to 25 ppm of sulfuric acid in the gas stream passing through the precipitator. The large majority of the sulfuric acid formed due to a flue gas conditioning system is removed in the precipitator.

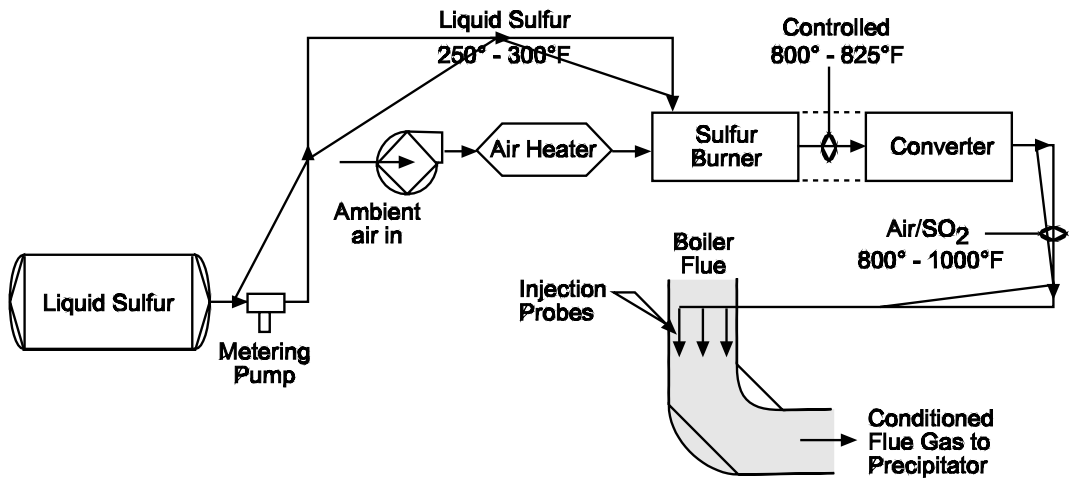

Figure 5-30. Sulfur trioxide conditioning system

Problem 5-5

A coal-fired utility boiler generates 5 ppm of sulfuric acid. Diagnostic tests have indicated that 17 ppm of sulfuric acid are needed in the gas stream to maintain the flyash resistivity in the moderate range. Calculate the sulfur required to operate a sulfur trioxide conditioning system for a period of one year. Assume that the boiler has a gas flow rate of 1.0 x 10^6 ACFM, the gas temperature is 310°F, the boiler operates 82% of the year, and the sulfur trioxide system is needed 85% of the operating time.

Solution:

Sulfur Trioxide System Operating Hours

$$\text{Operating Hours} = 8{,}760 \text{ hours total}\left(\frac{0.82 \text{ boiler hours}}{\text{total hours}}\right)\left(\frac{0.85 \text{ FGC hours}}{\text{boiler hours}}\right) = 6{,}106 \text{ FGC hours}$$

Sulfur Trioxide Demand, ppm

SO_3 needed = 17 ppm – 5 ppm = 12 ppm (1.2×10^{-5} lb moles $S0_3$/lb mole flue gas)

Sulfur Trioxide Injection Requirements, lb moles/hour

SO_3 need = 1.2×10^{-5} lb moles/lb mole flue gas

SO_3 need = 1×10^6 ACFM(528°R/770°R)(lb moles/384.5 SCF)(60 min/hour)(1.2 x 10^{-5})

SO_3 need = 1.28 lb moles/hour

Sulfur Required

Sulfur lb moles = SO_3 lb moles = 1.28 lb moles $S0_3$/hour

Sulfur required = (1.28 lb moles SO_3/hour)(6,106 hours)(32 lb/lb mole SO_3)(ton/2000)
= 125 tons/year

There are a number of sulfur trioxide conditioning systems in commercial service. The unit shown in Figure 5-31 stores the necessary sulfur in a pelletized form. The sulfur is fed to a melter and then oxidized to form sulfur trioxide. This approach avoids the possible problems and energy costs associated with storing sulfur in a molten form on a continuous basis.

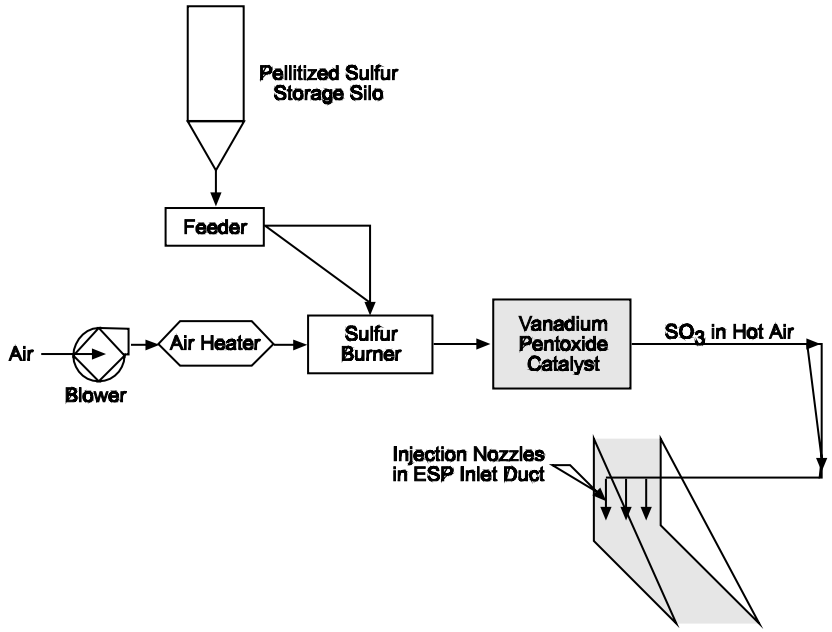

Figure 5-31. Pellitized sulfur type sulfur trioxide conditioning system

Another commercial version of a sulfur trioxide conditioning system uses a set of small catalyst chambers rather than a single large unit for oxidizing sulfur dioxide to sulfur trioxide. The sulfur dioxide gas formed in the sulfur burner is then distributed to a set of pipes leading the to precipitator inlet. Catalyst modules are present on each of the injection lines.

Ammonia flue gas conditioning (FGC) systems are very similar to the ammonia feed systems used for Selective Catalytic Reduction (SCR) and Selective Non-Catalytic Reduction (SNCR) used for nitrogen oxides control. The ammonia FGCs can use either anhydrous ammonia or aqueous ammonia as a feedstock. The ammonia is fed from the storage tank at a rate necessary to achieve a preset concentration level, normally 10 to 20 ppm. This level is well below the typical concentration levels in SCRs and SNCRs. The ammonia is diluted by a carrier gas, usually air, to a concentration well below its Lower Explosive Limit (LEL) of 15%. Ammonia feed concentrations are usually less than 3% by volume. The ammonia is then injected in the flue gas streams through a set of pipes mounted at the precipitator inlet. Due to the low ammonia concentrations, the large majority quickly reacts and nucleates on the surfaces of the flyash. Ammonia emission concentrations (slip levels) through the precipitator are usually near negligible levels.

Ammonia conditioning systems can be used as stand-alone units for cold side electrostatic precipitators subject to low resistivity related particulate matter emission problems. In this type of application, the main impact of the ammonia and its gas phase reaction procedures appears to be improved particle agglomeration of the dust on the collection plate surfaces. When used in conjunction with a sulfur trioxide conditioning system, ammonia units encourage the formation of dust layers with reduced resistivities.

5.3.7 Evaporative Coolers

Electrostatic precipitators are used for particulate matter control in some applications having flue gas temperatures as hot as 750°F. There are concerns that, in some site specific cases, chemical reactions within electrostatic precipitators and other air pollution control systems could contribute to the formation of dioxin-furan compounds. In those cases, the use of an evaporative cooler to minimize the flue gas temperatures to less than approximately 450°F may be desirable.

Evaporative cooling can be achieved in a specially designed evaporative cooling tower or by using water injection sprays near the inlet of the precipitator. It is important to use clean water for evaporative sprays. Suspended and dissolved solids in water evaporating to dryness can form small, difficult-to-control particulate matter.

5.3.8 Rapping Systems

The rapping intensities and frequencies must be adjusted for the approximate resistivity range that exists in the precipitator. If the resistivity is too low, the dust is weakly held and can be easily redispersed into the gas stream by excessive intensity or frequency of rapping. This is often indicated by routinely occurring puffs from the stack. If the resistivity is high, relatively high intensity and frequent rapping is needed. However, the mechanical limits of the rappers, rapper rods, and collection plates must be considered in maintaining this type of rapping practice.

The rapping frequency is not constant throughout the precipitator. The inlet fields should be rapped much more frequently than the middle and outlet fields. The calculated data shown in Problem 5-6 present some assumed field-by-field penetration values for a four-field unit with a gas flow rate of 250,000 ACFM and an inlet particulate matter loading of 2 grains per actual cubic foot. It is apparent that large quantities of particulate are captured in the inlet field, and frequent rapping is needed.

If the rapping is too frequent in the outlet fields, the accumulated dust layer between rapping cycles will be very thin. During rapping, these thin dust layers can be easily redispersed since they are not very cohesive. Rapping the thin dust layers too frequently can contribute to rapping reentrainment.

Problem 5-6

Estimate the quantities of dust in each field of a four-field electrostatic precipitator having efficiencies of 80%, 75%, 70%, and 65% respectively. Assume a gas flow rate of 250,000 ACFM and a particulate matter loading of 2 grains per actual cubic foot.

Field	Assumed Efficiency	Particulate Entering lb_m/hr	Particulate Leaving, lb_m/hr	Particulate Collected lb_m/hr
1 (inlet)	80	4,286	857	3,429
2 (middle)	75	857	214	643
3 (middle)	70	214	64	150
4 (outlet)	65	64	22	42

Due to the general pattern of particulate removal in a precipitator, the rapping frequency for the inlet field collection plates is usually once every 5 to 15 minutes. This means that the entire set of rappers on this field is activated once during each cycle of 5 to 15 minute duration. The outlet fields collection plates have cycle times that occur as often as one cycle per hour to as infrequently as one cycle every 24 hours.

The discharge electrode frame rappers and the gas distribution screen rappers are generally operated on a relatively high frequency ranging from cycle times of 5 minutes to more than 2 hours.

Many industrial processes served by electrostatic precipitators have process operating rate-related gas flow changes, changes in particulate matter loadings, and changes in particle characteristics. New microprocessor rapping system controllers have several rapping frequency programs. These can be selected manually or automatically based on the process operating conditions. These systems are very effective at tailoring the rapping practices to the prevailing operating conditions. Many of the systems also provide useful diagnostic data concerning the operating status of each of the rappers.

Rapping collection plates generally results in some rapping reentrainment regardless of the resistivity conditions and gas flow rates. Accordingly, collection plate rappers in different portions of the precipitator should not be activated simultaneously. The transient wave of particulate matter can impair the electrical performance of downstream precipitator fields. Most new microprocessor-based rapper controllers include features to preclude simultaneous rapping.

5.3.9 High Voltage Frame Support Insulators

The failure of any one of the electrical components within a field can result in the temporary loss of this field until the next off-line period when repairs can be completed. There are a variety of design approaches for minimizing the failure of high voltage frame support insulators. Most of these involve minimizing the quantities of moisture and solids that deposit on the inner and outer surfaces. Heated purge air can be supplied at a rate of 50 to 100 ACFM per insulator to the middle of the cylindrical insulator (Figure 5-32) to keep the inner surface hot and to reduce the particulate matter flowing upward into this area. In some units, unheated purge air is used with electrical resistance heaters (Figure 5-33) around the high voltage frame support insulators to prevent moisture accumulation on the exterior surface.

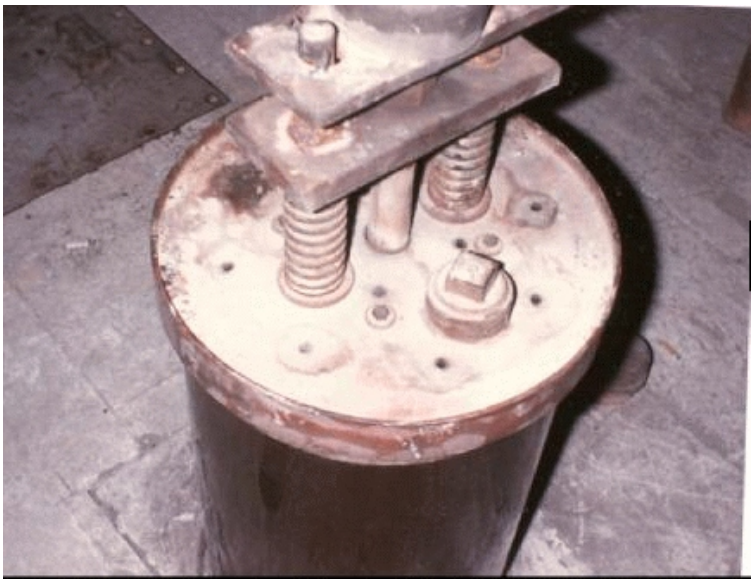

Figure 5-32. High voltage support insulator

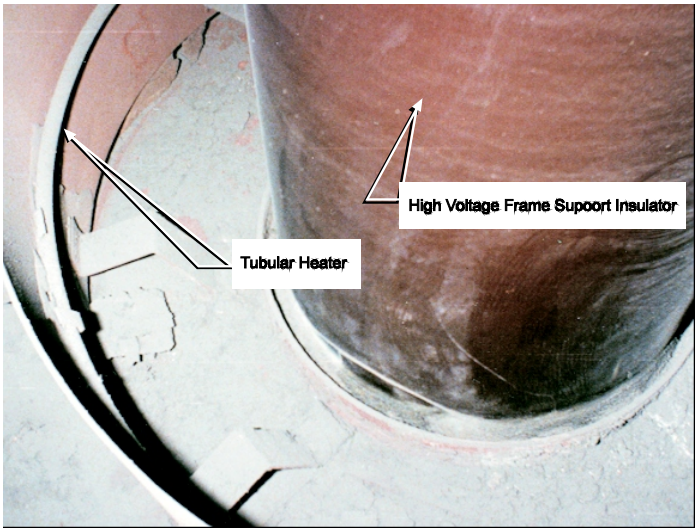

Figure 5-33. Electrical resistance heater for a high voltage support insulator

It is more difficult to protect anti-sway insulators because they are mounted immediately above the hopper area. It is not practical to supply a heated purge air stream or electrical heaters in this area. The insulator is also vulnerable to solids overflow and to air infiltration-related moisture condensation. Relatively long (> 12 inches) insulators are generally used to minimize the risk of short circuits and failure. In some designs, the anti-sway insulators have been eliminated by designing more rigid discharge electrode frame supports.

5.3.10 Discharge Electrodes

Discharge electrode designs have evolved substantially since the early 1970s when discharge wire failure was a common problem. The introduction of rigid discharge electrodes and electrode frames has substantially reduced this problem. The use of protective shrouds (shown in Figure 5-34) over the top and bottom 18 inches of the wire-type discharge electrodes has reduced the frequency of failure.

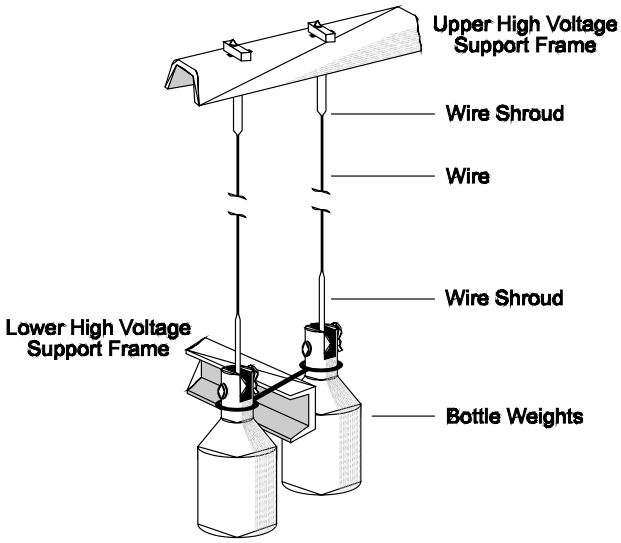

Figure 5-34. Protective shroud on a wire-type discharge electrode

Due to the improvements in discharge electrode design, present-day failures are usually due to either corrosion or misalignment problems. The failure of discharge wires has become a symptom of other problems rather than a fundamental problem.

5.3.11 Hoppers

The removal of solids from the hopper is the important third step in the overall electrostatic precipitation process. Failure to remove solids from the hoppers in a timely manner can cause collection plate misalignment and discharge electrode frame misalignment. Short circuit paths between the high voltage electrodes and the electrically grounded collection plates can result in the formation of large fused clinkers, which usually have to be removed manually. Hopper overflow can also cause deposition on anti-sway insulators.

There are a variety of design features that can reduce the vulnerability to hopper overflow. Hoppers should have steep sides to facilitate solids movement. They should have thermal insulation and an outer protective lagging to prevent heat loss. Hopper heaters are often mounted in the bottom portions of the hopper to provide supplemental heat in the area where convective and conductive cooling are most rapid. Maintaining proper solids temperatures in the hoppers is important because the hot area partially surrounding the deposited solids facilitates solids flow into the small throat at the bottom. If the solids and trapped air cool, the solids flow less readily and may bridge over the throat. The hopper partition plates, which divide the hopper into two halves to reduce gas sneakage flow through the hoppers, should not approach the throat too closely because this reduces the opening area for solids flowing toward the throat.

One of the most useful techniques for minimizing hopper overflow is to empty the hoppers as frequently as practicable. Hoppers are very effective "funnels," but undesirable storage vessels. It is especially important to empty the inlet field hoppers frequently due to the large quantities of dust collected in this portion of the precipitator.

5.3.12 Instrumentation

New state-of-the art automatic voltage controllers include digital gauges for all of the following electrical parameters of interest in the precipitator field.

- Primary voltage, volts A.C.
- Primary current, amperes A.C.
- Secondary voltage, kilovolts D.C.
- Secondary current, milliamps D.C.
- Spark rate
- SCR Conduction angle, degrees
- Field limiting condition
- Power input, kilowatts

In a few new systems, these parameters are logged and processed in data acquisition systems to provide routine operating records for the unit. In most existing units, the electrical data is logged manually by plant operators.

Information concerning the rappers is usually provided by instrumentation mounted in the rapper control panel. New microprocessor-based control cabinets provide visual information concerning the rapper program in use at the present time, the specific rappers being activated, the presence of any probable rapper activation faults, and the rapping intensities.

Gas stream temperature and oxygen monitors are often used upstream and downstream of electrostatic precipitators to detect the on-set of air infiltration problems. Air infiltration can increase gradually due to

wear of mechanical parts in the solids discharge system, deterioration of fabric type expansion joints on ductwork, and/or corrosion of exterior metal parts. The rate of infiltration can increase rapidly because the corrosion caused by the acid deposition in cold areas increases gaps and holes where air is entering. One way to identify the presence of significant air infiltration is to install gas stream temperature monitors immediately upstream and downstream of the precipitator. A change in the temperature drop across the unit at a given load condition provides one relatively inexpensive and useful indicator. Increases from the baseline range of temperature drops would indicate the need to identify and repair the infiltration sites.

Oxygen concentration measurements at the inlet and outlet of the units can also be used to identify increased air infiltration. An increase of more than 0.5% in the oxygen composition of the gas stream is generally associated with significant air infiltration-related problems. For example, a unit with an inlet concentration of 4% oxygen and an outlet concentration of 4.5% oxygen requires further attention.

Hopper level detectors are often used to provide an early warning of high solids levels in precipitator hoppers. It is important that the detectors be mounted in the proper location. If they are mounted too low in the hoppers, they alarm unnecessarily and may be ignored by the operators. If they are mounted too high in the hoppers, there may be insufficient time for the operator to respond to the alarm and begin removing solids from the hoppers.

Review Exercises

Types and Components

1. What type of electrostatic precipitator generally uses a presaturator chamber or presaturator water sprays before the unit? Select all that apply.
   a. Dry, negative corona
   b. Wet, negative corona
   c. Wet, positive corona
   d. Answers b and c

2. What are the typical superficial gas velocities through a dry, negative corona precipitator?
   a. 1 to 5 feet per second
   b. 2 to 10 feet per second
   c. 3 to 6 feet per second
   d. 1 to 5 feet per minute

3. What charge is imposed on a collection plate in a dry, negative corona precipitator or a wet, negative corona precipitator?
   a. Negative
   b. Positive
   c. None, the plates are electrically grounded.
   d. None of the above

4. What type of electrostatic precipitator is used to collect organic mists?
   a. Dry, negative corona
   b. Wet, negative corona
   c. Wet, positive corona
   d. Answers b and c

5. What type of electrostatic precipitator is least vulnerable to resistivity problems?
   a. Dry, negative corona
   b. Wet, negative corona
   c. Wet, positive corona
   d. Answers b and c

6. What is the purpose of the T-R set in dry, negative corona precipitators?
   a. Decrease the voltage and rectify the electricity to alternating current.
   b. Increase the voltage and rectify the electricity to alternating current.
   c. Increase the voltage and rectify the electricity to alternating current.
   d. Increase the voltage and rectify the electricity to direct current.

7. What is the normal current in an electrostatic field in good physical condition when the applied secondary voltage is less than the corona onset level?

   a. Less than 1 ampere
   b. Less than 0.1 ampere
   c. Zero
   d. None of the above

8. What problems can occur if moisture and/or conductive solids accumulate on the surfaces of the high voltage frame support insulators? Select all the answers that apply.

   a. The insulator can overheat and shatter.
   b. The field served by the insulator could trip offline due to the short circuit.
   c. The discharge wires in the field could be vulnerable to electrical sparking.

9. What fraction of the particulate matter entering the precipitator is usually collected in the inlet (first) field?

   a. 10% to 25%
   b. 25% to 50%
   c. 50% to 80%
   d. 80% to 99%

10. What is the purpose of rapping in dry, negative corona precipitators?

   a. Remove large clumps of agglomerated solids precipitated in the field.
   b. Keep the collection plate metal clean by intensely redispersing collected solids that have not fallen into the hopper.
   c. Keep the high voltage frame support insulators clean.
   d. Keep the anti-sway insulators clean.

Operating Principles

11. Under what conditions do dry, negative corona precipitators operate best?

   a. Low resistivity
   b. Moderate resistivity
   c. High resistivity

12. Under what conditions is the dust layer weakly held to the vertical collection plates in a dry, negative corona precipitator?

   a. Low resistivity
   b. Moderate resistivity
   c. High resistivity

13. What factors influence the dust layer resistivity for a precipitator operating at less then 350°F? Select all of the answers that apply.
    a. Gas temperature
    b. Sulfuric acid vapor concentration
    c. Water vapor concentration
    d. All of the above

14. The saturation charge is related to _____.
    a. The cube of the particle diameter
    b. The square of the particle diameter
    c. The first power of the particle diameter
    d. The square root of the particle diameter

15. Electrical charge is dissipated through dust layers on the collection plates of dry, negative corona precipitators based on _____. Select all of the answers that apply.
    a. Surface conduction
    b. Bulk conduction
    c. Electrical sparking

16. Resistivity usually _____ over the gas temperature range of 500°F to 800°F.
    a. Increases
    b. Decreases
    c. Remains unchanged

17. The secondary voltage is _____.
    a. The voltage applied on the discharge electrodes
    b. The voltage applied to the primary side of the T-R set
    c. The voltage applied by the back-up power supply used in the event that the primary circuit trips offline
    d. None of the above

18. What conditions are inappropriate for dry, negative corona electrostatic precipitators?
    a. Explosive gases or vapors
    b. Sticky particulate matter
    c. Gas streams vented back into occupied areas
    d. All of the above

19. Typical secondary voltages in a dry, negative corona precipitator and a wet, negative corona precipitators are in the range of _____.

a. 5,000 to 10,000 volts
b. 10,000 to 20,000 volts
c. 20,000 to 50,000 volts
d. 50,000 to 100,000 volts
e. 100,000 to 300,000 volts
f. 480 volts.

20. What is the difficult-to-control particle size range?

a. 0.1 to 0.5 micrometers
b. 0.5 to 2 micrometers
c. 2 to 5 micrometers
d. 5 to 10 micrometers

Capability and Sizing

21. What is the collection efficiency predicted by the Deutsch-Anderson equation for a precipitator having a collection area of 70,000 ft^2 and a gas flow rate of 440,000 ACFM? Assume an effective migration velocity of 0.5 ft/sec.

22 . What is the aspect ratio for a five-field electrostatic precipitator having collection plate heights of 30 ft, collection plate lengths of 9 ft, and a precipitator width (normal to gas flow) of 50 ft?

23. What is the average gas velocity passing through the precipitator described in Problem 22 assuming that the gas flow rate is 400,000 ACFM?

24. What is the collection plate area of a field having the following characteristics?

- Plate height: 40 ft
- Plate length: 6 ft
- Number of plates: 39
- Plate-to-plate spacing: 9 in.

25. What is the SCA (specific collection area) of a ginel-chamber, five-field precipitator having the following characteristics?

- Plate height: 40 ft
- Plate length: 6 ft
- Number of plates: 39
- Plate-to-plate spacing: 9 in.
- Number of fields in series: 5
- Average gas velocity: 4.2 ft/sec

26. An electrostatic precipitator collects 4,000 pounds of flyash per hour. There are four fields in series and a single hopper per field. Which of the following values approximates the quantity of flyash removed from the inlet hopper?

a. 1,000 pounds/hour

b. 2,800 pounds/hour

c. 500 pounds/hour

d. 1,200 pounds/hour

Review Answers

Types and Components

1. What type of electrostatic precipitator generally uses a presaturator chamber or presaturator water sprays before the unit?
   b. Wet, negative corona

2. What are the typical superficial gas velocities through a dry, negative corona precipitator?
   c. 3 to 6 feet per second

3. What charge is imposed on a collection plate in a dry, negative corona precipitator or a wet, negative corona precipitator?
   c. None, the plates are electrically grounded.

4. What type of electrostatic precipitator is used to collect organic mists?
   c. Wet, positive corona

5. What type of electrostatic precipitator is least vulnerable to resistivity problems?
   d. Answers b and c

6. What is the purpose of the T-R set in dry, negative corona precipitators?
   d. Increase the voltage and rectify the electricity to direct current.

7. What is the normal current in an electrostatic field in good physical condition when the applied secondary voltage is less than the corona onset level?
   c. Zero

8. What problems can occur if moisture and/or conductive solids accumulate on the surfaces of the high voltage frame support insulators?
   a. The insulator can overheat and shatter.
   b. The field served by the insulator could trip offline due to the short circuit.

9. What fraction of the particulate matter entering the precipitator is usually collected in the inlet (first) field?
   c. 50% to 80%

10. What is the purpose of rapping in dry, negative corona precipitators?
    a. Remove large clumps of agglomerated solids precipitated in the field.

Operating Principles

11. Under what conditions do dry, negative corona precipitators operate best?
    b. Moderate resistivity

12. Under what conditions is the dust layer weakly held to the vertical collection plates in a dry, negative corona precipitator?
    a. Low resistivity

13. What factors influence the dust layer resistivity for a precipitator operating at less then 350°F?
    d. All of the above

14. The saturation charge is related to _____.
    b. The square of the particle diameter

15. Electrical charge is dissipated through dust layers on the collection plates of dry, negative corona precipitators based on _____. Select all of the answers that apply.
    a. Surface conduction
    b. Bulk conduction

16. Resistivity usually _____ over the gas temperature range of 500°F to 800°F.
    b. Decreases

17. The secondary voltage is _____.
    a. The voltage applied on the discharge electrodes

18. What conditions are inappropriate for dry, negative corona electrostatic precipitators?
    d. All of the above

19. Typical secondary voltages in a dry, negative corona precipitator and a wet, negative corona precipitators are in the range of _____.
    c. 20,000 to 50,000 volts

20. What is the difficult-to-control particle size range?
    a. 0.1 to 0.5 micrometers

Capability and Sizing

21. What is the collection efficiency predicted by the Deutsch-Anderson equation for a precipitator having a collection area of 70,000 ft^2 and a gas flow rate of 440,000 ACFM? Assume an effective migration velocity of 0.5 ft/sec.

Solution:

$$e^{-w(A/G)}$$

$$-w(A/G) = 0.50 \text{ ft/sec } (70{,}000 \text{ ft}^2) / [(440{,}000 \text{ ft}^3/\text{min}) (1 \text{ min}/60 \text{ sec})]$$

$$(A/G) = 4.77$$

$$e^{-4.77}$$

22. What is the aspect ratio for a five-field electrostatic precipitator having collection plate heights of 30 ft, collection plate lengths of 9 ft, and a precipitator width (normal to gas flow) of 50 ft?

Answer: 1.5

Solution:

Aspect ratio is the sum of the field lengths divided by the collection plate height.

$$A.R. = \frac{5 \text{ fields} \times 9 \text{ ft/field}}{30 \text{ ft}} = 1.5$$

23. What is the average gas velocity passing through the precipitator described in Problem 22 assuming that the gas flow rate is 400,000 ACFM?

Answer: 266.67 ft/min or 4.44 ft/sec

Solution:
Velocity = gas flow rate/area

$$\text{Area for flow} = 30 \text{ ft} \times 50 \text{ ft} = 1{,}500 \text{ ft}^2$$

$$\text{Velocity} = \frac{400{,}000 \text{ ft}^3/\text{min}}{1{,}500 \text{ ft}^2}$$

$$= 266.67 \text{ ft/min or } 4.44 \text{ ft/sec}$$

24. What is the collection plate area of a field having the following characteristics?

- Plate height: 40 ft
- Plate length: 6 ft
- Number of plates: 39
- Plate-to-plate spacing: 9 in.

Answer: 18,240 ft^2

Solution:

Number of passages = (no. of plates 1) = 38

Field plate area = 2 (38 passages) (6 ft) (40 ft)

= 18,240 ft^2

25. What is the SCA (specific collection area) of a single-chamber, five-field precipitator having the following characteristics?

- Plate height: 40 ft
- Plate length: 6 ft
- Number of plates: 39
- Plate-to-plate spacing: 9 in.
- Number of fields in series: 5
- Average gas velocity: 4.2 ft/sec

Answer: 317.46 ft^2/1000 ACFM

Solution:

Total plate area = 5 fields (18,240 ft^2/field) = 91,200 ft^2

Gas flow rate = area × velocity

Area = 38 passages (0.75 ft/passage) (40 ft) = 1,140 ft^2

Gas flow rate = (1,140 ft^2) (4.2 ft/sec) (60 sec/min)

= 287,280 ft^3/min

SCA = area/gas flow rate

= 91,200 ft^2/287,280 ft^3/min

= 317.46 ft^2/1000 ACFM

26. An electrostatic precipitator collects 4,000 pounds of flyash per hour. There are four fields in series and a single hopper per field. Which of the following values approximates the quantity of flyash removed from the inlet hopper?

Answer: b. 2800 pounds.

An inlet field removes 50% to 80% of the inlet particulate matter

Bibliography

Beak, W., W. Krawcyzk, and J. Richards. *Identifying and Minimizing the Effects of Spatial/temporal Fly Ash Resistivity Variations to Reduce Emissions and Maintenance Requirements.* Paper presented at the Independent Power Generation Conference. New Orleans, LA, 1988.

Bickelhaupt, R.E. *A Technique for Predicting Fly Ash Resistivity*. EPA 600/7-79-204. 1979.

Colbert, T.S. *The Electrostatic Precipitator and its Power Supply: a Circuit Analysis.* Paper 79-9.2. Presented at the 72nd Annual Meeting of the Air Pollution Control Association. Cincinnati, OH. June, 1979.

Engelbrecht, H.L. *Increased Plate-to-Wire Spacing to Enhance Electrostatic Precipitator Performance.* Paper 83-55.6. Presented at the 76th Annual Meeting of the Air Pollution Control Association. June, 1983.

Eskra, B.J., and B.G. Mckinney. *One Year's Operating Experience with SO_3 Conditioning on a Large Coal-fired Unit's Electrostatic Precipitator.* Paper 82-49.3. Presented at the 75th Annual Meeting of the Air Pollution Control Association. June, 1982.

Feldman, P.L., and K.S. Kumar. *Effects of Wide Plate Spacings in Electrostatic Precipitators.* Paper 90-101.7. Presented at the Air and Waste Management Association Meeting. Pittsburgh, PA. June, 1990.

Fletcher, H.R. *Operating Experience at Detroit Edison with Various Flue Gas Conditioning Systems.* Paper 82-49.1. Presented at the 75th Annual Meeting of the Air Pollution Control Association. June, 1982.

Gooch, J.R., and H.M. Guillaume, Jr. *Electrostatic Precipitator Rapping Reentrainment and Computer Model Studies.* Electric Power Research Institute Publication FP-792, Vol. 3. 1978.

Hall, H.J. *Summary of Overall Concepts for Design, Energization, and Control of Electrostatic Precipitators.* Paper 83-57.6. Presented at the 76th Annual Meeting of the Air Pollution Control Association. June, 1983.

Humbert, C.O. *Electrostatic Precipitator Rappers: Their Function, Operation, and Maintenance.* Paper 83-57.3. Presented at the 76th Annual Meeting of the Air Pollution Control Association. June, 1983.

Jonelis, R.E., and J.A. Jonelis. *Economical, Innovative Methods of Straightening ESP Collector Plates So as to Achieve Alignment for the Purposes of Improving Particulate Control and Performance.* Paper 85-JPGC-APC-5. Presented at the American Society of Mechanical Engineers/IEEE Power Generation Conference. Milwaukee, WI. October, 1985.

Katz, J. *The Art of Electrostatic Precipitators*. Port Washington, NY: Scholium International. 1979.

Lawless, P. *Electrostatic Precipitator V-I and Performance Model: Users Manual*. EPA 600/R-92-104a. 1992.

Lurgi, G. *Corrosion-Proof Wet Precipitator.* 1988.

Makansi, J. *Particulate Control: Optimizing Precipitators and Fabric Filters for Today's Power Plants. Power:*S1-S16. 1986.

McDonald, J.R., and A.H. Dean. *A Manual for the Use of Electrostatic Precipitators to Collect Fly Ash Particles.* EPA 600/8-80-025. 1980.

Neundorfer, M. *Second Symposium on on the Transfer and Utilization of Particulate Control Technology*. Vol. 2. *Electrode Cleaning Systems: Optimizing Rapping Energy and Rapping Control.* EPA 600/9-9-80-039a. 1980.

Raymond, R.K. *Second Symposium on the Transfer and Utilization of Particulate Control Technology*. Vol. 2. *Electrostatic Precipitators: Electrical Problems and Solutions.* EPA 600/9-9-80-039a. 1980.

Schwab, M.J, and R. Johnson. *Numerical Design Method for Implementing Gas Distribution within Electrostatic Precipitators.* Paper presented at the 56th Annual Meeting, American Power Conference. Chicago, IL. 1994, April.

Spencer, H.W. *Electrostatic Precipitators: The Relationship of Ash Resistivity and Precipitator Electrical Operating Parameters.*

Steinsvaag, D. *Smoke Abatement for Textile Finishers.* American Dyestuff Reporter. September, 1992.

Szabo, M.F., and R.W. Gerstle. *Operation and Maintenance of Particulate Control Devices on Coal-fired Utility Boilers*. EPA 600/2-77-129. 1977.

Theodore, L., and A.J. Buonicore. *Industrial Air Pollution Equipment for Particulates*. Cleveland, OH: CRC Press, 1976.

Verhoff, F.H., and J.T. Banchero. *Chemical Engineering Progress* 70:71. 1974.

Weyers, L.L., and R.E. Cook. *Operating Experience with Flue Gas Conditioning Systems at Commonwealth Edison Company.* Santa Anna, CA: Wahlco, April, 1981.

White, H.J. *Fly Ash Resistivity.* Journal of the Air Pollution Control Association. 1977.

Chapter 6
Particulate Wet Scrubbers

Particulate wet scrubbers are a diverse set of control devices. Simple devices, such as spray tower scrubbers, are used for the collection of particulate matter larger than approximately 5 µm. Various scrubbing systems, such as tray tower scrubbers, mechanically aided scrubbers, and wet ionizing scrubbers, are used to collect particulate matter as small as 1 µm. Scrubbing systems, such as adjustable throat venturis and condensation scrubbers, are used for high efficiency collection of particulate matter, even in the < 1 m size range.

Particle size is an important factor in all types of scrubbing systems. This is because all particulate wet scrubbers use the same basic collection mechanisms interial impaction and Brownian motion, both of which are highly dependent on particle size.

Particulate matter wet scrubbers, like electrostatic precipitators and fabric filters, use a three-step process for the treatment of particulate-laden gas streams.

1. Particle capture in either droplets, liquid sheets, or liquid jets
2. Capture of the liquid droplets entrained in the gas stream
3. Removal and treatment of the particulate matter-contaminated liquid prior to discharge

Particle capture (Step 1) is accomplished in a contacting vessel, such as a venturi scrubber, a tray tower scrubber, or a spray tower scrubber. Mist eliminators built into the scrubber vessel (or provided as a separate vessel) are used to collect the entrained water droplets (Step 2) after the scrubber. Clarifiers, vacuum filters, and/or settling ponds are often used to treat the waste stream from the scrubber (Step 3). All scrubber systems have a number of important components including pumps, fans, alkaline feed systems, piping, and monitoring instruments.

6.1 TYPES AND COMPONENTS OF WET SCRUBBER SYSTEMS

Typical types and components of wet scrubber systems are introduced in this section to serve as a foundation for later discussions of operating principles, sizing, and design. These scrubber types and components are integrated into a moderately complex overall system. The capability of the scrubber systems depends on the extent to which these various components operate together.

6.1.1 Characteristics of Wet Scrubber Systems

A typical particulate matter wet scrubber system is illustrated in Figure 6-1. This system consists of a number of major component units.

- Evaporative cooler
- Scrubber vessel
- Mist eliminator
- Liquid recirculation equipment
- Alkali addition system
- Wastewater treatment system
- Instrumentation
- Ductwork, fan and stack

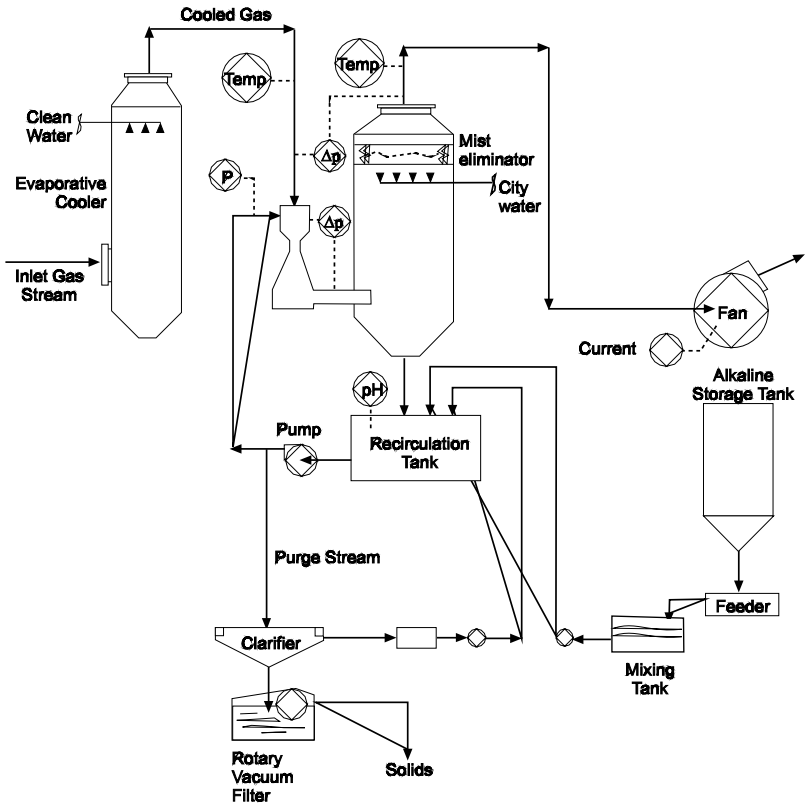

Figure 6-1. Example particulate matter wet scrubber system

Evaporative Cooler or Presaturator

The evaporative cooler can be as complex as a full evaporative cooling tower or as simple as a set of water injection nozzles in the ductwork leading to the scrubber. The primary purpose of the evaporative cooler is to reduce the gas temperature to protect temperature-sensitive components in the scrubber vessel, mist eliminators and other components. For example, it is common to have corrosion-resistant liners on the scrubber vessels that can volatilize at temperatures exceeding 400°F to 1000°F. Some scrubber vessels and many mist eliminators are fabricated with fiberglass reinforced plastics (FRP) that have temperature limitations of 180°F to 250°F. The evaporative cooler is provided to ensure that the gas temperatures in the scrubber vessel, mist eliminator, and other portions of the system do not exceed their design limitations even if the recirculation system in the scrubber fails.

The evaporative cooler provides a secondary benefit in particulate matter control systems. By cooling the gas stream prior to particulate matter removal, the evaporation of droplets in the scrubber vessel is significantly reduced. The mass flux of water vapor away from evaporating droplets impedes particle capture by the droplets. Accordingly, the minimization of evaporation has a slight beneficial impact on the particulate matter collection efficiency.

Scrubber Vessel

The scrubber vessel is designed to optimize the particle capture mechanisms discussed in Section 2. The gas stream is contacted by the liquid stream to achieve high efficiency particle inertial impaction and Brownian diffusion into the water droplets, water sheets, and/or water jets in the scrubber vessel. In some cases, it is also possible that electrostatic attraction provides slight additional particle capture.

The intensity of the liquid-gas contact varies substantially among the various types of scrubber vessels. The units with the largest differences between the particulate-laden gas stream and the liquid targets (droplets, sheets, jets) usually have the highest particulate matter collection efficiency in the difficult-to-control particle size range of 0.1 to 1 micrometer. As discussed in Section 2, this is the range where inertial impaction becomes progressively weaker and where Brownian motion is still relatively limited.

The selection of the type of scrubber vessel is based primarily on the particle size distribution of the gas stream generated by process equipment. Scrubbers with high intensity liquid-to-gas contact are used when the mass loadings in the difficult-to-control particle size range are high. Scrubbers with moderate-to-low intensity contact are selected when the mass loadings are primarily in the large size range, typically greater than 1 micrometer.

Several other factors must be considered in selecting the most appropriate type of scrubber vessel for a given industrial application.

- Requirements to control gaseous pollutants simultaneously with particulate matter
- Presence of potentially corrosive gaseous contaminants
- Cost of the scrubber system
- Physical size of the scrubber system

Mist Eliminator

Essentially all scrubber vessels generate relatively large water droplets that are reentrained in the gas stream. Many of these droplets capture particles and must be removed from the gas stream prior to discharge to the atmosphere. A mist eliminator is used for this purpose. The scrubber vessel shown in Figure 6-2 has a cyclonic mist eliminator with an additional mist eliminator mounted near the top of the mist eliminator vessel. In other commercial units, horizontal mist eliminator vessels (horizontal refers to gas flow pattern) are used for removal of the droplets.

Mist eliminators are usually equipped with one or more sets of spray nozzles to remove accumulated solids as the scrubber continues to operate. Solids build-up is due to impaction of solids-containing water droplets and due to the chemical precipitation of dissolved solids from the scrubbing liquid.

In addition to minimizing the carry-over of solids-containing droplets to the atmosphere, mist eliminators also protect downstream equipment, such as fans, from solids-containing droplets and minimize the amount of water lost from the system.

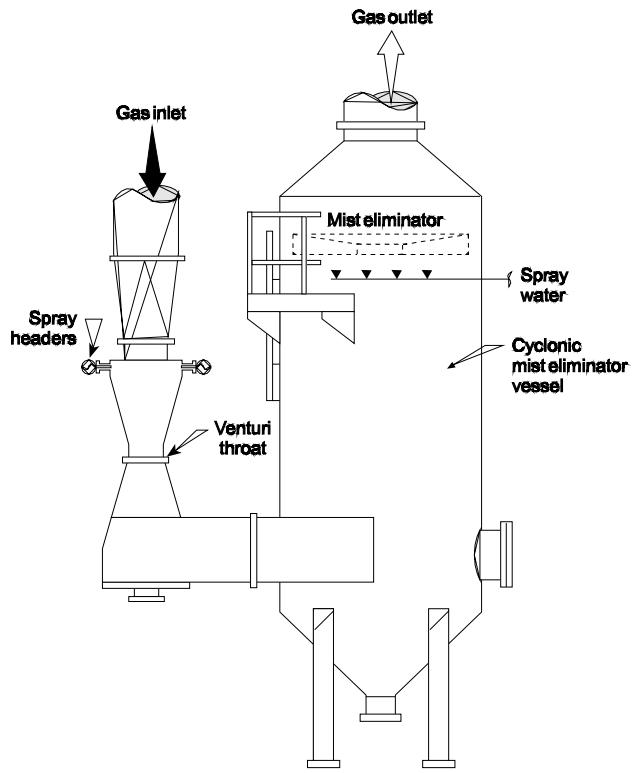

Figure 6-2. Venturi scrubber and mist eliminator vessel

Liquid Recirculation System

The scrubbing liquid is recirculated to minimize the amount of liquid that must be treated and discharged. The scrubbing liquid is collected in the sump of the scrubber and mist eliminator. Most systems use a recirculation tank having a liquid residence time of several minutes. This provides sufficient time to introduce alkali additives to adjust the pH back to the proper range, typically 5 to 9. The tank also supplies the recirculation pump used to recirculate the liquid back to the scrubber vessel.
The rate of recirculation liquid flow must be matched with the type of scrubber vessel and the concentrations of pollutants in the inlet gas stream. There must be sufficient liquid flow to provide good gas-liquid contact in the scrubber vessel.

Alkali Addition System

An alkali addition system is used on wet scrubber systems that collect acidic particulate matter or treat gas streams that have acidic gases or vapors that could absorb in the liquid stream. The most common acid gases include sulfur dioxide, hydrogen chloride, and hydrogen fluoride. Carbon dioxide formed in most combustion processes is also mildly acidic.

The most common alkalis used for neutralization of acidic material in scrubbers include lime, soda ash, and sodium hydroxide. In some cases, limestone and nalcohite are also used. All of these materials, with the exception of sodium hydroxide, are often stored and fed to the recirculation tank in a powder form. Sodium hydroxide is usually fed in solution. The rate of addition of alkali is controlled by a pH meter that is usually mounted in the scrubber recirculation tank or the recirculation pipe leading to the scrubber vessel.

Wastewater Treatment Systems

A small portion of the recirculation liquor is purged from the system in order to maintain proper solids levels in the liquor. This purge stream usually goes to a clarifier for removal of settleable solids. The clean overflow liquid from the clarifier is returned to the recirculation tank. The solid particles that settled by gravity are removed at the bottom in the underflow stream. The underflow is filtered in a rotary vacuum filter.

Instrumentation

Instruments used to monitor scrubber performance include static pressure drop gauges across the scrubber and the mist eliminator, recirculation liquid pH meters, outlet and inlet gas temperature gauges, and recirculation liquid flow rate gauges.

Opacity monitors are usually not present. The water droplets present in the stack gas scatter light and, therefore, make the use of monitors impractical.

Fans, Ductwork, and Stack

These components must be designed for more demanding service in wet scrubber systems than in fabric filter and electrostatic precipitator control systems. The static pressure drop can be very high in particulate matter wet scrubbers; therefore, the fans must be larger and have high motor horsepower. The fan housing and wheel must withstand the corrosive and erosive attack of contaminants in droplets penetrating the scrubber system.

In induced draft systems where the fan is downstream of the scrubber vessel, static pressures can range as low as –20 in. W.C. to less than –100 in. W.C. Ductwork at relative static pressures equal to or more negative than –20 in. W.C. are usually structurally reinforced to prevent deflection due to atmospheric pressure. The ductwork must also be capable of withstanding corrosion due to contaminants in the gas stream.

The stack must be properly sized to provide adequate dispersion, despite the disadvantage of cold gas streams with little to no thermal plume rise. The stacks must have adequate drainage to handle upsets in the scrubber and/or mist eliminator system causing excessive carry-over of droplets.

6.1.2 Types of Scrubber Vessels

A wide variety of scrubber vessels are used for particulate matter control. They differ with respect to their ability to collect small particulate matter, their ability to simultaneously control particulate matter and gaseous contaminants, their size, and their cost. The following list of scrubber types provides examples of many categories of particulate wet scrubbers.

1. Spray tower scrubbers
2. Mechanically aided scrubbers
3. Packed bed scrubbers
   a. Vertical packed bed
   b. Crossflow packed bed
   c. Woven fiber bed
   d. Mesh fiber bed
   e. Wet-ionizing

4. Tray Tower scrubbers
   a. Impingement tray
   b. Sieve tray
   c. Froth tower
   d. Catenary grid
   e. Moving bed
5. Gas-atomized
   a. Fixed throat venturi
   b. Adjustable throat venturi
   c. Rod deck
   d. Collision
   e. Orifice
6. Liquid atomized
7. Condensation growth
   a. Venturi scrubber
   b. Ejector

Spray Tower Scrubbers

A spray tower scrubber consists of an open vessel with an array of spray nozzles. The nozzles are arranged in a pattern that completely covers the gas flow path. In some cases, multiple spray headers are used in series to improve efficiency. Impaction of particulate matter occurs on the rapidly moving droplets. Spray tower scrubbers are effective only for particles greater than approximately 5 µm due to the limitations of achieving high droplet velocities in the spray nozzle. Despite this limitation, spray tower scrubbers are very useful for treating gas streams having high concentrations of large diameter particulate matter. They are also useful when it is necessary to control both particulate matter and gaseous pollutants.

A typical spray tower scrubber is shown in Figure 6-3. In this design, the spray nozzles are mounted in the inlet duct leading to a cyclonic chamber. Alternatively, the spray nozzles can be mounted in a cyclonic chamber: in a vertical, baffle-filled tower or in an open, vertical tower.

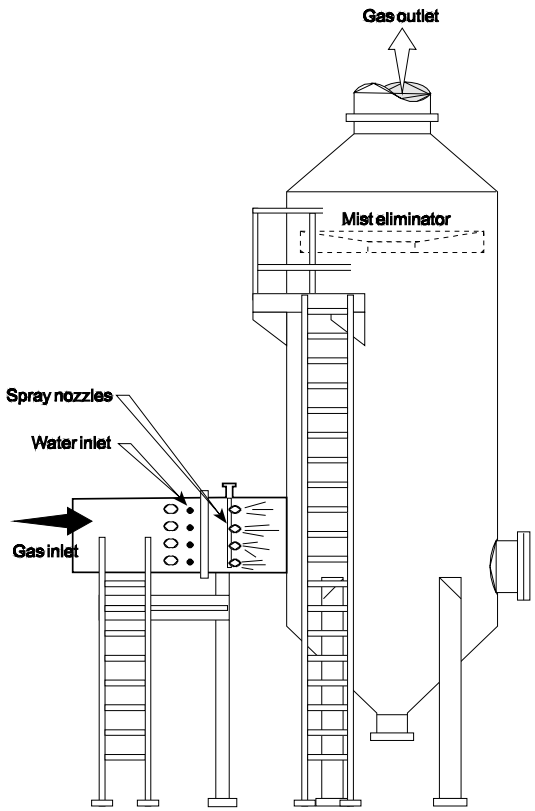

Figure 6-3. Spray tower scrubber (example)

One of the most important aspects of a spray tower scrubber is the type and arrangement of the spray nozzles used to inject scrubbing liquid into the gas stream. Full cone spray nozzles are used in spray scrubbers. They provide complete coverage of the intended target area, which is necessary to ensure maximum particle capture. Hollow cone nozzles are rarely used in this type of scrubber because they concentrate the droplets in the outer portions of the spray pattern, leaving the center of the pattern relatively dry.

Spray scrubbers operate with a flange-to-flange static pressure drop of 1 to 3 in. W.C. The static pressure drop is due to the normal flow resistance associated with the inlet ductwork, the mist eliminator (if present), and the outlet ductwork. The static pressure drop is not directly related to the particulate matter removal efficiency of the scrubber.

Spray tower scrubbers are the least expensive type of scrubbing vessel. The low cost is to due to the simplicity of the scrubber system components and shell.

Mechanically Aided Scrubbers

A mechanically aided scrubber uses mechanical energy to accelerate the gas stream to create conditions favorable for particle impaction. The fan-type mechanically aided scrubber shown in Figure 6-4 has a single spray nozzle in the inlet gas duct. This generates the liquid droplets that serve as the particle impaction targets. The gas stream is accelerated during movement through the fan.

A mechanically aided scrubber is limited to a particle size range greater than approximately 1 µm. This limit is due partially to the maximum differences in particle and droplet velocities that can be obtained in the co-current (liquid and gas streams move in the same direction) type of scrubbing system.

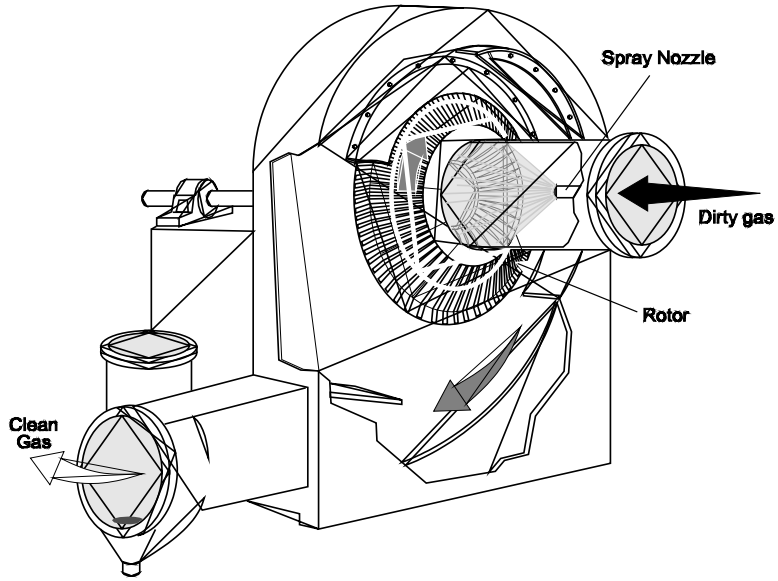

Figure 6-4. Mechanically aided scrubber

Mechanically aided scrubbers are usually limited to small-to-moderate gas flow rate applications. This is due to the limitations inherent in sizing the fan.

Packed Bed Scrubbers

In a typical packed bed scrubber, scrubbing liquid is introduced above the bed and trickles down over the packing in one or more beds arranged in series. The beds can be arranged in either a vertical tower or as a horizontal vessel. Packing in the beds can consist of raschig rings, pall rings, berl saddles, tellerettes, intalox saddles, or many other commercial materials. Some common types of packing materials are shown in Figure 6-5.

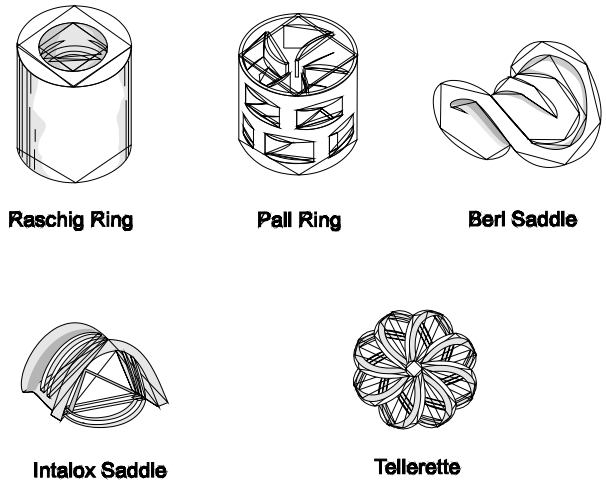

Figure 6-5. Common types of packing material

These packing materials are designed to provide the largest possible exposed liquid surface area per unit volume of bed. This is necessary to ensure effective gaseous absorption, the principal function of packed bed scrubbers.

These scrubbing systems are designed primarily for the absorption of gases and vapors. They have only a limited capability for particle removal. Removal efficiencies for particulate matter less than approximately 3 µm are very low. This is primarily due to the very low gas velocities through the bed. Particle impaction into the liquid layers coating the packing is very limited due to these low velocities.

A portion of the bed can become plugged if the particulate matter inlet concentrations are high. The scrubbing liquid flowing downward over the packing moves too slowly to purge out large quantities of particulate matter.

Vertical Packed Bed Scrubbers. Large, vertical packed bed scrubbers usually have several beds in series. Liquid redistributors are mounted at the top of the scrubber vessel and sometimes between the beds to ensure proper coverage of the packing material.

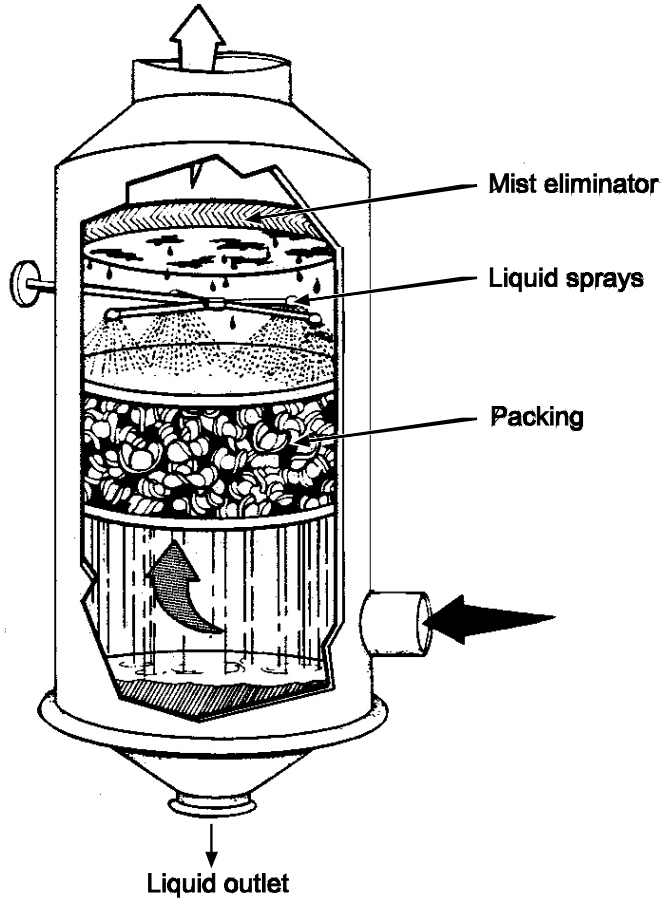

Figure 6-6. Vertical packed bed scrubber system

The performance of these redistributors and the liquid distributor at the top of the packed bed scrubber is critical for removing gaseous materials. Proper liquid distribution is slightly less important for particulate matter removal.

Crossflow Packed Bed Scrubbers. Crossflow scrubbers, such as the example unit shown in Figure 6-7, have vertical beds, and the gas stream passes in a horizontal direction. The scrubbing liquid is distributed on the top of the packing and passes downward in a crossflow orientation to the gas stream.

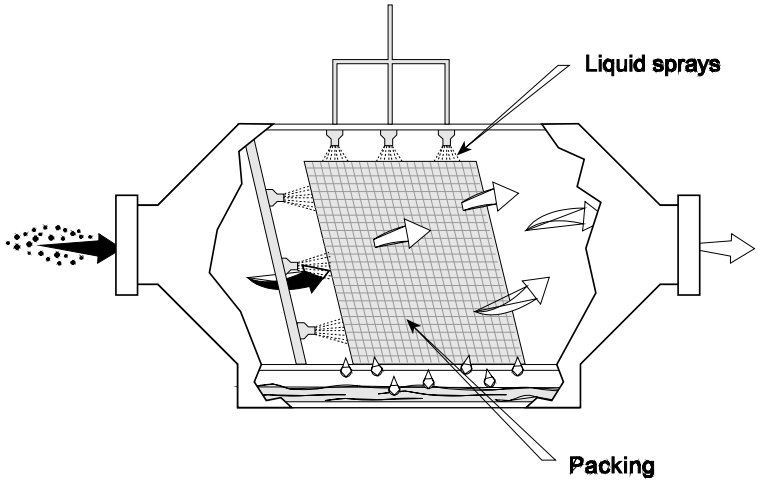

Figure 6-7. Crossflow packed bed scrubber

The performance characteristics of a crossflow scrubber with respect to particulate matter are very similar to the vertical tower packed bed scrubbers. However, these are sometimes advantageous due to their low profile. They can be retrofit into existing plant areas having limited vertical space. Crossflow packed beds also have vertically oriented mist eliminators that inherently drain better than horizontal mist eliminators.

Fiber Bed Scrubbers. Fiber bed scrubbers use one or more vertical mesh pads composed of interlaced synthetic fibers. Often, composite mesh pads are constructed of mesh pads of different fiber diameters and densities. The cross-section of an example fiber bed is illustrated in Figure 6-8. Scrubbing liquid can be sprayed either continuously or intermittently on the inlet side of each of the mesh pads.

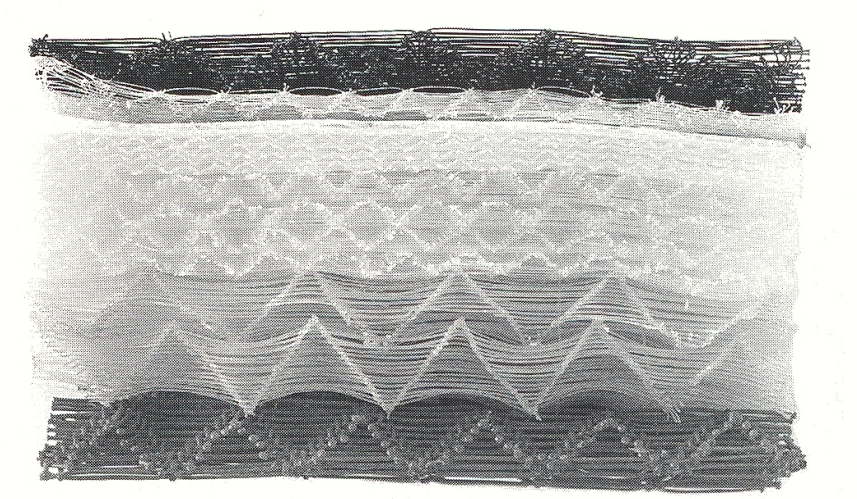

Figure 6-8. Composite fiber pad
(Reprinted courtesy of Kimre, Inc.)

Fiber bed scrubbers are designed exclusively in a crossflow orientation as shown in Figure 6-9. There are usually two to four separate beds in series. A open weave precollector bed is used in applications where heavy droplet loadings or large diameter droplets are expected in the gas stream. This type of scrubber is capable of efficient particle removal down to sizes approaching 1 micrometer. It is frequently used for the control of mists that can coalesce and drain from the mesh pad.

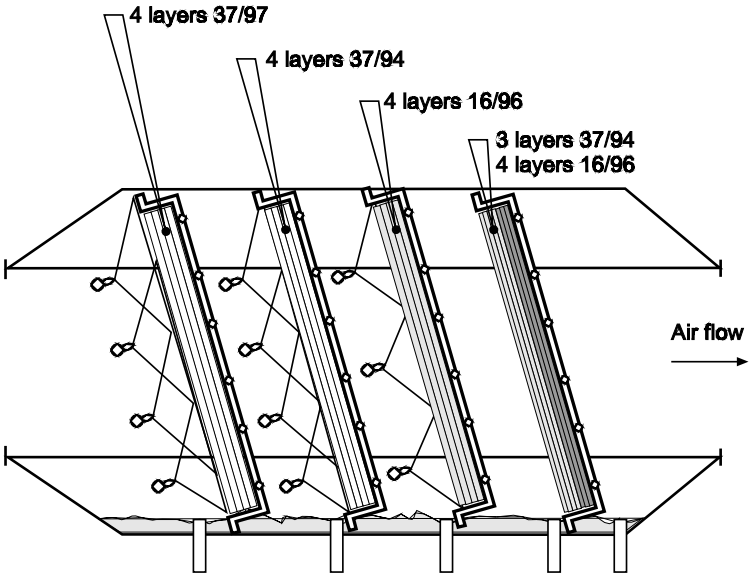

Figure 6-9. Four stage fiber bed scrubber
(Reprinted courtesy of Kimre, Inc.)

The gas velocities through the fiber pad are usually maintained in the range of 5 to 12 feet per second, depending on the fiber diameters and fiber pad design characteristics. The static pressire drops across each of the stages ranges from 0.2 to approximately 1 in. W.C. depending on the gas velocities and the fiber pad characteristics.

Wet-ionizing Scrubbers. Wet-ionizing scrubbers are the only type of particulate matter wet scrubber that uses electrostatic attraction as the primary technique for particle capture. The inlet gas stream passes through a short ionizer section composed of a number of high voltage discharge electrodes separated by small, grounded collection plates. The ionizer section is conceptually similar to a conventional precipitator field; however, the ionizer section is designed simply to impart an electrical charge to the particles. It is not designed to collect the particles. The ionizer section usually operates at secondary voltages of 20 to 30 kilovolts, D.C.

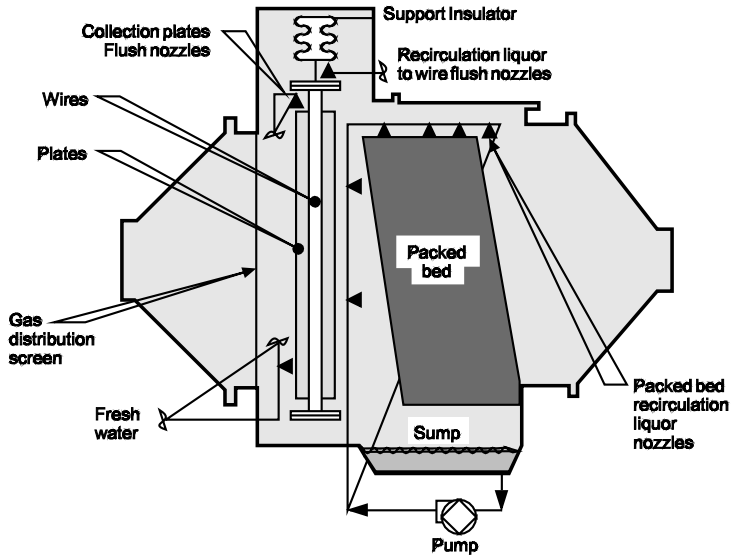

Figure 6-10. Wet-ionizing scrubber

Following the ionizer section, the gas stream passes through a crossflow scrubber section that is used for both particulate matter collection and gaseous absorption. Scrubbing liquid is distributed by means of a set of nozzles on the top and front of the bed. The electrostatically charged particles induce an opposite charge in the water layers coating the packing and are, therefore, attracted to and captured by the water layers.

A recirculation pump is used to recirculate scrubbing liquor from an internal sump back to the packed bed. A simplified drawing of a wet-ionizing scrubber is shown in Figure 6-10.

When necessary, scrubber modules like the one shown in Figure 6-10 can be arranged in series. This provides multiple opportunities to capture the particulate matter and minimizes problems caused by gas flow distribution at the inlet of the scrubber.

Tray Tower Scrubbers

Tray tower scrubbers are vertical towers with one or more trays for contacting the gas and liquid streams. The liquid stream enters from the top and flows downward over the trays. The gas moves in a counterflow direction. The principal collection mechanism for particulate matter is impaction. Tray tower scrubbers are usually selected for applications involving particulate matter greater than approximately 1 m. They have limited efficiency below 1 m due to the limits to the gas stream velocities through the openings in the trays.

When multiple trays are used, there are several opportunities to capture particulate matter. Particles that penetrate the first tray can be captured in the next tray. Accordingly, these scrubbers are less vulnerable to gas-liquid maldistribution than some other types.

Impingement Tray Scrubbers. A typical impingement tray scrubber is shown in Figure 6-11. The trays are metallic plates with numerous holes approximately 3/16 inches in diameter. Small baffle plates are mounted directly above each of the holes.

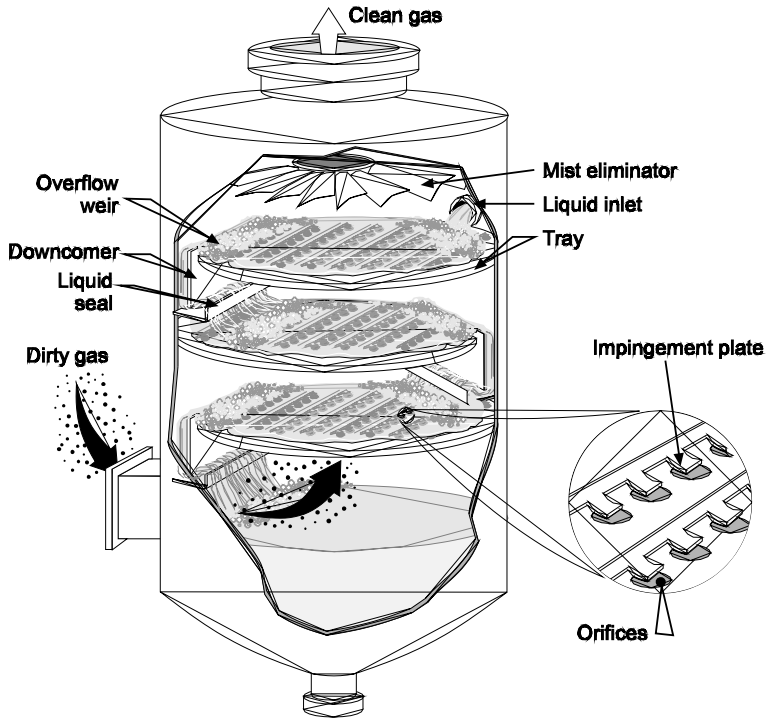

Figure 6-11. Impingement tray scrubber

Scrubbing liquid enters as a stream at the top of the unit. Overflow weirs on each of the trays set the height of the liquid on each tray to approximately 1 to 1.5 in. After passing across the tray, the liquid passes down a vertical passage called the downcomer. A U-shaped liquid seal at the bottom of each downcomer allows the liquid to flow freely to the next stage while preventing the gas stream from short-circuiting up the downcomer.

The gas stream is accelerated as it passes through the impingement tray orifices. The gas jets atomize a portion of the liquid above the tray. These droplets serve as the main impaction targets. Particles can also collect in liquid sheets.

The mist eliminators for tray tower scrubbers are usually mounted above the top tray. There must be sufficient space, termed freeboard, above the top tray so that the large quantities of scrubbing liquid entrained in the gas stream can fall out due to gravity before reaching the lower side of the mist eliminator.

The performance of impingement tray scrubbers is dependent on the physical condition of the tray and the orifices of the tray. Bowed or sloped trays will imbalance the height of the scrubbing liquid. The gas stream will preferentially pass through the orifices with the lowest liquid height because this is the low resistance path. The portion of the gas stream that continues to pass through the orifices with high liquid levels will be slow and ineffectual with respect to impaction.

Plugging the impingement orifices must be avoided. These scrubbers are vulnerable to plugging due to the very small diameters of the holes. Suspended solids can accumulate in these holes and harden, making it necessary to drill out or rod out the affected orifices. Due to the vulnerability to solids accumulation, the liquor recirculation system and treatment system are especially important. The suspended solids must be restricted to low levels by use of clean scrubbing liquid, to the extent possible, and by treatment of the recirculated liquor using clarifiers, filters, and other techniques.

Sieve Tray Scrubbers. Sieve tray scrubbers are conceptually similar to impingement tray scrubbers. The trays have large orifices and are, therefore, less vulnerable to orifice pluggage. However, the gas velocities are slightly lower than impingement tray scrubbers, which reduces the capability of the sieve tray scrubber. Usually, two or more trays are used in sieve plate units.

Catenary Grid Scrubbers. Catenary grid scrubbers have a set of catenary-shaped (saucer-like) wire mesh grid trays across a tray tower scrubber. The liquid is introduced at the top of the tray and flows downward from stage to stage without the need for side-mounted downcomers used on other types of tray tower scrubbers. The mixing action of the gas stream and the liquid on the trays creates a highly turbulent zone and causes droplet atomization. Particle impaction occurs in the droplets.

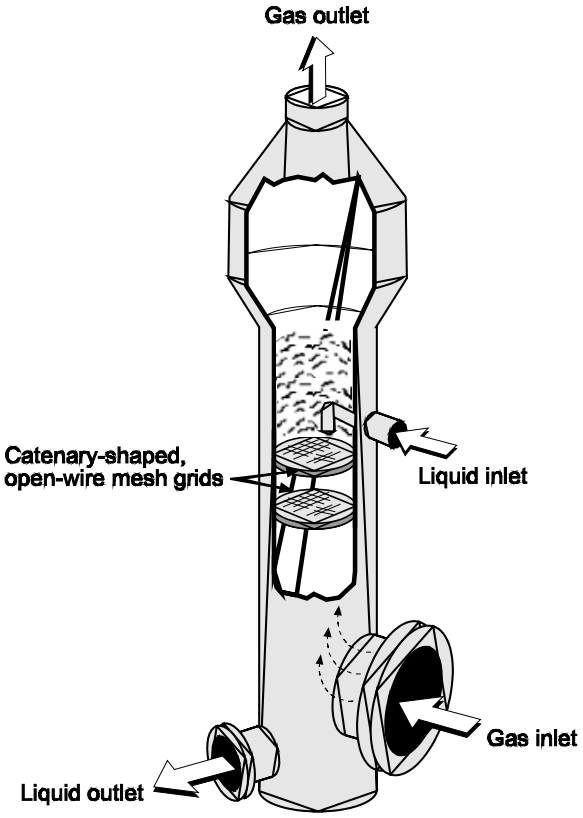

Figure 6-12. Catenary grid scrubber
(Reprinted courtesy of CECO Filters, Inc.)

Catenary grid systems are more tolerant of high suspended solids levels in the recirculation liquid than other types of tray tower scrubbers. The relatively open wire mesh stages are not highly prone to pluggage.

The superficial gas velocities through a catenary grid range from 12 to 20 feet per second. The upper end of this range is slightly higher than most other types of tray tower scrubbers. The static pressure drops range as low as 4 in. to more than 40 in. W.C. depending on the gas velocities and the liquid-to-gas ratios.

A conventional mist eliminator is used at the top of the catenary grid for the removal of entrained water droplets. An expanded area must often be provided to ensure that the gas stream velocities are slowed prior to entering the mist eliminator.

Moving Bed Scrubbers. Spherical, hollow packing, which is approximately the diameter of a ping-pong ball, is used in a moving bed scrubber. The bed is in an area between two open supporting grids and is filled 40 to 50% with mobile packing. Liquid is distributed across the top bed by spray nozzles. The gas flows in a counterflow direction from the bottom of the bed. Highly turbulent mixing occurs due to the motion of the packing material and aids in the formation of droplets and liquid sheets that can serve as impaction targets.

Moving bed scrubbers were originally designed to control sources of very sticky particulate matter, specifically, the organic aerosols emitted by Soderberg-type primary aluminum electrolytic cells. Due to the turbulent movement of the packing, the sticky material is continually removed from the surface of the packing. Due to their non-sticking character, moving bed scrubbers are also tolerant of high suspended solids levels in the recirculation liquid. Reactive slurries of lime and limestone can be used if there is a need to simultaneously control acid gases. The turbulent contact between gases and liquids created by the movement of the packing facilitates gases absorption into the scrubber liquid.

Moving bed scrubbers often have two to three beds in series in the same scrubber vessel. In some cases, an additional bed is used at the top of the tower for mist elimination.

A conventional mist eliminator can be used as the top of the scrubber vessel. There is no need for an enlarged mist eliminator section because the optimum velocity for the moving bed scrubber is similar to the optimum velocity range for conventional mist eliminators.

Froth Tower Scrubbers. Scrubbing liquid is injected into a gas stream in a manner that balances the gas and liquid momentum to create a highly turbulent froth zone (Myers and McIntosh, 1991). Particle impaction and gaseous absorption occur in the sheets of liquid within the froth.

The two scrubbers that use this scrubbing technique are: (1) reverse jets and (2) froth towers. The reverse jet scrubber injects a stream of liquid upward into a downward flowing gas stream. The spray characteristics and the liquid flow rate are maintained in a range in which a froth zone is created. The froth tower is a baffle tower with a descending stream of scrubbing liquid. The liquid flow rate and the gas flow area between the baffles are selected to ensure a froth zone on at least the top several baffle stages.

Gas-Atomized Scrubbers

The term *gas-atomized* indicates that the scrubber uses high energies in the gas stream to atomize the scrubber liquid used for particle capture. All gas-atomized scrubbers are designed to obtain high efficiency inertial impaction. Brownian motion contributes slightly to particle capture; however, gas atomized scrubbers are not designed to optimize diffusion mass transfer.

Fixed Throat Venturi Scrubbers. One of the most common types of gas-atomized scrubbers is the fixed throat venturi, such as the unit shown in Figure 6-13. To achieve the high gas velocities in a venturi, the entering gas stream passes into a converging section that has a small open area for gas flow. This accelerates the gas stream to velocities between 50 and 250 mph. Because the fixed throat has a constant open area, the actual gas velocity achieved in the venturi section depends on the gas flow rate. Particle collection efficiency is, therefore, also gas flow rate dependent. Fixed throat venturi scrubbers are used on sources at which the gas flow rate is relatively constant or where the particle size distribution is sufficiently large that some variations in pressure drop are tolerable.

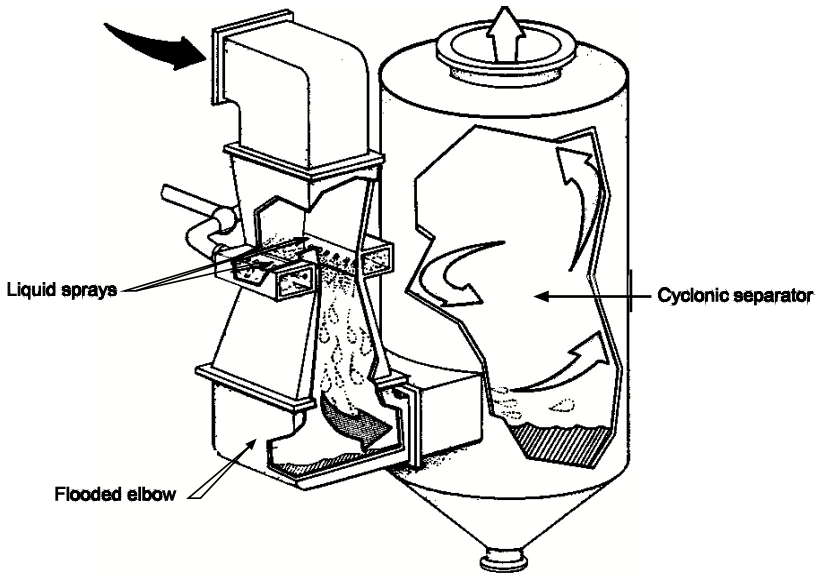

Figure 6-13. Fixed throat venturi scrubber

Because of the high gas velocities, the residence time of the gas stream in the venturi throat, where most particulate matter collection occurs, is only 0.001 to 0.005 sec. Proper gas-liquid distribution is essential in obtaining optimum performance of a fixed throat venturi scrubber.

Adjustable Throat Venturi Scrubbers. A typical adjustable throat venturi scrubber is shown in Figure 6-14. In this type of unit, the moveable dampers can vary the throat area in order to control the gas velocity.

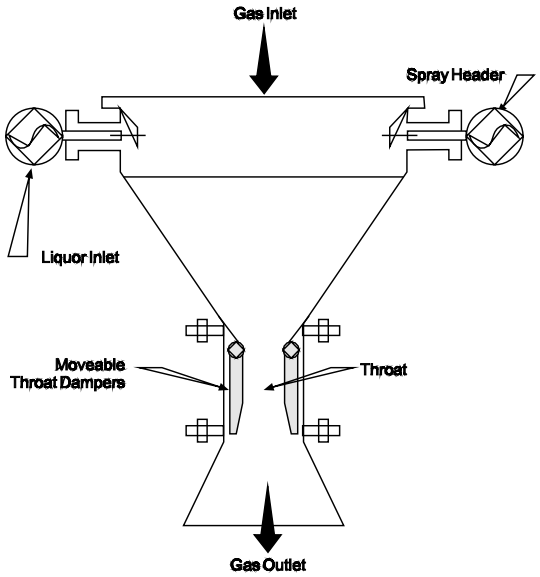

Figure 6-14. Adjustable throat venturi scrubber

The scrubbing liquid is injected into the gas stream just above the throat. The unit shown in Figure 6-14 uses spray headers to distribute the liquid on the side walls. The liquid is sheared off the side walls and entrained in the gas stream as it enters the throat. In other types of venturis, spray nozzles are used to distribute the liquid into the converging section of the scrubber. The atomization of the scrubbing liquid by the high-velocity gas stream provides droplets that serve as impaction targets.

Initially, the droplets have a low velocity in the direction of the gas flow. They accelerate rapidly in the gas stream. Impaction occurs on the droplets due to the large difference in the gas stream-particle velocities and the accelerating droplets. Once the droplets leave the throat area, they are moving at velocities close to the gas velocities and the remaining upcaptured particles. Impaction of the uncaptured particles into the droplets does not occur efficiently because they are moving at similar velocities and in a similar direction. Gas-atomized scrubbers use a high velocity gas stream to atomize the scrubbing liquid and to impact the particles in the liquid droplets that are formed in the high velocity zone. The effectiveness of gas-atomized scrubbers is related to the maximum differences in the droplet and particle (gas stream) velocities.

The typical static pressure drop across a venturi scrubber varies from a low of 5 in. W.C. to values exceeding 100 in. W.C. The static pressure drop is related to the gas velocities in the throat, the quantity of scrubbing liquid used, and the configuration of the throat. High static pressure drops are used only in situations demanding high efficiency removal of very small particulate matter.

There is a wide variety of adjustable throat mechanisms in addition to the type shown in Figure 6-14. The simplest is a metal plate that enters from one side of the venturi and extends across part of the throat. These simple plates are usually manually operated. Another style of adjustable throat has a flow restrictor that enters from the bottom of the throat as shown in Figure 6-15. As this flow restrictor advances, the area on either side is reduced, thereby, adjusting the gas flow rate. The flow restrictors are supported on a pipe that is raised or lowered by a hydraulic actuator.

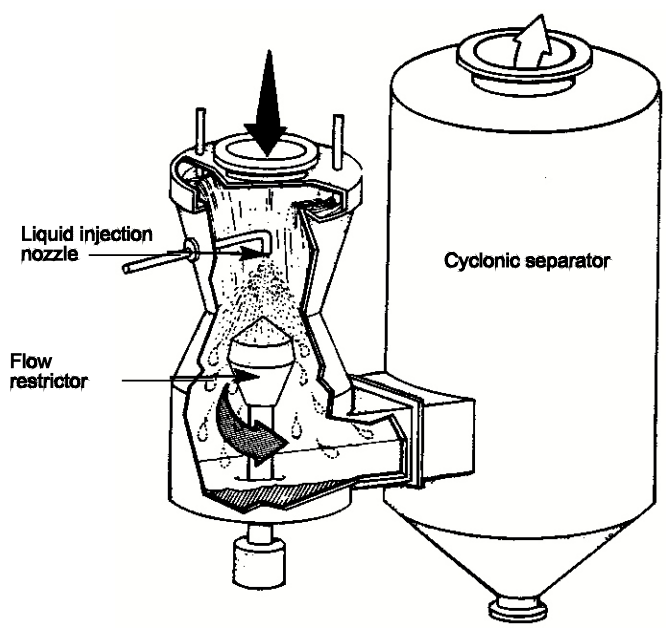

Figure 6-15. Flow restrictor-type adjustable throat venturi scrubber

Erosion conditions within the venturi throat can be severe. All adjustment throat mechanisms must be designed to withstand these conditions. They require frequent inspection and occasional replacement.

Proper liquid distribution across the inlet to the venturi throat is very important. Most of the particles that penetrate the throat will pass uncollected through the remainder of the scrubbing system. Obviously, portions of the venturi throat without any atomized scrubbing liquid have no capability for collecting particulate matter.

Rod Deck Scrubbers. Rod deck scrubbers are similar to venturi scrubbers in that they use high velocity gas streams to atomize liquid droplets and to impact particulate matter. A gas stream entering a rod deck scrubber is accelerated as it passes between the closely spaced rods shown in Figure 6-16.

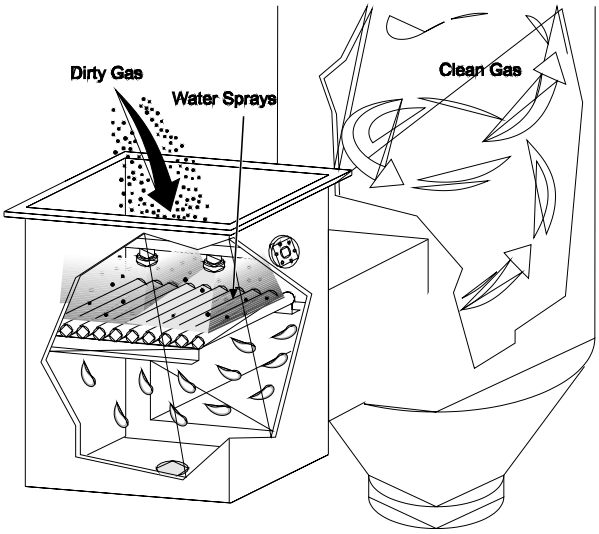

Figure 6-16. Rod deck scrubber

The liquid is supplied by a set of spray nozzles above the rod deck, which is positioned to fully irrigate the gas flow area. The high-velocity gases in the open area between the rods further atomize the sprayed water droplets. After the rod deck, the gas stream decelerates, turns, and passes into a mist eliminator vessel to remove the entrained water droplets.

Multiple decks of rods can be used to improve particulate removal capability. The decks can be equipped with actuators to modify the spacing between the decks and, thereby, adjust the static pressure drop across the unit.

The rods must be fabricated from abrasion resistant materials due to the high-velocity conditions. They must be replaced when they have significantly eroded.

Collision Scrubbers. In collision scrubbers, the gas streams are split into two separate streams. Each stream enters a venturi-like section for contacting the injected scrubbing liquid. These two sections are arranged in an opposed manner so that gas streams exiting each of the scrubbing liquid contact areas collide. Within the collision zone, the droplets and particles impact due to the large difference in velocity and trajectory. Collision scrubbers use a gas recirculation system to ensure adequate gas flow in the venturi contactors at a variety of inlet gas flow rates.

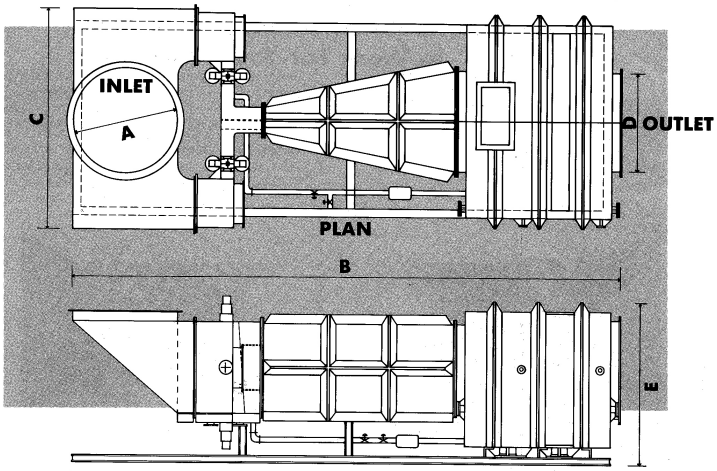

Figure 6-17. Collision scrubber
(Reprinted courtesy of Monsanto Enviro-Chem Systems Inc.)

The scrubber system uses a recirculation stream to maintain adequate velocities in each throat despite changes in the overall inlet gas flow system. The recirculation line has a modulating damper to control the rate of recirculated gas flow.

Orifice Scrubbers. In orifice scrubbers, the gas stream is forced to turn sharply directly above or through a pool of scrubbing liquid. The gas stream entrains and atomizes the scrubbing liquid. Impaction occurs in the droplets formed by the movement of the gas stream. The velocity of the gas over the pool of scrubbing liquid is controlled partially by the height of the pool. An example orifice scrubber system is shown in Figure 6-18.

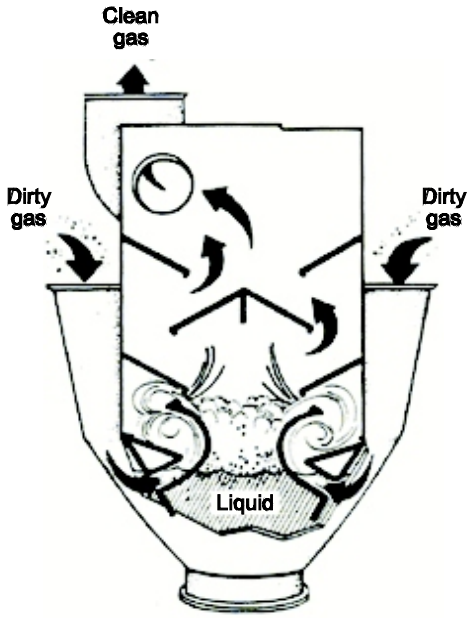

Figure 6-18. Orifice scrubber vessel
(Reprinted courtesy of Joy Energy Systems)

Orifice scrubbers are usually less vulnerable than fixed throat venturis to gas-liquid maldistribution; however, it is more difficult to achieve high gas velocities in this type of system. Orifice scrubbers inherently have a low profile design and can be easily retrofit into tight areas of existing plants.

Liquid Atomization Scrubbers

The scrubbing liquid is atomized to extremely small droplets of 5 to 50 micrometers using a two-fluid nozzle operating at high pressure. Particle impaction occurs in a contacting chamber due to the high velocity of the droplets exiting the fluid nozzle. This type of scrubber is capable of efficient particle removal down to a size of approximately 1 micrometer. An example of a high energy liquid atomization nozzle is shown in Figure 6-19.

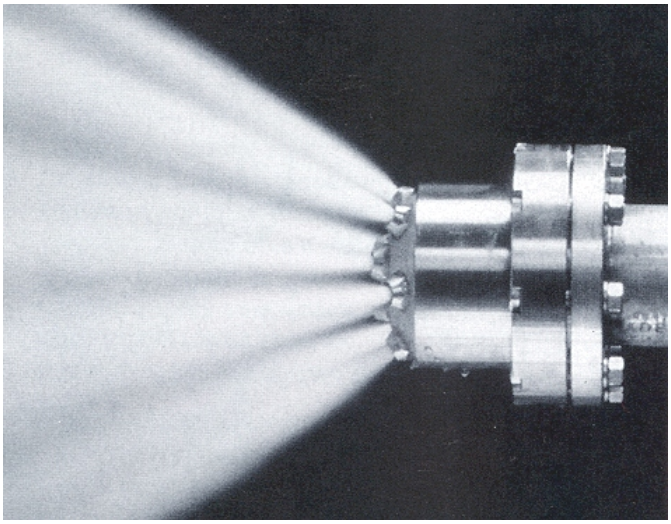

Figure 6-19. Nozzle in a high energy liquid atomization scrubber
(Reprinted courtesy of Turbosonics, Inc.)

The scrubber nozzles operate at pressures of 50 to 200 psig. A dedicated compressor is often used to supply compressed air at the necessary operating pressure. Because of the droplet size distributions created by this type of scrubber, an efficient mist eliminator is needed.

Condensation Growth Scrubbers

Condensation growth scrubbers are complex systems designed to improve particulate matter removal efficiencies in the submicrometer particle size range. Large quantities of water vapor are introduced into the particle-containing gas stream. Due to cooling, some of this water vapor condenses on the surfaces of the submicrometer particles, thereby, increasing their mass. The particles are collected in conventional scrubbers downstream of the vessel used for condensation growth.

Condenser/Venturi Scrubber Condensation Growth Scrubbers. Figure 6-20 shows a simplified flowchart for a condensation growth scrubbing system using a packed bed and a venturi scrubber in series. In this unit, water vapor is introduced by evaporating clean water injected into the very hot gas stream. This approach can be used for incinerators and other processes operating with inlet gas temperatures in excess of 1800°F. For other processes, it is necessary to inject low pressure steam to provide the necessary water vapor.

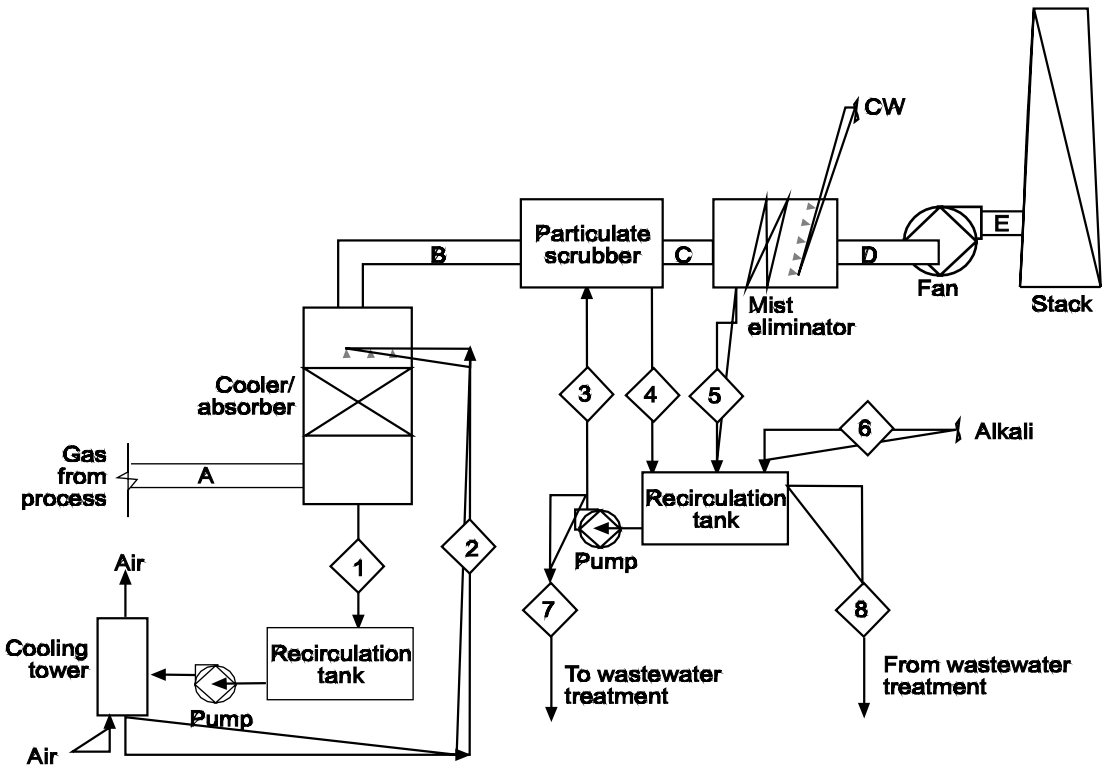

Figure 6-20. Example of a condensation growth scrubber system

Following the evaporative cooling or steam injection step, the water vapor content can range from 40% to 60% by volume of the gas stream. The water vapor is condensed in a packed bed vessel (as shown in Figure 6-20) or a spray tower scrubber upstream of the main particulate collection device. The extent of condensation is maximized by cooling the scrubbing liquor recirculating through the system. Sensible heat can be removed from the scrubber by means of a small indirect heat exchanger or a small cooling tower.

Particulate matter is removed in a venturi or other type of scrubber capable of high efficiency removal of small particulate matter. Static pressure drops of 30 to 60 in. W.C. may be necessary in the scrubbers depending on the resulting particle size distribution and on the removal efficiencies required.

High Energy Ejector Scrubbers. A high energy ejector scrubber uses a single high-pressure spray nozzle to inject liquid into the vessel. The reduced pressure adjacent to the high-pressure stream is sufficient to induce a gas flow from the process being controlled. The gas moving principles used in ejector scrubbers are identical to those used in laboratory faucet air suction lines. All the energy needed to operate the scrubbing system is supplied by the liquid stream rather than using energy supplied by the gas stream centrifugal fan.

Particulate matter is impacted in the droplets generated in the high-pressure nozzle. The differences in particle and droplet velocities, necessary for impaction, are due to the high-velocity droplets in the relatively slow-moving air stream.

High energy ejector scrubbers can be used for both particulate matter control and gaseous absorption. They are often arranged in series in order to generate the necessary static pressures for gas movement and to increase pollutant removal efficiencies.

6.1.3 Mist Eliminators

Most wet scrubbing systems generate liquid droplets that are entrained in the gas stream leaving the treatment area. These droplets include two separate distributions. There are large droplets that form in the scrubber vessels due to atomization of liquid sprayed by nozzles or by shearing of liquid from sheets and jets. Most of these droplets are in the range of 20 to 1,000 micrometers in diameter. These droplets serve as impaction targets in the scrubber vessel and, therefore, include the captured particulate matter. There is a second population of droplets due to the condensation of water vapor in the saturated gas zone of the scrubber vessel. These droplets are in the size range of 0.1 to 10 micrometers. These very small droplets contain little, if any solids.

The purpose of the mist eliminator is to remove the large, solids-containing droplets prior to gas stream discharge to the atmosphere. Solids from these droplets could accumulate in outlet ductwork, erode the fan wheel, contribute to stack corrosion, and create nuisance problems in the immediate vicinity of the stack discharge.

Mist eliminators in commercial use include, but are not limited to the following types.

- Cyclonic vessels
- Radial vanes
- Chevrons
- Mesh pads
- Fiber pads
- Woven pads

Normal static pressure drops across all these types of mist eliminators range from 0.5 to more than 4 in. W.C. Static pressure drop gauges are useful for monitoring the pressure drop and providing an early warning of solids accumulation.

Cyclonic Vessel Mist Eliminators

Cyclonic vessels have a tangential gas inlet and operate like a conventional large-diameter cyclone. Depending on the gas velocity, the gas stream spins one-half to two revolutions prior to discharge. They have reasonable efficiency when operated at close to the design inlet gas velocity. However, droplet removal decreases rapidly at gas flow rates less than 80% or more than 120% of the design value.

The gas flow rate sensitivity is the main disadvantage of cyclonic mist eliminators. The cost of a stand-alone vessel is another major disadvantage. All of the other types of mist eliminators can be installed in the outlet portion of the scrubber vessel and, therefore, do not require their own vessel. The main advantage of the cyclonic mist eliminator is its openness as shown in Figure 6-21. As long as the cyclonic vessel drain is properly sized and remains open, the mist eliminator is not vulnerable to plugging caused by excessive carryover of solids-containing droplets from the scrubber vessel.

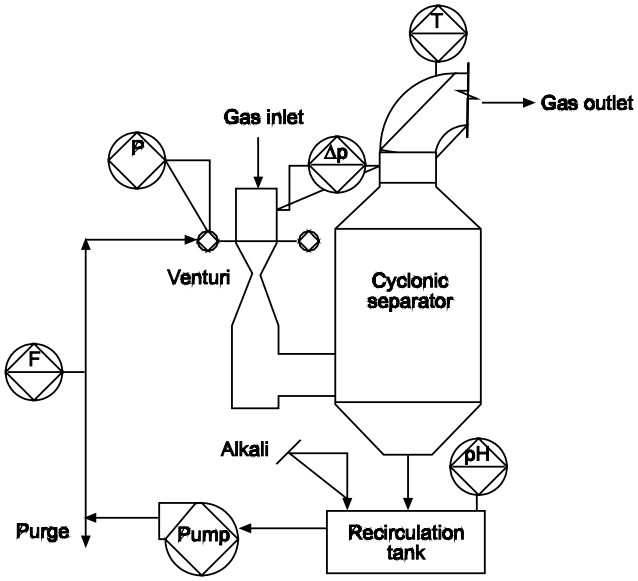

Figure 6-21. Cyclonic mist eliminator in a wet scrubber system

Due to the spinning action of the gas stream, it is often necessary to install anti-vortex baffles in the stack in order to eliminate cyclonic flow conditions at emission testing locations. It is also common to install liquid flow deflectors to prevent liquid collected on the inner cyclone wall from flowing across the tangential inlet duct and being reentrained into the gas stream.

Radial Vane Mist Eliminators

Radial vane mist eliminators have a single layer of overlapping baffles oriented across the gas stream. As the gas stream turns to pass around the baffles, droplets impact on the baffles and drain back into the gas stream. The gas velocities are usually maintained at less than 15 ft/sec to avoid liquid entrainment from the trailing edge of the mist eliminator blade. High velocities are usually caused by the unintentional build-up of solids on part of the radial vanes as shown in Figure 6-22.

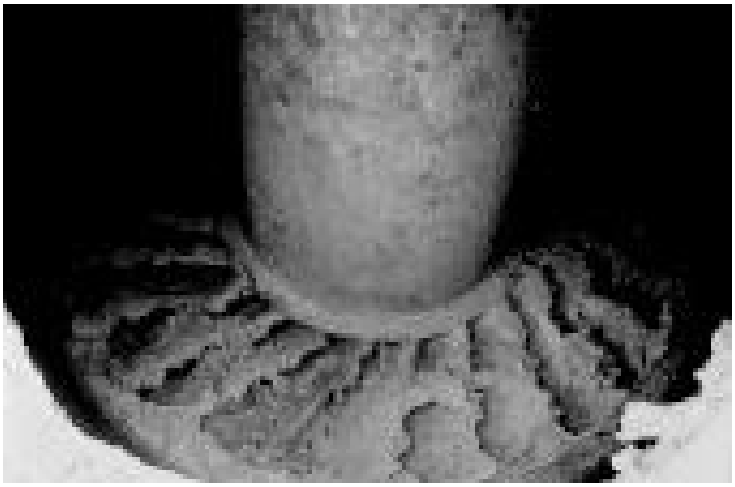

Figure 6-22. Radial vane mist eliminator with heavy solids accumulation

These deposits increase the velocities in the portion of the mist eliminator that is still open for flow. In order to minimize solids accumulation, clean water spray headers are placed on the inlet and/or outlet sides. These are activated intermittently on a once-per-shift or once-per-day rate depending on the severity of the solids problem.

Chevron Mist Eliminators

Chevrons are simply zig-zag baffles that force the gas to turn sharply several times while passing through. Droplets are captured on the chevron blades in the same manner as radial blade mist eliminators. However, with the chevron configuration, it is possible to force the gas to turn two or more times and, therefore, create more opportunities for droplet impaction. A standard three-pass chevron blade mist eliminator is shown in Figure 6-23.

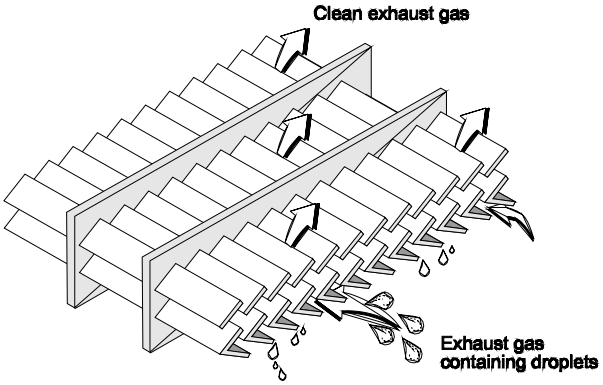

Figure 6-23. Chevron mist eliminator

Other common types of chevrons have two- and four-pass arrangements. Each manufacturer has a variety of designs for the chevron blades to minimize reentrainment and optimize the gas flow range.

Chevron mist eliminators can be installed in either a vertical or horizontal arrangement. In the vertical design, liquid draining from the chevron blades is opposed by the upward moving gas stream. In the horizontal arrangement, the liquid drains in a direction 90 degrees from the gas stream; therefore, less reentrainment of collected droplets occurs.

Essentially all of the chevron mist eliminator designs, regardless of vertical or horizontal orientation, are limited to gas velocities of less than approximately 20 ft/sec. Many of the chevrons have optimum performance in the 5 to 15 ft/sec range. At high velocities, liquid on the blades can be driven toward the outlet side of the chevron where it can be reentrained in the gas stream.

Solids accumulation on the chevron mist eliminators can create high velocities by restricting the amount of area open for gas flow. In applications where solids accumulation is possible, mist eliminator sprays are installed to clean the chevrons on a frequent basis. These sprays are activated on an hourly or shift basis, as necessary to maintain the static pressure drop across the mist eliminator in the design range. In most cases, the sprays are mounted on inlet side. However, in cases especially prone to solids accumulation, sprays are mounted on both the leading and trailing sides. The sprays can be activated either by timers or by static pressure sensors. Clean water is used for mist eliminator cleaning. The necessary water pressures depend on the placement of the spray nozzles. Values of 5 to 20 psig are common.

The chevron mist eliminators are fabricated in sections for shipment to the customer. They are mounted in a support frame that spans the scrubber vessel.

Mesh Pad Mist Eliminators

Mesh pads are randomly interlaced metal fibers. The pads can be up to 6 inches thick. As in the case with the chevrons, there is a maximum gas velocity above which reentrainment is possible. This maximum gas velocity depends on the density of the mesh (usually 5 - 9 lb_m/ft^3), on the materials of construction, and on the gas density. The maximum velocity is usually in the range of 12 ft/sec. A mesh pad mist eliminator pad is illustrated in Figure 6-24.

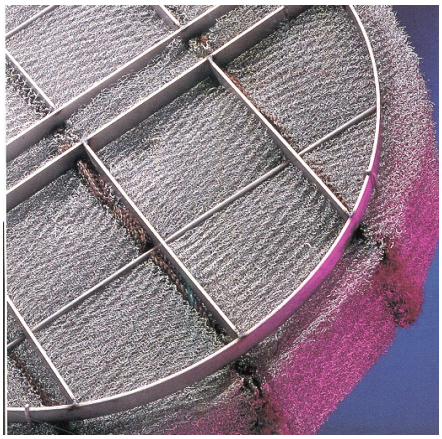

Figure 6-24. Mesh pad eliminator

The mesh pads are fabricated in sections. They are held in place by support frames mounted across the scrubber vessel being controlled. Spray nozzles are often mounted on the inlet side of the mesh pad to help remove accumulated solids.

Woven Pads

Woven pads have complex, interlaced synthetic fibers that serve as impaction targets. Mist eliminators composed of these materials are often layered in a manner identical to the composite pad shown earlier in Figure 6-8. The inlet side layers are open weaves that are capable of removing large quantities of large-diameter material without overloading. The middle and outlet side layers have more compact weaves, which have high removal efficiencies for the small liquid droplets. These units have maximum velocities of 8 to 15 ft/sec, depending on the pad construction characteristics.

6.1.4 Liquid Recirculation Systems, Alkali Addition Systems, and Wastewater Treatment Systems

Pumps

For scrubber applications, the most common pumps are (1) centrifugal, (2) positive displacement, and (3) progressing cavity. Centrifugal pumps are used almost exclusively for recirculation liquor streams and clarifier overflow streams.

A typical centrifugal pump is shown in Figure 6-25. The liquid enters axially (left to right in Figure 6-25) and is accelerated by the rotating impeller. As the liquid leaves the impeller radially, the liquid velocity decreases, and the pressure increases.

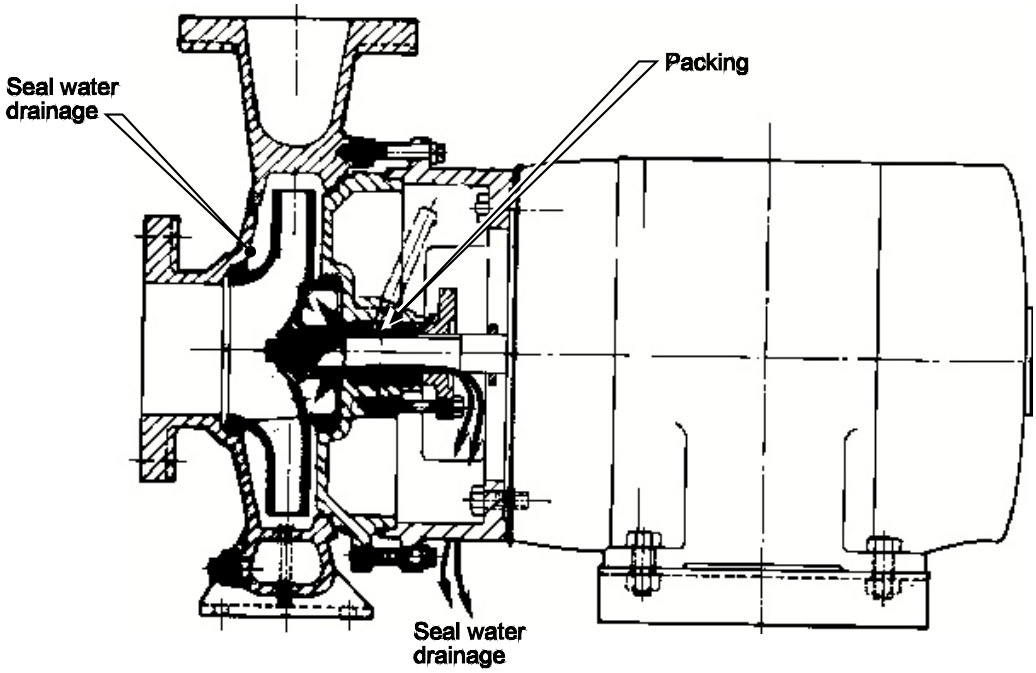

Figure 6-25. Centrifugal pump

Seal water is injected around the pump shaft, which extends from the drive motor to the pump housing. The seal water minimizes corrosion and erosion of the pump shaft by minimizing the leakage of the scrubber liquid out of the pump housing.

The pumping system may consist of a number of components, including the suction pipe, strainer, suction side check valve, discharge check valve, and discharge control valve. The strainer is used for removal of small bits of metal and other contaminants that can be caught in the liquid stream. Strainers are often removed when there is a tendency for suspended solids in the liquid stream to blind the strainer filter. The suction side check valve is used to reduce the risk of air infiltration into the suction side piping during an outage. The discharge valve is used to adjust liquid flow from the pump.

Positive displacement pumps, such as diaphragm pumps, can be used for movement of high solids content streams, such as the clarifier underflow. Progressive cavity pumps are used for movement of high solids streams and/or potentially clogging liquid streams.

Spray Nozzles and Headers

There are four common types of spray nozzles used in particulate wet scrubbers: (1) full cone, (2) hollow cone, (3) fine spray, and (4) air atomizing. Of these, the full cone nozzle is used most frequently due to the characteristics of its spray pattern. As illustrated in Figure 6-26, the full cone nozzle projects droplets across an entire circular area. This is necessary in many types of scrubbers, such as spray towers and venturis, to obtain effective gas-liquid contact.

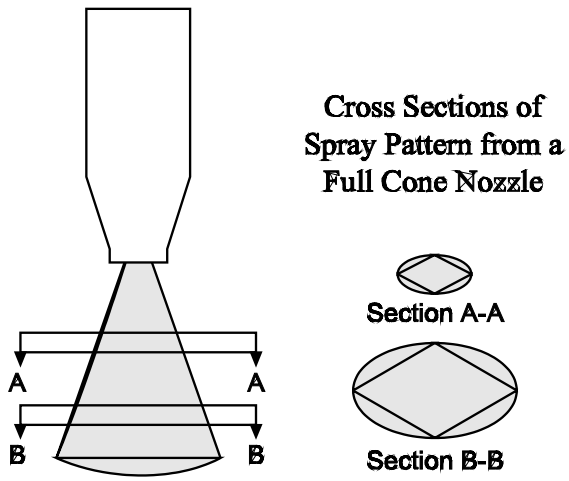

Figure 6-26. Spray pattern of full cone nozzle

The spray angle can be as important as the spray pattern. The design spray angle should be sufficiently large to provide full coverage of the gas stream. If the spray angle is small, a large number of nozzles are needed to ensure good gas-liquid contact. The spray angle is affected by the following factors.

- Nozzle orifice diameter
- Nozzle design
- Nozzle condition
- Liquid pressure
- Liquid viscosity
- Liquid surface tension

The spray angle usually increases slightly with the pressure of the liquid in the supply header. Liquids that have greater viscosity or a higher surface tension than pure water will change the spray angles indicated by the nozzle manufacturer. The presence of solids in the nozzle will usually decrease the spray angle or entirely distort the spray pattern. Erosion of the nozzle orifice will also have an adverse impact on the spray angle.

The droplets produced by full cone and hollow cone nozzles usually have diameters of 100 to 1,000 micrometers. The droplet size distributions are usually expressed in one or more of the following units of measure.

- Mass median diameter (MMD)
- Median volume diameter (MVD)
- Median number diameter (MND)
- Sauter mean diameter (SMD)

The mass median diameter and the median volume diameter express the droplet size against which the distribution is measured: 50% of the droplets are larger and 50% are smaller than the stated value. These two equivalent terms are the most commonly used measures of the droplet size distribution. The median number diameter deals with the distribution *by count:* 50% of the droplets by count are larger and 50% of the droplets by count are smaller than the median. The Sauter mean diameter expresses the droplet size distribution based on the surface area. The Sauter mean diameter for a nozzle is the diameter of the droplet having the same volume-to-surface area as the ratio of the volume and surface area of the entire liquid stream sprayed.

The liquid supply headers for sets of spray nozzles are often as important as the nozzles in ensuring good gas-liquid contact in the scrubber vessel. These headers must be designed to prevent solids accumulation that could partially or completely block pipes leading to individual nozzles. Clean-out traps are often provided to allow routine cleaning during offline periods.

Alkali Addition Systems

The most common alkalis used for neutralizing acidic constituents in the recirculation liquid stream include lime, soda ash, and sodium hydroxide. Powdered lime and soda ash are stored in silos in quantities that support routine operation for one week to one month. The solids are metered out using a weigh belt feeder that supplies the injection line. The rate of alkali injection is controlled by a pH meter and transducer mounted in the main liquid recirculation tank or the feed line to the scrubber vessel.

The alkali is injected into the scrubber system recirculation tank. The alkali requires several minutes of residence time in the tank for complete mixing and dissolution.

Wastewater Treatment Systems

There is a wide variety of wastewater treatment systems for particulate matter wet scrubber systems. Some small scrubbers at large industrial facilities discharge directly to the plant wastewater system rather than using a dedicated wastewater treatment system. Small scrubbers collecting nontoxic particulate matter, such as those at asphalt plants, sometimes use a small two-zone settling pond for wastewater treatment. In these cases, the effluent overflowing the second zone of the pond is returned to the scrubber system.

For large particulate matter wet scrubber systems, a small wastewater treatment system is installed. A clarifier is used for removal of the suspended solids that will settle by gravity. The overflow from the clarifier is returned to the scrubber recirculation tank. The clarifier underflow containing the concentrated solids is often sent to a rotary vacuum filter for removal of the suspended solids. The sludge from the rotary vacuum filter is sent to a landfill for disposal.

In some cases, a flocculent is added to the clarifier to optimize solids removal. However, addition of flocculates must not exceed the levels that cause an increase in the liquid surface tension. This can have an unintended detrimental effect on particulate removal efficiency of the scrubber by decreasing the effectiveness of particle impaction into the liquid droplets and by changing the droplet size distribution formed in the scrubber.

6.1.5 Fans, Ductwork, and Stacks

The gas handling components of a particulate matter wet scrubber system must be designed for the high negative static pressures that are present during routine operating periods. These components must also be designed for the high levels of entrained droplets, low pH levels, and highly corrosive gas concentrations that can be present during scrubber and/or process upsets.

Fans

Radial blade fans are most common downstream of particulate wet scrubbers due to their ability to withstand moderate solids and droplet loadings in the gas stream. The fan wheel and fan housing materials of construction are selected based on information concerning the expected gas stream temperatures and the peak concentrations of potentially corrosive materials.

The fans used on particulate matter wet scrubbers are usually larger and require more energy than fans for comparably sized fabric filter systems. This is due to the considerably high static pressures that must be generated in the fan to overcome the flow resistance of the scrubber.

Fans used on wet scrubber systems are often equipped with drains at the bottom of the fan housing to allow for the removal of moisture accumulating due to droplet entrainment in the gas stream or due to condensation of water vapor from the gas stream.

Ductwork

Ductwork requirements for high energy particulate wet scrubbers are more demanding than for other types of air pollution control systems. The ductwork must be reinforced to prevent deflection and collapse if the negative static pressure exceeds –20 in. W.C. As illustrated in Example 6-1, this pressure represents very high forces on the ductwork surface.

Problem 6-1

What is the force on a 1-foot length of rectangular ductwork that is 4 feet high and 3 feet wide if the static pressure inside the duct is –20 in. W.C.?

Solution:

Calculate the area of the one foot duct section.

- Area of sides = (2 sides)(4 ft high)(1 ft long) = 8 ft^2
- Area of top and bottom = (2 sides)(3 ft wide)(1 ft long)= 6 ft^2
- Total area = sides + top + bottom = 14 ft^2

Calculate the inward force on 1 square in. at –20 in. W.C.

- (-20 in. W.C.) (14.7psig/407 in. W.C.) = -0.72 lb_f/in^2

Calculate the total force on the 1-foot length of duct

- (-0.72 lb_f/in^2)(14 ft^2)(144 in^2/ft^2) = -1,456 lb_f

Failure to adequately reinforce the ductwork could result in damage to welds. Air infiltration through gaps in the ductwork welds could become severe due to the high negative pressures. Severe air infiltration reduces the amount of gas captured at the process and, therefore, contributes to fugitive emissions. Accordingly, proper design of the ductwork is important to the overall effectiveness of the wet scrubber system.

Stacks

Particulate matter wet scrubbers can have one or two stacks. The main stack is used to disperse the effluent stream of the scrubber system. This stack must be fabricated from materials that can withstand the contaminants that are emitted when scrubber and/or process upsets occur.

Bypass stacks are used upstream of the scrubber vessel when the gas stream being treated is very hot. The bypass duct is opened when there is a failure of the liquid recirculation line or emergency flush line. Without the liquid streams, the temperatures in the scrubber vessel could exceed the design limitations of the scrubber shell, mist eliminator, or corrosion resistant liners. The bypass stack is usually sealed by a butterfly damper or louver damper. These dampers must provide a tight gas seal to prevent air infiltration into the scrubber system during routine operating periods.

6.1.6 Instrumentation

Instruments are used throughout the scrubbing system to protect system components and to monitor performance. A partial list of the instruments includes the following:

Gas temperature monitor

- Scrubber inlet temperature monitor
- Scrubber outlet temperature monitor

Liquid flow rate monitor

- Recirculation liquid stream flow rate monitor
- Purge liquid stream flow rate monitor

Liquid pressure gauge

- Recirculation pump discharge gauge
- Scrubber liquid distribution header pressure gauge

Liquid pH monitor

- Recirculation tank or recirculation liquid stream pH monitor

Static pressure drop monitor

- Wet scrubber vessel (flange-to-flange) static pressure drop monitor
- Mist eliminator (media) static pressure drop monitor

The scrubber inlet temperature gauge is used to detect high gas temperatures that could damage scrubber system materials. Many scrubbers are constructed of fiberglass reinforced plastics (FRP) with temperature limits of 180°F to 250°F or have corrosion-resistant liners that have maximum temperature limits ranging from 400°F to 1000°F. In the event of high gas temperatures, emergency flush systems are included in many scrubbers to protect the system during an emergency shutdown.

The outlet gas temperature gauges protect the downstream fan. Loss of scrubbing liquid flow due to pump failure, pipe freezing, pipe breakage, or pipe blockage could result in higher than desirable gas temperatures. The scrubber outlet temperature data are also useful for evaluating scrubber system performance.

Liquid flow monitors are used to indicate liquid flow rate so that it can be kept in the intended operating range. The size of the facility and the characteristics of the liquid being monitored determine type of instrument used. Relatively clean liquid streams can be monitored by orifice meters, swinging vane meters, and rotameters. Magnetic flow meters and ultrasonic meters can be used on streams with moderate solids levels.

Liquid pressure gauges are used on supply headers to the scrubber to indicate problems such as nozzle pluggage, nozzle orifice erosion, and header pluggage. Pluggage problems are indicated by higher than normal pressures. Most liquid pressure gauges are direct indicating type instruments that must be checked while inspecting the scrubber system.

pH instruments are used to control the alkaline feed rate to the scrubber system. It is usually advantageous to maintain the pH at levels above 5 and below 9. At low pH levels, the scrubber component materials are vulnerable to corrosion. At high levels, calcium and magnesium compounds can precipitate from solution and create scale deposits in piping, nozzles, scrubber walls, and mist eliminators.

The static pressure gauge across the scrubber vessel is used primarily to evaluate routine performance. In larger units, the static pressure is sensed by a differential pressure transmitter, and an electrical signal is sent to a monitoring system in the control room. Direct indicating gauges such as manometers and Magnehelic® gauges are used in many smaller systems. Static pressure gauges are required by many U.S. EPA New Source Performance Standards (NSPS) and by many state-promulgated regulations.

Static pressure drop gauges are used on mist eliminators to indicate excessive solids build-up that could lead to droplet reentrainment and fan operating problems. These data are used to indicate the need for cleaning sprays.

6.2 PARTICULATE MATTER WET SCRUBBER OPERATING PRINCIPLES

The two particle capture mechanisms used in particulate wet scrubbers are inertial impaction and Brownian motion. These mechanisms, which were discussed in Chapter 2, are briefly reviewed in this section to illustrate important scrubber operating variables. The use of static pressure drop data to evaluate the performance of the scrubber is also addressed.

6.2.1 Particle Collection Mechanisms

Impaction

Impaction occurs when a particle has too much inertia to avoid a target that it is approaching. It crashes into the target instead of flowing around it on the gas streamlines. If the particle is retained by the target (in this case, a droplet), a successful impaction has occurred. The effectiveness of impaction is related to the impaction parameter shown in Equation 6-1.

$$K_I = \frac{C_c d^2 \rho_p v}{18 \mu_g D_c} \tag{6-1}$$

Where:

K_I = impaction parameter (dimensionless)

C_c = Cunningham slip correction factor (dimensionless)

d = physical particle diameter (cm)

ρ_p = particle density (gm/cm^3)

v = difference in velocities of particle and target (cm/sec)

D_c = target diameter (cm)

$_g$ = gas viscosity (gm/cm sec)

This equation indicates that impaction effectiveness is related to the square of the particle diameter. Impaction is much more efficient for large particles than for small particles, especially those particles less than 0.5 m.

The impaction parameter shown in Equation 6-1 also indicates that impaction is directly proportional to the difference in the velocities of the particle and the droplet or liquid sheet target. There are substantial differences among the various types of scrubbers with respect to this relative velocity term. Furthermore, the difference in velocity does not remain constant throughout some types of scrubbers.

For example, in venturi scrubbers there is a very large difference between particle velocity and droplet velocity at the inlet to the throat. However, a fraction of a second later when the gas stream reaches the throat outlet, the droplets have accelerated to a velocity near that of the particles in the gas stream. In venturi scrubbers, impaction is most efficient at the inlet to the throat, before the droplets have accelerated. In packed bed scrubbers, the difference in particle and target velocities is very low due to the low gas velocity. Accordingly, impaction is very limited for this category of scrubbers. In the packed bed,

this difference remains relatively constant throughout the bed, and impaction of relatively large particles is dependent partially on the height of the bed.

The effectiveness of impaction is inversely related to the diameter of the target. Small water droplets serve as better targets than large droplets. The formation of small droplets is favored by droplet atomization in high-velocity gas streams and droplet atomization in high-pressure nozzles. Low surface tension conditions in the liquid also favor small droplet size distributions.

Brownian motion

Brownian motion is the particle movement caused by the impact of gas molecules on the side of the particle. Only very small particles are affected by the molecular collisions. The effectiveness of Brownian motion is related to the particle diffusivity defined in Equation 6-2.

$$D_p = \frac{CKT}{3\pi\mu_g d_p} \tag{6-2}$$

Where:

D_p = diffusivity of particle (cm^2/sec)

K = Boltzmann constant (gm cm^2/sec^2 °K)

T = absolute temperature (°K)

d_p = particle diameter (cm)

$_g$ = gas viscosity (gm/cm•sec)

C_c = Cunningham slip correction factor (dimensionless)

Diffusion begins to be effective as a capture mechanism for particles less than approximately 0.3 µm, and it is significant for particles less than 0.1 µm. Most industrial sources of concern in the air pollution field do not generate large quantities of particulate matter in the less than 0.1 µm size range. In most cases, Brownian motion is not a major factor influencing overall scrubber collection efficiencies.

6.2.2 Liquid-to-Gas Ratio

Droplets or liquid sheets (surfaces of liquid jets or bubbles) are needed to serve as impaction targets in all wet scrubbing systems. The rate of liquid flow to a scrubber is often expressed in terms of the liquid-to-gas ratio with units of gallons per 1000 ACF. The gas flow rate portion of this term is usually evaluated at the scrubber outlet because test ports for gas velocity measurement are often available.

Most wet scrubber systems operate with liquid-to-gas ratios between 4 and 20 gal/1000 ACF. Higher values do not usually improve performance, and they may have a slightly adverse impact due to changes in the droplet size distribution formed in the scrubber. Low values can have a highly adverse impact because there are simply too few impaction targets available. At low liquid-to-gas ratio conditions, a portion of the particle-containing gas stream may pass through the collection zone without encountering a water droplet target.

The liquid-to-gas ratios for scrubbers that remove both particulate matter and gaseous pollutants must often be set to facilitate the gaseous pollutant removal. These liquid-to-gas ratios for gaseous absorption are often above the optimum levels for particulate collection.

6.2.3 Static Pressure Drop

The static pressure drop across scrubbers is due to the frictional losses of the gas stream moving through the ductwork and the scrubber, the energy required to accelerate the gas, and the energy required to

accelerate and atomize (if applicable) the liquid stream. The energy losses for all of these are related to the square of the gas velocity as indicated in Equation 6-3.

$$\Delta p \propto v^2 \tag{6-3}$$

Where: p = static pressure drop

v = gas velocity in scrubber

Static pressure drop equations have been derived for a number of scrubber types. For example, Yung et al. (1977) developed Equation 6-4 to describe the pressure drop across a venturi scrubber.

$$\Delta p = 0.00082 V^2 \frac{Q_L}{Q_G} \tag{6-4}$$

Where:

p = static pressure drop (cm W.C.)

v = gas velocity (cm/sec)

Q_L = liquid flow rate (cm^3/sec)

Q_G = gas flow rate (cm^3/sec)

This equation does not take into account the frictional losses of the gas stream in the inlet ductwork, in the outlet ductwork, and within the scrubber itself. Equation 6-4 indicates that the static pressure drop for a venturi scrubber is also directly related to the liquid-to-gas ratio.

Empirical Correlation Based on Pressure Drop

For scrubber systems using primarily impaction for particle capture, there is a logical relationship between the penetration and the static pressure drop. The penetration should decrease as the static pressure drop increases. This is because the effectiveness of impaction is directly proportional to the difference in the velocities of the rapidly moving particles and the slow-moving liquid droplets or sheets. High static pressure drop values are associated with high gas velocities through the scrubber. Due to the logical association between static pressure drop and penetration, the easily measured static pressure drop has been used as an indirect indicator and predictor of performance for a number of years.

In 1961, the general relationship was expressed as a formal theory, termed the contact power theory by Semrau. It was based on Bernoulli's mechanical energy balances for the liquid and gas streams passing through the scrubber and indicated that penetration (or efficiency) is a function only of the amount of energy expanded in the scrubber.

$$P_G = 0.158 \quad p \tag{6-5}$$

$$P_L = 0.583\ [Q_L/Q_G] \tag{6-6}$$

$$P_T = P_G + P_L \tag{6-7}$$

$$N_t = \quad (P_T)^{ó} \tag{6-8}$$

$$\eta = 1 - e^{-N_t} \tag{6-9}$$

Where:

p = static pressure drop (in. W.C.)

P_G = power input from gas stream (HP/1000 ACFM)

P_L = power input from liquid stream (HP/1000 ACFM)

Q_L/Q_G = liquid-to-gas ratio (gal/1000 ACFM)

N_t = number of transfer units (dimensionless)
= empirical constants (dimensionless)
= efficiency (percent)

Actually, the constant of 0.158 shown in Equation 6-5 is not a true constant. A check of the Bernoulli mechanical energy balance for the gas stream indicates that Equation 6-5 should be expressed as shown in Equation 6-10. The gas density must be taken into account (Richards, 1983). The value used by Semrau was the gas density at 32°F and 14.7 psia.

$$P_G = \left(\frac{\Delta p}{\rho_g}\right) G \qquad (6\text{-}10)$$

Where: P_G = power input
p = static pressure drop
$_g$ = gas density
G = gas flow rate

A number of correlations have been published that relate the power consumption in units of horsepower per 1000 ACFM and one of the measures of emissions such as outlet particulate concentration, number of transfer units, or removal efficiency. Four of these correlations are reproduced in Figures 6-27, 6-28, 6-29, and 6-30 in order to demonstrate their characteristics.

Figure 6-27 is the performance data for cyclonic spray tower scrubbers and venturi scrubbers serving ferrosilicon furnaces. Considering that the transfer units are a logarithmic function, there is considerable variability, especially for the cyclonic scrubbers.

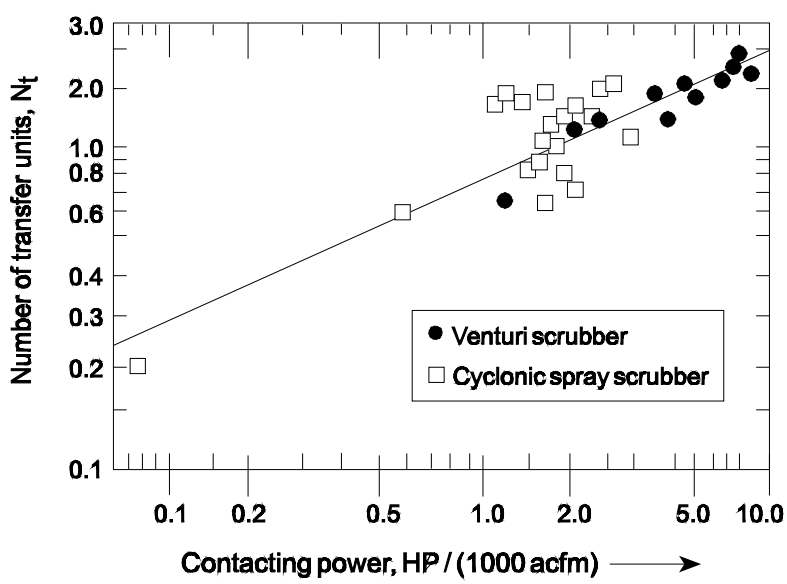

Figure 6-27. Relationship between contact power and number of transfer units, cyclonic and venturi scrubbers serving ferrosilicon furnaces

Data scatter is also evident in Figure 6-28 for the emissions data for flooded disc scrubbers (a type of adjustable throat venturi that is no longer manufactured) serving lime kilns at four separate kraft pulp mills. A 90% confidence interval for the emission data would demonstrate considerable variability of the data even near the mean pressure drop value (approximately 9 in. W.C.). It is difficult to use correlations of this nature to make accurate estimates of performance.

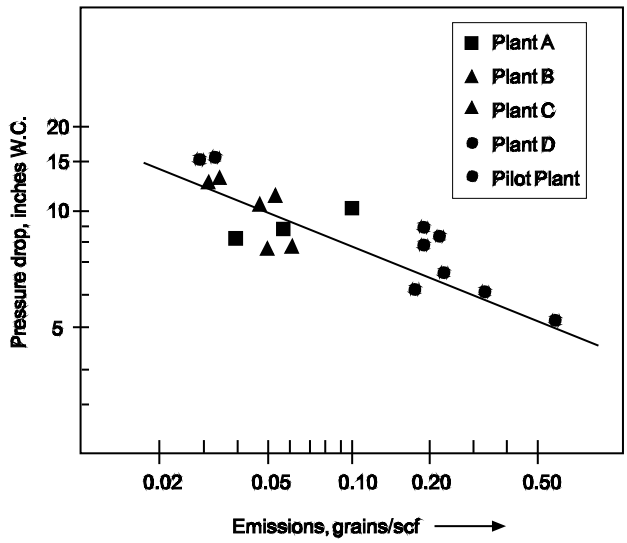

Figure 6-28. Relationship between pressure drop and particulate emissions for flooded disc scrubbers serving lime kilns (Walker and Hall, 1968)

Figure 6-29 is a plot of the emissions versus the static pressure drops of conventional venturi scrubbers serving a number of different coal thermal dryers. There is no apparent correlation in this data.

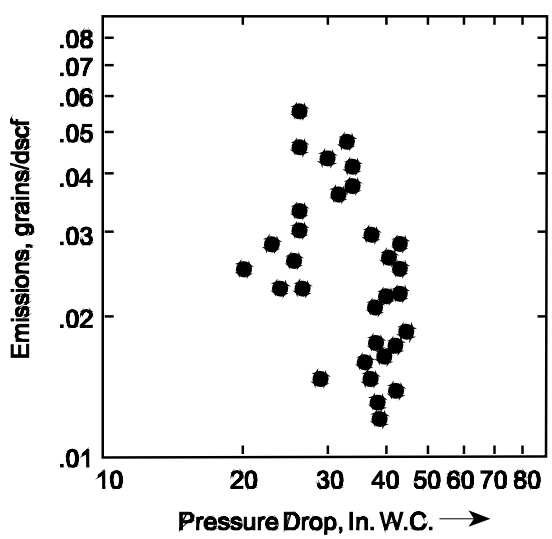

Figure 6-29. Particulate matter emissions versus pressure drop, venturi scrubber serving coal driers (Engineering Science, 1979)

Only the data shown in Figure 6-30 appear to have a correlation with a minimum amount of variability. These data were taken at three side-by-side venturi scrubber systems serving similar metallurgical furnaces. Furthermore, the tests used to compile the data were performed over a short time period, thereby avoiding variations due to changes in scrubber operating conditions.

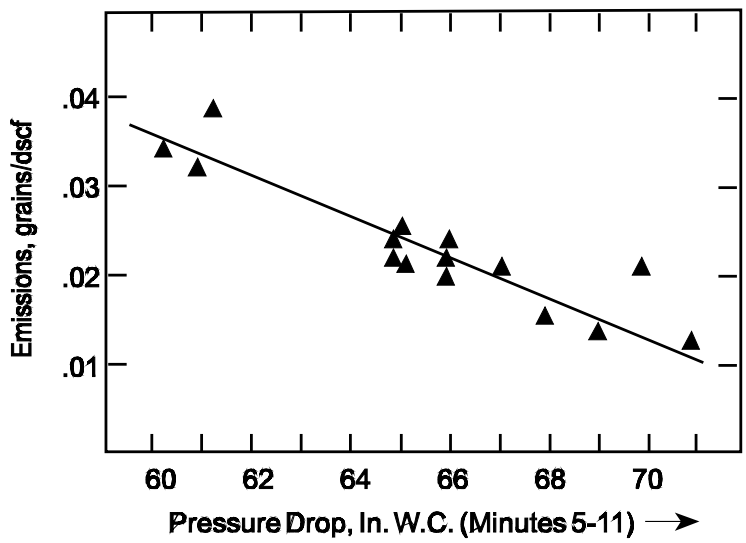

Figure 6-30. Emissions versus pressure drop for three venturi scrubbers serving Q-BOF processes

The underlying cause of the data scatter, which was apparent in Figures 6-27, 6-28, and 6-29, was due to differences in the particle size distribution from plant-to-plant over time. The static pressure drop correlations are based on the assumption that the particle size distribution is a constant. This is rarely accurate when data from different plants or processing units are combined into a single correlation. The acceptable correlation shown in Figure 6-30 appears to be one of the few cases in which data from different units can be combined into a single correlation. Overall, the inability to account for possible variations in the inlet particle size distribution to the scrubber is the major limitation of this type of correlation.

Some variations in particle size distribution are common in all processes due to slight changes in raw materials, operating conditions, and process loads. However, problems such as vapor nucleation and solids release during droplet evaporation can cause major changes in the quantity of particulate matter in the difficult-to-control size range of 0.1 to 2 µm. The aerosol formation mechanisms were discussed in Chapter 2.

Certain operating problems in wet scrubbers can also increase emissions without affecting the static pressure drop across the unit. For example, gas-liquid maldistribution in the scrubber throat can cause dramatically increased emissions with little, if any, change in the observed static pressure drop. Changes in the effectiveness of particle impaction into the droplet targets can also affect performance. Reduced capture effectiveness can be caused by changes in the surface tension of the droplets or by the presence of non-wettable materials coating the surfaces of the particles.

The correlations based on scrubber static pressure drop must be used with caution due to the possible shifts in particle size distribution and changes in emissions that can occur without significant changes in the static pressure drop.

6.2.4 Particulate Matter Wet Scrubber Capabilities and Limitations

Particulate matter wet scrubbers can provide high efficiency control in a wide variety of industrial applications. Certain types of scrubber systems can provide simultaneous control of both particulate matter and gaseous contaminants. Wet scrubbers are often the control device of choice if there is the potential for embers and/or explosive gases and vapors in the gas stream to be treated.

The main limitation that must be considered in selecting a specific type of wet scrubber is the particle control capability in the submicrometer size range. Many types of particulate wet scrubbers can have very limited efficiencies when the inlet gas stream has particles that are primarily in the difficult-to-control size range of 0.1 to 1.0 µm. Typical particle size-collection efficiency curves for the various types of particulate matter wet scrubbers are shown in Figure 6-31.

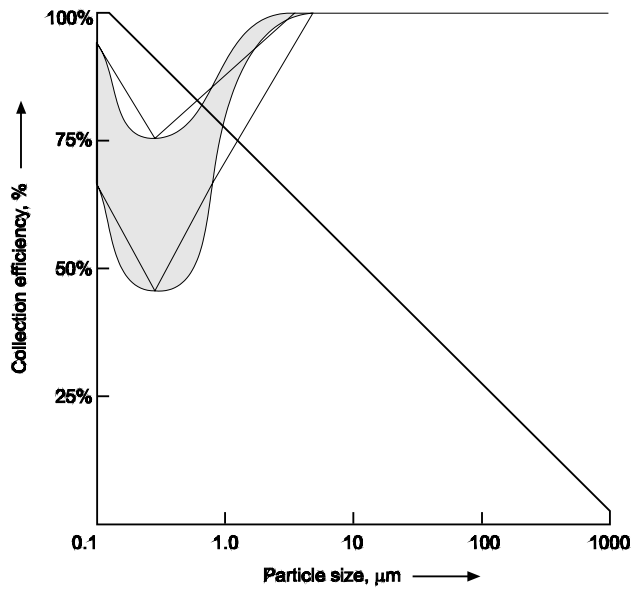

Figure 6-31. Particle size-collection efficiency relationships

The extent of the efficiency decrease in this size range depends primarily on the intensity of the gas liquid contact in the scrubber vessel. Scrubber vessel types that use high energies to develop large differences in the particles and the liquid targets have excellent inertial impaction efficiencies in the difficult to control range. Those scrubbers designed primarily for gaseous contaminant control have low differences in particle-liquid velocities and correspondingly have little or no particle collection in the difficult-to-control size range.

Another limitation of particulate matter wet scrubbers is the availability of water. Make-up water is needed to replace water evaporated with the effluent gas stream, water lost as part of the discharged wastewater, and water lost as part of sludge from rotary vacuum filters or similar processing units. In arid climates, there might be insufficient water to use a particulate matter wet scrubber.

The ability to economically dispose of the wastewater stream in an environmentally sound manner is another limitation of particulate matter wet scrubbers in some locations. The purge stream from the scrubber recirculation liquid stream might contain dissolved species that have poor leachability characteristics in disposal ponds.

Wet scrubbers usually generate very visible plumes composed of condensed water droplets. The highly visible water droplet plumes that can be quite persistent in cold weather and high humidity conditions can cause visibility problems for nearby roads and airports. Water droplet fallout from the plumes can, in unusual cases, cause freezing problems on walking surfaces and roadways near the facility.

6.3 PARTICULATE MATTER WET SCRUBBER SIZING AND DESIGN

This section concerns the evaluation of new scrubbing systems. The primary issues are (1) the ability of the scrubbing system to achieve the required particulate matter removal efficiency and (2) the adequacy of the mist eliminator to remove entrained droplets.

6.3.1 Particulate Matter Removal Capability

There are three general approaches to evaluating the capability of a scrubber system: (1) empirical evaluations based on previously installed scrubbers on similar sources, (2) pilot scale tests, and (3) theoretical penetration-particle size models.

Empirical Evaluation

Most scrubber manufacturers have extensive databases describing the performance of their various commercial brands of scrubbers on different types of industrial sources. These data provide a starting point in determining if a given type of scrubber system will be able to meet the performance requirements specified by the purchaser. Site-specific information is considered along with this historical performance data to determine if a scrubber would be appropriate. The most important site-specific data is the inlet particle size distribution. Unfortunately, these data are rarely available. Accordingly, the design review is limited to factors such as those listed below.

- Average and maximum gas flow rates
- Average and maximum inlet gas temperatures
- Concentrations of corrosive materials present in the inlet gas stream
- Concentrations of potentially explosive materials present in the inlet gas stream
- Availability of make-up water
- Purge liquid treatment and disposal requirements
- Process type, raw materials, and fuels
- Source operating schedule
- Area available for scrubber and waste water treatment
- Alkali supply requirements
- Particle size distribution (when available)
- Emission test data (when available)

This site-specific information is used in conjunction with the historical data base to determine if the scrubber is applicable to the process. The data also provide a basis for the design of the scrubber system components and for estimating the necessary static pressure drop.

The primary advantage of this approach is that scrubber system evaluation is based on actual emissions data obtained using test procedures identical to those to be applied to the new scrubber system. The

disadvantage is the inability, in many cases, to take into account site-specific factors that could affect the particle size distribution. Particle size is the single most important variable affecting particulate matter removal efficiency.

Furthermore, there can be significant process unit-to-process unit differences in the generated quantities of particulate in the difficult-to-control size range of 0.1 to 1 m.

Pilot Scale Tests

Pilot scale performance tests can be conducted when there is uncertainty concerning the applicability of a scrubber or the necessary operating conditions of a scrubber. These tests are preferably conducted on the specific source to be controlled, so that the actual particle size distribution and particle characteristics are inherently taken into account. If this is an entirely new application that has not yet been built, a similar, existing unit can be tested.

The tests are normally conducted using a small skid-mounted scrubber system capable of handling 500 to 2,000 ACFM. The gas is pulled from the effluent duct from the process source. The performance of the pilot scale scrubber system is determined using conventional U.S. EPA reference method emission tests.

The primary advantage of this approach is that the performance of a scrubber very similar to the proposed unit can be evaluated on the actual gas stream. Furthermore, a series of tests can be conducted relatively quickly to identify the optimal operating conditions such as static pressure drop. The main disadvantage is that the tests are expensive. Pilot scale tests usually indicate slightly higher particulate matter removal efficiencies than can be achieved by the full scale system because a variety of non-ideal gas flow conditions are more significant on the larger systems. Also, the particle size distribution in the pilot scale scrubber may be different than in the actual effluent gas stream due to errors in the way the slip stream is withdrawn from the main duct or due to changes in the gas stream while passing down the temporary ductwork to the pilot scrubber.

Theoretical Penetration Models

The collection efficiency of particulate matter wet scrubbers is highly dependent on particle size because of the inherent characteristics of the two primary capture mechanisms: impaction and Brownian motion. Theoretical models attempt to take impaction and diffusion into account based on the general particle and droplet movements expected in each type of scrubber. The models provide an estimate of the penetration value as a function of the particle size. The penetration versus particle size data can then be applied to the particle size distribution of a commercial system to estimate the overall penetration (emission) rate at the specific operating conditions.

Venturi Scrubbers

Penetration equations for a variety of scrubber types have been derived by Calvert et al. (1972) and are presented in the *Scrubber Handbook*. The penetration model for venturi scrubbers will be used as an example of this evaluation technique. The venturi scrubber model was originally published in the *Scrubber Handbook* and was subsequently refined and updated by Yung et al. (1977).

The model is based on impaction into droplets within the throat of the venturi scrubber. The simplified version of the model shown below is based on the assumption that the droplets accelerate to the velocity of the gas stream prior to leaving the throat (often termed the "infinite" throat model).

$$\log_{10} P_t(d_p) = -B \frac{4K_{po} + 4.2 - 5.02K_{po}^{0.5}\left(1 + \frac{0.7}{K_{po}}\right)\tan^{-1}\sqrt{\frac{K_{po}}{0.7}}}{K_{po} + 0.7} \tag{6-11}$$

Where:

$P_t(d_p)$ = penetration for particle size i

B = parameter defined in Equation 6-12

K_{po} = impaction parameter at throat entrance (dimensionless)

$$B = \left(\frac{L}{G}\right)\frac{\rho_l}{\rho_g C_D} \tag{6-12}$$

Where:

L/G = liquid to gas ratio (dimensionless)

$_{l,\ g}$ = liquid and gas density (e.g., kg/m^3)

C_D = drag coefficient (liquid at the throat)

$$K_{po} = \frac{d^2 v_{gt} C_c \rho_p}{9\mu_g d_d} \tag{6-13}$$

Where:

d = physical particle diameter (cm)

v_{gt} = gas velocity in throat (cm/sec)

$_g$ = gas viscosity (gm/cm×sec)

d_d = droplet diameter (cm)

C_c = Cunningham slip correction factor

ρ_p = Particle density (gm/cm^3)

$$C_D = 0.22 + \frac{24}{N_{RE,d}}\left(1 + 0.15\, N_{RE,d}^{0.6}\right) \tag{6-14}$$

Where:

$N_{RE,\ d}$ = Reynolds number of the droplet at the throat inlet (dimensionless)

$$C_c = 1 + \frac{(6.21 \times 10^{-4}\, T)}{d_p} \tag{6-15}$$

Where:

C_c = Cunningham slip correction factor

T = absolute gas temperature (°K)

d_p = particle diameter (micrometers)

$$d_p = d\sqrt{\rho_p} \tag{6-16}$$

Where:

d_p = aerodynamic diameter of particle (cm)
d = physical diameter of particle (cm)
$_p$ = density of particle (gm/cm^3)

Example calculations based on this venturi scrubber performance model are shown in Figure 6-32. There is a strong particle size dependence, with the penetration values dropping down toward 0.01 (99% efficiency) for the greater than 1 m size range.

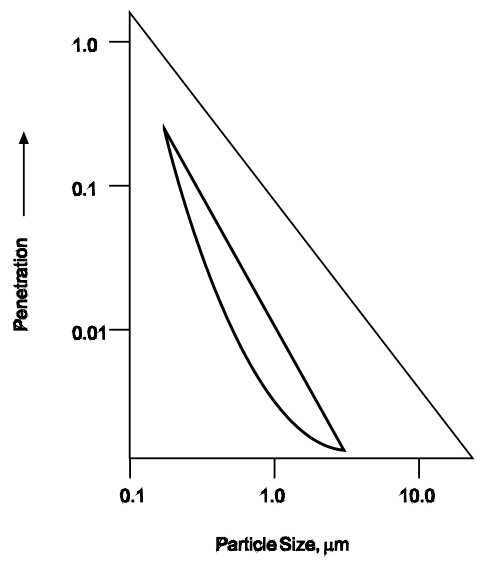

Figure 6-32. Penetration versus particle size for an example venturi scrubber (Yung et al., 1977)

Comparisons of the model results with actual scrubber system performance data indicate that the model sometimes predicts slightly higher-than-actual emissions in the submicrometer range, possibly due to the exclusion of diffusion collection mechanisms. The actual penetration of particles in the greater than 1 mm range is slightly greater than predicted. This may be due to one or more non-ideal flow conditions such as liquor maldistribution in the throat. The model often provides a good tool for evaluating the performance of a scrubber system serving a source with a known particle size distribution.

Problem 6-2

Using the spreadsheet version of the venturi scrubber model, calculate the removal efficiency for a 5.0 micrometer (physical diameter) particle.

The gas flow rate is 15,000 ACFM, the gas temperature is 68°F, the gas moisture content is 10%, the oxygen content is 20%, the barometric pressure is 30.5 in. Hg, and the gas static pressure is -0.8 in. W.C.

The venturi throat dimensions are 20cm x 24 cm and the liquid flow rate is 100 gal/min. Assume that the particle density is 1.1 gm/cm^3, the liquid droplet diameter is 0.1 cm, and the density of the liquid is 1.0 gm/cm^3.

Solution:

The collection efficiency for a 5.0 micrometer (physical diameter) particle is estimated at 98.2% by the venturi scrubber performance model.

Spray Tower Scrubbers

The equations provided by Yung et al. for spray tower scrubbers are provided in Equations 6-17 and 6-18. Equation 6-18 is based on the impaction parameter provided in Equation 6-1.

$$P_i = e^{-\left[\frac{0.75\, v_t \eta_i Z}{r_d (v_t - v_G)}\right]\left(\frac{L}{G}\right)} \tag{6-17}$$

$$\eta_i = \left[\frac{K_i}{(K_i + 0.7)}\right]^2 \tag{6-18}$$

Where:

P_i = penetration for particle size i

K_i = impaction parameter (dimensionless)

v_t = droplet terminal settling velocity (cm/sec)

$_i$ = efficiency due to impaction (dimensionless)

Z = scrubber height (cm)

r_d = droplet radius (cm)

v_G = gas superficial velocity (cm/sec)

L/G = liquid to gas ratio (dimensionless; i.e., liters/min per liters/min)

Data concerning the droplet radius can be obtained from the spray nozzle manufacturers. The droplet terminal settling velocity can be calculated based on the procedures summarized in Chapter 2. The remainder of the parameters necessary to perform this calculation are based on the readily available design data for the scrubber being analyzed.

Problem 6-3

Using the spray tower performance equations presented above, estimate the removal efficiency of a 4.0 micrometer (physical diameter) particle. The gas flow rate is 5,000 ACFM, gas temperature is 68°F, static pressure is 0 in. W.C., oxygen content of the gas is 15%, moisture content of the gas is 8%, and the barometric pressure is 27 in. Hg.

The scrubber height is 305 cm, with a gas velocity of 304.8 cm/sec. Use a particle density of 1.1 gm/cm^3, liquid density of 1.00 gm/cm^3, droplet diameter of 0.08 cm, and a liquid flow rate of 30 gal/min.

Solution:

The estimated collection efficiency for a particle with a physical diameter of 4.0 micrometers is 92.6%.

Tray Tower Scrubbers

The equation provided by Yung et al. for an impingement type tray tower scrubber is shown in Equation 6-19.

$$P_i = 1 - \left[\frac{K_i}{K_i + 0.7} \right]^2 \tag{6-19}$$

Where:

P_i = Penetration through an impingement plate scrubber of a particle with an aerodynamic diameter of i.

K_i = Impaction parameter of a particle with an aerodynamic diameter of i.

The impaction parameter is calculated based on Equation 6-1. All of the other parameters needed to calculated based on the design data for the specific scrubber being analyzed. The velocity term used in the impaction parameter should be the vena contracta velocity for the orifice. Yung et. al. recommend a value of 1.43 times the average velocity calculated by dividing the actual gas flow rate by the orifice area. The collector "diameter" used in the impaction parameter equation should be the diameter of the orifices in the impaction plate.

This equation is based on the assumption that there is a normal head of liquid across all of the orifices in the tray. The penetration approaches 1.0 (zero collection efficiency) if the tray is partially or completely dry.

Problem 6-4

Using the spreadsheet theoretical penetration model determine the collection efficiency of a particle having a 4 micrometer physical diameter. The gas flow rate is 6,000 ACFM, gas temperature is 77°F, gas moisture content is 5% and gas oxygen content is 20.9%. The bed height is 216 cm with a diameter of 108.5 cm. The packing material is 3.8 cm Stoneware Berl Saddles (bed porosity = 0.70) with a packing element width of 0.165 cm. Assume a particle density of 1.0 gm/cm^3 and no liquid hold-up in the bed.

Solution:

The estimated collection efficiency for a particle diameter of 4 micrometers is 93.8%.

Liquid-to-Gas Ratio

The liquid-to-gas ratio can be defined based either on the inlet or outlet gas flow rates. It can also be defined based on either actual or standard gas flow rates. Due to the differences in the format of this parameter, it is important to include a full set of units or other descriptive information to clarify the meaning of the parameter. In this course, the liquid-to-gas ratio is defined as indicated in Equation 6-20 and illustrated in Figure 6-33.

$$\frac{L}{G} = \frac{\text{Inlet Liquid Flow Rate (gpm)}}{\text{Outlet Gas Flow Rate (1000 ACFM)}} \tag{6-20}$$

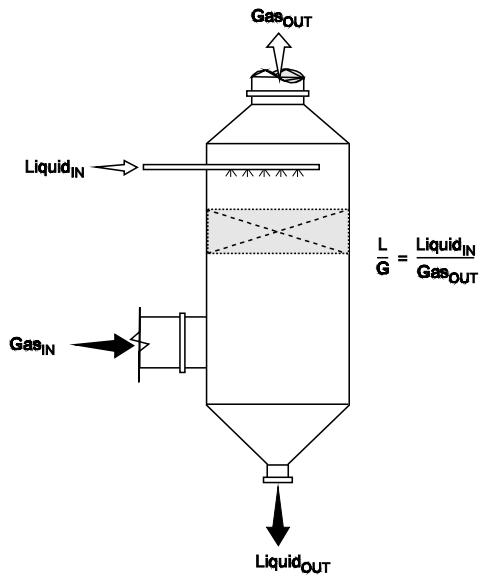

Figure 6-33. Definition of the liquid-to-gas ratio

The outlet gas flow rate is used because this value is readily measured as part of an emission test program. It is considerably easier to obtain an accurate flow measurement at the scrubber outlet, where particulate matter loading in the gas stream is reduced and good sampling ports are available. Most scrubber inlet ducts are not well suited for gas flow rate testing.

It is helpful to confirm that the liquid-to-gas ratio to be used on a scrubber system is above the minimum level necessary to ensure proper gas-liquid distribution. In most gas-atomized scrubbers, this minimum value is approximately 4 gallons per thousand ACF. In other type of scrubbers, the value is as low as 2 gallons per thousand ACF. Calculation of the liquid-to-gas ratio is illustrated in Problem 6-5.

Problem 6-5

What is the design liquid-to-gas ratio for the scrubber system that has an outlet gas flow rate of 15,000 ACFM, a pump discharge rate of 100 gpm, and a liquid purge rate of 10 gpm? The purge stream is withdrawn from the pump discharge side.

Solution

$$\text{Liquid-to-gas ratio} = \frac{\text{Inlet liquid flow (gpm)}}{\text{Outlet gas flow (1000 ACFM)}}$$

Inlet liquid flow = 100 gpm – 10 gpm = 90 gpm

Liquid-to-gas ratio = 90 gpm/15,000 ACFM= 0.006 gallons /ACF = 6 gallons/1000 ACF

The liquid-to-gas ratio is usually expressed in terms of thousands of ACF as a matter of convenience. This converts the common values of the parameter to simple, single- and double-digit values.

6.3.3 Liquid Purge Rates

A small portion of the recirculating liquid in a scrubber system must be purged for treatment. The treated liquid can then be returned to the system or replaced with make-up water. The liquid purge rate necessary to ensure long term proper performance of a system depends on one or more of the following factors.

- The rate of particulate matter capture
- The maximum concentration of suspended solids acceptable in a given scrubber system
- The rate of dissolved solids precipitation in the recirculated liquid due to the accumulation of calcium and/or magnesium ions
- The rate of chloride or fluoride ion accumulation in the scrubber liquid.

Problem 6-6 illustrates the calculations involved in evaluating the necessary liquid purge rate based on the particulate matter capture rates and maximum suspended solids levels.

Problem 6-6

Estimate the liquid purge rate and recirculation pump flow rate for a scrubber system treating a gas stream of 30,000 ACFM (inlet flow) with a particulate matter loading of 0.8 grains per ACF. Assume that the scrubber particulate matter removal efficiency is 95% and the maximum suspended solids level desirable in the scrubber is 2% by weight. Use a liquid-to-gas ratio of 8 gallons (inlet) per thousand ACF (outlet) and an outlet gas flow rate of 23,000 ACFM.

Solution:

The inlet particulate loading is calculated as

$$\text{Inlet mass} = 30{,}000\ \text{ACFM}\left(\frac{0.8\ \text{grains}}{\text{ACF}}\right)\left(\frac{\text{lb}}{7000\ \text{grains}}\right) = 3.43\frac{\text{lb}}{\text{min}}$$

Collected mass = 0.95 (Inlet Mass) = 3.26 lb/min

Purge solids of 3.26 lb/min are 2% of the total purge stream

Purge stream = (3.26 lb/min)/0.02 = 163 lb/min liquid

Purge stream with 2% suspended solids has a specific gravity of approximately $1.02\ \frac{\text{lb}_m\ \text{liquid}/\text{ft}^3}{\text{lb}_m\ \text{water}/\text{ft}^3}$

$$\text{Density of purge} = \left(\frac{8.46\ \text{lb}_m\ \text{water}}{\text{gal}}\right)(1.02)$$
$$= \frac{8.63\ \text{lb}_m}{\text{gal}}$$

$$\text{Purge stream} = \left(163\frac{\text{lb}_m}{\text{min}}\right)\left(\frac{\text{gal}}{8.63\ \text{lb}_m}\right) = 18.87\text{gpm}$$

This purge stream quantity is a significant fraction of the total flow through the system. At a liquid to-gas ratio of 8 gallons per thousand ACF, the recirculation stream to the scrubber is 184 gpm. Therefore, the total pump discharge flow must be 202.9 gpm.

6.3.4 Mist Eliminator Velocities

There are definite limits to the gas velocity through the mist eliminator. At high gas velocities, liquid can be forced toward the trailing edge of the mist eliminator elements and reentrained in the gas stream. General guidelines concerning the maximum velocities are presented in Table 6-1.

Table 6-1. Gas Velocities Through Mist Eliminators

Mist Eliminator Type	Orientation	Maximum Gas Velocity ft/sec
Chevron	Horizontal	15 – 20
Chevron	Vertical	12 – 15
Mesh Pad	Horizontal	15 – 23
Mesh Pad	Vertical	10 – 12
Woven Pad[1]	Vertical	8 – 15
Tube Bank	Horizontal	18 – 23
Tube Bank	Vertical	12 – 16

Source: Shifftner and Hesketh (1983)
1. Kimre Inc.

The actual maximum velocities that apply to the specific type of mist eliminator should be determined from the manufacturer's specification sheets. These data can then be used to confirm that the mist eliminator is located in an area with gas velocities below the maximum levels. The average gas velocity through the mist eliminator can be calculated simply by dividing the actual gas flow rate by the cross-sectional area of the mist eliminator as shown in Equation 6-21. The calculation of the mist eliminator velocity is illustrated in Example 6-7.

$$\text{Velocity} = \frac{\text{Gas flow rate (ACFM) (min/60 sec)}}{\text{Mist eliminator area (ft}^2\text{)}} \tag{6-21}$$

Problem 6-7

Estimate the gas velocity through a mist eliminator having a diameter of 6.5 feet, an average gas flow rate of 4,000 DSCFM, and a peak gas flow rate of 4,760 DSCFM. The peak gas stream temperature is 130°F, the static pressure during peak flow in the vessel is –30 in. W.C., and the barometric pressure is 29.4 in. Hg. The moisture content of the gas stream is 6%.

Solution:

The gas velocity should be evaluated under peak flow conditions because this is the time when reentrainment is most probable.

Convert the gas flow rate to actual conditions to evaluate velocity.

SCFM = DSCFM/[(100-%H_2O)/100] = 4760/0.94 = 5064 SCFM

Pressure at the mist eliminator inlet

$$= 29.4 \text{ in. Hg} + \left(-30\text{in. W.C.}\left(\frac{1\text{in. Hg}}{13.6\text{ in. W.C.}}\right)\right) = 27.19 \text{ in Hg}$$

ACFM = 5064 SCFM(29.92 in.Hg/27.19 in. Hg)(460°R + 130°F)/528°R = 6227 ACFM

Area of Mist Eliminator = 3.14 × (6.5 feet)^2/4 = 33.2 ft^2

Velocity = Flow/Area = (6227 ft ^{3}/min)/33.2 ft^2 =188 ft/min

= 3.13 feet per second

Note that the amount of area blocked by mist eliminator blades or any support frames is not taken into account in estimating the average velocity. Accordingly, the velocity estimated is lower than the actual velocity through the mist eliminator. However, this is taken into account when manufacturers publish their maximum velocity guidelines.

6.3.5 Alkali Requirements

Particulate matter wet scrubbers systems must include an alkali addition system if they are treating gas streams that have acid gases along with particulate, or that are collecting particulate matter or acid mists that are acidic in nature. The most common acidic gases are sulfur dioxide, hydrogen chloride, and hydrogen fluoride. Carbon dioxide, which is formed in all combustion processes involving fossil fuels, wood fuels, and waste fuels is also acidic. The alkali requirements are usually calculated based on the quantities of acidic gases captured and the molar ratios necessary for reactions such as 6-1, 6-2, and 6-3.

$SO_2 + Ca(OH)_2 + 0.5\ O_2 \longrightarrow (CaSO_4)_s + H_2O$ Reaction 6-1

$2HCl + Ca(OH)_2 \longrightarrow Ca^{++} + 2\ Cl^- + 2H_2O$ Reaction 6-2

$2HF + Ca(OH)_2 \longrightarrow Ca^{++} + 2\ F^- + 2H_2O$ Reaction 6-3

Problem 6-8

Calculate the amount of calcium hydroxide (lime) needed to neutralize the HCl absorbed from a gas stream having 50 ppm HCl and a flow rate of 10,000 SCFM. Assume an HCl removal efficiency of 95%.

Solution:

The quantity of HCl absorbed in the scrubbing liquid is calculated as follows.

$$50\text{ppm HCl} = \frac{0.00005\ \text{lb mole HCl}}{1.0\ \text{lb mole total}}$$

$$\text{HCl} = 10{,}000\ \text{SCFM}\left(\frac{\text{lb mole}}{385.4\ \text{SCF}}\right)\left(\frac{0.00005\ \text{lb mole HCl}}{\text{lb mole total}}\right)(95\%\ \text{removal efficiency})$$

HCl = 0.00123 lb mole HCl/min

$$Ca(OH)_2\ \text{req'd} = \left(\frac{1\ \text{lb mole } Ca(OH)_2}{2\ \text{lb mole HCl}}\right)\left(\frac{0.00123\ \text{lb mole HCl}}{\text{min}}\right) = \frac{0.00062\ \text{lb mole } Ca(OH)_2}{\text{min}}$$

$Ca(OH)_2$ req'd = (0.00062 lb mole/min)(74 lb/lb mole) = 0.046 lb/min = 2.75 lb/hr

The alkali feed system should be designed to provide sufficient alkali during times of peak acidic gas concentrations. In some processes, the acid gas concentration can vary by more than a factor of 2. If these peaks last for long periods of time, the alkali system must have sufficient capacity to prevent severe pH excursions to values less than approximately 5. At these levels, the rate of corrosion begins to accelerate, especially in the presence of chlorides and fluorides.

6.3.6 Instrumentation

The selection and mounting of instrumentation is important in ensuring that the particulate control system operates at its maximum capability. The types of instruments that are used include static pressure drop gauges, temperature gauges, liquid flow rate gauges, liquid pressure gauges, and pH gauges. Opacity monitoring instruments are not used on particulate matter wet scrubber systems because the condensed water droplets often present in the gas stream scatter light. It is not possible to differentiate between light scattering due to particulate matter or due to water droplets.

The types of instruments that are necessary for a particulate matter wet scrubber system depend, in part, on the size of the unit, the toxicity of the pollutants being collected, the variability of operating conditions, and the susceptibility to performance problems. Instruments in particulate matter wet scrubber systems usually include one or more of the following monitors.

- Scrubber vessel static pressure drop gauge
- Mist eliminator static pressure drop gauge
- Outlet gas temperature
- Recirculation liquid pH
- Fan motor current

Static pressure drop gauges should be mounted across the entire scrubber system, spanning the inlet duct to the outlet duct. In this position, the gauges measure the flange-to-flange static pressure drop. This value takes into account the energy losses involved in re-accelerating the gas stream in the exit ductwork from the scrubber vessel. The flange-to-flange pressure drop also takes into account the effect of any mist eliminators mounted directly in the scrubber vessel. It is possible to install the static pressure drop gauge directly across the gas-liquid contact zone (such as the venturi throat); however, non-ideal gas flow conditions near the surface of the scrubber wall and the presence of high levels of scrubbing liquid affect both the accuracy and reliability of these static pressure measurements. The inlet and outlet ductwork are usually less vulnerable to measurement problems.

The static pressure drop across the mist eliminator provides an excellent indicator of the physical condition of the mist eliminator. The static pressure drop is strictly a function of the geometry of the mist eliminator, the gas flow rate through the mist eliminator, and the gas density. Accordingly, the static pressure drop should be a relatively constant value. If an increase in the pressure drop occurs, it may be necessary to activate the cleaning system more frequently or for a longer operating time. Values well below the baseline range suggest that part of the mist eliminator has fallen apart or otherwise been damaged. Structural failure of the mist eliminator is possible due to the forces that can be imposed on the surface when it is significantly blinded. For example, a 6-ft diameter mist eliminator immediately upstream of a fan with an inlet static pressure of -10 in. W.C. can create a force of over 1,400 lb_f on the surface. Corrosion-related weakening of the supporting frame on the mist eliminator can cause the entire mist eliminator to break into parts and be pulled toward the fan. Also, some mist eliminators constructed of FRP (fiberglass-reinforced plastics) and other synthetic materials can suffer adhesive failure if there is a gas temperature spike. This can cause part of the mist eliminator to break away. The gaps left in the mist eliminator have a very low static pressure drop, and most of the gas stream channels through this area. Accordingly, the effectiveness of the mist eliminator is compromised.

Due to the turbulent mixing of the gas and liquid streams in a venturi throat, it is not usually practical to install a window and simply observe the maldistribution condition. Instead, it is necessary to use indirect indicators. One of the best indirect indicators is the outlet gas temperature monitor. When the gas-liquid distribution is good, the outlet gas stream temperature will be at the *adiabatic saturation temperature*. This simply means that the gas stream is saturated with water vapor (100% relative humidity). The adiabatic saturation temperature is easily calculated using a procedure illustrated in the psychrometric chart in Figure 6-34. The starting point in the procedure is a point on the psychrometric chart defined by the inlet gas stream dry bulb temperature and absolute humidity (generally estimated based on information concerning the process). From the point established by these two conditions, follow a parallel adiabatic saturation line until the 100% relative humidity line is reached. The adiabatic saturation temperature is indicated on the psychrometric chart.

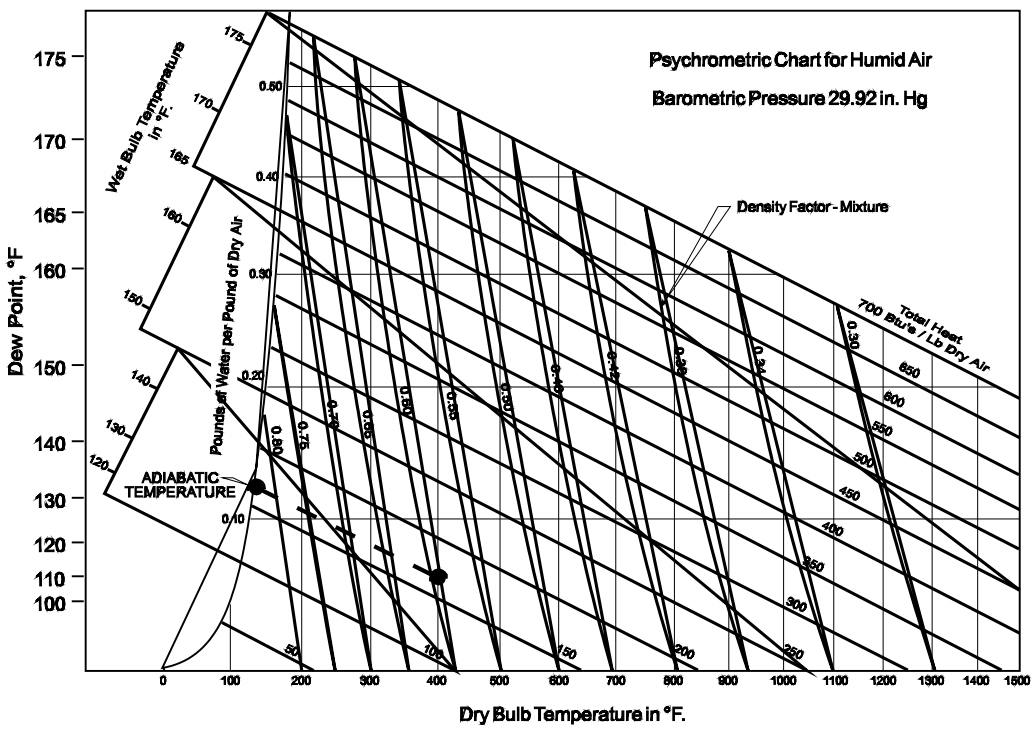

Figure 6-34. Psychrometric chart method of estimating adiabatic saturation temperature

Scrubber outlet gas temperatures more than 5°F to 10°F above the adiabatic saturation temperature are often associated with significant maldistribution. This is because maldistribution conditions that cause poor heat transfer from the gas to the liquid also cause poor contact between the particle-laden gas stream and the liquid stream in the scrubber.

It should be noted that the techniques described earlier are not especially sensitive indicators of maldistribution in venturi scrubbers. Impaction virtually ceases after the venturi throat. However, heat transfer from the gas and liquid streams can continue until the gas stream passes through the mist eliminator.

The recirculation liquid pH monitor provides essential information for scrubbers absorbing acid gases and/or acidic particulate matter. The pH must usually be maintained above approximately 5 to minimize vulnerability to corrosion and reduced acid gas absorption. If the pH exceeds levels of approximately 9, there is some vulnerability to chemical precipitation (often termed scaling) of calcium and magnesium compounds. These solids can build-up in spray nozzles and in the scrubbing vessels and disrupt gas-liquid distribution.

pH monitors are often mounted in areas shielded from high velocity, swirling liquid currents in the recirculation tank. They are also mounted at an elevation and position in the tank where there is a minimal risk of encapsulation in precipitated and settled solids.

Fan motor current meters are used to provide an indirect indication of gas flow through the scrubber system. Increased motor currents are associated with increased flow. These instruments are relatively simple and easy to maintain.

Review Exercises

Types and Components of Particulate Wet Scrubbers

1. What is the average residence time of the gas stream in the throat of a venturi scrubber throat?
   a. 0.1 to 0.5 seconds
   b. 1 to 10 seconds
   c. 10 to 50 seconds
   d. 0.001 to 0.005 seconds

2. What is the typical static pressure drop across a mist eliminator?
   a. 0.1 to 0.4 in. W.C.
   b. 0.5 to 4 in. W.C
   c. 4 to 8 psia
   d. 4 to 8 kPa

3. There are more than fifteen categories of particulate matter scrubber designs. What is one of the features that can be used to determine which categories are more efficient for particles in the difficult–to-control size range?
   a. Relative difference in velocities of the particles in the gas stream and the liquid targets used for collection.
   b. Liquid-to-gas ratio
   c. Droplet size distribution generated by the scrubber
   d. Liquid surface tension maintained by use of flocculants

4. What is the purpose of the evaporative cooler or presaturator often used upstream of a particulate wet scrubber? Select all that apply.
   a. Protection of heat sensitive components in the scrubber vessel
   b. Optimize inertial impaction into droplet targets
   c. Increase the gas velocity through the scrubber
   d. All of the above

5. What is the normal pH range in a particulate matter wet scrubber?
   a. 1 to 5
   b. 5 to 9
   c. 9 to 11
   d. 11 to 14

6. Select the factor(s) that often affect the necessary purge rate in a wet scrubber system. Select all that apply.
   a. Particulate loading in the gas stream being treated
   b. Hydrogen chloride concentration in the gas stream being treated
   c. Maximum suspended solids levels in the recirculated liquid stream
   d. All of the above

7. What size of droplets are usually controlled by a mist eliminator?
   a. 0.1 to 1 micrometer
   b. 1 to 50 micrometers
   c. 20 to 1000 micrometers
   d. 1000 to 10,000 micrometers

8. What type of wet scrubbers are primarily designed for the removal of gaseous air contaminants? Select all that apply.
   a. Packed bed scrubbers
   b. Collision scrubbers
   c. Mechanically aided scrubbers
   d. Crossflow packed bed scrubbers

9. What type of wet scrubbers are primarily designed for the removal of mists? Select all that apply.
   a. Fiber bed scrubber
   b. Mesh bed scrubbers
   c. Spray tower scrubbers
   d. Impingement tray tower scrubbers

Operating Principles of Particulate Wet Scrubbers

10. What is the most important factor affecting the ability of a particulate matter wet scrubber to achieve high removal efficiencies?
    a. Particle size
    b. Static pressure drop
    c. Droplet size distribution
    d. Droplet surface tension

11. What is the difficult-to-control particle size range?
    a. 0.1 to 1.0 micrometers
    b. 1 to 5 micrometers
    c. 5 to 20 micrometers
    d. 20 to 50 micrometers

12. What is the main particle collection mechanism used in particulate matter wet scrubbers?
    a. Brownian motion
    b. Electrostatic attraction
    c. Inertial impaction
    d. Coagulation

13. What variables can affect the adequacy of a correlation between scrubber static pressure drop and the particulate matter removal efficiency? Select all that apply.

    a. Particle size distribution
    b. Adequacy of gas-liquid maldistribution
    c. Droplet surface tension
    d. Condensation of vapors in the scrubber
    e. All of the above

Sizing and Design of Particulate Wet Scrubbers

14. Calculate the liquid-to-gas ratio for a scrubber system with a gas flow rate of 4,000 ft^3/sec and a recirculation liquor flow rate of 2,000 gal/min. Is this value in the normal range for a particulate matter wet scrubber?

15. A chevron mist eliminator is 8 ft in diameter. The gas flow rate through the scrubber system has been measured at 60,500 ACFM

    a. What is the average velocity through the mist eliminator?
    b. What is the average velocity if 40% of the mist eliminator is completely blocked due to solids accumulation? Is this velocity within the normal operating range of a vertically mounted chevron mist eliminator?

16. What is the most difficult-to-collect particle size range for a venturi scrubber?

    a. 0.01 to 0.05 m
    b. 0.1 to 2 m
    c. 2 to 10 m
    d. 10 to 100 m
    e. 0.0001 to 0.002 cm

17. A scrubber system has an inlet dry bulb temperature of 600°F and an inlet absolute humidity of 0.05 lbs of water per pound of dry air. What is the adiabatic saturation temperature for this gas stream? Use the psychometric chart presented in Figure 6-35.

18. The baseline pressure drop across a mist eliminator is 1.2 in. W.C. at a gas flow rate of 30,000 ACFM. The static pressure drop is now 2.2 in. W.C., and the gas flow rate is 34,000 ACFM. Is there any reason to suspect pluggage of the mist eliminator?

Review Answers

Types and Components of Particulate Wet Scrubbers

1. What is the average residence time of the gas stream in the throat of a venturi scrubber throat?
   d. 0.001 to 0.005 seconds

2. What is the typical static pressure drop across a mist eliminator?
   b. 0.5 to 4 in. W.C

3. There are more than fifteen categories of particulate matter scrubber designs. What is one of the features that can be used to determine which categories are more efficient for particles in the difficult –to-control size range?
   a. Relative difference in velocities of the particles in the gas stream and the liquid targets used for collection.

4. What is the purpose of the evaporative cooler or presaturator often used upstream of a particulate matter wet scrubber? Select all that apply.
   a. Protection of heat sensitive components in the scrubber vessel
   b. Optimize inertial impaction into droplet targets

5. What is the normal pH range in a particulate wet scrubber?
   b. 5 to 9

6. Select the factor(s) that often affect the necessary purge rate in a wet scrubber system. Select all that apply.
   d. All of the above

7. What size of droplets are usually controlled by a mist eliminator?
   c. 20 to 1000 micrometers

8. What type of wet scrubbers are primarily designed for the removal of gaseous air contaminants? Select all that apply.
   a. Packed bed scrubbers
   d. Crossflow packed bed scrubbers

9. What type of wet scrubbers are primarily designed for the removal of mists? Select all that apply.
   a. Fiber bed scrubber
   b. Mesh bed scrubbers

Operating Principles of Particulate Matter Wet Scrubbers

10. What is the most important factor affecting the ability of a particulate matter wet scrubber to achieve high removal efficiencies?
    a. Particle size

11. What is the difficult-to-control particle size range?

    a. 0.1 to 1.0 micrometers

12. What is the main particle collection mechanism used in particulate matter wet scrubbers?

    c. Inertial impaction

13. What variables can affect the adequacy of a correlation between scrubber static pressure drop and the particulate matter removal efficiency? Select all that apply.

    e. All of the above

Sizing and Design of Particulate Wet Scrubbers

14. Calculate the liquid-to-gas ratio for a scrubber system with a gas flow rate of 4,000 ft^3/sec and a recirculation liquor flow rate of 2,000 gal/min. Is this value in the normal range for a particulate wet scrubber?

    Answer: 8.33 gal/1000 ACF

    Gas flow rate = (4,000 ft^3/sec) (60 sec/min) = 240,000 ft^3/min

    Liquid-to-gas ratio = (gal/min)/(ACF/min)

$$= \frac{2{,}000 \text{ gal/min}}{240{,}000 \text{ ft}^3\text{/min}}$$

$$= 8.33 \text{ gal/1000 ACF}$$

    This is in the normal range of 4 - 20 gal/1000 ACF.

15. A chevron mist eliminator is 8 ft in diameter. The gas flow rate through the scrubber system has been measured at 60,500 ACFM.

    a. 20.0 ft/sec
    b. 33.3 ft/sec

    This is not within the normal operating range for this type of mist eliminator.

Solution for Part a:

Average velocity through mist eliminator = Gas flow rate/area

Mist eliminator area = $D^2/4 = 3.14\ (8\ ft)^2/4 = 50.2\ ft^2$

$$\text{Velocity} = \frac{60{,}500 \text{ ft}^3\text{/min}}{50.2 \text{ ft}^2}$$

$$= 1{,}200 \text{ ft/min} = 20.0 \text{ ft/sec}$$

Solution for Part b:

Average velocity with 40% blockage = 100% open velocity/0.6

$$= \frac{(20.0\ \text{ft/sec})}{0.6} = 33.3\ \text{ft/sec}$$

This is **not** within the normal range for a vertically mounted chevron mist eliminator.

16. What is the most difficult-to-collect particle size range for a venturi scrubber?

    b. 0.1 to 2µm

17. A scrubber system has an inlet dry bulb temperature of 600°F and an inlet absolute humidity of 0.05 lbs. of water per pound of dry air. What is the adiabatic saturation temperature for this gas stream? Use the psychometric chart presented in Figure 6-35.

    Answer: The adiabatic saturation temperature is approximately 138°F.

18. The baseline pressure drop across a mist eliminator is 1.2 in. W.C. at a gas flow rate of 30,000 ACFM. The static pressure drop is now 2.2 in. W.C., and the gas flow rate is 34,000 ACFM. Is there any reason to suspect pluggage of the mist eliminator?

    Yes. The increase in static pressure drop could not be caused by the slightly increased gas flow rate. The static pressure drop due to gas flow rate increases as the square of the gas flow rate. Accordingly, this could only cause a 28% increase. The observed static pressure drop has increased 83%.

Bibliography

Calvert, S., J. Goldschmid, D. Leith, and D. Mehta. *Scrubber Handbook*. Vol. l, *Wet Scrubber System Study*. EPA-R2-72-118a. 1972.

Engineering Science. *Scrubber Emissions Correlation Final Report*. U.S. EPA Contract 68-01-4146, Task Order 49. 1979.

Ensor, D.S. *Ceilcote Ionizing Wet Scrubber Evaluation*. EPA 600/7-79-246. 1979.

Myers, J.R., and D. McIntosh. *The Dynawave Scrubber: a Highly Efficient Gas Cleaning*. Paper presented at the American Institute of Chemical Engineers Midwest Regional Meeting. St. Louis, MO. February, 1991.

Radian Corporation. *Economic and Technical Evaluation of a Hydro-Sonic Free-Jet Scrubber for a Hazardous Waste Incinerator*. Report DCN 87-213-071-05. 1987.

Richards, J. *Wet Scrubber Inspection and Evaluation Manual*. PA 340/1-83-022. 1983.

Schifftner, K. *Flux Force Condensation Scrubbers for Utilization on Municipal Solid Waste Incinerators*. Paper presented at the Joint American Society of Mechanical Engineers/IEEE Power Generation Conference. Dallas, TX. October, 1989.

Schifftner, K.C., and H.E. Hesketh. *Wet Scrubbers*. Ann Arbor Science. Ann Arbor, MI. 1983.

Schifftner, K.C., and R.G. Patterson. *Engineering Efficient Hospital Waste Incinerator Scrubbers*. Paper presented at the First National Symposium on Incineration of Infectious Wastes. Washington, D.C. May, 1988.

Semrau, K.T. C*orrelation of Dust Scrubber Efficiencies*. Journal of the Air Pollution Control Association 10:200-207. 1961.

U.S. Environmental Protection Agency. 1982. *Control Techniques for Particulate Emissions from Stationary Sources*. Vol. 1, *Wet Scrubbers*. EPA 450/3-81-005a.

Walker, A.B., and R.M. Hall. *Operating Experience with a Flooded Disc Scrubber: a New Variable Throat Orifice Contactor*. Journal of the Air Pollution Control Association 18:319-323. 1968.

Yung, S., S. Calvert, and H.F. Barbarika. *Venturi Scrubber Performance Model*. EPA 600/2-77-172. 1977.

Chapter 7
Mechanical Collectors

Mechanical collectors use inertial force to separate particles from a rotating gas stream. There are two main types of mechanical collectors: (1) large diameter cyclones and (2) small diameter multi-cyclones. Large diameter cyclones are used for the collection of large diameter particulate matter that would otherwise settle out near the source and create a nuisance in the immediate area. Multi-cyclone collectors are groups of small diameter cyclones that have better particulate removal capability than large diameter cyclones. The multi-cyclone units are used as stand-alone collectors on sources generating moderate-to-large particulate matter. They are also used as precollectors in fabric filters and electrostatic precipitators.

7.1 TYPES AND COMPONENTS OF MECHANICAL COLLECTORS

7.1.1 Large Diameter Cyclones

The inlet gas stream enters the large diameter cyclone through a tangentially mounted duct that imparts a spin to the gas stream. The inlet duct is usually at the top of the cyclone body, but large diameter cyclones may also have bottom inlets. Both arrangements are shown in Figure 7-1.

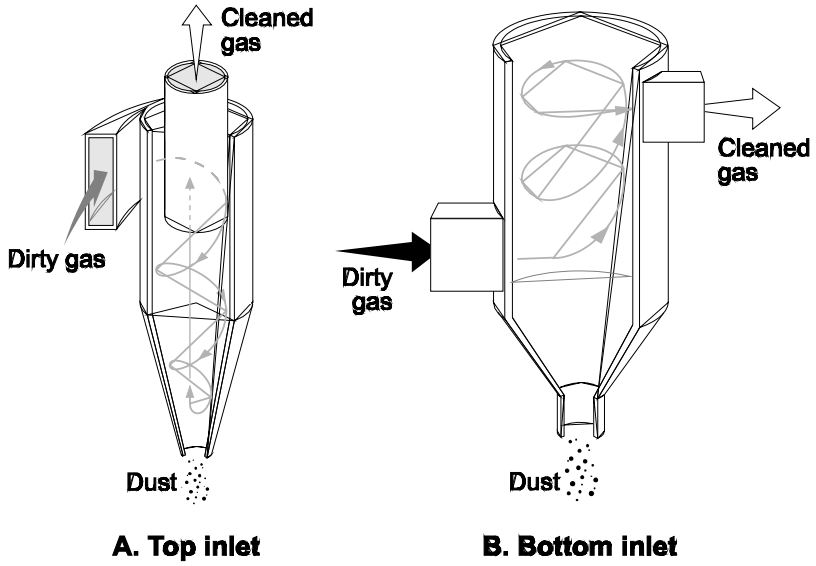

Figure 7-1. Large diameter cyclones

With the normal inlet gas stream velocity of 20 to 50 ft/sec, the gas stream spins approximately one-half to two complete rotations within the cyclone body of both types of units shown in Figure 7-1. An increase in the gas inlet velocity increases the spinning action of the gas stream, thereby improving inertial separation of the particles.

The gas flow pattern in a bottom inlet large diameter cyclone is relatively simple. The inlet gas stream begins to spin in the cyclone body because of the tangential inlet duct configuration. The gas stream forms an ascending vortex that rises up in the cyclone body to the outlet duct at the top of the unit. The particles that migrate across the gas streamlines settle by gravity when they approach the surface of the cyclone body where the gas velocity is low.

In the top inlet design, the gas stream spins in two separate vortices. The inlet stream creates an outer vortex due to the tangential location of the inlet duct and due to the presence of the outlet tube extension that prevents gas movement into the center of the cyclone body. As the gas stream passes down the cyclone body, it turns 180° and forms an inner vortex that moves toward the gas outlet tube at the top of the cyclone. The outlet tube must extend sufficiently far into the cyclone to facilitate formation of the outer vortex and to prevent a "short circuit" path for the gas stream.

The particles that have migrated toward the outer portion of the outer vortex break away from the gas stream when it turns 180° to enter the inner vortex. Due to their inertia, the particles continue to move downward toward the cyclone hopper (often termed the cone) as the gas stream turns from the outer vortex to the inner vortex. The movement of the particles toward the hopper is controlled partially by inertial forces. The force of gravity also assists in particle movement toward the hopper.

Top-inlet, large-diameter cyclones can have a number of different inlet designs as shown in Figure 7-2. The most common design is the simple tangential inlet (A). The deflector vane (B) reduces the gas stream turbulence at the inlet and can reduce the overall pressure drop. However, the deflector vanes can also impair vortex formation and thereby reduce particulate collection. Helical inlets (C) have been used in an attempt to reduce cyclone pressure drop and to improve performance. Involute entries (D) can also reduce turbulence-related pressure drop at the inlet. However, they usually provide improved efficiency due to the manner in which the outer vortex develops.

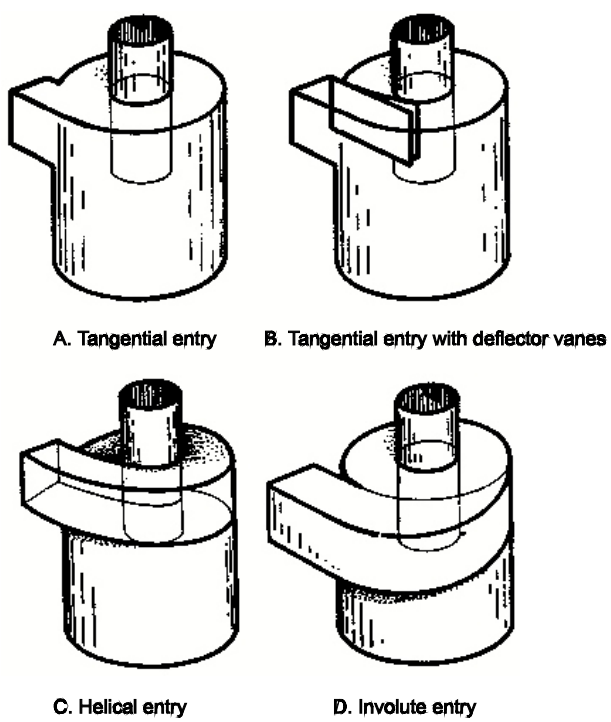

Figure 7-2. Types of cyclone inlets

The dust discharge system for a large diameter cyclone consists of a conical bottom section and a solids discharge valve. Four common types of solids discharge valves used on large diameter cyclones are shown in Figure 7-3.

A solids discharge valve with good sealing characteristics is needed on negative pressure units (fan downstream from the cyclone) to prevent air infiltration in the bottom of the cyclone, which could disrupt the vortices in the cyclone. The slide gate (A), the rotary discharge valve (B), and the double flapper valve (D) are all capable of providing an airtight seal. The screw conveyor arrangement (C) cannot provide an airtight seal unless a solids discharge valve is placed between the bottom of the cyclone and the screw conveyor.

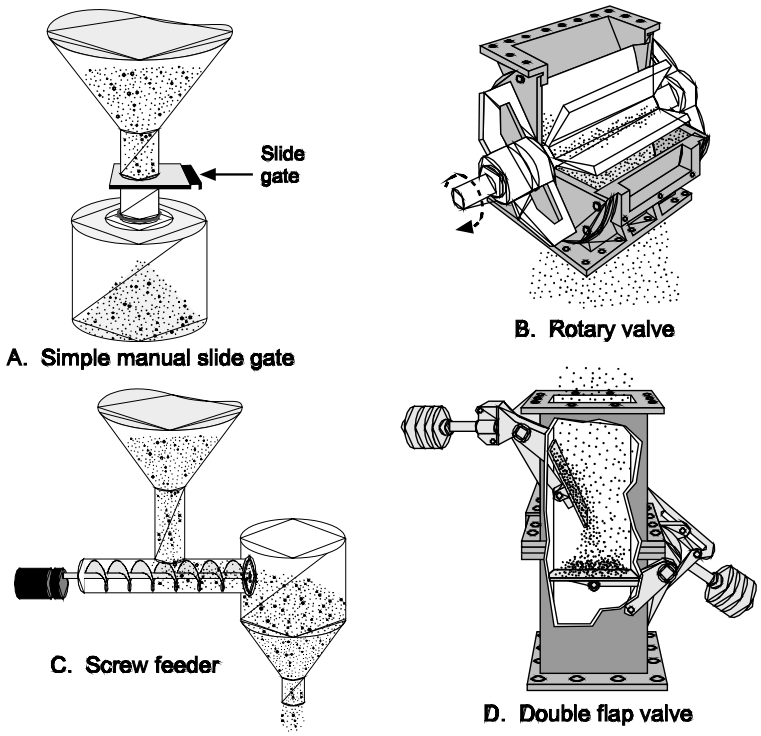

Figure 7-3. Four types of solids discharge valves

A solids discharge valve is not needed for positive pressure cyclones as long as there is a way to contain the particulate matter being discharged from the conical section. It is designed to channel the dust toward the solids discharge valve, to prevent the vortices from reentraining particulate from the hopper area, and to facilitate the transition gas movement from the descending outer vortex to the ascending inner vortex. The outlet gas tube is an important consideration in the design of a large diameter cyclone. Some of the energy due to the radial motion of the ascending gases can be recovered by (1) scroll devices or (2) outlet drums placed on top of the outlet tube. These two cyclone enhancements, which are shown in Figure 7-4, are essentially flow straighteners that can effectively reduce the overall pressure drop across the unit without affecting the particulate matter removal efficiency.

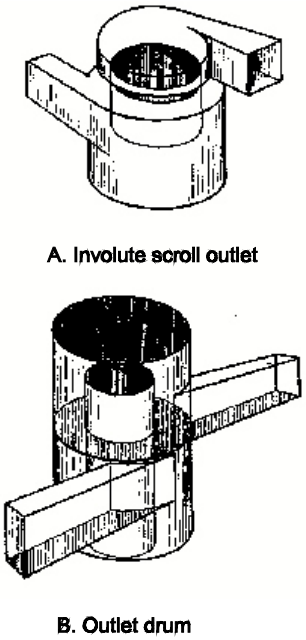

Figure 7-4. Special outlet configurations for
large diameter cyclones

Large diameter cyclones can be used in series or parallel arrangements in order to increase particulate matter removal efficiency or to increase gas flow capability. A series arrangement of two cyclones of equal size. A parallel arrangement of four cyclones of equal size are shown in Figure 7-5.

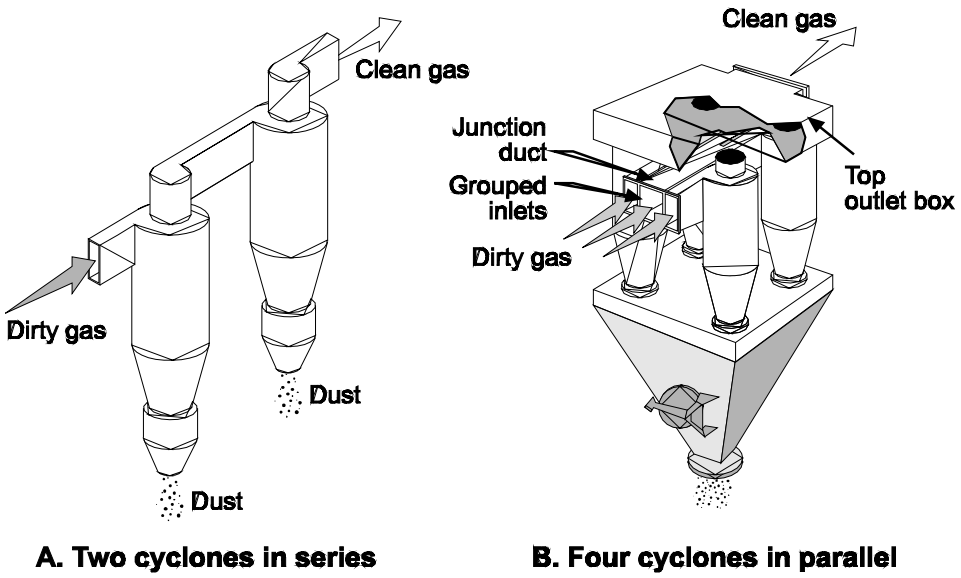

Figure 7-5. Series and parallel arrangements of cyclones
Two cyclones in series – Four cyclones in parallel

7.1.2 Small Diameter Multi-Cyclone Collectors

The particulate matter removal capability of a small diameter cyclone is greater than that of a large diameter cyclone because the gas stream is forced to spin in small vortices. The gas stream has a high radial velocity in the small cyclone; therefore, the particles are subjected to greater inertial force. However, it is not possible to handle a large gas stream in a single small diameter tube. In order to treat the entire gas stream, a large number of small diameter tubes can be used in a single multi-cyclone collector in which the tubes are in a parallel arrangement. Multi-cyclone collectors have cyclone tubes that range in size from 6 to 12 in. in diameter. A small multi-cyclone collector, such as the one shown in Figure 7-6, can have as few as 16 tubes. Large units may have several hundred tubes.

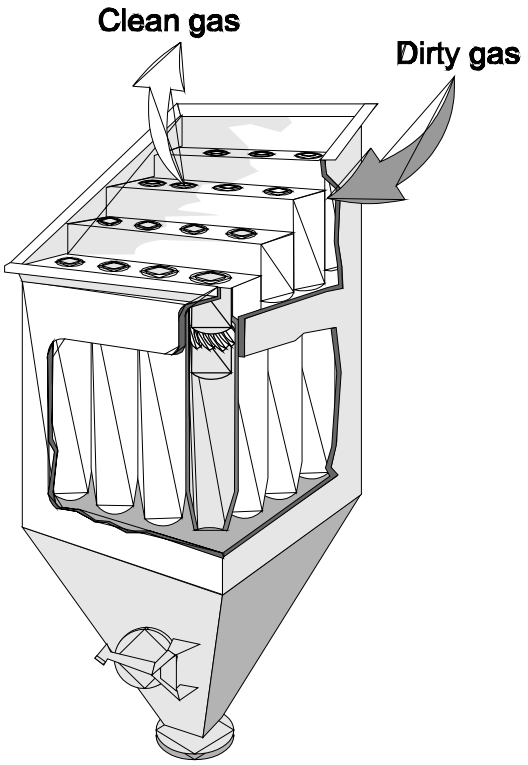

Figure 7-6. Multi-cyclone collector

Cyclone tubes used in multi-cyclone collectors have axial inlets and outlets. As shown in Figure 7-7, the spinning motion of the gas stream is created as the gas entering the tube passes over a set of spinner vanes. Approximately 90% of the total pressure drop of the tube is due to these vanes.

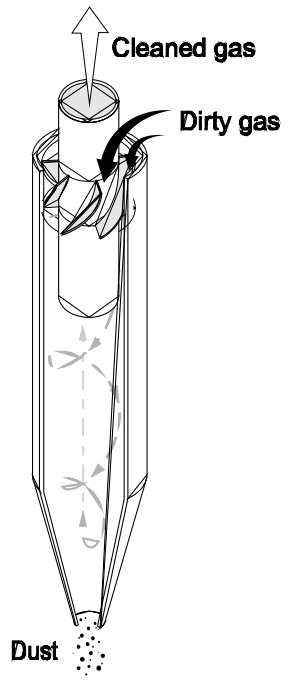

Figure 7-7. Small diameter cyclone tube for a multi-cyclone collector

The vortices in the multi-cyclone tubes are similar to those in a large diameter cyclone. The inlet gas stream forms an outer vortex. This vortex dissipates near the conical bottom of the tube. An inner vortex is formed and ascends to the outlet tube.

Particulate matter that separates from the gas stream near the bottom of the tube falls through the dust outlet and enters a hopper (or hoppers) below the set of tubes. A solids discharge valve below the hopper is necessary to prevent air infiltration upward through the hopper area.

The multi-cyclone tubes rest on a horizontal metal plate which is termed the dirty side tube sheet. In some designs, a gasket (Figure 7-8) is used underneath the cyclone tube in order to prevent gas movement from the inlet duct to the hopper area.

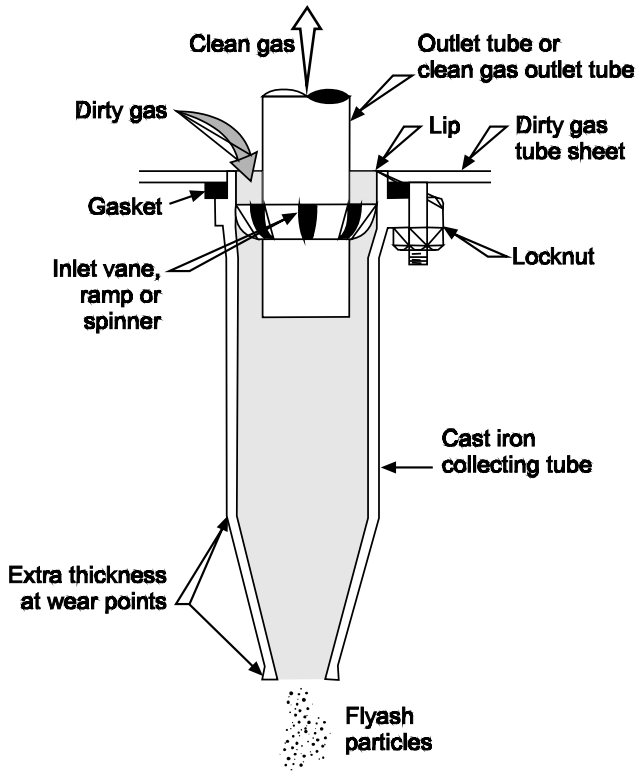

Figure 7-8. Gasket between a multi-cyclone tube and a dirty side tube sheet (Reprinted by permission of Schmidt Associates, Inc.)

The outlet tubes are fabricated from erosion-resistant materials because they are exposed to the particulate-laden inlet gas stream. The outlet tubes extend upward through a second metal plate, which is usually designed in a step fashion (Figure 7-6) or as a steep slope. This metal plate is termed the clean side tube sheet since it separates the inlet gas stream from the outlet gas stream. The configuration of the clean side tube sheet ensures that the inlet gas stream is divided relatively uniformly among the rows of cyclone tubes in the collector.

There must be a seal between the outlet gas tubes and the clean side tube sheet. In some units, the outlet tube is seal-welded to the tube sheet. Alternatively, the outlet tube can have a gasketed seal. Both arrangements are shown in Figure 7-9.

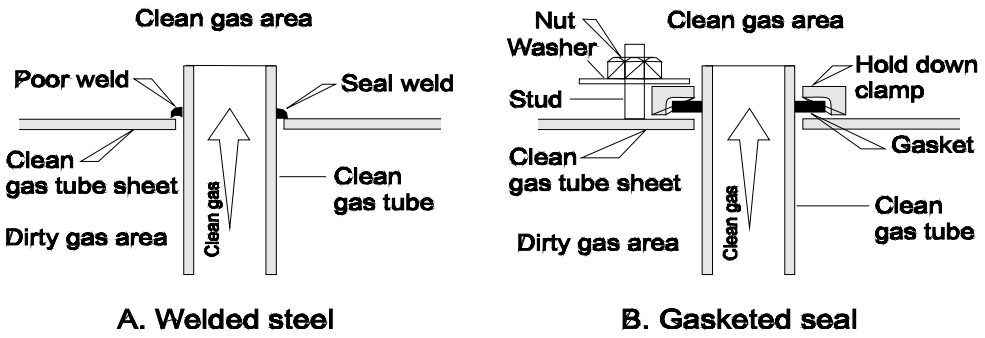

Figure 7-9. Outlet tube: clean side tube sheet seals for multi-cyclone collectors
(Reprinted by permission of Schmidt Associates, Inc.)

Instrumentation for multi-cyclones is usually very limited. Most multi-cyclone collectors are equipped only with differential pressure gauges to monitor the pressure drop across the unit.

7.2 OPERATING PRINCIPLES

7.2.1 Particle Collection

Steps in Particulate Matter Control

All mechanical collectors use inertial force to separate particles from a gas stream. Because the inertial force is applied in a spinning gas stream, the inertial force is often termed centrifugal force. The first step in particle capture is the accumulation of particles along the inner wall of the cyclone due to centrifugal force.

For vertically oriented cyclones, settling the particles into a hopper is the second step in the overall process of particle capture. However, unlike electrostatic precipitators and fabric filters, there is little if any particle agglomeration to facilitate gravity settling until the particles reach the cyclone tube discharge. The particles settle at a rate that is dependent partially on their terminal settling velocities. As discussed in Section 2, these settling rates are quite small for particles less than 10 micrometers. Fortunately, most particles in vertical cyclones also retain some momentum toward the hopper due to the motion of the gas stream passing through the cyclone. The combined effect of gravity settling and the momentum from the gas stream are sufficient to transport the particles from the cyclone wall to the cyclone tube discharge, and eventually the hopper.

The third step is the overall particulate matter control process is the removal of accumulated solids from the hoppers. This is an especially important step in mechanical collectors because the cyclone outlets extend directly into the hoppers. The presence of high solids levels due to hopper discharge problems could block the outlets and make the cyclone entirely ineffective for particulate removal.

Particle Inertial Separation

The movement of particles due to inertial force in a spinning gas stream is estimated using Equation 7-1, the expression for centrifugal force (previously presented as Equation 2-23).

$$F_c = \frac{m_p \ u_T^{\ 2}}{R} \tag{7-1}$$

Where:

F_c = centrifugal force (gm/cm•sec^2)

m_p = mass of the particle (gm)

u_T = tangential velocity of the gas (gm/sec)

R = cylinder radius (cm)

Expressing the mass of the particle (m_p) in Equation 7-1 in terms of the particle density and the particle volume (see Equations 2-3 and 2-4) yields the following equation:

$$F_c = \frac{\frac{\pi}{6} d^3 \rho_p u_T^{\ 2}}{R} \tag{7-2}$$

Where:

d = physical particle diameter (cm)

p = particle density (gm/cm^3)

The tangential velocity term, u_T, takes into account the velocity of the gas stream spinning in the cyclone. Small diameter cyclones with high gas stream velocities will exert larger centrifugal forces than large diameter cyclones with low gas velocities.

Following the derivation shown in Chapter 2, the terminal migration velocity of particles across the gas stream toward the cyclone outer wall, as shown in Figure 7-10, are calculated by relating the centrifugal force (here, Equation 7-2; presented earlier as Equation 2-24) with the drag force. In the laminar flow range, the expression of the migration velocity is expressed as shown here in Equation 7-3 (presented earlier as Equation 2-25).

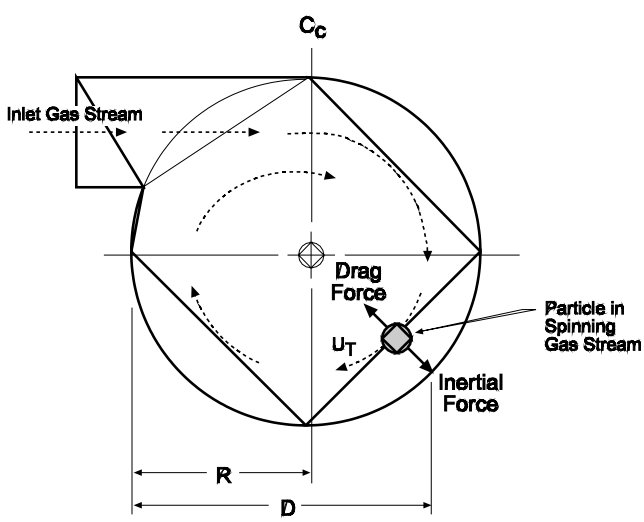

Figure 7-10. View of spinning gas in a cyclone (top view)

$$v_c = \frac{d^2 \rho_p u_T^2 C_c}{18 \mu R} \tag{7-3}$$

Where:

v_c = migration velocity ($gm^2/cm \cdot sec$)
d = physical particle diameter (cm)
$_p$ = particle density (gm/cm^3)
u_T = tangential velocity of the gas (gm/sec)
C_c = Cunningham correction factor (dimensionless)
μ = fluid viscosity (gm/cm•sec)
R = cylinder radius (cm)

This equation illustrates that velocity of the particle moving across the gas stream lines in the cyclone and toward the cyclone wall is proportional to the square of the particle size. This means that cyclones will be substantially more effective for large particles than for small particles. At any given particle size, the particle radial velocity will be proportional to the square of the gas stream tangential velocity and inversely proportional to the cyclone radius. These two parameters determine the extent to which the gas stream is spinning within the cyclone. High velocities increase the spinning action and therefore increase particle radial velocity and particle collection. A small cyclone radius makes the gas stream turn more sharply and, therefore, also increase cyclone efficiency.

It should be noted that this expression for the particle migration velocity only applies if the particle Reynolds number is less than 1. Mechanical collectors are often designed to collect very large particles that would not have such low Reynolds numbers. An accurate expression for the movement of these large particles can be derived by relating the centrifugal force equation (Equation 7-1) with the force of drag in the transitional and turbulent Reynolds number ranges (Equations 2-16 and 2-17). This is not essential for small diameter cyclones because all of the particles that are in the transitional and turbulent ranges are collected with close to 100% efficiency.

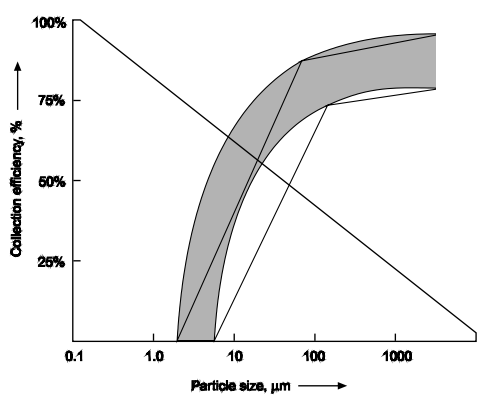

Figure 7-11. Particle size-collection efficiency relationship for cyclonic collectors

The particle size-efficiency curve shown as Figure 7-11 illustrates the sharp decrease in efficiency as the particle size decreases.

It is apparent from this general performance curve and the other size-efficiency curves presented in this section that conventional mechanical collectors are not intended for collecting particles smaller than

approximately 3 micrometers. However, there is a category of high efficiency small diameter cyclones that have good removal efficiencies down to approximately 1 micrometer. The enhanced performance is due to very high velocities in the small diameter cyclonic tube.

7.2.2 Static Pressure Drop

The pressure drop across a cyclone is an important parameter for purchasers of mechanical collectors. Increased pressure drop means greater costs for power to move exhaust gas through the control device. With cyclones, an increase in pressure drop usually means that there will be an improvement in collection efficiency. For these reasons, there have been many attempts to predict pressure drops from design variables.

One of the simplest pressure drop equations that correlates reasonably well with the experimental data (Leith, 1973) was developed by Shepard and Lapple (1939).

$$\Delta p = \left(\frac{v_i^2 \rho_g}{2g\rho_m}\right)\left(\frac{H_c B_c K_c}{D_c^2}\right) \tag{7-4}$$

Where:

- p = pressure drop (in. W.C.)
- $_g$ = gas density (lb_m/ft^3)
- $_m$ = density of measuring manometer fluid used to measure v_i (lb_m/ft^3)
- g = gravitational constant (ft/sec^2)
- K_c = empirical constant (16 for cyclone with tangential inlet, 7.5 for cyclone with inlet vane)
- H_c B_c = inlet height and inlet width (ft)
- D_c = cyclone body diameter (ft)

Leith (1973) found a correlation coefficient of 0.77 between experimental data and calculations based on Equation 7-4. Perfect correlation equals 1.0. None of the pressure drop equations was found to have better than a 0.80 correlation coefficient. Another expression frequently used is given in Equation 7-5.

$$\Delta p = \frac{0.0027Q^2}{k_c D_e B_c H_c \left(\frac{L_c}{D_c}\right)^{\frac{1}{3}} \left(\frac{Z_c}{D_c}\right)^{\frac{1}{3}}} \tag{7-5}$$

Where:

- p = pressure drop (cm W.C.)
- Q = volumetric flow rate (ft^3/min)
- k_c = dimensionless factor that is descriptive of the cyclone inlet vanes (1.0 for vanes that do not expand the entering gas or touch the outlet wall, 2.0 for vanes that expand and touch the outlet wall)
- D_e = outlet tube diameter (cm)
- H_c, B_c = inlet height and inlet width (cm)
- Z_c = height of cyclone bottom cone (cm)
- L_c = height of cyclone body (cm)
- D_c = cyclone body diameter (cm)

When compared to experimental data, this equation was found to have a correlation coefficient of only 0.53 (Leith, 1973).

It should be noted from both of these equations that the pressure drop is a function of the square of the inlet velocity. Most of the empirical pressure drop equations have the following form:

$$\Delta p = K_c \rho_g v_i^2 \tag{7-6}$$

Where:

p = pressure drop (in. W.C.)
K_c = proportionality factor (dimensionless)
$_g$ = gas density (lb_m/ft^3)
v_i = inlet gas velocity (ft/sec)

If the pressure drop is measured in inches of water, K_c can vary from 0.013 to 0.024. Velocities for cyclones range from 20 to 70 ft/sec, although common velocities range from 50 to 60 ft/sec. At velocities greater than 80 ft/sec, turbulence increases in the cyclone, and efficiency decreases significantly. At high loads of particulate matter and high velocities, scouring of the cyclones by the particles also increases rapidly. To minimize erosion in such cases, cyclones are designed for lower inlet velocities.

Typical pressure drops for low efficiency, large diameter cyclones are in the range of 1 to 3 in. W.C. Multi-cyclone collectors usually have pressure drops in the range of 2 to 6 in. W.C.

7.2.3 Capabilities and Limitations of Cyclonic Collectors

The primary limitation of cyclonic collectors is their inability to capture small particles. Current environmental regulations require much more efficient collection of these small particles than are capable by cyclonic collectors. In addition, collection efficiency is substantially reduced at low gas flow rates due to the decreased particle inertia.

Sources emitting stringy material can cause build-up of material in the inlet vanes of multi-cyclone collectors. Partially blocked inlet spinner vanes do not generate the cyclonic flow patterns necessary for proper inertial separation.

Mechanical collectors in general are not useful for the collection of sticky particulate matter. The main difficulties associated with these materials involve removal from the hoppers and build-up along the inner wall of the cyclone. Examples of hard-to-collect sticky material include partially polymerized oils, condensed high molecular weight organics, and ammonium sulfate and bisulfate particles.

Small diameter cyclones, including all multi-cyclone collectors, are vulnerable to severe erosion when treating gas streams having very large diameter particulate matter. Particles over twenty micrometers are very abrasive at the high tangential velocities achieved in the small diameter cyclones. The abrasiveness of particulate matter increases with the square of the particle diameter. Accordingly, cyclones handling particles in the twenty to more than one hundred micrometer size range can be vulnerable to high erosion rates.

Mechanical collectors are occasionally used as precollectors in air pollution control systems vulnerable to ember entrainment. While the embers do not damage mechanical collector components, the hoppers must be properly designed to prevent the accumulation of combustible material that could be ignited. Simmering fires in the mechanical collector hoppers could warp the tube sheet supporting the multi-cyclone tubes, crack welds and gaskets used to seal the tubes to the tube sheet, and damage the hopper casings.

7.3 CAPABILITY AND SIZING OF MECHANICAL COLLECTORS

7.3.1 Collection Efficiency

A number of formulations have been developed for determining the cyclone collection efficiency, n_i, for a particle of a given size. These approaches are applicable to both large diameter cyclones used as stand-alone collectors and small diameter cyclones used as part of a multi-cyclone collector.

An excellent discussion and comparison of these theories is given by Leith. Figure 7-12 (reproduced from Leith's *Cyclone Performance and Design)* estimates the applicability of several theories for the calculated efficiency of a simple cyclone. All these theories show a strong dependence on particle size.

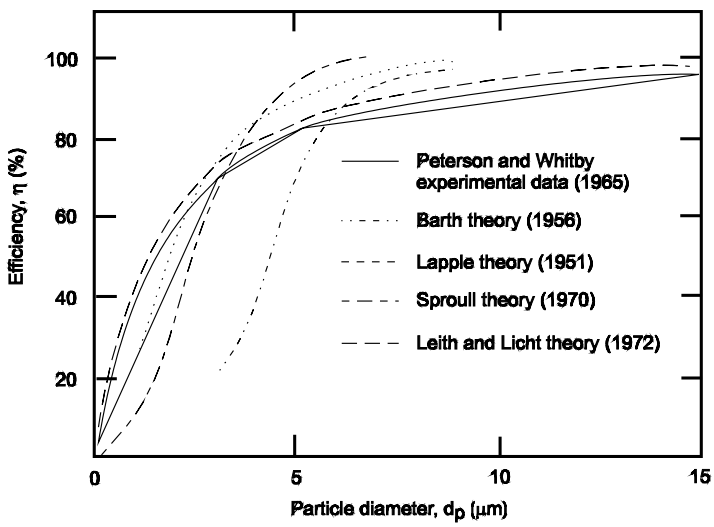

Figure 7-12. Cyclone efficiency versus particle size, experimental results, and theoretical predictions

This section will describe two methods of estimating cyclone efficiency: (1) the Leith and Licht equation and (2) the Lapple graphical method. Each approach provides a removal efficiency for a given particle size.

The fractional efficiency equation of Leith and Licht is similar to many equations developed for particulate control devices.

$$n_i = 1 - e^{-2[CY]^{(1/(2n+2))}} \tag{7-7}$$

Where:

n_i = efficiency for particle diameter i (dimensionless)
C = cyclone dimension factor (dimensionless)
= impaction parameter (dimensionless)
n = vortex exponent (dimensionless)

$$C = \frac{8\,K_c}{K_a\,K_b} \tag{7-8}$$

Where:

C = cyclone dimension factor i (dimensionless)

K_a = cyclone inlet height divided by the cyclone diameter a/d (dimensionless)

K_b = cyclone inlet width divided by the cyclone diameter b/d (dimensionless)

K_c = cyclone volume constant (Equation 7-16) (dimensionless)

$$n = \frac{(12\,D)^{0.14}}{2.5} \tag{7-9}$$

Where:

D = cyclone body diameter (feet)

$$\frac{1-n_1}{1-n_2} = \left(\frac{T_1}{T_2}\right)^{0.3} \tag{7-10}$$

Where:

n_1 = vortex index at ambient temperature (dimensionless)

n_2 = vortex index at elevated temperature (dimensionless)

T_1 = ambient absolute temperature (°R)

T_2 = elevated absolute temperature (°R)

$$l = 2.3D_e\left(\frac{D^2}{ab}\right)^{0.333} \tag{7-11}$$

Where:

l = natural length – distance below gas outlet where vortex turns (feet)

D_e = gas outlet diameter (feet)

D = cyclone body diameter (feet)

a = cyclone inlet height (feet)

b = cyclone inlet width (feet)

H S = overall cyclone height outlet length (7-12)

If l < (H-S), calculate V_{nl}:

$$V_{nl} = \frac{\pi D^2}{4}(h-S) + \left(\frac{\pi D^2}{4}\right)\left(\frac{(l+S-h)}{3}\right)\left(1.0 + \frac{d}{D} + \frac{d^2}{D^2}\right) - \left(\frac{\pi D_e{}^2 l}{4}\right) \tag{7-13}$$

$$d = D - (D-B)\left(\frac{S+l-h}{H-h}\right) \tag{7-14}$$

Where:

V_{nl} = volume of cyclone at natural length (ft^3)
D = cyclone body diameter (feet)
h = height of upper cylindrical body of cyclone (feet)
S = outlet length (feet)
l = natural length – distance below gas outlet where vortex turns (feet)
D_e = gas outlet diameter (feet)
H = overall cyclone height (feet)

If l > (H-S), calculate V_H:

$$V_H = \frac{\pi D^2}{4}(h-S) + \frac{\pi D^2}{4}\left(\frac{H-h}{3}\right)\left(1.0 + \frac{B}{D} + \frac{B^2}{D^2}\right) - \frac{\pi D_e{}^2}{4}(H-S) \tag{7-15}$$

Where:

V_H = volume of cyclone below exit duct (ft^3)
B = outlet duct diameter for dust (feet)

Calculate the K_C, using either V_{nl} or V_H as appropriate.

$$K_c = \frac{V_s + \frac{V_{nl}}{2}}{D^3} \text{ or } \frac{V_s + \frac{V_H}{2}}{D^3} \tag{7-16}$$

Where:

K_c = cyclone volume constant
V_s = annular shaped volume above exit duct to midlevel of entrance duct (ft^3)
V_{nl} = volume of cyclone at natural length (ft^3)

$$V_s = \frac{\pi\left(S - \frac{a}{2}\right)\left(D^2 - D_e{}^2\right)}{4} \tag{7-17}$$

$$C = \frac{8K_c}{K_a K_b} \tag{7-18}$$

$$u_{T_2} = \frac{Q}{ab} \tag{7-19}$$

Where:

a = inlet height (ft)

b = inlet width (ft)

Q = gas flow rate (ACFM)

$$\Psi = \frac{\rho_p d_p^2 u_{T_2} (n+1)}{18\mu D} \tag{7-20}$$

Where:

= cyclone inertial impaction parameter (dimensionless)

$_p$ = particle density (gm/cm^3)

d_p = particle diameter (cm)

u_{T2} = tangential velocity of particle at cyclone wall (cm/sec)

= gas viscosity (gm/cm•sec)

D = cyclone body diameter (feet)

n = vortex exponent (dimensionless)

K_a = cyclone inlet height divided by cyclone body diameter (dimensionless)

K_b = cyclone inlet width divided by cyclone body diameter (dimensionless)

Q = gas flow rate (ACFM)

It is apparent that the collection efficiency is related to the square of the particle diameter and is directly proportional to the inlet gas velocity. Collection efficiency is inversely proportional to the diameter of the cyclone. The method has also been extended by Koch (1977) to provide a graphical method of optimizing certain parameters of cyclone design.

An older method of calculating cyclone fractional efficiency and overall efficiency was developed by Lapple (1975). The first step in this procedure is the calculation of the particle size collected with 50% efficiency (termed the cut diameter) using Equation 7-21.

$$[d_p]_{50} = \sqrt{\frac{9\mu B_c}{2\pi n_t v_i (\rho_p - \rho_g)}} \tag{7-21}$$

Where:

$[d_p]_{cut}$ = cut diameter (ft)
μ = gas viscosity (lb_m/sec•ft)
n_t = effective number of turns (0.5 to 3 for common cyclones)
v_i = inlet gas velocity (ft/sec)
$_p$ = particle density (lb_m/ft^3)
$_g$ = gas density (lb_m/ft^3)
B_c = cyclone inlet width (ft)

The cut diameter is a characteristic of the cyclonic control device and should not be confused with the geometric mean particle diameter of the particle size distribution. The cut diameter takes into account the gas stream inlet velocity, the cyclone inlet width, the gas viscosity, and other factors that influence particle removal in the cyclone.

A particle size-removal efficiency curve for the cyclonic collector is prepared by calculating ratios of particle size to the cut diameter, $[d_p]_i/[d_p]_{cut}$ and applying the curve shown in Figure 7-13. As a universal curve for common cyclones, this correlation has been found to agree within 5% at a $[d_p]_i/[d_p]_{cut}$ ratio near 1.0. This empirical curve takes into account the dependence of cyclonic performance on the square of the particle diameter.

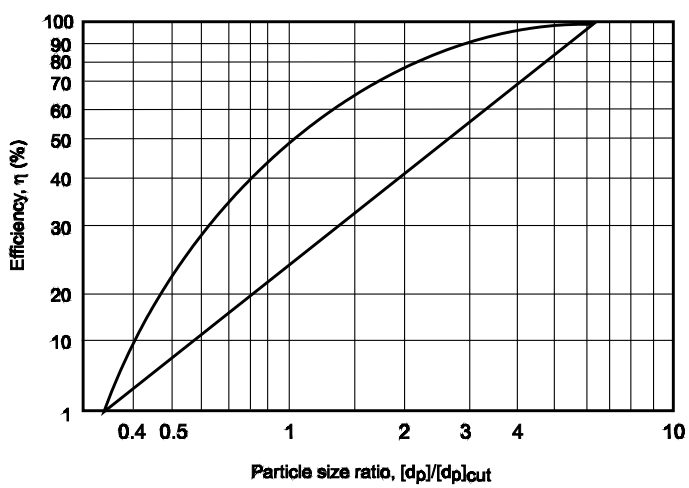

Figure 7-13. Cyclone efficiency versus particle size ratio (Lapple, 1975)

The following procedures are followed to calculate the particle size - removal efficiency curve:

- Calculate the $[d_p]_{cut}$ for the cyclone being evaluated.
- Calculate several values of the ratio $[d_p]_i/[d_p]_{cut}$ over the particle size range of interest.
- Plot the efficiency for each $[d_p]_i$ determined from Figure 7-13.

The plotted efficiency values will give the estimated performance characteristics of the cyclone at the operating conditions used to estimate $[d_p]_{cut}$. Because this procedure only gives a very approximate estimate, a range of cut diameters is often used instead of a single value. Maximum and minimum efficiency curves determined from these values will then give a range of efficiencies for evaluation purposes.

Problem 7-1

Use of the Cut Diameter Procedure for Estimating Cyclone Efficiency

Assume that a large diameter cyclone is being used for the removal of grain dust in the range of 8 to 100 m in diameter. What is the particle size-removal efficiency curve for the cyclone if it has a diameter of 1 ft, an inlet gas velocity of 50 ft/sec, and an operating temperature of 68°F?

Assume a particle density of 80 lb_m/ft^3 and a gas density of 0.075 lb_m/ft^3.

Use a gas viscosity of 1.2×10^{-5} lb_m/sec ft.

The cyclone has an inlet width of one foot.

The first step in using the cut diameter approach is to estimate the cut diameter under the stated operating conditions. The cut diameter is calculated using Equation 7-21. The particle size-efficiency estimates are shown in Table 7-1.

$$[d_p]_{cut} = \sqrt{\frac{9\mu B_c}{2\pi n_t v_i(\rho_p - \rho_g)}}$$

Where:

$[d_p]_{cut}$ = cut diameter (ft)

= gas viscosity, 1.2 10^{-5} lb_m/sec•ft

n_t = effective number of turns (one for large cyclone)

v_i = inlet gas velocity, 50 ft/sec

$_p$ = particle density, 80 lb_m/ft^3

$_g$ = gas density, 0.075 lb_m/ft^3

B_c = cyclone inlet width, 1 ft

$[d_p]_{cut}$ = 0.0000656 ft = 20.0 m

Table 7-1. Efficiency Estimates, Problem 7-1

$[d_p]_i$, m	$[d_p]_i/[d_p]_{cut}$ (based on $[d_p]_{cut}$ = 20.0)	Efficiency, $[d_p]_i$ (based on Fig. 7-13)
8	0.40	9
12	0.60	28
20	1.00	50
30	1.50	67
50	2.50	85
100	5.00	98

Problem 7-2

Use of the Cut Diameter Procedure for Estimating Cyclone Efficiency

What is the effect on the cyclone evaluated in Problem 7-1 if the inlet velocity decreases from 50 ft/sec to 30 ft/sec due to a drop in the gas flow rate?

The revised cut diameter for this operating condition is 25.8 m. The particle size-efficiency estimates are shown in Table 7-2.

Table 7-2. Efficiency Estimates, Problem 7-2

$[d_p]_i$, m	$[d_p]_i/[d_p]_{cut}$ (based on $[d_p]_{cut}$ = 25.8)	Efficiency, $[d_p]_i$ (based on Fig. 7-13)
8	0.31	0
12	0.47	18
20	0.78	38
30	1.16	54
50	1.94	78
100	3.88	96

The resulting efficiency curves for Problems 7-1 and 7-2 are shown in Figure 7-14. These curves illustrate the importance of particle size and inlet velocity (gas flow rate) on cyclone performance.

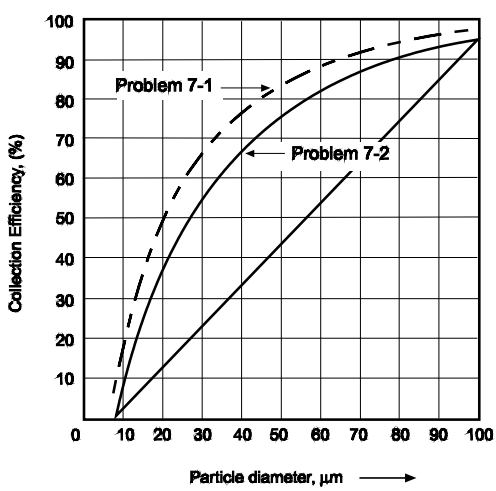

Figure 7-14. Problems 7-1 and 7-2 efficiency curves

The two efficiency estimation procedures discussed in this section provide a general means of evaluating the extent to which changes in operating conditions can affect cyclone performance. However, they are rarely used to estimate mass emissions from actual systems for the following reasons.

- Inlet particle size data is rarely available.
- Cyclonic collectors are often used as precollectors for more efficient particulate collectors.

- The Lapple cut diameter method is based on particle size data obtained in the 1940s and 1950s, well before the development of accurate particulate measurement techniques.

Conventional emission testing procedures are generally used for evaluating the performance of large cyclonic systems. Small systems are often evaluated using visible emission observations and routine inspection techniques.

Cyclones and multi-cyclones are not highly efficient for the collection of small particles that are largely responsible for light scattering. Accordingly, the presence of a high stack opacity from a cyclonic collector is usually indicative of process conditions that are creating particle size distributions smaller than the design range of the cyclonic collector. This could be due to a variety of process conditions such as incomplete combustion and/or vapor nucleation. These conditions must be evaluated as part of the process equipment inspection. Usually, changes in the operating conditions of the cyclonic collector will not significantly affect the emission opacity.

7.3.2 Instrumentation

There are usually few instruments on mechanical collectors, due primarily to their small size and service requirements. On moderate-to-large systems, the following instruments might be useful.

Large Diameter Cyclones
- Static pressure drop gauges

Multi-Cyclones
- Static pressure drop gauges
- Inlet and outlet temperature gauges (combustion source applications)

Large diameter cyclones and multi-cyclonic collectors are usually not equipped with opacity monitors due to the limited light-scattering characteristics of the moderate-to-large diameter particulate collected in these units. The only direct indicator of performance is the deposition of large diameter material in areas immediately adjacent to the cyclonic collector stack or vent. In some cases, the large particulate matter also impacts on adjacent structural columns, building walls, and other vertical surfaces.

Static Pressure Drop Gauges

The static pressure drop across the unit is dependent mainly on the inlet gas velocity and the physical conditions of the cyclonic collector. The inlet gas velocity is dependent directly on the gas flow rate, which in turn is a function of the process operating rate. At a given process operating rate, the pressure drop is dependent almost exclusively on the physical condition of the collector. This fact can be used to evaluate mechanical problems within the collector that could impair performance. An increase in the pressure drop at a given process operating rate could indicate solids plugging at the inlet to the cyclonic tube of multi-cyclone collectors. A decrease in the pressure drop at a given process operating rate could be due to a variety of problems.

- Erosion of the outlet tubes in large diameter cyclones and multi-cyclone collectors
- Failure of one or more of the gaskets on the clean side tube sheet of multi-cyclone collectors
- Erosion of the axial inlet spinner vanes in multi-cyclone tubes

The static pressure gauge provides the only data that can be used to readily identify these problems while the unit is operational. This relatively inexpensive instrument is very useful.

Inlet and Outlet Gas Temperature Gauges

Air infiltration is a common problem with multi-cyclone collectors serving combustion sources. It is caused by frequent thermal expansion and contraction as the boiler load varies, by erosion of the solid

discharge valve, and by aging of the high temperature gaskets. Air leaking into the hopper area of the multi-cyclone collector can significantly reduce the particulate removal efficiency. The inrushing air reentrains particulate from the hopper and disrupts the vortices in the cyclone tubes as it moves upward toward the outlet tubes.

The onset of air infiltration problems can be readily identified by the gas temperature drop across the unit. The relatively cold ambient air dilutes the flue gas stream and increases the temperature drop across the unit. A multi-cyclone collector with a gas temperature drop of more than 25°F probably has significant air infiltration, assuming that the temperature data are correct and representative. Increases in the gas temperature drop of 5 to 10°F from the baseline range (at a given boiler load) are also indicative of significant air infiltration. The cost of the temperature gauges at the inlet and outlet is relatively small compared to the benefits provided with respect to the early identification of air infiltration problems. The temperature gauges are usually mounted in the inlet and outlet ductwork.

Hopper Design

The hoppers of multi-cyclone collectors should be designed to minimize solids discharge problems. As stated earlier, solids accumulation in the hoppers can block the cyclone tube outlets of both large diameter cyclones and small multi-cyclone tubes. Several hopper design features are used to minimize hopper solids overflow.

- Properly sealing solids discharge valve
- Adequately sized hopper throat
- Adequately sloped hopper walls
- Strike plates and/or vibrators (large systems only)
- Thermal insulation around the hopper walls (units operating at elevated gas temperatures)

Mechanical collectors generally use rotary discharge valves or double flapper valves (see earlier discussion) for the discharge of solids from the hoppers. These valves must be well maintained to minimize air infiltration up through the hopper and into the cyclone tubes. It is important to note that most mechanical collectors are located on the inlet (upstream) side of the fan and operate with negative static pressures in the range of –2 to –10 in. W.C. in the hopper area. The solids discharge valve must be in good condition to maintain an air seal with these moderately high negative static pressures.

The hopper throat must be sized to allow for adequate solids flow. Solids bridging in the hoppers might occur when the throat is undersized. The necessary size of the throat depends on the sizes of particles collected, the tendency of particles to agglomerate in the hopper, and the temperature of the solids being withdrawn from the hopper. It is common practice to use throats of at least 10 inches diameter. In some large units, the throats are in the range of 12 to 24 inches.

The hopper walls must be sloped properly to allow for solids movement toward the hopper throat. Generally hopper valley angles are at least 60 degrees. This severe slope minimizes the tendency for material to cling to the walls. It is also helpful to minimize protrusions into the hopper from the wall. Obstacles such as U-shaped hand holds can provide an initial site for solids accumulation and bridging even when the hopper walls are properly sloped.

Strike plates are reinforced, “anvil-like” plates mounted on the exterior hopper walls in an area near the hopper throat. These plates protrude through any thermal insulation and outer lagging present around the hopper wall. The purpose of these plates is to provide a site where operators can apply a moderate force to dislodge solids accumulating on the side walls or bridging over the hopper throats. Without these strike plates, operators might be tempted to use a sledge hammer on the unreinforced hopper wall. Over time, the use of a sledge hammer on the unprotected hopper wall causes it to bulge inward. The hammer-

related deflections can choke off the approach to the throat and provide sites for more severe solids accumulation. Mounting a strike plate provides an inexpensive means to minimize this hopper discharge problem.

On large mechanical collector systems, an electric vibrator can be used in lieu of a strike plate or in combination with the strike plate. The electric vibrator is used whenever the solids discharge valves are operating in order to gently force solids in the hopper to flow toward the hopper throat. Electrical vibrators are usually not economically reasonable for very small mechanical collector systems.

Thermal insulation is used around most mechanical collectors serving combustion sources. This helps to keep the solids hot and free flowing in the hoppers. It also minimizes stresses caused when the interior surface of metal is exposed to the 250°F to 600°F gas stream temperature while the exterior surface is exposed to ambient temperatures. It is common to install 2 to 4 inches of either mineral wool or fiberglass as insulating material around hoppers. In some cases, designers include an air gap and air stops under the thermal insulation to improve the insulating effect.

Large multi-cyclone collectors can be vulnerable to a gas flow problem termed cross-hopper gas movement. The potential for the gas flow problem is created by the unequal heights of the outlet tubes as shown in Figure 7-15.

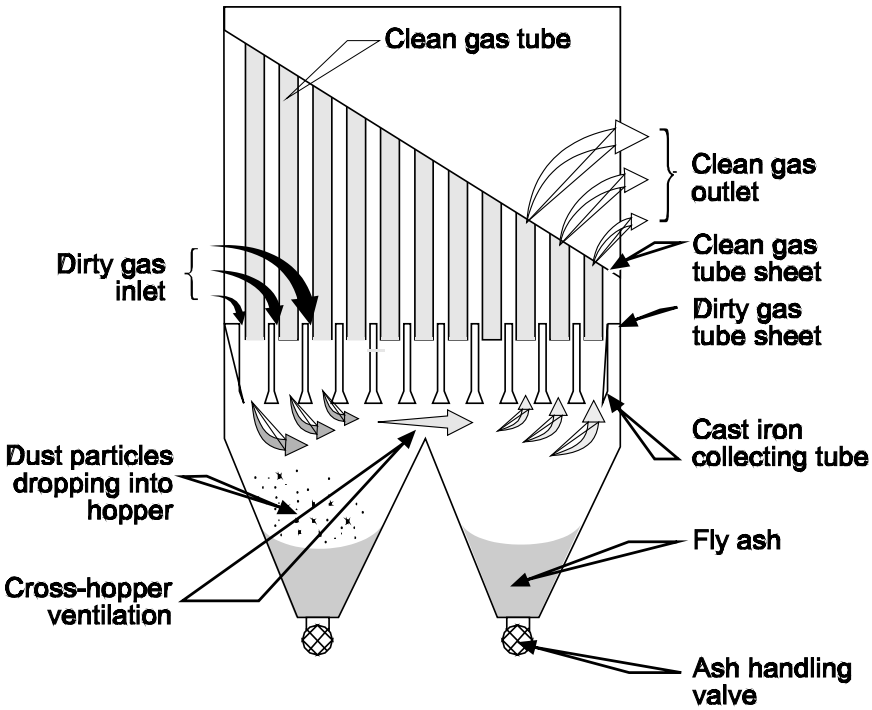

Figure 7-15. Cross-hopper gas flow (Reprinted by permission of Schmidt Associates, Inc.)

The gas in the first several rows of the collectors has higher gas flow resistance in the outlet tubes than the gas in the last several rows. Accordingly, the path of least resistance for the gas in the first several rows can be to pass downward through the dust discharge points, across the hopper, and up through the tubes in the back rows. This flow pattern has an impact that is very similar to air infiltration. The gas passing across the top of the hopper can reentrain particulate matter and disrupt the vortices in the tubes subject to

the upward flow. It is usually corrected by placing gas flow-restricting baffles in the hoppers (Figure 7-16).

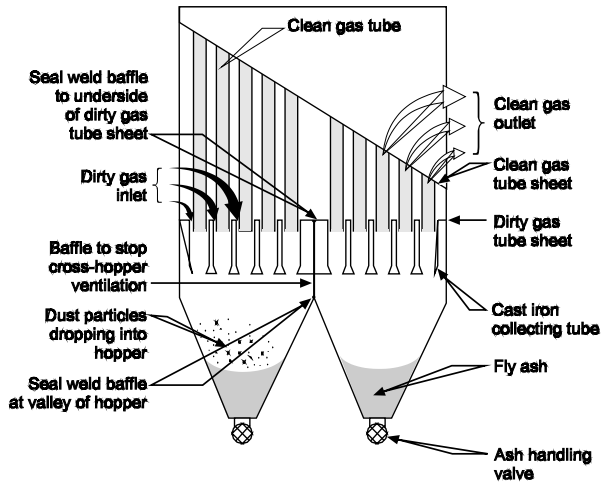

Figure 7-16. Hopper baffles to prevent cross-hopper flow
(Reprinted by permission of Schmidt Associates, Inc.)

An alternative technique for treating cross-hopper flow is to withdraw a small gas stream from the hopper area as shown in Figure 7-17 and treat this gas stream in a separate collector. Particulate matter removal problems are eliminated by capturing the gas moving across the hopper and the ambient air leaking into the hopper.

The gas stream withdrawn from the hopper does not have the opportunity to rise upward through the back rows of tubes and disrupt the vortices. A small pulse jet baghouse is often used to treat this gas stream withdrawn from the multi-cyclone hopper. The quantity of gas treated in these units is usually 10% to 20% of the total gas stream. These units are often termed side-stream or hopper ventilation systems. There are a number of side-stream systems. The main differences between the systems involve the gas pick-up design in the hopper.

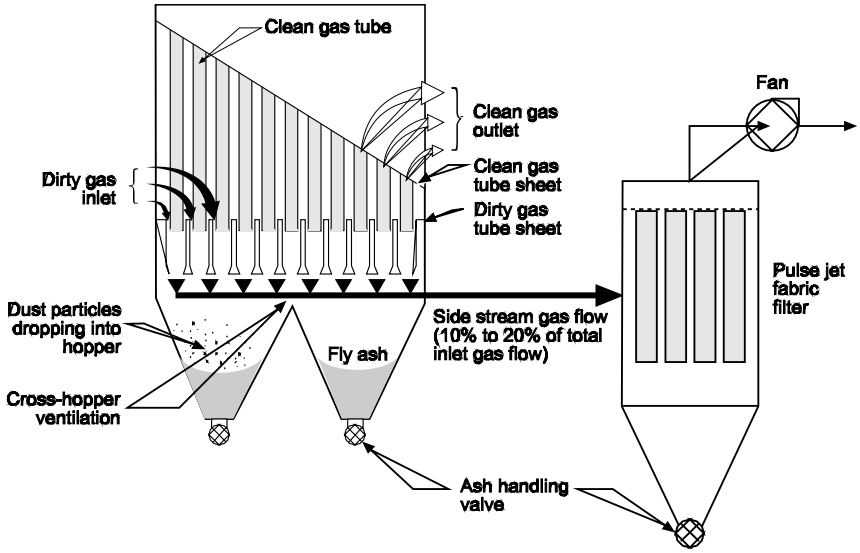

Figure 7-17. Side stream baghouses

Review Exercises

Types and Components of Mechanical Collectors

1. What is the normal range of inlet gas stream velocities to large diameter cyclones?
   a. 5 to 10 feet per second
   b. 20 to 50 feet per second
   c. 5 to 10 feet per minute
   d. 20 to 50 feet per minute

2. What is the purpose of using a solids discharge valve on the hoppers of both large diameter cyclones and multi-cyclone collectors? Select all that apply.
   a. Minimize air infiltration into the cyclone
   b. Minimize the risk of fires
   c. Maintain solids flow out of the hopper
   d. Answers b and c
   e. Answers a, b, and c

3. What design feature initiates the spinning gas flow in a large diameter cyclone?
   a. Spinner vanes
   b. Gravity
   c. Tangential gas inlet
   d. None of the above

4. Which type of mechanical collectors has higher radial velocities?
   a. Large diameter cyclones
   b. Multi-cyclones

5. What is the purpose of the clean side tube sheet in a multi-cyclone collector?
   a. Support the cyclone tubes
   b. Separate the inlet gas stream from the outlet (treated) gas stream
   c. Separate the outlet (treated) gas stream from the hopper
   d. None of the above

6. Approximately what percentage of the multi-cyclone unit static pressure drop occurs across the spinner vanes?
   a. 25%
   b. 50%
   c. 75%
   d. 90%
   e. 95%

7. What is the typical number of complete turns (360 degree) achieved in a large diameter cyclone operating with a normal inlet gas velocity?
   a. One-half to three
   b. Two to five
   c. Five to ten
   d. Greater than ten

8. What is the typical range in the diameters of multi-cyclone tubes?
   a. 1 to 6 inches
   b. 6 to 12 inches
   c. 12 to 18 inches
   d. 18 to 24 inches

9. Must multi-cyclone tubes be oriented vertically (inlet at top, cyclone discharge at bottom) in order to operate properly?
   a. Yes
   b. No

10. Why is it important to fabricate the outlet extension tubes of multi-cyclone collectors from abrasion resistant material?
   a. Minimize abrasion caused by the inlet gas stream
   b. Minimize abrasion caused by the outlet gas stream
   c. Minimize fracturing the inlet particulate matter
   d. All of the above.

Operating Principles of Mechanical Collectors

11. The performance of a mechanical collector is related to the _____ of the particle diameter.
   a. First power
   b. Second power
   c. Third power
   d. Performance is independent of particle size

12. The performance of a mechanical collector is related to the _____ of the radial gas velocity.
   a. First power
   b. Second power
   c. Third power
   d. Performance is independent of radial gas velocity

13. Static pressure drop across a mechanical collector is related to the _____ of the gas flow rate.
   a. First power
   b. Second power
   c. Third power
   d. Static pressure drop is independent of gas flow rate

14. Typical static pressure drops in a multi-cyclone collector are _____.
    a. 1 to 3 in. W.C.
    b. 2 to 6 in. W.C.
    c. 1 to 3 psig
    d. 2 to 6 psig

15. Multi-cyclone collectors are capable of effectively removing particles down to approximately _____ micrometers.
    a. 0.5 micrometers
    b. 3 micrometers
    c. 10 micrometers
    d. 20 micrometers
    e. 50 micrometers

Design and Sizing of Mechanical Collectors

16. What is the particle size-removal efficiency curve for a large diameter cyclone if it has a diameter of 1 ft, an inlet gas velocity of 42 ft/sec, and an operating temperature of 200°F? The material being processed has sizes ranging from 10 to 100 micrometers. The particle density is 70 lbs/ft^3. If necessary to solve the problem, assume that the water vapor content is 10%, and the oxygen concentration is 6%. Assume the gas stream spins one complete rotation within the cyclone.

17. What is the effect on the cyclone evaluated in Problem 16 if the inlet velocity increases from 42 ft/sec to 50 ft/sec due to an increase in the gas flow rate?

18. Using the mass distribution shown in the following table, calculate the overall particulate matter collection efficiency for the cyclone operating in accordance with the conditions in Problem 17.

Particulate Mass Distribution	
Size Range	**% of Mass**
5 to 15	1
15 to <25	3
25 to <35	9
35 to <45	13
45 to <55	24
55 to <65	29
65 to <75	15
75 to < 85	4
85 to <115	2
Total	100%

19. Using the Leith-Licht equations (7-7 through 7-21) in the form of the spreadsheet provided, calculate the efficiency for removing a 7 micrometer sized particle in a cyclone having the following dimensions and gas flow conditions.

$_p$	= particle density = 65 lb_m/ft^3
a	= cyclone inlet height = 2 feet
b	= cyclone inlet width = 1 foot
D	= cyclone body diameter = 4 feet
H	= overall cyclone height = 8 feet
h	= height of upper cylindrical body of cyclone = 2.5 feet
B	= outlet duct diameter for dust = 1 foot
S	= outlet length = 1.5 feet
D_e	= gas outlet diameter = 1 foot
Q	= gas flow rate = 2000 ACFM
	= gas viscosity = 1.5×10^{-5} lb/ft-sec
T	= gas temperature = 150°F
O_2	= oxygen concentration = 20.9%
H_2O	= moisture concentration = 5%

20. Estimate the static pressure drop across a mechanical collector using the equation proposed by Leith (provided below). Use the following data in solving the problem.

$$\Delta p = \frac{0.0027Q^{2}}{k_c D_e B_c H_c \left(\frac{L_c}{D_c}\right)^{\frac{1}{3}} \left(\frac{Z_c}{D_c}\right)^{\frac{1}{3}}}$$

Where:

Δp	= pressure drop
Q	= volumetric flow rate = 2,000 ACFM
k_c	= dimensionless factor that is descriptive of the cyclone = 2
Z_c	= height of cyclone bottom cone = 2 feet
L_c	= height of cyclone body = 4 feet
D_c	= cyclone body diameter = 1foot
H_c, B_c	= inlet height and inlet width = 0.5 and 0.5 feet
D_e	= outlet tube diameter = 0.25 feet

Review Answers

Types and Components of Mechanical Collectors

1. What is the normal range of inlet gas stream velocities to large diameter cyclones?

   b. 20 to 50 feet per second

2. What is the purpose of using a solids discharge valve on the hoppers of both large diameter cyclones and multi-cyclone collectors? Select all that apply.

   e. Answers a, b, and c

3. What design feature initiates the spinning gas flow in a large diameter cyclone?

   c. Tangential gas inlet

4. Which type of mechanical collectors has higher radial velocities?

   b. Multi-cyclones

5. What is the purpose of the clean side tube sheet in a multi-cyclone collector?

   b. Separate the inlet gas stream from the outlet (treated) gas stream

6. Approximately what percentage of the multi-cyclone unit static pressure drop occurs across the spinner vanes?

   d. 90%

7. What is the typical number of complete turns (360 degree) achieved in a large diameter cyclone operating with a normal inlet gas velocity?

   a. One-half to two

8. What is the typical range in the diameters of multi-cyclone tubes?

   b. 6 to 12 inches

9. Must multi-cyclone tubes be oriented vertically (inlet at top, cyclone discharge at bottom) in order to operate properly?

   b. No

10. Why is it important to fabricate the outlet extension tubes of multi-cyclone collectors from abrasion resistant material?

    a. Minimize abrasion caused by the inlet gas stream

Operating Principles of Mechanical Collectors

11. The performance of a mechanical collector is related to the _____ of the particle diameter.

    b. Second power

12. The performance of a mechanical collector is related to the _____ of the radial gas velocity.

    b. Second power

13. Static pressure drop across a mechanical collector is related to the _____ of the gas flow rate.

    b. Second power

14. Typical static pressure drops in a multi-cyclone collector are _____.

    b. 2 to 6 in. W.C.

15. Multi-cyclone collectors are capable of effectively removing particles down to approximately _____ micrometers.

    b. 3 micrometers

Design and Sizing of Mechanical Collectors

16. What is the particle size-removal efficiency curve for a large diameter cyclone if it has a diameter of 1 ft, an inlet gas velocity of 42 ft/sec, and an operating temperature of 200°F? The material being processed has sizes ranging from 10 to 100 micrometers. The particle density is 70 lbs/ft^3. If necessary to solve the problem, assume that the water vapor content is 10%, and the oxygen concentration is 6%. Assume the gas stream spins one complete rotation within the cyclone.

    Solution:

    The first step in using the cut diameter approach is to estimate the cut diameter under the stated operating conditions. The cut diameter is calculated using Equation 7-21. The particle size-efficiency estimates are shown in the table provided in this solution.

    The gas viscosity at 200°F can be estimated using Equation 2-8.

    $$\mu = 51.05 + 0.207T_s + 3.24x10^{-5}(T_s)^2 - 74.14x + 53.417y$$

    Where:

    μ = fluid viscosity (micropoise)
    T_s = stack temperature (°R)
    x = water vapor content of gas stream (fraction)
    y = oxygen content of gas stream (fraction)

    $= 197 \times 10^{-6}$ gm/cm-sec $= 1.33 \times 10^{-5}$ lb_m/ft-sec

    The air density at 200°F can be calculated from the ideal gas flow or by using following ratio.

$$\rho_{air@200F} = \rho_{air@68F}\left(\frac{528\ °R}{460\ °R + 200\ °F}\right)$$

$$\rho_{air@200F} = 0.075\ \frac{lb_m}{ft^3}\left(\frac{528\ °R}{460\ °R + 200\ °F}\right) = 0.06\ \frac{lb_m}{ft^3}$$

$$[d_p]_{cut} = \sqrt{\frac{9\mu B_c}{2\pi n_t v_i(\rho_p - \rho_g)}}$$

n_t = effective number of turns (one for large cyclone)
v_i = inlet gas velocity, 42 ft/sec
$_p$ = particle density, 70 lb_m/ft^3
$_g$ = gas density, 0.060 lb_m/ft^3
B_c = cyclone inlet width, 1 ft
$[d_p]_{cut}$ = 0.0000804 ft = 24.5 m

Efficiency Estimates		
$[d_p]_i$, m	$[d_p]_i/[d_p]_{cut}$ (based on $[d_p]_{cut}$ = 24.5)	Efficiency, $[d_p]_i$ (based on Fig. 7-13)
10	0.41	11
20	0.82	41
30	1.22	55
40	1.63	68
50	2.04	78
60	2.45	84
70	2.86	90
80	3.27	92
100	4.08	96

17. What is the effect on the cyclone evaluated in Problem 16 if the inlet velocity increases from 42 ft/sec to 50 ft/sec due to an increase in the gas flow rate?

Solution:

The gas viscosity and gas density remain the same from Problem 16.

n_t = effective number of turns (one for large cyclone)
v_i = inlet gas velocity, 50 ft/sec
$_p$ = particle density, 70 lb_m/ft^3
$_g$ = gas density, 0.060 lb_m/ft^3
B_c = cyclone inlet width, 1 ft
$[d_p]_{cut}$ = 0.0000738 ft = 22.5 m

Efficiency Estimates		
$[d_p]_i$, m	$[d_p]_i/[d_p]_{cut}$ (based on $[d_p]_{cut}$ = 22.5)	Efficiency, $[d_p]_i$ (based on Fig. 7-13)
10	0.44	14
20	0.89	43
30	1.33	58
40	1.78	72
50	2.22	82
60	2.67	88
70	3.11	92
80	3.56	94
100	4.44	97

18. Using the mass distribution shown in the following table, calculate the overall particulate matter collection efficiency for the cyclone operating in accordance with the conditions in Problem 17.

Particulate Matter Distribution	
Size Range	% of Mass
5 to 15	1
15 to <25	3
25 to <35	9
35 to <45	13
45 to <55	24
55 to <65	29
65 to <75	15
75 to < 85	4
85 to <115	2
Total	100%

Solution:

The mass distribution should be multiplied by the efficiency values determined in Problem 17.

Calculation of Overall Particulate Matter Collection Efficiency				
Size Range	**% of Mass**	**Mid-Range Size**	**Efficiency (from Problem 17)**	**% of Mass Collected**
5 to 15	1	10	14	0.1
15 to <25	3	20	43	1.3
25 to <35	9	30	58	5.2
35 to <45	13	40	72	9.4
45 to <55	24	50	82	19.7
55 to <65	29	60	88	25.5
65 to <75	15	70	92	13.8
75 to < 85	4	80	94	3.8
85 to <115	2	100	97	1.9
Total	100%	N/A	N/A	80.7

The overall mass efficiency calculated by this approach is 80.7%.

19. Using the Leith-Licht equations (7-5 through 7-21) in the form of the spreadsheet provided, calculate the efficiency for removing a 7 micrometer sized particle in a cyclone having the following dimensions and gas flow conditions.

Where:

$_p$ = particle density = 65 lb_m/ft^3
a = cyclone inlet height = 2 ft
b = cyclone inlet width = 1 ft
D = cyclone body diameter = 4 ft
H = overall cyclone height = 8 ft
h = height of upper cylindrical body of cyclone = 2.5 ft
B = outlet duct diameter for dust = 1 ft
S = outlet length = 1.5 feet
D_e = gas outlet diameter = 1 ft
d_p = particle diameter = 7 micrometers
Q = gas flow rate = 2000 ACFM
= gas viscosity = 1.5 x 10^{-5} lb/ft-sec
T = Gas temperature = 150°F
O_2 = oxygen concentration = 20.9%
H_2O = moisture concentration = 5%

Solution:

The Leith-Licht equation is used to estimate the efficiency for a given particle size. The collection efficiency is 0.48 (fractional) or, 48%.

20. Estimate the static pressure drop across a mechanical collector using the equation proposed by Leith (Provided below). Use the following data in solving the problem.

$$\Delta p = \frac{0.0027Q^{2}}{k_c D_e B_c H_c \left(\frac{L_c}{D_c}\right)^{\frac{1}{3}} \left(\frac{Z_c}{D_c}\right)^{\frac{1}{3}}}$$

Solution:

It is necessary to convert all of the dimensions to centimeters.

p	= pressure drop (cm W.C.)
Q	= volumetric flow rate = 2,000 ACFM
k_c	= dimensionless factor which is descriptive of the cyclone = 2
Z_c	= height of cyclone bottom cone = 2 ft = 60.96 cm
L_c	= height of cyclone body = 4 ft = 121.92 cm
D_c	= cyclone body diameter = 1 ft = 30.48 cm
H_c B_c	= inlet height and inlet width = 0.5 and 0.5 ft = 15.24 cm
D_e	= outlet tube diameter = 0.25 ft = 7.62 cm

Static pressure drop = 1.53 cm of water = 0.602 in W.C.

Bibliography

Koch, W.L., and D. Leith. *New Design Approach Boosts Cyclone Efficiency.* Chemical Engineering. (November, 1977): 79-88.

Lapple, C.E. *Processes Use Many Collection Types.* Chemical Engineering 58:145-151. 1951.

Leith, D., and D. Mehta. *Cyclone Performance and Design.* Atmospheric Environment 7:527-549. 1973.

Shepard, C.B., and C.E. Lapple. *Flow Pattern and Pressure Drop in Cyclone Dust Collectors.* Industrial Engineering Chemistry 31:972-984. 1939.

Chapter 8

Particulate Matter Emission Testing and Monitoring

Regulatory agencies and industrial facility operators must also have an understanding of particulate matter testing and monitoring to confirm that the sampling ports and continuous emission monitors are properly located and meet U.S. EPA specifications. This chapter provides an introduction to emission testing and opacity monitoring. For more detailed information, students are encouraged to take, EPA APTI Course 450, *Source Sampling for Particulate Pollutants*; and, EPA APTI Course 474, *Continuous Emissions Monitoring*.

8.1 PARTICLE SIZE DISTRIBUTION MEASUREMENT

Particle size distribution is one of the most important factors affecting the performance of particulate matter control systems. Measurement of the size distribution is often necessary in order to prepare equipment design specifications or to analyze performance of existing systems.

Several alternative methods are used to evaluate the particle size distribution of particulate matter in industrial gas streams. An ideal particle measuring device would be able to do the following:

- Measure the exact size of each particle
- Report data instantaneously without averaging data over some specified time interval
- Determine the complete composition of each particle including shape, density, and chemical nature

It would be an extremely difficult task to produce such an instrument. At this time, there are devices that incorporate only one or two of these ideal functions. Various sizing techniques will be examined and compared to such an ideal device, listing advantages and disadvantages of each. While this discussion is not intended to be exhaustive, it will review the more commonly employed methods.

8.1.1 Cascade Impactors

Cascade impactors are used most frequently to determine the particle size distribution of exhaust streams from industrial sources. Cascade impactors utilize the inertia of the particles to separate the particulate matter in the sample gas stream into a number of size categories. Impactors measure the aerodynamic diameter of the particles.

The mechanism by which an impactor operates is illustrated in Figure 8-1. This impactor is constructed using a succession of stages, each containing orifice openings with an impaction slide or collection plate behind the openings. In each stage, the gas stream passes through the orifice opening and forms a jet that is directed toward the impaction plate. The larger particles will impact on the plate if their inertia is large enough to overcome the drag of the air stream as it moves around the plate. Since each successive orifice opening is smaller than those on the preceding stage, the velocity of the air stream, and therefore that of the dispersed particles, is increased as the gas stream advances through the impactor. Consequently, smaller particles eventually acquire enough momentum to break away from the gas streamlines to impact on a plate. A complete particle size classification of the gas stream is therefore achieved.

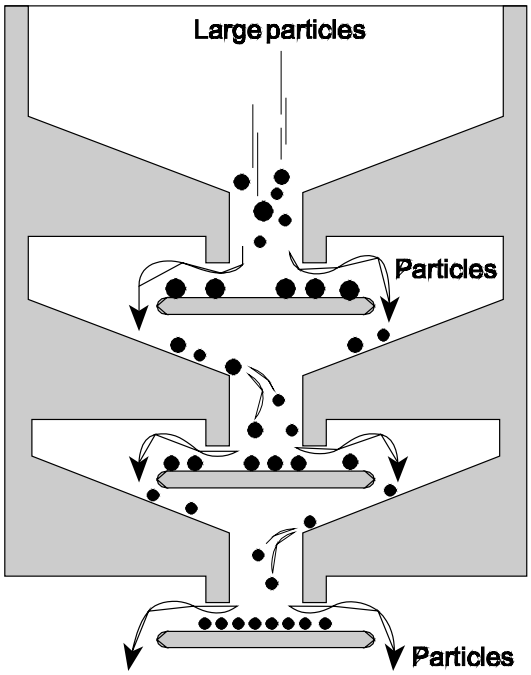

Figure 8-1. Schematic diagram, operation of a cascade impactor

Typical impactors consist of a series of stacked stages and collection surfaces. Depending on the calibration requirements, each stage contains from one to as many as 400 precisely drilled jet orifices, identical in diameter in each stage but decreasing in diameter in each succeeding stage (Figure 8-2).

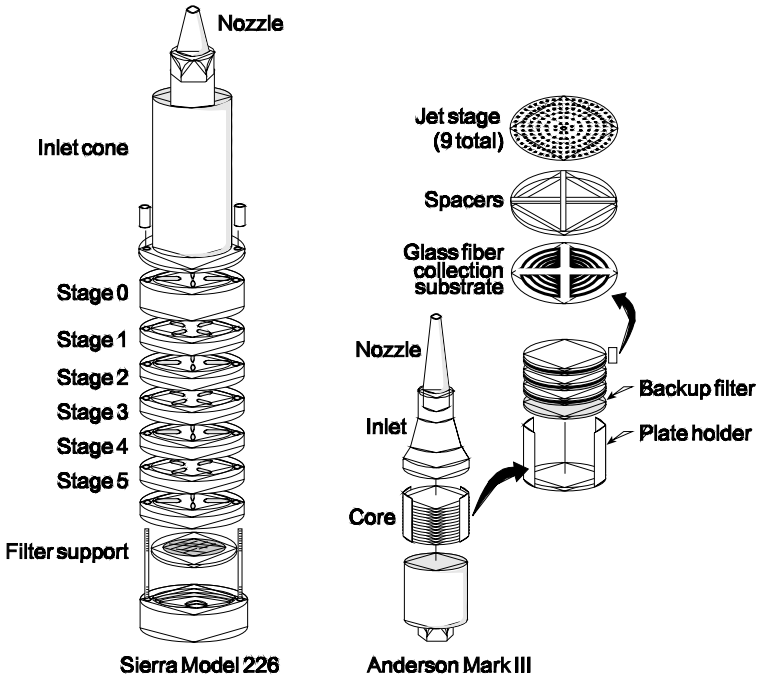

Figure 8-2. Sketches of two commercial types of cascade impactors

Particles are collected on preweighed individual stages, usually filters made of glass fiber or thin metal foil. The sampling period is usually in the range of 5 minutes to 30 minutes depending on the concentration of particulate matter in the gas stream being tested. It is important to avoid excessively long sampling periods because this can lead to the reentrainment of particles initially captured on each stage. This results in a bias to lower-than-true measured particle sizes.

Once the sampling is complete, the collection filters are conditioned and reweighed, yielding particle size distribution data for the various collection stages. Occasionally, there are some dusts that are very difficult to collect and, therefore, require grease on the collection filter for adequate particle capture.

Once the particles have been partitioned into discrete ranges, chemical analyses can be performed on the collected particles.

The effective range for measuring the aerodynamic diameter is generally between 0.3 and 20 m. However, some cascade manufacturers have achieved size fractionalization as small as 0.02 m with the use of 20 or more stages. Factors limiting the accuracy of cascade impactors include particle bounce on the impactor stages, particle reentrainment from the impactor stages, and particle agglomerate fracturing in the impactor jets. The latter problem is caused by the high velocities created by the jets in subsequent stages. Other practical problems include the nucleation of vapors due to heat transfer to the large metal cascade impactor sampling heads and air infiltration into one of more of the numerous sealing surfaces of cascade impactor heads.

Impactors are one of the most commonly used devices for determining particle size because of the impactor's compact arrangement and the readily available sampling equipment.

8.1.2 Microscopy

Various types of microscopy analyses can be performed on samples obtained on filters. The filters are exposed to the gas stream using one of the emission testing procedures described later in this section. The representativeness of the sample on the filter depends in part on the characteristics of the sampling equipment and in part on the adequacy of the sampling procedures. It is important to minimize the sampling times to avoid overloading the filter. Particles should be deposited as a single layer on the filter to the extent possible. The sampling times are usually in the range of one to five minutes.

There are several common types of microscopic analyses used to evaluate particle size. Polarizing light microscopy (PLM) uses visible light that is focused on the particle and magnified in a set of lenses mounted in a conventional microscope (Figure 8-3). With the appropriate lenses and sample preparation techniques, PLM analyses can be used to size particles as small as 3 micrometers.

The size of a particle is estimated by comparing each particle to a scale in the eyepiece, usually calibrated to micrometers. Each particle, presented in a fixed area of the eyepiece, is sized and tallied into a number of size categories. The number of particles sized may range from 100 to several thousand per sample depending on the accuracy desired. This method can be time consuming and extremely tedious. Training is needed to properly identify and size particles using this technique.

The particles are usually collected by deposition on a glass slide or filter. The glass slide or filter is subsequently analyzed by a microscope in the lab. The analyses of size distribution of particles collected in the field and transported to the lab must be viewed with caution. First of all, it is difficult to collect a truly representative sample, and then it is almost impossible to maintain the original size distribution after transfering the samples to laboratory conditions. For example, laboratory measurements cannot determine whether some of the particles existed in the process stream as agglomerates of smaller particles. In spite of the limitations of the microscopic method, this method is useful in the determination of some properties of interest.

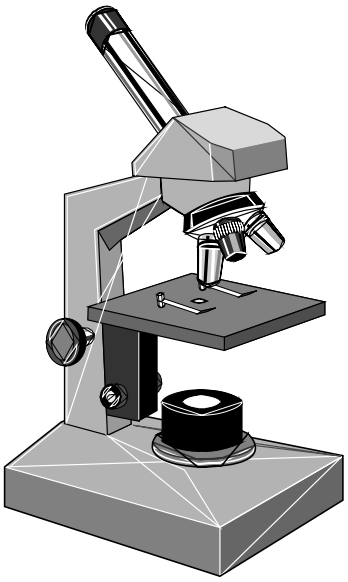

Figure 8-3. Optical microscope used for PLM analyses

Generally speaking, the chemical composition of the particle can not be determined by using an optical microscope. However, a subsequent chemical analysis can be performed on the sample.

Scanning electron microscopy (SEM) can provide greater magnification of the particles than with PLM. With SEM, magnifications of up to a factor of 20,000 is possible. It is possible to resolve particles as small as 0.3 micrometers with normal electron beam energy levels. Furthermore, an electron beam "microprobe" can be used to obtain elemental chemical analyses of individual small particles and even localized areas of large particles. The electron beam analyses are usually termed *Energy Dispersive X-Ray Spectroscopy* or EDX.

As in the case with PLM, particle size distributions determined by SEM involve the comparison of the projected area of the particle with a calibrated graticle mounted into the viewing port for the SEM. A photomicrograph of a sample of flyash on a filter is provided in Figure 8-4.

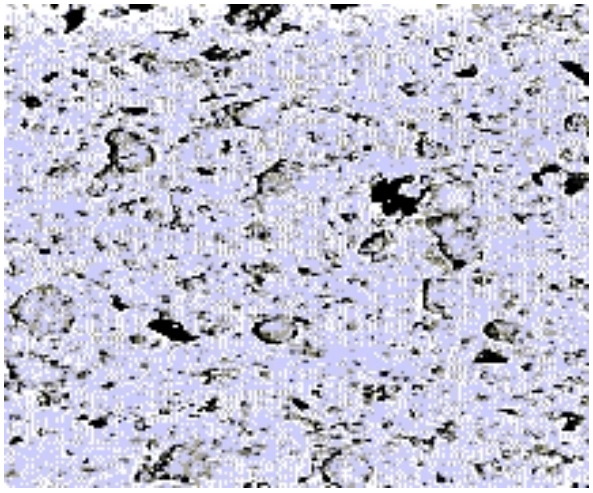

Figure 8-4. SEM photomicrograph of flyash
(Reprinted courtesy of Research Triangle Institute, Inc.)

Typically, 400 or more particles per filter sample section are individually counted to compile a particle size distribution estimate.

8.1.3 Optical Counters

Optical particle counters have not been widely used for particle sizing because they cannot be directly applied to the stack exhaust gas stream. The sample must be extracted, cooled, and diluted before entering the counter. This procedure must be done with extreme care to avoid introducing serious errors in the analyses. A major benefit of an optical counter is the ability to observe emission (particle) fluctuations on a real time, instantaneous basis. Particle sizes as small as 0.3 µm can be determined with an optical counter.

Optical particle counters work on the principle of light scattering. Each particle in a continuously flowing sample stream passes through a small illuminated viewing chamber. Light scattered by the particle is observed by the photodetector during the time the particle is in the viewing chamber (Figure 8-5). The intensity of the scattered light is a function of particle size, shape, and index of refraction. Optical counters give reliable particle size information only when one particle is in the viewing chamber at a time. The simultaneous presence of more than one particle can be interpreted by the photodetector as a larger sized particle. This error can be minimized by maintaining sample dilution ratios to ensure less than 300 particles per cubic centimeter.

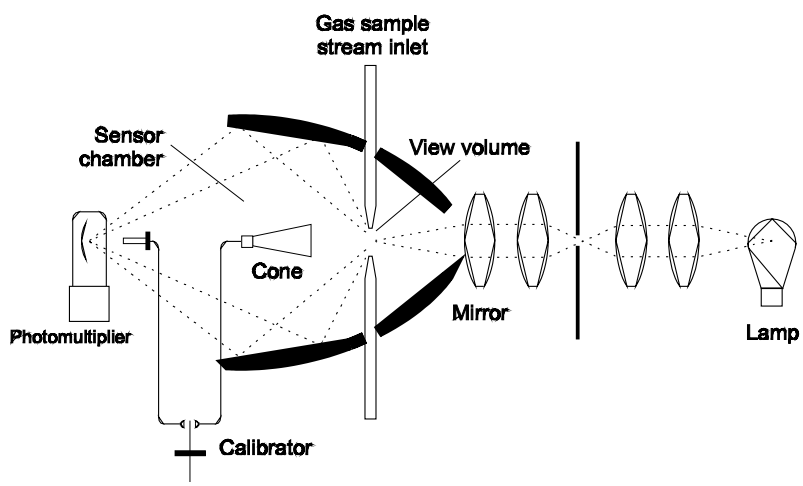

Figure 8-5. Operating principle for an optical particle counter

A drawback of the optical counter is the dependence of the instrument calibration on the index of refraction and the shape of the particle. Errors in counting can also occur due to the presence of high concentrations of very small particles, which are sensitive to the light wavelength used.

8.1.4 Electrical Aerosol Analyzer

The electrical aerosol analyzer (EAA) is an aerosol size distribution measuring device that was commercially developed at the University of Minnesota. The EAA uses an electrical field set at an intensity dependent upon the size and mass of the particle to measure the mobility of a charged aerosol. The analyzer operates by first placing a unipolar charge on the aerosol being measured and then measuring the resulting mobility distribution of the charged particle by means of a mobility analyzer.

One type of EAA is shown in Figure 8-6 (Hewitt, 1957).

Charged particles enter through a narrow passage (A) and experience a radial force toward the central cylinder due to the applied field. The mobility of the charged particles can be measured by moving the sampling groove (B) axially or by varying the applied field.

The EAA has been used for source analysis by pulling a sample from the stack and introducing the gas stream into the analyzer. The instrument requires that enough particles pass through the chamber so that a charge can be detected. The concentration range for the most efficient operation of the EAA is from 1 to 1000 g/m^3. Since stack gas concentrations usually exceed 1000 g/m^3, sample dilution with clean air is required (U.S. EPA, 1979). No information on the chemical composition of the particles is obtainable since the particles are not collected. The major advantage of the EAA is that the instrument can measure particles from 0.003 to 1.0 m in diameter.

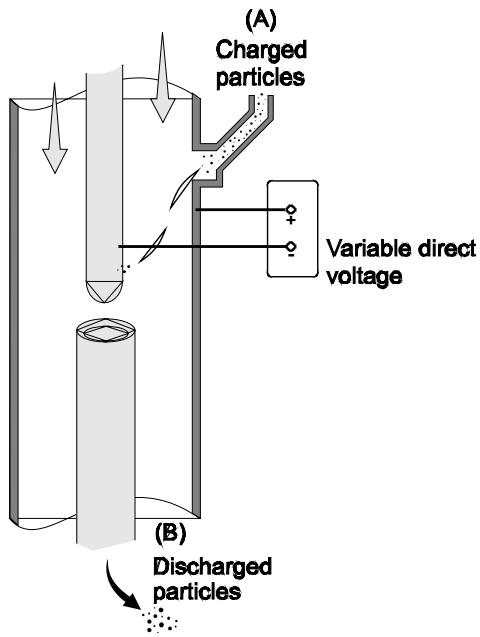

Figure 8-6. Coaxial cylinder mobility analyzer

8.2 EMISSION TESTING PROCEDURES

Compliance with particulate matter emission regulations is typically determined using one of the four U.S. EPA Reference Methods (40 CFR Part 60, Appendix A) intended for particulate matter collection. In these methods, the particulate matter emissions are measured during a set of three one-hour measurements and converted to units such as the following:

- Pounds of particulate matter emitted per hour
- Pounds of particulate matter emitted per million Btu's of heat input into a boiler
- Grains (1/7000th of a pound) of particulate matter per standard cubic meter
- Micrograms of particulate matter per standard cubic meter
- Micrograms of particulate matter per standard cubic meter corrected to 7% oxygen

The data from the three runs of the test are averaged, and the result is compared against the regulatory limit to determine if the source is in compliance.

8.2.1 General Testing Requirements

Particulate matter is especially difficult to collect from a flowing gas stream because some of the particles have significant inertia and may not remain in the gas streamlines while passing around bends or other flow disturbances. The particles can stratify on one side or portion of the gas stream due to their inertia. In order to minimize these problems, all U.S. EPA Reference Methods for particulate matter testing require that the sampling location comply with U.S. EPAMethod 1. This method requires traversing of the sampling location to obtain samples at a number of properly located points. It also specifies that the sampling location be a distance of at least eight stack (or duct) diameters downstream and two stack (or duct) diameters upstream from any flow disturbance. This is often termed the **eight-and-two criteria**. Flow disturbances include but are not necessarily limited to the following:

- Bend
- Expansion
- Contraction
- Visible flame

When the sampling location meets the eight-and-two criteria, the emission test can be conducted with the minimum number of sampling points at that sampling location. Twelve sampling points are required for ducts or stacks greater than 2ft diameter or equivalent diameter (see U.S. EPA Method 1 for ducts less than 2 ft in diameter). The equivalent diameter for rectangular ducts and stacks is calculated using the standard equation for hydraulic diameter.

$$D_e = \frac{2LW}{(L+W)} \tag{8-1}$$

Where:

D_e = equivalent diameter
L = length of rectangular duct or stack
W = width of rectangular duct or stack

U.S. EPA Method 1 permits an alternative approach when it is not possible to satisfy the eight-and-two criteria. To ensure representative sampling when flow disturbances are encountered, U.S. EPA Method 1 requires additional sampling points. The number of points depends on the distance to the closest upstream or downstream flow disturbance. This requirement is specified in Figure 8-7 (Figure 1-1 of U.S. EPA Method 1). Figure 8-7 is use after accurately measuring the distance of the sampling location to upstream and downstream disturbances. The minimum number of points that must be used is indicated by Problem 8-1 shown in Figure 8-8. In the example, the distance to the upstream disturbance is the controlling factor, and the emission test must be conducted using 20 sampling points. Two sampling points 90° apart are needed for circular ducts. Therefore, 10 sampling points per traverse are needed.

The sampling points must divide the stack or duct into equal areas to ensure that the test provides representative data. In the case of rectangular sampling locations, the sampling points divide the cross-sectional area of the sampling location into a number of equal area rectangles. The layout of the sampling grid is specified in Table 1-1 of U.S. EPA Method 1. In the case of circular stacks or ducts, the pattern of the sampling points is based on equal areas of concentric circles. These sampling locations are specified in Table 1-2 of U.S. EPA Method 1, which is reproduced in Figure 8-9, along with an example location pattern when 12 sampling points (six on each traverse) are required.

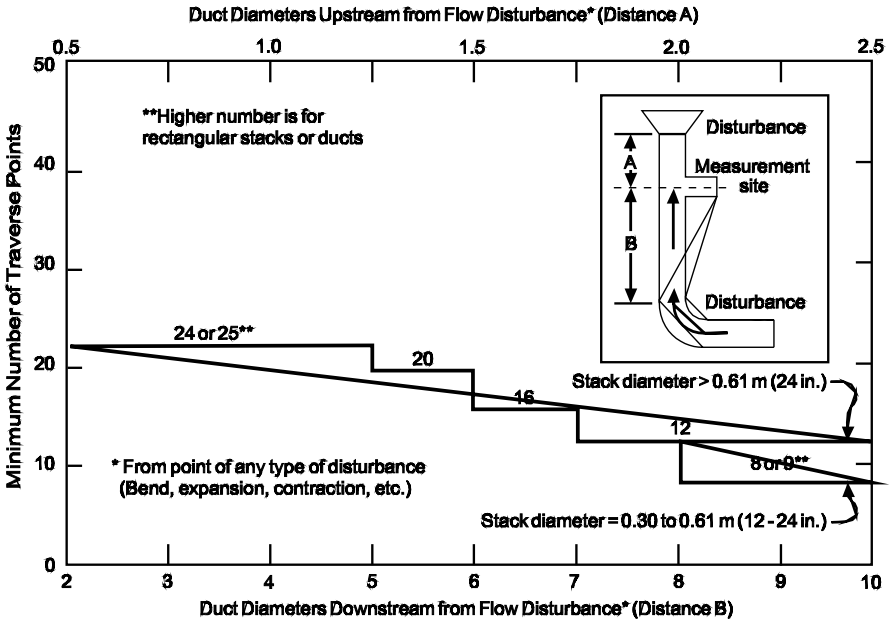

Figure 8-7. Minimum number of traverse points for particulate traverse (Figure 1-1, U.S. EPA Method 1, 40 CFR Part 60, Appendix A)

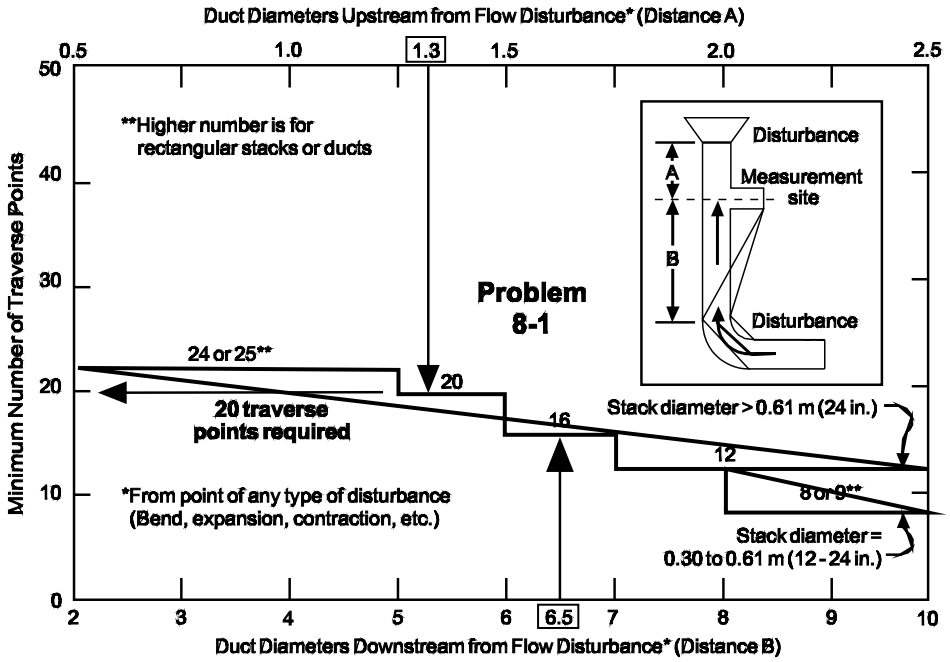

Figure 8-8. Example calculation of the number of sampling points

Pt. 60, App. Meth. 1

Traverse Point	Distance, % of diameter
1	4.4
2	14.6
3	29.6
4	70.4
5	85.4
6	95.6

40 CFR Ch. 1 (7-1-89 Edition)

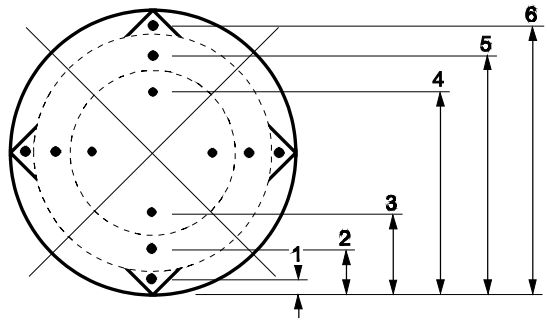

Table 1-2. Location of Traverse Points in Circular Stacks
(Percent of stack diameter from inside wall to traverse point)

Traverse point on a diameter	Number of traverse points on a diameter											
	2	4	6	8	10	12	14	16	18	20	22	24
1	14.6	6.7	4.4	3.2	2.6	2.1	1.8	1.6	1.4	1.3	1.1	1.1
2	85.4	25.0	14.6	10.5	8.2	6.7	5.7	4.9	4.4	3.9	3.5	3.2
3		75.0	29.6	19.4	14.6	11.8	9.9	8.5	7.5	6.7	6.0	5.5
4		93.3	70.4	32.3	22.6	17.7	14.6	12.5	10.9	9.7	8.7	7.9
5			85.4	67.7	34.2	25.0	20.1	16.9	14.6	12.9	11.6	10.5
6			95.6	80.6	65.8	35.6	26.9	22.0	18.8	16.5	14.6	13.2
7				89.5	77.4	64.4	36.6	28.3	23.6	20.4	18.0	16.1
8				96.8	85.4	75.0	63.4	37.5	29.6	25.0	21.8	19.4
9					91.8	82.3	73.1	62.5	38.2	30.6	26.2	23.0
10					97.4	88.2	79.9	71.7	61.8	38.8	31.5	27.2
11						93.3	85.4	78.0	70.4	61.2	39.3	32.3
12						97.9	90.1	83.1	76.4	69.4	60.7	39.8
13							94.3	87.5	81.2	75.0	68.5	60.2
14							98.2	91.5	85.4	79.6	73.8	67.7
15								95.1	89.1	83.5	78.2	72.8
16								98.4	92.5	87.1	82.0	77.0
17									95.6	90.3	85.4	80.6
18									98.6	93.3	88.4	83.9
19										96.1	91.3	86.8
20										98.7	94.0	89.5
21											96.5	92.1
22											98.9	94.5
23												96.8
24												98.9

Figure 8-9. Location of traverse points in a circular stack (Figure 1-3 and Table 1-2 of Method 1, 40 CFR Appendix A, respectively)

At most sampling locations, the gas stream flow is essentially parallel to the side of the stack or duct as shown in Figure 8-10a. However, the gas flow can swirl as shown in Figure 8-10b if the gas stream enters the stack tangentially, or the gas stream passes through equipment such as radial vane mist eliminators which can induce a swirling action. This is termed **cyclonic flow**, and it could prevent accurate particulate matter emission testing. Accordingly, U.S. EPA Method 1 requires a cyclonic flow check prior to the emission test. If the cyclonic flow severity exceeds the value specified in Method 1, the testing organization must either find another sampling location, eliminate the cyclonic flow, or use a complicated sampling procedure called the "alignment" approach. This ensures that the sampling nozzle is oriented properly with respect to the gas stream movement at each sampling point.

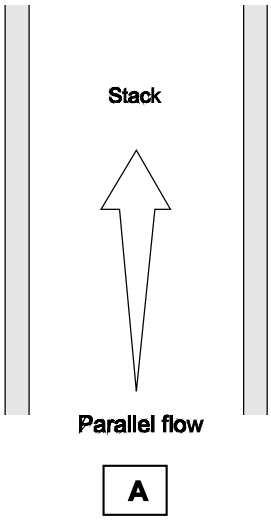

Figure 8-10a. Parallel flow

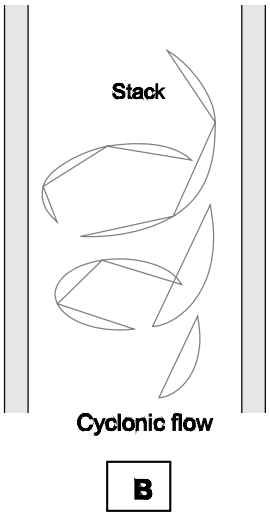

Figure 8-10b. Cyclonic flow

The concentration of the particulate matter in the gas stream collected through the sample probe is determined by the particulate matter sampling system. The total gas flow rate must be measured in order to convert this sample gas particulate matter concentration into one or more of the data formats presented earlier, such as the concentration of particulate matter in the actual gas stream or the total emission rate per hour. The total gas flow rate is determined by U.S. EPA Method 2 which is conducted simultaneously with the particulate matter emission test. The probe used for the U.S. EPA Method 2 gas flow rate measurement is mounted near the probe for the particulate matter sampling train so that the particulate matter sample and the gas flow rate measurement can be made at the same points while traversing the sampling location. U.S. EPA Method 2 specifies that either a standard pitot tube or a Type S pitot tube be used for the gas flow measurements. An illustration of the probe portion of a Type S pitot tube in front of a particulate matter sampling probe nozzle is shown in Figure 8-11.

The U.S. EPA Method 2 data is recorded on a form similar to the one shown in Figure 8-12. The data needed to calculate the gas flow rate includes the point-by-point velocity pressures, gas stream temperatures, and stack absolute pressures.

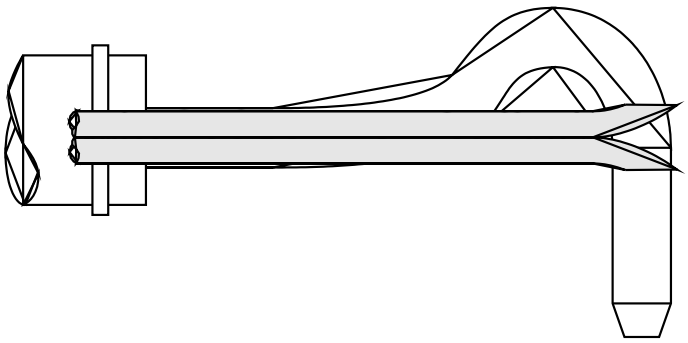

Figure 8-11. Type S pitot tube and sampling nozzle

The total gas flow rate at the sample location is calculated using Equations 8-2 and 8-3.

$$v_s \text{ (average)} = K_p C_p \left(\sqrt{\Delta p}\right)_{avg.} \sqrt{\frac{T_s}{P_s M_s}} \tag{8-2}$$

Where:

v_s = stack gas velocity (average) (ft/sec)
K_p = pitot tube constant (U.S. EPA Method 2), 85.49
C_p = pitot tube coefficient (dimensionless)
$\left(\sqrt{\Delta p}\right)_{Avg.}$ = average of square roots of velocity pressure (in H_20)
M_s = gas stream molecular weight (U.S. EPA Method 3) (lb/lb-mole)
T_s = stack absolute temperature (average) – (°R)
P_s = stack absolute pressure (average) – (in. H_g)

$$Q_s \text{ (average)} = 3600\left(1 - B_{ws}\right) v_s A_s \frac{T_{Std}}{P_{Std}} \frac{P_s}{T_s} \tag{8-3}$$

Where:

Q_s = dry volumetric stack gas flow rate corrected to standard conditions (dscf/hr)
B_{ws} = water vapor content of gas stream (U.S. EPA Method 4), proportion by volume
A_s = area of sampling location (ft^2)
T_{Std} = standard temperature (528°R)
P_{Std} = standard pressure (29.92 in. H_g)
P_s = absolute pressure of gas stream at sampling location (in. H_g)
T_s = stack absolute temperature (average) (°R)

It is apparent that the calculation of the gas flow rate from the pitot tube velocity pressure data also requires information concerning the gas stream molecular weight and moisture content. These are determined using U.S. EPA Methods 3 and 4, which also must be conducted simultaneously with the particulate matter sampling and velocity measurements. The gas molecular weight (dry basis) is determined by measuring the carbon dioxide, oxygen, and carbon monoxide concentrations.

The average molecular weight on a dry basis is determined using Equation 8-4. The molecular weight on a wet basis is calculated by factoring in the moisture content of the stack gas as shown in Equation 8-5.

$$M_d = 0.44\ (\%CO_2) + 0.32\ (\%O_2) + 0.28\ (\%N_2 + \%CO) \tag{8-4}$$

$$M_s = M_d\left(1 - B_{ws}\right) + 18B_{ws} \tag{8-5}$$

The moisture content of the sample gas stream enters the calculations of the gas flow rate in several places. Obviously, this must be measured accurately in order to avoid errors in calculating the total particulate matter emission rate. Moisture content in many industrial gas streams can vary from a low of less than 1% by volume to more than 50% by volume. Moisture is measured using U.S. EPA Method 4. The moisture in the sample gas stream of the particulate matter sampling system is removed by means of condensation in cold impingers and desiccation in a packed impinger bed. The moisture content is determined volumetrically and gravimetrically.

Environmental Protection Agency

Plant	Pt. 60, App. A, Meth. 2
Date Run No.	
Stack Diameter or Dimensions, m (in.)	
Barometric Pressure, mm Hg (in. Hg)	
Cross Sectional Area, m^2 (ft^2)	
Operators	
Pitot Tube I.D. No.	
Avg. Coefficient, C_p =	
Last Date Calibrated	Schematic of Stack Cross Section

Traverse Point No.	Velocity Head, Δp mm (in.) W.C.	Stack Temperature t_s °C (F) T_s °K (R)	Pg mm Hg (in. Hg)	$\sqrt{\Delta p}$
	Average			

Figure 8-12. Velocity traverse form

A schematic of a complete particulate matter sampling train is shown in Figure 8-13. As shown in the upper left of this drawing, the pitot tube for the U.S. EPA Method 2 gas flow rate measurement is mounted close to the probe for the particulate matter sampling train. The moisture in the sample gas stream is removed in a set of impingers immersed in ice. The last impinger in the series is filled with a desiccant to complete the moisture collection.

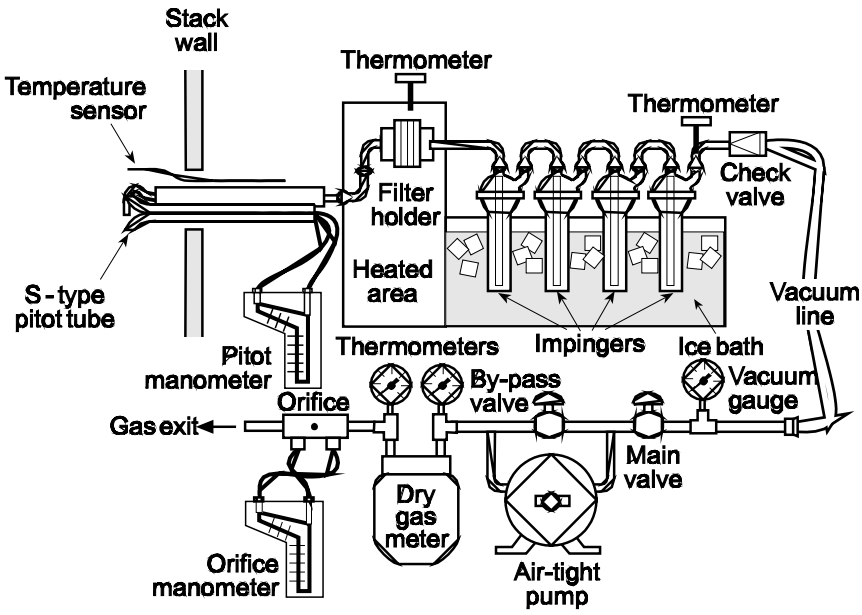

Figure 8-13. Complete sampling train for particulate emission testing (Figure 5-1, 40 CFR 60 Appendix A)

It is important to note that the sample gas is pulled through the sampling train by means of a vacuum pump at the end of the sampling assembly. The entire sampling train with the exception of the dry gas meter and the orifice are under negative pressure. This means that ambient air could leak into the sample line and create a significant error in determining the particulate matter concentration in the sample gas stream. Accordingly, all of the U.S. EPA Reference Methods for determining particulate matter emissions include a requirement for leak checking the sampling train immediately following the emission test run (three runs per test). Some of the most common leak sites include the tops of the impingers, the pipe fittings after the filter (U.S. EPA Method 5 type particulate matter measurement), and the connection at the end of the sampling probe.

The sample gas flow rate through the particulate matter sampling train must be adjusted as the probe is moved from point to point during traversing of the sampling location. Due to the inertial properties of the particulate matter, the velocity of the sample gas entering the end of the probe must be approximately equal to the velocity of the gas stream at the sampling point. When the velocity of the gas entering the sampling nozzle is exactly equal to the velocity of the gas stream, *isokinetic sampling* is achieved. If the velocity into the nozzle is too high, the gas will be pulled in from too large of an area. This is called *over-isokinetic sampling*. It leads to lower-than-actual particulate matter measurements since many of the large particles fly past the sample probe as the gas is drawn into the probe. Gas velocities into the nozzle that are too low can also cause significant errors. This is termed *under-isokinetic sampling*. Under-isokinetic sampling results in greater-than-actual particulate matter concentrations since large particles fly into the probe as part of the gas stream flows around the probe. During most particulate matter emission tests, the sampling velocities must be maintained at an average of 90% to 110% of the isokinetic rate in order to avoid these errors. This is accomplished by choosing a probe nozzle with the appropriate diameter and by adjusting the sampling gas flow rate while moving from point to point.

Both over-isokinetic and under-isokinetic sampling are illustrated in Figure 8-14.

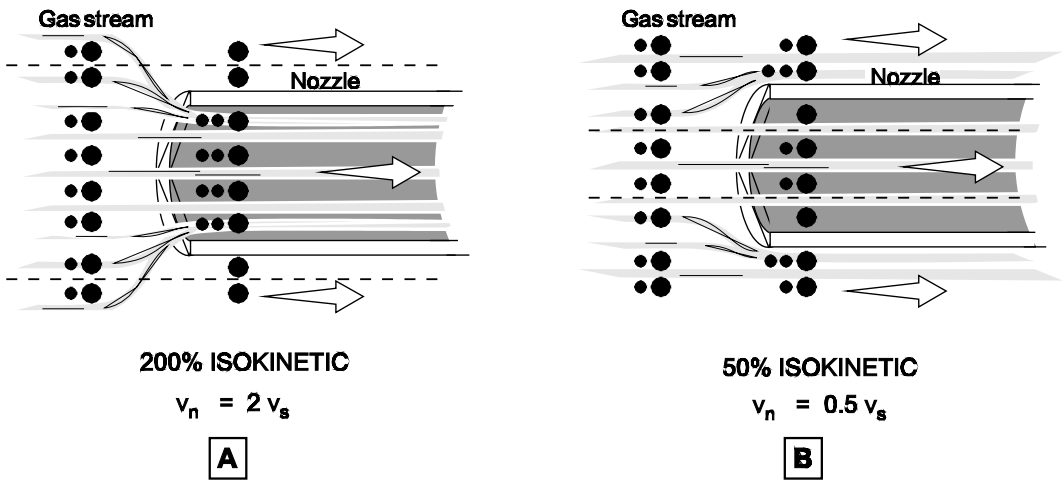

Figure 8-14. Isokinetic sampling bias

8.2.2 Total Particulate Matter Emissions

There are two main test procedures used for measuring total particulate emissions: U.S. EPA Methods 5 and Method 17. They differ with respect to the means used to filter the particulate from the sample gas stream.

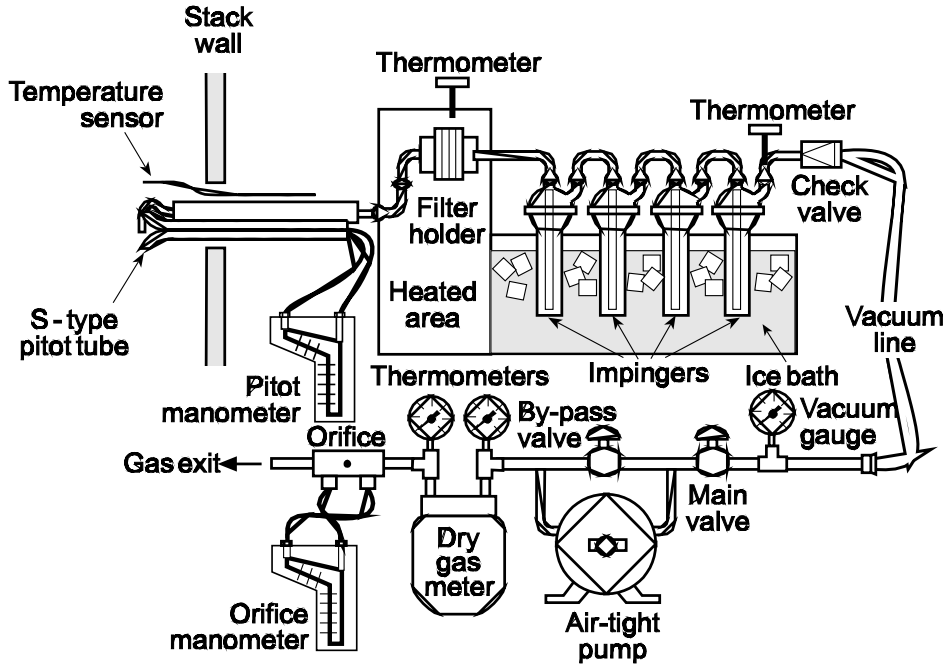

Figure 8-15. Method 5 particulate sampling train
(Figure 5-1, 40 CFR 60 Appendix A)

The U.S. EPA Method 5 sampling train is shown in Figure 8-15. The filter is kept in a hot box which must be maintained at 248 ± 25°F. The probe is also heated to this temperature. The total quantity of particulate matter captured during the emission measurement run is determined by adding the weight gain of the filter and the quantity of solids washed from the nozzle, the probe, and the front half of the filter holder. Only pollutants that are in a solid and/or liquid form at 248 ± 25°F are captured in these areas. Vapor phase materials that can pass through the probe and filter at this temperature are captured in the impingers. The impinger "catch" is not usually counted as particulate matter.

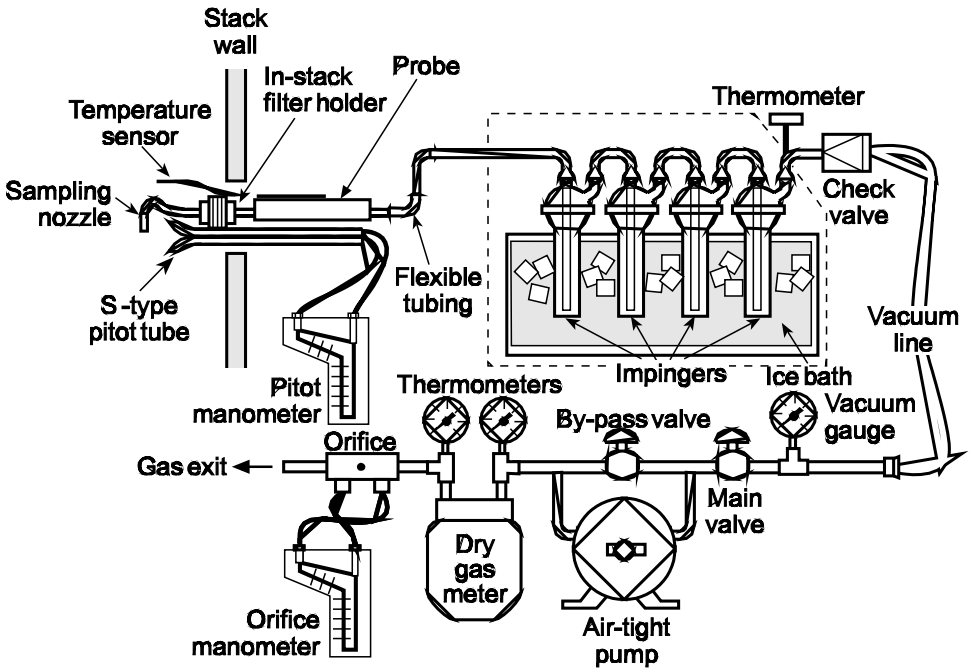

Figure 8-16. Method 17 particulate sampling train
(Figure 17-1, 40 CFR 60 Appendix A)

The U.S. EPA Method 17 sampling train is shown in Figure 8-16. In this case, the particulate matter filter is mounted in a holder that is inserted in the stack. With this approach, the filter is at approximately the same temperature as the stack gases being tested. The particulate matter concentration measured using U.S. EPA Method 17 can be different than that measured by U.S. EPA Method 5 since particulate matter can both condense and vaporize depending on the temperature. The temperature range that is permissible for a U.S. EPA Method 17 test depends on the specific requirements included in the regulations for the type of source being tested.

The total particulate matter emissions calculated from U.S. EPA Method 5 and Method 17 data are based on measurements from U.S. EPA Methods 2 through 4, which are conducted simultaneously.

8.2.3 PM_{10} Particulate Matter Emissions

In 1986, the U.S. Environmental Protection Agency revised the National Ambient Air Quality Standards (NAAQS). The total suspended particulate matter concentration was dropped in favor of an ambient standard based on the concentration of particles less than or equal to 10 m in diameter. This is called the **PM_{10} standard**. This standard was promulgated since health effects research had demonstrated that particles less than 10 m were primarily responsible for adverse health effects. Also, the ambient concentrations of total particulate matter in some rural areas and arid areas were dominated by relatively

non-toxic emissions from roads and from natural sources. Many states have now revised the particulate matter emission regulations to limit emissions of particulate matter less than 10 m rather than the total particulate matter emissions. Accordingly, the U.S. EPA has developed and promulgated two reference methods to permit the measurement of PM_{10} particulate matter emissions from stationary sources. These methods are 201 and 201A (40 CFR Appendix A). They are similar to the other particulate matter emission measurement methods in that they also use U.S. EPA Methods 1 through 4 to determine the appropriate sampling location and to provide the supporting data for the calculations. They differ from total suspended particulate matter emission measurement techniques in that large particles are removed before the sample gas reaches the filter.

A U.S. EPA Method 201A sampling assembly is shown in Figure 8-17. The gas stream enters through a nozzle, which is identical to that used in Methods 5 and 17. The sample gas then enters a cyclone which removes the particulate matter larger than 10 m.

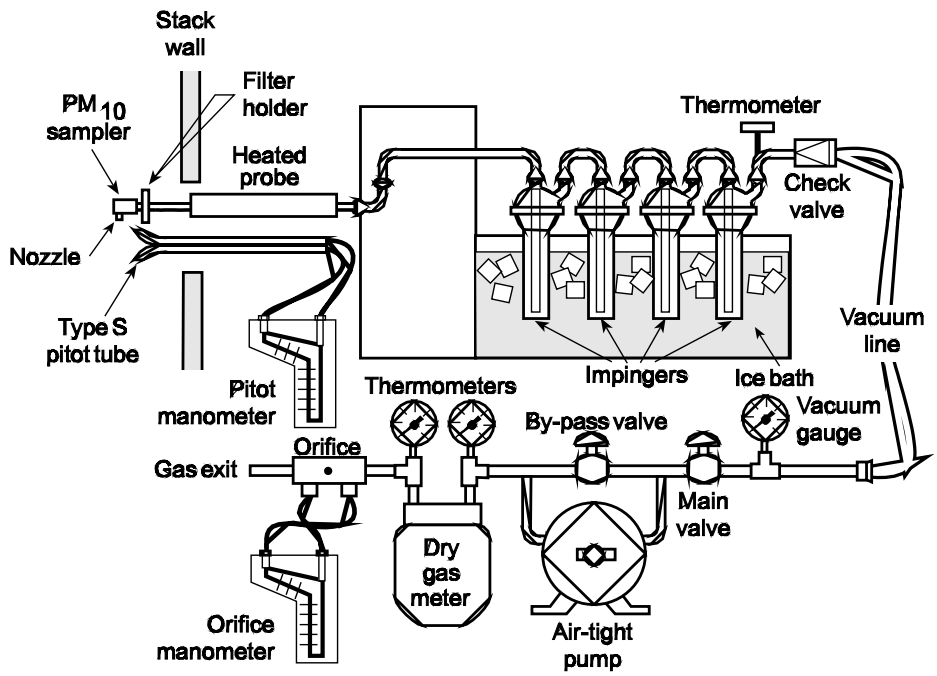

Figure 8-17. Method 201A particulate sampling train
(Figure 17-1, 40 CFR 60 Appendix A)

This large material is collected in a cone-shaped receiver at the bottom of the cyclone. The sample gas with particulate equal to or less than 10 m passes through the downcomer in the cyclone that leads to the filter. All particulate in the downcomer, on the filter, and in the front half of the filter holder is counted as PM_{10} particulate. The 201A test is conceptually similar to U.S. EPA Method 17 in that the cyclone and filter holder are usually mounted in the stack. When used in this manner, the particulate determined by U.S. EPA Method 201A are those materials that are in a solid or liquid form at the stack temperature.

The performance of the cyclone is strongly dependent on the gas flow rate. Accordingly, Method 201A includes specifications concerning the acceptable minimum and maximum gas flow rates for the sampling train. The sample gas flow rate must be maintained in this range and must also provide for isokinetic sampling conditions at the nozzle. Since it is difficult to balance these two gas flow requirements, the method allows for a wider range of isokinetic conditions than U.S. EPA Methods 5 and 17. During a Method 201A test, the isokinetic range is 80% to 120%.

The alternative method for determining PM_{10} emissions is Method 201. This method has a sample gas recirculation loop to maintain the gas flow rate through the cyclone at optimum conditions. Otherwise, this method is identical to U.S. EPA Method 201A.

8.2.4 $PM_{2.5}$ Particulate Matter

In 1997, the U.S. EPA promulgated new National Ambient Air Quality Standards concerning $PM_{2.5}$ particulate matter. This is solid and liquid particles having an aerodynamic diameter equal to or less than 2.5 micrometers. The test procedure being developed for $PM_{2.5}$ is an extension of Method 201A used for the measurement of PM_{10} particulate matter. The EPA proposed sampling train is based on a dual cyclone approach originally developed by Southern Research Institute (1) and modified by Air Control Techniques P.C. (2). This sampling train is illustrated in Figure 8-18.

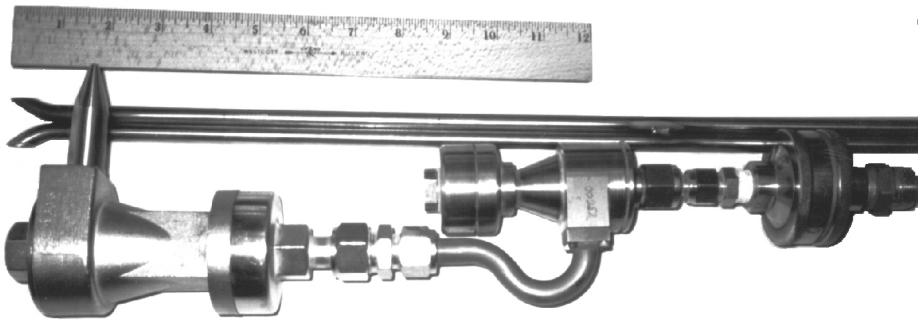

Figure 8-18. Dual cyclone sampling head for PM_{10} and $PM_{2.5}$

This sampling system consists of a nozzle, a PM_{10} cut size cyclone identical to the one used in U.S. EPA Method 201A, a $PM_{2.5}$ cut size cyclone, and a filter. Using this sampling system, the particulate matter captured in the gas stream is separated into the following size fractions.

- Supercoarse particulate matter larger than 10 micrometers
- Coarse particulate matter larger than 2.5 micrometers and equal to or less than 10 micrometers
- Fine particulate matter equal to or less than 2.5 micrometers

The material equal to or less than 2.5 micrometers (filter and filter inlet) is defined as $PM_{2.5}$ particulate matter. PM_{10} consists of the fine particulate matter plus the coarse particulate matter ($PM_{2.5}$ cyclone, filter, and filter inlet). Total filterable particulate matter consists of the combined material in all three size categories.

One of the advantages of this sampling approach is that it is possible to obtain emissions data in the PM_{10} and $PM_{2.5}$ size categories simultaneously. Furthermore, separate emission measurements are obtained for the fine and coarse fractions of PM_{10}. The sampling train can be used to acquire sufficiently large sample quantities to facilitate detailed chemical analyses. This is important because there is increasing interest in the specific chemical species present in the fine particulate matter fraction.

The development of this method has allowed the direct measurement of $PM_{2.5}$ emissions from a variety of stationary sources. These emission data are needed to develop effective control strategies to achieve $PM_{2.5}$ NAAQS in the future.

8.3 EMISSION MONITORING

8.3.1 Opacity

Particles entrained in a gas stream scatter visible light. The extent to which the intensity of the light beam is reduced is described by the Beer-Lambert law shown as Equation 8-6, which indicates that the extent of light reduction is exponentially related to the particle concentration.

$$T = \frac{I}{I_o} = e^{-\alpha c l} \tag{8-6}$$

Where:

T = light transmittance

I = intensity of the light energy leaving the gas

I_o = intensity of the light energy entering the gas

= attenuation coefficient

c = concentration of the pollutant

l = distance the light beam travels through the gas

The most convenient way to express the reduction in light intensity is the opacity. This term is defined in Equation 8-7.

$$\text{Opacity} = 100 - \text{Transmittance (\%)} \tag{8-7}$$

If there is no reduction in light intensity, the transmittance is 100% and the opacity is zero. If all the light is scattered, the transmittance is zero and the opacity is 100%. High opacity is generally associated with high particulate matter concentrations. Accordingly, opacity is used as an indirect indicator of particulate emissions in some regulations and as a separately enforceable requirement in other regulations.

However, in most cases, it is not possible to directly correlate the opacity and the particulate emissions measured by the reference methods described earlier in this section. This is partially because the attenuation coefficient, , in the Beer-Lambert law is dependent on the wavelength of light and on the characteristics of the particles. One of the most important factors is the particle size distribution. The particle size distribution is rarely measured and can vary substantially due to process and control system operating conditions. A large number of relatively expensive emission tests would be necessary to characterize an accurate and precise opacity-particulate mass emission correlation for a specific source.

Nevertheless, opacity is a very useful diagnostic and enforcement tool. It can be determined manually using U.S. EPA Method 9 and instrumentally using opacity monitors operating in accordance with 40 CFR Appendix B, Performance Specification 1.

A simplified schematic of a continuous opacity monitor is shown in Figure 8-19. Visible light from a specially designed lamp passes through a beam splitter. Part of the light beam goes directly to the detector as an indication of the initial light intensity. The remainder of the light beam passes across the stack, is reflected over the retroreflector, passes across the stack a second time, and strikes the detector. The difference between the two light beam intensities is used as a measure of the light transmittance. Blowers and filters (not shown in Figure 8-19) are used to keep optical windows (not shown) on both the source and retroreflector clean.

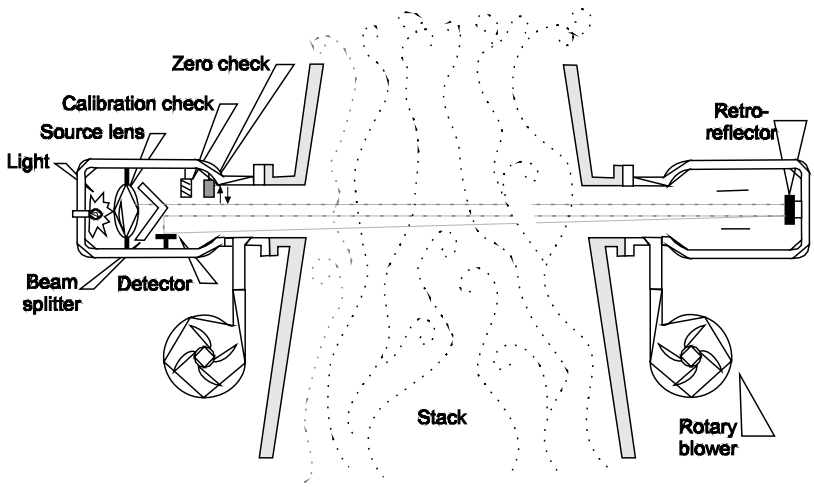

Figure 8-19. Double-pass opacity monitor

The following seven items are the main design criteria for opacity monitors:

1. **Spectral response** - Maximum sensitivity of the system must be between 500 and 600 nanometers (nm). No more than 10% of the response can be outside the range of 400 to 700 nanometers.

2. **Angle of projection** - The light beam must be within an angle of 5°.

3. **Angle of view** - The detector must have an angle of view within 5°.

4. **Calibration error** - The instrument must be within 3% of the opacity indicated by calibration neutral density filters.

5. **Response time** - A step change in opacity must be identified at least 95% in less than 10 seconds.

6. **Sampling** - One measuring cycle every 10 seconds is required, and there must be at least one data point recorded every 6 minutes.

7. **System operation check** - There must be a way to check the "active" elements of the system in the zero and calibration procedures.

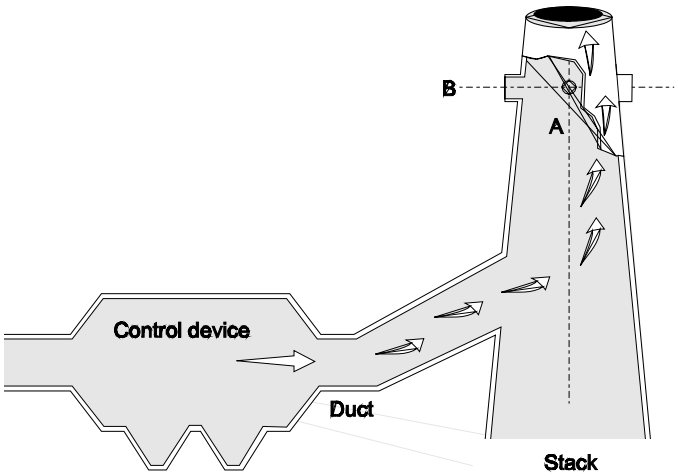

Figure 8-20. Siting for opacity monitor

The spectral response is important since the wavelength band specified is in the visible range where none of the common pollutant gases (except the dimmer of nitrogen dioxide) absorb light. At wavelengths above 700 nm, water and carbon dioxide (two common components of combustion gases) absorb light. Below 340 nm, sulfur dioxide absorbs light. The visible range of 400 to 700 nm is also identical to the visible light that is inherently used in U.S. EPA Method 9 visible emission observations.

The angle of projection and view are important since the detector should not be exposed to light that has been scattered by particulate matter in the gas stream. The 5° values are based on the need to maintain an accurate instrument without unnecessary, costly optical components.

The continuous opacity monitor must be located in a position where it provides a representative measurement of the in-stack opacity. It is usually mounted in a position as far as possible from upstream and downstream flow disturbances, which could cause stratification of the particulate matter in the gas stream. It is generally mounted in the plane of the bend when it is installed downstream from a turn. The importance of this siting criteria is illustrated by Figure 8-20 which shows alternative positions A and B.

In position A, the monitor would not see the high concentration stream of particulate matter which has stratified on the right side of the stack due to the inertia of the particles entering the stack from the elbow to the left. By mounting the instrument in position B, its field of view crosses this high concentration area.

In order to be used for compliance monitoring, the continuous opacity monitor must successfully complete the requirements included in Performance Specification 1. During a one week test, the instrument system must have zero drift less than or equal to 2% opacity, a calibration drift less than or equal to 2% opacity, and a response time of 10 seconds or less.

Once operational, opacity monitors require routine servicing to ensure proper performance. The instruments can be vulnerable to several problems, most of which cause higher-than-actual opacity readings:

- Excessive dirt accumulation on the optical windows
- Misalignment of the source and retroreflector modules
- Electronic drift due to high temperatures at the instrument location
- Lamp failure
- Data recorder failure

8.3.2 Particulate Matter Continuous Emission Monitors

There are a variety of instruments that are being developed and used to provide a continuous measurement of the particulate matter mass emissions (Particulate CEMs). There are four different types of instruments being evaluated for possible application in future emission monitoring applications.

- Light scattering instruments
- Beta gauge instruments
- Scintillation monitors
- Oscillating microbalance instruments

The light scattering instruments operate on entirely different principles than opacity monitors used to measure opacity. The light scattering particulate matter CEMs measure the quantity of light that is scattered in specific directions from the surfaces of particles passing through the detection area. The detection area is a small zone located several feet within the stack or duct being monitored. Unlike transmissiometers used to measure opacity, light scattering particulate matter CEMs do not use a light beam passing across the entire stack or duct.

The scattered light energy received at the detector is amplified to provide a signal proportional to the particulate matter mass in the sensor zone. One commercial type of light scattering particulate matter CEMs is illustrated in Figure 8-21.

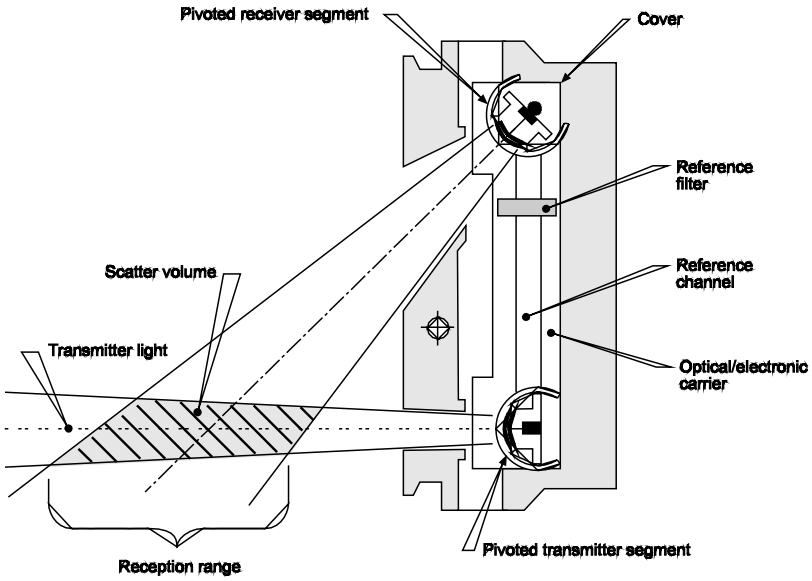

Figure 8-21. Light scattering type particulate CEM
(Reproduced courtesy of Sick, Inc.)

Light scattering particulate matter CEMs detect both solid and liquid particles. They can not distinguish between the presence of solid particles and condensed uncombined water droplets. However, the instruments can be designed to operate on a small slip stream extracted from the stack and dried before entering the sensor area. These types of extractive light scattering particulate matter CEMs are being considered for some wet stack applications.

Scintillation particulate CEMs operate in a manner that is conceptually similar to transmissometers. The scintillation monitors generate a light beam that is projected across the stack or duct being monitored.

However, unlike transmissometers, the wavelength of the scintillation instrument light source is modulated at a high frequency. The instrument detector obtains a frequency dependent light signal that is proportional to the mass concentration of particulate matter passing through the light beam. Figure 8-22 illustrates a commercially available scintillation instrument.

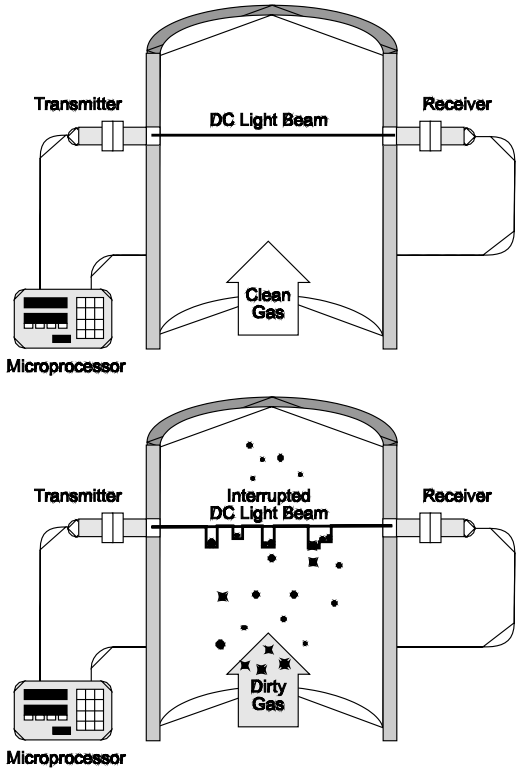

Figure 8-22. Scintillation monitor
(Reproduced courtesy of BHA, Inc.)

Like all light scattering instruments, the scintillation instrument is moderately sensitive to the particle size distribution. It also can not distinguish between solid particles and droplets of uncombined water. All particles and droplets that are capable of scattering light are detected with this instrument.

A beta gauge instrument collects a sample of particulate matter on a filter and exposes the sample to low levels of beta radiation. The amount of radiation absorbed by the sample is proportional to the mass of solids on the filter. All beta gauge instruments extract the sample from one or more points in the stack or duct being monitored. The samples are accumulated on the filter surface for periods ranging from 1 minute to more than twenty minutes depending on the concentration of solids in the gas stream. Once there is sufficient sample, the sample gas stream is interruped and the sample and filter are exposed to beta radiation. A beta ray detector below the filter is used to compare the energy levels with the collected solids with a baseline energy level obtained when the filter was clean. One commercial type of beta gauge particulate matter CEMS is shown in Figure 8-23.

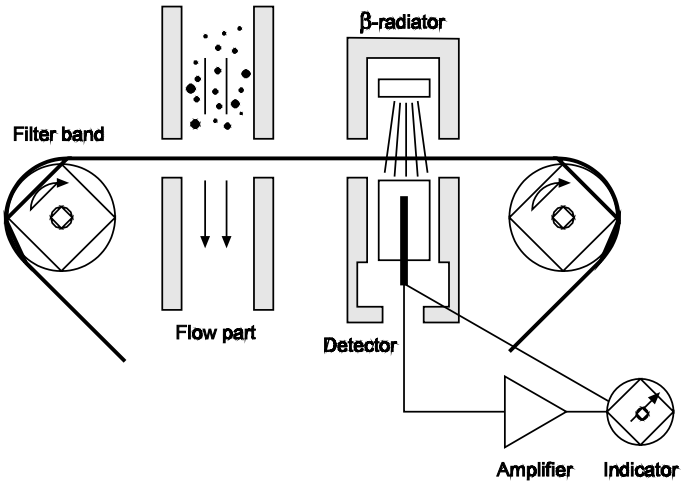

Figure 8-23. Beta gauge instrument
(Reproduced courtesy of Durag, Inc.)

Due to the need to acquire a sample, the beta gauge instruments provide mass concentration data over discrete averaging periods. The accuracy of the mass concentration measurement depends on the extent of beta ray energy absorption by the solids and on the accuracy of the measured sample gas flow rate transporting the solids from the stack to the filter. One of the advantages of the beta gauge instruments is that they are not highly dependent on variations in the particle size distribution of the solids being collected.

An oscillating microbalance particulate matter CEMS uses an extractive system to collect a sample on a small detector that oscillates initially at a known frequency. The accumulation of solids on this detector changes the frequency of oscillation. The measured change in frequency is fundamentally related to the mass quantity. A commercially available oscillating microbalance instrument is illustrated in Figure 8-24.

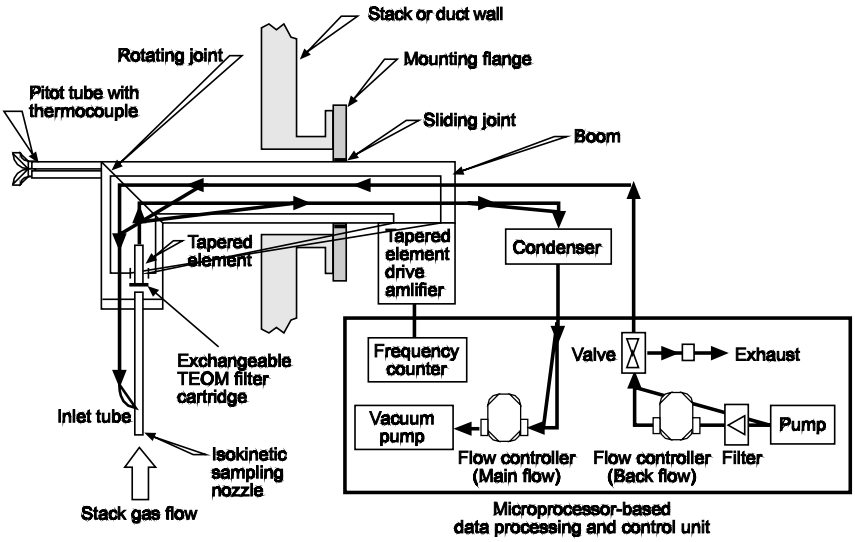

Figure 8-24. Oscillating microbalance particulate CEMS
(Reproduced courtesy of Rupprecht & Patashnick Co., Inc.)

The accuracy of the mass concentration measurement is dependent on the accuracy of the sample gas flow rate. This type of unit provides a mass concentration measurement that is independent of the particle size distribution. When the sample gas stream is dried prior to deposition on the detector, the instrument can detect solid particles independent of uncombined water droplets. However, as is the case with all drying systems, care is needed in drying to avoid the volatilization of particles composed, in part, of compounds such as ammonium nitrate and low molecular weight orgnic compounds.

Review Exercises

1. What is the normal range of applicability of cascade impactors?
   a. 10 m - 100 m
   b. 1 m - 20 m
   c. 0.5 m - 20 m
   d. 0.3 m - 20 m
   e. 0.005 m - 3 m

2. What is the normal range of applicability of optical microscopes?
   a. > 10 m
   b. > 3 m
   c. > 1 m
   d. > 0.3 m
   e. > 0.005 m

3. What is the normal filter temperature in a U.S. EPA Method 5 sampling train?
   a. 400°F
   b. 320°F
   c. 248°F
   d. 168°F
   e. 68°F
   f. 20°C

4. What types of problems affect the accuracy of cascade impactors for measuring the particle size distribution?
   a. Particle bounce
   b. Particle fracturing
   c. Stage reentrainment
   d. All of the above

5. What filterable particulate measurement method uses an in-stack filter? Select all that apply.
   a. Method 5
   b. Method 17
   c. Method 201A
   d. Dual Cyclone (Method 201B)
   e. All of the above

6. What EPA method concerns the proper location for emission testing
   a. Method 1
   b. Method 2
   c. Method 3
   d. Method 4
   e. Method 5
   f. Method 101A

7. A transmissometer is mounted downstream of a 90˚ elbow in a duct. How should the transmissometer be mounted?
   a. In the plane of the bend
   b. 90˚ to the plane of the bend
   c. Either a or b

8. What EPA method concerns visible emission observations?
   a. Method 1
   b. Method 3
   c. Method 6
   d. Method 9

9. PM_{10} particulate matter can be divided into which two size categories?
   a. Supercoarse and coarse
   b. Coarse and fine
   c. Fine and ultrafine
   d. None of the above

10. An observer is attempting to make a U.S. EPA Method 9 opacity observation of a stack. Inadvertently, the observer selects an observation site where there are two identical stacks along the line-of-sight. Therefore, the light reaching the observer is passing through two plumes. Both of these plumes have an opacity of 20%. What is the opacity seen by the observer?
    a. 20%
    b. 24.5%
    c. 36%
    d. 40%
    e. 52.5%
    f. 80%

Review Answers

1. What is the normal range of applicability of cascade impactors?

   d. 0.3 m - 20 m

2. What is the normal range of applicability of optical microscopes?

   b. > 3 m

3. What is the normal filter temperature in a U.S. EPA Method 5 sampling train?

   c. 248°F

4. What types of problems affect the accuracy of cascade impactors for measuring the particle size distribution?

   d. All of the above

5. What filterable particulate measurement method uses an in-stack filter? Select all that apply.

   b. Method 17
   c. Method 201A
   d. Dual Cyclone (Method 201B)

6. What EPA method concerns the proper location for emission testing

   a. Method 1

7 . A transmissometer is mounted downstream of a 90 elbow in a duct. How should the transmissometer be mounted?

   a. In the plane of the bend

8. What EPA method concerns visible emission observations?

   d. Method 9

9. PM_{10} particulate matter can be divided into which two size categories?

   b. Coarse and fine

10. An observer is attempting to make a U.S. EPA Method 9 opacity observation of a stack. Inadvertently, the observer selects an observation site where there are two identical stacks along the line-of-sight. Therefore, the light reaching the observer is passing through two plumes. Both of these plumes have an opacity of 20%. What is the opacity seen by the observer?

    c. 36%

Solution:

Basis: 100 units of light are approaching the first plume. Transmittance through first plume is 80 units of light.

Light approaching the second plume is 80 units.
Transmittance is 80% through second plume.
Light leaving second plume is 64 units.

Total transmittance through both plumes is 64%. So the opacity is approximately 36%.

Bibliography

Hewitt, G.W. *The Charging of Small Particles for Electrostatic Precipitation.* Paper No. 73-283. Presented at the AIEE Winter General Meeting. New York, NY, 1957.

U.S. Environmental Protection Agency. *Guidelines for Particulate Sampling in Gaseous Effluents from Industrial Processes.* EPA 600/7-79-028. 1979.

References

1. Southern Research Institute, *PM_{10} and $PM_{2.5}$ Measurement Methods, Draft Report.* 1989.

2. *Air Control Techniques, $PM_{2.5}$ Test Protocol.* Portland Cement Association Research Publication 2081. 1996.